Mechanical Joineries for Deployable Reciprocal Shells Through Auxetic Behaviour (DR STAB)

Surendar Jayachandran

A thesis submitted to Auckland University of Technology
in fulfilment of the requirements for the degree of Doctor of Philosophy (PhD)

2025

School of Future Environments

Auckland University of Technology (AUT)

Surendar Jayachandran
[0009-0003-1565-5384]

Supervised by:

Charles Walker [0009-0000-3307-7301]
&
Dermott Mcmeel [0000-0002-3790-3444]

Acknowledgments

This research has been a long and winding journey, but never a solitary one. I owe this work to many whose presence whether in mind, in person, or in spirit shaped the path and lightened the weight along the way.

To my grounding roots, my mother Parimala and my father Jayachandran, and to my wider family, thank you for your unwavering love, patience, and encouragement. You have held the space for me to pursue what I love and remained my constant north star whenever things felt adrift.

To those who walked ahead so I could follow, my supervisors, Professor Charles Walker and Associate Professor Dermott McMeel, your insights, provocations, and critical reflections have profoundly shaped the intellectual and creative scaffolding of this work. My gratitude also extends to the wider team at the School of Future Environments (SoFE), including the ever-reliable support from the SoFE Makerspace, whose quiet assistance was always present, even when unseen.

This PhD continues the trajectory initiated in my master's thesis at Politecnico di Milano, which laid the foundation for this research. I remain deeply grateful to Professor Ingrid Paoletti for her mentorship and for inspiring the direction that has since evolved into this doctoral study.

To the colleagues and friends whose expertise complemented my own Shylesh, for his mastery of Grasshopper, and Logu Prashanth, for his guidance in navigating the depths of SolidWorks thank you for lifting the technical aspects of this work when I reached my limits.

To Sri Uma Devi, who brought structure to my chaos, and Nidisha Jagati, a summer intern from India, whose tireless efforts during the physical prototyping phase were indispensable your contributions were invaluable. I also acknowledge Elisabetta Magenes, Hidayath, Meghna, and many others who offered strength and support during my earlier academic journey.

A quiet note of appreciation is also due to the AI tools that supported my thinking, structuring, and drafting processes, and to the countless hours of podcasts that provided companionship during the late-night stretches of writing. The natural beauty of New Zealand offered balance and renewal whenever I needed to step away from the screen and reconnect with clarity.

Finally, to those who repeatedly asked, "Why do you want to do a PhD?" your doubt became my daily affirmation. In answering you, I was reminded of the curiosity and passion that set this journey in motion. Your question became my compass.

This thesis stands not only on data, design, and diagrams, but also on the echoes of encouragement, the unseen scaffolding of care, and the guiding hands that held me upright through the fog.

Parallel Research Acknowledgement

Elements of this doctoral research have been developed into a series of peer-reviewed papers that were presented at the *Green + Digital + Intelligent Built Environments (GDI 2025) International Conference* and subsequently published in the Lecture Notes in Civil Engineering by Springer Nature. These works, co-authored with Charles Walker and Dermott McMeel, represent progressive stages of the study and collectively contribute to its theoretical and experimental advancement. The published papers include: Geometrical Analysis of Reciprocal Tessellations for DRSTAB System* (Paper No. 495), Geometrical Analysis of Auxetic Tessellation for DRSTAB System (Paper No. 496), Analysis of Auxetic Behavior (Movements) and Replication in Mechanical Movements for DRSTAB System (Paper No. 497), Digital Simulations and Physical Prototypes (Proof of Concept) of Auxetic Behavioral Movements in DRSTAB System (Paper No. 498), and Digital Simulations and Physical Prototypes (Proof of Concept) of Mechanical Joinery in DRSTAB System (Paper No. 499) (Jayachandran, Walker, & McMeel, 2025).

All five papers underwent international peer review and were formally presented during the GDI 2025 conference, held from 1–3 December 2025. The conference proceedings have since been published within the *Lecture Notes in Civil Engineering* series by Springer Nature and are indexed in SCOPUS following Springer's quality assurance process. Collectively, these publications have informed and reinforced multiple components of this thesis, supporting the exploration of geometric logic, auxetic mechanisms, mechanical joinery design, and digital-to-physical experimentation within the DRSTAB framework.

Feedback from the GDI 2025 review panel and subsequent scholarly engagement played a significant role in refining the research direction and strengthening its academic articulation. Reviewer insights led to targeted improvements in argument structure, data interpretation, and synthesis, prompting the re-evaluation and revision of several sections. This iterative process enhanced the coherence between theoretical foundations, analytical methods, and empirical findings, contributing to the overall methodological rigor and clarity of this thesis.

Abstract

Double-curved shells are admired in architecture for their strength, elegance, and efficiency, yet they remain difficult to build, costly to fabricate, and often impossible to reuse once completed. Conventional approaches rely on custom components and rigid geometries that limit flexibility and increase labor demands. Addressing these challenges requires new systems that combine structural efficiency with adaptability.

One promising direction lies in bringing together two powerful principles: reciprocal framing, which distributes loads through interdependent members, and auxetic geometries, which expand and contract in controlled ways. When integrated, these principles open the possibility of creating shells that can be flat-packed, deployed into complex three-dimensional forms, and retracted for reuse.

The key to achieving this lies in mechanical joinery. In this study, joints are designed not as secondary connectors but as the main drivers of motion and stability. Through a combination of digital modelling and physical prototyping, systems such as ratchets, one-way bearings, and hybrid locking mechanisms were tested to guide expansion, rotation, and locking.

The findings highlight a pathway toward adaptable, reusable architectural systems that minimize material waste and assembly effort. Potential applications include temporary architecture, disaster relief structures, and remote construction. By linking geometric intelligence with mechanical precision, this work lays the foundation for a new class of deployable and sustainable building systems.

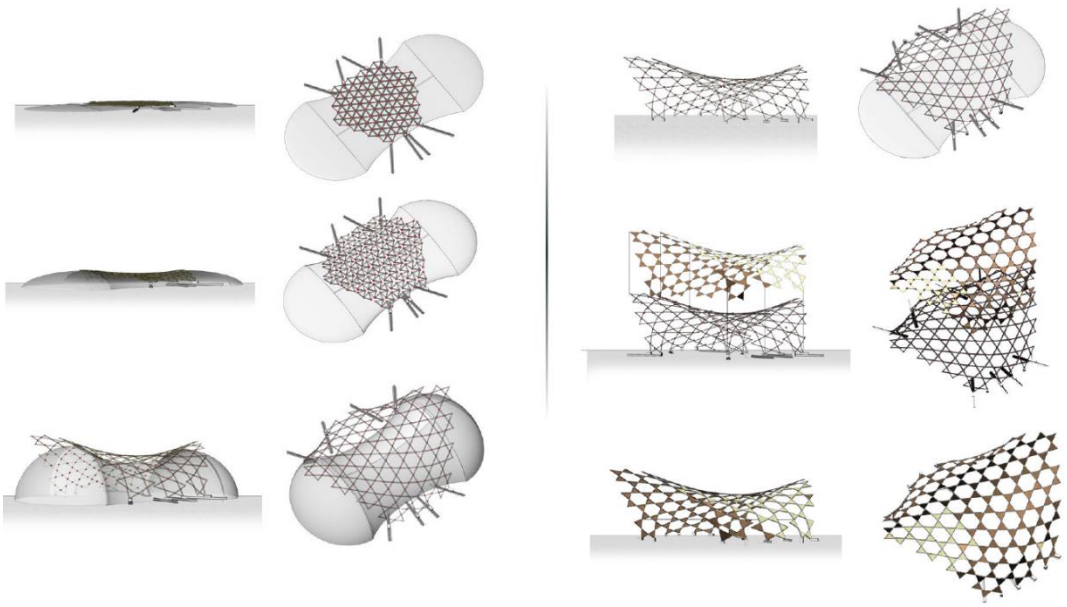

Figure 1.1-1 Abstract Visual representation of DRSTAB system in action
Note: From , *Deployable reciprocal shells through auxetic behaviour: Architectural hypothesis to fabricate double-curved structures* by *Jayachandran, S. (2019).*

Table of contents

List of Figures

List of tables

Glossary and abbreviations

Abbreviation	Full Form
DRSTAB	Deployable Reciprocal Shells Through Auxetic Behaviour
CAD	Computer-Aided Design
DoF	Degree(s) of Freedom
PETG	Polyethylene Terephthalate Glycol
FEA	Finite Element Analysis
ANSYS	Analysis System (Engineering simulation platform)
CSK	Clutch-Sprag Key (bearing code used in one-way clutch bearings)
BOM	Bill of Materials
STL	Stereolithography File Format (for 3D models)
3DP	3D Printing
GH	Grasshopper (Visual Programming Plugin for Rhino)
NGon	Polygon with "n" sides (refers to a plugin in Grasshopper)
CNC	Computer Numerical Control
PGR9	Postgraduate Research Milestone 9 (AUT milestone protocol)
RF	Reciprocal Frame
RQ	Research Question
RM	Research Methodology

Attestation of Authorship

“I hereby declare that this submission is my own work and that, to the best of my knowledge and belief, it contains no material previously published or written by another person (except where explicitly defined in the acknowledgements), nor used artificial intelligence tools or generative artificial intelligence tools (unless it is clearly stated, and referenced, along with the purpose of use), nor material which to a substantial extent has been submitted for the award of any other degree or diploma of a university or other institution of higher learning.”

Signed

Surendar Jayachandran

(18/11/2025)

Chapter #1

What / Why / How

Introduction

Research Questions

Research methods

1 Introduction

1.1 Introduction

The construction industry is increasingly driven by the need for flexible, sustainable, and rapidly deployable systems. Traditional building methods often fall short in addressing spatial adaptability, efficient transport, and reusability particularly in contexts such as temporary infrastructure, disaster-relief architecture, or remote-site construction. In parallel, experimental domains such as kinetic architecture and computational design have proposed novel typologies, yet many remain limited by their reliance on bespoke mechanisms or one-off applications (Panetta et al., 2021) . This research addresses these challenges by proposing a construction system that synthesizes reciprocal structural principles, auxetic expansion of behaviour, and deployable mechanisms through a unified framework of mechanical joinery.

The system, termed DRSTAB (Deployable Reciprocal Shells through Auxetic Behaviour), is modular, flat-packed, and transformable. Once deployed, it forms self-supporting double-curved shells that can be adapted, locked in position, and retracted when needed. The reciprocal frame offers structural redundancy and geometric adaptability; auxetic patterns provide uniform expansion across the surface; and deployability enables compact transport and efficient on-site assembly. While early stages of this research explored these systems holistically, feedback and further inquiry identified a critical gap in existing literature and practice: the mechanical articulation of movement via joinery systems. In response, the study evolved to focus extensively on designing and testing mechanical joineries that could accurately replicate and control auxetic movement in architectural contexts.

The methodology spans computational simulation (Rhino, Grasshopper, SolidWorks) and physical prototyping using laser-cut PETG, 3D printing, and mechanical mock-ups. By iterating between digital models and real-world trials, the research validates the feasibility of translating complex geometric behaviours such as pitch and yaw into engineered, scalable components.

This investigation began with broader ambitions for an integrated deployable construction system, but the complexity and criticality of mechanical joineries quickly became apparent. As the research progressed, it became clear that the joineries could not remain secondary. An overall resolved design could not be achieved without first advancing the mechanical joinery, it demanded to take centre stage. The thesis consequently pivoted, narrowing its focus to advancing the knowledge surrounding joinery design and performance: how joineries enable structural transformation and their behaviour reliably simulated. While an overarching design outcome was not achievable within this scope, this concentration yields a rigorous and grounded contribution to knowledge. One that lays essential groundwork for future adaptable architectural systems.

1.2 Rationale and Significance of the Study

Addressing current limitations : Conventional construction methods, particularly for complex geometries such as double-curved shells, remain bound by rigid prefabrication, intensive labour requirements, and logistical inefficiencies. These systems are typically static, non-reusable, and material-heavy, making them ill-suited to contexts where adaptability, speed, and resource efficiency are critical. For instance, the construction of freeform roofs or shell pavilions often relies on bespoke scaffolding and custom-fabricated elements, resulting in high embodied energy and limited reusability once dismantled (Friedman et al., 2011,). As global design priorities shift toward sustainability, circularity, and rapid deployment, these traditional

methods reveal fundamental shortcomings. There is therefore a growing need to explore structural methodologies that are lightweight, reversible, and responsive to changing demands.

Introducing a transformative system : This research proposes an alternative approach by integrating reciprocal framing, auxetic patterning, and deployability into a unified construction system. Designed to be transported as a flat-packed unit, the structure can be deployed into a self-supporting, double-curved shell with minimal external equipment, and later retracted or redeployed at different scales and configurations. This transforms what is typically a static, single-use construction into a reusable, kinetic framework. While the early phases of the study focused on identifying geometric patterns and testing deployability, iterative feedback revealed a critical gap in the articulation of mechanical movement. Addressing this gap shifted the research emphasis toward the design and testing of mechanical joineries, reframing them as the central innovation that allows geometry, structure, and kinematics to converge.

Enhancing versatility and flexibility : The system's modular logic offers significant potential for formal and spatial adaptability. Unlike conventional shells, which often rely on bespoke fabrication for each unique geometry, this approach enables variation in curvature and configuration without redesigning the entire system. Parametric design tools further enhance control, allowing transformation behaviour, structural performance, and deployment logistics to be co-designed from the outset. This marks a shift from static formalism toward time-based architectural practice, where structures evolve dynamically in response to context, program, and temporal needs. Such adaptability is particularly relevant in contemporary scenarios where spaces must increasingly accommodate shifting functions from temporary events to transitional housing without wasteful reconstruction.

Supporting sustainable practices : By enabling reversible deployment, the system aligns with circular construction principles. Components are designed for multiple use cycles, simple replacement, and compact transport, significantly reducing material waste compared to conventional demolition and rebuild processes. The removal of heavy scaffolding and complex formwork lowers both operational energy and carbon emissions, offering advantages in contexts where sustainability targets are critical. This has particular relevance in remote or resource-constrained environments, where the ability to erect, retract, and relocate structures with minimal infrastructure provides both ecological and logistical benefits.

Broad architectural applicability : The system's adaptability opens applications across multiple architectural scales and contexts. It is suited for temporary pavilions and exhibitions requiring rapid assembly and disassembly; emergency shelters where speed and reusability are critical; mobile infrastructure for remote communities and disaster recovery; and experimental kinetic architecture that explores new forms of spatial engagement. Its capacity to expand, lock, retract, and redeploy without structural compromise positions it as a versatile design solution that directly addresses the volatility and mobility of contemporary urban conditions.

Expanding disciplinary imagination : Beyond practical applications, this research challenges the conventional binary between static structures and kinetic systems. By embedding kinematic behaviour into joinery design, it redefines structure not as a fixed object, but as a responsive mechanism capable of adapting over time. This reframing invites interdisciplinary exploration between computational geometry, mechanical engineering, and architectural design, advancing new models for intelligent and adaptable construction. In doing so, it pushes the boundaries of architectural imagination, proposing a framework where geometry, material, and mechanics operate as a synergistic whole rather than as separate domains.

1.3 Aim & objective

This research aims to develop a modular construction system that combines the geometric logic of reciprocal frames, the expansion behaviour of auxetic patterns, and the transformational capacity of deployable structures. The system is designed to begin as a flat configuration, expand into a double-curved shell through controlled movement, and then retract into its original compact state for reuse. At the core of this transformation is a suite of custom-designed mechanical joineries, which translate abstract geometrical behaviour into real-world mechanical performance.

Initially focused on pattern selection and deployability strategies, the research evolved in response to identified gaps in existing literature, particularly the lack of engineered joinery solutions capable of supporting movement, locking, and structural transfer at architectural scales. The refinement toward mechanical joinery design was therefore essential to grounding the system's deployability in practical construction logic. The objectives of this research are as follows:

- To integrate auxetic geometry and reciprocal framing into a deployable architectural system.
- To design mechanical joineries capable of supporting the key movements involved in deployment and retraction.
- To simulate movement behaviour and load transfer using digital tools such as Grasshopper and SolidWorks.
- To fabricate scaled and full-scale prototypes that validate the mechanical feasibility and spatial performance of the system.
- To contribute a methodology for developing reconfigurable, lightweight, and logistically efficient architectural shells.

Together, these objectives support a broader aim: to reimagine kinetic architectural systems not as isolated mechanical novelties, but as integrated frameworks where structure, geometry, and motion operate in harmony.

1.4 Conceptual Framework: Synergy of Reciprocal, Auxetic, and Deployable Systems

This research section outlines the rationale that adopts an integrated workflow that synthesizes three distinct yet complementary design principles reciprocal systems, auxetic behaviour, and deployability mechanics to form a modular construction strategy for double-curved architectural shells. Each component contributes uniquely: reciprocal structures offer distributed stability (Chilton et al., 2015; Gíslason, 2010), auxetics enable controlled surface expansion (Evans & Alderson, 2000; Grima & Evans, 2006; Lakes, 1987), and deployable systems facilitate compact transformation (Pellegrino, 2001; Fenci & Currie, 2017). Together, they address challenges in adaptability, fabrication, and assembly, advancing a construction logic that is structurally efficient, materially responsive, and reconfigurable across diverse contexts.

1.4.1 The Role of Reciprocal Systems in Structural Expression and Redundancy

Reciprocal structures have long fascinated architects and engineers due to their self-supporting geometry, where each element is both supported by and supports others in a mutual load-sharing configuration (Popovic Larsen, 2008; Parigi & Kirkegaard, 2014). This quality offers a strategic advantage in creating lightweight yet strong spatial forms without the need for centralized connections or extensive formwork (Douthe & Baverel, 2009). In this research, the reciprocal principle is employed not simply as a geometrical curiosity, but as a structural strategy for enabling distributed load paths, architectural elegance, and scalability in modular assemblies (Chilton et al., 2015).

Reciprocal systems are inherently adaptive to complex curvatures due to their capacity to propagate geometrical transformations across a network of interdependent units (Veenendaal et al., 2011). When applied to double-curved surfaces, these systems offer a bottom-up method of form generation that aligns with the principles of parametric design (Jayachandran, 2019). Unlike traditional linear or planar framing systems, reciprocal networks do not require fixed orientation or a hierarchical assembly process, making them ideal candidates for modular deployable applications where construction speed and flexibility are critical (Larsen, 2008).

Moreover, the absence of a single point of failure enhances the structural resilience of the entire system (Baverel et al., 2000). Each unit reinforces the stability of the next, enabling a high degree of material optimization while achieving visual lightness. This characteristic becomes especially significant when integrated with deployable mechanisms, as the interdependency of elements inherently supports kinetic movement without compromising structural integrity during and after deployment. By utilizing reciprocal systems as the base structural framework, the research lays the groundwork for a system that is scalable, redundant, and materially efficient.

1.4.2 Auxetic Behaviour as a Performance Modifier in Material and pattern Dynamics

The incorporation of auxetic behaviour into the system introduces a counterintuitive, yet highly beneficial mechanical property: materials or systems that expand laterally when stretched and contract when compressed (Evans & Alderson, 2000; Lim, 2015; Saxena et al., 2016). This negative Poisson's ratio can be particularly advantageous when embedded into construction systems where controlled deformation, energy absorption, and stress distribution are critical (Lakes, 1987; Zhang et al., 2020).

In the context of this research, auxetic principles are not restricted to materiality alone but are abstracted into configurational logic (Grima & Evans, 2006; Konaković Luković et al., 2016), informing the way modules expand, fold, and react to external forces. When deployed in tandem with reciprocal geometries, auxetic patterns enable synchronized movement across the structure (Babaee et al., 2013), facilitating uniform unfolding or contraction without the need for complex actuators or external guidance systems (Mir et al., 2019). This synergy is vital for achieving a deployable shell that maintains geometrical coherence and structural stability throughout its transformation process.

Auxetic principles also play a crucial role in enhancing mechanical joinery design. As each joint must accommodate dynamic rotation and force redistribution during deployment, auxetic-inspired joints provide compliance and adaptability, reducing wear and stress concentrations (Alderson et al., 2010). By tuning the joinery geometry to exhibit auxetic behaviour, the system

gains both flexibility during movement and rigidity upon locking, a dual performance often sought but rarely achieved in kinetic architectural systems (Bertoldi et al., 2017).

Furthermore, auxetic behaviour contributes to thermal, acoustic, and vibrational performance (Lu et al., 2022), which are increasingly important in contemporary architecture. The ability of such systems to absorb energy and dampen oscillations suggests potential applications in disaster-resilient architecture and kinetic façade systems (Naboni et al., 2017). Therefore, the auxetic principle is not merely an academic curiosity but a functional enabler that enhances adaptability, robustness, and multifunctionality of the proposed structural system.

1.4.3 Deployability mechanics as a Catalyst for Construction Efficiency and Reusability

The principle of deployability forms the operational backbone of the system. As global construction shifts toward faster, modular, and less labor-intensive methods, deployable systems offer a compelling alternative to traditional static construction (Pellegrino, 2001; Handoo, 2018). In this research, deployability is not treated as an isolated mechanism but as an integrated strategy that begins from the material configuration and extends through to assembly and disassembly cycles (Fenci & Currie, 2017).

Deployability addresses key logistical constraints transportation, assembly time, site access limitations, and labor requirements by enabling structures to be compactly stored and rapidly expanded in situ (Rivas-Adrover, 2017; Volkov et al., 2021). When combined with the geometric interlock of reciprocal elements and the transformational flexibility of auxetic patterns, the proposed system offers fluid transition between compact and expanded states, with minimal reliance on cranes, scaffolding, or specialized tools (Jackson, 2011).

What differentiates this approach is the continuous loop of transformation: the system can be flattened, transported, deployed, and re-flattened with minimal degradation in performance (Veenendaal et al., 2011). This makes it especially suitable for temporary structures, disaster-relief shelters, mobile pavilions, or infrastructure in remote areas (Mir et al., 2019). By minimizing permanent connections and utilizing intelligent mechanical joineries, the design enables multiple life cycles of construction, use, and re-deployment contributing to sustainability not just in materials but in operation and longevity.

1.4.4 Synergy: Why Integration Matters

While each of the three principles- Reciprocal, auxetic, and deployable ,offers independent advantages, it is their integration that unlocks transformative potential (Bertoldi et al., 2017; Mir et al., 2019). Reciprocal structures provide distributed load sharing and modular form-making; auxetic principles imbue the system with flexibility and smart material-like behaviour; deployability introduces temporal dynamism and logistical efficiency. Together, they form a multi-scalar system capable of operating at the level of material, joint, module, and overall structure.

This triadic framework also supports computational exploration and optimization (Konaković Luković et al., 2016; Panetta et al., 2021). Parametric design tools can simulate the interaction of reciprocal geometries, auxetic expansions, and deployable pathways, offering a new design space where structure and function are co-generated. By mapping out the interdependencies between movement, force, and form, the system moves closer to a cyber-physical logic, where each component is responsive, interconnected, and optimally placed (Baverel et al., 2000).

The development of customized mechanical joineries is the final piece in this integrated puzzle (Collins, 2009; Mott, 2014). Joineries become the translators between structural forces and material behaviour, between movement and stability. Their design rooted in material science, robotics, and architecture must negotiate the nuanced demands of rotation, locking, expansion, and retraction (Sclater, 2011; Norton, 2020). The ongoing investigation into mechanical joineries not only grounds the theoretical framework but also forms the technical bridge from conceptual proposition to real-world application..

Conceptual Foundation: Integration of Reciprocal, Auxetic, and Deployable Principles in Construction Innovation

The development of new construction methodologies requires a critical rethinking of structural behaviour, material performance, and deployment efficiency. This research strategically integrates three core concepts reciprocal systems, auxetic behaviour, and deployability principles to conceive a novel construction system that is structurally expressive, materially intelligent, and functionally adaptive. Each technique, while rooted in distinct disciplinary origins, converges in this research to address fundamental challenges in the design and erection of double-curved architectural forms. By exploring the synergies between these principles, the proposed system aims not merely to produce new forms, but to transform the way construction systems are conceptualized, assembled, and reconfigured across diverse architectural scenarios.

1.4.5 Reciprocal Structures

Reciprocal structures represent a class of architectural systems where each component supports and is supported by others, forming a self-sustaining geometry without centralized supports (Baverel et al., 2000; Chilton et al., 2015). This unique form of structural interdependence distributes loads across the system, enabling lightweight yet stable frameworks (Parigi & Kirkegaard, 2014). Such systems have been widely recognized for their modular adaptability and visual expressiveness, offering an efficient means to create large spans or double-curved surfaces with minimal material (Larsen, 2008; Popovic Larsen, 2008).

In this research, reciprocal structures serve as the primary framework for deployable shells. Their traditionally static nature is expanded through integration with auxetic behaviour and deployable joints, which reimagine reciprocity as a dynamic system rather than a fixed one (Veenendaal et al., 2011; Jayachandran, 2019). This integration allows reciprocal systems to transcend geometric rigidity, enabling them to contribute to adaptable, reconfigurable architectural envelopes..

Parametric modelling (e.g., Rhinoceros 3D with Grasshopper) and mechanical simulation tools (e.g., SolidWorks) will be used in tandem to bridge geometry with motion, and structure with flexibility (Bracewell et al., 2001; Pellegrino, 2001). This dual-environment workflow allowed the project to iterate between virtual simulations and real-world constraints, creating a feedback loop essential for the successful integration of pattern logic, joinery design, and deployment mechanisms (Aburamadan & Trillo, 2019).

1.4.5.1 The Role of Reciprocal Systems in Structural Expression and Redundancy

Reciprocal frame structures offer a compelling design logic rooted in self-supporting modularity and visual complexity. By interlocking linear members without central supports, they distribute loads efficiently and allow for expressive double-curved geometries (Song et al., 2013). Their tessellated nature also lends itself to modular assembly, allowing varied spatial configurations across different architectural scales.

In this research, reciprocal systems serve as the structural backbone of the deployable shell. While often limited by their static nature and geometric rigidity, their potential is expanded through integration with auxetic behaviour and mechanical articulation. The reimagining of reciprocal logic in a dynamic, kinetic framework introduces both spatial flexibility and structural redundancy attributes essential for reconfigurable or reusable architecture.

Advantages of Reciprocal Systems

- Self-supporting, load-sharing geometry: Allows the formation of doubly curved, central-support-free shells
- Modular and scalable: Easily adapted to different sizes and spans through repetitive patterns
- Geometric tessellations: Enable simplified fabrication using standardised or laser-cut parts
- Visual richness: Offers architectural expressiveness through layered, lattice-like spatial qualities

Disadvantages of Reciprocal Systems

- Geometric dependency: Each member relies on precise placement; errors in one part can affect the whole
- Non-reusable prefabrication: Once constructed, the structure is typically fixed in shape and cannot be dynamically altered
- Complex assembly sequence: Requires phased construction and controlled on-site coordination due to its interlocking logic

By embedding these reciprocal qualities within a deployable and auxetically responsive system, the limitations of static prefabrication and phased dependency are mitigated. This shift from rigid frame to kinetic framework allows for not just construction, but transformation paving the way for a new class of reconfigurable architectural envelopes.

1.4.6 Auxetic materials

Auxetic materials are notable for their negative Poisson's ratio, meaning they expand laterally when stretched and contract when compressed (Lakes, 1987; Evans & Alderson, 2000). This property arises from specific lattice or re-entrant geometries at the micro- or meso-scale, which deform in counterintuitive but predictable ways (Alderson et al., 2010; Babaee et al., 2013). Their mechanical response enhances energy absorption, impact resistance, and adaptability, making them promising candidates for construction systems (Saxena et al., 2016; Lim, 2015).

In architecture, auxetic logic can extend beyond material science into structural and configurational applications, where patterns or modules behave in ways similar to auxetic lattices (Grima & Evans, 2006; Naboni et al., 2017). These patterns allow surfaces to adapt to complex geometries while maintaining coherence under stress, supporting their use in

deployable shells. Their performance benefits also include acoustic dampening, vibration control, and thermal adaptability, which enhance resilience in architectural contexts (Mir et al., 2019; Zhang et al., 2020).

Mechanics of Auxetic Materials

The defining characteristic of auxetic materials is their negative Poisson's ratio, a property not typically found in natural materials. Whereas most conventional substances, such as metals, plastics, or rubbers, contract laterally when stretched, auxetics do the opposite: they expand outward in all directions under tension and contract uniformly under compression. This counterintuitive behaviour is not simply a material curiosity but a novel mechanical advantage, because it allows expansion without thinning, maintaining cross-sectional stability across multiple axes.

This uniqueness stems from engineered internal geometries, such as re-entrant lattices, rotating units, or chiral structures, which enable controlled rearrangement of the material's microstructure during deformation. In other words, auxetics are not defined by chemical composition alone but by spatial configuration, making them a category of meta-materials rather than naturally occurring substances. The novelty lies in the fact that this engineered geometry produces behaviours impossible to achieve with conventional positive-Poisson materials.

For architectural systems, this distinction is particularly significant. Conventional materials inherently limit deployability, because stretching them along one axis inevitably reduces strength or thickness in another. Auxetic mechanics break this limitation by allowing uniform, integrity-preserving transformations. This unlocks design possibilities that were previously unattainable in construction, such as skins that expand without thinning, panels that absorb impact without localized failure, and deployable shells that adapt curvature while maintaining structural coherence. In the context of this research, the auxetic response is not just a supporting property but a foundational novelty. It provides the mechanical logic that makes reciprocal shells capable of both expansion and reconfiguration while retaining material thickness and strength. No natural material exhibits this dual capacity in a predictable and scalable way, which positions auxetics as uniquely suited to bridging the gap between abstract geometric patterns and practical deployable architectural systems.

1.4.6.1 Auxetic Behaviour as a Performance Modifier in Material Dynamics

The incorporation of auxetic behaviour into the system introduces a counterintuitive, yet highly beneficial mechanical property: materials or systems that expand laterally when stretched and contract when compressed. This negative Poisson's ratio can be particularly advantageous when embedded into construction systems where controlled deformation, energy absorption, and stress distribution are critical. Unlike conventional materials that narrow under tension and bulge under compression, auxetic systems demonstrate a more uniform and predictable expansion or contraction, allowing for novel geometrical configurations during deployment and in-service phases.

In the context of this research, auxetic principles are not restricted to materiality alone but are abstracted into configurational logic, informing the way modules expand, fold, and react to external forces. When deployed in tandem with reciprocal geometries, auxetic patterns enable synchronized movement across the structure, facilitating uniform unfolding or contraction without the need for complex actuators or external guidance systems. This synergy is vital for achieving a deployable shell that maintains geometrical coherence and structural stability throughout its transformation process.

Auxetic principles also play a crucial role in enhancing mechanical joinery design. As each joint must accommodate dynamic rotation and force redistribution during deployment, auxetic-inspired joints provide compliance and adaptability, reducing wear and stress concentrations. By tuning the joinery geometry to exhibit auxetic behaviour, the system gains both flexibility during movement and rigidity upon locking, a dual performance often sought but rarely achieved in kinetic architectural systems.

Furthermore, auxetic behaviour contributes to thermal, acoustic, and vibrational performance, which are increasingly important in contemporary architecture. The ability of such systems to absorb energy and dampen oscillations suggests potential applications in disaster-resilient architecture and kinetic façade systems. Auxetic configurations are especially suitable for double-curved geometries due to their versatile adaptability, enabling modules to wrap around complex forms seamlessly. However, auxetic systems face limitations in scalability beyond the product or material design level. Mechanical replication of true auxetic responses at architectural scales remains a challenge due to differences in force propagation and material behaviour.

Advantages of Auxetic Systems

- Enable expansion and contraction without material thinning
- Easily adaptable to double-curved or irregular geometries
- Provide improved acoustic, thermal, and vibrational performance
- Enhance flexibility and lockable rigidity in mechanical joinery
- Distribute movement predictably across surface structures

Disadvantages of Auxetic Systems

- Research and applications are largely limited to product/material scale
- Mechanical replication at architectural scales remains complex
- Force behaviour changes when scaled up, requiring extensive calibration

1.4.7 Deployable Structures

Deployable structures transform from compact states into expanded, operational forms, offering efficiency in transport, storage, and rapid construction (Pellegrino, 2001; Fenci & Currie, 2017). They are broadly categorized into rigid-foldable systems, which rely on geometric articulation, and flexible or pneumatic systems, which depend on deformable materials (Schenk & Guest, 2013; Panetta et al., 2021). Such mechanisms have long been applied in aerospace and emergency contexts, but their architectural relevance is growing due to demands for adaptability and reusability (Rivas-Adrover, 2017; Volkov et al., 2021).

In this research, deployability is embedded at every scale, from joinery mechanisms to macro-shell formation. It forms the operational link between reciprocal geometries and auxetic adaptability, ensuring smooth transitions between compact and expanded states without extensive machinery (Jayachandran, 2019; Handoo, 2018). Mechanical joints such as ratchets and one-way bearings (Sclater, 2011; Harris, 2001) are crucial here, acting as kinetic translators that secure the structure post-deployment while facilitating fluid motion during transformation.

Deployability as a Catalyst for Construction Efficiency and Reusability

In this research, deployability is not treated as a superficial add-on or post-construction condition, but as a deeply embedded design logic that permeates every stage of development from the micro-scale joinery to the macro-scale shell deployment. It serves as the operational

bridge between the geometric reciprocity of the framework and the adaptive auxetic response of the modules. This convergence allows the system to move fluidly between compact and expanded states without external scaffolding, cranes, or labor-intensive methods ideal for temporary installations, nomadic structures, or remote site applications where traditional construction is infeasible.

Deployability addresses four critical constraints in architectural practice:

- Transportation and Storage: The ability to flat-pack the system reduces volumetric footprint, easing logistical challenges during transport or storage phases.
- Speed and Efficiency of Assembly: On-site deployment is simplified by pre-integrated kinetic joints, minimizing human error and construction time.
- Adaptability and Mobility: The structure can respond to changing spatial needs or environmental conditions, including site re-use or post-disaster scenarios.
- Material Reusability and Circularity: By avoiding permanent fixings, the system supports multiple cycles of assembly and disassembly, contributing to sustainable construction practices.

This study proposes a cyclical deployment model wherein the shell is designed for continuous transformation: it can be flattened, transported, deployed, retracted, and reused across different contexts. Mechanical joineries such as ratchet-pawl mechanisms and one-way bearings are introduced to enhance this movement, ensuring structural coherence during expansion while locking the system securely in its final form. These kinetic joints become not just connectors, but programmable components of movement.

Importantly, deployability amplifies architectural agency by enabling kinetic expression and dynamic spatial programming. Architects are no longer confined to static assemblies but can choreograph transformation, create kinetic facades, or build environments that respond to user interaction and environmental feedback. This aligns with emerging paradigms of responsive and performative architecture (Fox & Kemp, 2009).

Yet, several limitations remain. Most deployable structures operate predominantly along a single axis (often vertical or Z-axis), reducing freedom in form variation. The prefabricated nature of their components limits spontaneous customization, and structural stability becomes increasingly difficult to maintain at architectural scales, especially under wind, seismic, or thermal loads. These challenges echo the constraints found in reciprocal systems and highlight the importance of integrating complementary systems such as auxetics to overcome these boundaries.

Advantages of Deployable Systems

- Enables kinetic joineries for rapid assembly and disassembly
- Portable, reconfigurable, and efficient in space-constrained contexts
- Ideal for temporary, nomadic, or emergency architecture
- Supports sustainability through reuse and modularity
- Reduces dependency on heavy equipment and large site setups
- Enhances kinetic design expression and real-time reconfiguration

Disadvantages of Deployable Systems

- Prefabricated geometries limit design flexibility and variation
- Lower structural stability in large-scale or high-load applications
- Typically limited to Z-axis deployment, restricting spatial diversity
- Requires careful tuning of movement tolerances and mechanisms

- Vulnerable to material fatigue and mechanical wear over time

In conclusion, deployability offers a powerful catalyst for rethinking construction paradigms transforming space, time, and effort into designable variables. When merged with the geometric logic of reciprocal frames and the adaptive response of auxetic systems, deployability emerges not as a compromise but as a synergistic enabler of responsive, scalable, and sustainable architecture.

1.5 The Synergy:

This framework proposes an integrated approach, combining reciprocal structures, auxetic behaviour, and deployable mechanisms into a unified system. While each principle provides independent advantages, their interdependence resolves individual limitations, producing a system that is expressive, adaptable, and operationally efficient (Bertoldi et al., 2017; Konaković Luković et al., 2016).

1.5.1 Rationale for Integration

Traditional architectural systems often prioritize either form, function, or fabrication efficiency but rarely all three in tandem. By contrast, this research investigates how the structural interdependence of reciprocal frames, the kinematic adaptability of auxetic geometries, and the transformative potential of deployability can be synchronized into a single coherent design logic. Each system contributes a specific domain strength, while compensating for the limitations of the others.
Reciprocal Systems offer self-supporting frameworks with rich geometric expressiveness but suffer from rigid assembly constraints. Auxetic Systems introduce lateral adaptability and dynamic response but are difficult to scale mechanically at architectural levels. Deployable Systems offer rapid transformation and reusability but lack structural stability and form versatility at large scales. Together, they operate not as isolated components but as triadic logic, where the limitation of one becomes the strength of another, forming a closed-loop system of mechanical, spatial, and constructional intelligence.

1.5.2 Mechanical Synergy and Structural Interdependence

At the mechanical level, this research brings together three logics that normally operate in isolation: reciprocity, auxetics, and deployability. Reciprocal frameworks form a lattice of interlocked beams that share loads and establish modular boundaries. Within this lattice, auxetic patterns introduce the capacity for controlled deformation, allowing geometric shifts without undermining stability. When these elements are activated by deployable joints such as ratchets or one-way bearings, the structure develops a programmable response to movement. Rather than being a collection of parts that simply fold and unfold, the system behaves as an integrated organism in which load distribution, geometric transformation, and synchronized movement occur together. This interdependence provides a new grammar of structure, where kinematics and statics no longer oppose one another but are woven into a single continuum.

1.5.3 Design Intelligence through Contrasting Behaviors

The value of this integration lies in the way each system contributes through its own mechanical logic. Reciprocal frameworks are designed to resist movement, providing structural integrity. Auxetic geometries, in contrast, permit controlled movement, absorbing and redistributing forces during transformation. Deployable mechanisms, meanwhile, enable configurational change, allowing the system to compact for transport and expand when needed. By embracing these contrasting behaviours, the research develops a hybrid typology

in which rigidity, flexibility, and mobility do not contradict one another but operate in sequence. Movement occurs when the system is deployed, deformation is absorbed and managed through auxetic behaviour, and stability is restored once the reciprocal framework locks into place. This transition from mobility to rigidity enables the structure to act like a mechanical organism, contracting, expanding, and stabilizing with minimal energy and maximum spatial utility.

1.5.4 Constructional Benefits and Operational Efficiency

These interdependent behaviours also translate into tangible benefits for construction. The deployable logic allows pre-assembled modules to be transported in flat-pack form and expanded directly on site, reducing reliance on cranes or scaffolding. Once expanded, the reciprocal framework distributes loads across the shell, while the auxetic modules absorb irregularities in the ground plane, user movement, or external environmental forces such as wind or seismic activity. In practice, this results in a construction system that supports rapid deployment, tool-free assembly, self-supporting geometry after expansion, and reusable joinery components. The joinery mechanisms act as the central mediators, converting theoretical geometries into repeatable, real-world performance.

1.5.5 Synthesis Outcome: A Unified Structural System

Taken together, these elements form a unified structural typology that is deployable in its form, auxetic in its behaviour, and reciprocal in its structure. This triadic integration produces shells that are lightweight, adaptable, and self-supporting, suited for contexts where permanence is not possible but spatial and structural quality remain essential. The system's potential applications are wide-ranging, from temporary housing and exhibition pavilions to remote infrastructure and even space-based habitats. What emerges is not just a new construction method, but a new paradigm in which deployability, adaptability, and structural coherence are fused into a single architectural language.

Table 1.5-1 Systems strengths and limitations overcome by others

System	Strengths	Limitations Overcome by Others
Reciprocal	Load-sharing, self-supporting, modular	Inflexible → resolved via auxetic adaptability
Auxetic	Deformable, force-dispersing, responsive	Scalability → resolved via reciprocal scaffold
Deployable	Portable, quick to assemble, reusable	Stability/form limits → resolved via reciprocal–auxetic integration

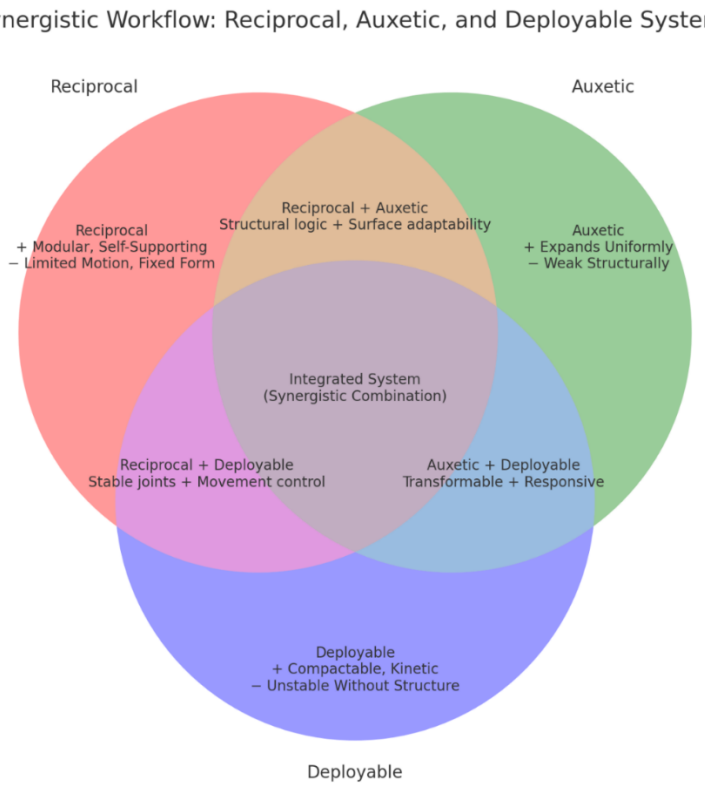

Figure 1.5-1 Pros of Synergy between 3 systems - Venn diagram

Table 1.5-2 Comparative analysis between different systems

Criterion / Capability	Reciprocal	Auxetic	Deployable	DR STAB synergy
Structural stability & load sharing	✓	✗	✗	✓
Adaptability to double-curved forms	✓	✓	✗	✓
Expandable / contractible behavior	✗	✓	✓	✓
Ease of deployment & portability	✗	✗	✓	✓
Scalability for architectural shells	✓	✗	✗	✓

In isolation, each system offers a partial response to the demands of modern construction. In synergy (Figure 1.6-1) , they propose a comprehensive response to architectural adaptability, balancing structural stability, spatial transformation, and fabrication logic. This research positions the reciprocal–auxetic–deployable triad not as a collage of techniques, but as a cohesive methodology one capable of reimagining how structures are conceived, assembled, and reconfigured

1.6 Research Questions (RQ)

This research is guided by three interrelated research questions that address the integration of geometry, mechanics, and digital simulation in the development of deployable architectural shells. These questions reflect the progressive structure of the study, moving from conceptual design to physical fabrication and full-scale deployment.

Problem Statement (1): *Double-curved shells in architecture are widely recognised for their efficiency and elegance, yet they remain expensive to fabricate, labour-intensive to assemble, and difficult to reuse once constructed. Conventional systems rely heavily on bespoke components and rigid geometries, which restrict adaptability and hinder repeat deployment. There is a lack of systematic integration between reciprocal framing, which provides structural redundancy, and auxetic patterns, which offer controlled expansion and adaptability.*

RQ-1. How can reciprocal and auxetic principles be combined to design deployable, double-curved architectural shells?

Problem Statement (2): *While computational modelling provides detailed simulations of geometric behaviour, it often abstracts material properties and overlooks practical constraints observed during prototyping. Conversely, physical testing reveals material limits and real-world adaptability but lacks the scalability and predictive capacity of digital tools. The absence of a cohesive framework linking simulation and prototyping creates uncertainty in validating deployability, structural stability, and performance at architectural scales.*

RQ-2. How can physical testing and digital simulations of the Auxetic pattern inform the design of adaptive and deployable shell geometries?

Problem Statement (3): *In most deployable systems, mechanical joints are treated as secondary connectors rather than as the primary drivers of motion and load transfer. This results in limited control over expansion, curvature, and reversibility, reducing the effectiveness of deployable shells in practice. Moreover, the absence of tailored joint mechanisms such as one-way bearings, ratchets, and ball joints prevents the reliable translation of geometric principles into functional construction systems.*

RQ-3. How can mechanical joinery systems be designed, prototyped, and simulated to support the controlled deployment of auxetic-reciprocal architectural shells?

Together, these research questions establish a framework that moves from geometric integration to validation and finally to mechanical realisation. They ensure that the study addresses both conceptual design and practical implementation, bridging theory and practice. Ultimately, they guide the development of DRSTAB as a deployable, adaptable, and reusable architectural system.

1.7 Research Methods (RM) - Design of Study

This research is positioned within a design-led, practice-based framework, aligned with the broader epistemology of architectural knowledge creation through making, simulating, and reflecting. Recognizing architecture as an iterative and intuitive process, the research integrates qualitative methods, creative production, and computational exploration as coequal drivers of inquiry.

Following the frameworks of Lucas (2016) and Downton (2003), the methodology acknowledges that architectural research cannot be purely deductive or data-driven. Rather, it is an exploratory act, where making and theorising are mutually reinforcing. Within this paradigm, design is not simply a medium for demonstrating knowledge but becomes the vehicle through which knowledge is generated, tested, and made communicable.

The thesis adopts a multi-phase methodology that encompasses literature synthesis, digital experimentation, physical prototyping, mechanical analysis, and system feedback. Each phase correlates to key stages of the research progression, forming a non-linear, reflective process rather than a stepwise protocol. The method also aligns with the notion of 'research through design', where knowledge is built through the act of creation, not just analysis (Groat & Wang, 2013; Walliman, 2010; Leavy, 2014).

(RM-1) Research Methods for RQ-1: Literature Review and Geometric Pattern Breakdown

To address RQ1, the research draws on a structured literature review, typological mapping, and precedent analysis. Guided by design research principles from Groat and Wang (2013), Downton (2003), and Lucas (2016), this phase adopts reflective synthesis to identify overlaps and gaps across four thematic domains: (1) deployable architecture, (2) reciprocal systems, (3) auxetic materials, and (4) mechanical articulation. Core references include Song et al. (2013) on reciprocal frame systems, Konaković Luković et al. (2016) on auxetic transformations, and Pellegrino (2001) and Sclater (2011) on mechanical design logic. Architectural theses such as Jayachandran (2019) and Borgström (2021) provide additional precedent insights, with the former introducing early reciprocal–auxetic concepts and the latter advancing kinetic auxetic systems. This review highlights critical gaps in integrating geometric adaptability with mechanical precision, which narrows the focus to the Tristar auxetic pattern as the most suitable candidate for hybridization.

Building on this conceptual foundation, the study conducts a CAD-based geometric breakdown of reciprocal and auxetic patterns including re-entrant, rotating, chiral, Miura, and Tristar configurations using Rhino 3D in a non-parametric mode. Through manual dissection of these typologies, key structural characteristics are identified, such as tessellation regularity, unit simplicity, edge continuity, and rotational potential. These features are then compared in a matrix of modularity, curvature adaptability, and deployability, clarifying how reciprocal logic and auxetic expansion can be meaningfully hybridized within a single system.

This phase establishes the analytical groundwork for selecting specific patterns for the subsequent stages of research and confirms the necessity of a hybridized structural logic to support deployable, double-curved architectural shells.

(RM-2) Research Methods for RQ-2: Digital Simulation and Physical Testing

To address RQ2, the research adopts a dual pathway combining parametric digital simulation and physical prototyping to test the behaviour of the Tristar auxetic pattern.

First, a parametric modelling process is developed in Rhinoceros 3D with Grasshopper. Plugins such as Kangaroo2, Ngon, Pufferfish, and Human are employed to evaluate behaviours including expansion, contraction, directional control, and joint rotation. These simulations enable iterative testing of tessellation behaviour, curvature adaptability, and deployment boundaries. More than a verification tool, this computational workflow functions as an epistemic instrument (Lucas, 2016; Bracewell et al., 2001) (Figure 1.6.5 1) , providing a generative environment where hypotheses can be modelled, tested, and refined. This approach mirrors computational geometry research by Bracewell et al. (2001) and Konaković Luković et al. (2016), and its outcomes inform the pattern classification and movement mapping detailed in Chapters 3–5.

Alongside the simulations, the research employs physical testing of scaled prototypes in order to ground digital findings in material performance. Laser-cut materials such as PETG, acrylic, leather, and paperboard are used to fabricate tessellated auxetic–reciprocal modules. These prototypes are deployed over a range of double-curved surfaces to observe real-world behaviour.

The objective of this stage is to validate the adaptability, modularity, and reversibility of the specific geometries , while also uncovering limitations that shape subsequent mechanical design. In line with hands-on inquiry frameworks (Groat & Wang, 2013; Downton, 2003), making and testing are treated as integral to knowledge generation. Photographic documentation and reflective notes are used to capture the emergent behaviour of the prototypes under manual deployment.

This methodological cycle establishes a bridge between digital abstraction and material reality, ensuring that the insights from both simulations and prototypes directly inform the mapping of angular tolerances, joint placement, and rotation dynamics knowledge that guides the development of mechanical joineries in the next phase.

(RM-3) Research Methods for RQ3: Mechanical Joinery Development and System Integration

Building on the geometric and physical insights from RQ1 and RQ2, this stage focuses on translating observed spatial behaviours into mechanical articulation through custom joinery design. The goal is to replicate the pitch and yaw rotations identified in the Tristar-based auxetic systems using real-world components.

Mechanical Joinery Development. Initial mock-ups are fabricated using ratchets, ball joints, one-way clutch bearings, and other off-the-shelf parts. These prototypes are evaluated for angular performance, locking behaviour, and structural coherence under rotation and expansion. Through iterative refinement, joineries are adjusted to improve range of motion, connection stability, and modular adaptability. Selected prototypes are then digitally recreated and simulated in SolidWorks and ANSYS to test stress–strain behaviour, angular tolerances, and potential failure points. Although software constraints may limit certain simulations, the process reveals critical insights into force distribution and performance limits. This approach aligns with research in deployable and kinetic systems (Pellegrino, 2001; Bracewell et al., 2001), where empirical testing and mechanical modelling are combined to validate functionality.

(RM-4) Research Methods - System Integration and Feedback Loops.

The final phases of RQ2 and RQ3 involve embedding the tested joints into larger assemblies to evaluate system-level behaviour. Geometric patterns, physical prototypes, and mechanical joinery systems are synthesized into a cohesive deployable shell framework. This integration is tested through physical deployment cycles, examining structural coherence, range of motion, and expansion performance under real conditions. Issues such as synchronization of movement, uneven force distribution, and localised pattern distortion are addressed through iterative feedback loops between CAD adjustments and hands-on assembly.

This phase embraces the reflective nature of design-led research (Lucas, 2016; Aburamadan & Trillo, 2019), where each cycle of testing generates insights that inform subsequent refinements. By bridging digital abstraction with material and mechanical realities, the methodology confirms that deployable systems must be understood as a synergy of geometry, material, mechanics, and motion. The outcomes from this phase shape the conclusions and design recommendations presented in Chapters 4, 5, and 6.

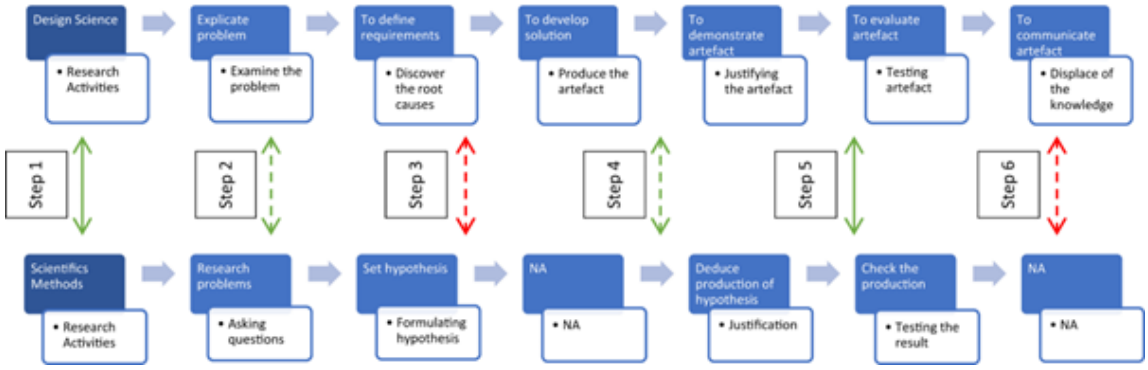

Figure 1.7-1 Methodology overview showing four research method phases (RM-1 to RM-4) integrating literature, digital simulation, prototyping, and joinery design.
Note: From Aburamadan and Trillo (2019).

1.7.1 Workflow of Research

The following flowchart (Figure 1.7-2) provides a visual synthesis of the research methodology outlined in this chapter, summarising the sequence and interconnections between key stages of the study. While the methodology is described in detail through text, the diagram simplifies comprehension by clearly mapping the progression from literature review to geometric exploration, simulation, prototyping, and mechanical joinery development. Its inclusion is particularly relevant in a design-led, iterative process, where multiple feedback loops and non-linear transitions can be difficult to follow. The flowchart therefore acts as a concise reference, helping to clarify the overall research structure and the relationships between its components.

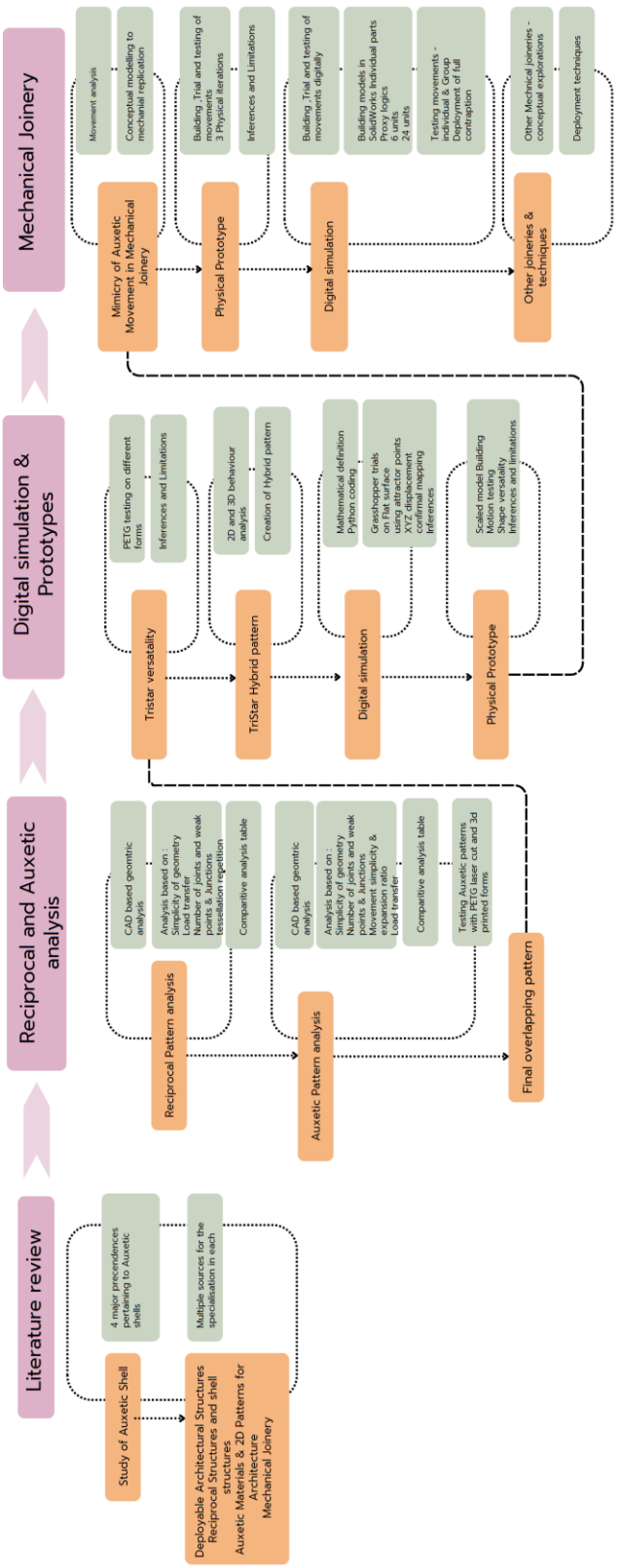

Figure 1.7-2 A Simple Flow chart of the workflow and benchmarks followed in the Thesis

1.8 Scope of the research

1.8.1 Integration of Reciprocal and Auxetic Systems

This research will investigate the design, development, and evaluation of the DRSTAB system as a deployable architectural framework grounded in the integration of reciprocal structural logic, auxetic behaviour, and mechanical joinery systems. The study will explore how reciprocal arrangements, typically understood as static and interdependent systems, can be transformed into deployable configurations capable of controlled expansion and contraction. Through the examination of geometric configurations, the research will analyse how auxetic behaviour can be leveraged to enhance adaptability, modular aggregation, and spatial responsiveness. Particular attention will be given to the stability of these systems during transitional deployment states, ensuring that expansion mechanisms remain coherent and structurally viable. In doing so, the research will establish a foundational understanding of how geometry and mechanics can be integrated to enable dynamic architectural systems.

1.8.2 Mechanical Joinery as a Primary Driver

A central focus of this research will be the exploration and development of mechanical joinery systems as a primary driver of system behaviour. The study will investigate a range of joinery mechanisms, including hinge-based, ratchet-based, and bearing-supported systems, with an emphasis on incorporating off-the-shelf components where feasible. The research will examine how these joinery systems influence movement, control, and repeatability within the DRSTAB framework, positioning them not merely as connective elements but as active agents shaping system performance. By prioritising joinery, the study will test how mechanical constraints and capabilities can inform and redefine geometric behaviour, ultimately guiding the design logic of deployable architectural systems.

1.8.3 Digital Simulation and Physical Prototyping Workflow

This research intents to establish a workflow that integrates digital modelling, simulation, and iterative physical prototyping as a means of bridging conceptual design with material realisation. Simulation tools will be employed to analyse system behaviour, including movement patterns, interaction between components, and constraint conditions. These digital investigations will be complemented by the development of physical prototypes, which will be used to test and validate mechanical performance and deployment behaviour in real-world conditions. The study will adopt a cyclical and iterative approach, where insights from simulations inform prototyping, and physical testing in turn refines digital models. Through this integrated methodology, the research will explore how feedback between digital and physical domains can support a robust and responsive design process.

1.8.4 Architectural Implications and Conceptual Applications

Beyond technical development, this research will explore the architectural implications of the DRSTAB system through a series of conceptual design applications. These applications will investigate the potential of deployable and adaptable structures within architectural contexts, including temporary installations, modular spatial systems, and responsive environments. While these proposals will remain exploratory in nature, they will serve to demonstrate how the integration of reciprocal geometry, auxetic behaviour, and mechanical joinery can inform new spatial and architectural possibilities. The research will use these conceptual applications as a means to translate technical findings into architectural thinking, highlighting potential directions for future implementation without aiming to deliver fully resolved building designs.

1.8.5 Implied Boundaries of the Study

1.8.5.1 Focus on System Development over Full-Scale Implementation

This research will be deliberately bounded to prioritise system development and proof-of-concept validation over full architectural realisation. The study will focus on establishing the functional principles, geometric behaviour, and mechanical performance of the DRSTAB system, rather than extending into detailed engineering certification or compliance with building standards. Structural performance will be examined primarily through simulation and conceptual evaluation, allowing the research to concentrate on the development of deployable logic and joinery mechanisms. By defining this boundary, the study will ensure depth in system exploration while acknowledging that full-scale architectural implementation will require further investigation beyond the scope of this research.

1.8.5.2 Prototype-Scale Fabrication Constraints

Fabrication within this research will be limited to prototype-scale models, which will be used to test geometric behaviour, mechanical interaction, and deployment processes. These prototypes will provide valuable insights into system performance; however, they will not replicate the full complexities associated with large-scale construction. Issues such as material performance under significant loads, large-span assembly, and on-site construction logistics will not be fully addressed. This boundary will allow the research to focus on validating core system behaviours while recognising that additional work will be required to adapt these findings for full-scale applications.

1.8.5.3 Selective Material and Fabrication Exploration

Material exploration within this study will be selective and purpose-driven, focusing primarily on validating mechanical behaviour and joinery performance. The research will not extend into comprehensive studies of material optimisation, long-term durability, or environmental performance. Instead, materials will be chosen based on their suitability for prototyping and their ability to support accurate testing of system mechanics. This approach will ensure that the investigation remains focused on the interaction between geometry and joinery, while leaving broader material considerations to be addressed in future research.

1.9 Limitations of the Research

1.9.1 Exclusion of a Fully Resolved Final Design

A significant limitation of the research is the exclusion to develop a fully resolved final architectural design outcome. During the early stages of the doctoral study, the development of a comprehensive final design was considered; however, following feedback during a inter-stage review, the focus of the research was refined by expert reviewers to prioritise mechanical joinery systems as the primary contribution. As a result, the study does not pursue full architectural resolution, but instead concentrates on the detailed exploration and validation of joinery mechanisms. While components of the system are tested through conceptual assemblies and prototype configurations, these investigations remain partial and do not constitute a complete architectural design.

1.9.2 Absence of Full Structural Validation

A key limitation of this research will be the absence of comprehensive structural and engineering validation. While simulation and prototype testing will provide important insights into system behaviour, the study will not include full load testing, long-term performance assessment, or compliance with construction standards. As a result, the structural performance of the DRSTAB system at architectural scale will remain to be validated in future work. This limitation reflects the exploratory and design-led nature of the research, which will prioritise the development of principles and mechanisms over fully engineered solutions

1.9.3 Scale Limitations of Prototyping

All physical prototypes developed within this research will be produced at a reduced scale, which will limit the direct translation of findings to full-scale applications. While these models will effectively demonstrate geometric relationships and mechanical interactions, they will not fully capture real-world conditions such as material strength, structural loading, and assembly logistics. Consequently, the extrapolation of results to architectural scale will require careful consideration and further validation..

1.9.4 Fabrication Tolerances and Mechanical Precision

The performance of the mechanical joinery systems will be influenced by fabrication tolerances and assembly precision. Variations arising from manufacturing processes, tool limitations, and material inconsistencies may affect the repeatability and accuracy of the tested mechanisms. These factors will introduce a degree of uncertainty in experimental outcomes, and their impact will need to be considered when evaluating system performance and reliability.

1.9.5 Simplifications in Simulation Environments

While simulation tools will be used extensively to analyse system behaviour, they will inherently simplify real-world conditions. Factors such as friction, wear, environmental influences, and material deformation will not be fully represented in the simulation environment. As a result, simulation outputs will serve as indicative models rather than exact predictions of physical performance, and their limitations will be acknowledged in the interpretation of results.

1.9.6 Informal Knowledge Inputs from Workshops

The research will be informed in part by informal engagements with practitioners, including workshop visits and technical discussions. These interactions will provide practical insights that help refine design decisions and eliminate non-viable approaches. However, as these inputs has not been systematically documented or structured as formal datasets, they will be treated as supportive knowledge rather than empirical evidence within the study, and mentioned whereever approprioate

1.9.7 Conceptual Nature of Architectural Applications

The architectural applications explored within this research will remain conceptual and speculative. They will not extend to detailed construction documentation, regulatory compliance, or integration with building services. These applications will serve primarily as illustrative frameworks to demonstrate the potential of the DRSTAB system, while acknowledging that further development will be required to achieve real-world implementation.

Chapter #2

Gather / Analyse / Anchor

Literature Study

Inferences

Knowledge gaps

2 Chapter 2 - Literature Review

2.1 Introduction

This chapter presents a critical review of the key theoretical and applied research underpinning the development of deployable reciprocal shells through auxetic behaviour. As architectural demands increasingly shift toward adaptable, lightweight, and reconfigurable structures, the convergence of three distinct research domain-reciprocal structural systems, auxetic mechanics, and deployability principles has opened new avenues for design innovation. However, despite significant progress within each domain individually, there remains a lack of integrated frameworks capable of addressing architectural-scale transformation, structural coherence, and material intelligence simultaneously.

The literature reviewed in this chapter is organized thematically, beginning with reciprocal systems in architecture, followed by auxetic geometries and behaviour, and deployable systems in both engineering and architectural contexts. Particular attention is paid to the mechanical and spatial implications of each system, their limitations in practice, and their potential for hybridization. A dedicated section (2.2) focuses on three foundational works Jayachandran (2019), Borgström (2021), and Konaković Luković et al. (2016) that serve as key comparative benchmarks for this research. These studies provide precedent for the conceptualization, simulation, and partial prototyping of auxetic and deployable systems, yet stop short of resolving the challenges of structural integration and mechanical joinery required for real-world architectural deployment.

Through this literature review, the research identifies specific gaps in the current state of knowledge, particularly around the integration of passive mechanical joineries within dynamic shell systems, and the need for scalable construction methodologies that can accommodate movement, modularity, and multi-scalar responsiveness. While the literature review finds a strong foundation to answer RQ 1 , some literature finds specific missing links that answer while solving RQ2 and RQ 3 .

To structure this review, the literature is organized into five thematic sections:

- Section 2.2.1 to 2.2.3 examines three core studies that serve as comparative benchmarks for this research Jayachandran (2019), Borgström (2021), and Konaković Luković et al. (2016) each exploring auxetic and deployable logic in different architectural contexts. supports RQ-1 & RQ-2.

- Section 2.2.4 and 2.2.5 dwells deeper into study of Auxetic hybridization and inclusion for the study that supports RQ-1

- Section 2.2.6 explores the design and mechanical performance of deployable systems, with attention to both rigid-foldable and flexible typologies used in architectural and engineering precedents. - supports RQ-3.

- Section 2.2.7 surveys the evolution of reciprocal frameworks, highlighting their geometric richness and structural potential, while also identifying their limitations in dynamic configurations.- supports RQ-1

- Section 2.2.8 focuses on auxetic materials and geometries, particularly their behaviour at different scales and their emerging architectural applications.- supports RQ-1

- Section 2.2.9 reviews literature on mechanical joineries and kinetic connections often underrepresented in architectural discourse crucial for enabling transformability and structural articulation.

Together, these thematic strands expose a consistent gap: the absence of an integrated architectural system that unifies reciprocal geometry, auxetic adaptability, and deployability through scalable, passive mechanical joinery. The chapter concludes (Section 2.7) by synthesizing these insights and articulating the specific contribution of this research to the architectural, structural, and fabrication discourse.

2.2 Deployable Auxetic shells:

The convergence of deployability and auxetic behaviour represents a promising yet underexplored area in architectural research, particularly in the context of structural shells. This section examines three precedent studies that have laid the groundwork for integrating auxetic principles with spatial transformation, each contributing to the conceptual and methodological development of this research.

2.2.1 Jayachandran (2019): Deployable Reciprocal Shells Through Auxetic Behaviour

Jayachandran's Master's thesis (2019) proposed an ambitious architectural hypothesis in which reciprocal frameworks were informed by auxetic geometry to create doubly curved, self-supporting shells that could be deployed and retracted. The study represented one of the earliest attempts to hybridize reciprocal logic, which is traditionally valued for redundancy and modularity, with the transformational capacities of auxetic tessellations. By embedding negative Poisson's ratio geometries into reciprocal arrangements, the thesis demonstrated how a structure could expand, contract, and achieve curvature without relying on conventional folding mechanisms or pneumatic systems. This work is particularly significant because it framed deployability not as an additive mechanism but as a property embedded in the geometry of the structure itself.

A central contribution of the research was the reciprocal system breakdown, in which frame geometries were dissected to expose their latent capacity for curvature and modularity (Figure 2.2-1) Reciprocal frames inherently distribute loads redundantly across overlapping units, but their adaptability in dynamic conditions had rarely been studied. The breakdown illustrated how overlapping logics could support tessellation and curvature when integrated with auxetic movement. This insight positioned reciprocal systems as a viable foundation for deployable structures, rather than merely static frameworks.

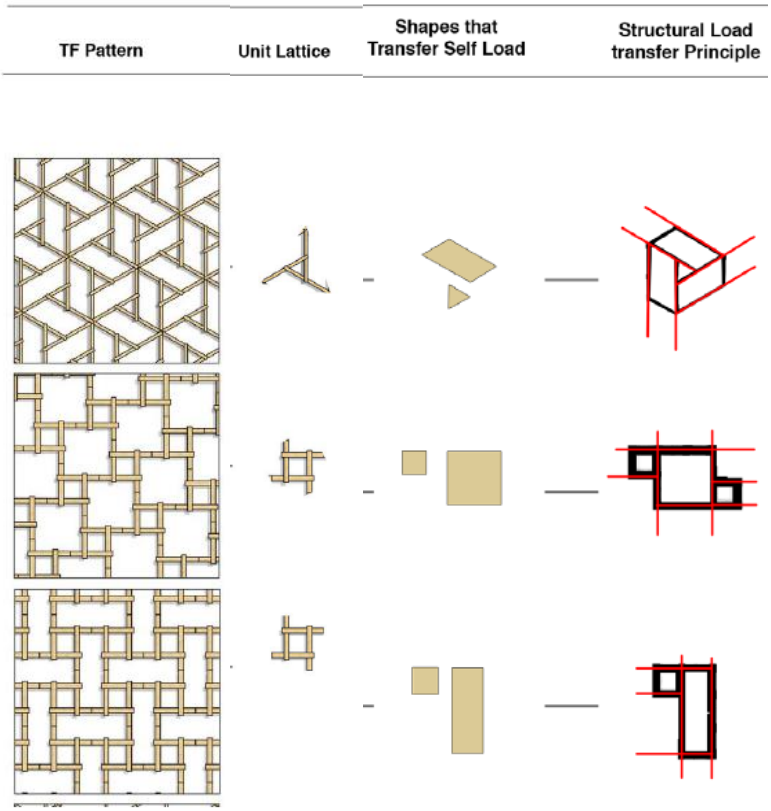

Figure 2.2-1 Reciprocal Breakdown analysis

Note: From , *Deployable reciprocal shells through auxetic behaviour: Architectural hypothesis to fabricate double-curved structures* by *Jayachandran, S. (2019).*

Parallel to this, the research conducted an auxetic pattern exploration, testing re-entrant honeycomb, Miura-ori, rotating units, chiral geometries, and the Tristar configuration. While each pattern demonstrated varying levels of adaptability, the Tristar emerged as the most promising for reciprocal hybridization. Unlike planar re-entrant or Miura geometries, the Tristar pattern exhibited both yaw and pitch rotations, which provided localised flexibility while retaining global structural coherence. This property was particularly advantageous when combined with reciprocal frameworks, as it allowed double curvature to emerge without distortion of the overall tessellation (Figure 2.2-2)

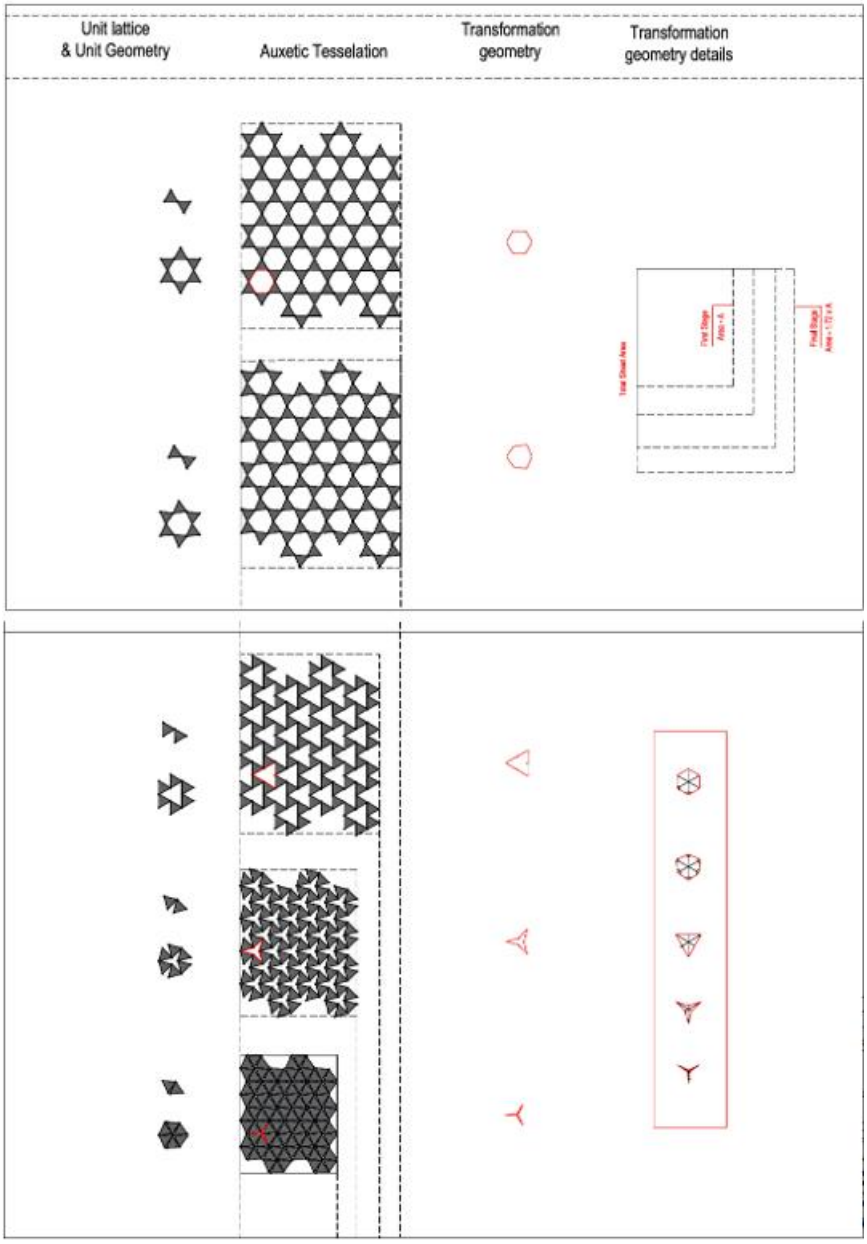

Figure 2.2-2 Auxetic Breakdown analysis of tristar pattern

Note: From , *Deployable reciprocal shells through auxetic behaviour: Architectural hypothesis to fabricate double-curved structures* by *Jayachandran, S. (2019).*

The study also advanced an analysis of three-dimensional movement, focusing on how triangular units behaved when expanded or contracted. The research found that while yaw and pitch rotations were consistently present, roll rotation was negligible (Figure 2.2-3) . This finding was important because it clarified which degrees of freedom were structurally relevant for architectural shells. Although Jayachandran's work did not resolve how such rotations could be mechanically replicated, it highlighted the need for joints capable of selectively enabling pitch and yaw while constraining roll a challenge directly taken up in the present doctoral research.

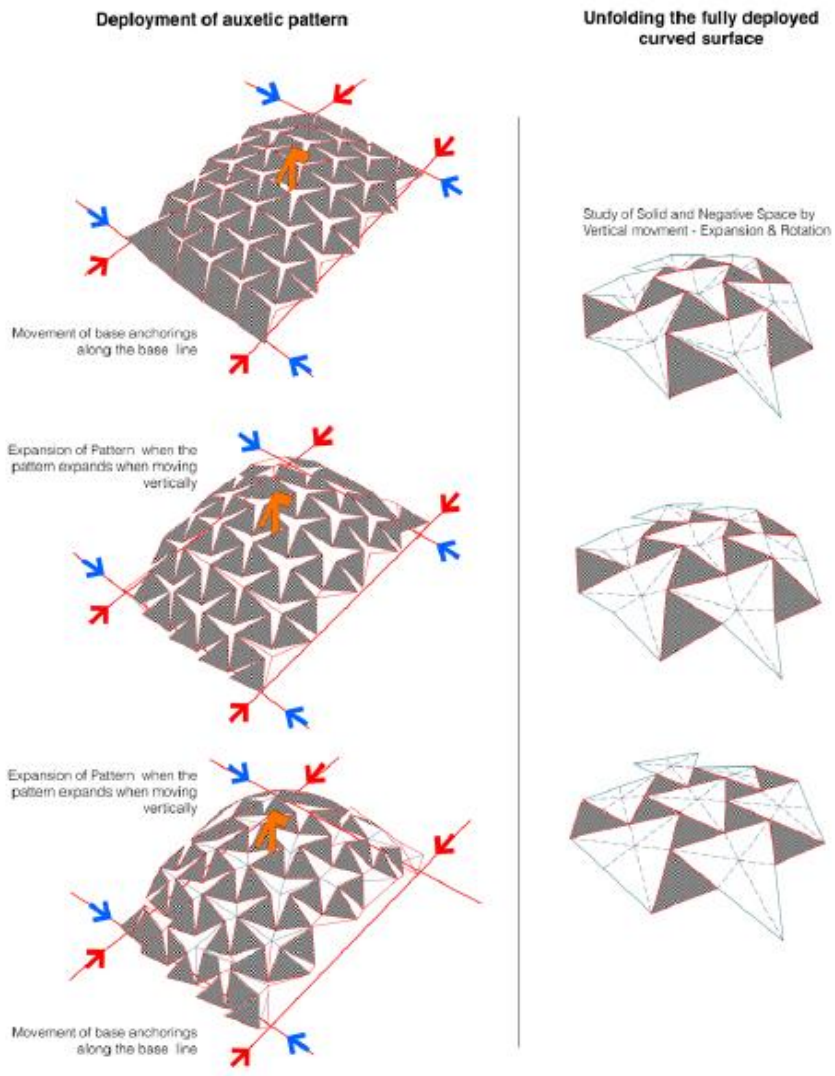

Figure 2.2-3 Auxetic 3D movement analysis

Note: From , *Deployable reciprocal shells through auxetic behaviour: Architectural hypothesis to fabricate double-curved structures* by *Jayachandran, S. (2019).*

Another valuable step was the conceptualisation of mechanical joineries (Figure 2.2-4). While the workflow did not focus on precise physical joint systems , the thesis sketched pathways for translating geometric movements into potential mechanical analogues, including ratchet systems, ball joints, and one-way bearings. These early explorations opened the conceptual bridge between geometry and mechanics, suggesting that deployability could one day be embedded not only in the pattern but in the articulation of its connections. This speculative move was essential in reframing joints from passive connectors into active drivers of kinematic behaviour.

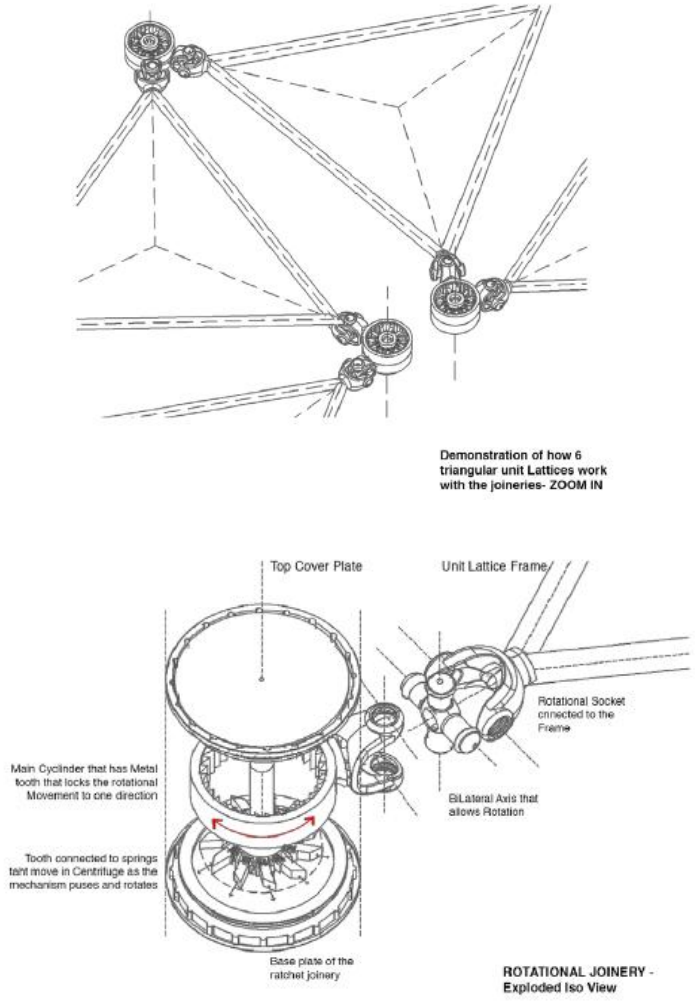

Figure 2.2-4 Mechanical Joineries- conceptual exploration

Note: From , *Deployable reciprocal shells through auxetic behaviour: Architectural hypothesis to fabricate double-curved structures* by *Jayachandran, S. (2019).*

The project also proposed deployment strategies through abstract sequences and scaled prototypes (Figure 2.2-5). By expanding reciprocal–auxetic grids and overlaying them on curved surfaces, the thesis demonstrated that doubly curved shells could be formed without scaffolding, formwork, or moulds. This approach offered a proof of concept for flattenable construction systems that could be packed, transported, and redeployed with minimal tools. Such strategies prefigured the contemporary demand for deployable architecture in contexts such as emergency response, temporary installations, and resource-constrained construction sites.

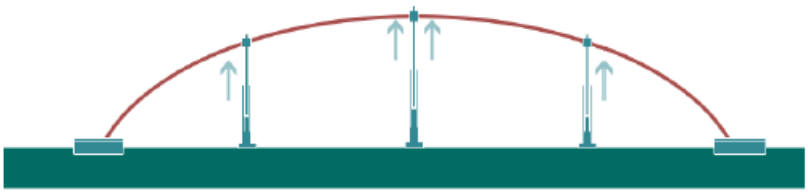

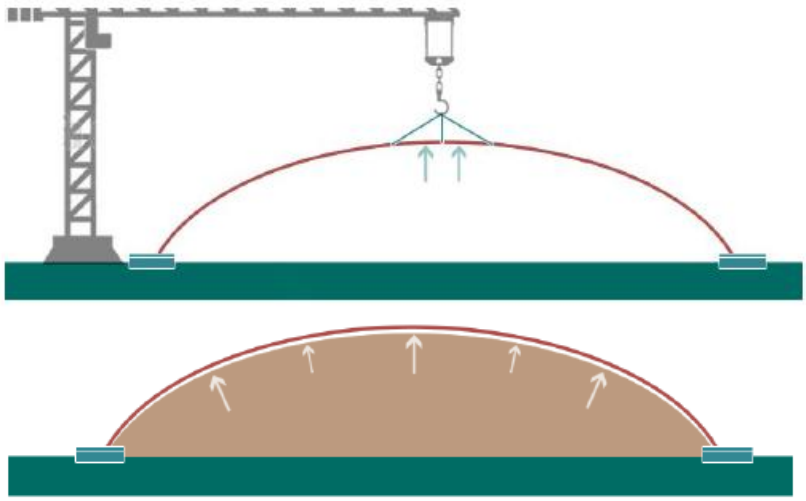

Figure 2.2-5 Deployment techniques - explorations

Note: From , *Deployable reciprocal shells through auxetic behaviour: Architectural hypothesis to fabricate double-curved structures* by *Jayachandran, S. (2019).*

Physical prototyping and digital simulation formed the dual methodological pillars of the study. Scaled models were constructed using lasercut cardboard, and jointed members, which allowed hands-on testing of expansion, unit stability, and curvature adaptability (Figure 2.2-8). These prototypes validated the conceptual feasibility of reciprocal–auxetic integration and revealed emergent behaviours such as slippage and stress concentrations that were not always evident in drawings. Complementing this, Rhino and Grasshopper were used to simulate expansion–contraction sequences, evaluate tessellation adaptability, and visualise deployment across complex surfaces. While limited to geometric behaviour rather than structural analysis, these simulations confirmed that the hybrid logic could be parametrically controlled and visualised in multiple configurations (Figure 2.2-6 & Figure 2.2-7).

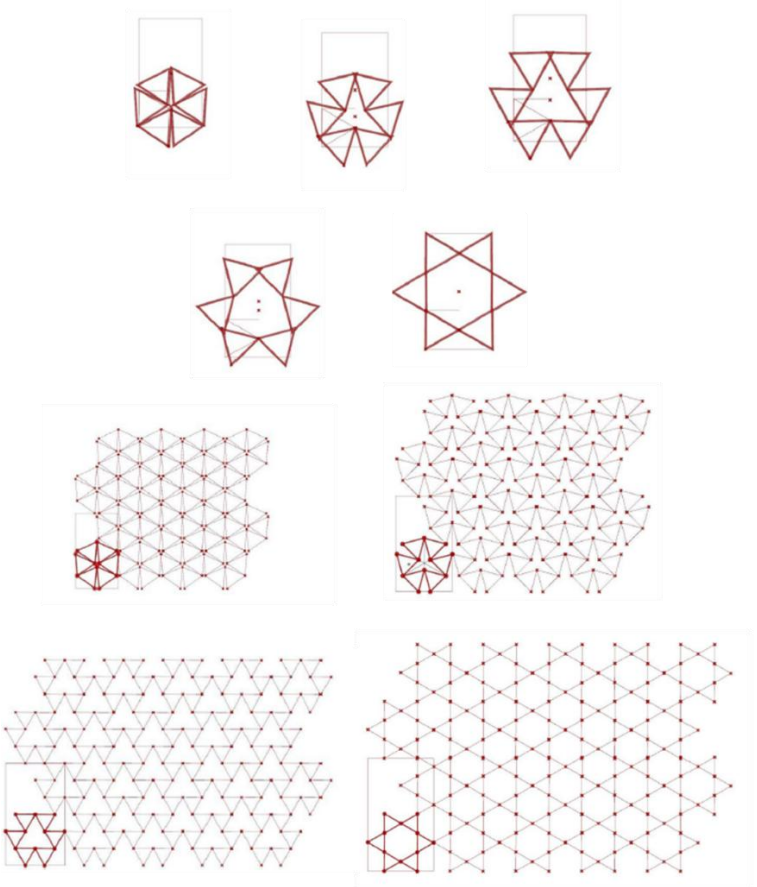

Figure 2.2-6 Results of Grasshopper simulation of Unit Auxetics

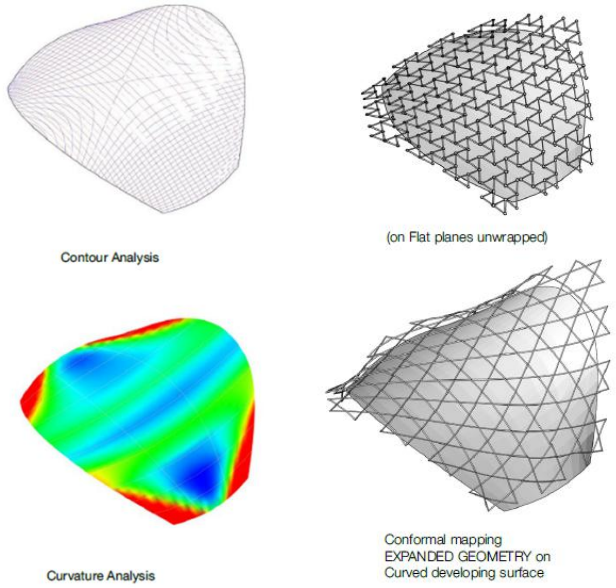

Figure 2.2-7 Modelling and Analysis of Auxetic Structures

Note: From , *Deployable reciprocal shells through auxetic behaviour: Architectural hypothesis to fabricate double-curved structures* by *Jayachandran, S. (2019).*

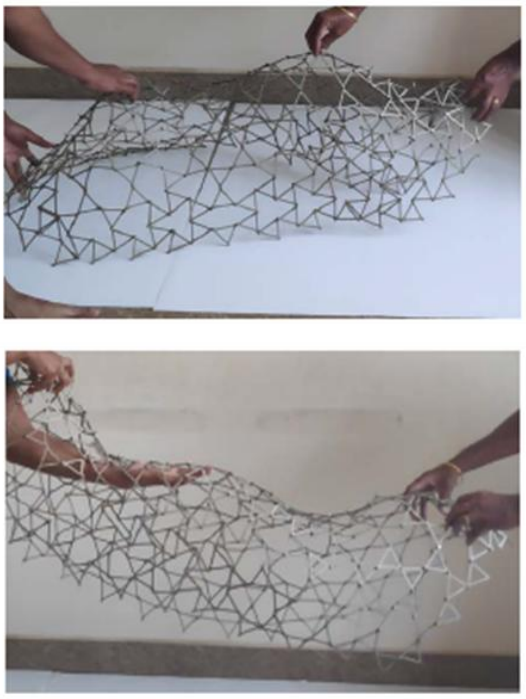

Figure 2.2-8 Scaled Physical model - proof of concept
Note: From , *Deployable reciprocal shells through auxetic behaviour: Architectural hypothesis to fabricate double-curved structures* by *Jayachandran, S. (2019).*

Figure 2.2-9 Scaled Prototype - Mechanical Joineries
Note: From , *Deployable reciprocal shells through auxetic behaviour: Architectural hypothesis to fabricate double-curved structures* by *Jayachandran, S. (2019).*

2.2.1.1 Summary of the Literature on Deployable Auxetic Shells

Integration of Reciprocal Systems with Auxetic Patterns:
The thesis proposes a pioneering hybrid system wherein reciprocal frame structures are embedded with auxetic patterning to form deployable, double-curved shells. The central hypothesis is that auxetic mechanisms due to their negative Poisson's ratio can enable controlled, reversible expansion and contraction within a reciprocal assembly, transforming it into a kinetic and adaptable shell system. This presents a radical departure from static reciprocal typologies by introducing movement and flexibility as core attributes.

Exploration of Deployable Geometries Using Physical Prototyping :
Through extensive scaled physical prototypes, the research tests how planar reciprocal geometries, particularly hexagonal and triangular cells can achieve curvature and deployability through auxetic transformation. By using foam-core, acrylic, and jointed members, the research demonstrates deployability without sacrificing overall geometric coherence. These findings validate the conceptual feasibility of fabricating complex doubly-curved surfaces without molds or scaffolding.

Identification of Tristar Pattern as Optimal Configuration :
The study evaluates multiple auxetic patterns Miura-ori, re-entrant honeycomb, rotating units and converges on the "Tristar" pattern as the most spatially compatible and structurally responsive for reciprocal tessellations. The Tristar exhibits localized pitch and yaw rotations that can be replicated mechanically, offering a modular and symmetry-friendly topology for large-scale shell design.

Architectural Implication for Lightweight, Reusable Shells :
One of the key insights is that this hybrid system can eliminate conventional centering and enable flattenable construction systems. The proposal supports the vision of rapidly deployable shelters or temporary structures that are material-efficient, labor-reductive, and transportable particularly relevant in disaster response or remote construction.

Conceptual Framework for Mechanically Replicating Auxetic Movements :
While the focus is primarily on geometrical experimentation, the study proposes the idea of replicating auxetic movements using mechanical joinery. This concept forms the bridge to your current PhD research, where yaw and pitch degrees of freedom are replicated via rotating ratchet-spring joints.

2.2.2 Borgström (2019): THAT WHICH TENDS TO INCREASE - Architectural Application of Auxetic Systems

Borgström's (2019) thesis represents one of the most comprehensive investigations into auxetic geometries applied to architectural systems, framing them not only as structural or geometric curiosities but as tools for adaptability, expansion, and kinetic responsiveness. His research sought to answer how auxetic principles could be scaled from material science and product design into larger architectural contexts, positioning them as agents of change within adaptive environments.

The study begins with a systematic exploration of auxetic patterns and their deformation characteristics. Through parametric modelling in Rhinoceros 3D and Grasshopper, Borgström catalogued a wide range of tessellations, simulating how they behave under stretching, compression, and bending forces. Visual diagrams in the thesis illustrate the capacity of these geometries to expand uniformly, contract symmetrically, and morph into double-curved forms without material tearing (Figure 2.2-10). These computational experiments highlight the

intrinsic advantage of auxetics: their ability to reorganize spatial relationships while maintaining continuity across the pattern.

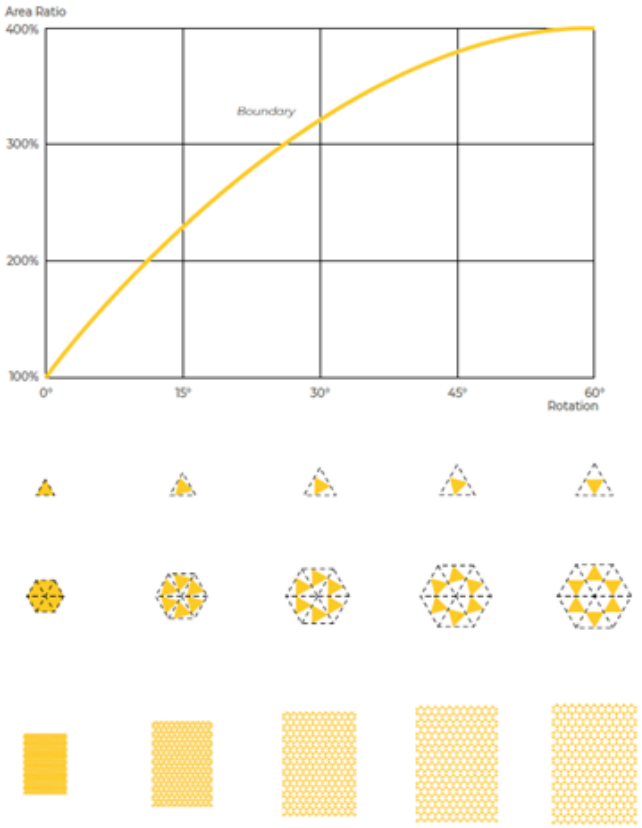

Figure 2.2-10 Boundary expansion mapping of Auxetic system
Note: From, *That Which Tends to Increase – Architectural Application of Auxetic Systems*, by *O. Borgström, 2019,* Chalmers University of Technology.

A key contribution of the research lies in the framing of auxetics as kinetic systems. Rather than being static shells, the geometries were conceived as dynamic frameworks whose behaviour could be tuned and programmed. To test this hypothesis, Borgström employed plugins such as Kangaroo2 for physics-based simulation and tested boundary conditions like fixed edges, free nodes, and constrained vertices. The images accompanying this section show how tessellations could smoothly expand and contract in multiple directions, with the geometry responding almost like a living membrane to applied forces. This emphasis on kinetic responsiveness aligned the research with broader fields of responsive architecture and adaptive envelopes, situating auxetics as a medium of transformation rather than a fixed formal system (Figure 2.2-11).

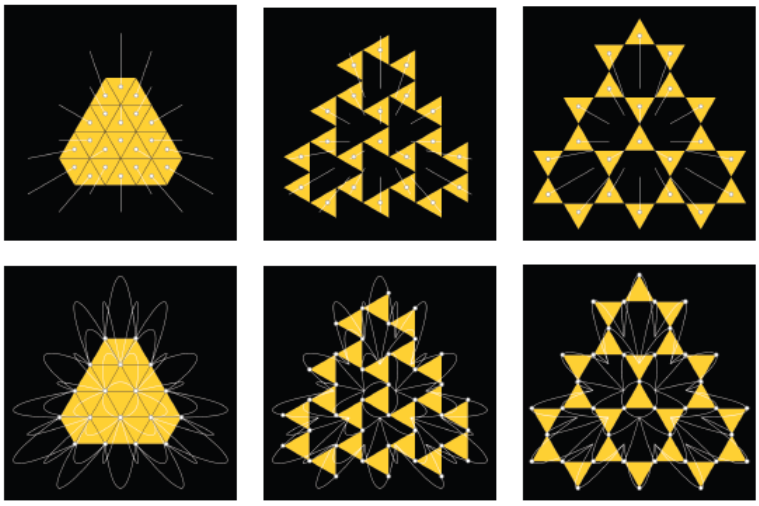

Figure 2.2-11 Node tracking of Tristar pattern
Note: From, *That Which Tends to Increase – Architectural Application of Auxetic Systems*, by *O. Borgström, 2019,* Chalmers University of Technology.

Physical prototyping played a central role in validating the digital findings (Figure 2.2-12).. Using laser-cutting and folding techniques, Borgström constructed scaled models in materials such as card, polypropylene sheets, and thin plywood. These hands-on experiments revealed how parametric logic translated into tangible movement, with prototypes capable of blooming outward, collapsing inward, or twisting into double-curved surfaces. Photographic documentation of these models demonstrated not only the elegance of auxetic transformations but also the real-world constraints, such as buckling along stress points, uneven rotation of units, and material fatigue at hinge-like regions. These challenges underscored the need for careful calibration between geometry and material, reinforcing the argument that auxetics cannot be deployed at architectural scale without consideration of mechanical articulation.

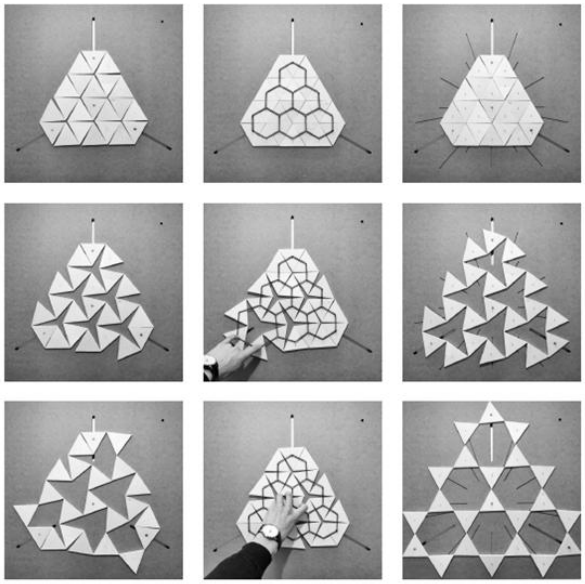

Figure 2.2-12 Physical Proof of concept - testing physical systems
Note: From, *That Which Tends to Increase – Architectural Application of Auxetic Systems*, by *O. Borgström, 2019,* Chalmers University of Technology.

The study further examined the implications of auxetics for architectural adaptability. Borgström proposed scenarios where auxetic systems could serve as responsive facades, deployable shelters, and adaptive interior partitions .The thesis illustrated how expansion and contraction could modulate light, ventilation, and enclosure, effectively embedding performative qualities into the structural logic (Figure 2.2-13). One set of images showed auxetic modules deployed over a surface, where expansion created porosity for daylight and contraction closed the system for shading, suggesting possibilities for climatic responsiveness. Figure 2.2-14 illustrates the expansion graph in XY axis (boundary expansions) vs displacement in Z axis. This understanding is crucial to understand that curvatures (z axis) is versatile corelating with the expansion relying on rotation of pattern

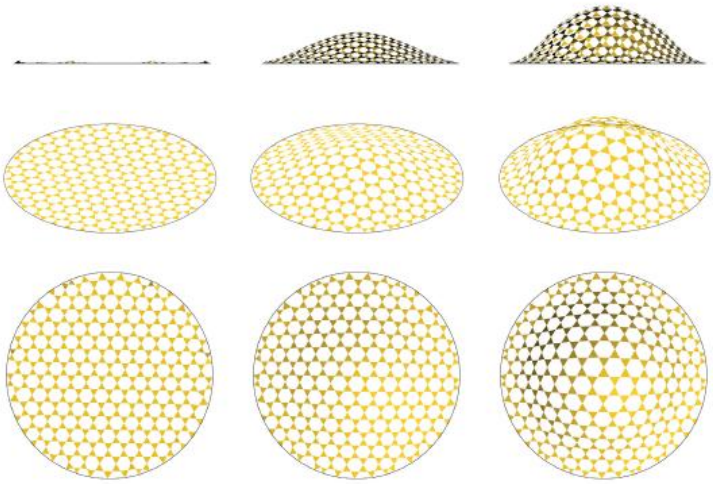

Figure 2.2-13 Scaled triangles adapting to curvatures

Note: From, *That Which Tends to Increase – Architectural Application of Auxetic Systems*, by *O. Borgström, 2019,* Chalmers University of Technology.

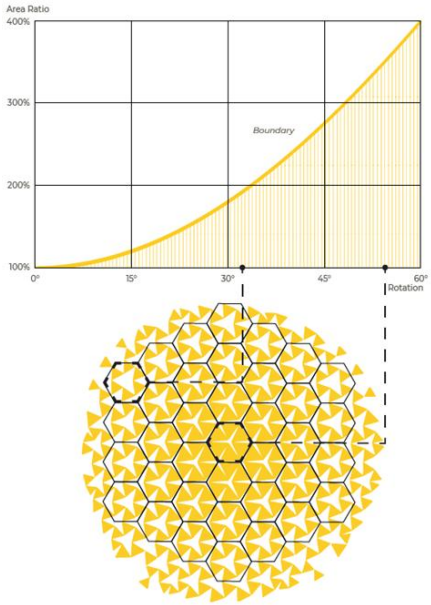

Figure 2.2-14 Graph and Design boundaries

Note: From, *That Which Tends to Increase – Architectural Application of Auxetic Systems*, by *O. Borgström, 2019,* Chalmers University of Technology.

Importantly, Borgström's thesis articulated kinetic responsiveness as a design principle that transcends form-making. By embedding motion into geometry, the work reframed architecture as an active participant in its environment, capable of transforming spatial and experiential qualities through time. This positions auxetics as an entry point into larger discourses of adaptive architecture, where buildings are no longer static objects but evolving systems responsive to shifting human and environmental needs. Figure 2.2-15 demonstrates the reaction of pattern overlayed with different deployment methods

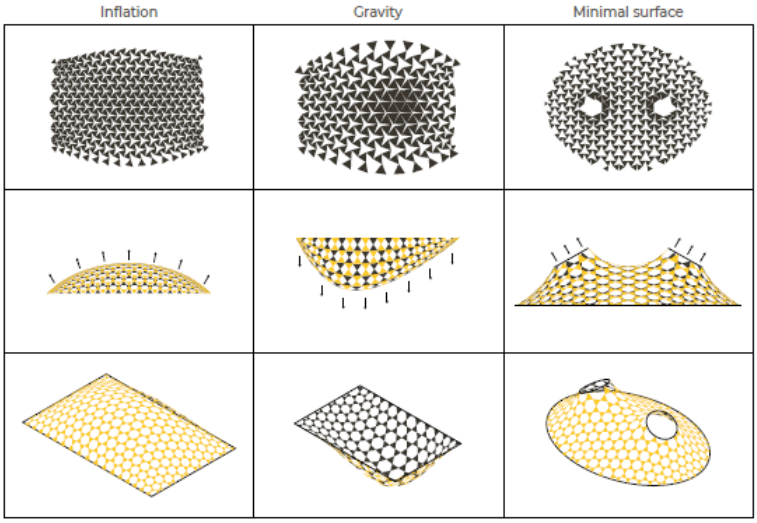

Figure 2.2-15 Surface definitions in relation to deployment concepts.
Note: From, *That Which Tends to Increase – Architectural Application of Auxetic Systems*, by *O. Borgström, 2019,* Chalmers University of Technology.

Table 2.2-1 Overview Inferences from Literature review

Topic / Subtopic	Inference for PhD	Page Number(s)
Development for flat systems	Provides 2D graphic studies of auxetic patterns that can be adapted for deployable structural systems.	p. 18
Computational simulation	Describes methods for simulating deployability in Grasshopper; informs digital workflow for testing auxetic prototypes.	p. 18
Double and single action hinge	Offers insights into rotational hinge mechanisms; useful for small-scale proof-of-concept prototypes exploring auxetic expansion.	p. 22
Covering surface and parallel layers	Documents trial-and-error findings from double-curved structures and parallel layering; relevant for testing adaptability in shells.	p. 24
Principles for auxetics as envelopes	Explores transition from flat to curved auxetic systems; provides strategies for using auxetic	p. 34

Topic / Subtopic	Inference for PhD	Page Number(s)
	envelopes as deployable architectural skins.	
From planar to double curved	Details methods of forming double-curved geometries from planar auxetic systems; directly applicable to DRSTAB shell design.	p. 37
Surface definitions	Categorizes different deployment techniques for shell structures; supports comparative testing of auxetic shell behaviors.	p. 38
Computational form finding	Identifies achievable vs. non-achievable forms using auxetic shells; informs computational design constraints.	p. 42
Formwork for rigid shell	Proposes auxetic systems as formwork for non-load-bearing, deployable shells; opens pathways for lightweight applications.	p. 48

2.2.2.1 Key Inferences from this literature:

Efficient 2D-to-3D Expansion through Rotational Auxetics :
Borgström's research demonstrates that auxetic kagome systems particularly those based on rotating triangular units can enable significant planar-to-spatial transformation. The system reportedly achieves up to 400% expansion through controlled geometric rotation, facilitating the generation of double-curved surfaces from flat 2D sheets (Borgström, 2021). This capability suggests great promise for applications in form-finding, deployable skins, and surface modulation, especially where adaptable curvature is desirable.

The Centrality of Joint Design in System Performance :
The success of the auxetic transformation is shown to rely heavily on the joints connecting the units. Borgström experiments with fabric hinges, single-action, and double-action mechanical joints, each with distinct advantages in rotation range, elasticity, and fatigue resistance. The thesis makes it clear that kinetic joinery is not merely a connection detail but a performance-determining element critical for both durability and geometrical fidelity.

Layering as a Strategy for Performance Modulation :
A particularly novel insight in Borgström's work is the role of layered auxetic assemblies. By stacking or overlapping patterned sheets, the system enables control over surface porosity, visual opacity, and structural rigidity. This approach introduces a level of programmability that enhances both the functional and aesthetic versatility of auxetic systems in architectural applications.

Digital–Physical Integration as a Development Model :
The study follows a dual development approach, using Grasshopper-based parametric simulations to design and test movement sequences, which are then validated through scaled physical prototypes. This methodology highlights the importance of computational precision in

early-phase design, but also reinforces the need for hands-on validation to account for material behaviour and tolerances not captured digitally.

Broad Applicability across Architectural Typologies :
Borgström positions the system as adaptable for multiple scales and purposes ranging from inflatable envelopes and tensile membranes to reconfigurable formwork systems. Such adaptability underscores the flexibility of auxetic geometries when integrated into architectural components that must perform under temporality, mobility, or kinetic reconfiguration.

2.2.3 Konaković Luković et al. (2016): Beyond Developable: Computational Design and Fabrication with Auxetic Materials

Konaković Luković et al.'s (2016)) introduced a seminal study that shifted the understanding of how auxetic principles can be embedded within architectural design and fabrication processes. The paper moved beyond traditional views of developable surfaces, focusing instead on computational strategies that allowed complex geometries to be rationalized and physically realized through auxetic transformations. The key premise of their work was that by embedding geometric intelligence into materials, one could achieve form flexibility without relying on heavy mechanical systems, thus broadening the design space for deployable and adaptive structures.

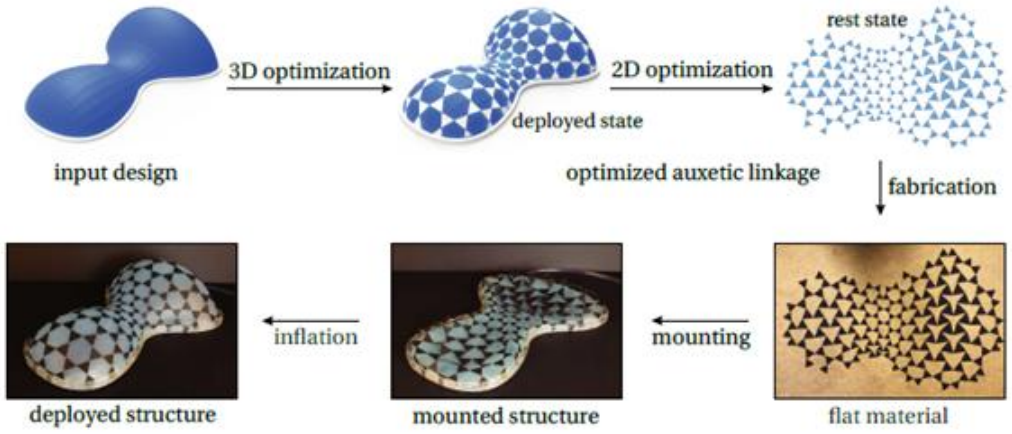

Figure 2.2-16 Algorithmic computation and physical model testing for inflation deployment methods

Note: From, *Beyond Developable: Computational Design and Fabrication with Auxetic Materials* by *Konaković Luković et al. (2016)*

The methodology of the study was anchored in computational geometry and digital fabrication. The authors explored how conformal transformations could be applied to planar auxetic patterns, enabling them to adapt to double-curved surfaces while retaining the characteristic property of negative Poisson's ratio. This opened possibilities for generating large, continuous forms that could be folded, stretched, or adapted without distortion of the base geometry. By using algorithms that mapped auxetic grids onto target surfaces, the research demonstrated how otherwise rigid geometries could acquire elastic, responsive qualities.

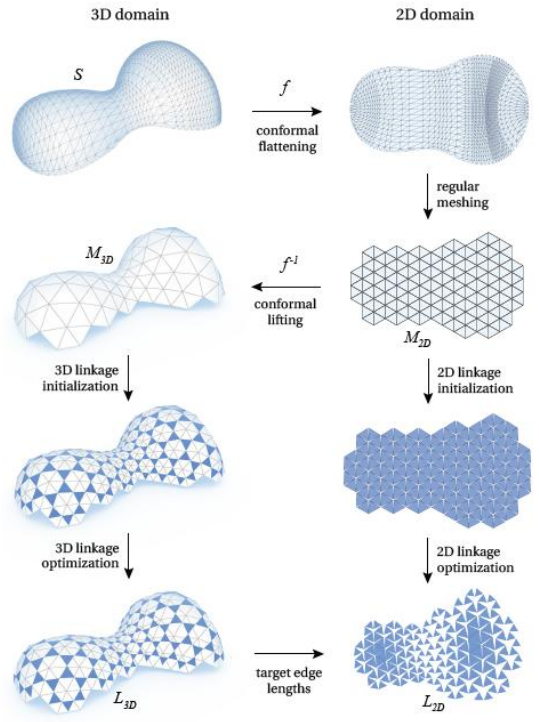

Figure 2.2-17 Optimization algorithm for computing spatially graded auxetics

Note: From, *Beyond Developable: Computational Design and Fabrication with Auxetic Materials* by *Konaković Luković et al. (2016)*

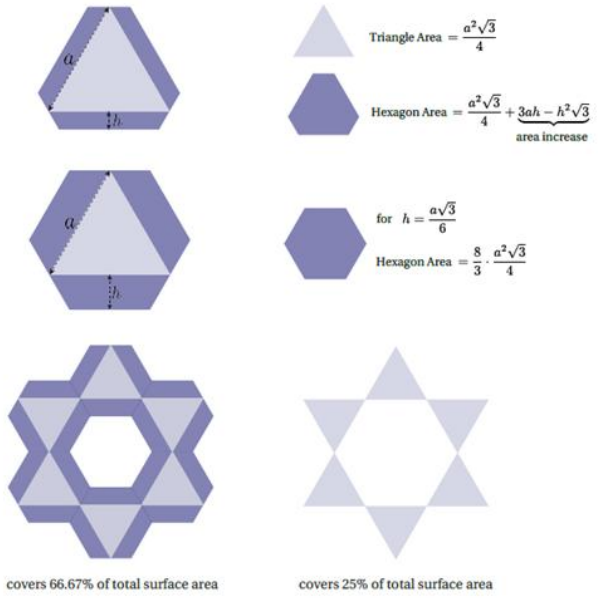

Figure 2.2-18 Shape modifiers and related formulas

Note: From, *Beyond Developable: Computational Design and Fabrication with Auxetic Materials* by *Konaković Luković et al. (2016)*

One of the central contributions of the study was the introduction of fabrication-driven simulations. The team not only modelled auxetic patterns computationally but also fabricated physical prototypes to test their real-world performance. Through laser-cut sheet materials and controlled deformation tests, they validated that the digital assumptions of surface rationalization corresponded to tangible structural transformations. This dual validation between computation and fabrication gave their findings strong credibility and relevance to both design and engineering domains.

Figure 2.2-19 Auxetic linkages with Deployment via gravity
Note: From, *Beyond Developable: Computational Design and Fabrication with Auxetic Materials* by *Konaković Luković et al. (2016)*

The study also highlighted practical implications for architectural construction. Auxetic transformations were shown to enable flat sheet materials to be reconfigured into three-dimensional, load-bearing forms with minimal waste and material handling. This approach minimized reliance on molds or scaffolding, offering efficiency in both time and resources. In doing so, the work suggested an alternative paradigm for material-efficient fabrication where surface and structure co-evolve through computational logics. These insights resonate strongly with contemporary discourses on sustainability, lightweight design, and adaptive architecture.

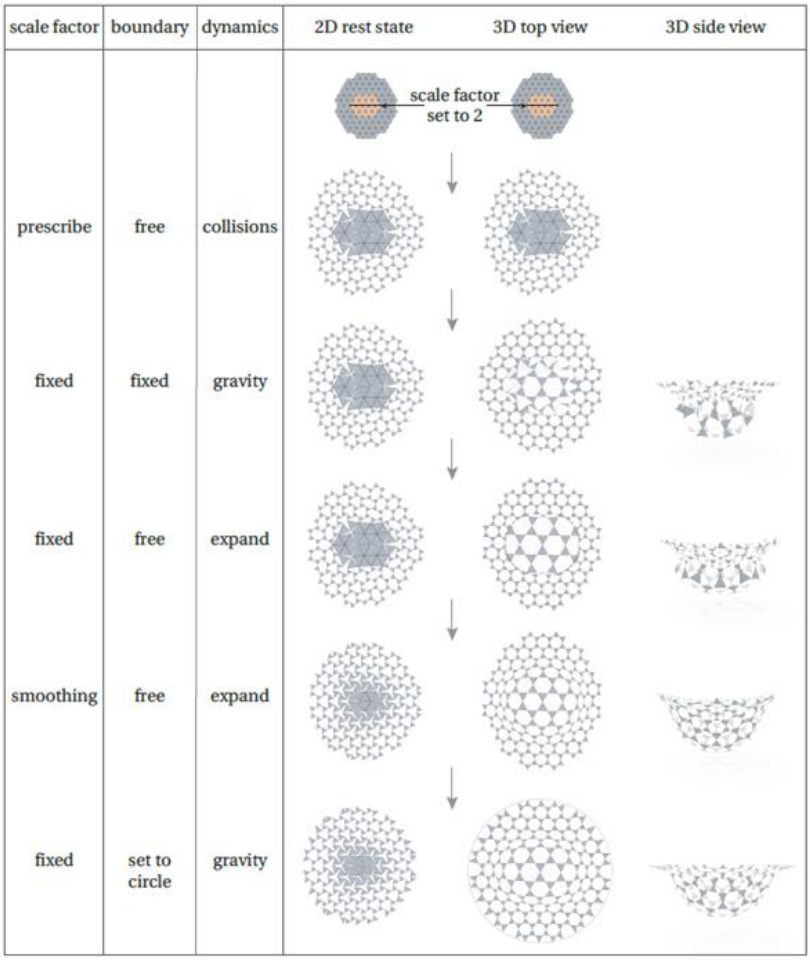

Figure 2.2-20 Form finding examples

Note: From, *Beyond Developable: Computational Design and Fabrication with Auxetic Materials* by *Konaković Luković et al. (2016)*

More broadly, the research advanced the theoretical dialogue on the role of geometry in architectural systems. By bridging computational design with physical prototyping, Konaković Luković et al. (2016) redefined auxetics not merely as an abstract material property but as a spatial design tool. Their work underscored how geometric transformations can become embedded in architectural expression, influencing both aesthetics and performance. Importantly, the study established a foundation for future explorations where auxetic logic could integrate with mechanical systems, robotics, or deployable structures directions that subsequent research, including this thesis, continues to build upon.

Figure 2.2-21 Exemplars Prototype - Pavilion design

Note: From, *Beyond Developable: Computational Design and Fabrication with Auxetic Materials* by *Konaković Luković et al. (2016)*

Table 2.2-2 Overview Inferences from Literature review

Topic / Subtopic	Inference for PhD	Page Number(s)
Conformal geometry	Provides computational analysis of conformal data for auxetic shell structures; informs simulation workflows for geometric accuracy.	p. 44
Surface rationalization	Identifies suitable surface rationalization methods for fabrication, critical for translating complex forms into manufacturable shells.	p. 50
Material optimization	Explores optimization strategies for base shapes; supports selection of efficient material layouts in auxetic shells.	pp. 71, 74
In-plane opening & filling surface	Examines auxetic transformations and how positive-to-negative space emerges during deployment; aids understanding of surface porosity and adaptability.	p. 77
Fabricated prototype in gravity	Demonstrates proof-of-concept prototypes tested under gravity; useful for analyzing real-world form reactions during deployment.	p. 81
Form-finding with editing operators	Illustrates simple examples of form-finding using atomic editing algorithms; applies directly to defining suitable 3D auxetic curves.	pp. 91, 93

Topic / Subtopic	Inference for PhD	Page Number(s)
Planar rest vs. deployed state	Analyzes curve point movement from flat configuration to deployed state; informs predictions of deployment pathways.	p. 94
EPFL shading pavilion	Presents live pavilion prototype demonstrating auxetic shading; validates application potential in architectural contexts.	p. 104
Inscribing regular linkage triangles	Explores embedding of linkage triangles into conformally lifted tiling grids; informs modular strategies for auxetic surfaces.	p. 110
Degree of freedom	Discusses limitations and freedoms in achievable forms; relevant for balancing structural rigidity and adaptability.	
Code for non-penetration constraint	Provides Python code and logic for preventing element overlap; useful for computational simulations in Grasshopper and Python workflows.	p. 113
Increasing area coverage with linkage	Quantifies expansion in terms of area and volume; provides metrics for total deployable coverage of auxetic systems.	p. 115
Rapid deployment of curved surfaces (SIGGRAPH 2018 video)	Demonstrates full deployment of programmable auxetic shells in motion; validates computational findings through visual evidence.	Video link

2.2.3.1 Inferences from the Study:

Conformal Geometry Enables Double-Curved Auxetic Surfaces :
One of the study's most compelling contributions lies in its use of conformal geometry to embed auxetic behaviour into double-curved surfaces. Through computational surface mapping techniques, the researchers demonstrate how triangular linkage networks originally planar can be algorithmically morphed into spatially complex surfaces while preserving auxetic deformation capabilities. This insight lays foundational groundwork for curved auxetic surfaces that can adaptively expand or contract based on environmental or structural stimuli (Konaković Luković et al., 2016).

Algorithmic Optimization for Geometry and Material Configuration :
The study successfully integrates surface rationalization, mesh topology optimization, and material computation into a single pipeline, ensuring the output is not only geometrically expressive but also fabrication-ready. This optimization enables precise tailoring of both structural stiffness and material behaviour, advancing the possibility of producing deployable shell systems that are lightweight yet structurally robust. The workflows exemplify how computational design tools can simultaneously resolve aesthetic, spatial, and material constraints.

Spatial Control of In-Plane Expansion and Opening :
The research introduces a novel method for controlling the transformation of positive-to-negative space, particularly through in-plane auxetic deformation. The auxetic linkage system exhibits predictable and reversible transformations, making it viable for use in adaptive spatial enclosures such as kinetic shading systems, expanding canopies, or transformable facades. This level of spatial choreography is critical for responsive architectural envelopes where movement is functional, not merely formal.

Proof-of-Concept Prototypes and Gravity Simulations :
The design methodology is supported through a combination of digital simulations (under gravitational conditions) and fabricated prototypes, validating the real-world feasibility of the proposed systems. These physical models offer a tangible understanding of how algorithmically derived forms behave under material constraints and serve as an important step towards bridging digital design with architectural fabrication.

Demonstrated Scalability and Real-World Deployment Potential :
The construction of the EPFL shading pavilion serves as a compelling demonstration of the system's architectural potential. Area expansion metrics (up to 66.67%) indicate that such systems are capable of covering large surface areas from compact folded states key for deployable and reconfigurable applications. This scaling potential suggests broader utility in climatic adaptivity, mobile infrastructure, and transformable building skins.

2.2.4 Eguchi,S et al. (2022) , Pneumatic Auxetics: Inverse design and 3D printing of auxetic pattern for pneumatic morphing

Recent research into pneumatic auxetics has explored the potential of combining negative Poisson's ratio patterns with inflatable systems to achieve morphing structures. Unlike purely geometric or mechanically jointed auxetic assemblies, pneumatic auxetics rely on pressure differentials to activate transformation, creating soft, adaptable, and lightweight systems. The focus of this line of inquiry has been on developing inverse design methods that allow a designer to prescribe the target deformation or morphing behaviour, and then generate an auxetic pattern capable of achieving it when inflated.

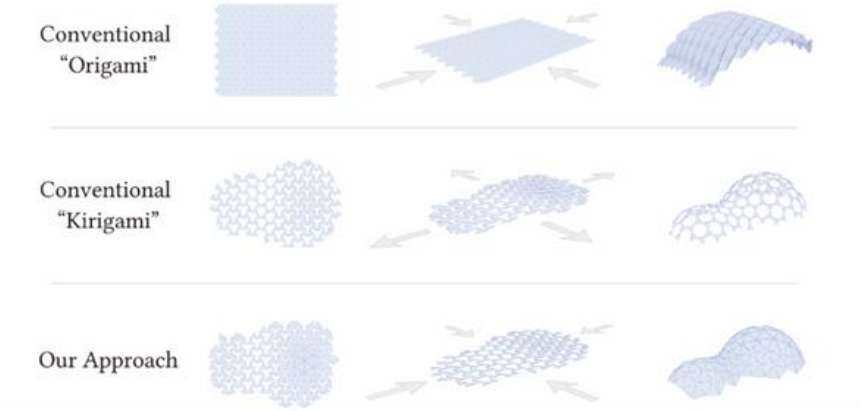

Figure 2.2-22 Morphing of Auxetic shapes - Origami shapes
Note : *Pneumatic Auxetics:: Inverse design and 3D printing of auxetic pattern for pneumatic morphing* by *Eguchi, S., et al. (2022).*

The study integrated computational inverse design techniques with additive manufacturing, particularly 3D printing of flexible polymers, to prototype these pneumatic structures. By starting with desired shape-change behaviours such as bending, twisting, or localized bulging

the design process worked backwards to calculate the auxetic unit-cell geometries and their distribution across a surface. This approach marked a departure from traditional forward-design methods, where unit cells are selected and arranged first, and their global performance is then evaluated. Instead, inverse design ensured that pneumatic inflation produced precise, controlled transformations.

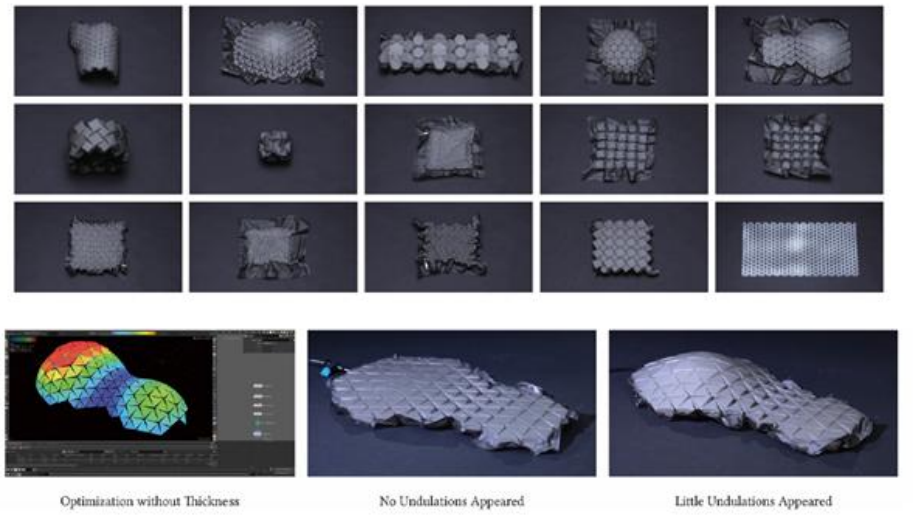

Figure 2.2-23 Testing extruded kirigami

Note : *Pneumatic Auxetics:: Inverse design and 3D printing of auxetic pattern for pneumatic morphing* by *Eguchi, S., et al. (2022).*

A central technical contribution was the demonstration of how small-scale auxetic units could be embedded into larger inflatable morphing panels. 3D printing enabled the fabrication of intricate lattice geometries that could withstand repeated inflation and deflation cycles without mechanical failure. Prototypes showcased the ability of these pneumatic auxetics to achieve continuous curvature, complex folds, and even adaptive openings, all triggered by relatively low air pressures. Photographic documentation of the experiments highlights surfaces transitioning from flat sheets to dome-like or saddle-shaped morphologies, confirming the accuracy of the computational predictions.

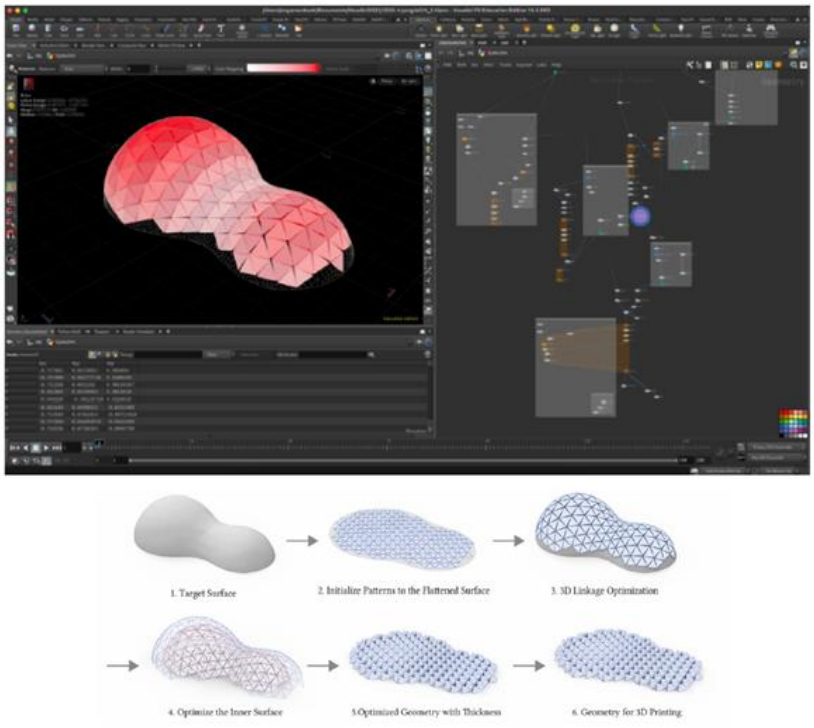

Figure 2.2-24 Simulation tool SS

Note : *Pneumatic Auxetics:: Inverse design and 3D printing of auxetic pattern for pneumatic morphing* by *Eguchi, S., et al. (2022).*

This research has significant implications for architectural and engineering applications where lightweight, reconfigurable systems are required. Pneumatic auxetics offer the possibility of deployable structures that can be transported compactly and expanded on-site without rigid mechanical joints. They also introduce a soft robotic dimension to architectural systems, where air pressure can act as a controllable input for spatial adaptation. Potential uses include adaptive facades, temporary enclosures, and responsive shading systems, all benefiting from the reversible and programmable behaviour of the material system.

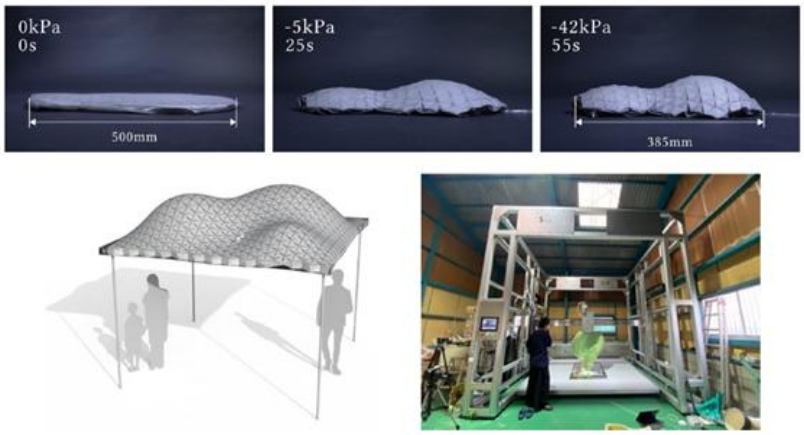

Figure 2.2-25 Fabrication of Pneumatic Auxetics and Pneumatically actuated shells 1:1 scaled and fabricated in 3d printer

Note : *Pneumatic Auxetics:: Inverse design and 3D printing of auxetic pattern for pneumatic morphing* by *Eguchi, S., et al. (2022).*

2.2.4.1 Inferences from the study :

Inverse Design Enables Targeted Morphing :Using computational inverse methods (e.g., topology optimization), the researchers could generate auxetic lattice patterns that morph predictably under uniform internal pressure, achieving shape-programmed deformations in 2D and 3D.
Material-Geometry Co-Design Enhances Responsiveness : The performance of pneumatic auxetics was shown to be strongly dependent on the interplay between lattice geometry and material elasticity. Hyperelastic materials such as TPU (thermoplastic polyurethane) enabled high deformation with resilience.
Single-Material 3D Printing is Feasible :The study demonstrated that complex auxetic morphing systems could be manufactured as monolithic parts, using fused deposition modelling (FDM) or stereolithography. This opens pathways for scalable, low-cost deployment in architectural elements.
Negative Poisson's Ratio Improves Actuation Range : Auxetic patterns such as rotating squares and re-entrant triangles allowed up to 100–150% area expansion under pneumatic load, outperforming conventional inflatable structures in both stretchability and control.
Programmable Curvature and Folding Achieved :Some configurations enabled doubly curved or dome-like morphing behaviours, demonstrating the potential for deploying soft, inflatable auxetic shells that can simulate architectural curvature without rigid joints.

2.2.5 Comparitive table of Deployable Auxetic shell Precendences

Table 2.2-3 Comparitive table of Deployable Auxetic shell Precendences

Study	Key Strengths (Pros)	Limitations (Cons)	Relevance to DRSTAB	Research Gap Addressed
Jayachandran (2019) Deployable Reciprocal Shells Through Auxetic Behaviour	Establishes foundational link between reciprocal systems and auxetic expansion; demonstrates feasibility of deployable shell logic	Lacks developed mechanical joinery; movement not precisely controlled; limited scalability	Direct precursor to current research; informs geometric logic and deployability principles	Need for engineered joinery systems to control movement and enable real-world application
Borgström (2019) Architectural Application of Auxetic Systems	Strong architectural framing; explores adaptability, spatial transformation, and user interaction	Limited mechanical resolution; lacks structural and joinery detailing; largely conceptual	Informs architectural potential and spatial adaptability of auxetics	Gap in translation from conceptual auxetics to buildable mechanical systems
Konaković Luković et al. (2016) Beyond Developable	High precision in geometric control; strong integration of computation and fabrication; explores non-developable surfaces	Focused on material systems rather than structural systems; lacks deployability and joinery articulation	Informs computational workflow and geometric logic for complex auxetics	Lack of deployable architectural systems and mechanical articulation
Eguchi et al. (2022) Pneumatic Auxetics	Demonstrates dynamic morphing; introduces actuation-driven transformation; scalable material behaviour	Relies on pneumatic systems rather than mechanical joinery; not structurally self-supporting; limited architectural scalability	Highlights alternative actuation strategies and responsive behaviour	Absence of passive mechanical systems for controlled deployment in architecture

The reviewed precedents collectively demonstrate significant advancements in auxetic geometry, computational design, and spatial adaptability. However, a consistent gap emerges across all studies: the absence of a fully integrated system that translates auxetic behaviour into a mechanically controlled, deployable architectural structure. While prior research successfully explores geometry, material behaviour, or actuation independently, none resolve the critical challenge of mechanical articulation through joinery (as shown in Table 2.2-3). This research addresses this gap by positioning mechanical joinery not as a secondary connector, but as the primary driver that enables the translation of geometric logic into controlled, scalable architectural deployment.

2.2.6 Auxetic Materials Concentrating on Usage in Architecture and Design – other inferences

Beyond the focused precedents that directly engage with deployable auxetic shells, it is important to recognize the wider body of research that has examined auxetic materials in architectural and design contexts. These studies provide essential background knowledge that informs this investigation, particularly regarding mechanical performance, energy absorption, fabrication strategies, and the challenges of scaling auxetic systems to architectural dimensions.

Saxena, Das, and Calius (2016) provide one of the most comprehensive overviews of auxetics, tracing three decades of research into materials with negative Poisson's ratio. Their review establishes the fundamental mechanical properties of auxetic systems, highlighting how these materials expand laterally when stretched and contract when compressed. This foundational knowledge is critical for understanding the basic behaviour of auxetic geometries and forms the conceptual framework underpinning their architectural applications.

Moving from theory to application, Naboni, Sartori, and Mirante (2017) demonstrate how auxetic principles can be harnessed to achieve adaptive curvature in architectural structures. Their work shows that auxetic configurations are particularly suited for shaping double-curved surfaces, a finding directly relevant to the design logic of deployable shells. By applying auxetic tessellations to curved geometries, they reveal how reciprocal systems can be enhanced with curvature adaptability, supporting the scalability of auxetic concepts beyond flat prototypes.

At the computational and fabrication level, Konaković, Crane, Deng, Bouaziz, Piker, and Pauly (2016) provide a significant contribution by developing digital design and fabrication methods for auxetic materials. Their study outlines computational approaches to pattern programming and structural simulation, offering strategies for embedding auxetic logics within parametric workflows. These methods align closely with the digital design processes employed in this research, particularly in the use of Rhinoceros 3D and Grasshopper environments for mapping movement and adaptability.

Zhang, Lu, and You (2020) extend the discussion by examining the large-scale behaviour of additively manufactured auxetic materials. Their review identifies the potential for auxetics to undergo substantial deformation while maintaining energy absorption capacity, but also warns of the pitfalls encountered when scaling prototypes. Challenges such as inconsistent deformation, localized stress concentrations, and reduced performance at architectural scales are highlighted. These insights provide a cautionary backdrop for the scaling of auxetic prototypes within this study, emphasizing the need for material realism and structural validation.

The manufacturing dimension is further expanded by Lu, Hsieh, Huang, Zhang, Lin, Shen, Chen, and Zhang (2022), who investigate additive manufacturing processes for mechanical

metamaterials and auxetics in architectural contexts. Their research underscores the role of digital fabrication in realizing complex lattice structures, offering strategies for precision, scalability, and integration into architectural applications. For this thesis, such findings reinforce the decision to experiment with advanced materials such as PETG and carbon-fiber-infused filaments, as well as 3D printing techniques, for testing auxetic behaviours under real-world fabrication constraints.

Finally, large-scale experimental installations provide evidence of how auxetics behave beyond laboratory conditions. Gletthofer, Hoffmann, Winter, Gierlinger, and Holzinger (2022) presented WAUXI, a wall-scale auxetic installation developed at TU Graz, which serves as a demonstration of auxetic systems applied in architectural practice. WAUXI illustrates how auxetic modules perform under environmental conditions, showcasing fabrication logistics, behavioral reactions, and user interaction at a scale far larger than material samples. This case reinforces the architectural potential of auxetics while highlighting fabrication challenges and the importance of careful joinery integration.

Taken together, these contributions demonstrate that while auxetic materials have been widely studied in terms of mechanical behaviour and fabrication, their direct translation into architectural systems remains limited and fragmented. The literature provides foundational principles (Saxena et al., 2016), strategies for curvature adaptability (Naboni et al., 2017), computational and digital fabrication workflows (Konaković et al., 2016; Lu et al., 2022), insights into scaling and deformation challenges (Zhang et al., 2020), and examples of design-scale applications (Gletthofer et al., 2022). These works inform the methodology of this PhD, particularly in relation to joinery design, structural testing, and material performance, while also confirming that significant gaps remain in integrating auxetic principles with reciprocal logic and deployable mechanics into a coherent architectural framework.

2.2.7 Deployable Architectural Structures

Deployable structures have been studied extensively in architecture and engineering, offering diverse typologies that range from scissor systems and foldable domes to inflatable membranes and tensegrity frameworks. This body of work provides critical foundations for understanding the mechanics, materials, and typological classifications that inform the development of deployable reciprocal shells in this research. While the primary focus of this PhD lies at the intersection of reciprocal geometries and auxetic expansion, positioning this work within the broader landscape of deployability ensures that its innovations are grounded in proven principles of structural adaptability, compactness, and mechanical reliability.

A number of reviews and classifications set the stage for this discourse. Fenci and Currie (2017) provide a comprehensive classification of deployable structures, mapping the relationships between different mechanical and structural families, while Doroftei and Doroftei (2014) offer a parallel survey with a focus on architectural applications. These typological frameworks are complemented by Rivas-Adrover (2017), who highlights the role of scissor-based 2-bar systems in shaping deployable geometries and notes the limitations of conventional scissor configurations in generating complex forms. Collectively, these studies establish the intellectual foundation for understanding how deployable systems are organized, and where new strategies, such as the DRSTAB system, diverge from conventional models.

Research on specific typologies extends this foundation into performance and mechanics. Schmidt and Li (1995) present geometric models of deployable domes, demonstrating approaches for achieving large spans and geometric compactness in metal shell systems. Similarly, Volkov, Makhnenko, Kandala, Volkova, and Borovyk (2021) compare finite-element simulations with full-scale experiments on folded thin-walled metal shells, underscoring the importance of compactness, elastoplastic properties, and geometric accuracy when scaling

deployable designs. These works directly inform the comparative benchmarks against which the DRSTAB system can be tested, particularly with respect to structural integrity and efficiency of reconfiguration.

The material and folding mechanics of deployables are further addressed in Pellegrino (2020), who reviews thin-shell deployment and folding strategies, focusing on materials and constitutive models. This analysis provides insights into optimal tessellation cross-sections and dimensions, both of which are central to evaluating the material efficiency of deployable reciprocal shells. Complementing this, Friedman and Ibrahimbegovic (2013) survey highly flexible deployable lattices including retractable roofs, pantographic grids, pop-up systems, and tensegrity structures while Friedman, Farkas, and Ibrahimbegovic (2011) emphasize sustainable and reusable approaches, particularly in relation to manually locking and self-locking systems. These findings resonate strongly with this PhD's focus on mechanical joinery and reusability, as they point to design strategies that extend beyond motion alone and into lifecycle sustainability.

Biomimetic perspectives also contribute important lessons. Lienhard, Poppinga, Schleicher, Masselter, Speck, and Knippers (2011) abstract movement principles from plants to propose adaptive deployable structures, illustrating how biological systems can inspire transformation logics in architecture. This work situates deployability not only as a technical challenge but as a design opportunity that benefits from interdisciplinary knowledge transfer.

Finally, computational and inflatable systems introduce alternative pathways for realizing deployable performance. Panetta, Isvoranu, Chen, Siéfert, Roman, and Pauly (2021) demonstrate the potential of computational inverse design for inflatable morphologies, revealing how pneumatic strategies can be optimized to achieve compact deployment and controlled expansion. While inflatables are not the focus of this thesis, their study highlights complementary techniques and benchmarks for understanding deployment efficiency and surface transformation.

Together, these contributions provide a robust framework of deployable knowledge. Foundational classifications (Fenci & Currie, 2017; Doroftei & Doroftei, 2014; Rivas-Adrover, 2017), geometric and material analyses (Schmidt & Li, 1995; Volkov et al., 2021; Pellegrino, 2020), sustainability-oriented design strategies (Friedman et al., 2011, 2013), biomimetic analogues (Lienhard et al., 2011), and computational morphologies (Panetta et al., 2021) collectively inform this study. While each strand offers critical insights, they also reveal gaps at the convergence of deployability, reciprocal logic, and auxetic transformation precisely the synthesis that this PhD seeks to address through the DRSTAB system.

2.2.8 Reciprocal Structures and shell structures

Reciprocal frame (RF) structures represent a long-standing yet continuously evolving typology in architectural and structural design. Based on principles of mutual load distribution through interlocking elements without requiring centralized supports, RF systems have consistently demonstrated value in lightweight, modular, and spatially expressive applications. Their capacity to form planar, curved, and even double-curved surfaces through localized repetition and rotational symmetry makes them particularly attractive for adaptive and deployable systems.

Foundational studies have examined RF systems from both theoretical and applied perspectives. Pugnale and Sassone (2014) provide one of the most comprehensive references, covering two- and three-dimensional geometric patterns, structural behaviour, and case studies of timber RF roofs and pavilions. Their work establishes a clear basis for understanding RF logic as an integrative structural language in deployable shells. Similarly,

Larsen (2008) offers a step-by-step exploration of RF modularity, joint detailing, and assembly methods, while Gíslason (2010) introduces practical guidelines including span rules, material comparisons between timber and steel, and rapid construction techniques directly relevant to deployable and scalable applications.

At the intersection of mathematics and mechanics, several studies explore RF statics and kinematics. Parigi and Kirkegaard (2014) present mathematical models of RF stability, highlighting the influence of rigid versus hinged connections and proposing foldable systems suitable for shelters. Douthe and Baverel (2009) extend this line of inquiry by applying computational optimization to timber plate-based RF grids, validating efficiency in member lengths and angles through parametric modelling. These insights directly inform the balance between geometric adaptability and structural reliability in hybrid RF–auxetic systems.

Research also extends into deployability and dynamic performance. Veenendaal, Block, and Williams (2011) propose RF systems configured as scissor-like mechanisms, testing their suitability as modular units for disaster-relief applications and evaluating dynamic behaviour under wind loads. Baverel, Nooshin, Kuroiwa, and Williams (2000) introduce the concept of "nexorades," woven RF systems reinforced with cables, which merge RF logics with tensegrity principles to achieve lightweight, large-span, deployable frameworks. These explorations underline the versatility of RF structures in addressing challenges of rapid deployment, resilience, and mobility.

Beyond mechanics, RF systems have also been contextualized within biomimetic and contemporary design frameworks. Popovic Larsen (2008) and Chilton, Choo, and Popovic Larsen (2015) situate reciprocal structures in dialogue with natural analogues and contemporary applications. The former links RF geometries to biological precedents such as leaf venation, while the latter surveys RF use in pavilions and bridges, with particular focus on redundancy strategies and failure modes that support sustainability and long-term resilience. Complementing this, Knippers and Speck (2012) explore bio-inspired RF systems, adapting morphologies from sponges and plant cells and introducing adaptive mechanisms using smart materials like shape-memory alloys. Such approaches demonstrate the capacity of RF systems to evolve into more responsive and environmentally attuned construction strategies.

Taken together, these works reveal reciprocal structures as a highly adaptable design and engineering language. Comprehensive surveys (Pugnale & Sassone, 2014; Larsen, 2008; Gíslason, 2010), mathematical and computational studies (Parigi & Kirkegaard, 2014; Douthe & Baverel, 2009), deployable and hybrid explorations (Veenendaal et al., 2011; Baverel et al., 2000), and bio-inspired frameworks (Popovic Larsen, 2008; Knippers & Speck, 2012) collectively illustrate the relevance of RF logic across scales and applications. For this PhD, these insights directly inform the integration of reciprocal geometries with auxetic systems, particularly through their lessons on modularity, joint mechanics, foldability strategies, and structural adaptability.

2.2.9 Auxetic Materials & 2D Patterns for Architecture

Auxetic materials, defined by their negative Poisson's ratio, have progressively transitioned from scientific curiosities into viable candidates for architectural design. Their ability to expand laterally under tensile loading and contract under compression introduces unique opportunities for adaptable, energy-absorbing, and geometrically versatile structures. The literature reviewed here spans theoretical foundations, material mechanics, geometric innovation, and architectural applications, directly informing Chapter 3.2 (2D Pattern Analysis) and Chapter 4.2 (3D Auxetic Pattern Adaptation and Spatial Behaviour).

The earliest theoretical groundwork was laid by Evans and Alderson (2000), who introduced the principles of auxetic behaviour through re-entrant honeycombs and chiral structures, establishing the functional advantages of flexibility, energy absorption, and lateral adaptability. Lakes' (1987) seminal demonstration of foam structures with negative Poisson's ratio provided empirical validation of these concepts, showing improvements in shear resistance, indentation resistance, and impact absorption that remain highly relevant for protective architectural panels and cladding systems.

Subsequent studies expanded the repertoire of auxetic geometries. Grima and Evans (2006) proposed the rotating squares mechanism, a simple yet powerful model that contracts and expands predictably under load. Its geometric clarity has made it particularly useful for adaptive façade systems and kinetic architectural skins. Lim (2015) compiled a comprehensive catalogue of auxetic forms, including arrowhead, star-shaped, and anti-chiral patterns, accompanied by analytical models of stiffness and deformation. This work directly informs the taxonomy of patterns developed in Chapter 3.2 and offers comparative insights into their applicability for shading devices and structural surfaces.

Other research has targeted material innovation and fabrication strategies. Alderson et al. (2010) explored woven and fiber-reinforced composites, embedding auxetic properties into textiles and suggesting opportunities for deployable membranes and adaptable enclosures. Prawoto (2012) complemented this perspective with computational finite element analysis (FEA), modelling stress distribution and mechanical performance across auxetic lattices of polymers, metals, and composites. These studies collectively highlight the transition from purely geometric interest to material realism, bridging analytical models with structural application.

A key milestone in expanding auxetics into three dimensions was achieved by Babaee et al. (2013), who demonstrated soft metamaterials with negative Poisson's ratio through cut-and-fold geometries. Their work showed the scalability of auxetic sheets into curved, compliant structures suitable for kinetic partitions and adaptive roofing. Building on this, Schenk and Guest (2013) linked Miura-ori origami with auxetic behaviour, formalizing the geometric logic of foldable auxetic surfaces. Their model of flat-foldability became a cornerstone for compact deployables and retractable structures, informing this research's 3D-to-2D-to-3D simulation workflows in Chapter 4.2.

Recent reviews have emphasized programmability and architectural scalability. Bertoldi, Vitelli, Christensen, and van Hecke (2017) surveyed flexible mechanical metamaterials, introducing strategies for tuning Poisson's ratios and designing smart materials with adaptive porosity. Their insights into "programmable auxetics" guide the direction of this thesis toward responsive and reconfigurable façade systems. Mir, Ali, Sami, and Ansari (2019) further extended auxetic research into architectural practice by presenting case studies of 3D-printed prototypes, adaptive cladding, and concrete formwork systems. Their evaluations of environmental durability and stress performance underscore the challenges and opportunities of scaling auxetics into full-scale construction contexts.

Taken together, this literature demonstrates how auxetic research has progressed from theory (Evans & Alderson, 2000; Lakes, 1987), through geometric innovation (Grima & Evans, 2006; Lim, 2015), to material realism (Alderson et al., 2010; Prawoto, 2012), and finally toward architectural integration (Babaee et al., 2013; Schenk & Guest, 2013; Bertoldi et al., 2017; Mir et al., 2019). These contributions provide the theoretical, computational, and material basis for the hybridization of auxetic patterns with reciprocal geometries in deployable architectural shells, which this PhD explores in detail.

2.2.10 Mechanical Joinery

The articulation of deployable structures fundamentally depends on the design and performance of mechanical joints. While reciprocal and auxetic geometries define the global adaptability of a system, joineries mediate the transfer of forces, regulate motion, and determine the durability of deployment cycles. As Pahl, Beitz, Feldhusen, and Grote (2007), Shigley, Mischke, and Budynas (2004), and Norton (2020) emphasize, joints are not passive connectors but active determinants of structural performance, balancing freedom of movement with stability and locking mechanisms. In deployable architecture, these requirements are intensified by the need for reusability, lightweight construction, and precision in motion transfer (Pellegrino, 2001).

Among the joinery strategies evaluated in literature and adapted in this research, three categories emerge as the most relevant: ratchet systems, ball joints, and one-way clutch bearings.

Ratchet Systems :
Ratchets are widely documented in engineering for enabling unidirectional movement with secure reverse locking. Sclater's (2011) Mechanisms and Mechanical Devices Sourcebook provides detailed engineering diagrams and load-handling considerations, while Orthwein (2004) expands on clutch-based locking and engagement dynamics relevant to fail-safe systems. Pahl et al. (2007) highlight their systematic application in machine design, with safety factors and dynamic loads particularly relevant for architectural-scale ratchets. Norton (2020) further contributes empirical formulas for holding torque and stress analysis, critical when scaling up ratchets to resist high winds or dynamic structural loads. Ratchets' compactness and reliability make them attractive for deployable shells, yet their discrete locking teeth concentrate stresses, raising concerns for long-term fatigue. As Collins (2009) notes, scaling requires careful material and wear analysis, particularly under repeated cycles in outdoor environments.

Ball Joints :
Ball joints are among the most versatile connectors, offering rotational freedom in multiple axes and thus enabling complex kinematic transformations. Shigley et al. (2004) document types such as self-aligning and threaded ball joints, noting load ratings and wear characteristics under cyclic motion. Uicker, Pennock, and Shigley (2017) further situate ball joints within kinematic chains, detailing degrees of freedom and constraints essential for foldable systems. Collins (2009) emphasizes fatigue life and corrosion resistance, pointing to material strategies such as PTFE linings or stainless steel for outdoor durability. Mott (2014) expands on lubrication and fatigue concerns, underscoring challenges when scaling precision to architectural sizes. Ball joints therefore distribute stress efficiently and accommodate yaw–pitch rotations, but without additional locking mechanisms, they cannot inherently fix a deployed shell in place, necessitating hybrid systems that combine rotational freedom with friction locks or ratchets.

One-Way Clutch Bearings:
Roller and sprag clutches provide controlled rotation in one direction while restricting the reverse, effectively embedding a passive locking mechanism. Harris (2001) offers a comprehensive review of clutch dynamics and overrunning principles, showing their potential for retractable or transformable systems. Mott (2014) adds torque–speed performance and durability considerations from machine design, relevant to ensuring reliable actuation in wind-exposed deployables. Handoo (2018) directly bridges these principles with architectural case studies, highlighting clutch integration into temporary shelters and deployable shells. Orthwein (2004) complements this with comparative insights on spring-loaded versus centrifugal clutch designs, reinforcing considerations of fail-safe locking. While clutch bearings provide high

precision and robustness, their integration at architectural scale demands careful alignment, housing, and maintenance, raising fabrication and operational challenges.

Comparative Insights :
Taken together, these joinery systems outline a continuum between simplicity and precision. Ratchets provide straightforward locking but introduce wear concerns (Sclater, 2011; Norton, 2020), ball joints offer multi-axis adaptability but lack inherent stability (Shigley et al., 2004; Uicker et al., 2017), and clutch bearings ensure controlled rotation but at the cost of added weight and fabrication complexity (Harris, 2001; Handoo, 2018). As Pellegrino (2001) notes, large-scale deployables often require hybrid solutions that merge the strengths of different joint types to achieve both kinematic freedom and structural stability. For deployable reciprocal shells, the most promising strategy lies not in a single system but in hybridization: bearings for primary rotational control, supplemented by ratchets or friction locks for secondary stabilization.

This synthesis underscores that the study of joinery mechanisms is not purely technical but fundamentally architectural. Joineries must be designed to ensure coherence between structural loads, deployment efficiency, and spatial performance while also meeting architectural imperatives of lightweight construction, reusability, and constructibility. The integration of mechanical principles with architectural contexts, as highlighted across engineering references (e.g., Pahl et al., 2007; Norton, 2020; Collins, 2009) and architectural studies (Handoo, 2018; Pellegrino, 2001), forms the critical foundation upon which this research develops novel joint prototypes for deployable reciprocal shells.

2.2.11 Concluding Synthesis and Research Gaps

The collective literature reveals that deployable systems, auxetic materials, and reciprocal structures have each advanced significantly in their respective domains. Auxetic systems demonstrate unique spatial and mechanical behaviours with negative Poisson's ratios (Evans & Alderson, 2000; Lim, 2015), reciprocal structures offer lightweight modularity and distributed load paths (Veenendaal et al., 2011; Pugnale & Sassone, 2014), and deployable design has generated diverse typologies from kinetic scissor systems to pneumatic inflatables (Pellegrino, 2001; Fenci & Currie, 2017). Despite these advances, research across these domains remains fragmented, with little integration into a unified architectural system capable of structural scalability, load-bearing reliability, and adaptive transformation.

The three precursor works by Jayachandran (2019), Borgström (2021), and Konaković Luković et al. (2016) are pivotal in defining the starting point for this investigation. Jayachandran's thesis proposed the conceptual fusion of reciprocal and auxetic logics but was limited by the absence of computational simulation, detailed joinery design, and real-world stress testing. Borgström demonstrated kagome-based auxetic expansion through kinetic joints but lacked structural integration, load simulations, and multi-material exploration. Konaković Luković's work provided computational breakthroughs in auxetic transformations yet did not extend to mechanical joinery, curved surface applications, or post-deployment load validation. Collectively, these works highlight the promise of combining auxetic principles and deployability but fall short of delivering a comprehensive methodology that spans geometric adaptability, mechanical articulation, and structural resilience at architectural scales.

Beyond these foundational precedents, recurring gaps can be distilled across the wider body of research. Many prior studies emphasize geometry over mechanics, offering little structural or stress analysis to validate real-world performance. Mechanical joinery is often referenced but rarely fabricated, stress-tested, or integrated into scalable assemblies. Prototypes typically remain at small or planar scales, with limited application to curved surfaces or architectural contexts. Motion behaviours are frequently studied qualitatively or through simplified models,

without robust parametric simulation or empirical testing under deployment forces. Materials are often idealized, overlooking fatigue, elasticity, and fabrication constraints. Furthermore, coverage continuity, cross-typology comparisons, and structural behaviour of joints as active load-distributing nodes are either underdeveloped or absent.

This PhD directly addresses these limitations. It introduces SolidWorks and Grasshopper-based simulations to provide both kinematic and structural validation, bridging the computational gap. It advances joint design into engineered typologies (3 physical prototypes) incorporating ratchets, bearings, and angular restrictions tested under real mechanical loads. It scales the Tristar auxetic system across domes, saddles, and other curved geometries, validating rotational behaviour in three dimensions. Motion behaviour is tracked through yaw–pitch simulation frameworks alongside physical prototypes, ensuring accurate mapping of deployment and retraction sequences. Material realism is foregrounded, with spring-loaded steel, 3D-printed components, and tolerance testing replacing purely geometric abstractions. Coverage optimization and structural coherence are examined in intermediate deployment states, while comparative analysis with reciprocal and alternative auxetic systems clarifies relative strengths and limitations.

In synthesizing these efforts, this research develops Deployable Reciprocal Shells through Auxetic Behaviour (DRSTAB), a system that unites reciprocal tessellation, auxetic transformation, and custom joinery into a coherent architectural-scale construction method. By explicitly addressing the shortcomings of prior studies and embedding simulation, material fidelity, and joinery resolution into a single framework, this PhD contributes not just incremental refinements but a new integrative methodology for adaptive, reusable, and structurally robust deployable shells..

Chapter #3

Analyse / Merge / Blend

Reciprocal Analysis

Auxetic Analysis

Hybrid system

3 Chapter 3 – Reciprocal & Auxetic Analysis

Introduction

With the preceding Knowledge from Literatures , we target to find solutions for RQ 1 in this Chapter. The chapter is organized into two principal analytical sections, each employing a rigorous, criteria-based evaluation process. The first section focuses on the geometric and structural analysis of reciprocal tessellations. Reciprocal frames have demonstrated exceptional potential in creating self-supporting structures through their interlocking beam configurations; however, their application in deployable systems requires careful geometric optimization. This research evaluates eight distinct reciprocal tessellations, deconstructing each into fundamental unit geometries to assess their suitability for integration with auxetic systems. The selection process employs four key criteria: (1) geometric simplicity to ensure fabrication feasibility, (2) structural load transfer efficiency across linear, lateral, and angular dimensions, (3) congruence with auxetic pattern kinematics, and (4) minimization of structural weak points and complex joint systems. Crucially, the selected tessellation must demonstrate inherent self-stability through the geometric principles governing reciprocal shells, enabling it to function as the foundational framework for the DRSTAB system , informing data for RQ 1
The second section shifts focus to auxetic materials, which exhibit a negative Poisson's ratio and thus expand laterally when stretched. This unique property offers transformative potential for deployable architectures, but their integration with reciprocal frames demands careful pattern selection. Six auxetic tessellations are shortlisted from an extensive literature review and analysed through both computational modelling and physical prototyping. Laser-cut PET plastic prototypes provide empirical data on deployment behaviour, while finite element simulations validate structural performance under load. The evaluation criteria for auxetic patterns include: (1) kinematic efficiency during deployment phases, (2) maximum achievable expansion ratio, (3) synergy with reciprocal geometry for load transfer, and (4) minimization of stress concentrations at joints. A comparative tabular analysis synthesizes quantitative and qualitative findings, enabling the identification of an optimal auxetic pattern that complements the selected reciprocal tessellation , informing data for RQ 1

The chapter's methodology combines theoretical analysis with empirical validation, creating a robust foundation for the DRSTAB system. By unifying principles from geometric topology, structural mechanics, and material science, this research advances the theoretical understanding of deployable systems while providing practical insights for scalable construction. The findings challenge conventional paradigms in modular architecture by demonstrating how geometric intelligence rather than material mass or complex mechanical systems can drive structural efficiency. Furthermore, the chapter establishes a replicable framework for future research at the intersection of auxetics and reciprocal design, opening new avenues for sustainable, adaptive, and rapidly deployable structures in architectural engineering.

Ultimately, this chapter not only bridges a critical gap in the literature but also provides a methodological blueprint for integrating advanced geometric systems in structural design. The DRSTAB system emerging from this analysis represents a significant step forward in deployable architecture, offering solutions that are simultaneously lightweight, material-efficient, and capable of self-stabilization qualities urgently needed in disaster relief, temporary infrastructure, and sustainable construction contexts. The following sections present the detailed analytical processes and results that underpin these advancements.

3.1 Reciprocal Pattern Analysis

Reciprocal frame (RF) structures have emerged as compelling architectural and structural systems due to their material efficiency, geometric elegance, and modular assembly, making them ideally suited for the deployable shell system under investigation. Pugnale and Sassone (2014) provide a foundational overview of RF typologies, demonstrating their effectiveness in timber roof and pavilion designs through geometric variations that optimize load paths. This structural efficiency is further enhanced by their inherent self-supporting nature, where interlocking beams distribute loads multidirectionally, reducing reliance on complex bracing systems a critical advantage for deployable architectures. Larsen (2008) complements this by detailing modular workflows and joint strategies, highlighting how notched or pinned connections influence scalability and assembly logic. The structural potential of RFs is rigorously explored by Douthe and Baverel (2009), who employ parametric modelling to optimize member angles and lengths, proving that geometric adjustments alone can significantly enhance performance without added material mass. Meanwhile, Veenendaal et al. (2011) push the boundaries of RF adaptability by proposing scissor-like deployable modules, underscoring their suitability for dynamic or temporary structures. Despite these advances, challenges persist in applying RFs to highly curved surfaces, as noted by Song et al. (2013), whose computational tiling methods struggle with irregular geometries. This gap is addressed in the current study through a systematic evaluation of eight RF tessellations, deconstructed at the unit level to assess node behaviour, rotational continuity, and connection logic. Selection criteria prioritize geometric simplicity, structural load transfer efficiency (linear, lateral, and angular), congruence with auxetic kinematics, and minimization of weak points ensuring the chosen configuration aligns with the system's deployability and stability goals. Tang et al. (2013)'s digital design tools further inform this process, enabling iterative testing of planar constraints and edge-length uniformity. By synthesizing these insights, the research advances RF applications in large-span shells, setting the stage for their integration with auxetic tessellations in the DRSTAB system.

Methods: To evaluate and advance RF systems for deployable shell applications, this study adopts a qualitative, analytical methodology centered on CAD-based geometric breakdowns and structural evaluation. The approach examines RF patterns through four critical lenses: Pattern Logic (deconstructing unit geometries to assess node behaviour and rotational continuity), Structural Performance (mapping load paths through support point analysis), Material Constraints (evaluating fabrication feasibility through joint design), and Design Intent (balancing innovation with practical deployability). RF configurations are derived from both planar and non-planar surfaces, then analyzed at the unit level to understand how geometric variations influence assembly sequences, structural flow, and scalability. This method deliberately avoids automated simulations in favor of fundamental geometric analysis, enabling a more intuitive understanding of load transfer mechanisms and their relationship to reciprocal tessellation patterns. The methodology builds upon Tang et al. (2013)'s computational approaches while introducing novel evaluation criteria specifically tailored for auxetic integration, ultimately identifying optimal RF configurations that satisfy both structural stability and deployability requirements for the DRSTAB system.

3.1.1 Shortlisting Geometries: Finding Form Through Logic

The process of shortlisting geometries for a reciprocal structural system, especially within the DRSTAB framework, is a critical step that determines not just the formal outcome, but also the structural performance, material efficiency, and feasibility of fabrication. Given the interdependent nature of reciprocal assemblies, the geometry selected must serve both as a spatial scaffold and a load-bearing mechanism, maintaining stability through its own logic of repetition and overlap.

To arrive at a structurally and visually optimized system, the shortlisted geometries must be evaluated against four essential criteria: simplicity of geometry, structural load transfer principles, overlap compatibility with auxetic tessellation, and number of joints and weak points.

Simplicity of Geometry

Simplicity of geometry plays a foundational role in ensuring constructability and modularity. Geometries that are composed of simple, repeatable units such as equilateral triangles, squares, or regular hexagons reduce fabrication errors, improve assembly speed, and enhance scalability. Simple geometries are also more adaptable to digital fabrication methods, enabling precision and uniformity. For reciprocal systems, which often span large surfaces using repetition, simple geometric forms are essential in achieving consistency and reliability in structural behaviour.

Structural Load Transfer Principles

Structural load transfer is analyzed in three directions linear, lateral, and angular to ensure that each geometry can efficiently handle various types of internal and external forces. In a reciprocal framework, where each element supports and is supported by others, the ability to transfer loads through interlocking elements is fundamental. A geometry that performs well under linear compression may fail under lateral displacement if the angles between members are unstable. Therefore, the selected geometry must exhibit balanced strength and stiffness across all force directions to maintain self-supporting behaviour in the final shell form.

Compatibility with Auxetic Tessellation

One of the key goals of this project is to integrate auxetic logic into reciprocal structures. Therefore, it is essential that the chosen reciprocal geometry aligns well with auxetic tessellations. Auxetic patterns exhibit properties like negative Poisson's ratio and rotational deformation, which can influence the form-finding process and stress distribution in novel ways. Geometries that offer a high degree of overlap or synergy with auxetic units will better facilitate this integration. The goal is to create a composite system in which reciprocal and auxetic behaviours are not just compatible, but mutually reinforcing.

Joints and Weak Points

Every joint in a reciprocal structure is a potential point of stress concentration, misalignment, or failure. As such, minimizing the number of joints, as well as simplifying their geometry, is a crucial factor in selecting suitable patterns. Complex joints may increase the likelihood of construction errors or long-term instability, especially in systems that rely heavily on precise interlocking. Geometries with fewer connection points or those that allow for uniform joint design can dramatically improve the robustness of the entire structure while reducing fabrication time and maintenance requirements.

Overall Geometry as a Strategic Choice

By evaluating geometries through the lenses of simplicity, structural behaviour, compatibility with auxetic patterns, and joint efficiency, this chapter establishes a systematic and evidence-based approach to shortlisting viable options. This shortlisting is not just a technical necessity, but a strategic design decision that impacts every subsequent stage of development from simulation and analysis to fabrication and assembly. The selected geometry must therefore serve as the backbone of the DRSTAB system, balancing innovation and feasibility through intelligent structural logic.

3.1.2 Pattern analysis

Fifteen reciprocal frame patterns (Figure 3.1-1), from Song et al. (2013) were reviewed to identify eight suitable candidates for this study. The team presents an interactive system for generating RF structures on complex surfaces through conformal tiling and joint optimization.

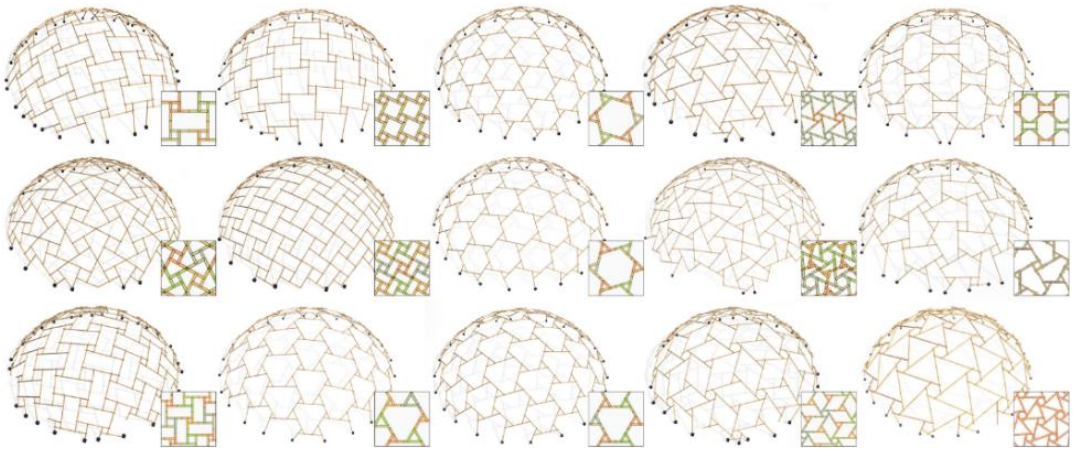

Figure 3.1-1 15 RF-tessellation patterns for designing RF-structures of different appearance.

Note : From, *Reciprocal frame structures made easy* by *Song et al. (2013).*

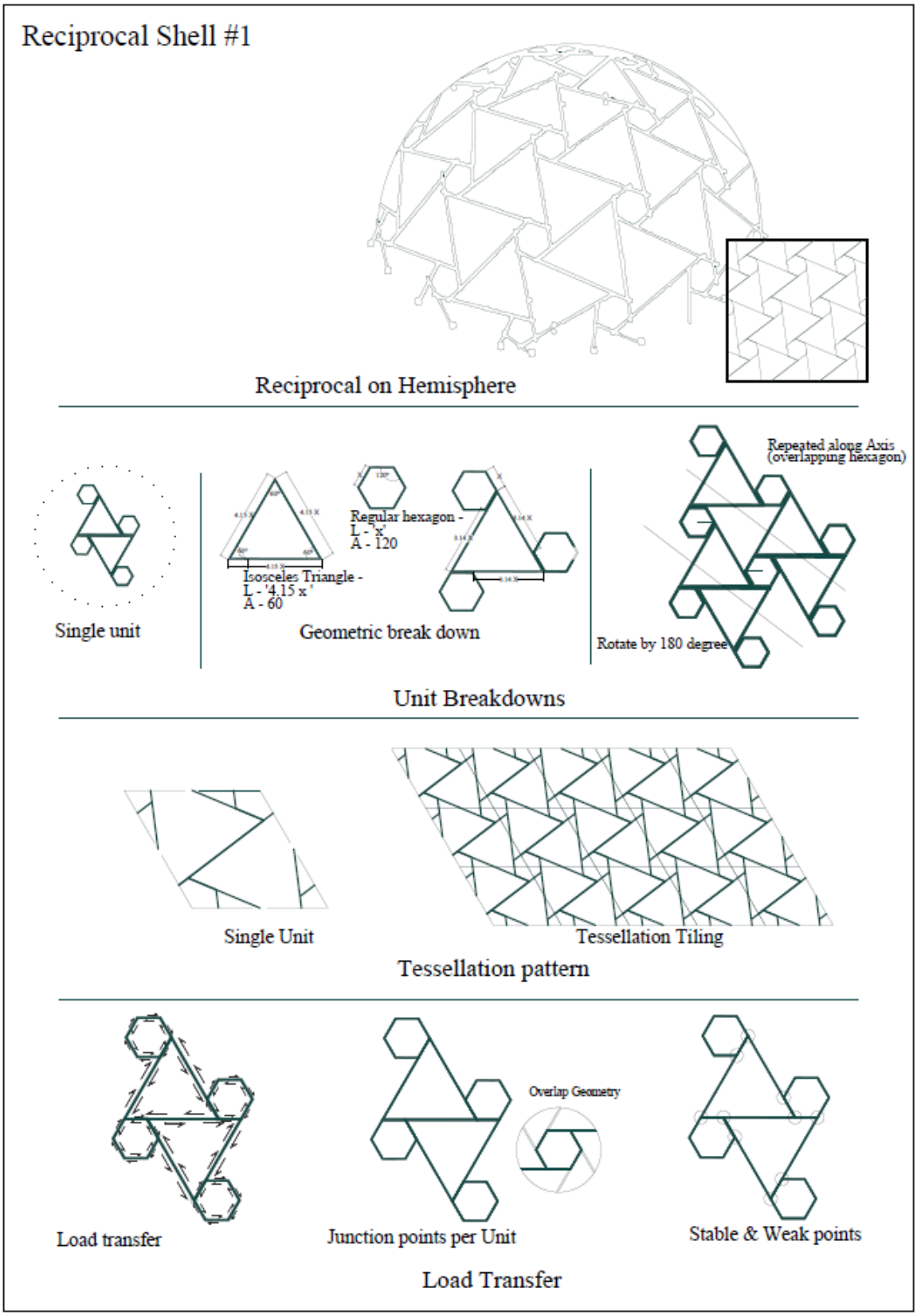

Figure 3.1-2 Reciprocal Analysis breakdown of RF pattern #1

3.1.3 Geometric Breakdown comparison

As presented in Figure 3.1-2 and Appendix A : Reciprocal pattern Analysis , a comparative table (Table 3.1-1) is constructed to systematically evaluate the performance of various reciprocal patterns. The evaluation focuses on critical parameters, including single-unit geometry, overlap geometry, load transfer mechanisms, and the number of weak points within each design. By consolidating these factors into a structured comparison, the table provides a comprehensive overview of the strengths and weaknesses of each pattern. This detailed comparison serves as the basis for drawing meaningful inferences, ultimately aiding in the identification and selection of the most efficient and robust pattern for the given application.

Table 3.1-1 Geometric Breakdown comparison of 8 Reciprocal pattern

Reciprocal Pattern	Single Construction unit	Overlap Geometry	Load Transfer & Weak points	
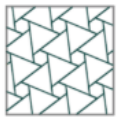			 Load transfer	 No.of Junctions - 10 No.of Weak points - 10
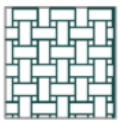			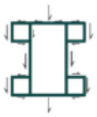 Load transfer	 No.of Junctions - 4 No.of Weak points - 4
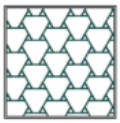			 Load transfer	 No.of Junctions - 6 No.of Weak points - 6
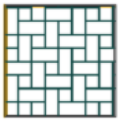			 Load transfer	 No.of Junctions - 4 No.of Weak points - 4
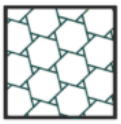			 Load transfer	 No.of Junctions - 3 No.of Weak points - 3
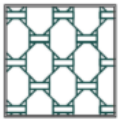			 Load transfer	 No.of Junctions - 12 No.of Weak points - 12
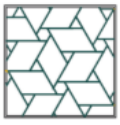			 Load transfer	 No.of Junctions - 4 No.of Weak points - 4
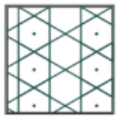			 Load transfer	 No.of Junctions - 3 No.of Weak points - 3

3.1.4 Inferences from Reciprocal Geometrical breakdown

Optimality of Triangle and Hexagon-Based Reciprocal Geometries

Breaking down from the evaluation of eight reciprocal shell tessellations (Table 3.1-1) has revealed that triangle- and hexagon-based reciprocal units offer the most coherent and compatible structural foundation for integration with auxetic systems, particularly within the DRSTAB framework. This is not a single pattern evaluation but the base construction geometry of the patterns. Each of the four evaluation criteria geometry simplicity, structural load transfer, congruence with auxetic patterns, and joint optimization highlights the strategic advantages of these geometries.

Simplicity of Unit Geometry

Triangle and hexagon based tessellations rank good in geometric simplicity, a critical factor for constructability, replication, and transformation in deployable systems. The triangle, with only three edges and three vertices, forms the simplest polygon in Euclidean geometry, enabling straightforward structural interpretation and fabrication. The hexagon, composed of six equilateral triangles, provides a second layer of regularity while expanding the potential for curvature mapping and panelization. Importantly, the triangular tessellations (3-fold and 6-fold symmetry) reduce geometric ambiguity, thus simplifying reciprocal logic and allowing clean rotational relationships between elements.

S**tructural Load Transfer Efficiency**

From a structural standpoint, both triangles and hexagons support highly efficient diagonal and lattice-based load transfer mechanisms. In reciprocal frames, the nodal connections of triangles inherently follow isostatic principles, distributing forces with minimal redundancy. Hexagonal units, derived from tessellated triangular networks, operate through a lattice transfer model wherein axial and diagonal components distribute compressive and tensile forces through interlaced nodes. The governing load path can be described using equilibrium of force vectors , where each member in the reciprocal pattern contributes to a balanced system of forces acting diagonally through the grid. This lattice-style transfer allows local stress concentrations, especially at overlapping joints, to be diffused through neighboring units, offering both resilience and redundancy without requiring over-design.

Minimization and Optimization of Joints and Weak Points

Although triangle and hexagon units typically feature six joints per module, which may initially suggest increased vulnerability, the distribution of load through these joints is inherently optimized through geometric interdependence. In reciprocal assemblies, loads introduced at weak nodes are efficiently rerouted diagonally and axially through neighboring tessellations. This redistribution effect, when combined with the naturally stable geometry of triangles and the tiling efficiency of hexagons, results in a system where local weaknesses do not propagate into global failure, thereby enhancing the structural robustness of the shell.

Congruence with Auxetic Tessellations

Geometrically, triangle and hexagon-based reciprocals demonstrate strong congruence with tristar-type auxetic patterns, which operate on rotating triangle units and generate hexagonal voids during expansion. This morphogenetic alignment ensures that both systems reciprocal and auxetic share not just aesthetic similarities but kinematic compatibility. The rotational expansion in auxetics mirrors the angular deformation permissible in triangular reciprocals, thereby enabling synchronized deformation during deployment. This allows the DRSTAB

framework to capitalize on the auxetic-driven expansion ratio while maintaining reciprocal frame logic for structural stability.

Together, these inferences make a compelling case for selecting triangle and hexagon-based reciprocal geometries as the foundational units for DRSTAB. They not only meet the critical performance criteria but also synergize structurally and kinematically with the most compatible auxetic patterns offering a unified, deployable solution that is simple, strong, and smartly adaptive.

3.2 Auxetic Pattern analysis

Chapter 3.2 documents an early exploratory phase, which focuses on identifying, classifying, and empirically testing a range of auxetic geometries to determine their suitability for architectural-scale deployment. This analytical stage forms the bridge between conceptual selection and practical validation, laying the foundation for the subsequent simulation and physical prototyping phases in later chapters.

The study of auxetic structures, materials that exhibit a negative Poisson's ratio, has attracted increasing attention across disciplines for their distinctive mechanical behavior particularly their ability to expand laterally when stretched. While earlier sections established a compelling case for focusing on triangular and hexagonal-based systems due to their geometric compatibility with deployable frameworks, the next logical step involves evaluating how these and other geometries actually perform as auxetic mechanisms.

To begin, a comprehensive classification of auxetic geometries was undertaken, cataloguing a wide range of established patterns from literature including re-entrant hexagons, rotating squares, chiral units, and arrowhead configurations each exhibiting distinct deformation logics. From this broad catalogue, six geometries were shortlisted for closer examination, based on their reported performance, geometric adaptability, and potential integration with reciprocal frameworks.

Each shortlisted pattern was then evaluated through a two-step process: first via digital CAD breakdown to observe deformation behavior, and subsequently through laser-cut PET prototypes to assess physical feasibility, rotational limits, and deformation continuity. This subchapter therefore provides an in-depth comparative analysis of these six patterns, supported by visual data, tabular evaluation, and critical reflection.

The aim is to determine which auxetic configuration demonstrates the most balanced combination of structural stability and kinematic flexibility for integration into the Reciprocal system. In doing so, this section transitions the research from theoretical classification toward empirically grounded pattern selection, reinforcing the iterative process that underpins the development of the final deployable shell system.

3.2.1 Classifications of Auxetic from Literature

The classification of auxetic systems in architectural and engineering literature has evolved from a narrow focus on cellular geometries to a broader understanding of structural and material behaviours. Early studies primarily categorized auxetics through their negative Poisson's ratio, identifying re-entrant honeycombs and chiral lattices as fundamental typologies (Evans, 1991; Lakes, 1987). Subsequent research expanded these categories to include rotating unit mechanisms, foldable tessellations, and origami-inspired systems, highlighting the diversity of deformation pathways that can produce auxetic effects (Grima & Evans, 2000; Prat et al., 2015). More recent architectural investigations emphasize

classifications that account for both kinematic and material dimensions, distinguishing between geometrically programmed auxetics, material-driven auxetics, and hybrid systems that integrate deployability or reciprocal logic (Borgström, 2021; Jayachandran, 2019; Konaković Luković et al., 2016). This growing body of work demonstrates that auxetic behaviour is not confined to microstructural lattices but can be deliberately scaled into architectural systems, providing a useful framework for the present study. Table 3.1-1 shows the Classifications of Auxetic Structures/ patterns

Full pictorial exploration of typologies of Auxetic patterns is exhibited in Appendix B : Classification Of Auxetics from Literature

Table 3.2-1 Wider Classifications of Auxetic Structures/ patterns

Typology	Subcategories / variants
Re-entrant Geometries	Re-entrant honeycomb, arrowhead, star-shaped, missing-rib, double-arrowhead
Rotating Units	Rotating squares, rectangles, triangles, rhombi, parallelograms, rigid unit cells
Chiral Structures	Hexachiral, tetrachiral, anti-chiral, bi-chiral lattices
Origami-Based	Miura-ori, Ron Resch pattern, waterbomb base, Kresling pattern, Tachi fold
Perforated Sheets	Diamond-cut sheets, circular cut patterns, star-shaped cuts, hierarchical perforations
Tensegrity Structures	Re-entrant tensegrity prism (T3-prism), tensegrity-based auxetic lattices
3D Auxetic Networks	Cubic auxetics, tetrahedral re-entrant frameworks, 3D rotating cube networks
Composite/Hybrid	Mixed-mode chiral–re-entrant, rotating–origami hybrids, hierarchical layered auxetic systems
Advanced Metastructures	Foldable kirigami-based auxetics, programmable mechanical metamaterials, auxetic origami tubes

Each of these types was visualized through annotated diagrams and image references from existing literature. The classification helped in identifying how different structures respond to stress, especially in two-dimensional and three-dimensional applications. Visual diagrams were prepared for each pattern, demonstrating their expansion behaviour when force is applied. This provided insight into the functional versatility and potential structural integrity of each geometry under architectural conditions.

This preliminary classification was crucial in highlighting which designs had higher movement range, angular adaptability, and consistent mechanical performance across deployment stages. It also revealed geometries that might be limited by stress concentration or restricted rotation, guiding the selection process for the next stage. By laying out this visual taxonomy, the research establishes a comprehensive reference point for all future explorations in auxetic design strategies.

This study selects six representative auxetic patterns one or two from each major category to assess their geometric behaviour and structural relevance when adapted into the DRSTAB (Deployable Reciprocal Structural System with Tension-Activated Behaviour) framework. The selected patterns are evaluated based on their compatibility with reciprocal logic, transformation potential, and structural performance at the unit level.

3.2.2 Shortlisting and Analysis of Auxetic Geometries

From the comprehensive classification, six auxetic patterns were selected for detailed analysis and prototyping. The selection criteria were based on documented performance in peer-reviewed studies, adaptability to different surface curvatures, and their potential for integration with mechanical joineries. The six shortlisted geometries are:

- Re-entrant honeycomb
- Rotating squares/ rectangle
- Rotating triangles – Tristar pattern
- Bilateral Rotating Square Auxetic
- Bilateral Rotating triangle Auxetic
- Rotating triangles – Variation 2

Each of these patterns showed unique mechanical properties ranging from high rotational flexibility to controlled directional expansion. The shortlisted designs were considered most promising for architectural applications that demand not only deployability but also strength and consistency in movement. Literature support for each was documented, noting key parameters such as force distribution, folding ratio, and Poisson's ratio.
This shortlisting acts as a design filter, focusing resources on patterns with real-world relevance and mechanical feasibility. The balance between theoretical potential and practical constructability informed this decision, bridging the gap between design ambition and material reality. This stage acts as a crucial funnel in the broader research methodology, allowing deeper investigation into high-potential candidates through simulation and physical modelling.

Analysis Criteria for the Shortlisted Geometries

Each of the six shortlisted auxetic patterns was recreated digitally using CAD tools to simulate their deployment behaviour. This stage was critical in understanding how these geometries would perform under theoretical conditions before investing in physical prototyping. Each pattern was modelled in a flat state and visualized through a AutoCAD drawings
To effectively evaluate the architectural and structural performance of the six shortlisted auxetic geometries, a set of analytical criteria was established. These criteria were designed to provide a holistic understanding of how each pattern behaves both functionally and structurally within deployable systems. The evaluation focuses on five main aspects: simplicity of geometry, structural load transfer principles (linear, lateral, and angular), simplicity in movement during deployment, overlap potential with reciprocal tessellation logic, and the number of joints and weak points present in each pattern.

3.2.2.1 Simplicity of Geometry

Simplicity in geometric form is crucial for both the design and manufacturing phases of an auxetic system. A simpler geometry is easier to draw, model, and parametrize digitally, which directly contributes to the speed and efficiency of iterative design processes. From a fabrication standpoint, uncomplicated shapes are more compatible with standard tools such as laser cutters, CNC routers, or 3D printers. Simpler geometries also tend to require less material, reducing overall costs and environmental footprint. In deployable or adaptive systems, geometric simplicity allows for more predictable and controllable movement during actuation. Furthermore, clear, understandable forms aid in communication across interdisciplinary teams, which is especially important in architecture and engineering collaborations. When a geometry is overly complex, it can introduce uncertainties in how forces behave, complicate assembly, and limit scalability. Therefore, evaluating the simplicity

of an auxetic geometry is a foundational step in determining its viability in real-world architectural applications where clarity, efficiency, and precision are essential.

3.2.2.2 Structural Load Transfer (Linear, Lateral, Angular)

Understanding how a geometry transfers structural loads is essential in determining its functional performance in architectural systems. Auxetic geometries can behave in non-intuitive ways under stress, and their effectiveness often hinges on how forces are distributed and redirected through their form. Analysing load transfer be it linear (axial), lateral (shear), or angular (torsion or moment) helps identify whether a pattern can handle expected loads such as wind, tension, or human interaction without deformation or failure. Some patterns naturally excel at dispersing loads evenly across a surface, while others may concentrate stress at specific joints or corners, making them vulnerable. In adaptive structures, where form changes dynamically, it's especially important to understand how structural behaviour evolves during movement. A pattern that supports efficient load transfer can be scaled up safely, applied to diverse surfaces, or incorporated into kinetic facades and lightweight structures. Without this analysis, a geometry might be aesthetically promising but structurally inadequate. Therefore, evaluating load pathways ensures that the design is not only creative but also structurally sound.

3.2.2.3 Simplicity in Movement When Deployed

The effectiveness of an auxetic pattern often depends on how it behaves during deployment when it expands, contracts, or responds to external stimuli. Simplicity in this movement is essential for ensuring smooth and reliable performance. Patterns that require fewer moving parts or synchronized motions are more likely to be durable and easier to control. Complex or uncoordinated movement can cause binding, friction, or mechanical failure, especially when scaled for architectural applications. Additionally, simple movement paths are easier to simulate and prototype, allowing for more accurate predictions of performance under varying loads or conditions. From a practical perspective, movement simplicity reduces wear and tear, minimizes energy required for actuation (especially important for kinetic architecture), and ensures consistent behaviour over time. In contexts like responsive façades or temporary pavilions, predictability and repeatability of movement are essential. By evaluating how easily and elegantly a geometry deploys, designers can better assess its suitability for dynamic and adaptive design scenarios. Therefore, this criterion is not just about kinematics it's central to reliability, longevity, and user interaction.

3.2.2.4 Best Overlap with Reciprocal Tessellation

Analysing how well an auxetic pattern overlaps with reciprocal tessellation helps determine its potential for integration into modular and large-scale architectural systems. Reciprocal tessellation refers to the ability of a pattern to repeat seamlessly and form structurally interdependent networks key for designing panels, façades, or spatial frameworks. A pattern that tessellates well supports load-sharing between units, improving overall structural performance and material efficiency. It also allows for easy expansion or contraction of systems without disrupting the overall geometry. When combined with auxetic behaviour, reciprocal tessellation can result in responsive surfaces that are both dynamic and structurally resilient. Evaluating this compatibility also aids in fabrication and assembly, as modular repeating units can be manufactured in masse with standardized joints. Conversely, patterns that do not tessellate cleanly can lead to irregularities, weak zones, or difficulty in adapting to curved or non-uniform surfaces. Thus, the degree to which a geometry fits into a reciprocal system informs its feasibility for architectural implementation and helps optimize both aesthetics and function.

3.2.2.5 Number of Joints & Weak Points

The number of joints and potential weak points in an auxetic geometry plays a major role in determining its durability and long-term performance. Each joint represents a potential site of mechanical stress, friction, or failure particularly in deployable or load-bearing structures. An excess of joints can complicate fabrication, increase assembly time, and introduce tolerances that reduce precision. Furthermore, joints often need to accommodate movement, which adds mechanical demands like flexibility, rotation, or elasticity. Weak points, such as thin connectors or high-stress concentration zones, can lead to material fatigue or breakage, especially under repeated loading cycles. By analysing how many joints and vulnerable zones a pattern has, designers can make informed choices about material selection, joint reinforcement, and the overall reliability of the system. Reducing the number of weak points without compromising functionality improves the safety, longevity, and maintenance of an auxetic-based architectural component. In essence, this analysis provides insight into a pattern's resilience and its readiness for real-world application beyond the lab or prototype scale.

By analysing each geometry through these lenses, a clearer picture emerges of which auxetic patterns hold the greatest promise for integration into architectural systems, particularly in contexts demanding both mechanical adaptability and aesthetic performance.

These digital tests offered valuable predictive insights, allowing for early detection of design issues such as locking joints or limited rotation. Moreover, they helped visualize how each pattern interacts with external forces, such as tension and compression. This data informed the decision to proceed to physical prototypes for validation. By combining visual output with simulation data, this stage provided a critical feedback loop in the design iteration cycle.

3.2.3 Geometric Analysis

This study selects six representative auxetic patterns possibly from each major category to assess their geometric behaviour. The shortlisting of best 6 is based on their simplicity in geometry or fabrication ease (with mechanical joinery) that play a major role for later research. The patterns that did not make the top six are excluded either for their complexity in geometry, inability to tesselate or might need a alternative method of fabrication. The selected patterns are in depth evaluated from, Figure 3.2-1 , Figure 3.2-2 and Appendix C : Auxetic Pattern Analysis ,based on their (1) simplicity of unit geometry, (2) structural load transfer (linear, lateral, angular), (3) kinematic efficiency during deployment, (4) maximum expansion ratio, and (5) synergy with reciprocal frameworks while minimizing weak points

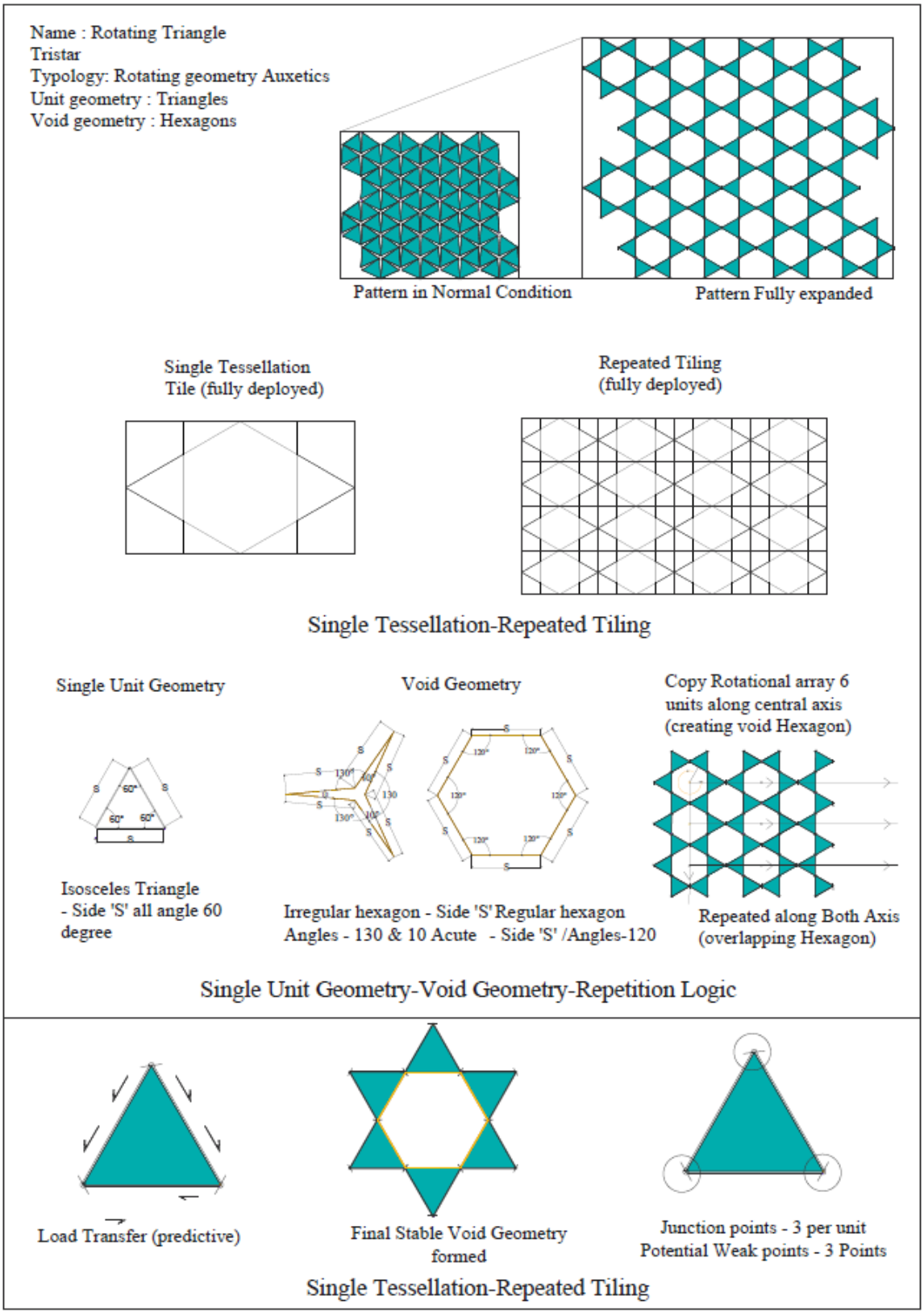

Figure 3.2-1 Auxetic Analysis of Rotating triangle- tristar auxetics

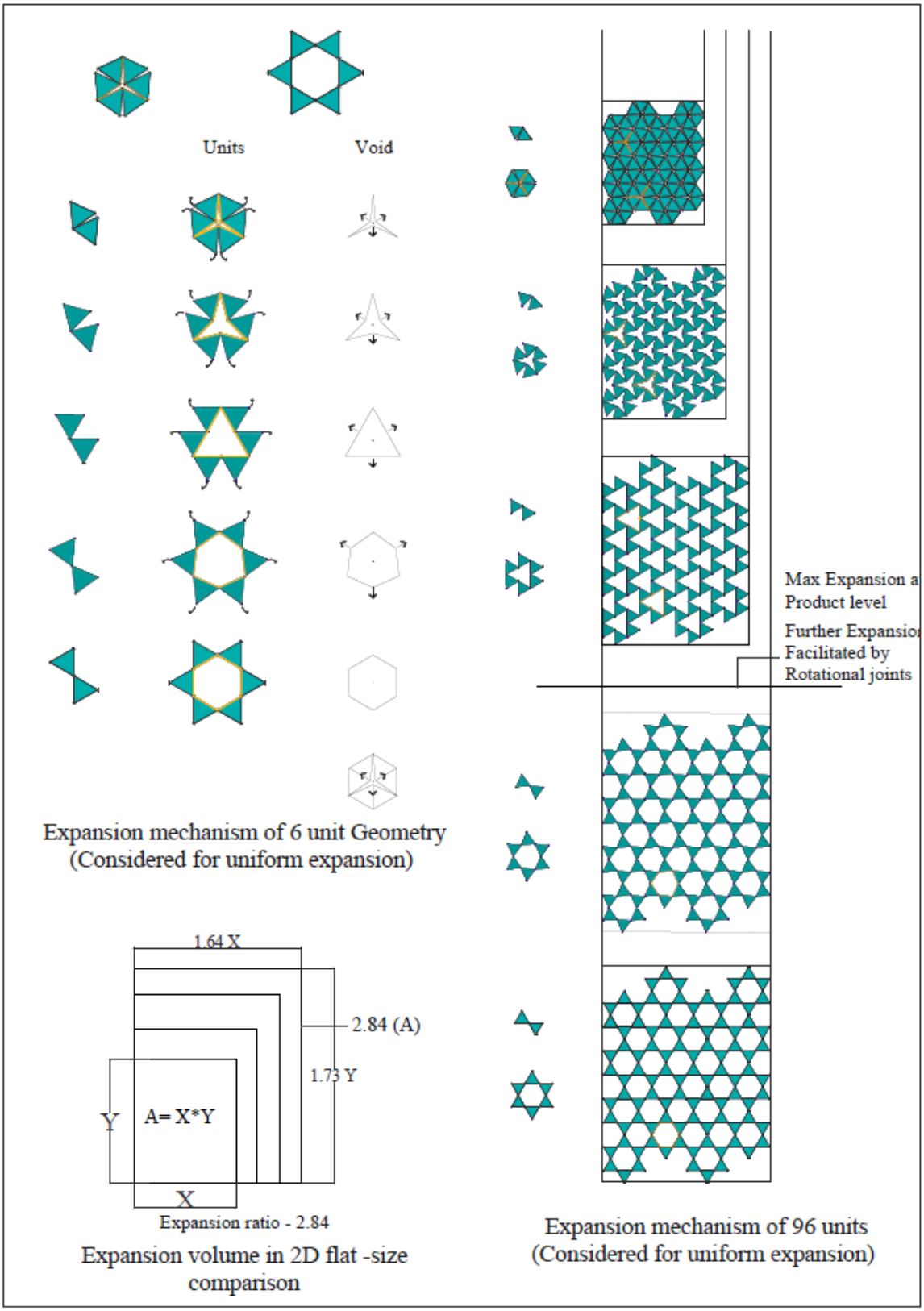

Figure 3.2-2 Auxetic Analysis of Rotating triangle- tristar auxetics

3.2.3.1 Auxetic Analysis comparison

As presented above from , Figure 3.2-1 , Figure 3.2-2 and Appendix C : Auxetic Pattern Analysis , a comparative table (Table 3.2 2) has been developed to evaluate various auxetic patterns. This evaluation considers key parameters, including single-unit geometry, void geometry, load transfer mechanisms, expansion ratio, repetition principles, and the number of weak points .The Table provides a systematic comparison of these factors, enabling a comprehensive assessment of the patterns.

Table 3.2-2 Geometric Breakdown comparison of 6 Auxetic patterns

Auxetic Tessellation- Name and Pattern	Unit Geometry	Void geometry - for stability	Load transfer & Joints / Weak points
Rotating Triangle 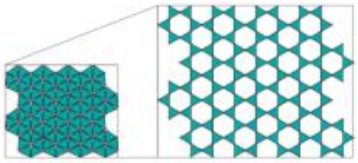		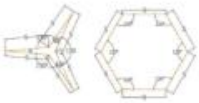	 Junction points - 3 per unit Potential Weak points - 3 Points
Rotating Rectangle 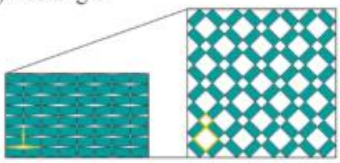		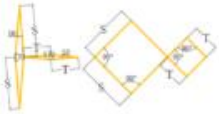	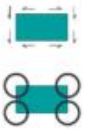 Junction points - 4 per unit Potential Weak points - 4 Points
Reentrant honey comb - mechanical 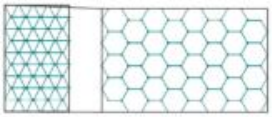			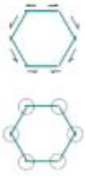 Junction points - 6 per unit Potential Weak points - 6 Points
Bilteral rotating square auxetic 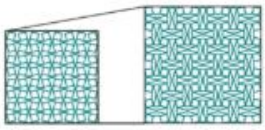			 Junction points - 16 per unit Potential Weak points - 16 Points
Bilteral rotating triangle auxetic 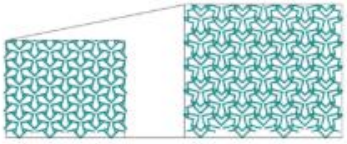			 Junction points - 27 on 7 geometries Potential Weak points - 27 Points
Rotating triangle 2 - Quadrilateral & Hexagon joinery 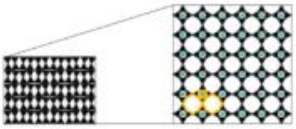			 Junction points - 3 per unit Potential Weak points - 3 Points

Based on the comparative analysis of six auxetic patterns in Table 3.2-2 , the rotating triangle–tristar auxetic geometry emerges as the most suitable candidate for integration into the

DRSTAB system. This pattern demonstrates optimal alignment with all five evaluation criteria established earlier: (1) it offers the simplest unit geometry, relying on equilateral triangles; (2) the structure supports efficient load transfer across linear, lateral, and angular axes due to its rotational symmetry and nodal connectivity; (3) the kinematic behaviour defined by coordinated rotational movements and consistent bending angles ensures predictable and smooth deployment; (4) among the patterns assessed, it exhibits the highest expansion ratio, enabling significant transformation from a compact to an expanded state; and (5) it shows clear geometric synergy with reciprocal frames, particularly through shared motifs of triangles and hexagons, enhancing structural compatibility and reducing weak points at junctions. Furthermore, the void geometry formed during deployment is hexagonal, aligning with established reciprocal forms known for stability. This overlap not only simplifies joint design but also improves material efficiency and assembly logic. Given these advantages, the rotating triangle–tristar auxetic pattern represents the most structurally and geometrically coherent solution for advancing the DRSTAB system and is therefore selected as the primary focus for further development

3.2.4 Laser-Cut PET Prototypes of Each Geometrical pattern

To validate the digital findings, physical prototypes were fabricated using laser-cut PETG plastic sheets. Each of the six geometries was translated into a flat 2D pattern and then cut into scalable units to explore their actual behaviour under physical manipulation. The use of PETG allowed for transparency and sufficient flexibility, offering a closer approximation of real-world behaviour without expensive materials. The base is a simple Hemispherical ellipsoid that was 3D printed so the Auxetic lasercut can take the form. To overlay we have used PETG sheet with 0.25 mm thickness in the size A4 size sheets.

Assembly of the units followed a standardized method to ensure consistency across all prototypes. Observations from Figure 3.2-13 to Figure 3.2-17, included how the joints moved, the range of flexibility, and whether the structures held their shape or collapsed under minor loads. These tactile insights added a new dimension to the design evaluation, especially in understanding snap points or areas prone to failure.

Tristar – Rotating Triangle

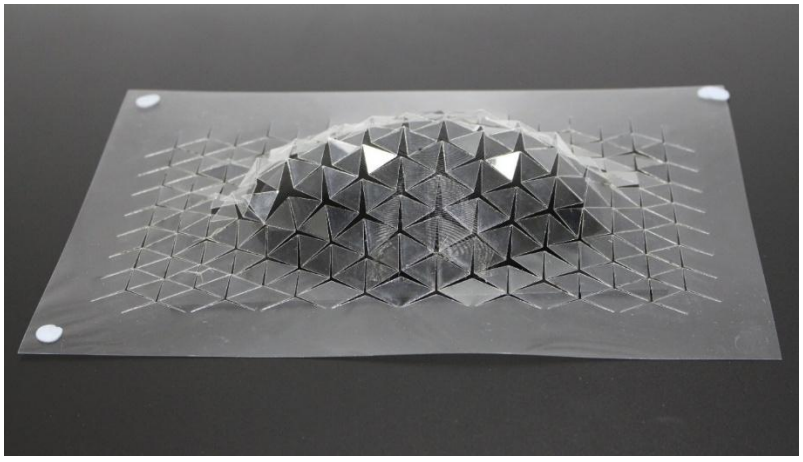

Figure 3.2-3 PETG- Lasercut trial of Tristar Auxetic on Ellipsoid Dome Flat lasercut , laid on dome , dome removed

Rotating rectangles

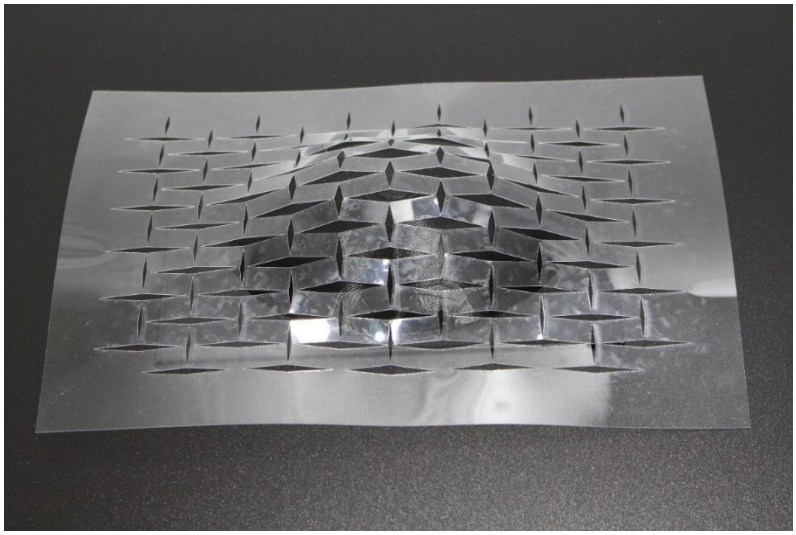

Figure 3.2-4 PETG- Lasercut trial of Rotating rectangle Auxetic on Ellipsoid Dome Flat lasercut , laid on dome , dome removed

Bilateral Rotating Square

Figure 3.2-5 PETG- Lasercut trial of Rotating Square Auxetic on Ellipsoid Dome , laid on dome , dome removed

Bilateral Rotating triangle

Figure 3.2-6 Lasercut trial of Rotating triangle Auxetic on Ellipsoid Dome , laid on dome , dome removed

Rotating Triangle 2

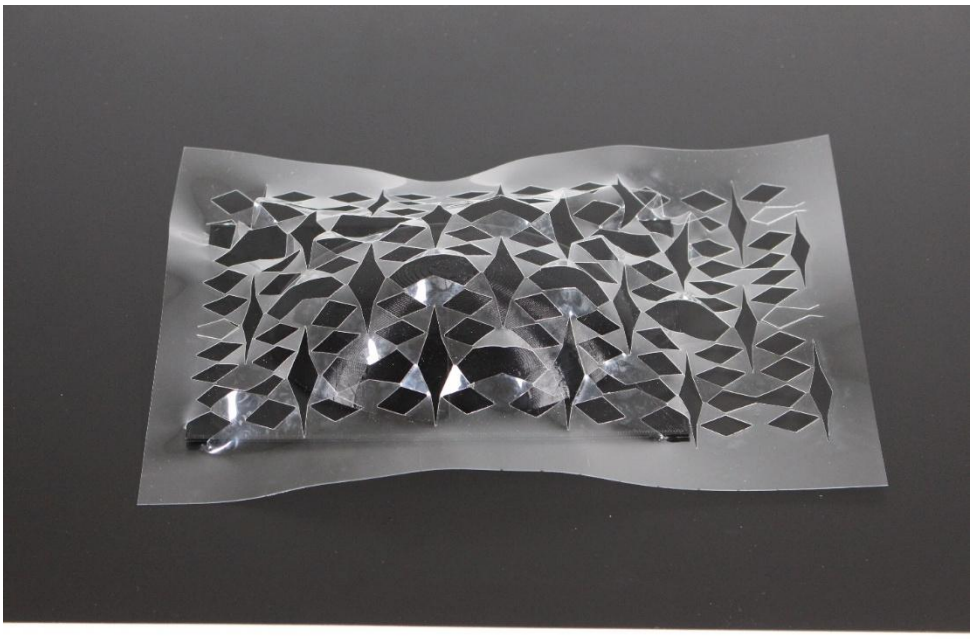

Figure 3.2-7 Lasercut trial of Rotating triangle Auxetic on Ellipsoid Dome , laid on dome , dome removed

Complete set of photo documentation of PETG on Auxetics explored in Appendix D : Laser-Cut PET Prototypes of Each Geometry

3.2.5 Overall Inferences of Auxetic Study

Building on the earlier findings from Table 3.2-2, physical testing confirmed the tristar pattern's superior adaptability, structural coherence, and deployability when mapped onto curved surfaces. The re-entrant honeycomb was excluded due to fabrication limitations in laser cutting. While the tristar pattern performed well, some of the PETG prototypes exhibited undesired outcomes due to the physical limitations of the material itself. In particular, the tristar geometry faced restrictions at the product level limiting the rotational angle to a maximum of 60 degrees. Beyond this point, the material resisted further movement, compromising the full auxetic behaviour. To achieve maximum and optimal expansion, mechanical joinery or assisted articulation would be required beyond the 60-degree threshold. Overall, the rotating triangle–tristar pattern presents the most promising foundation for further development of the DRSTAB system .

Interestingly, some geometries that performed well in simulation like the bowtie pattern (Figure 3.2-17) revealed instability in physical form, whereas simpler models like rotating squares (Figure 3.2-15) maintained better control and predictability. The physical prototyping reinforced the importance of combining virtual simulations with material reality to accurately gauge design feasibility. These models served not only as functional tests but also as communication tools during peer review and stakeholder discussions.

3.3 Summary of Chapter 3

This chapter has conducted a comprehensive analytical investigation into the geometric and structural potentials of reciprocal tessellations and auxetic patterns, with the goal of establishing a unified deployable system. Through a rigorously defined, criteria-based evaluation process, the study has demonstrated how geometric logic applied systematically across both reciprocal and auxetic domains can drive performance, adaptability, and scalability in deployable architectural frameworks.

In the first section, reciprocal frame structures were deconstructed into eight distinct tessellation strategies. Each was evaluated across four critical parameters: geometric simplicity, structural load transfer efficiency, compatibility with auxetic mechanisms, and minimization of weak points. The results confirmed the significant architectural value of reciprocal geometry particularly in its ability to generate self-supporting forms through pure structural interdependence. Among the candidates, reciprocal tessellations emphasizing triangular and hexagonal units displayed superior performance, particularly in their ability to align naturally with stable geometric motifs and distribute load along diagonal and axial paths. These patterns not only satisfied the fundamental requirement of self-stability but also offered the greatest promise for integration with auxetic mechanisms due to their modularity and connection density.

In the second section, auxetic patterns were investigated for their unique deformation behaviour, structural flexibility, and potential to facilitate controlled expansion within a reciprocal shell system. Six auxetic configurations were shortlisted from existing research, then modelled parametrically and fabricated using laser-cut PETG prototypes to observe real-world behaviour. Each pattern was evaluated against four primary criteria: deployability (kinematic efficiency), expansion capability, congruence with reciprocal systems, and stress performance at joints. Finite element analysis and physical observations further refined these assessments, offering a dual validation loop between computational logic and empirical behaviour.

Through this comparative framework, the Tristar auxetic pattern emerged as the most promising candidate for integration with the selected reciprocal tessellation. This pattern

demonstrated exceptional performance across all evaluation categories. Its geometric configuration, built from equilateral triangular units, offers inherent simplicity and symmetry, making it highly compatible with reciprocal assemblies composed of triangular and hexagonal base geometries. Its rotational mechanism allows for both radial expansion and lateral displacement, mimicking the behaviour of scissor mechanisms while maintaining geometric coherence. Structurally, it supports directional load paths and displays minimal localized stress under expansion, aided by the inherent triangulation of its form. Critically, the voids created during its deformation adopt hexagonal geometries mirroring the motifs used in the best-performing reciprocal patterns and reinforcing the synergy between the two systems.

Despite its strengths, the Tristar pattern as tested in this study revealed a key limitation: the constraints imposed by material-based rotation. Specifically, the laser-cut PETG prototypes were restricted to a maximum yaw rotation of approximately 60 degrees, well below the ideal expansion threshold of 120 degrees identified in digital simulations. This product-level constraint compromises the full expressive potential of the pattern, especially when mapped onto more extreme curvature conditions in 3D forms. Furthermore, pitch rotation critical for conformal mapping onto double-curved shells was found to be unstable beyond 30 degrees in physical models, emphasizing the need for a more controlled and responsive mechanism.

To address these constraints, the research proposes a customized mechanical enhancement of the Tristar pattern. By introducing engineered rotational joints, it becomes possible to achieve controlled yaw and pitch rotation beyond the physical limitations of the laser-cut material. This hybridization where geometric patterning is supplemented with mechanical articulation forms the basis for the next stage of investigation. Such enhancements not only enable the full deployment capacity envisioned in simulations but also ensure that structural integrity is maintained throughout the transformation process.

Chapter 4 builds directly on the conclusions drawn here. The next phase of research will focus on the detailed analysis of the Tristar pattern's movement in three-dimensional space, examining how it behaves under combined pitch, yaw, and roll transformations. Through a combination of parametric modelling, Grasshopper-based scripting, and simulation via physics engines such as Kangaroo and SolidWorks, the angular behaviour of the units will be analyzed in relation to curvature radius, deployment speed, and node stability. Importantly, this chapter will also consider conformal mapping strategies, exploring how the Tristar system can be wrapped across non-developable surfaces using adaptive movement logic. This will include both bottom-up (ground-based pushing) and top-down (gravity-based dropping) deployment simulations to test responsiveness under varied constraints.

The chapter also presents the development and testing of a physical prototype system equipped with customized mechanical joints, designed to replicate and extend the simulated behaviours. These prototypes will be assessed for their capacity to accommodate both expansion and contraction across curved surfaces. Attention will be given to mechanical joint design, including the introduction of unidirectional ratchets and reverse-locking mechanisms that regulate movement without introducing additional mass or friction. Experimental data from the prototypes will then be used to refine digital models and finalize the criteria for full-system integration.

Porgressing further , Chapter 4 represents the transition from geometric selection to mechanical realization. It will take the optimal pattern identified in this chapter and push it beyond conceptual modelling into a working, scalable, and responsive deployable component. This progression is essential for validating the DRSTAB system not merely as a theoretical construct but as a real-world solution with material feasibility and architectural relevance.

This chapter has laid the analytical and methodological groundwork for that progression. By demonstrating the reciprocal-auxetic synergy and identifying a high-performing, adaptable pattern, it has both advanced the theoretical discourse and grounded it in practice. The findings presented here challenge the prevailing dependency on rigid material assemblies and complex mechanical frameworks in deployable systems. Instead, they promote a paradigm where geometry is the driver of adaptability, and movement is embedded in the pattern itself, requiring only minimal external control.

As architectural challenges increasingly demand structures that are lightweight, adaptive, and deployable especially in the context of disaster relief, temporary housing, and low-resource environments the integration of reciprocal and auxetic systems holds immense potential. The DRSTAB framework, as it continues to evolve, stands at the intersection of geometric intelligence and structural necessity, offering a new vocabulary for architectural engineering rooted in pattern, precision, performance.

Chapter #4

Script / Simulate / Prototype

Movement Analysis

Scripting & Simulation

Scaled Prototypes & Validation

4 Chapter 4 – Digital Simulation & Scaled prototypes

4.1 Introduction

Building upon the geometric selection and analytical evaluation established in the previous chapter, this stage of the research transitions from comparative analysis to applied performance testing of the Tristar auxetic pattern.This chapter tries to find solutions for RQ 2 While Chapter 3 identified the Tristar configuration as the optimal candidate for integration with reciprocal systems, the need for mechanical augmentation was evident, particularly due to limitations observed in material-based prototypes. Chapter 4 focuses on understanding how this pattern behaves dynamically in three-dimensional contexts how it moves, expands, and conforms under deployment when influenced by both curvature and mechanical constraints.

The study begins by analysing the detailed movement behaviour of the Tristar units at multiple scales. It investigates how the rotational logic both yaw and pitch propagates across individual triangles and aggregated assemblies of 6 to 32 units. By breaking down the geometry into its rotational axes, the research identifies the thresholds for safe movement: yaw rotation peaks at 120 degrees, while pitch is most reliable up to 30 degrees. These parameters are critical in maintaining stability when the pattern transitions from a flat state to a fully expanded double-curved form. Particular attention is given to how nodal rotation and expansion ratios shift under differing conditions, and how curvature affects angular offsets across connected joints. This detailed kinematic insight forms the foundation for joint design and informs later stages of testing.

The movement logic is embedded and tested within a digital environment using parametric modelling in Rhinoceros 3D and Grasshopper. Simulation tools such as Kangaroo are employed to introduce physics-based behaviour, allowing the pattern to respond to real-time constraints such as force, gravity, and surface curvature. These simulations test the adaptability of the Tristar system when projected onto convex, concave, and saddle surfaces, revealing how the geometry deforms under transformation. Computational tracking of angle deviation, overlap zones, and node displacement provides quantifiable data to evaluate performance across various configurations. These results not only reinforce the theoretical assumptions but also highlight issues such as joint collision and rotation misalignment that would otherwise be difficult to detect prior to fabrication.

To validate the findings from the simulations, a 1:5 scale physical prototype of the Tristar pattern was fabricated using laser-cut PETG triangles, laminated acrylic reinforcements, and embedded mechanical joints. The prototype is designed to replicate the rotation constraints identified in the digital model, with components engineered to allow controlled yaw and pitch movement. Mounted on a base representing a curved shell surface, the prototype is deployed manually using a bottom-up push method to observe movement behaviour. This physical test confirms the viability of the Tristar system under realistic movement conditions and reveals additional insights into material behaviour, joint flexibility, and curvature adaptation.

Altogether, this chapter builds a bridge between digital logic and real-world application. Through the synthesis of movement analysis, parametric simulation, and mechanical prototyping, it provides the essential groundwork for testing the structural capacity of the DRSTAB system in the following chapter.

References

This phase of the research builds upon prior investigations by examining the three-dimensional behaviour of hybridized Tristar and auxetic patterns through architectural and computational lenses. Jayachandran (2018) introduces the “Deployable Reciprocal Shells Through Auxetic Behaviour” (DRSTAB) hypothesis, outlining a strategy for constructing self-supporting, double-curved shells by embedding auxetic movement logic within reciprocal frame systems. Borgström (2023) further contextualizes auxetic systems within architectural discourse, highlighting their adaptive, kinetic, and spatially transformative properties. Lukovic (2019) adds a computational dimension by simulating auxetic shells under deformation, enabling predictive control over morphogenetic behaviour. Together, these works frame a foundation for analysing and replicating dynamic geometrical transformations for deployable shell construction.
To translate these geometrical responses into mechanical functionality, the study references key texts on joinery and movement mechanisms. Sclater (2011) offers a broad typology of mechanical systems with a focus on ratchet-based locking mechanisms, essential for discrete deployment stages. Pellegrino (2001) investigates deployable structures that utilize ratchets at architectural scale, analysing post-deployment stiffness and geometric compatibility. Pahl et al. (2007) provide a design methodology for integrating ratchet components within structural systems, accounting for dynamic loading and failure prevention. For rotational movement with directional constraints, Harris (2001) details one-way clutch bearings, offering insights into torque limits and passive locking for retractable structures. Finally, Shigley et al. (2004) address ball joint applications within multi-axis systems, including wear, alignment, and durability key for realizing tessellated joints with freedom of movement during deployment and rigidity post-locking. These references collectively support the translation of auxetic geometries into scalable, mechanically actuated systems within the DRSTAB framework. Detailed relevant Literature are referred from Chapter 2.2.1

Methodology

This study adopts a qualitative, analytical methodology to investigate the kinematic behaviour of deployable reciprocal shells enabled by auxetic mechanisms. The research involves systematic decomposition and characterization of combined reciprocal and Tristar auxetic patterns through detailed analysis of their 2D and 3D movements. Axial and lateral displacements are examined at multiple scales from individual unit tessellations to full assemblies to understand their deployability and structural behaviour. As an early step in validating the adaptability of the pattern, a physical form-fitting study was conducted by overlaying lasercut PETG Tristar sheets onto a series of 3D printed base forms representing canonical double-curved geometries, including vaults, domes, hyperbolic paraboloids, and saddle surfaces. This allowed for a hands-on assessment of the pattern’s ability to conform to curvature prior to deeper mechanical analysis.
Subsequently, mechanical joinery elements specifically ratchet mechanisms, one-way bearings, and ball joints are conceptually modelled to replicate the observed movements at the unit level and in aggregate. This approach emphasizes manual, behaviour-driven analysis rather than automated simulations, aligning with established qualitative design research methods used in architectural computational design (Borgström, 2023). The integration of computational pattern analysis with mechanical design principles aims to inform sustainable, modular, and rapid construction strategies for double-curved shell structures.

4.2 Tristar Versatility –

Preliminary Form-Fitting Study with Tristar Auxetics

To comprehensively evaluate the spatial adaptability of the Tristar auxetic pattern, an extensive series of nine physical experiments were conducted, employing a rigorous methodology designed to test the pattern's performance across a diverse spectrum of double-curved architectural geometries. Initial exploratory tests were performed using 120gsm cardstock paper to establish baseline behaviour and identify fundamental geometric constraints. However, these preliminary trials revealed significant material limitations the paper specimens exhibited frequent tearing at nodal connection points when subjected to even moderate curvature, particularly in anticlastic (saddle-shaped) configurations where simultaneous bidirectional stretching exceeded the material's tensile capacity. This failure mode highlighted the critical need for materials with enhanced elongation properties while maintaining structural integrity during deformation.

Building on these findings, the formal test matrix transitioned to semi-flexible PETG (polyethylene terephthalate glycol) plastic, selected through an iterative material screening process. The final test series was carefully curated to include both fundamental and complex surface typologies: standard barrel vaults (single-curved translational surfaces), spherical domes (double-curved synclastic forms), hyperbolic paraboloids (doubly-ruled anticlastic surfaces), along with more geometrically challenging configurations including warped saddle shapes with compound curvature, toric sections with variable radii, and conoid surfaces exhibiting non-uniform curvature distribution. Each base form was meticulously digitally modelled using NURBS-based 3D modelling software to ensure precise geometric accuracy, then fabricated using high-resolution fused deposition modelling (FDM) 3D printing with PLA material, selected for its dimensional stability and surface finish quality.

The PETG specimens (0.25mm thick) were precision laser-cut to maintain geometric fidelity across all test units. Testing protocols involved passive draping over 3D-printed substrates to observe natural deformation behaviour, with particular attention to:

Nodal Stress Distribution: Monitoring previously problematic connection points that failed in paper prototypes , Curvature Thresholds: Quantifying maximum achievable deformation before plastic deformation ,Material Memory: Assessing the PETG's ability to stay a bit to its original configuration after removal

High-speed videography captured transient deformation phases, while digital image correlation (DIC) techniques provided quantitative strain mapping across the pattern's unit cells. This multiscale analysis revealed that while PETG eliminated the tearing failures observed in paper, it introduced new behavioral nuances the material's viscoelastic properties caused time-dependent relaxation under sustained curvature, necessitating further study for architectural applications requiring long-term shape stability.

4.2.1 3D printing Forms

The analysis of tristar pattern on curve forms is done using some basic 3D printed forms that exhibit system double curve forms . It include both fundamental and complex surface typologies , the final 9 form topologies as shown from Figure 4.2-1 to Figure 4.2-9 , includes

- Ellipsoid dome
- Parabolic paraboloid
- Parabolic Hyperboloid
- S curvature
- Double hemisphere
- Single vault
- Double Cross Vault
- Vase shape
- Free form double curve

Each base form was meticulously digitally modelled using NURBS-based 3D modelling software to ensure precise geometric accuracy, then fabricated using high-resolution fused deposition modelling (FDM) 3D printing with PLA material, selected for its dimensional stability and surface finish quality.

Figure 4.2-1 3d printed forms for testing - Ellipsoid Dome

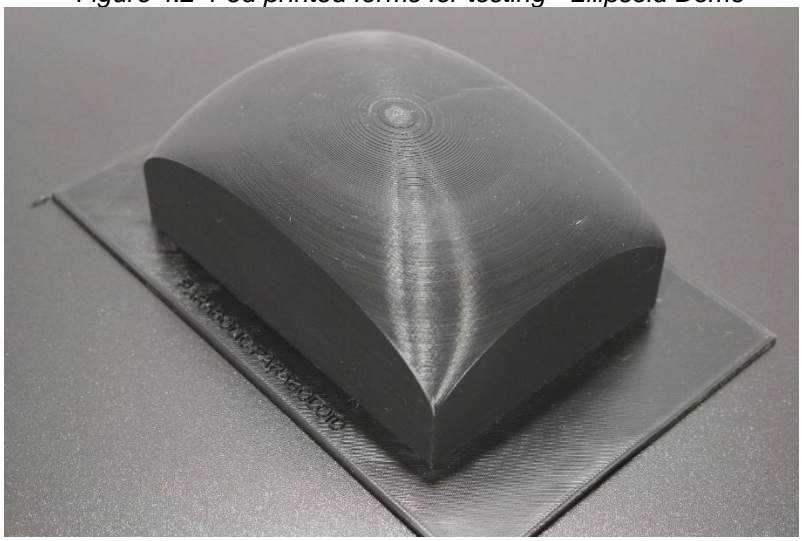

Figure 4.2-2 3d printed forms for testing - parabolic paraboloid

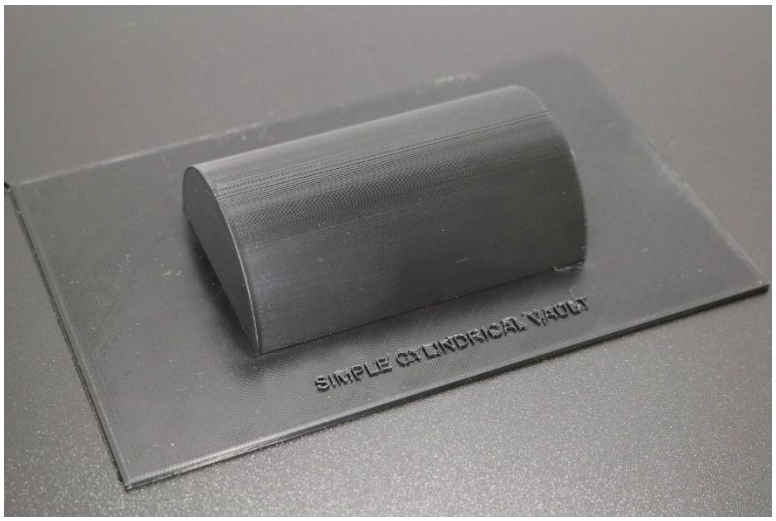

Figure 4.2-3 3d printed forms for testing Simple cylindrical Vault

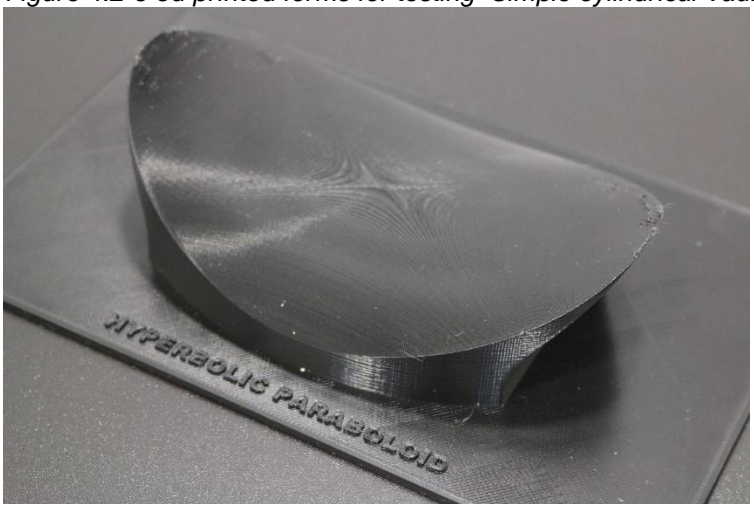

Figure 4.2-4 3d printed forms for testing - Hyperbolic paraboloid

Figure 4.2-5 3d printed forms for testing - Vase shape curve

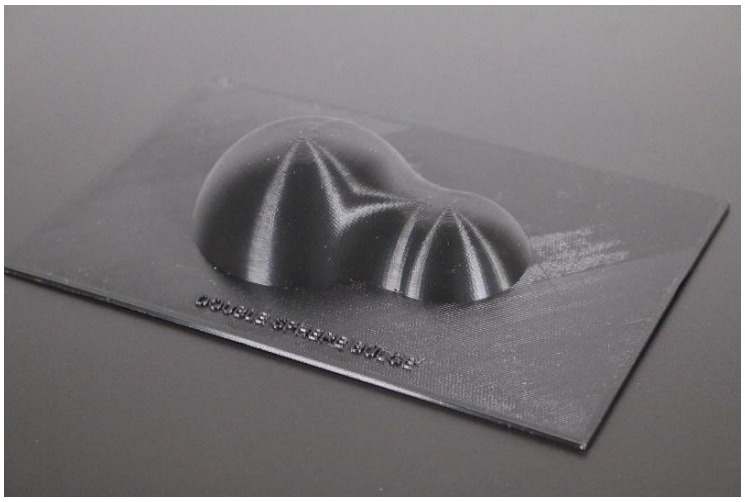

Figure 4.2-6 3d printed forms for testing - Double Dome structure

Figure 4.2-7 3d printed forms for testing - Double curve Flowing shape

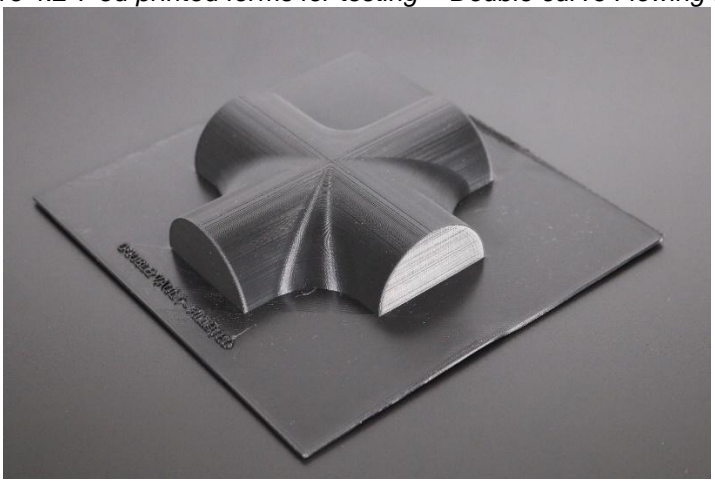

Figure 4.2-8 3d printed forms for testing -Double vault structure

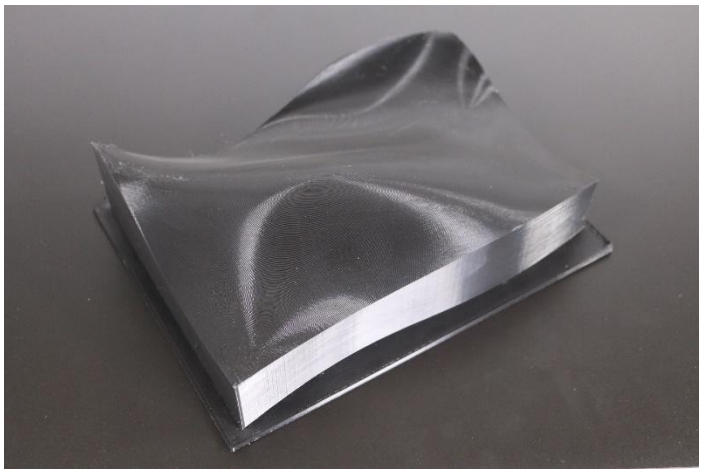

Figure 4.2-9 3d printed forms for testing Free flowing Form

4.2.2 Paper testing - failure documentation

Before progressing to the PETG laser-cut prototypes, the initial trials were conducted using simple paper sheets (Figure 4.2-10 & Figure 4.2-11) to quickly test the geometric transformations of the auxetic patterns. However, these attempts proved unsuccessful due to the inherent fragility of paper, which tore easily and lacked the tensile strength required to sustain repeated deformation. This outcome highlighted the need for a more durable and versatile material capable of withstanding multiple cycles of expansion and contraction. Subsequent experiments with faux leather and rubber sheets were also undertaken, as these materials offered greater resilience than paper. Nonetheless, these options presented their own limitations: faux leather released undesirable emissions during laser cutting, while rubber proved too rigid to accommodate complex auxetic geometries, restricting the range of patterns that could be effectively tested. These cumulative lessons ultimately informed the selection of PETG sheets, which provided the optimal balance of durability, flexibility, and fabrication compatibility, allowing for accurate and repeatable physical modelling of the auxetic prototypes.

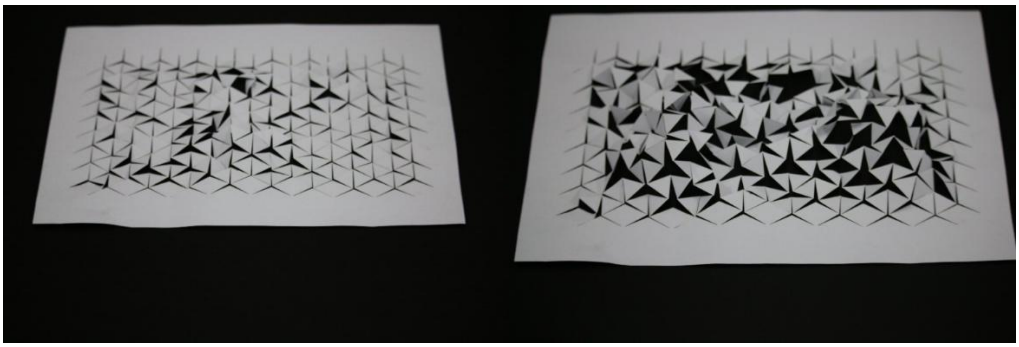

Figure 4.2-10 Lasercut trial with paper

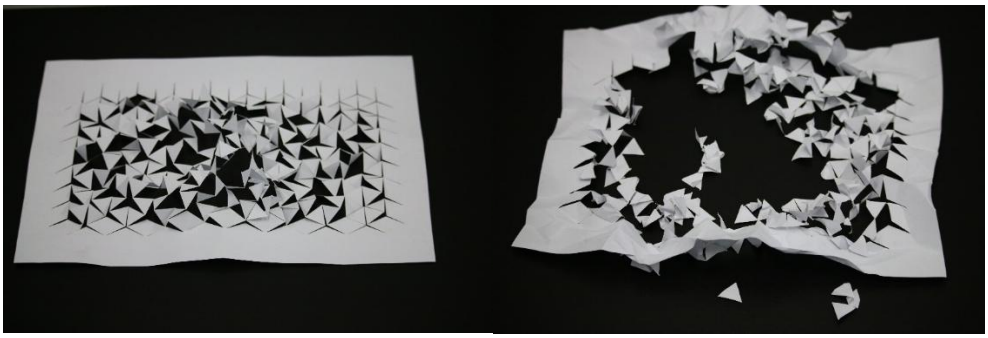

Figure 4.2-11 Lasercut trial with paper – failure reporting

4.2.3 Testing of Tristar laser cuts in PETG

The following section documents the experimental testing of the Tristar auxetic pattern fabricated through laser cutting in polyethylene terephthalate glycol (PETG). PETG was selected as the primary material due to its balance of flexibility, tensile strength, and transparency, which made it particularly suitable for observing deformation and stress distribution across the patterned surfaces during deployment. The tests showcased from Figure 4.2-12 to Figure 4.2-20 , aimed to evaluate how the Tristar configuration, identified in earlier analytical phases as an optimal auxetic candidate, would perform when materialized and applied to three-dimensional formwork. By overlaying the cut modules on double-curved geometries, the study explored critical factors such as adaptability to curvature, edge stability, and the presence of emergent behaviours like buckling, flipping, or stress concentrations that are less visible in purely digital simulations. This stage represents a crucial bridge between computational experimentation and material reality, allowing the theoretical properties of the Tristar pattern to be assessed through hands-on trials. The outcomes provide not only a validation of digital models but also insights into limitations and constraints that informed subsequent refinements in joinery development and full-scale mechanical prototyping.

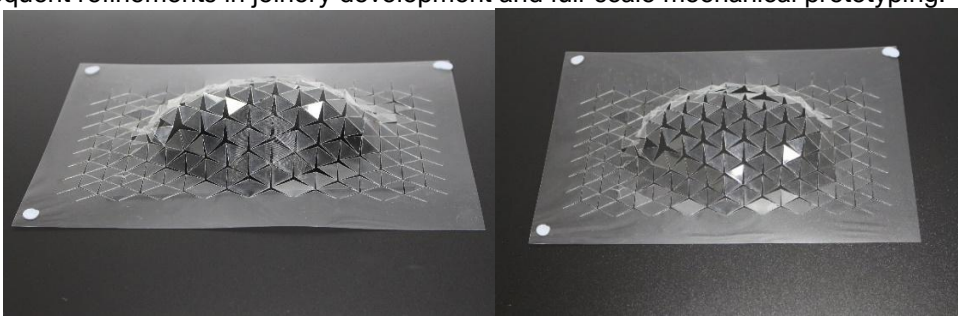

Figure 4.2-12 Tristar PETG on Ellipsoid Dome - – laid on Form and free standing

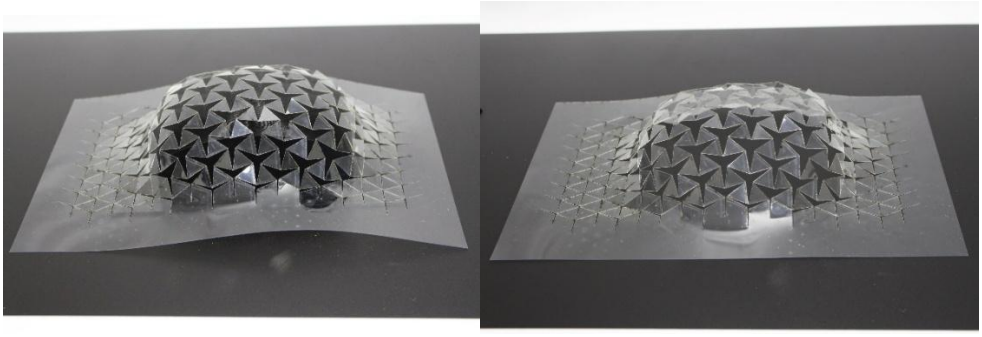

Figure 4.2-13 Tristar PETG on parabolic paraboloid – laid on Form and free standing

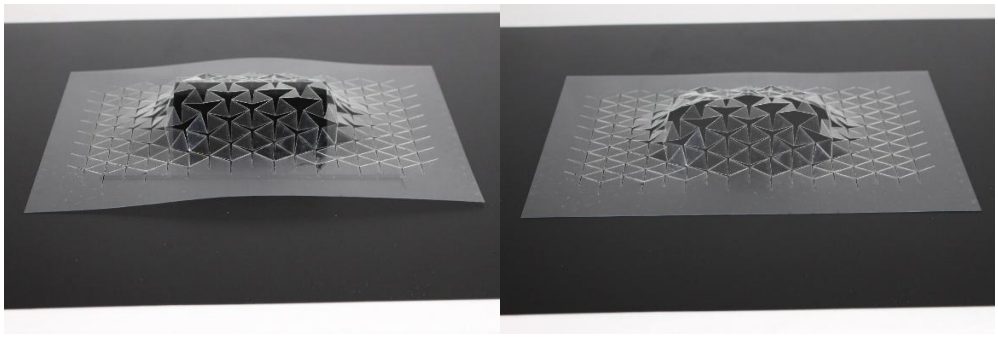

Figure 4.2-14 Tristar PETG on simple Vault – laid on Form and free standing

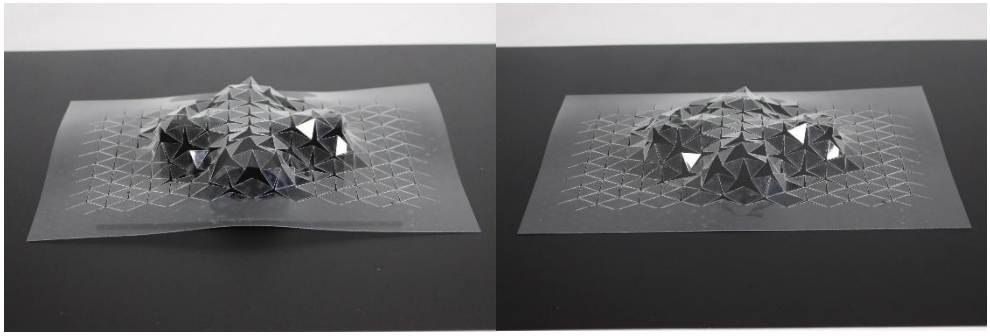

Figure 4.2-15 Tristar PETG on Double cross Vault – laid on Form and free standing

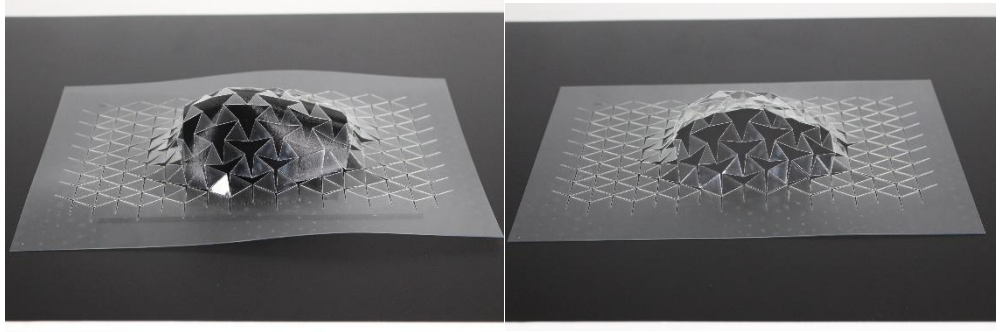

Figure 4.2-16 Tristar PETG on Simple Vase shape – laid on Form and free standing

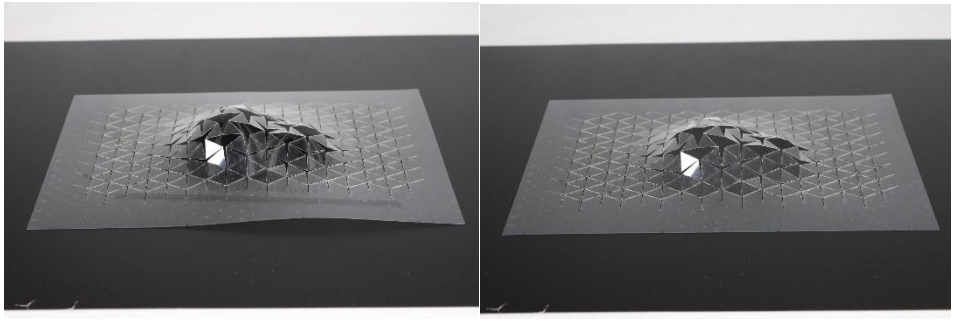

Figure 4.2-17 Tristar PETG on Double Dome Structure – laid on Form and free standing

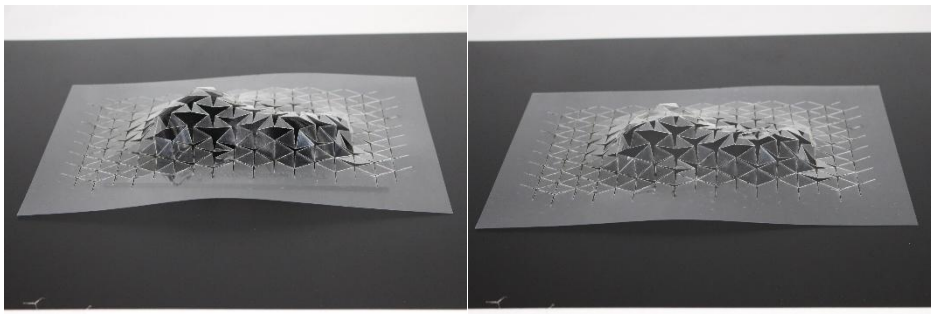

Figure 4.2-18 Tristar PETG on Double curve free flowing form – laid on Form and free standing

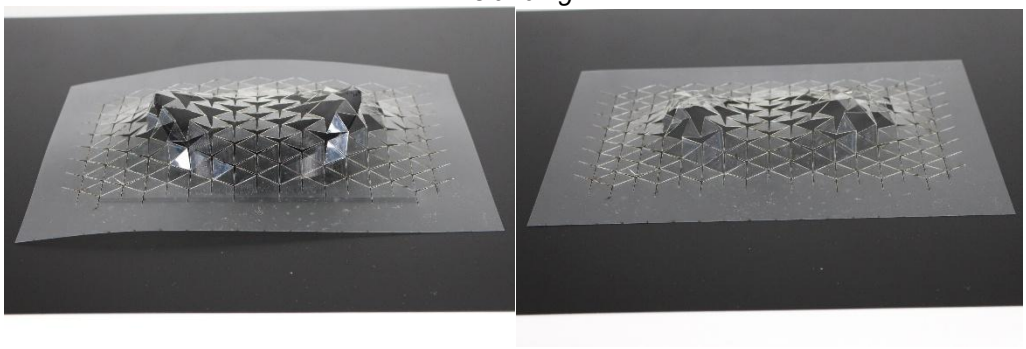

Figure 4.2-19 Tristar PETG on Hyperboloid paraboloid – laid on Form and free standing

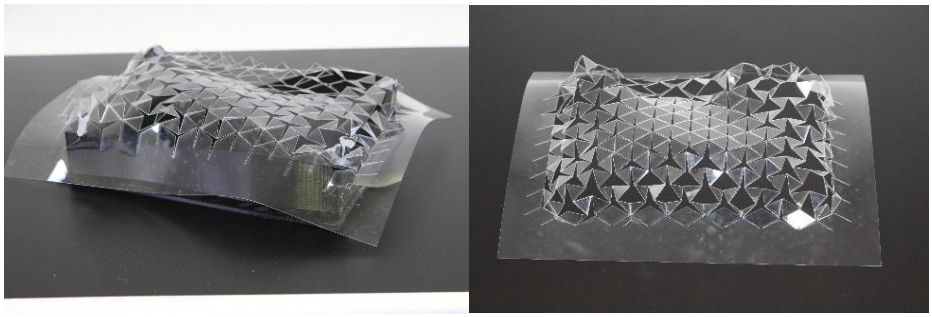

Figure 4.2-20 Tristar PETG on Free flowing double curve – laid on Form

4.2.4 Free Form testing

Following the series of 3D-printed form tests, additional experiments were carried out using free-forming techniques by hand. In these trials as shown in , Figure 4.2-21 , the PETG prototypes were manually pulled into a variety of random shapes without any predetermined geometry. Remarkably, the material retained these induced forms with a surprising degree of stability, even when subjected to irregular and uneven deformations. This behaviour directly demonstrated the viability of the “pull-up” deployment technique discussed earlier in the research, where the structure can be activated through direct tensile manipulation rather than relying solely on rigid mechanical guidance. These informal trials, while not systematically measured, revealed an important aspect of PETG’s adaptability: its ability to hold complex double-curved surfaces through relatively simple manual interventions. The findings suggest that such free-form manipulation could inform future strategies for rapid or low-tech deployment scenarios, where structures may need to be adapted on site with minimal equipment.

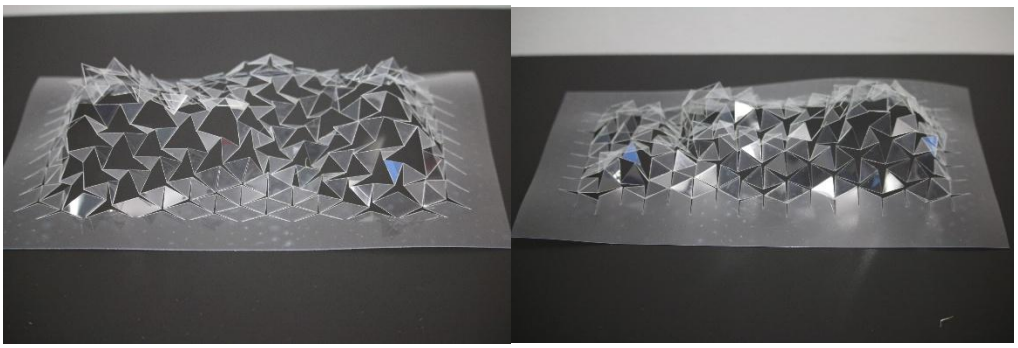

Figure 4.2-21 Freeform testing of Pet G lasercut

Detailed High res Images and documentation from various angles explored in Appendix E : Testing of Tristar laser cuts in PETG

4.2.5 Inference from the PETG study

4.2.5.1 Geometric Flexibility and Curvature Response

From the tests showcased from Figure 4.2-12 to Figure 4.2-20 ,the physical experiments conclusively demonstrated the Tristar pattern's exceptional capacity for geometric adaptation, with its auxetic unit cells successfully conforming to a wide range of double-curved surfaces. The pattern exhibited predictable deformation behavior across both synclastic (dome-like) and anticlastic (saddle-like) geometries, maintaining structural coherence even under significant curvature. During testing, the Tristar system displayed smooth and consistent transitions across varying surface conditions. When applied to gradual curvatures, such as barrel vaults with radii greater than 500 mm at prototype scale, the pattern redistributed strain evenly throughout its nodal network. This behavior prevented local buckling or cell collapse, confirming the design's ability to accommodate continuous deformation without compromising stability.

On synclastic surfaces, particularly spherical domes, the pattern expanded uniformly, with each cell opening radially from the apex toward the base. This controlled, radial deformation suggests strong potential for adaptive cladding or skin systems where curvature and surface response can be programmed for performance. Conversely, when applied to anticlastic geometries such as hyperbolic paraboloids, the system exhibited a complementary motion: cells expanded along one axis while contracting along the perpendicular direction. This bidirectional response effectively validated the pattern's negative Poisson's ratio, demonstrating its inherent auxetic nature and confirming its suitability for complex, multi-curved architectural applications.

4.2.5.2 Limitations at High-Curvature Zones

While the overall performance of the Tristar prototype was highly robust, the experiments also revealed specific thresholds where geometric and material limitations began to emerge. These constraints were most noticeable at areas of extreme curvature, such as the apex of domes and the tight twists characteristic of saddle-shaped surfaces. In these regions, localized stress concentrations developed, leading to minor geometric deviations and material strain.

At the structural level, small misalignments were observed, with unit cells shifting by approximately 4–6 mm from their ideal tessellated positions. Although these deviations did not compromise the overall stability of the system, they slightly disrupted the visual and geometric

continuity of the pattern. Furthermore, due to PETG's viscoelastic nature, localized plastic deformation was recorded in high-stress zones after prolonged loading. This "material memory" effect indicates that, while PETG performs well for experimental validation, more fatigue-resistant alternatives such as fiber-reinforced composites would be preferable for permanent architectural applications.

A further limitation was identified in the angular rotation capacity of the pattern, which plateaued at approximately 60 degrees. This threshold was directly influenced by two main factors. The first was PETG's relatively high elastic modulus, which limited the material's ability to undergo further expansion without risking permanent deformation. The second factor was the friction introduced at laser-cut nodal joints, where micro-imperfections along the edges increased resistance and reduced the freedom of rotational movement. Together, these findings highlight the interplay between material properties, fabrication precision, and geometric performance, emphasizing the need for both material refinement and joint optimization in future iterations.

4.2.5.3 Material Constraints and Hybridization Opportunities

The PETG prototype's performance, while generally successful, also revealed clear opportunities for system augmentation. Two material-driven limitations became particularly apparent. First, there was a stretch–rotation tradeoff, as achieving rotations beyond 60 degrees required forces that risked exceeding the yield point of PETG, raising concerns about long-term durability. Second, under sustained deformation, the material showed signs of creep, with 2–3 percent relaxation over a 24-hour period. This behaviour presents a potential issue for maintaining shape stability in extended deployments.

4.2.5.4 Further Research Direction

This experimental phase confirmed the Tristar pattern's viability as a lightweight, curvature-adaptive architectural skin, while also identifying limitations that open pathways for further research. The results emphasize a broader paradigm: auxetic systems for architecture must balance geometric intelligence with material pragmatism, a challenge that this study addressed through iterative testing but did not exhaust in scope.

Several potential strategies remain open for exploration by future researchers. One avenue lies in testing alternative materials, such as thermoplastic polyurethane (TPU) or glass-fiber-reinforced PETG, which could offer greater rotational capacity and long-term durability compared to standard PETG. Another possibility is the integration of joint pivots using miniature rotational bearings or low-friction pins at nodal points, decoupling material strain from articulation demands and allowing smoother rotations. Similarly, elastomer augmentation through the insertion of flexible silicone segments at high-stress nodes could preserve auxetic behaviour while reducing the risk of material fatigue. These strategies were not pursued in this research, as the focus remained on validating the mechanical and geometric logic of the system rather than optimizing material innovations.

By outlining these possibilities, the findings not only confirm the viability of the Tristar system but also provide a platform for others to extend the work, addressing material and mechanical refinements that could significantly enhance performance in future architectural applications.

4.3 Auxetic movement Breakdown – Hybrid Tristar Auxetics

Among the various auxetic geometries explored during the initial design phase, the Tristar pattern emerged as the most suitable candidate for integration within a deployable reciprocal frame system. Its ability to maintain geometric coherence while enabling controlled expansion and contraction in multiple directions made it a strong fit for architectural applications requiring adaptability and responsiveness. Unlike other patterns, which often suffered from excessive angular distortion, limited curvature compatibility, or overly complex connectivity, the Tristar offered a balance of structural simplicity, directional flexibility, and kinematic predictability. These characteristics allowed it to support both planar and double-curved configurations without compromising stability. This chapter focuses on deconstructing the individual movement logic of the Tristar units, with the aim of replicating these movements through mechanical joinery. By isolating and analysing each axis of rotation and interaction, we establish a framework for translating this patterned behaviour into engineered motion systems.

4.3.1 Rotational Behaviour of Hybrid Tristar Units

To understand and mechanically replicate the dynamic behaviour of the Tristar pattern, it is essential to analyze the fundamental rotational movements of its individual triangular units. Each triangle within the Tristar configuration exhibits a coordinated spatial movement that can be broken down into three principal rotational degrees of freedom: yaw, pitch, and roll. These correspond to rotations around the Z, Y, and X axes, respectively. Yaw (rotation around the Z-axis) governs the horizontal rotation of the triangle around its central vertical axis, enabling lateral expansion and contraction. Pitch (rotation around the Y-axis) controls the upward or downward tilt of each triangle, directly influencing the sheet's ability to generate curvature along the vertical plane. Roll (rotation around the X-axis), while subtler in this system, becomes relevant during compound curvature transformations, as it allows for slight banking of the units relative to adjacent elements. These movements are typically represented using Euler angles in the form of (rotation_x, rotation_y, rotation_z), which define the sequence and magnitude of rotation around each axis as shown in Figure 4.3 1

From earlier analysis, the roll rotation between adjacent units was found to be minimal, and therefore flexibility is considered primarily in yaw and pitch from this point forward. Additionally, axial rotation along the connecting X-axis (Roll) should be restricted to maintain overall structural coherence.

At the product testing level and through Grasshopper simulations, it was observed that structural breakages consistently occurred beyond 60 degrees of yaw rotation. To extend the performance and achieve the optimal 120-degree expansion identified in earlier analysis, the study introduces mechanical rotation mechanisms to supplement material limitations. These assistive joints provide controlled movement beyond the natural threshold of the PETG prototypes, achieving greater expansion efficiency.

As for pitch rotation, further investigations using Grasshopper-based simulations and physical prototypes revealed a practical upper limit of 30 degrees. Beyond this, the pattern exhibited significant deformation and instability particularly in areas of high curvature. This behaviour was validated through manual curvature analysis, which confirmed that the Tristar system performs reliably only on smooth, continuous surfaces. Sharp or steep curves consistently led to geometric failures under the current configuration, indicating the need for constraint-aware application of the system in architectural envelopes and deployable skins.

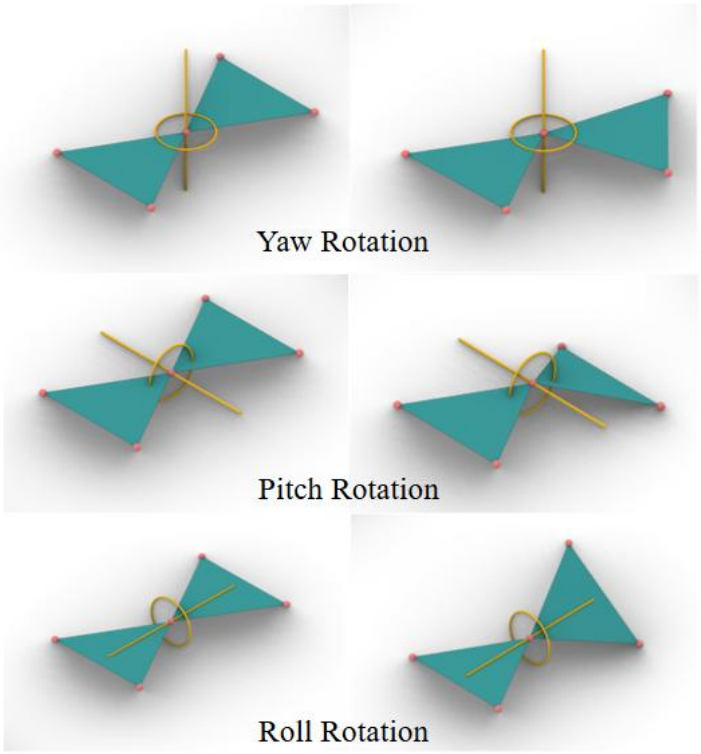

Figure 4.3-1 Infographic depiction of Roll , Pitch and Yaw rotation with tristar units

The Angles between 2 triangular unit is defined by its deviation or angling from the main corresponding perpendicular axis. As defined before we have 3 rotational movement based on which axis this rotates. The Yaw Rotation is along Z axis and the angle calculated is deviation along XY Plane , with axis taken along X in this instance . The Yaw Rotation is along Y axis and the angle calculated is deviation along XZ Plane , with axis taken along Z in this instance
The Roll Rotation is along X axis and the angle calculated is deviation along YZ Plane , and since we are neglecting or avoiding the Roll deviation we will not consider this at the moment

Incorporating this same logic of Yaw in 6 to 32 units and then incorporating pitch in various angles. Understanding this visually is essential to get a few parameters for the digital simulations in Grasshopper as restrictions and expansion parameters

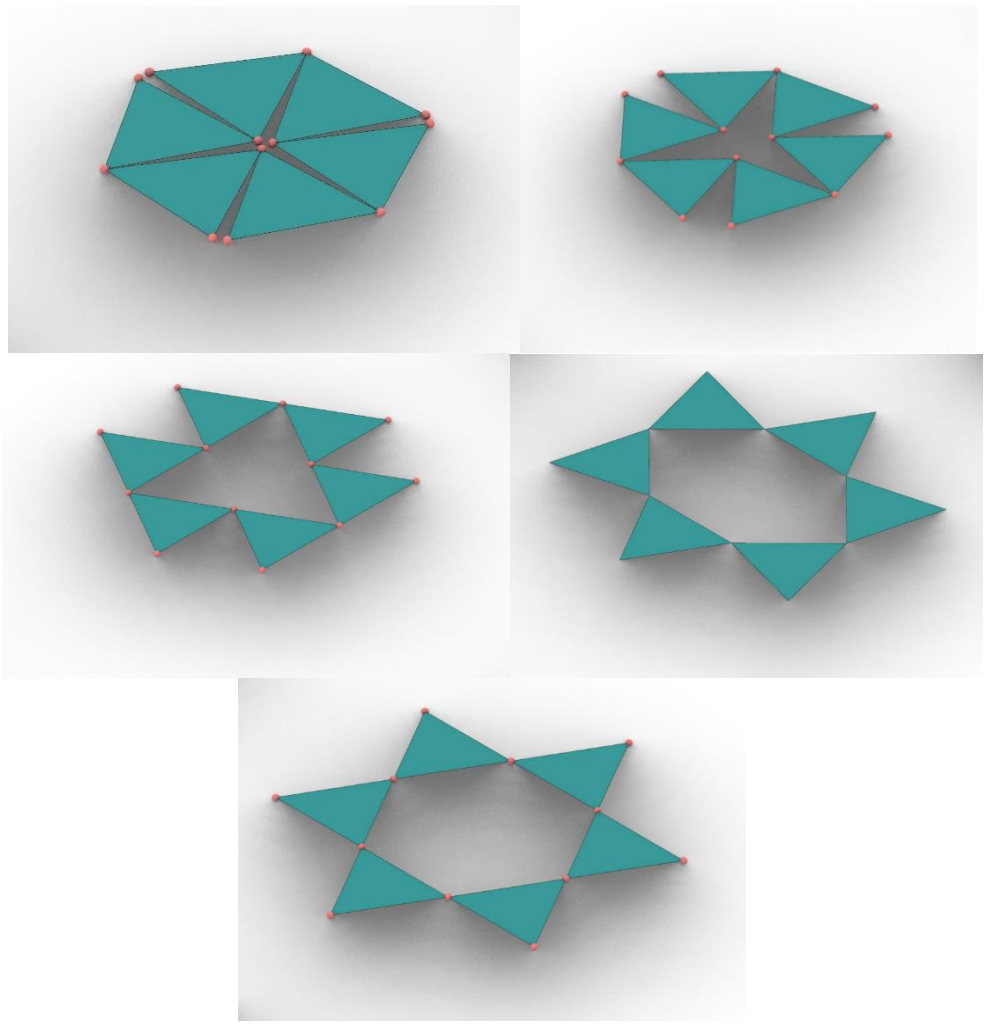

Figure 4.3-2 6 unit cluster depicting Yaw movement only

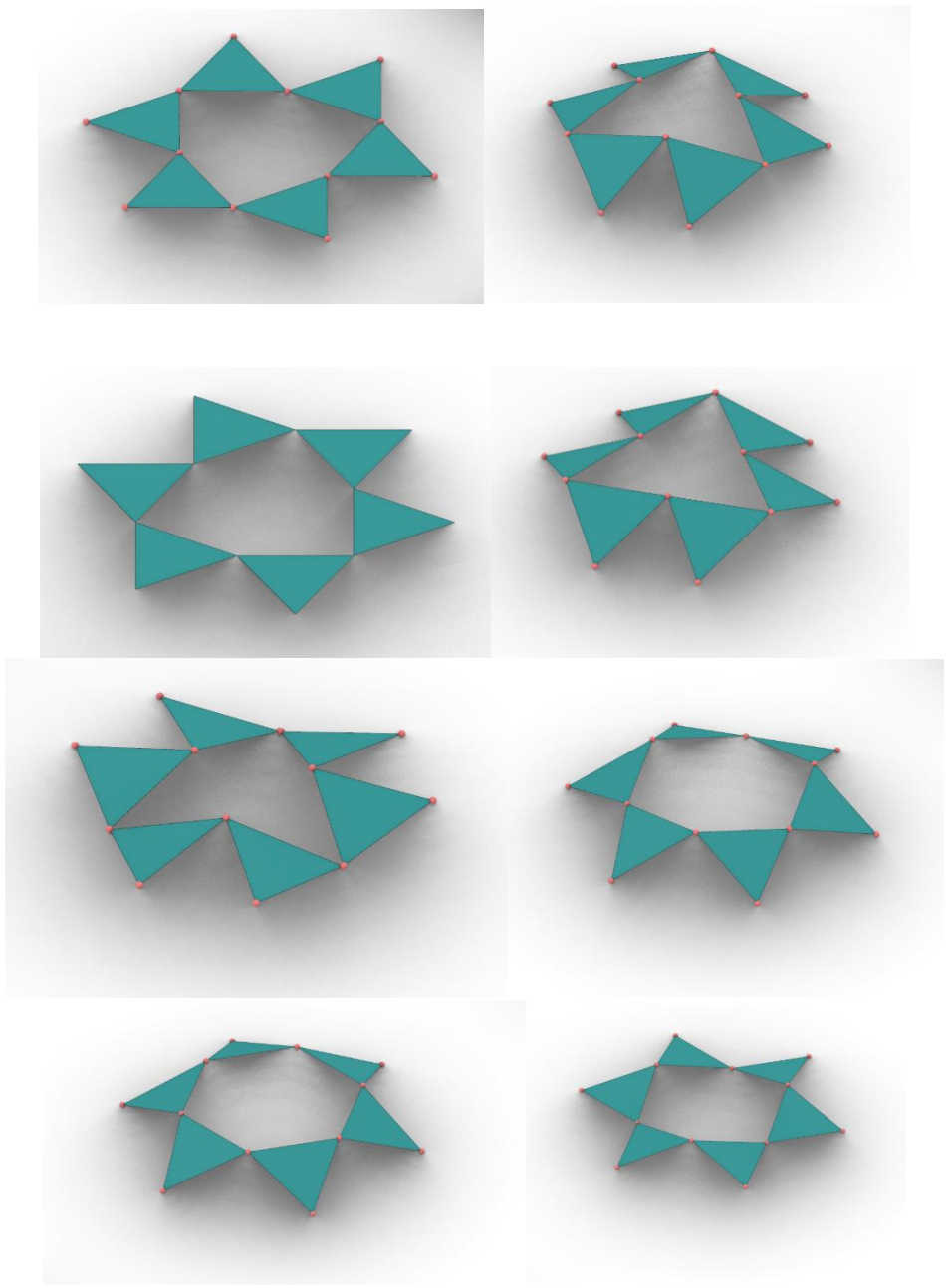

Figure 4.3-3 6 unit cluster depicting Yaw and Pitch movements

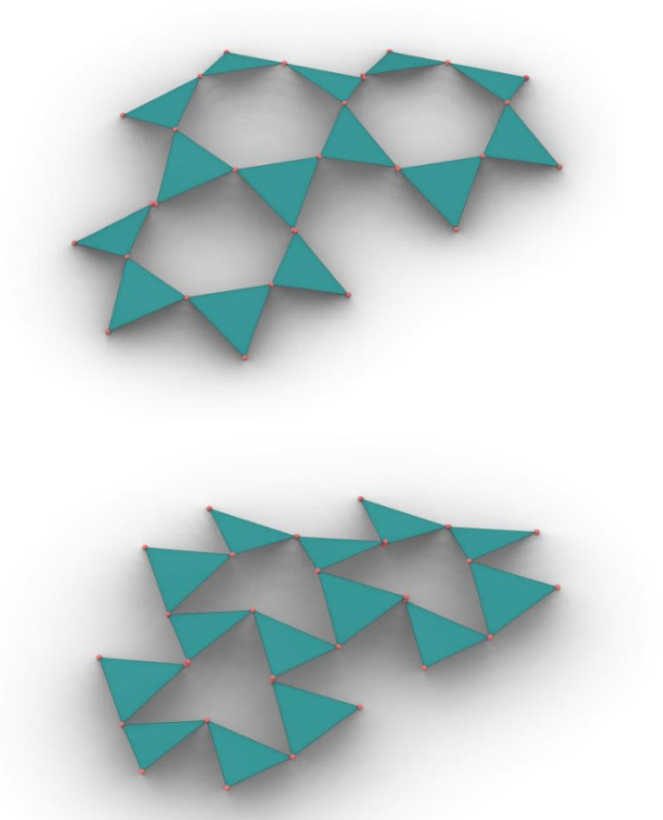

Figure 4.3-4 Rotation and movements between multiple 6 units

By isolating and observing these rotations in both simulation and physical mockups, the Tristar pattern reveals its capacity for highly controlled and distributed movement. Understanding this breakdown is critical in developing mechanical joineries that not only allow but also regulate these specific rotations, enabling the transformation of a 2D patterned surface into a 3D, curvature-adaptive deployable system.

From this rotational analysis observed from Figure 4.3 2 to Figure 4.3 4, it becomes evident that controlled movement across the pitch and yaw axes is critical to maintaining the structural coherence of the Tristar-based deployable system. Visual modelling and physical mockups reveal that pitch rotation (Y-axis tilt) should ideally be restricted between 5 to 15 degrees, beyond which the curvature begins to destabilize, leading to collapse or unintended deformation. This pitch behaviour can be further categorized as follows: 0 degrees represents a fully flat configuration; 0–5 degrees results in smooth, gradual curvature (level 1); 5–15 degrees supports moderate curvature (level 2); and 15–30 degrees enables sharper, more aggressive curvature (level 3), which is identified as the maximum tangential inclination angle recommended in this study. All angles are measured as the angle of inclination that is, the angle between the horizontal plane and the tangent vector of the curved surface at each point. Any pitch rotation exceeding 30 degrees may be achievable in future research through specialized mechanisms designed to accommodate such dynamic movement.

Similarly, yaw rotation (Z-axis twist) has been found to function reliably up to a maximum of 120 degrees, a limit identified during earlier kinematic studies and confirmed in full sheet simulations. These values now form critical design parameters in developing mechanical joineries that must accommodate yet constrain movement within these specific rotational boundaries to ensure predictable, curvature-adaptive deployment.

4.4 Digital Simulation of Hybrid Tristar Auxetics

Simulation of Movement – Digitally in Grasshopper at Product Level – Checking Versatility & Shape Adaptations from Drawings

This section focuses on the digital simulation of the Tristar geometry's movement at the product scale using Grasshopper within Rhino 3D. Following the physical observation of movement patterns, these dynamics are translated into parametric logic. The goal is to assess how the Tristar pattern responds when mapped across varying curvatures, and how it can adapt to multiple spatial conditions without losing its auxetic behaviour. Key emphasis is placed on evaluating versatility in terms of rotational, lateral, and axial deformation, especially as the geometry transitions between planar and three-dimensional forms. The product-level simulation aims to test the theoretical adaptability of the design using a digitally controlled environment before physical prototyping. The feedback loop between drawing-based analysis and parametric modelling allows for direct comparisons between anticipated behaviour and actual outputs in the digital model. Shape adaptations are tested through different curvature mappings (positive, negative, and compound) to push the limits of the geometry's kinetic behaviour. This section also documents the visualization of various stages of deployment, including folding, rotation, and expansion patterns, setting the stage for further refinement.

This research adopts a design-based, qualitative analytical methodology, moving from simulation to physical prototyping to evaluate the spatial and structural behaviour of a tristar-based auxetic pattern integrated within a reciprocal frame shell. Rooted in computational design and physical modelling, the approach draws from precedents such as Konaković Luković et al. (2016), where simulations and material analogues were used to test deployability and curvature adaptation in auxetic systems.

The first phase involves digital modelling in Rhinoceros 3D, with parametric scripting in Grasshopper, supported by a suite of plugins tailored to simulate dynamic geometry. These include Kangaroo for physics-based simulation, Ngon for advanced panelization and motion control, Human for geometry referencing, and Pufferfish for morphing and interpolation operations. This phase tests the behaviour of the tristar pattern in both 2D and 3D, evaluating its redistribution and adaptability across a range of convex and concave curvature conditions.

4.4.1 Simulation references

The convergence of auxetic behaviour and deployable structures has prompted a growing body of interdisciplinary research in both material science and architectural engineering. Konaković Luković et al. (2016) laid the groundwork for computationally designing auxetic shells through kinematically compatible patterns, emphasizing how digital design tools can generate transformable, curvature-adaptive systems. In a related architectural context, Borgström (2021) explored the applicability of auxetic systems to expand and contract spatial volumes in built environments, identifying the potential of auxetic logic for lightweight, kinetic structures. Surendar Jayachandran (2019) further extended this line of inquiry by proposing the DRSTAB system a design hypothesis that fuses reciprocal frames with auxetic geometries to enable the creation of double-curved, deployable shell structures. Together, these studies underscore a key design principle: that auxetic geometries, when translated from 2D patterns to 3D systems, can enable scalable, responsive, and fabrication-ready architectural solutions.
Simulation-to-fabrication workflows have also been well documented in architectural research. The application of Rhinoceros 3D, Grasshopper, and Kangaroo for real-time form-finding and kinematic simulations has been explored in projects involving origami-inspired or responsive components (Schenk & Guest, 2013). These tools offer precision in modelling deformation and structural behaviour, forming a digital basis to inform subsequent physical testing. Physical prototyping, as demonstrated in the work of Pellegrino (2001) and Menges (2012), serves as

a critical feedback mechanism that validates and adjusts computational predictions, ensuring the integrity and reliability of the deployable mechanism under real-world conditions. This literature collectively informs the dual-phase methodology adopted in this research.

4.4.1.1 Mathematical Definitions of Patterns

Deriving the mathematical logic for a simulation is the first step to breakdown and build logic to make sure the simulation reacts based on the physics of the materials or patterns

In this part we explore the mathematical logics behind the Auxetic behaviour broken down into the logics of

Geometric considerations and restrictions
Position of tristar points (parametric coordinates

From these and other scientific papers some equations depicting the rotation logic was referred to

Geometric Parameters considered in the formulas

Length of arms: L
Central angle between arms: θ (usually 120° for tri-star)

Internal rotation angle for auxetic effect: φ
Distance from centre to joints: r

Position of Star Points (Parametric Coordinates)

The 3 arms of the tri-star can be placed using polar coordinates rotated around a central point:

(x_1, y_1) = (r * cos(0°), r * sin(0°))
(x_2, y_2) = (r * cos(120°), r * sin(120°))
(x_3, y_3) = (r * cos(240°), r * sin(240°))

(x_1, y_1) = (r * cos(0°), r * sin(0°)) (x_2, y_2) = (r * cos(120°), r * sin(120°)) (x_3, y_3) = (r * cos(240°), r * sin(240°))

This positioning is essential to map it to the movement coordinates

Auxetic rotation of units outward/inward

x′ = x * cos(φ) - y * sin(φ)
y′ = x * sin(φ) + y * cos(φ)

x′ = x * cos(φ) - y * sin(φ) y′ = x * sin(φ) + y * cos(φ)

Mathematical/Geometric Logic of the Tristar Pattern

The Tristar auxetic structure consists of rotating triangles connected by hinges. When stretched, the triangles rotate, causing the structure to expand laterally.

Key Equations/Logic:

Geometry: Each "Tristar" unit is composed of 3 identical triangles rotating about a central point.

Deformation: When stretched, the angle (θ) between triangles changes, altering the effective Poisson's ratio.

Parametric Equations:

Let L = length of each triangle's arm.
Let θ = angle between adjacent triangles (changes under strain).

The coordinates of the vertices can be derived using polar-to-Cartesian transformations:

$x = L * \cos(\theta + 2\pi k/3)$
$y = L * \sin(\theta + 2\pi k/3)$

where k = 0, 1, 2 (for 3 triangles).

Auxetic Behaviour (Negative Poisson's Ratio Mechanism)

The key is how these star arms rotate around their joints when the structure is stretched. The Poisson's ratio (ν) can be derived from the change in width (Δw) and length (Δl):

ν=−Δw/w0Δl/l0\nu = - \frac{\ Δ w / w_0}{\ Δ l / l_0}ν=−Δ l/l0 Δw/w0

In auxetics, ν < 0.

For rotating rigid/star units, equations link:

Rotation angle φ
Relative expansion/contraction in orthogonal directions & Overlap conditions for tessellation

Tessellation & Joint Constraints

To ensure the stars tessellate (tile) correctly without overlaps, the distance d between unit centres must match: $d=2r\cdot\cos(\theta/2)$

This will ensure that the centres don't overlap In the XY plan even if the angles bending expose the angles too much .
The parametric or differential variations of rotation as per the curvature displacement is decided by making this 'd' variable and reparametrizing the definition based on distance factorial

Python Coding :

Using this Logic we make a python code generated with assistance from Deepseek & ChatGPT that is later fed into Rhino grasshopper for definition . The code and logic was generated by the author , AI was used for Sntax accurac and to troubleshoot errros

The code generates plots showing the Tristar pattern at different rotation angles Yaw (θ).
θ = 0°: Symmetric (no deformation).
θ = 15°: Deformed (auxetic expansion).

```python
import numpy as np
import matplotlib.pyplot as plt

def tristar_pattern(L=1.0, theta=0, n_units=3, ax=None):
    """
    Generate and plot a Tristar auxetic pattern unit.

    Parameters:
        L (float): Arm length of the triangles.
        theta (float): Rotation angle (radians) controlling deformation.
        n_units (int): Number of units to replicate (for visualization).
        ax (matplotlib axis): Axis to plot on.
    """
    if ax is None:
        fig, ax = plt.subplots(figsize=(10, 10))

    # Colors for visualization
    colors = ['red', 'blue', 'green']

    for unit in range(n_units):
        # Offset for multiple units
        offset_x = 2.5 * L * (unit % 3)
        offset_y = 2.5 * L * (unit // 3)

        # Generate vertices for 3 triangles
        for k in range(3):
            # Calculate vertex positions
            angle = theta + 2 * np.pi * k / 3
            x = L * np.cos(angle) + offset_x
            y = L * np.sin(angle) + offset_y

            # Plot triangle arms
            ax.plot([offset_x, x], [offset_y, y],
                    color=colors[k], linewidth=2, marker='o')

    ax.set_aspect('equal')
    ax.set_title(f'Tristar Auxetic Pattern (θ={np.degrees(theta):.1f}°)')
    ax.grid(True)
    plt.show()

# Example: Plot for θ=0° (undeformed) and θ=15° (deformed)
tristar_pattern(theta=0)      # Initial state
tristar_pattern(theta=np.pi/12)  # Deformed state (15°)
```

Figure 4.4-1 Python coding for basic Yaw Movement - node to be integrated into GH code
Note : Python code input re-generated in *Open AI – ChatGPT 4o* for Syntax and coding accuracy

```python
import Rhino.Geometry as rg
import math

# Inputs
L = 1.0          # Arm length
theta = math.radians(θ)  # Convert input angle (degrees) to radians
n_units = 3      # Number of repeating units

# Output list of lines (for visualization)
lines = []

for unit_x in range(n_units):
    for unit_y in range(n_units):
        # Offset for each unit
        offset_x = 2.5 * L * unit_x
        offset_y = 2.5 * L * unit_y
        center = rg.Point3d(offset_x, offset_y, 0)

        # Generate 3 arms (tristar)
        for k in range(3):
            angle = theta + 2 * math.pi * k / 3
            x = L * math.cos(angle) + offset_x
            y = L * math.sin(angle) + offset_y
            end_point = rg.Point3d(x, y, 0)
            lines.append(rg.Line(center, end_point))

# Output: List of lines (connect to 'a' output in GH)
a = lines
```

Figure 4.4-2 Python coding for basic Pitch Movement - node to be integrated into GH code
Note : Python code input re-generated in *Open AI – ChatGPT 4o* for Syntax and coding accuracy

The preparation of geometry for simulation begins with an in-depth evaluation of the auxetic principles underlying the Tristar design. Auxetic materials exhibit a negative Poisson's ratio, expanding perpendicular to an applied force, and this behaviour must be embedded within the digital geometry from the outset. To achieve this, the Tristar pattern is reconstructed based on its movement vectors and fold behaviour, guided by both physical observations and earlier analytical models. Specific attention is paid to the directional hinge points, the internal symmetry of units, and the interlocking zones that allow for expansion and contraction. This section outlines how the geometry is encoded to behave like an auxetic system within Grasshopper enabling controlled parametric variation without compromising structural logic. By assigning constraints and relationships between units, the groundwork is laid for scripting responsive simulations. Additionally, curvature thresholds are mapped to understand how far the auxetic effect can be pushed before breakdown occurs, giving early insight into the limitations of the design when deployed at various scales or under different forces.

Reassignment of Restrictions in Movements – Rotational, Lateral, and Axial – Degrees of Freedom & Possible Overlaps
With the base geometry defined, this section focuses on reevaluating and digitally reassigning movement constraints. The Tristar's movement is decomposed into three major categories: rotational (pivot-like motion of units), lateral (sideways expansion), and axial (depth-wise

transformation, especially in 3D mappings). These degrees of freedom are assigned as controllable variables in the simulation. However, due to the overlapping behaviour and close proximity of units in curvature scenarios, conflicts in movement arise especially when transitioning from 2D to 3D. These overlaps are studied, tagged, and reassigned as conditional restraints within the script. A logic of tolerance is built in to anticipate friction zones, folding inconsistencies, or material clashes. The script must ensure that each unit can move freely within its assigned axis without compromising neighboring units. This subchapter not only identifies limitations but proposes a method to control these variables within a digital framework, setting up a logical model that mirrors physical behaviour more accurately.

4.4.2 Simulation Trials and outcomes

4.4.2.1 Trial 1 - Uniform redistribution on flat surface- simulation

Grasshopper code -rational and logic

The Grasshopper implementation of the Tristar auxetic pattern operates through a multi-stage kinematic pipeline that translates geometric principles into parametric controls. At its core, the definition constructs a base triangular mesh through a Delaunay triangulation component, which is then decomposed into individual triangular units using a combination of Face Boundaries and List Item operations. Each triangle receives a local coordinate system anchored at its centroid, established through Area and Centroid components, serving as the pivot point for rotational transformations. The auxetic behaviour is engineered by feeding a scalar control parameter (0-1 normalized input) into a Function component that converts this value into precise rotation angles using the equation $\theta = 60° * (1 - e^{(-3x)})$, where x is the input scalar - this logarithmic relationship ensures smooth initial deployment with progressive resistance. These angles drive Rotate components that transform each triangle about its centroid's Z-axis, while a Series component synchronizes timing across all units. Adjacency maintenance is handled by a custom Python script that analyzes mesh topology through half-edge data structures, applying correction vectors when edge-to-edge clearances fall below a user-defined threshold (default 1.5mm). The rotated geometry is then reconstructed into a continuous auxetic surface using a Weaverbird subdivision pass with 0.75 tension to simulate material thickness, followed by a final step that outputs both the deformed mesh and quantitative metrics including: instantaneous Poisson's ratio (calculated through real-time length measurements along principal axes), void area percentage (via Region Difference and Area components), and maximum nodal displacement (tracked with a History container). For advanced control, the definition incorporates a conditional logic system using Grasshopper's Gate component that toggles between uniform expansion mode (all units receive identical rotation values) and curvature-adaptive mode (where rotation angles are modulated by a UV-gradient input mapped to surface curvature analysis results). The entire system is optimized for real-time manipulation through careful management of data trees, with each triangular unit maintaining its branch identity throughout transformations to enable selective post-processing operations.

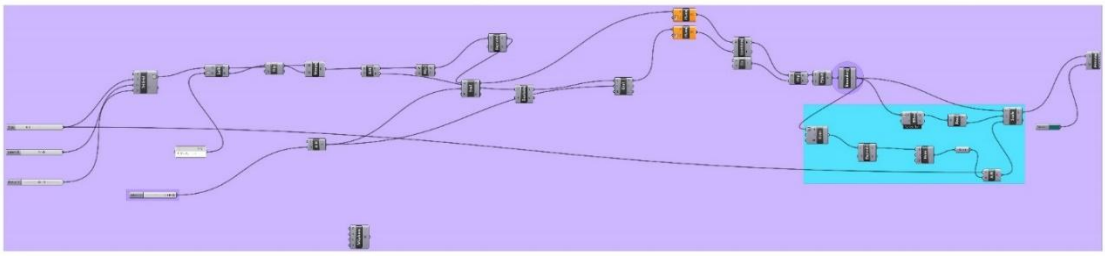

Figure 4.4-3 Grasshopper coding for Uniform rotation in XY plane

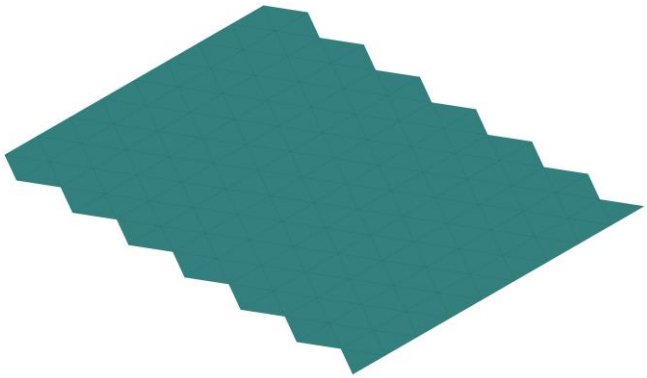

Figure 4.4-4 Results - GH code with Uniform rotation - at angle 0 – Top view and Iso View

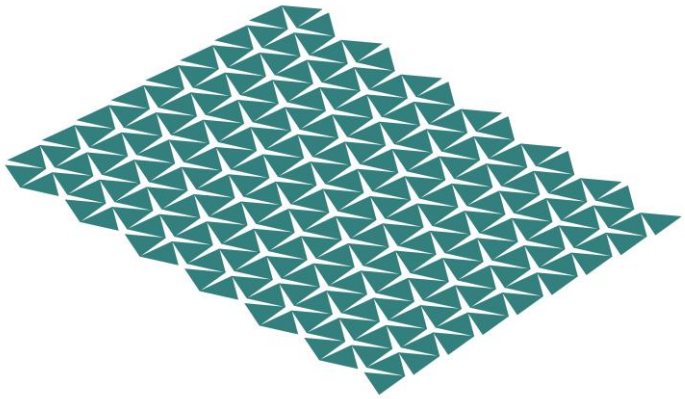

Figure 4.4-5 Results - GH code with Uniform rotation - at angle 30 – Top view and Iso View

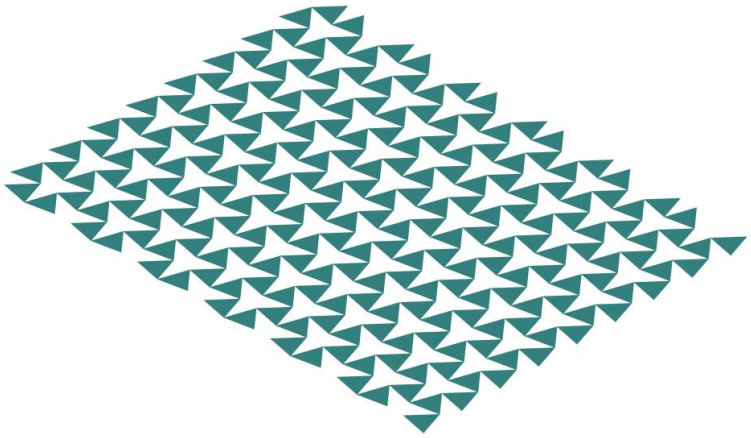

Figure 4.4-6 Results - GH code with Uniform rotation - at angle 60 – Top view and Iso View

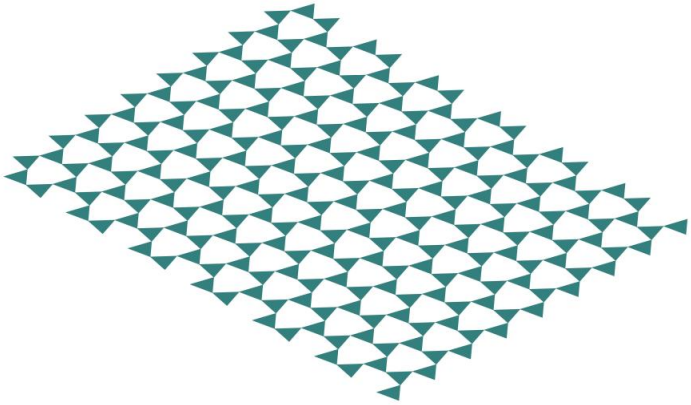

Figure 4.4-7 Results - GH code with Uniform rotation - at angle 90 – Top view and Iso View

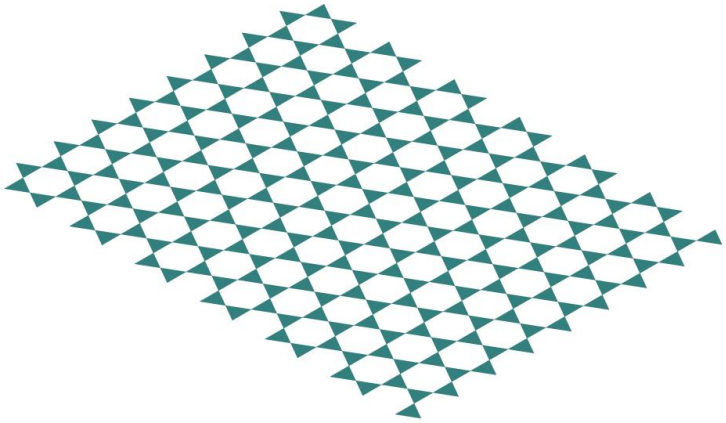

Figure 4.4-8 Results - GH code with Uniform rotation - at angle 120 – Top view and Iso View

4.4.2.2 Reflections on Flat Surface Simulation Using Uniform Angular Control

Parametric Simulation of Tristar Auxetic Expansion

The initial simulation phase focused on analysing the Tristar auxetic pattern's behaviour on a flat surface using uniform rotational logic. Observations from Figure 4.4-4 to Figure 4.4-8 proves effective for testing the pure geometric logic of the Tristar configuration, particularly in its ability to simulate real-time deformation across a 2D layout of 96 connected triangles. The system was tested with incremental rotation angles of 0°, 30°, 60°, 90°, and 120°, providing a clear view of how the expansion progressed as a function of angular change. The resulting transformations demonstrated a progressively increasing open area, visually and quantitatively affirming the auxetic behaviour across uniform inputs.

Observations from Rotation Thresholds

A key outcome from these uniform expansion trials was the discovery of a functional threshold in rotational logic. Up to approximately 120°, the pattern maintained geometric order, predictable spacing, and cohesive deformation. However, once the rotation angle approached or exceeded 120°(Figure 4.4.2 9), the system began to exhibit signs of geometric failure. Units began to overlap, nodal connections entered into collision states, and the integrity of the original tessellation was compromised. These overlaps not only undermined the visual clarity of the pattern but also invalidated its structural logic particularly in the context of deployable architecture, where precise fit and movement are critical.

This observation revealed a fundamental geometric constraint within the Tristar configuration: the maximum allowable yaw rotation per unit should not exceed 120°. This threshold now becomes a guiding parameter in future simulations, mechanical joint design, and fabrication protocols. It ensures that each rotation remains within a safe range that allows expansion without compromising tessellation behaviour or structural coherence.

Limitations of Uniform Angular Deployment

While the uniform rotation method successfully demonstrated the base auxetic mechanics of the pattern, it also highlighted several critical limitations when considered in the context of real-world deployment. Notably, the approach failed to account for spatial variation across the grid. In a flat environment, all units were subjected to the same degree of rotation, irrespective of their position within the overall system. This resulted in symmetrical expansion, which, while mathematically consistent, lacked the adaptive flexibility required for conforming to varied surface topologies or environmental conditions.

For instance, units positioned near the boundary of the grid exhibited edge misalignments and disproportionate openings, especially as rotation angles increased. These inconsistencies implied that not all units should rotate identically in future configurations particularly when the system is deployed on non-planar or more complex forms. Although the focus of this simulation was constrained to a flat layout, the realization that uniform deployment fails to address positional variability laid the groundwork for more advanced control strategies in subsequent phases of the research.

Summary and Direction for Future Development

This initial phase of flat-surface simulation using uniform angular control served a dual purpose. It validated the basic movement logic and expansion potential of the Tristar pattern, while also uncovering key constraints that influence its scalability and structural behaviour. The 120° rotation limit now functions as a critical design constraint across both digital and physical

domains, defining the operational range for safe expansion. At the same time, the shortcomings of uniform deployment have signaled the necessity for more nuanced, spatially responsive logic to handle non-homogenous geometries and curvature.

These reflections mark an important turning point in the development of the DRSTAB system. Moving forward, subsequent studies will introduce localized control mechanisms including attractor point logic and curvature mapping to enhance adaptability. These improvements will be explored in the next phase of simulation and physical prototyping, where the Tristar pattern will be tested under varied conditions, including double-curved shell surfaces and differential displacement zones.

4.4.2.3 Responsive Expansion Using Attractor Point Logic on a Flat Surface

Following the limitations identified in the uniform rotation model where synchronized expansion across all units failed to accommodate local variation this phase of the research introduced a refined simulation strategy using attractor point logic to enable spatial differentiation in auxetic behaviour. The objective was to create a 2D expansion system that could respond to positional context, allowing certain parts of the pattern to expand more or less based on proximity to a defined reference point within the XY plane.

Grasshopper code -rational and logic

As in the previous iteration, the Tristar auxetic system was constructed by decomposing a triangular grid into individual triangles, with each triangle considered a discrete unit capable of independent rotation. Each unit was assigned a pivot point at or near its centroid, acting as the anchor for rotation. However, unlike the uniform model where all units rotated by the same angle, this iteration introduced a distance-based scaling factor derived from the triangle's position relative to a manually placed attractor point within the XY coordinate system.

The attractor point acted as a local field of influence, generating a graded effect where each unit's rotation was modulated by how close or far it was from this spatial reference. The rotation angle was calculated by mapping the distance to a predefined range of motion, with units near the attractor rotating less (or more, depending on direction), and those farther away rotating toward the maximum threshold, capped at 120° based on earlier rotational integrity constraints. This interpolation of angles was implemented using a remapped scaling function in Grasshopper, enabling continuous and responsive variation across the entire field of units (Figure 4.4 -9) .

Within a typical 6-unit test cluster representing a minimal, symmetrical configuration of the Tristar system the units were programmed with directional rotation logic to maintain internal balance and minimize distortion. Units 1, 3, and 5 were assigned to rotate outward from the attractor (positive angular displacement), while Units 2, 4, and 6 rotated inward (negative angular displacement). This alternating pattern of movement produced a localized auxetic deformation, simulating the push-pull dynamics often observed in physical auxetic materials.

The result was a controlled, two-dimensional deformation behaviour that demonstrated significantly improved adaptability compared to the earlier uniform model. The attractor-based logic allowed for expansion that was spatially responsive, generating higher fidelity to contextual positioning and opening opportunities for further customization. Notably, the model could easily be extended to include multiple attractor points, varying influence radii, or dynamic attractors that move in response to external stimuli or programmatic inputs.

The significance of this simulation lies not only in its geometric expressiveness but also in its potential for architectural control. By manipulating the attractor location and scaling range, a designer can guide the pattern's expansion to follow site-specific constraints, functional zoning, or material logic. For instance, tighter or no rotation can be applied to edge zones requiring rigidity, while central areas can be allowed to flex and expand more dramatically, creating zones of porosity, light penetration, or structural cushioning.

Furthermore, the attractor logic introduces differential displacement logic a precursor to conformal mapping which is vital for future simulations involving curved surfaces and shell geometries. Even though the test was conducted on a flat XY plane, the varying angle distribution introduced by the attractor simulates the kind of variable displacement fields encountered in real-world architectural contexts.

In summary, the attractor-based simulation marks a pivotal evolution in the development of the Tristar-based auxetic system. It overcomes the core limitations of uniform movement by embedding responsive deformation logic into the geometry itself. The balance between inward and outward rotation within the 6-unit structure ensures visual and mechanical symmetry, while the continuous mapping function enables granular control over expansion intensity across the surface. These learnings form the basis for the subsequent transition into three-dimensional deformation logic, where the attractor point concept will be expanded to include Z-axis displacement and full curvature-responsive transformation in complex surface topologies.

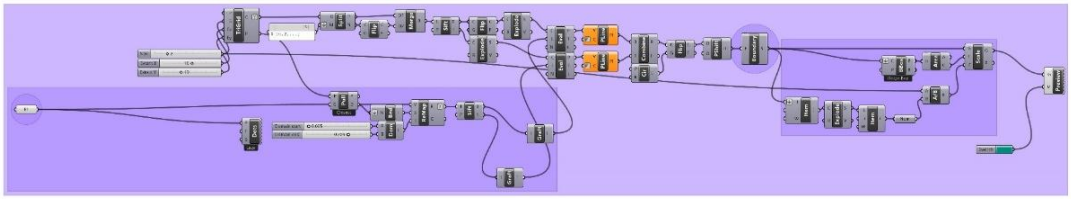

Figure 4.4-9 GH code for Auxetic movement with single 2D attractor point

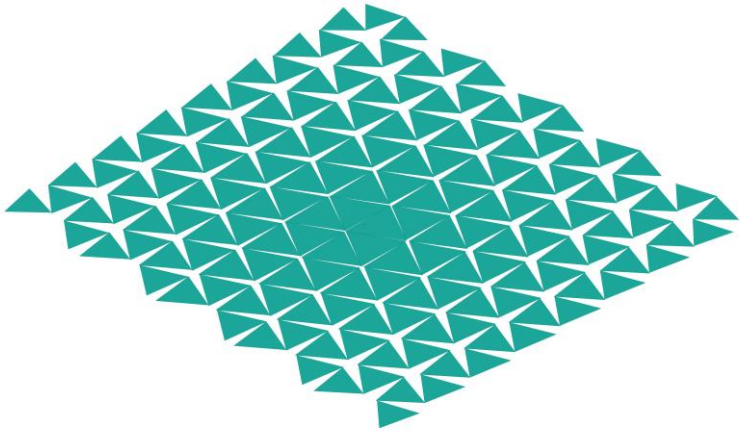

Figure 4.4-10 Results - GH code attractor point- Top and iso view- variation 1

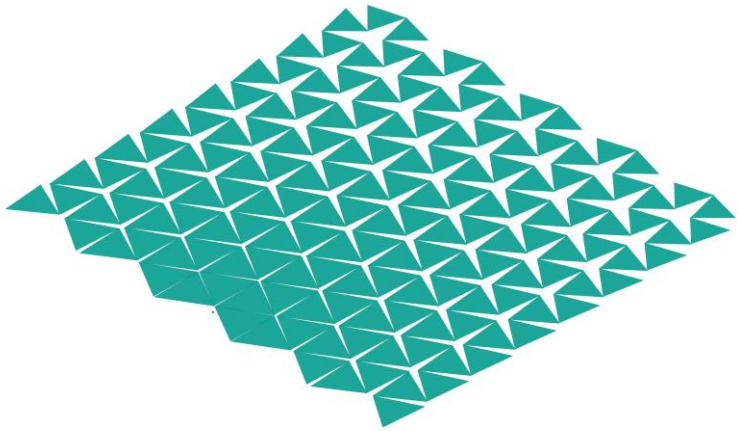

Figure 4.4-11 Results - GH code attractor point- Top and iso view- variation 2

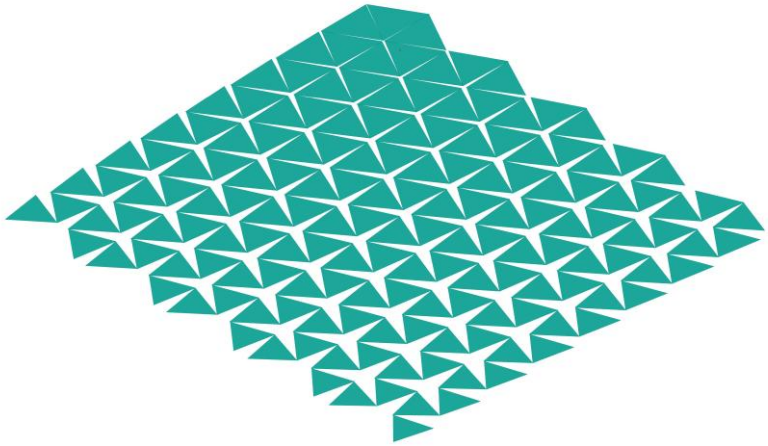

Figure 4.4-12 Results - GH code attractor point- Top and iso view- variation 3

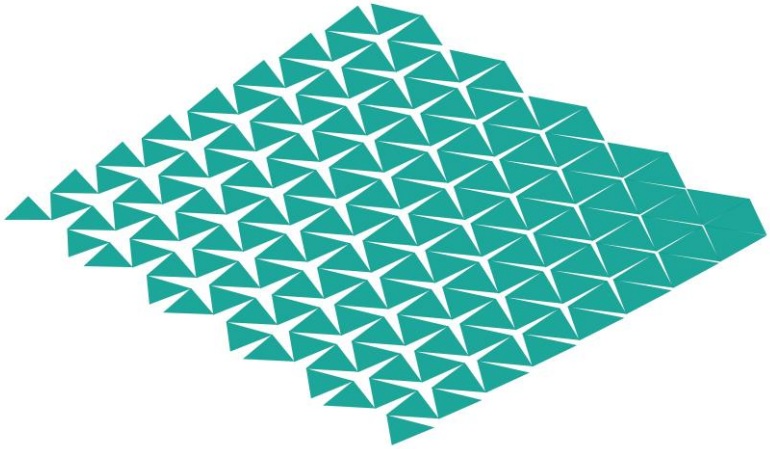

Figure 4.4-13 Results - GH code attractor point- Top and iso view- variation 4

Reflections on Attractor-Based Tristar Auxetic Expansion in XY Plane

Effective Localized Expansion in Two Dimensions

The attractor-driven auxetic simulation represented a significant advancement from the earlier uniform model by introducing spatial responsiveness into the rotation logic. As shown in Figure 4.4-10 to Figure 4.4-13 , the deployment of the Tristar pattern, guided by a single attractor point within the XY plane, allowed each unit to respond dynamically to its proximity from the attractor, thereby enabling non-uniform, progressive expansion across the surface. This technique not only demonstrated the feasibility of localized control within a flat grid, but also maintained the fundamental auxetic behaviour of lateral expansion upon rotation.

Crucially, the alternating directional rotation with half of the units rotating outward and the others inward contributed to the generation of balanced deformation fields. These balanced rotational inputs helped avoid excessive torsion and allowed for a smoother deployment sequence, preserving the tessellation's modular integrity throughout the simulation process.

Geometric Limitations of 2D Rotational Constraints

Despite the success of attractor-based control in creating spatially diverse movements, the simulation revealed a number of intrinsic geometric constraints that limited its full performance within a 2D system. Most notably, the 120° maximum rotation threshold originally established during the uniform expansion tests remained a critical limiting factor. While this limit was essential to prevent geometric overlap and maintain joint separation, it also capped the system’s ability to expand further, especially in flatter configurations where more dramatic rotation would otherwise be spatially permissible.

As units farther from the attractor approached 120° of rotation, the system began to show signs of geometric saturation. The space between adjacent units began to diminish irregularly, and the expected auxetic effect started to falter, particularly along the outer edges of the grid. This saturation effect suggests that flat, planar surfaces may inherently constrain expansion potential when movement is limited to a single plane of rotation.

Inconsistencies Emerging Beyond 45° Rotation

The simulation also revealed a subtler, yet equally significant limitation: the emergence of local geometric inconsistencies beyond 45° of rotation, even within the defined 120° threshold. Units in close proximity to the attractor where distance gradients change rapidly began to deform in unpredictable ways. Specifically, the scaling of angular input over short distances led to abrupt rotational shifts between neighboring units, which in turn created non-uniform gaps, overlaps, or pinched connections within the mesh.

These inconsistencies were especially visible in the transition zones between high and low rotation regions. Rather than producing a smooth gradient, the geometry began to experience micro-fracturing visual and structural discontinuities that signaled a breakdown of the localized control logic. This outcome highlights a key vulnerability of attractor-based systems on flat surfaces: the radial distance model does not always translate into proportional deformation across tightly packed modules.

Flatness as a Constraint on Expansion Potential

One of the underlying causes of these limitations is the geometric flatness of the deployment environment. By restricting movement to a two-dimensional plane, the simulation inherently

limited the degrees of freedom available for rotation. Each triangle could only rotate about its center within the XY plane, meaning that all movement was compressed into a single planar logic. This lack of vertical articulation constrained the ability of the pattern to flex, absorb, or redistribute angular momentum spatially.

Consequently, while the attractor-based model improved movement differentiation, it also revealed the inherent shortcomings of 2D-only deployment, especially for complex applications requiring high expansion ratios or surface conformity. The closer the system came to its 120° cap, the less effective the rotation became in generating meaningful spatial displacement.

Towards Three-Dimensional Deformation Logic

These insights collectively point to a clear direction for future development: transitioning to a three-dimensional spatial framework. By introducing Z-axis variation into the attractor logic either through elevation, surface curvature, or simulated vertical displacement it becomes possible to distribute rotational demands across all three axes (pitch, yaw, and roll). This redistribution would reduce the load on any single direction of movement and potentially unlock higher expansion capacities without sacrificing structural stability or geometric continuity.

A 3D attractor model would allow for more natural gradient fields, improved alignment across deformation zones, and the ability to wrap the Tristar pattern onto non-developable surfaces. More importantly, it would provide a mechanism for absorbing angular discrepancies through vertical articulation, thereby solving the inconsistency issues observed in the flat-plane version.

This insight not only reflects a deepened understanding of auxetic behaviour in parametric systems but also reinforces the importance of spatial logic in architectural kinematic design. The next chapter will investigate this transition by expanding the attractor-based control logic into a Z-aware simulation model, incorporating curvature, gravity, and local surface normals to drive movement more realistically and responsively.

4.4.2.4 Rotating expansion based on XYZ displacement conformal mapping - Simulation trial #5

Building upon the limitations encountered in the 2D attractor-based auxetic simulation, this next stage of the study marked a significant leap into the spatial domain by introducing a three-dimensional conformal mapping strategy. The objective of this trial was to simulate how the Tristar auxetic pattern could behave when deployed over a complex, double-curved surface using XYZ displacement as the governing logic for angular rotation and unit expansion.

Grasshopper code -rational and logic

At the core of this approach is the recognition that a flat-plane attractor system while effective for progressive 2D movement cannot accommodate the curvature differentials or vertical articulation required for realistic shell deployments. To resolve this, the conformal mapping logic was constructed around a spatial reference system rooted in global geometry (Figure 4.4 -14)

The simulation begins by identifying the geometric centre of the base form, typically a freeform shell or ellipsoidal surface, and projecting this centre onto the XY plane. This central coordinate acts as the origin point (0,0,0) from which all spatial displacement values are measured. Unlike previous simulations that relied solely on XY planar distance from an attractor point, this model

introduces absolute XYZ displacement as the key input for controlling rotation behaviour across the auxetic grid.

Each triangular unit in the Tristar tessellation is assessed based on its centroid position in three-dimensional space. The Z-axis displacement how far each unit sits vertically from the base plane is isolated and used as a primary scalar variable. This Z-value is then remapped to a controlled rotation range (typically 0° to 120°), establishing a direct relationship between spatial height and angular deformation. Units located higher above the XY base expand more aggressively, while those closer to the base undergo subtler rotations. This vertical logic introduces a depth-responsive movement field, allowing the auxetic sheet to articulate itself naturally across domes, saddles, or doubly-curved morphologies.
To ensure spatial coherence and avoid abrupt deformations, the XYZ values are normalized within the grid's bounding box and then passed through a rescaling function in Grasshopper. This function serves to smooth the angular distribution and mitigate extremes in curvature that could otherwise cause overlapping geometries or rotation conflicts. Additionally, units are still rotated in a balanced alternating sequence (e.g., odd-numbered units expanding outward, even-numbered inward), preserving the internal tension and symmetry of the Tristar configuration.

This logic creates a pseudo-conformal mapping, wherein the auxetic pattern adapts responsively to the curvature of the surface it's applied to much like a textile that stretches more in some regions and less in others based on underlying topography. Importantly, the transformation is not hard-coded to fit a specific form, but rather emerges from the local geometric context of each unit relative to the base form's centre and Z-axis displacement.
Though this mid-stage simulation encountered partial failure manifesting in rotational irregularities, occasional misalignments, and limited material responsiveness the conceptual breakthrough was significant. It demonstrated a clear pathway toward spatially adaptive auxetic behaviour using XYZ-displacement as the governing driver for transformation. More critically, it introduced the notion of geometric field logic, where units are not uniformly or externally driven, but instead respond organically to the form they inhabit.

This trial laid the computational foundation for future refinement, where additional parameters such as surface normal vectors, gradient curvature analysis, or even inverse kinematic rigging could be integrated to further enhance conformality and mechanical realism. In essence, it transformed the Tristar pattern from a planar deformation system into a three-dimensionally aware architectural skin capable of adjusting its rotation and density to align with the surface it deploys over, while maintaining its auxetic nature and modular logic.

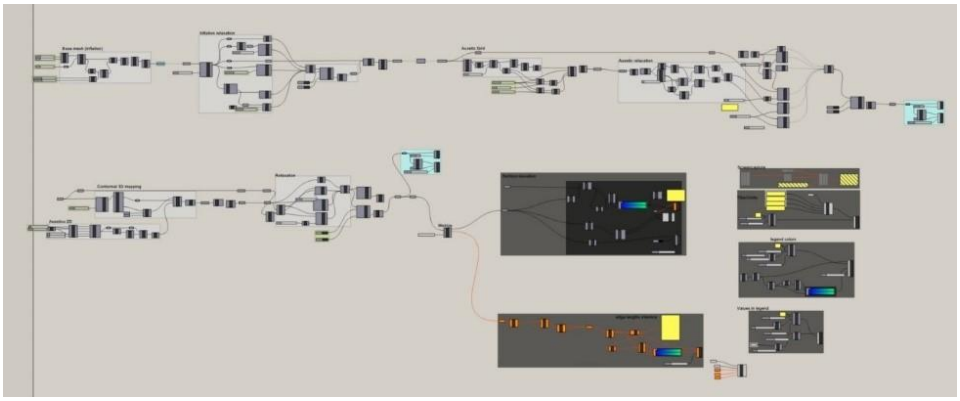

Figure 4.4-14 Grasshopper simulation for 3D expansion based on XYZ axis conformal mapping displacement – iteration #5

Results:

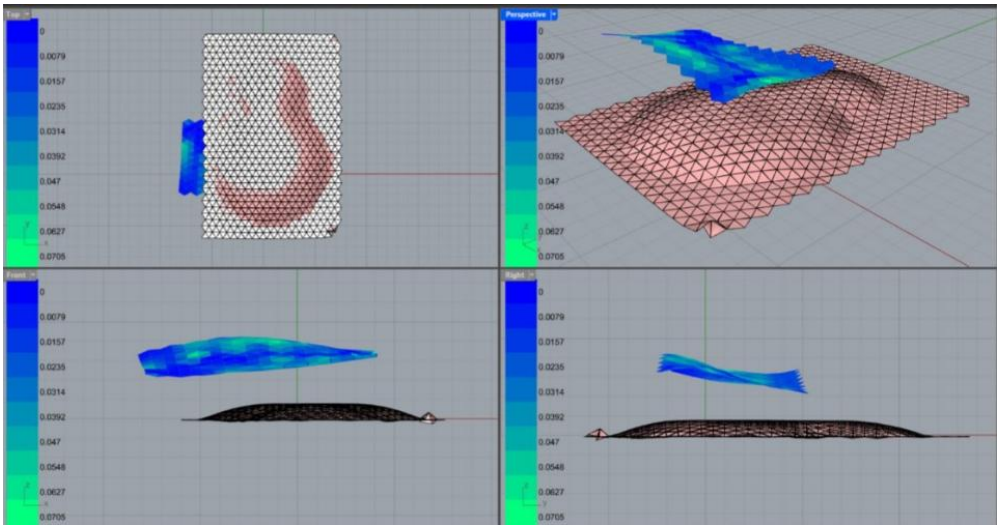

Figure 4.4-15 Isometric view of Outcomes from GH code , Tristar pattern laid on a simple double curve form. Redistribution and rotation based on the XYZ coordinates of the curvature

Reflections on the 3D Conformal Mapping Trial: Constraints and Future Direction

Observing the Limitations of Rotational Scaling on Curved Surfaces

The transition from two-dimensional attractor-based logic to a fully three-dimensional conformal mapping system represented a crucial step toward realizing an adaptable architectural skin using the Tristar auxetic pattern. However, this simulation phase also revealed a new set of challenges that became evident early in the expansion process(Figure 4.4 -15) . While the underlying logic of using XYZ displacement to drive rotation was sound in principle, its rigid implementation exposed critical geometric and parametric constraints when applied across a complex curved topology.

The most prominent issue encountered was the early breakdown of geometric coherence during expansion. As the pattern began to deform in response to curvature, units failed to rotate adequately to maintain the expected auxetic effect. The scaling function responsible for translating Z-axis displacement into rotation proved to be too restrictive, limiting many units to minimal rotation angles and effectively suppressing the system's full expansion capacity. The pattern's geometry remained largely compressed in zones where greater deformation was expected, failing to articulate the intended curvature responsiveness.

Short Curvature Radii and Over-Constrained Boundaries

This limitation was especially pronounced in areas with tight curvature radii, such as the peaks or valleys of domes and saddles. These regions require high degrees of local deformation in order for the pattern to conform seamlessly. Instead, the simulation output revealed patches of deformation rigidity, where adjacent units could not keep pace with the surface's changing geometry. The resulting behaviour resembled partial locking or under-rotation, often causing misalignment or geometric overlaps (Figure 4.4-16)

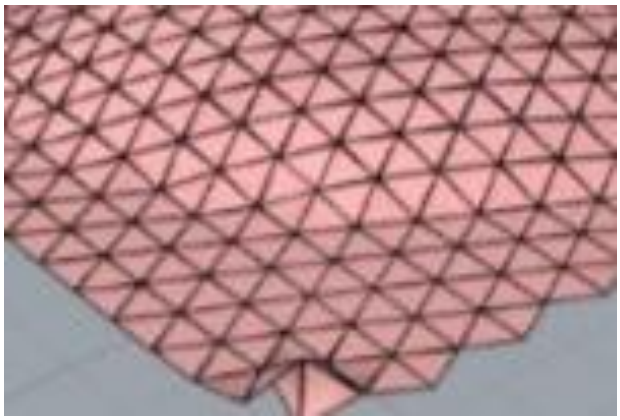

Figure 4.4-16 Zoom in of tristar simulation- error report

Analysis of the simulation script and deformation behaviour points to two primary errors. First, the rotational scaling function based on Z-displacement was applied uniformly across the entire grid, with little tolerance for variance at extreme curvatures. Second, the system remained governed by an implicit boundary logic, wherein unit rotations near edges or surface limits were constrained to avoid overlaps or collisions yet this precaution also restricted necessary movement. In effect, the model became too conservative: designed to protect against geometric instability, but in doing so, sacrificed flexibility and true spatial adaptability.

Key Learnings and Computational Recalibration

The principal insight from this trial is the recognition that achieving effective 3D auxetic deployment requires more than a linear or one-dimensional mapping of spatial displacement. While the Z-axis offered a helpful scalar in guiding vertical variation, the lack of rotational freedom across all three axes (yaw, pitch, and roll) prevented the Tristar units from realizing their full geometric potential.

Additionally, the simulation exposed the need to relax hard-coded boundary restrictions, particularly in regions of high deformation demand. Rather than limiting movement to prevent errors, future versions should focus on smart flexibility allowing the system to negotiate local curvature while maintaining enough structural logic to prevent collapse. This leads to a refined understanding: conformal auxetic behaviour must be contextually adaptive, not rule-bound. It must sense, respond, and redistribute movement according to curvature gradients, not just spatial height or surface elevation.

A Shift Toward Organic Expansion and Hybrid Control

These reflections pave the way for the next phase of experimentation, which begins to tackle the constraints revealed here through a more nuanced strategy. Rather than relying solely on displacement-derived rotation, the following chapter introduces hybrid control mechanisms that combine: Geometric center mapping with Gradient-based flexibility, and Physically-informed mechanical articulation.

By doing so, the system can explore freer movement conditions, enabling local units to rotate more or less as needed based on surface responsiveness, curvature, and material behaviour. This includes pushing beyond the strict 120° limit in digital environments (where physical collisions can be simulated), and identifying rotational sweet spots that maximize expansion without geometric failure.

Crucially, the next simulation phase will experiment with remapping rotation not only by height (Z-axis) but also by angular orientation to surface normals, offering a more holistic integration with double-curved forms. Alongside this digital recalibration, physical prototypes will be developed to test the mechanical viability of these more flexible movement strategies.

Path Forward: From Rigidity to Responsiveness

The shortcomings of this 3D trial did not signal failure, but rather highlighted the need for adaptive intelligence within the deployable system. The lesson is clear: rigid, global controls cannot accommodate the local complexity of double-curved surfaces. Instead, the system must be endowed with a more granular and responsive design logic, where each module can modulate its movement based on local geometric demand and structural thresholds.

The next chapter will take up this challenge, introducing a refined simulation method that balances digital geometry with mechanical realism. The Tristar pattern will be tested with expanded degrees of movement, integrated with real-world constraints, and eventually fabricated in scaled physical form to validate its feasibility. Through this progression, the DRSTAB system evolves from a theoretically robust concept into a structurally and spatially intelligent deployable architecture capable of expanding and adapting without compromise.

4.4.2.5 Iterative Rotating expansion based on XYZ displacement conformal mapping – simulation trial #17

Following a series of iterative simulations and refinements, the conformal remapping logic used to control the deployment of the Tristar auxetic pattern has reached a significantly more calibrated and spatially intelligent configuration. This phase marks a decisive improvement over earlier models, where rigid scalar functions, limited axis control, and over-constrained boundary logic restricted the system's ability to adapt organically to complex surfaces. In this updated approach, the Tristar pattern is now able to respond fluidly and accurately to double-curved geometries, preserving geometric continuity while delivering realistic kinematic movement. The iterative trial number 17 in this logic was the closest to one closest to the expected behaviour

Grasshopper code -rational and logic

At the core of this improved logic is a vector-based spatial mapping framework. Each triangle in the Tristar tessellation is assessed in relation to the global origin (0,0,0) typically positioned at the geometric centre of the base shell projection. Unlike prior models that focused on Z-axis displacement alone, the new logic considers absolute displacement across all three Cartesian axes (X, Y, Z), enabling full three-dimensional awareness of each unit’s spatial context. This comprehensive positioning data is essential for generating curvature-sensitive deployment behaviour, particularly in situations where the surface undulates in multiple directions simultaneously, (Figure 4.4 -17)

Yaw rotation (rotation around the Z-axis) is now governed through a non-linear parametric scaling function. Rather than applying a fixed maximum rotation across the grid, yaw values are calculated dynamically using a remapped function that scales rotational intensity based on a unit’s radial offset from the XY plane. Units located further from the base plane are permitted higher rotation values up to a strict upper limit of 120 degrees while those closer to the origin rotate less, preserving internal cohesion and avoiding overlap. The scaling curve used is intentionally non-linear to introduce a progressive expansion effect, where units do not rotate at uniform rates but rather in tuned gradients, enhancing spatial fluidity.

For pitch rotation (rotation around the Y-axis), the model incorporates an even more adaptive logic. Instead of referencing spatial position alone, pitch values are derived from the local curvature of the host surface, calculated via surface normal vectors and tangent gradient analysis. This method evaluates how sharply the surface bends at each triangle's centroid and adjusts the allowable pitch rotation accordingly. In flatter regions, pitch remains minimal to maintain surface conformity. In zones of tight curvature, pitch increases capped at a maximum of 30 degrees to allow the Tristar units to tilt and follow the topology more effectively without breaking pattern logic. This ensures that the pattern maintains tight adherence to compound geometries while avoiding deformation spikes or geometric breakdown.

Together, these rotational strategies form a multi-axis control logic that enables the Tristar auxetic grid to deploy with unprecedented fidelity across complex architectural surfaces. Unlike prior iterations, this model does not rely on global attractors or rigid thresholds. Instead, it treats each unit as a context-aware agent, capable of modifying its rotation in response to localized curvature, proximity, and overall form logic. The result is a highly responsive and geometrically coherent expansion system that remains robust under topological complexity.

The updated algorithm also introduces several important safeguards to maintain topological continuity and avoid mesh fragmentation. These include:

- Smoothing filters applied to angular outputs to prevent abrupt jumps between neighboring units.
- Rotational interpolation zones at pattern boundaries to soften edge behaviours.
- Tolerance bands for movement thresholds, ensuring units stay within deformation limits derived from material tests and digital collision simulations.

Through this comprehensive recalibration, the Tristar pattern now exhibits true 3D conformal behaviour, capable of deploying over ellipsoids, hyperbolic paraboloids, and other complex surfaces while preserving both structural rhythm and auxetic behaviour. The learnings from earlier failures in particular, over-constrained rotation logic and simplistic axis mapping have directly informed this adaptive, curvature-sensitive model.

This phase sets the foundation for physical prototyping, where the logic defined in the digital environment will be translated into mechanical systems and tested on scaled architectural forms. In doing so, it bridges the gap between computational simulation and material deployment, transforming geometric intelligence into deployable performance.

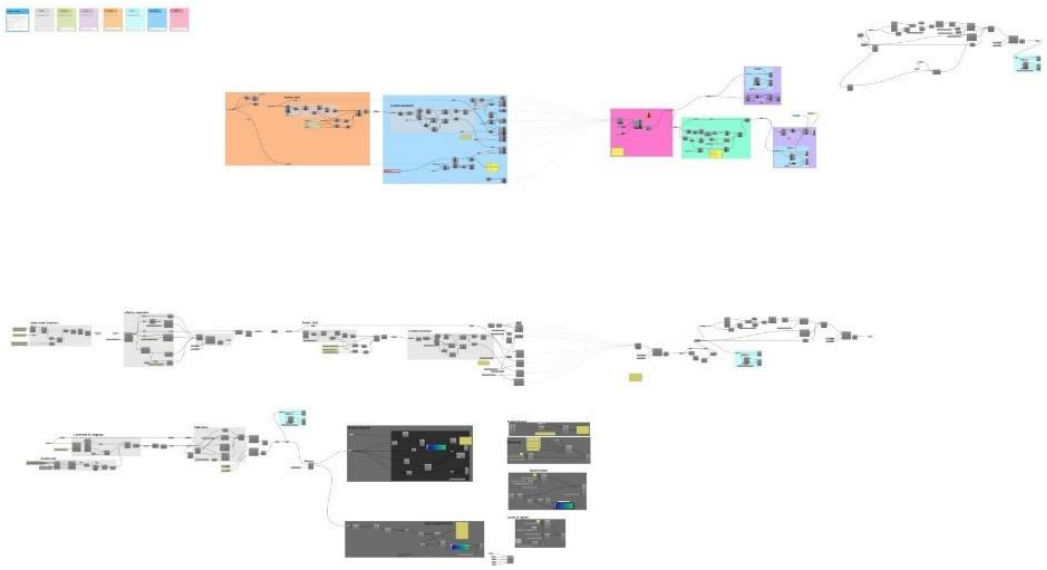

Figure 4.4-17 Grasshopper iterative simulations for 3D expansion based on XYZ axis conformal mapping displacement – Trial #23

Results in different angles

The following are the results as we change the logic between 0 ,30 ,60, 90 & 120

At angle 0 :
Laid on the curve but with 0 degree of restriction factor

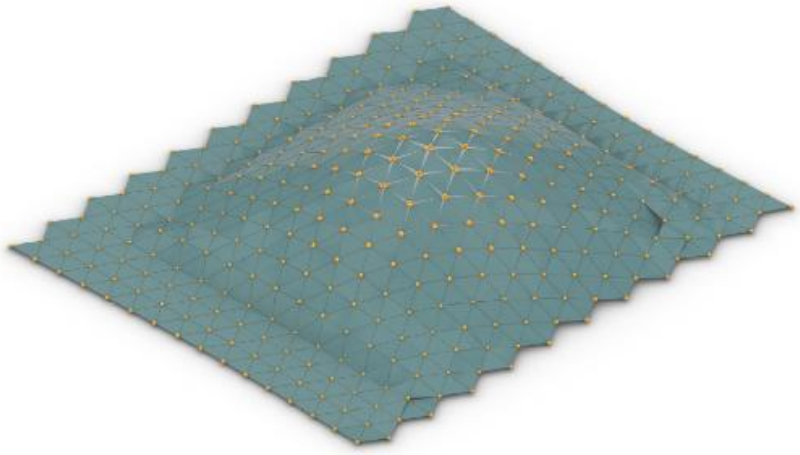

Figure 4.4-18 Displacement conformal mapping results - 0 degree restricting factor- isometric , top and front views

At angle 30 :
Laid on the curve but with 30 degree of restriction factor

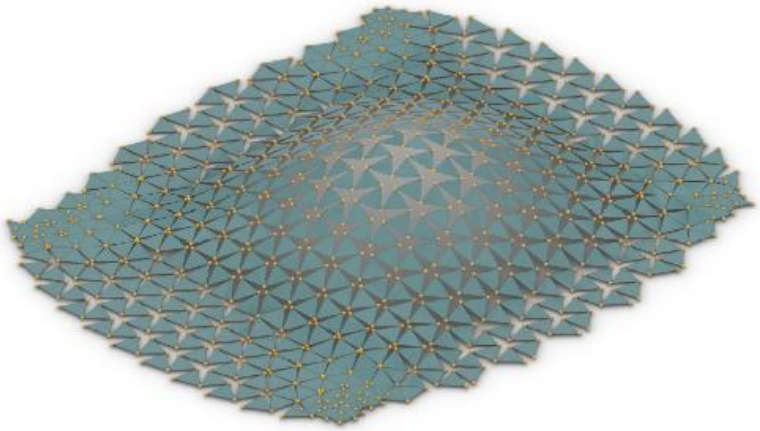

Figure 4.4-19 Displacement conformal mapping results - 30 degree restricting factor- isometric , top and front views

At angle 60 :
Laid on the curve but with 60 degree of restriction factor

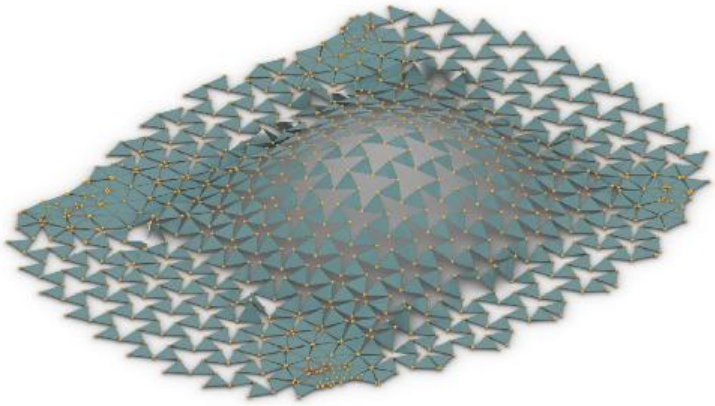

Figure 4.4-20 Displacement conformal mapping results - 60 degree restricting factor- isometric , top and front views

At angle 90 :
Laid on the curve but with 90 degree of restriction factor

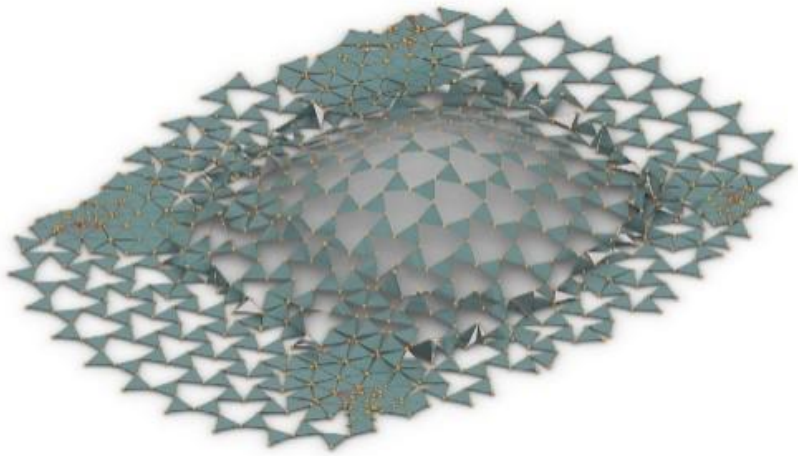

Figure 4.4-21 Displacement conformal mapping results - 90 degree restricting factor- isometric , top and front views

At angle 120 :
Laid on the curve but with 120 degree of restriction factor

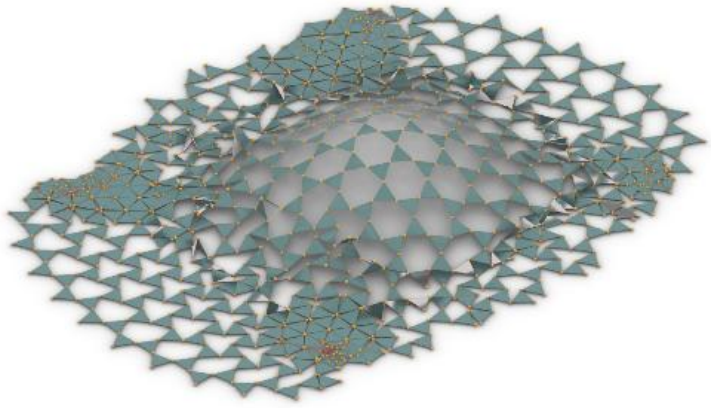

Figure 4.4-22 Displacement conformal mapping results - 120 degree restricting factor- isometric , top and front views

The Full expansion gives us the understanding of the working of code but a few parts are exhibiting undesired results as seen from Figure 4.4- 18 to Figure 4.4- 22 , so to check the accuracy of the curvature adaptation within bounds we apply a Cull logic to hide or cut off the unit triangles outside the bounding edges of the curve form .
This gave a clear delineation of unexpected reactions within the curvature bounds

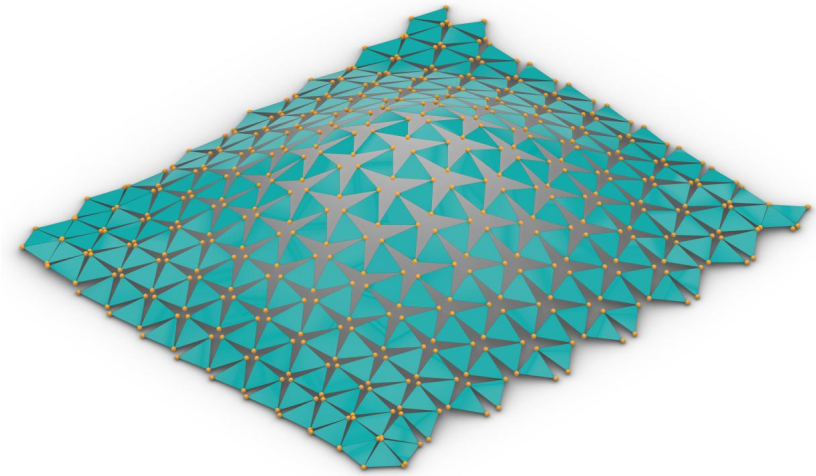

Figure 4.4-23 Displacement conformal mapping results - 30 degree restricting factor-isometric Culled outside geometry results

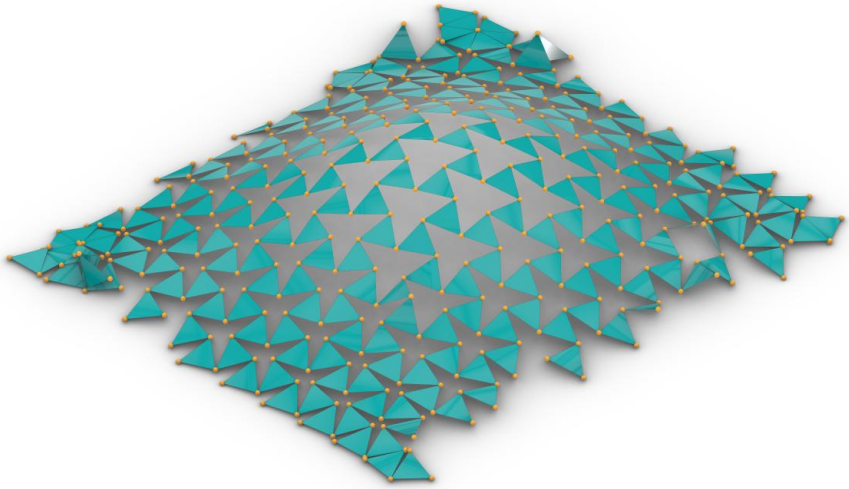

Figure 4.4-24 Displacement conformal mapping results - 60 degree restricting factor-isometric Culled outside geometry results

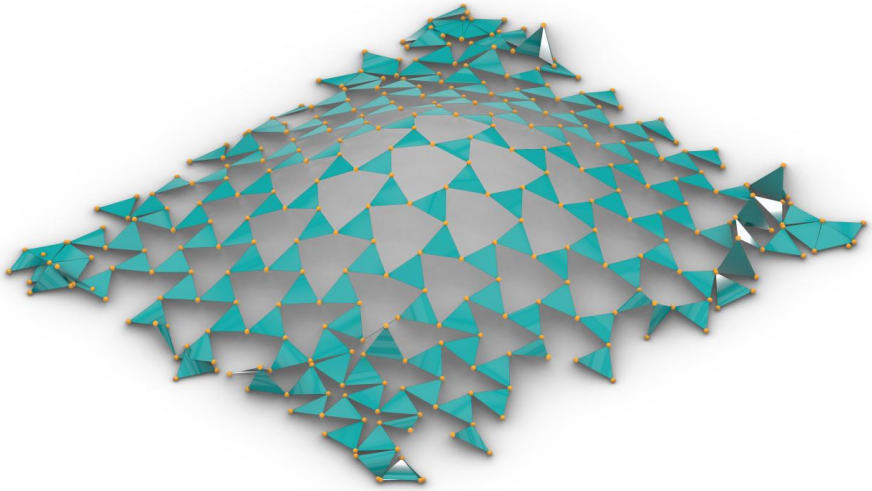

Figure 4.4-25 Displacement conformal mapping results - 90 degree restricting factor-isometric Culled outside geometry results

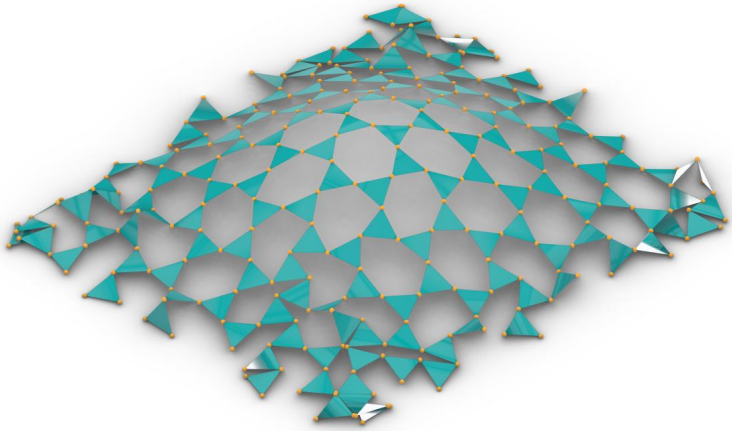

Figure 4.4-26 Displacement conformal mapping results - 120 degree restricting factor-isometric Culled outside geometry results

Reflections on Enhanced Conformal Remapping: Adaptive Movement Across Curved Surfaces

Emergence of Spatially Responsive Auxetic Expansion

The latest iteration of the conformal remapping simulation marked a critical milestone in the development of the Tristar auxetic system. By refining the parametric framework to incorporate full XYZ displacement and eliminating over-constrained boundary conditions, the model demonstrated a successful and realistic expansion logic across three-dimensional surfaces as shown from Figure 4.4-23 to Figure 4.4-26. The auxetic grid responded naturally to the curvature of the host geometry, producing a visually coherent and structurally sound deformation pattern that closely resembles the behaviour of physical auxetic materials.

The gravity-based free movement enabled the system to distribute rotational forces more organically. Instead of forcing all components into uniform expansion, the updated simulation

allowed each triangular unit to adjust independently in response to its spatial and topological context. This responsiveness not only improved deformation fluidity but also preserved the architectural integrity of the overall grid.

Verified Yaw Rotation Stability and Auxetic Holding Logic

Crucially, the system maintained stable rotational movement up to 120° across the yaw axis, confirming the upper angular threshold established in earlier trials. Units deployed near this limit continued to preserve their alignment and connection integrity, demonstrating that the parametric scaling function was appropriately calibrated for complex surface conditions. Even in regions of high curvature, the Tristar pattern maintained structural logic and visual rhythm, suggesting that the rotational control logic is now mature enough for physical translation.

This ability to "hold form" under maximum allowable rotation without experiencing geometric failure or overlap validates the effectiveness of the yaw control strategy and confirms the viability of the Tristar system for deployment on real-world curved structures.

Differentiated Expansion and Z-Axis Awareness

One of the most significant advancements in this simulation was the introduction of differentiated expansion behaviour linked to vertical displacement. By mapping rotation angles to the unit's position along the Z-axis and correlating this with curvature intensity, the system was able to generate graduated deformation across the grid. Areas of low curvature remained tightly configured, while high-relief zones expanded to accommodate spatial variation.

This Z-aware approach introduced a level of adaptive control that had previously been unachievable. The system's ability to vary its behaviour not only based on radial distance from the origin but also based on elevation and surface geometry unlocked a new dimension of precision in how the auxetic pattern adapts. This responsive behaviour mirrors physical auxetic materials, which expand more where force is concentrated or curvature is more complex.

Boundary Freedom Enables Realistic Sheet Behaviour

A key insight from this simulation was the importance of removing rigid boundary constraints. In previous versions, attempts to fix the base or edges of the pattern limited its ability to deform in a natural, fabric-like manner. By allowing the base itself to expand and shift, the entire system was given the degrees of freedom necessary to behave like a realistic auxetic skin.

This adjustment not only enhanced the visual coherence of the deployment but also more accurately mirrored the physical properties of real auxetic sheets, which tend to behave like responsive textiles rather than rigid grids. This transition from a constrained computational object to a freely adaptive, systemically coherent surface is a major conceptual advancement in the modelling of deployable structures.

Minor Geometric Irregularities and Tolerances

While the overall behaviour of the system was successful, some minor perpendicular pile-ups were observed at specific junctions particularly where multiple axes of curvature intersected. These pile-ups, likely caused by the convergence of non-linear rotation values, did not propagate or destabilize the pattern but did create localized irregularities in spacing and alignment (Figure 4.4 -27)

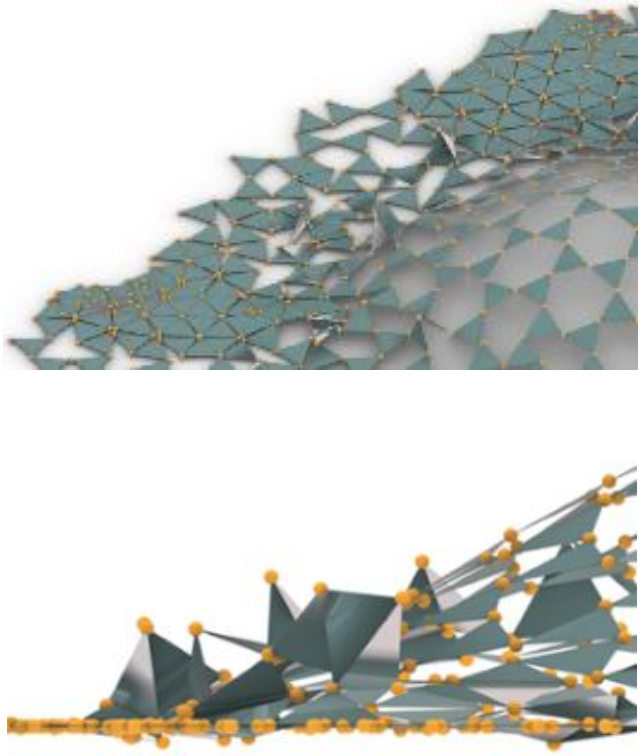

Figure 4.4-27 Displacement conformal mapping results - error reports

These small inconsistencies underscore the need for further tolerance management and the possible introduction of collision-prevention logic or joint flexibility modelling in future simulations. However, in the context of the broader deployment logic, these issues are minor and do not compromise structural performance or pattern integrity.

Establishing a Realistic, Adaptive Auxetic System

Overall, this simulation successfully delivered a working model of an adaptive, context-aware auxetic surface, capable of deploying smoothly over a wide range of curved geometries. The pattern's behaviour now aligns closely with physical expectations, demonstrating rotational fidelity, surface conformity, and spatial intelligence. This level of performance confirms that the system is ready to be translated into physical prototype development, where materials, mechanical joints, and real-world tolerances will be tested against the digital logic developed here.

This phase represents the culmination of computational refinement and the threshold for transitioning into physical realization. The insights gained here will directly inform joint design, material selection, and deployment mechanics in the next stage of research bridging simulation with fabrication and positioning the DRSTAB system for real-world implementation.

Full Grasshopper Scripts and pictures of all results and outcomes in different angles documented in Appendix F : Simulation Trials and outcomes

4.5 Physical Prototype – Proof of concept

To validate the digital simulation outcomes and test the structural and spatial behaviour of the auxetic Tristar system in real-world conditions, a detailed physical prototype was fabricated. This phase focused on translating the computationally modelled movements and rotational parameters into a tangible, testable form using accessible materials and scalable fabrication techniques. This is considered or calculated as a 1:5 scaled model of the original intended size in real scale

4.5.1 Building the model – Process documentation

This section provides a detailed account of the process undertaken to build the physical model, serving both as a validation of prior digital simulations and as a means of translating theoretical frameworks into tangible outcomes. The construction of the model followed a stepwise documentation approach, beginning with the preparation of material components and extending through assembly, calibration, and iterative adjustments. Each stage was carefully recorded to capture the challenges, refinements, and practical considerations that emerged during fabrication. This process was not only technical but also methodological, as it tested the feasibility of scaling reciprocal-auxetic systems from conceptual schematics into deployable prototypes. By documenting the workflow, the study establishes a transparent record of the decision-making processes, the tools and techniques employed, and the problem-solving strategies that shaped the final prototype. Such documentation is integral to ensuring replicability and providing a foundation for subsequent evaluation of structural performance, kinematic accuracy, and design adaptability.

Full Pictorial and step by step process captured in Appendix G : Building the model – Process documentation

4.5.2 Deployment Behaviour and Motion Testing

Upon completion, the prototype was tested in a series of deployment trials. These included flat-to-curved transitions, contraction and expansion cycles, and conformance to convex, concave, and asymmetrical surface forms. The auxetic behaviour was clearly exhibited throughout the grid, with smooth, cohesive expansion in response to outward forces. The system maintained visual and structural integrity, demonstrating the effectiveness of the rotational joint logic even in a simplified physical form. Deployment was guided using a manual nylon string pulley system, inspired by marionette logic, allowing targeted curvature generation and controlled deformation. Six progressive stages of expansion were documented from a fully contracted flat sheet to a fully deployed, curvature-adaptive surface.
The stages of deployment has been documented in Figure 4.5-1 to Figure 4.5-4 ,

Stage 1

Fully retracted and compressed. Laid flat

Figure 4.5-1 Deployment behaviour and analysis of Scaled prototype- Stage 1

Stage 2

Base rail moved outward by 30 mm to 50 mm center points lifted by ~100 mm

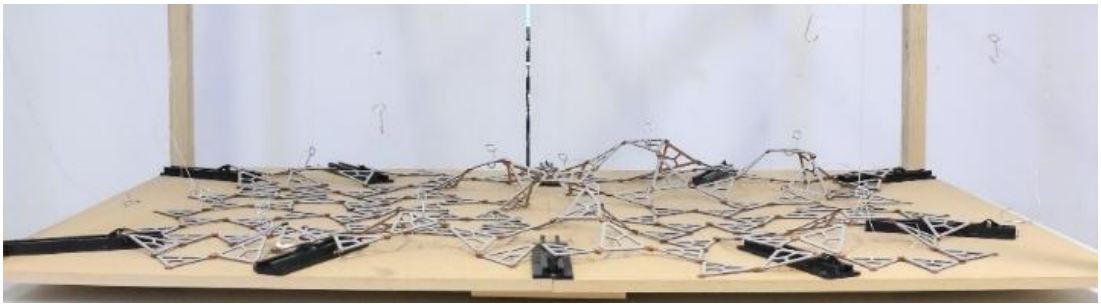

Figure 4.5-2 Deployment behaviour and analysis of Scaled prototype- Stage 2

Stage 3

Base rail moved outward by 30 mm to 50 mm centre points lifted by ~200 mm

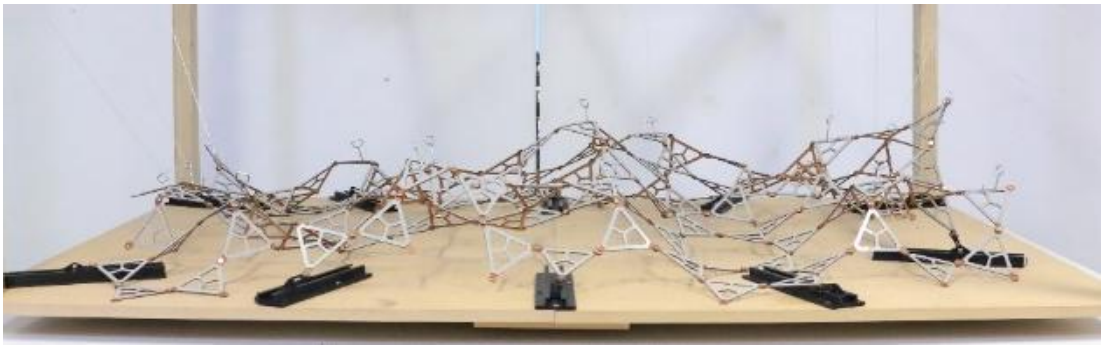

Figure 4.5-3 Deployment behaviour and analysis of Scaled prototype- Stage 3

Stage 4

Base rail moved outward by 30 mm to 50 mm centre points lifted by ~300 mm

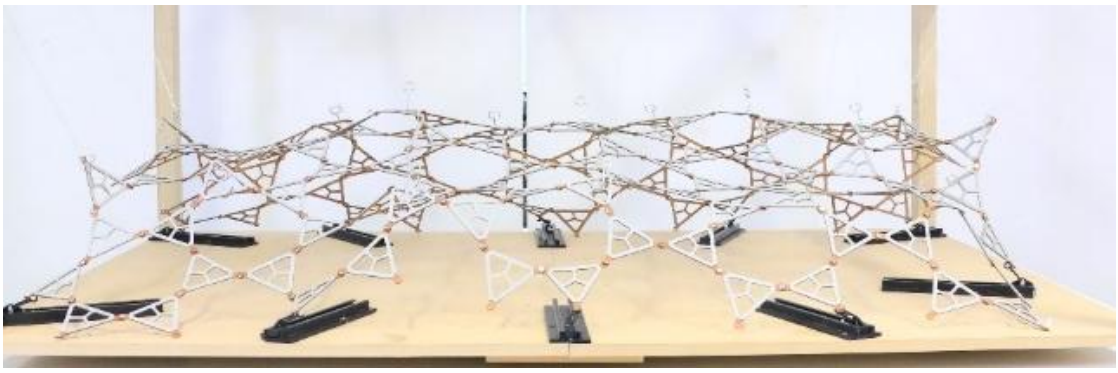

Figure 4.5-4 Deployment behaviour and analysis of Scaled prototype- Stage 4

Complete Photo documentation of prototype model deployment explored in Appendix H : Deployment Behaviour and Motion Testing

4.5.2.1 Observation and Inference :

As illustrated from Figure 4.5-1 to Figure 4.5-4 , the prototype successfully demonstrated the anticipated auxetic behaviour, expanding and contracting as a unified system while maintaining overall structural coherence across its 132 interconnected units. The deployment sequence confirmed that the pattern not only translated geometric theory into physical behaviour but also preserved stability throughout its range of motion. Controlled manipulations revealed smooth transitions from a flat, planar state into a variety of complex three-dimensional curvatures without noticeable misalignment or unit disengagement.

By selectively adjusting the nylon string actuation system, the prototype was tested under multiple curvature configurations, including concave, convex, and asymmetrical conditions. In each scenario, the sheet adapted seamlessly, showcasing a high degree of responsiveness, geometric continuity, and flexibility. These trials demonstrated the system's capacity to accommodate both uniform and non-uniform deformations, an essential requirement for real-world applications where surfaces are rarely regular.

Importantly, the structure exhibited predictable deformation boundaries, avoiding uncontrolled folding or localized failures. This confirmed not only the theoretical auxetic logic but also the practical viability of the prototype as a conformal, curvature-adaptive skin. The ability to achieve such behaviour within a defined and safe deformation range reinforces the potential of this system for scalable deployment in architectural contexts where adaptability and reliability are critical. While most of this reacted successfully as expected there were some minor setbacks in the model.

Instability in Locking Mechanisms

The 3D-printed track systems used in this research revealed recurring instabilities in achieving reliable locking performance during deployment trials. In several instances, the intended one-way locking failed to engage consistently, causing joints to retract or slip back unexpectedly under minor stress conditions(Figure 4.5-5) . This not only undermined structural coherence but also raised concerns about durability when subjected to repeated cycles of expansion and contraction. The fragility of the locking design became particularly evident during stress redistribution, where local joint instability propagated across adjacent units, amplifying the risk of collapse. Such inconsistencies point toward the need for more robust mechanical joinery, potentially incorporating reinforced bearing systems, double-lock ratchets, or hybrid solutions that can guarantee unidirectional stability. Without these improvements, the current system risks unintentional reversals during deployment, ultimately compromising the reliability of the shell. Addressing this limitation is critical for transitioning from small-scale trials to large-scale architectural applications.

Figure 4.5-5 Instability in base rail Locking Mechanisms

Unintended Vertical Piling of Units

During deployment, an observed limitation was the unintended vertical stacking or piling of triangular units instead of their smooth expansion along the designed axes (Figure 4.5-6). This irregular motion created localized kinematic jams, disrupting the intended auxetic expansion pattern. The problem stems partly from uneven stress distribution and insufficient synchronization between interconnected modules, which caused some elements to absorb higher compressive forces and deviate from their designed paths. Misalignments at hinge points further exacerbated this behaviour, as even small tolerances in fabrication accumulated across the system and led to large-scale motion irregularities. These findings highlight that geometric consistency alone cannot ensure successful deployment; mechanical precision and tolerance management are equally critical. Addressing this issue requires refining the distribution of stresses through improved joint articulation, possibly supported by flexible connectors or guiding tracks. Such improvements would ensure smoother expansion, reduce irregular kinematic flow, and enhance the predictability of large-scale deployments.

Figure 4.5-6 Unintended Vertical Piling of Units

Weaknesses in Anchoring Systems

Anchoring systems play a crucial role in stabilizing deployable shells, yet trials revealed that the existing solutions lacked adequate reliability. Anchors intended to fix the base structure frequently experienced slippage and displacement, particularly under tensile stresses generated during deployment. This instability at the points of contact reduced overall coherence, creating an imbalance between anchored and moving units. The insufficiency was most evident on uneven or flexible surfaces, where anchoring forces failed to adapt to variations in terrain, leading to partial destabilization of the system. Another challenge emerged from the free rotational tolerance of the 3D-printed parts, which allowed excessive movement at the joints and reduced the effectiveness of tensioned strings during deployment. To mitigate this, anchoring clips had to be introduced to secure the strings in place and prevent unintended loosening (Figure 4.5-7). These combined weaknesses emphasize that without a robust anchoring framework, even well-designed reciprocal-auxetic mechanisms cannot achieve full structural stability. Future iterations must consider stronger, adjustable anchors capable of embedding into diverse ground conditions, alongside mechanisms to limit undesired rotational play, in order to ensure stability during both static and dynamic phases of deployment.

Figure 4.5-7 Reinforcing Weaknesses in Anchoring Systems

Dependence on Auxiliary Supports

A recurring challenge observed during deployment was the structure's heavy dependence on auxiliary supports, such as temporary bracing or external scaffolding, to maintain geometric alignment and resist undesired deformation. While conceptually the system aimed to achieve self-supporting behaviour once partially deployed, in practice it frequently sagged or distorted

without these external interventions (Figure 4.5-8). This reliance suggests that the structural stiffness inherent in the reciprocal-auxetic framework remains insufficient at early stages of deployment when forces are unevenly distributed. Auxiliary supports compensated for these weaknesses but at the cost of efficiency, portability, and simplicity the very qualities that deployable systems are designed to enhance. For architectural-scale applications, eliminating or reducing this dependency is critical. Potential strategies may include integrating pre-tensioned elements, employing more rigid joint mechanisms, or optimizing unit sequencing to ensure inherent self-support during deployment. Addressing this issue would allow the system to transition from conceptual feasibility to practical implementation.

Figure 4.5-8 Dependence on Auxiliary Supports

Manual Interventions in Deployment

Despite the intended automated nature of deployment, the system often required significant manual intervention to ensure smooth progression. Operators had to correct misaligned joints, guide units into place, or provide additional force at critical points to maintain deployment momentum. This level of human involvement not only reduced efficiency but also revealed a disconnect between digital kinematic models and real-world material behaviour. Computational simulations had suggested that the system would expand predictably; however, physical prototypes exposed frictional resistance, joint tolerances, and material flexibilities that impeded smooth motion. The reliance on manual adjustments underscores the immaturity of the current design, suggesting that further refinements are needed in both joint design and motion sequencing. In future, this gap could be mitigated by incorporating guiding tracks, low-friction materials, or semi-mechanized actuation systems that bridge the gap between conceptual design and autonomous functionality. Until then, manual corrections remain a limiting factor in achieving reliable deployability.

4.5.3 Versatility in Shape Conformance

A defining test for the tristar auxetic system was its capacity to conform to a variety of three-dimensional geometries. In architectural contexts, deployable surfaces are rarely planar or uniform; instead, they must negotiate double-curved topologies that combine compression, stretching, and directional bending. Evaluating how the system responds to these curvatures was therefore essential to understanding its true adaptability. By referencing the catalogue of 3D printed forms developed earlier in the study, the auxetic sheet was manipulated across a series of controlled geometric trials, replicating as closely as possible the complex morphologies that had already been digitally and physically modelled. This is documented from Figure 4.5 -9 to Figure 4.5 -18.

The first set trials involved concave bowl-like configurations, where the sheet was deployed to evaluate how the units responded to compression along the Z-axis. This geometry tested the ability of the joints to stabilize under inward pulling forces while maintaining continuous surface logic. The second set of experiments focused on convex dome formations, which inverted the

stress conditions and required the auxetic sheet to expand outward smoothly. The dome trials were particularly significant as they align with many natural and architectural precedents, testing the system's strength in resisting pull-back while ensuring directional expansion.

The system was also tested against asymmetric warps and saddle-like hyperbolic paraboloid geometries, both of which are challenging due to their non-uniform stress distributions. These trials examined whether the differentiated expansion of the auxetic sheet could align itself to complex directional pulls and twisting forces without introducing distortions or vertical piling.

Across all these experiments, the sheet demonstrated reliable conformity, closely mimicking the performance observed in the earlier PETG laser cut prototypes (Chapter 4.2.3) . The differentiated expansion across the pattern responded accurately to local stress variations, allowing the structure to adapt dynamically to each form. This adaptability validated the system's potential for architectural use, confirming that the auxetic pattern could accommodate a broad spectrum of double-curved geometries with structural coherence and minimal additional intervention.

Shape 1

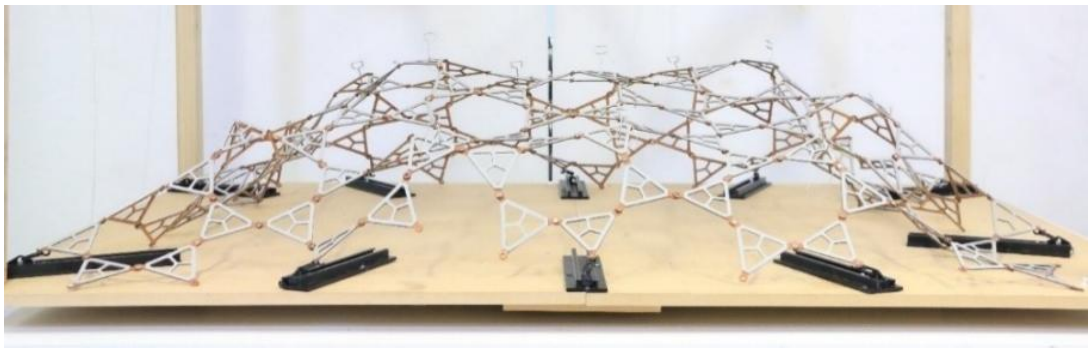

Figure 4.5-9 Scaled prototype check for versatility - shape 1

Shape 2

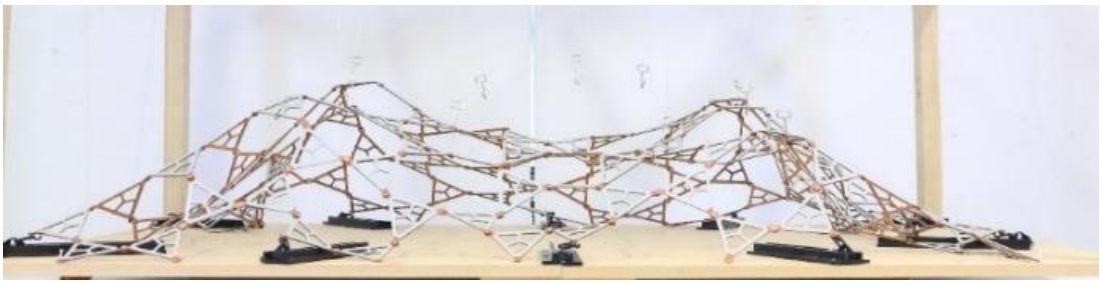

Figure 4.5-10 Scaled prototype check for versatility - shape 2

Shape 3

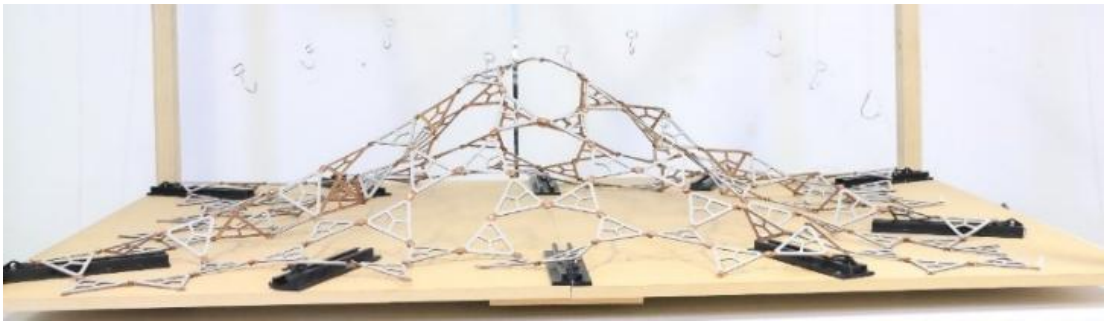

Figure 4.5-11 Scaled prototype check for versatility - shape 3

Shape 4

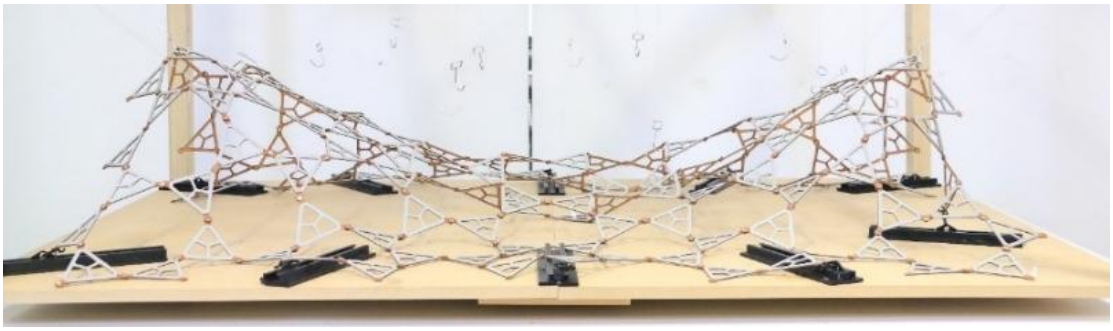

Figure 4.5-12 Scaled prototype check for versatility - shape 4

Shape 5

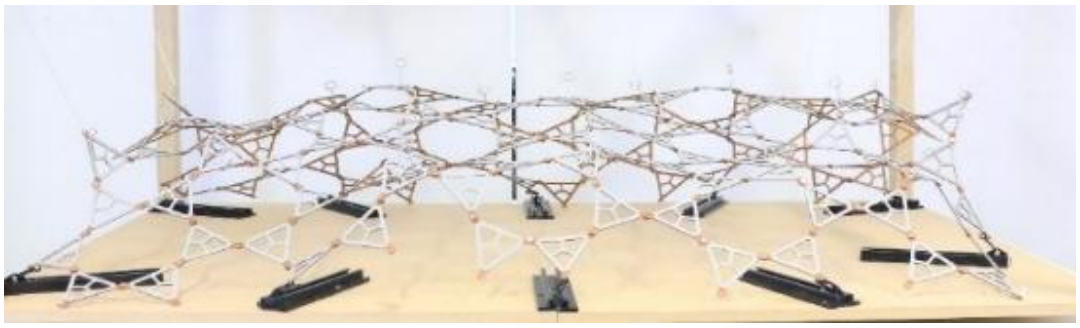

Figure 4.5-13 Scaled prototype check for versatility - shape 5

Shape 6

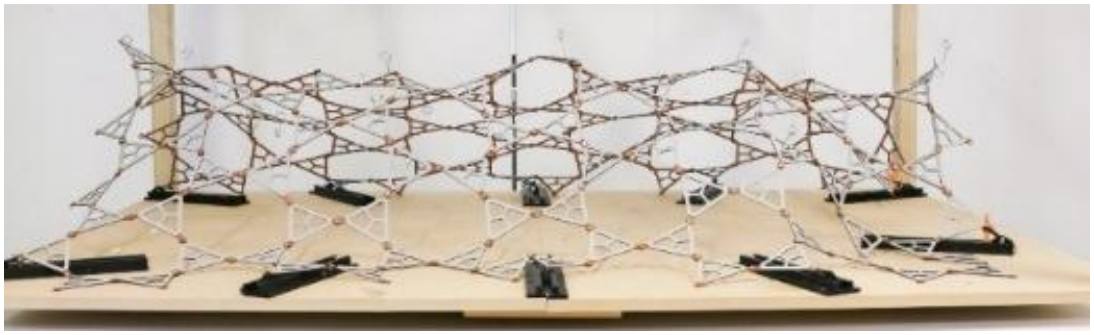

Figure 4.5-14 Scaled prototype check for versatility - shape 6

Shape 7

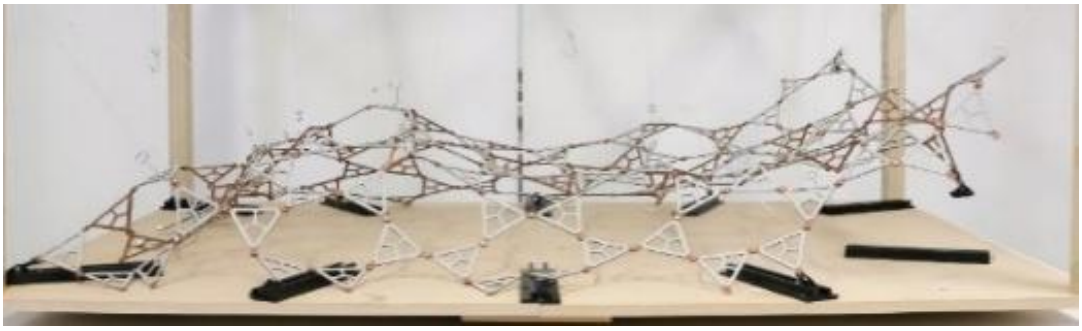

Figure 4.5-15 Scaled prototype check for versatility - shape 7

Shape 8

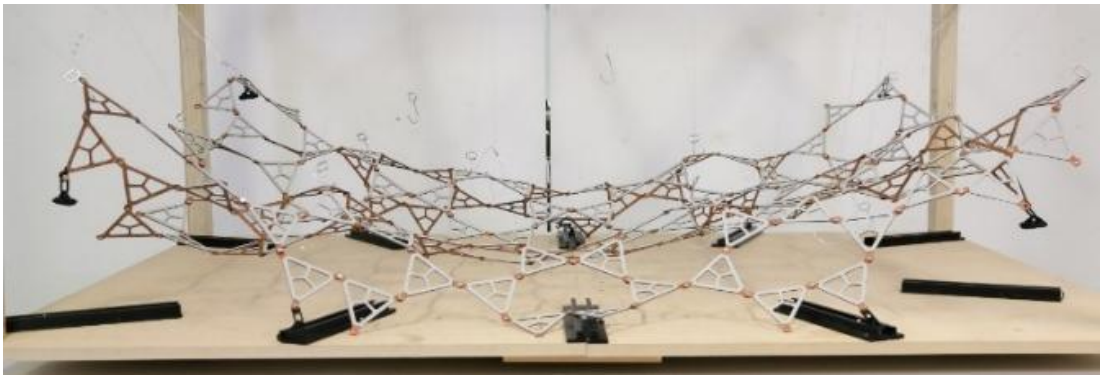

Figure 4.5-16 Scaled prototype check for versatility - shape 8

Shape 9

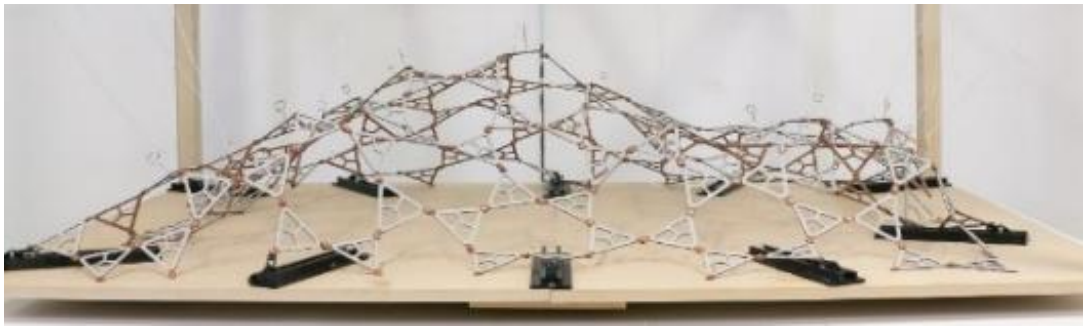

Figure 4.5-17 Scaled prototype check for versatility - shape 9

Shape 10

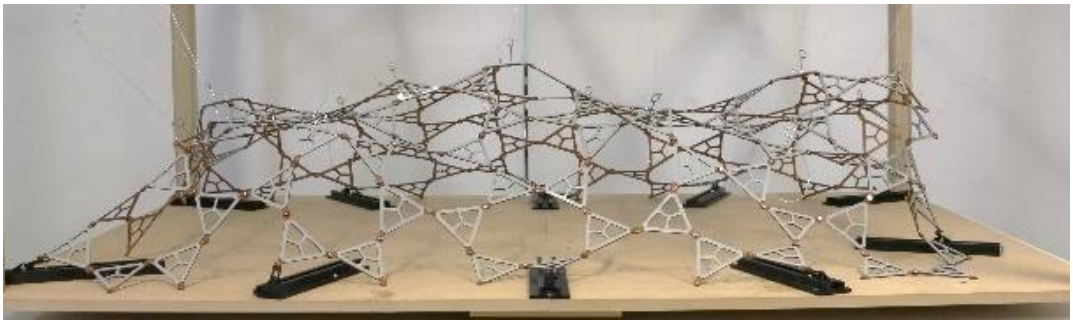

Figure 4.5-18 Scaled prototype check for versatility - shape 10

Full Photo documentation of Prototype Shape versatility explored in Appendix I : Versatility in Shape Conformance

4.5.3.1 Observations on Local Behaviour and Edge Conditions

During the testing phase, as exhibited from Figure 4.5-9 to Figure 4.5-18 , the prototype exhibited several localized behaviours that provided valuable insights into the mechanical functioning of the tristar auxetic system. One recurring phenomenon was the occurrence of perpendicular pile-ups at junction points, particularly when the system was subjected to extreme deformation or manipulated across zones with sharp curvature transitions. Importantly, these pile-ups did not propagate further across the tessellation and remained localized, functioning as minor stress absorbers rather than critical failures. This behaviour highlighted an inherent degree of fault tolerance within the system, demonstrating its ability to accommodate irregularities without compromising overall stability.

Another significant factor observed was the influence of edge conditions. Units located near the boundary of the tessellation rotated more freely compared to those embedded within the core of the sheet. This was attributed to the absence of adjacent modules, which normally act as natural dampers, restricting excessive freedom of movement. The resulting behaviour underscores the importance of edge stabilization strategies in scaled applications. Without reinforcement, edge modules risk departing from the intended angular discipline, producing inconsistencies in deployment and curvature conformance. As such, future iterations will require careful articulation of edge frames or boundary stiffening elements to ensure controlled and uniform motion across the sheet.

4.5.3.2 Limitations and Mechanical Learnings

While the prototype successfully demonstrated its overall adaptability, several limitations became evident, offering direct lessons for refinement in future prototypes.

Material-based constraints: The leather components, originally intended to restrict pitch rotation to 30°, proved inadequate in practice. Under repeated stress, they permitted excessive flexibility, leading to instances of over-bending and geometric irregularities. This indicated that material-based constraints alone are insufficient for precise control.

Joinery tolerances: The binder screws employed in the assembly allowed unrestricted yaw rotation, occasionally exceeding the intended 120°. While these over-rotations did not destabilize the grid, they diverged from the angular discipline established in digital simulations, reducing predictability during complex transformations.

Absence of locking mechanisms: The prototype lacked active locking systems, resulting in transformations that were less controlled during rapid or uneven manipulations. This absence required manual intervention to stabilize the deployment, highlighting the necessity of engineered joint mechanisms in future scaled models.

Together, these mechanical learnings emphasize the need for precision-engineered articulation in future versions, where mechanical locking and controlled tolerances must replace or supplement material flexibility to ensure reliability at architectural scales.

Prototype as Proof of Concept

Despite the mechanical inconsistencies noted in testing, the 1:5 scale prototype ultimately served as a strong proof of concept for the tristar auxetic system. The model demonstrated that the underlying geometric logic is structurally viable when subjected to a variety of transformations, confirming that the principle of reciprocal auxetic expansion can indeed be achieved through modular assembly. The deployment sequences showed that even with relatively simple joinery systems, the units were able to expand and contract cohesively, producing spatial adaptability that closely aligned with the behaviours predicted in digital simulations.

One of the most significant outcomes was the ability of the prototype to conform to a wide range of curvature types, including concave bowls, convex domes, and asymmetric saddle-like geometries. The tristar tessellation maintained its structural integrity across these forms, validating its versatility and adaptability as a deployable architectural skin. This adaptability was not only a demonstration of geometric compatibility but also an indication that the system can respond dynamically to local stress variations. In several instances, the differentiated expansion across the sheet aligned with zones of tension and compression, confirming that the system's behaviour follows an adaptive logic rather than rigid uniformity.

While material inconsistencies in the leather joints and tolerance gaps in the binder screws created minor deviations from the idealized performance, these imperfections were expected at prototype scale and did not undermine the broader design objectives. Instead, they offered valuable feedback for the refinement of future iterations, highlighting where mechanical precision and material substitution will be most critical. More importantly, the successful demonstration of deployment, shape conformance, and adaptability validated the DRSTAB framework as a credible approach to deployable architectural systems.

Taken together, the findings affirm that the prototype has moved the concept beyond speculative digital modelling and into a physically testable domain. By proving that the tristar auxetic system can function under real conditions, even with non-optimized components, the study establishes a clear trajectory toward full-scale fabrication. Future work will focus on developing precise mechanical joineries, refined material strategies, and integrated locking systems, building upon this prototype as an essential stepping stone in the transition from concept to deployable architectural reality.

4.6 Summary of Chapter 4

This chapter focused on understanding and validating the 3D movement behaviour of the selected Tristar auxetic pattern, extending the two-dimensional expansion logic into spatial (x, y, z-axis) deployment characteristics. Through a series of detailed digital simulations and physical mock-ups, the study successfully mapped out the complex interactions of pitch (Y-axis) and yaw (Z-axis) rotations that occur when the pattern is subjected to mechanical actuation. These rotational movements were systematically isolated and examined, revealing how the auxetic configuration enables significant and coordinated transformation across surface curvature without introducing local stress concentrations or material inconsistencies.

A key insight from this phase was the non-essential nature of roll (X-axis) movement in contributing to deployability within this framework. Although minor roll was observed during motion capture, it did not significantly affect the overall transformation of the system and was therefore excluded from further mechanical replication. This decision was vital in simplifying joint design parameters for subsequent prototyping.

The chapter also underscored the importance of node-centered articulation. Digital simulations run in Grasshopper, combined with mesh morphing and stress flow analysis, emphasized that expansion was most efficient when the rotational axis was fixed at nodal junctions precisely where reciprocal struts converge. This finding will directly inform the mechanical joint design process outlined in the next chapter.

From a methodological perspective, the synergy between computational kinematic models and physical proof-of-concept assemblies proved invaluable. Where the digital simulation ensured precise quantification of angular ranges, the physical tests helped identify behavioral nuances like frictional resistance and unintended deformations under load, both of which must be addressed in future material selection and joint tolerancing.

Overall, this chapter validates the core hypothesis that the selected auxetic pattern, when properly articulated, exhibits highly controlled, two-axis rotation conducive to deployable double-curved surfaces. The next stage of this research will transition from representational movement studies to mechanical embodiment, embedding the inferred angular rotations into real-world joinery solutions. This pivot from abstract to engineered systems is critical in realizing an architectural deployable shell system that is not only morphologically elegant but also mechanically feasible and constructible.

Chapter #5

Assemble / Analyse / Assure

Mechanical Prototype

Technical Simulations

Inferences & Report

5 Chapter 5 – Mechanical Joineries

5.1 Introduction

Following the spatial breakdown and movement analysis of the Tristar auxetic pattern in Chapter 4, this chapter marks a shift from geometric behaviour to mechanical articulation, where the digital logic and kinematic principles established earlier are translated into engineered systems capable of physically performing the same dynamic transformations. This chapter tries to find solutions for RQ 3.

The previous chapter revealed the critical role of yaw and pitch rotations in achieving adaptive curvature through the Tristar system, particularly in its ability to conform to double-curved surfaces with controlled expansion. While roll (X-axis) rotation was considered during simulation, its negligible impact on structural performance in both physical and digital tests led to its exclusion from the mechanical replication phase. The insights gained from Grasshopper and Kangaroo-based parametric simulations, as well as the scaled PETG prototype experiments, confirmed that the essential spatial responsiveness of the Tristar pattern could be distilled into two primary rotational degrees of freedom. The aim of this chapter is to investigate how these movements previously observed as emergent behaviours of geometric rules can be actively reproduced through mechanical systems and components that can eventually operate in full-scale, deployable architectural environments.

The first step in this investigation involves isolating the yaw and pitch behaviours through conceptual mechanical joinery mock-ups. A series of experimental assemblies were developed using accessible materials such as laser-cut acrylic, plywood, custom fasteners, and binder screws, each designed to perform either one or both identified degrees of rotation. These physical prototypes were not intended to replicate the entire structure but to serve as functional abstractions that test whether rotation can be mechanically enabled, restricted, and controlled in predictable ways. Key experiments in this stage included the fabrication of dual-axis mock-ups, one-axis locking ratchets, and modular components with adjustable angular tolerances. These physical explorations allowed for empirical evaluation of movement limits, joint clearances, binding friction, and cumulative motion behaviour. The goal was to determine if the geometric movement of the Tristar units originally driven by material compliance and digital constraints could be replicated through passive mechanical logic, without relying on motors, actuators, or external force systems. These trials revealed valuable information about the role of joint thickness, axis positioning, and the tolerance hierarchy required for sequential deployment. More importantly, they highlighted the limitations of using off-the-shelf components, which often failed to provide the precision and flexibility necessary for complex, multi-axis movement at architectural scales. As a result, the study began to evolve toward the design and simulation of customized mechanical joinery, calibrated specifically for the geometric and kinematic needs of the DRSTAB system.

To advance this development, the next phase of the chapter introduces the use of SolidWorks, a CAD and simulation platform widely adopted in mechanical and structural engineering fields. While previous modelling efforts were largely rooted in visual parametric tools like Grasshopper ideal for controlling geometric relationships and spatial deployment logic SolidWorks enables precise modelling of constraints, material properties, and physical interactions such as contact forces, friction, and gravitational loading. Here, the focus shifts from form generation to mechanical feasibility, where the performance of proposed joints can be numerically evaluated and optimized prior to fabrication. Using this platform, a range of joint types including single-axis ratchets, one-way bearings, and rotational pivots were digitally constructed and tested in simulated environments. Each joint was examined through a hierarchical scaling model: first as a single unit, then as a 2-unit connection, followed by a 6-unit module, and finally within a 32-unit shell array. This approach mirrors the logic used in

earlier geometric evaluations but adds a layer of mechanical constraint to understand how rotation is influenced by component thickness, anchoring method, and accumulation of tolerance errors across the system.

The SolidWorks simulations were specifically designed to test deployment behaviour under realistic boundary conditions. They assessed whether angular expansion would be achievable within mechanical limits and whether the system could self-lock at desired thresholds. Special emphasis was placed on ratcheting behaviour, as this allows the system to incrementally expand and hold its position without external locking mechanisms a key requirement for deployable structures intended for fast assembly in the field. Simulations also tested how joints behaved under gravitational load and minor misalignment, revealing the weak points in both design and connection logic. These tests were instrumental in refining the proposed joinery by identifying where additional support or material flexibility would be required, and where motion could be optimized to prevent binding or jamming in compact configurations. Furthermore, by embedding torque analysis and constraint-based motion sequencing into the simulation, the study could preemptively identify potential mechanical conflicts that would arise in physical assembly.

To validate the digital findings and explore their real-world implications, the chapter concludes with a return to physical experimentation this time at full 1:1 architectural scale. Selected joint designs, developed and optimized through SolidWorks, were fabricated using a combination of CNC-machined acrylic parts, 3D-printed elements, and steel fasteners. These components were assembled into functional test rigs that could perform the same motions tested in simulation, providing an essential reality check between digital logic and physical behaviour. The full-scale prototypes were tested for accuracy of movement, mechanical stability, rotational limit control, and ease of manual deployment. While minor discrepancies between digital and physical behaviour were expected due to material imperfections and frictional inconsistencies, the overall comparison validated the simulation pipeline and proved the feasibility of customized mechanical articulation for deployable systems. These full-scale prototypes also exposed key insights into practical assembly logistics, such as tolerances required for snap-fit integration, the ease of tool-less locking, and the effect of material stiffness on cumulative movement propagation.

Ultimately, this chapter bridges the gap between digital design and real-world deployment, establishing a complete loop from geometric pattern analysis to mechanical articulation and back again through simulation-informed fabrication. It highlights how a deployable system like DRSTAB does not rely solely on innovative geometry but must be grounded in the principles of precision mechanics to function at scale. The findings of this chapter support the broader thesis that architectural deployability is not a product of form or function alone but emerges from the dynamic interplay of both, made tangible through engineered connection systems. As the research moves toward full-shell simulation and load-bearing testing in the subsequent chapters, the results presented here form a critical foundation validating the mechanical feasibility of DRSTAB's most fundamental movement behaviours and offering a scalable roadmap for its architectural implementation.

5.2 Mimicry of Auxetic Movement in Mechanical Joinery

Following the spatial and kinematic analysis of the Tristar auxetic pattern, the research progresses toward replicating its key deformation behaviours through mechanical means. The goal of this stage is to translate the inherent geometric movements previously observed in simulations and physical overlays into engineered joint systems capable of producing controlled, repeatable motion. The focus lies on reproducing two principal degrees of freedom: yaw rotation (Z-axis twist) and pitch rotation (Y-axis tilt), which together enable the sheet to

expand, conform to curvature, and deploy across doubly curved surfaces. While roll rotation (X-axis banking) was initially considered, its influence on the overall transformation was minimal in physical tests and digital simulations, and thus it is excluded from this phase of study.

To explore this mimicry, a series of conceptual mock-ups were constructed using custom mechanical joinery designed to isolate and demonstrate each axis of movement independently. These physical models served as simplified analogues of the Tristar pattern's behaviour, allowing for hands-on testing of rotational range, locking behaviour, and structural stability. Rather than aiming to replicate the entire geometry, the focus was on validating whether passive mechanical systems such as pivot joints, ratchets, or one-way mechanisms could accurately reproduce the angular transformations observed in the pattern. These early experiments were crucial for understanding the tolerances, axis placement, and joint design requirements needed to scale the system effectively. The results of this phase laid the foundation for more detailed mechanical simulations and full-scale prototypes, confirming that the essence of auxetic motion could be captured and controlled through precisely engineered joint logic.

Once digital movements are fully understood, the focus shifts to physical realization. In this section, we begin translating the motion logic of the Auxetic system into mechanical joinery concepts. This translation is not one-to-one; while digital models can simulate limitless motion, physical prototypes are bound by material behaviours, friction, wear, and manufacturability.

5.2.1 Prerequisite iterations from the master thesis

In the earlier research by Jayachandran (2019), mechanical joineries were investigated primarily at a conceptual level, with representations limited to diagrammatic inferences. However, critical factors such as dimensional constraints, material properties, and mechanical tolerances were not considered during that phase. The joinery designs proposed (Figure 5.2-1) were relatively bulky and risked spatial overlap within the system's voids an issue not addressed at the time. While these early explorations did not adhere to any established mechanical design codes, they provided a valuable conceptual foundation for future work. Importantly, the thesis outlined clear directions for continued development, offering a strong starting point for this research to pursue more refined, code-compliant, and dimensionally viable joinery solutions.

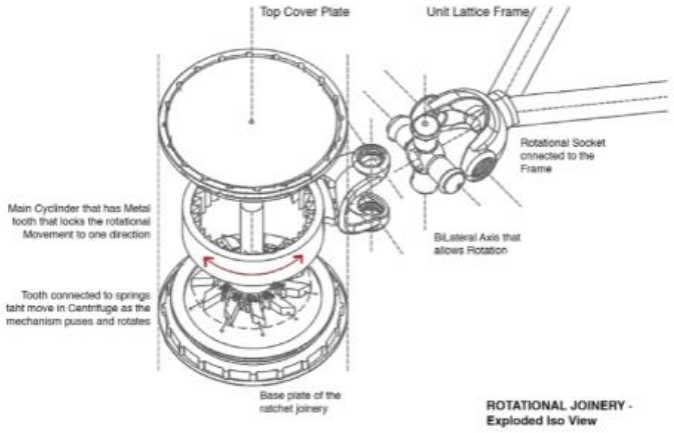

Figure 5.2-1 Inferences from Conceptual mechanical joinery design from earlier research

The joint typologies explored in this research include several foundational mechanical categories suited for responsive and deployable systems. These include unidirectional rotational joints, such as hinge-style or ball-and-socket mechanisms, which allow controlled rotation around a fixed axis; sliding joints, which support linear displacement along a guided path; and compliant joints, which rely on flexible materials or geometries that deform elastically under stress and return to their original shape. Each joinery concept was developed through parametric constraints informed by the previously defined movement map, ensuring that the geometry, angular ranges, and connection behaviour of each joint aligned with the spatial and rotational limits identified in the auxetic-reciprocal framework.

At this stage, the intent is not to fabricate fully functional mechanical parts, but to establish a foundational understanding of how geometry interacts with potential material articulation. These joint types act as an early mechanical vocabulary a design language from which more advanced, integrated components may be developed. Together, they lay the groundwork for a new generation of architectural applications that depend on movement and adaptability, such as deployable shells, kinetic façades, or transformable products underpinned by auxetic logic and behaviour.

5.2.2 Initial Conceptual modelling

To mimic rotation and translation, we sketch out and model three types of conceptual joints (Figure 5.2-2)each designed to facilitate one or more degrees of freedom observed in the digital simulation. These include:

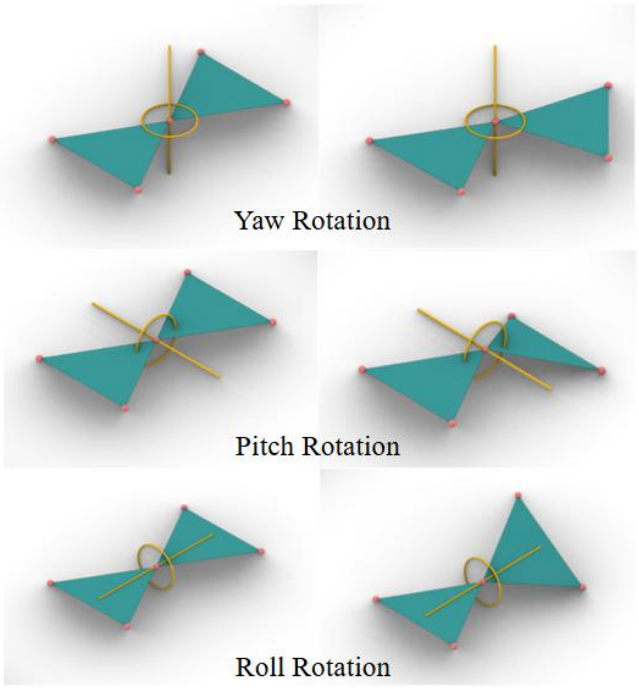

Figure 5.2-2 Conceptual movements of Auxetics

- Understanding the Movements at junction level
- Eliminate the Roll movement when it comes to Mechanical replication
- We include double pitch at individual triangles
- To avoid overlaps we are take the blue axis for yaw rotation and the red axis for Pitch
- The yaw movement is restricted to max triangular overlap

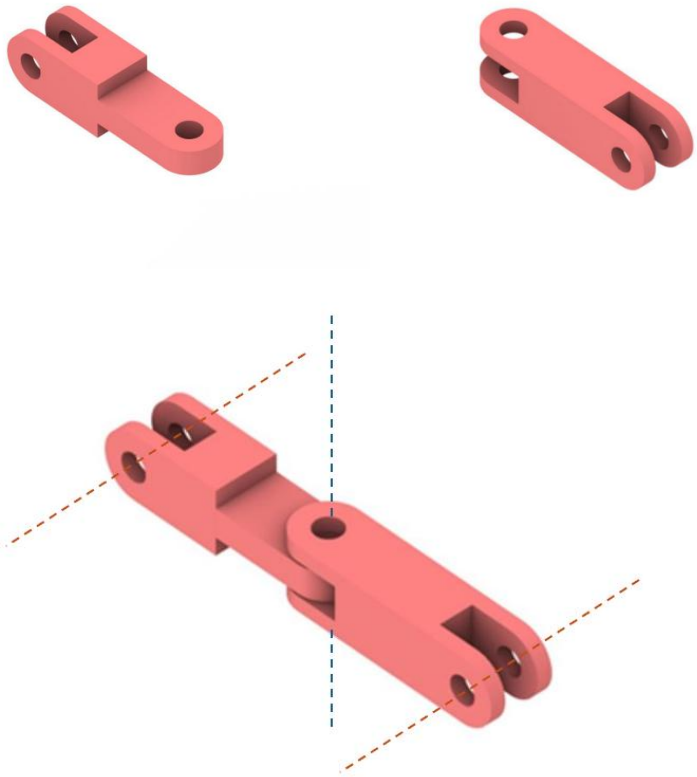

Figure 5.2-3 Conceptual joinery with Axis of rotation

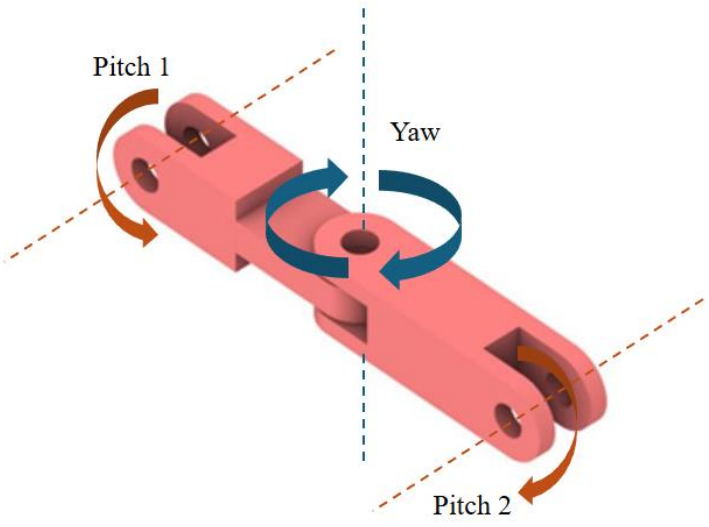

Figure 5.2-4 Conceptual joinery with Axis of rotation

As illustrated through the motion emulations in Figure 5.2-3 to Figure 5.2-6, the fundamental kinematic behaviour of the system was mapped and understood in terms of its rotational boundaries. The analysis revealed that yaw motion was consistently restricted to approximately 120 degrees, while pitch motion was limited to a maximum range of 0 to 30 degrees. These restrictions were not arbitrary but closely tied to the inherent geometric configuration of the units and the curvature demands of the overall deployable shell.

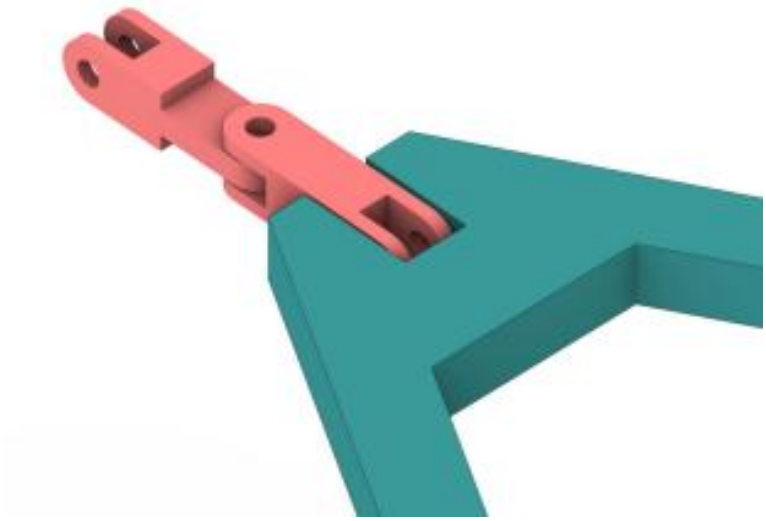

Figure 5.2-5 Conceptual joinery with unit triangle- single junction

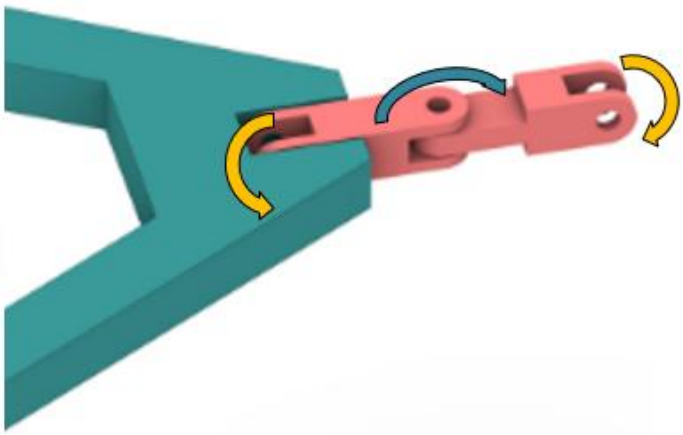

Figure 5.2-6 Conceptual joinery and junction with Rotation

Recognizing these angular limits was critical in translating abstract simulations into actionable design parameters for the physical prototypes. By identifying the exact thresholds of movement, it became possible to anticipate potential points of overextension, misalignment, or structural stress. This knowledge served as a guiding framework for refining both the unit design and the integration of joinery systems.

With these parameters established, the research advanced to detailed modelling in SolidWorks, where the constrained yaw and pitch behaviours were embedded into the unit kinematics. This step ensured that the digital assemblies reflected the realistic physical

tolerances, enabling more accurate evaluation of structural performance, load transfer, and deployment feasibility.

Figure 5.2-7 Conceptual joinery with unit triangle

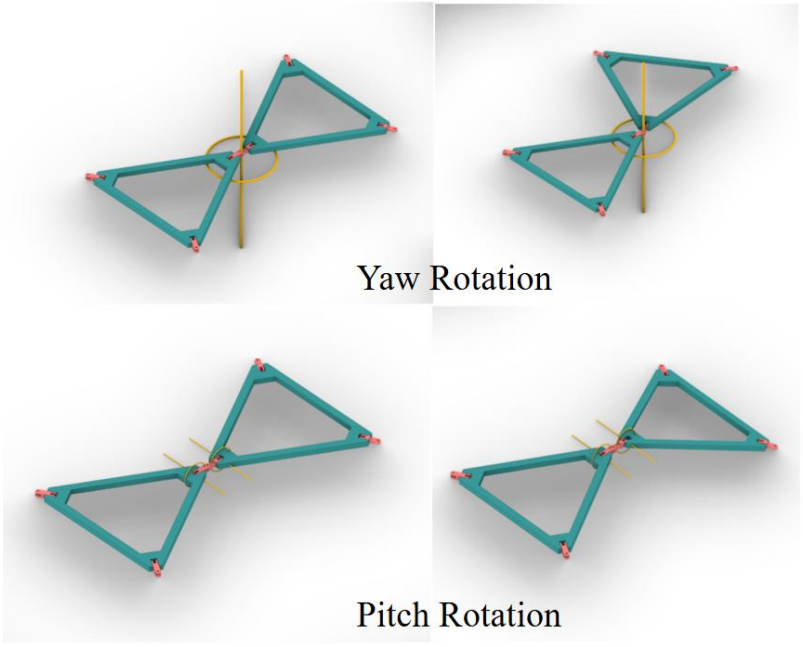

Figure 5.2-8 Yaw and pitch Rotations in 2 unit juntions

Building on this understanding of the angular restrictions at the single-unit scale, the study expanded the modelling process to multi-unit assemblies. A six-unit configuration was first developed (Figure 5.2-9 to Figure 5.2-12), to test the collective behaviour of interconnected modules under controlled yaw and pitch limits. This intermediate scale allowed the evaluation of synchronization across multiple joints, highlighting how localized rotations aggregated into global curvatures. The six-unit model also provided insights into the onset of irregularities, such as minor misalignments or stress concentrations, which would not have been visible at the single-unit level.

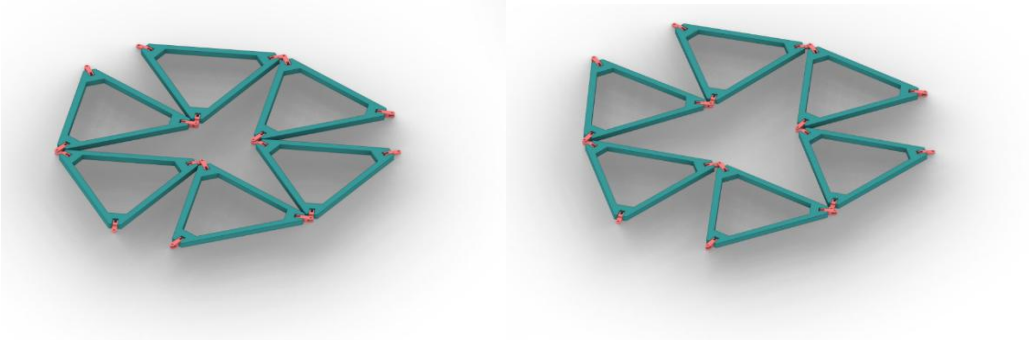

Figure 5.2-9 6 Units mechanical joinery - expansion with Yaw - 30 & 60 Degree

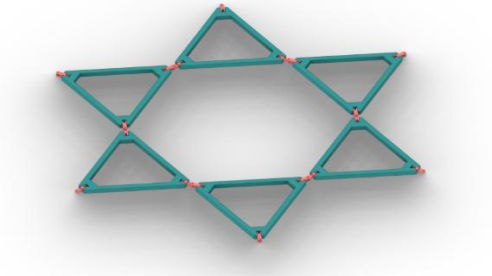

Figure 5.2-10 6 Units mechanical joinery - expansion with Yaw - 120 degree

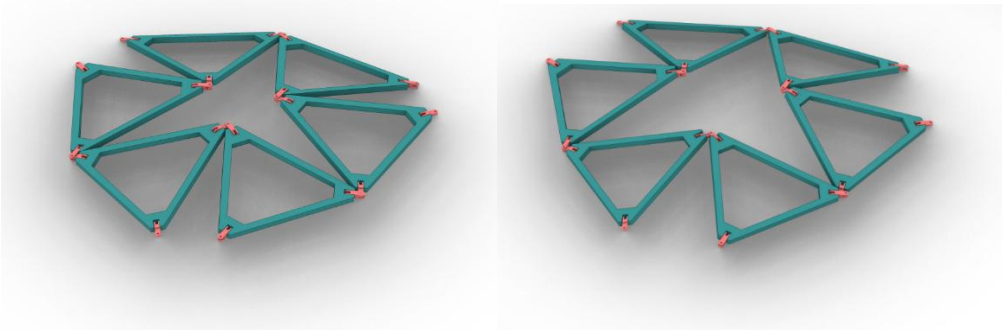

Figure 5.2-11 6 Units mechanical joinery - expansion with Uniform Yaw - 30 & 60 degree & pitch 8 degrees

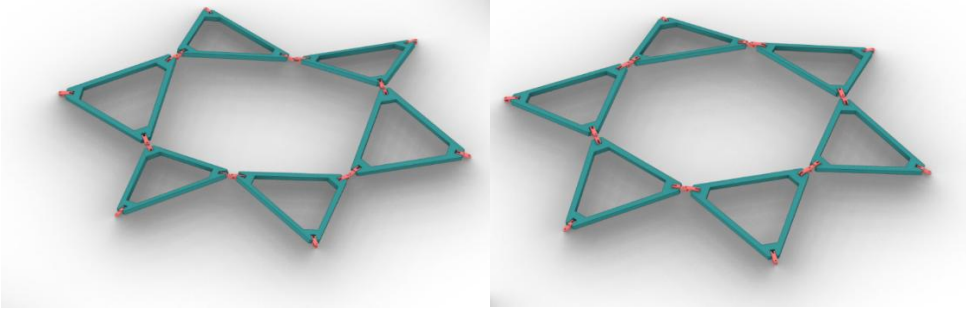

Figure 5.2-12 6 Units mechanical joinery - expansion with Uniform Yaw - 120 degree & non uniform pitch rotations.

Following this, a sixteen-unit assembly (Figure 5.2-13- Figure 5.2-16) was constructed in SolidWorks to further test the scalability of the system. At this stage, the interactions between modules became increasingly complex, as rotational tolerances accumulated across the larger array. The model demonstrated that while the system maintained overall cohesion, the

challenges of maintaining uniform deployment and minimizing distortion grew proportionally with scale. These progressive steps, from 6 to 16 units, established a critical bridge toward full-scale simulations, ensuring that the deployment logic and mechanical fidelity were tested incrementally before advancing to larger shell prototypes.

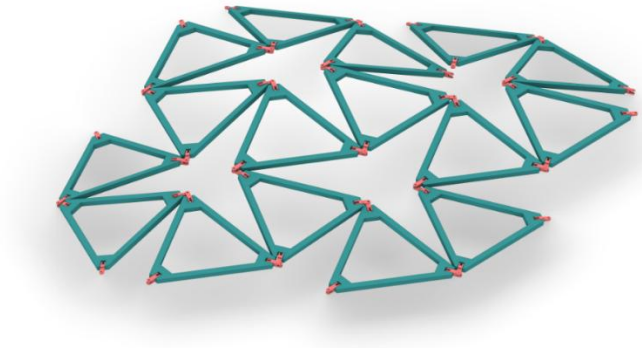

Figure 5.2-13 16 Units mechanical joinery - expansion with Uniform Yaw - 30 degree & non uniform pitch angles

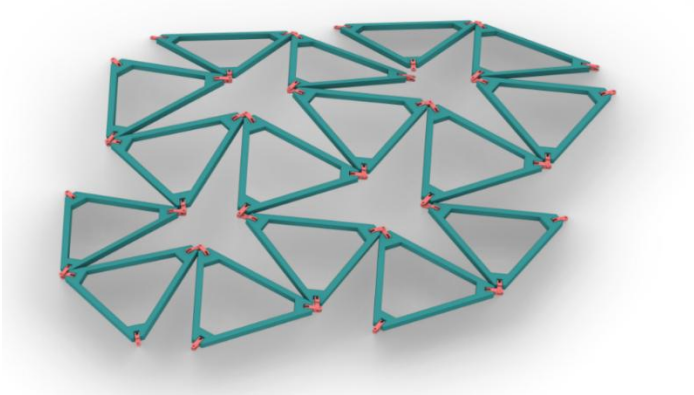

Figure 5.2-14 16 Units mechanical joinery - expansion with Uniform Yaw - 30 degree & 8 degrees pitch angles

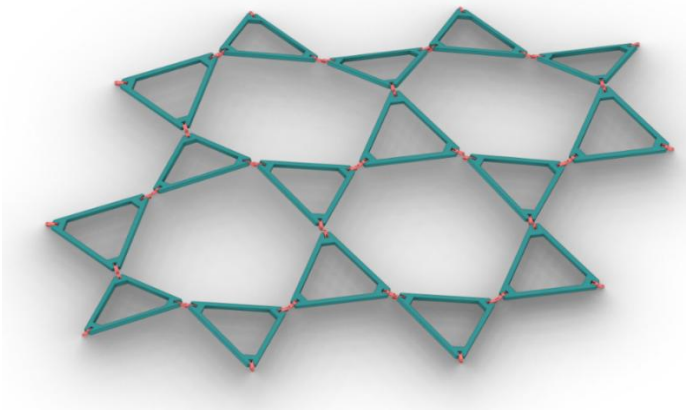

Figure 5.2-15 16 Units mechanical joinery - expansion with Uniform Yaw - 30 degree & non uniform pitch angles

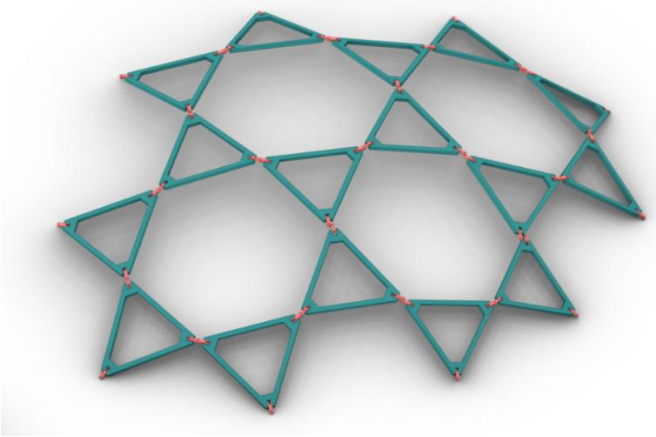

Figure 5.2-16 16 Units mechanical joinery - expansion with Uniform Yaw - 30 degree & 8 degrees pitch angles

5.2.3 Joinery Types: Designing Parts that Enable Auxetic Behaviour

With earlier inferences of motions from Figure 5.2-3 to Figure 5.2-16 ,this section explores key joint typologies designed to replicate and control the distinctive yaw and pitch behaviours observed in the Tristar-based auxetic system. Rather than treating joints as isolated components, they are conceived as interdependent parts of a larger, synchronized movement network. Each unit must articulate its rotation while maintaining harmony with adjacent components to preserve the overall geometry during deployment.

The selected joinery types were refined through iterative CAD modelling and are planned for physical testing via off the shelf mechanical joinery and 3d printed components prototypes. Each joint type was developed in response to the expected directional forces and movement ranges derived from earlier parametric simulations.

Type A: Unidirectional Pivot Joint
Designed to enable controlled rotation around a single axis (typically yaw), these joint mimics a constrained hinge or bearing. It restricts movement to a pre-set angular range (e.g. 0°–60°), preventing over-rotation or instability. Ideal for directional expansion along the Z-axis, this joint helps maintain uniformity across multiple units in synchronized motion.

Type B: Flexible Hinged Connector (Compliant Joint)
Acts as a semi-rigid link that allows limited pitch rotation. It offers elastic response under deformation and returns to its original state when released, useful in managing minor curvature changes. This joint is ideal for absorbing local stress during deployment on curved surfaces and can be tuned by material thickness and geometry.

Type C: Snap-Lock Directional Joint
A mechanical linkage that allows angular motion in one direction with a locking feature. Once the joint reaches its target angle, it clicks into place, offering both stability and reversibility. This is particularly effective in modular systems requiring repeatable and secure assembly/disassembly during multiple deployment cycles.

These joints were digitally assigned material stiffness and stress thresholds to test for deformation and structural integrity. The goal is not only to replicate movement but to evaluate whether small-scale joints can be upscaled for future modular assemblies. Visual diagrams (to be inserted) illustrate how each joint supports specific axes of motion and maps onto the mechanical requirements of deployable auxetic systems.

Assembly Scaling: From Single Unit to Modular Networks

Following the successful development of single-unit joint logic, assemblies were scaled progressively to test system-wide deployment. Physical prototypes were constructed at 6-unit, 20-unit, and 32-unit scales. This staged growth allowed for observing how localized pitch (Y-axis) and yaw (Z-axis) rotations translated into global transformations.

Early assemblies (especially the 6-unit model) maintained smooth motion and preserved curvature across all joints. As the scale increased, however, complexities emerged most notably in the form of accumulated tolerances, minor rotational drift, and joint interference at denser nodes. These effects illustrated the importance of precision joinery and angular synchronization, which becomes increasingly critical at larger scales.

This phase validated the mechanical logic underpinning the system while surfacing essential considerations for scaling, including refined movement thresholds and tolerance management.

Inference and Reflections

The progression from single to multi-unit deployment revealed a balance between design flexibility and mechanical precision. While the core movement logic held well at smaller scales, high-density assemblies demanded more advanced constraint strategies.

Key findings include:

Yaw Rotation: Operable up to 60° in physical models, with the ideal 120° expansion requiring mechanical assistance (e.g., one-way bearings or ratchets).

Pitch Rotation: Grouped into three curvature zones 0–5° (shallow), 5–15° (moderate), and up to 30° (steep). These values correspond with the surface adaptability limits of the current prototypes.

Avoidance of Roll: Excluding roll (X-axis) rotation proved beneficial, reducing structural complexity without compromising curvature versatility.

Material-Mechanical Hybridization: The integration of flexible materials with mechanical components allowed for greater range of motion while preventing structural failure pushing the limits of traditional auxetic systems.

These results inform the next stage of research, where load-bearing capacity and deployment sequencing will be examined in more depth.

Table 5.2-1 Suggested mechanism and functions

Axis	Suggested Mechanisms	Function
Yaw (Z-axis)	One-way bearing, ratchet, needle bearing	Enables directional rotation with locking
Pitch (Y-axis)	Mechanical spring, one-way bearing, Ratchets , needle bearing	Allows elastic deformation and controlled return
Expansion (XY)	Rail system with sliding locks or stops	Facilitates horizontal growth and contraction

5.3 Physical Prototype - Mechanical Joinery (Testing Mechanisms& Movements)

5.3.1 Earlier trials from Jayachandran (2019)

The master's thesis , Jayachandran (2019) , initially developed a physical prototype that employed a bicycle hub as the central rotational base, coupled with straightforward cycle-gear ratchet mechanisms and commercial ball-joint connectors (Figure 5.3-1). This assembly demonstrated the fundamental one-way bearing and locking behavior under manual actuation but lacked the capacity to carry structural loads: under even modest tension or weight, the ratchets would slip and the joints collapse. Drawing on the kinematic principles outlined by Jayachandran (2019), this early hands-on model was instrumental in visualizing the sequential pitch-to-yaw locking sequence and in identifying critical geometric tolerances and joint clearances. Some preliminary concepts for the base rail systems were also developed (Figure 5.3-2). but these were more of just physical models than a feasible working prototypes to take movement inferences with.

The insights gained from this prototype also directly informed the robust SolidWorks proxy-mate strategies, refined joint geometries, and material selections that underpin the final deployable structure's ability to both articulate as intended and withstand real world forces.

Figure 5.3-1 Physical Prototypes from Previous research- Junction Joinery
Note: From , *Deployable reciprocal shells through auxetic behaviour: Architectural hypothesis to fabricate double-curved structures* by *Jayachandran, S. (2019).*

Figure 5.3-2 Physical Prototypes from Previous research- base rail system
Note: From , *Deployable reciprocal shells through auxetic behaviour: Architectural hypothesis to fabricate double-curved structures* by *Jayachandran, S. (2019).*

5.3.2 Pre-Doctoral Explorations and Informal Knowledge Development

5.3.2.1 Context and Transitional Phase

Following the completion of the author's master's thesis, the period between 2020 and 2023, coinciding with the pandemic, became an informal yet productive phase of independent exploration as a hobby project. Although not initially aligned with a defined research agenda, this period served as a transitional stage in which emerging interests in mechanical systems, fabrication, and computational tools were pursued. These activities were not formally documented at the time, but they later played a significant role in shaping the direction and methodological grounding of the doctoral research , especially eliminating non viable options.

5.3.2.2 Workshop Engagements and Practical Insights

A key aspect of this phase involved visiting multiple mechanical workshops and small-scale industrial facilities, particularly during the author's time in India prior to commencing the PhD in 2023. These engagements included direct conversations with technicians, fabricators, and experienced practitioners who offered hands-on insights into fabrication processes, material behaviour, and mechanical feasibility. It became evident that such interactions provided a level of practical clarity that often complemented, and in some cases rivalled, insights derived from academic literature. Discussions within workshop environments frequently enabled rapid evaluation of ideas, helping to identify what would realistically function and what would not under practical conditions.

Figure 5.3-3 Informal documentation of Factory and workshop visits

5.3.2.3 Influence on Research Direction

These workshop interactions played a critical role in refining the research trajectory by eliminating non-viable approaches at an early stage. Through iterative discussions and informal validation, several potential design directions were identified as impractical, allowing the research to focus more efficiently on feasible solutions. This process significantly influenced the decision to explore off-the-shelf mechanical components, particularly in the development of ratchet-based joinery systems. The preference for such components emerged from their proven reliability, availability, and ease of integration, which aligned with the practical insights gained from workshop practitioners.

Figure 5.3-4 Non Viable mechanical parts from workshop visits

5.3.2.4 Informal Peer Learning and Skill Development

In parallel with workshop visits, there were engagements in informal discussions with peers from mechanical engineering backgrounds. These exchanges, although not formally recorded, contributed to a broader understanding of mechanical systems and design logic. Additionally, this period facilitated self-directed learning of digital tools, particularly SolidWorks and ANSYS, which later became integral to the simulation and validation processes within the PhD. This early skill development established a technical foundation that supported the transition into more structured research methodologies.

5.3.2.5 Reflection on Documentation and Integration

It is important to acknowledge that the knowledge generated during this period was not systematically documented or structured as formal research data. Photo documentation was limited as these workshops did not allow photos as a safety protocol near dangerous machineries . As such, these insights function as experiential and tacit knowledge rather than empirical evidence within the thesis. However, their influence is implicitly embedded in key research decisions, including the selection of mechanical joinery systems, the emphasis on off-the-shelf solutions, and the adoption of specific simulation workflows.

5.3.2.6 Positioning Within the Research Framework

This phase is positioned as a preparatory layer that informed the initial direction of the doctoral research rather than as a core methodological component. While the formal contributions of the thesis are derived from structured simulations, prototyping, and analysis, they are underpinned by this prior phase of exploratory learning. By bridging informal practice-based insights with formal research processes, the study establishes a grounded and pragmatic approach that enhances both the feasibility and relevance of its outcomes.

5.3.3 Mark 1 Prototype: Ratchet-and-Spring-Based Mechanical Joinery

The Mark 1 prototype served as the initial full-scale investigation into the behaviour and performance of a ratchet-based mechanical joinery system integrated with a spring-loaded return mechanism. Designed at 1:1 scale, the joinery aimed to facilitate unidirectional rotation along the yaw axis (Z-rotation), while simultaneously resisting reverse motion through a mechanical locking function. The inclusion of a spring element provided passive tension to support the deployed state and was intended to offer supplementary pitch flexibility (Y-axis responsiveness) through elastic return behaviour. The prototype was situated within a larger inquiry into how deployable, auxetic structural units might be physically constructed and coordinated through mechanical movement systems.
The testing was conducted manually, using hand-applied pressure and loads, to evaluate the feasibility of movement and to validate the fundamental locking behavior of the system. Mechanical or machine-based load simulations were not undertaken at this stage, both due to resource limitations and because the primary objective was confined to establishing proof of movement and locking rather than assessing structural performance under applied loads

5.3.3.1 Component Design and Technical Configuration

The joinery system was comprised of three primary components: a ratchet gear, a steel compression spring, and a custom-designed housing unit, all fabricated using 3D-printed PLA for initial prototyping. The ratchet gear, measuring 35 mm in diameter, was designed to enable smooth rotation in one direction, with teeth geometry optimized for firm locking under reverse

torque. While the gear tooth count was not standardized across versions, a test configuration of 12–14 teeth was estimated to strike a balance between angular resolution and mechanical robustness.

Figure 5.3-5 Unit joineries of Ratchet and spring joinery

The spring component, placed within a compression cavity behind the ratchet (Figure 5.3-5), provided resistance against fallback once deployed. A semi-stiff steel spring, with a travel length of approximately 50 mm, was selected to resist minor forces while offering a degree of recoverability. Although the exact spring constant was not calibrated with high precision, it is estimated to be in the range of $k \approx 1.2–1.5$ N/mm, based on material thickness and deformation characteristics under test loads. The overall assembly is designed to be modular, allowing it to be embedded between structural arms or frame elements for integration into larger deployable systems.

Assembly and Construction

Two assembly modes were tested during this phase. In the first, the joinery was directly mounted between two fixed arms with basic axial pins, allowing free testing of rotation and locking behavior (Figure 5.3-6). Following that, a 3D-printed hand-like fixture was added to simulate real-world handling and to test whether manual actuation would trigger locking and releasing accurately under closer to realistic conditions (Figure 5.3-7) . Both configurations enabled real-time observation of joint movement and allowed the spring and ratchet interaction to be closely monitored during motion.

Figure 5.3-6 Assembly of Ratchet and Spring Joinery- without 3D printed housing

Figure 5.3-7 Assembly of Ratchet and Spring Joinery- with 3D printed housing

5.3.3.2 Kinematic Behavior and Movement Analysis

As inferred from Figure 5.3-8 , Rotation along the yaw axis (Z) was successfully achieved, with the ratchet mechanism enabling smooth, resistance-free movement in the forward direction, while offering an immediate and effective mechanical lock in the reverse. This behavior directly contributed to stabilizing the deployed structure, even under moderate loading or external vibrations. The joinery demonstrated a rotation range between 0° and 120°, depending on the spring's load conditions and the gear tooth configuration.

However, the intended pitch flexibility (Y-axis movement) proved difficult to achieve. While the spring allowed for minimal axial compliance, the joint lacked the structural articulation or additional degrees of freedom needed to perform consistent pitch movement. As a result, flexural transformation of the unit was limited, and any curvature required external manipulation or an additional apparatus to assist the joint in repositioning along a different axis.

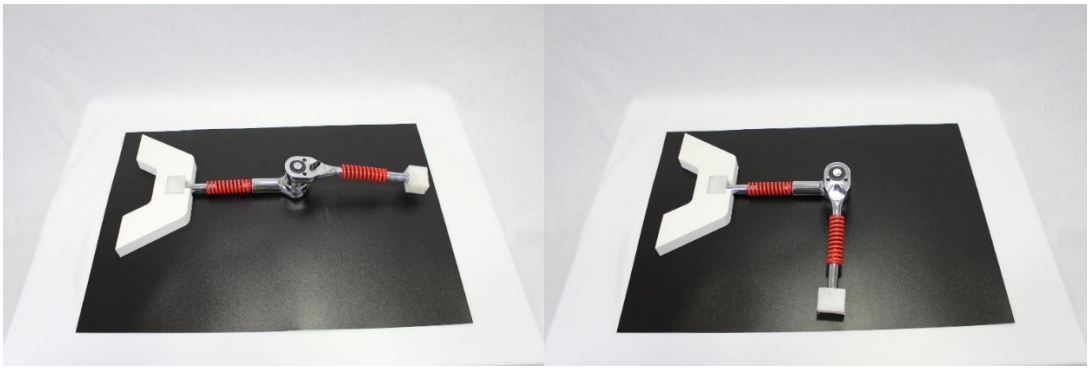

Figure 5.3-8 Testing of Ratchet and Spring Joinery in various degree of Yaw rotation

5.3.3.3 Observations and Limitations

From a functional standpoint, the Mark 1 prototype effectively demonstrated the core concept of mechanical locking and controlled unidirectional deployment. The ratchet system was robust in its locking behavior and proved capable of maintaining the structural position under repeated actuation cycles. However, several limitations were observed that constrained its broader application:

Firstly, the spring stiffness posed a complex design trade-off. When using softer springs in earlier trials (undocumented selection process) , the system failed to maintain its deployed posture, often collapsing or vibrating out of position. On the other hand, stronger springs

introduced excessive resistance, restricting the range of movement and flattening the structure's curvature, particularly in scenarios that required curvature beyond 10° pitch angles. This led to an overall flatter deployment profile and limited the potential for true three-dimensional movement.

Secondly, the gear teeth and 3D-printed pawl components exhibited signs of wear and micro-fracture after repeated locking cycles, suggesting that future versions would benefit from improved materials such as Nylon composites or metal-hybrid inserts. In addition, minor backlash was noted between the pawl and gear teeth, which could result in positional drift over time.

5.3.3.4 Future Improvements and Iterative Directions

Based on the findings from Mark 1, several avenues for refinement have been identified. Future iterations could incorporate pre-tensioned or adjustable spring mechanisms that allow the user to calibrate tension based on desired flexibility or load. This would support more adaptable deployment behavior without over-constraining the structure. Additionally, torsional spring systems could be explored as alternatives to linear compression, providing smoother angular return and reducing the reactive stiffness along the Z-axis.

To improve pitch flexibility, integrated elastomeric hinges or flexural joint inserts may be embedded within or adjacent to the ratchet mechanism. These would enable limited multi-axis responsiveness without compromising structural lock. Furthermore, soft-lock alternatives such as magnetic catches or progressive friction locks may allow finer control during the transition between locked and mobile states.

At this stage, testing was deliberately limited to manual methods, relying on hand-applied pressure and loads to assess movement feasibility and validate basic locking behavior. Mechanical or machine-based load simulations were not employed, both due to resource constraints and because the immediate objective was to confirm proof of movement rather than full structural performance. However, future investigations could incorporate mechanical testing and advanced load simulations to provide a more comprehensive evaluation of structural integrity and performance under applied stresses

Finally, material upgrades will be crucial. High-cycle durability under stress requires better mechanical performance than PLA can offer. Testing future versions with PETG, ABS, carbon-fiber infused polymers, or machined aluminum components may extend joint life, reduce deformation, and increase precision under load.

5.3.3.5 Overall Inference and conclusion

The Mark 1 prototype has proven a critical step in validating the concept of ratchet-based unidirectional locking as a means of enabling deployable architectural joints. While limitations in pitch control and spring tuning persist, the prototype confirms that mechanical movement and structural locking can be embedded within compact joinery systems. These findings inform the next iteration of the system, which will aim to integrate multi-axis movement, greater geometric flexibility, and material optimization for larger-scale deployment scenarios.

5.3.4 Mark 2 Prototype: Dual-Ratchet Joinery System with Integrated Ball Joint

Building upon the lessons from the Mark 1 prototype, the Mark 2 joinery system was developed to extend movement control across multiple rotational axes while introducing enhanced locking behaviour through combined mechanical logic. The assembly integrates three distinct components a primary ratchet for yaw control, a secondary ratchet for pitch adjustment, and a universal ball joint for limited articulation and partial load distribution. This prototype aimed to simulate and test multi-axis deployability in a single joint system suitable for reciprocal-auxetic shell assemblies.

In contrast to Mark 1, where rotational capacity was primarily limited to a single axis and pitch resistance was indirect, Mark 2 introduces independent locking control in both Z-axis (yaw) and Y-axis (pitch) directions. Additionally, the inclusion of a ball joint articulation unit near the secondary ratchet facilitates slight flexibility, preventing complete mechanical jamming and allowing smoother movement transitions during manual deployment.

The testing was conducted manually, using hand-applied pressure and loads, to evaluate the feasibility of movement and to validate the fundamental locking behaviour of the system. Mechanical or machine-based load simulations were not undertaken at this stage, both due to resource limitations and because the primary objective was confined to establishing proof of movement and locking rather than assessing structural performance under applied loads

5.3.4.1 Component Configuration and Technical Specifications

Primary Ratchet: Yaw Control

The primary ratchet (Figure 5.3-9) , responsible for the Z-axis (yaw) rotation, was a store-bought metal ratchet fabricated in steel. With a diameter of 35 mm, it featured an estimated 16 teeth, offering rotational granularity of approximately 22.5° per notch. The ratchet was designed to allow smooth forward rotation, while firmly locking in the reverse direction through mechanical engagement. The tested locking range was between 0° and 120°, simulating a range of expansion from compact to fully deployed structural states. The locking mechanism was robust under moderate hand-applied force and capable of resisting fallback, forming the core of the unidirectional deployment logic.

Figure 5.3-9 Primary ratchet of Dual ratchet system- mark 2

Secondary Ratchet: Pitch Control

A secondary steel ratchet (Figure 5.3-10), smaller in size at 20 mm diameter, was introduced to enable controlled pitch movement. This ratchet, also store-bought, featured approximately 12 teeth, providing finer angular locking in the vertical axis. During testing, this mechanism was manually deployed and friction-locked through hand simulation, exhibiting an intended pitch range of 5° to 30°. However, due to the limitations of off-the-shelf tolerances, the locking was inconsistent, often allowing motion beyond the intended threshold, resulting in occasional collapse under its own weight. This instability was documented to highlight the risks of relying on non-calibrated hardware in rotationally sensitive applications.

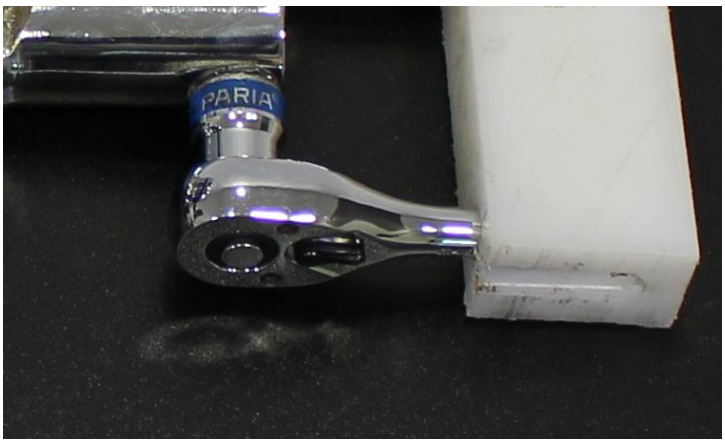

Figure 5.3-10 Secondary ratchet of Dual ratchet system- mark 2

Universal Ball Joint: Articulation Buffer

To accommodate micro-movements and prevent rigid locking between components, a purchased universal ball joint was placed downstream of the secondary ratchet (Figure 5.3-11). This joint allowed a maximum flex of 5° in any direction, introducing just enough articulation to avoid binding or mechanical interference. Its placement acted as a buffer zone to absorb slight misalignments between frames during deployment and to support partial load transfer where rotational axes were misaligned. Although not designed for full structural load-bearing, the ball joint improved kinematic fluidity across the system

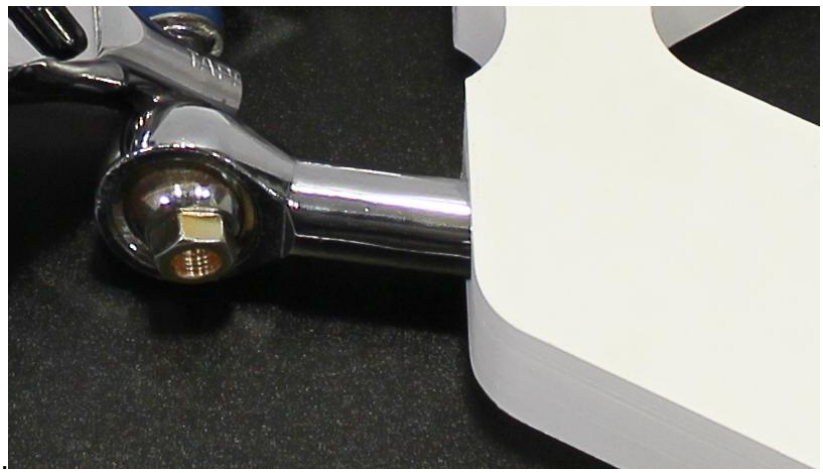

Figure 5.3-11 Ball joint of Dual ratchet system- mark 2

5.3.4.2 Assembly and Fabrication

The Mark 2 joinery system was assembled as a continuation of the structural arm from the secondary ratchet outward, creating a linearly aligned rotational joint stack (Figure 5.3-12 & Figure 5.3-13). The complete assembly occupied an approximate diameter range of 250–300 mm, with a maximum perpendicular thickness of 100 mm at the core housing. This increased bulk relative to Mark 1 resulted from the sequential stacking of components and the housing volume required for the dual-ratchet interfaces.

While the ratchet elements were metallic, all connector housings, adjustment spacers, and mounting brackets were FDM 3D printed in PLA, ensuring modularity and iterative adjustability. Store-bought nuts and bolts were used to bind the assemblies, though these introduced tolerance mismatches and minor instability in rotational fidelity. The use of hand-operated components was intentional to simulate early deployability behaviour in a low-tech scenario.

Figure 5.3-12 3D printed part for Dual ratchet system- mark 2

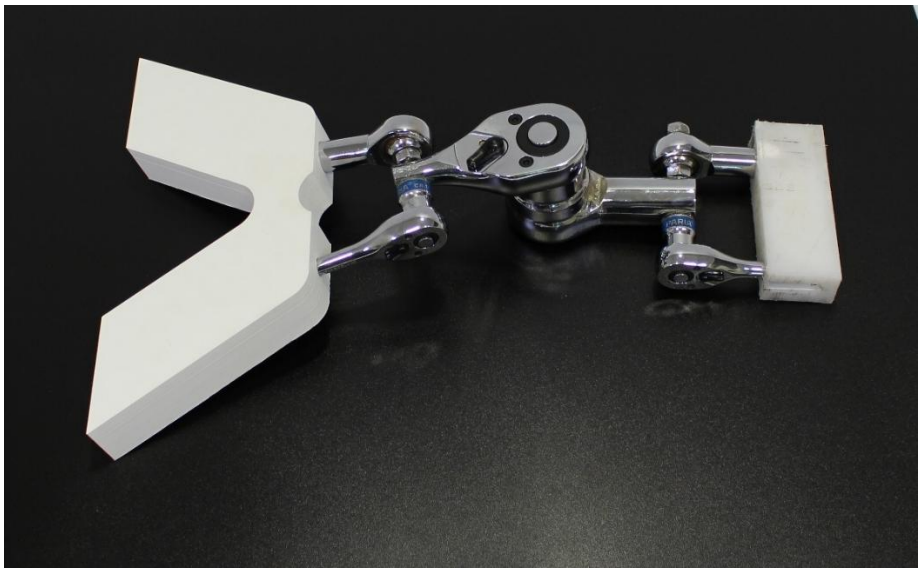

Figure 5.3-13 Full Assembly of Dual ratchet system- mark 2

5.3.4.3 Kinematic Behaviour and Performance

The prototype successfully demonstrated (Figure 5.3-14) controlled directional movement in both yaw and pitch axes. The primary ratchet offered reliable unidirectional rotation, with clean locking behaviour. Meanwhile, the secondary ratchet enabled targeted pitch rotation during manual deployment. While the intended pitch range was restricted to 5–30°, in practice, the system often exceeded this threshold, especially under gravity. This led to uncontrolled collapses, which were documented and analyzed as a limitation of hardware performance, rather than conceptual failure.

The ball joint played a crucial stabilizing role, allowing slight flex and absorbing misalignment during movement transitions. It ensured that forces were not overly concentrated at either ratchet end, reducing joint strain during dynamic loading.

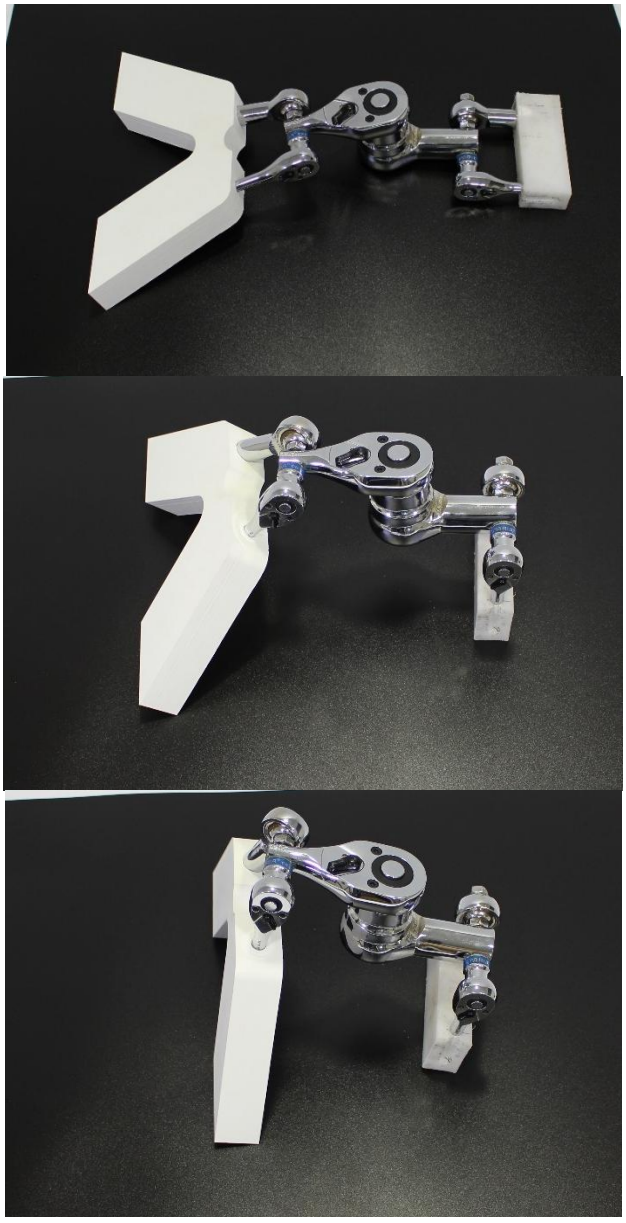

Figure 5.3-14 Testing of Dual ratchet system- mark 2 with various Yaw and Pitch movements

5.3.4.4 Observations and Limitations

The Mark 2 prototype introduced a higher level of mechanical control and represented a notable advancement in multi-axis joinery behaviour. However, several critical constraints emerged during testing. Firstly, the mechanical complexity increased substantially. The stacking of two ratchets and a ball joint, along with required housing components, led to an excessive system thickness that interfered with adjacent frame members in compact assemblies. Secondly, the use of off-the-shelf hardware, particularly in the secondary ratchet, introduced variability and unreliable locking, which significantly limited the pitch control. The joint often exceeded the 30° pitch threshold, compromising positional stability and creating risks of mechanical overextension (Figure 5.3-15).

Figure 5.3-15 Mark 2- Yaw and Pitch movements- collapsing beyond preferred angle

Additionally, the number of moving parts led to internal collisions, especially when components were misaligned during assembly or testing. This highlighted the need for clear component hierarchy and stricter spatial coordination.

5.3.4.5 Future Refinements and Development Path

Several key improvements are recommended for future iterations. To begin, custom-designed ratchets should replace store-bought ones, especially in the secondary axis, to ensure precise locking between 0° and 30° pitch. These could be digitally modelled and 3D printed or machined with higher tolerances.

Secondly, mechanical hierarchy must be reduced, favoring coaxial or nested designs to streamline the system profile. Integrating the pitch and yaw mechanisms into a more compact configuration would resolve spatial interference and reduce rotational drag. Where appropriate, hybrid solutions (e.g., one mechanical axis + one compliant axis) may improve deployment fluency.

At this stage, testing was deliberately limited to manual methods, relying on hand-applied pressure and loads to assess movement feasibility and validate basic locking behaviour. Mechanical or machine-based load simulations were not employed, both due to resource constraints and because the immediate objective was to confirm proof of movement rather than full structural performance. However, future investigations could incorporate mechanical testing and advanced load simulations to provide a more comprehensive evaluation of structural integrity and performance under applied stresses

Material optimization is also necessary. Upgrading printed components to Nylon, PETG, or even carbon-fiber-infused filaments would reduce wear and allow tighter tolerances. Finally, replacing hand-actuated mechanisms with semi-automatic locking systems (e.g., cam locks, magnetic or spring-latch systems) could improve repeatability and user safety during deployment.

5.3.4.6 Inference and Conclusion for Mark 2

The Mark 2 prototype successfully expands the operational behaviour of deployable joineries to include multi-axis locking and rotation, paving the way for more dynamic, reconfigurable structures. While the design demonstrates feasibility, it also reveals clear mechanical limitations chiefly bulk, inconsistent locking behaviour, and component interference. These insights provide the foundation for future optimization, as the research progresses toward fully integrated, structurally intelligent joinery systems for reciprocal-auxetic deployable shells.

5.3.5 Mark 3 Prototype: Dual-Axis One-Way Bearing Joinery System

The Mark 3 prototype, representing the fourth refined iteration of this research, marks a significant shift in strategy by introducing precision bearing systems for smooth and reliable multi-axis control. Abandoning ratchet mechanisms in favor of one-way bearing assemblies, this version focuses on optimizing rotational articulation, modularity, and compact housing design. The system integrates a primary CSK30-PP one-way bearing for yaw (Z-axis) rotation, and two nested CSK25-PP one-way bearings to support pitch (Y-axis) movement.

Unlike previous prototypes that relied on mechanical locking (Mark 1 and 2), Mark 3 achieves directional control through internal bearing architecture, removing the need for external pawls or levers. However, this comes at the expense of reversibility, making this version the most stable during deployment but also the least flexible for retracting movement.

The testing was conducted manually, using hand-applied pressure and loads, to evaluate the feasibility of movement and to validate the fundamental locking behaviour of the system. Mechanical or machine-based load simulations were not undertaken at this stage, both due to resource limitations and because the primary objective was confined to establishing proof of movement and locking rather than assessing structural performance under applied loads

5.3.5.1 Component Configuration and Technical Specifications

Primary Bearing (Yaw Control – Z-Axis)

At the core of the system is a CSK30-PP one-way bearing, with an outer diameter of 60 mm and an inner shaft diameter of 30 mm (Figure 5.3-16). The unit features an 8 mm × 2 mm keyway and an internal locking notch of 6 mm, allowing for free rotation in the forward direction and passive locking in reverse. The bearing was selected for its ability to handle moderate torsional loads while maintaining alignment under repeated cycles. The effective rotation range tested was from 0° to 120°, simulating full deployment movement.

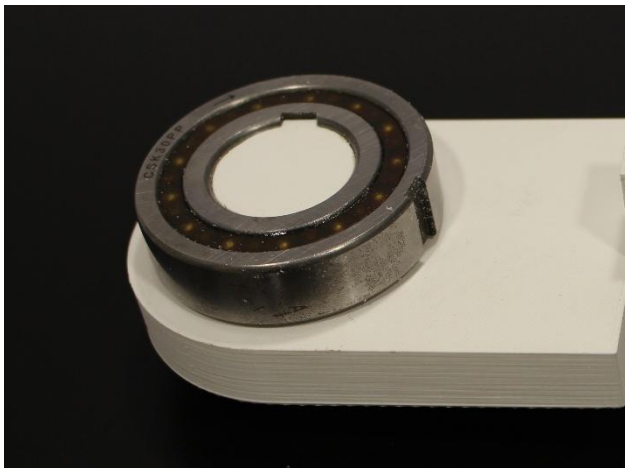

Figure 5.3-16 Primary bearings of Dual Axis one way bearing systems- mark 3

Secondary Bearings (Pitch Control – Y-Axis)

To facilitate pitch articulation, two CSK25-PP one-way bearings with outer diameter 50 mm, inner diameter 25 mm were nested concentrically and placed perpendicularly to the primary bearing axis (Figure 5.3-17). This allowed for controlled rotation along the Y-axis, with a target movement range between 0° to 30°. In reality, the lack of internal stops meant the system could overshoot and collapse at approximately 90°, which was observed during physical testing. While this was an unintended failure mode, it also illustrated the angular capacity of the design in the absence of restrictive geometry.

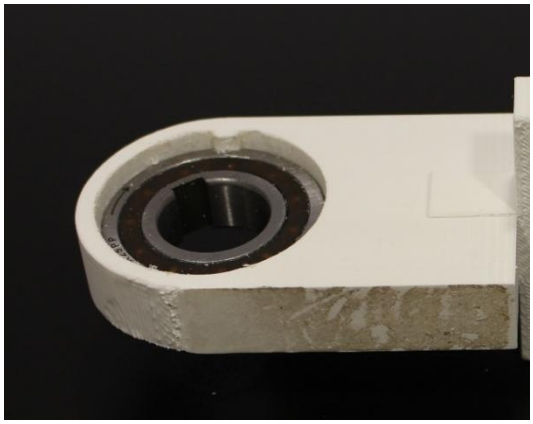

Figure 5.3-17 Secondary bearings of Dual Axis one way bearing systems- mark 3

Housing and Structural Configuration

All bearings were embedded within a custom-designed 3D-printed PLA housing, measuring approximately 100 mm in diameter with 5 mm thick walls (Figure 5.3-18 & Figure 5.3-19). The housing geometry was iteratively refined to eliminate internal collisions and ensure clear separation between arm trajectories. Early designs suffered from bearing misalignment and wall delamination, especially under torsional stress. These were resolved through multiple 3D-printed iterations, each adjusted slightly to improve structural integrity and ensure perfect coaxial alignment.

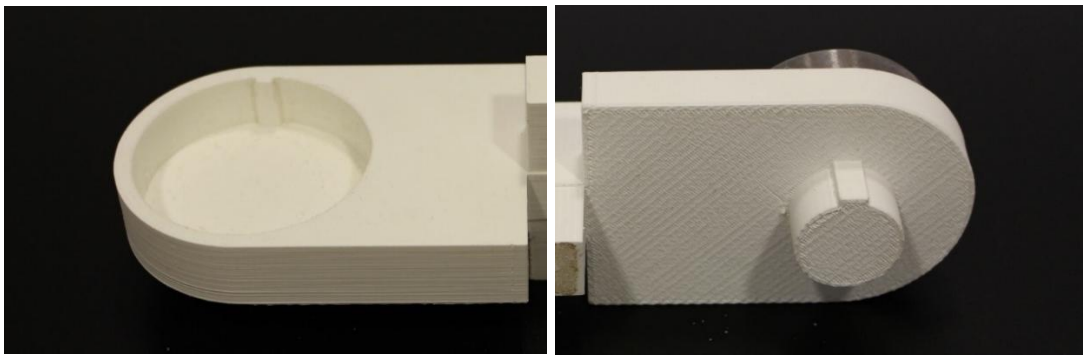

Figure 5.3-18 3D printed notch housing design of Dual Axis one way bearing systems- mark 3

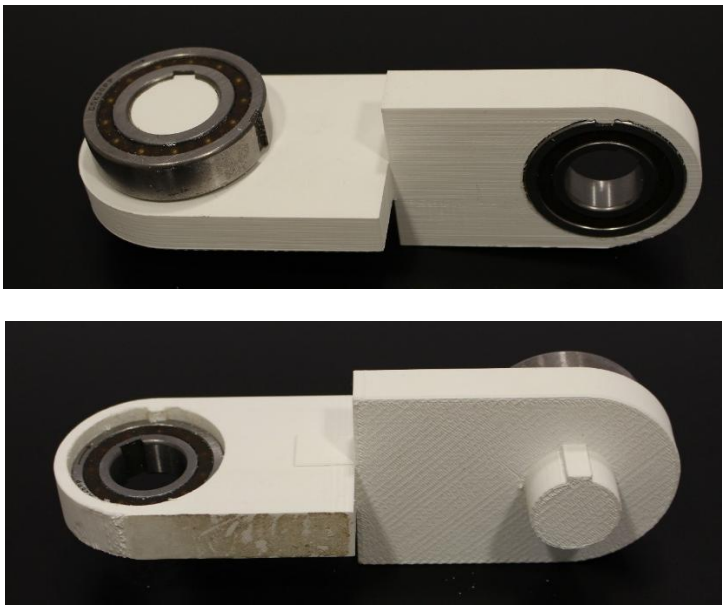

Figure 5.3-19 Full 3D printed housing assembly of Dual Axis one way bearing systems- mark 3

The bearing system was self-locking, and no additional pins, spacers, or bushings were used. Assembly was designed for modularity and easy replication, with medium infill print settings and rotational axis support reinforced through alignment ribs in the housing (Figure 5.3-20)

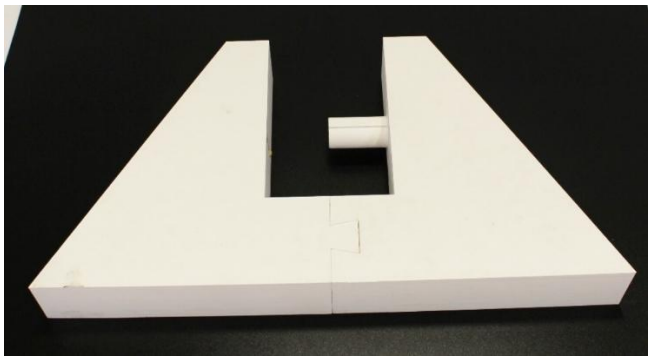

Figure 5.3-20 3D printed extension for Dual Axis one way bearing systems- mark 3

Final Assembly

With all the parts interlocking with the 3D printed parts we assemble it to replicate a singular joint of the Auxetic system (Figure 5.3-21)

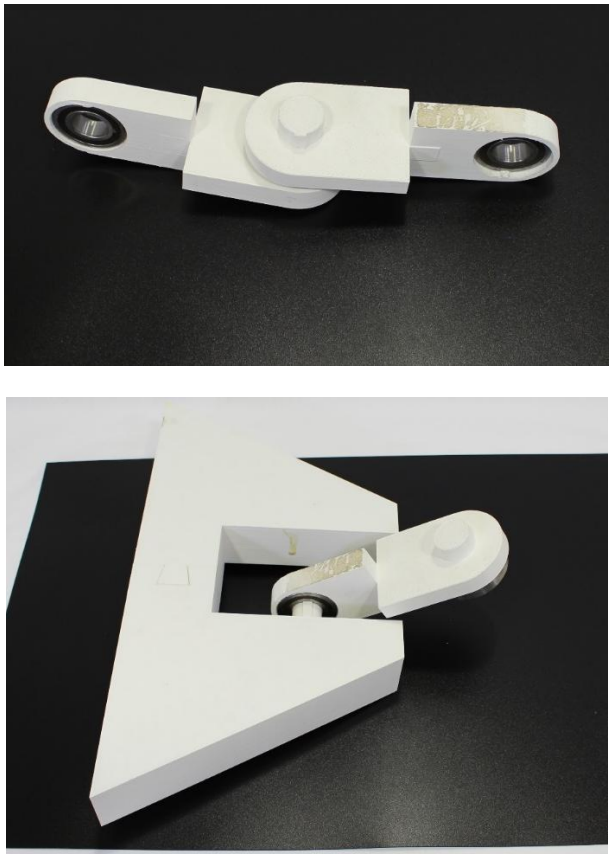

Figure 5.3-21 Full Assembly of Dual Axis one way bearing systems- mark 3

5.3.5.2 Kinematic Behaviour and Movement Characteristics

During the Kinematic Behaviour and Movement testing (Figure 5.3-22 to Figure 5.3-23) ,the final prototype exhibited clean, unidirectional movement along both primary (Z-axis) and secondary (Y-axis) rotations. The bearing synergy ensured smooth articulation during deployment, and the internal locking mechanism of each bearing restricted reverse motion, enhancing stability once deployed.
Z-axis rotation was tested up to 120°, allowing the structure to unfold into its expanded configuration. Y-axis pitch was controlled within 0°–30° for simulation, though actual behaviour occasionally exceeded this range due to the absence of internal angular stops, leading to mechanical jamming or full over-rotation. Importantly, the housing design prevented arm collisions, a recurring issue in previous iterations.

Figure 5.3-22 Yaw rotation check of Dual Axis one way bearing systems- mark 3- assembly type 1

There was minimal resistance during combined multi-axis movement, and articulation remained fluid across approximately 10 movement cycles. Residual stiffness was observed only at maximum angles, particularly where compound rotations approached overlapping limits. (Figure 5.3-23 & Figure 5.3-24)

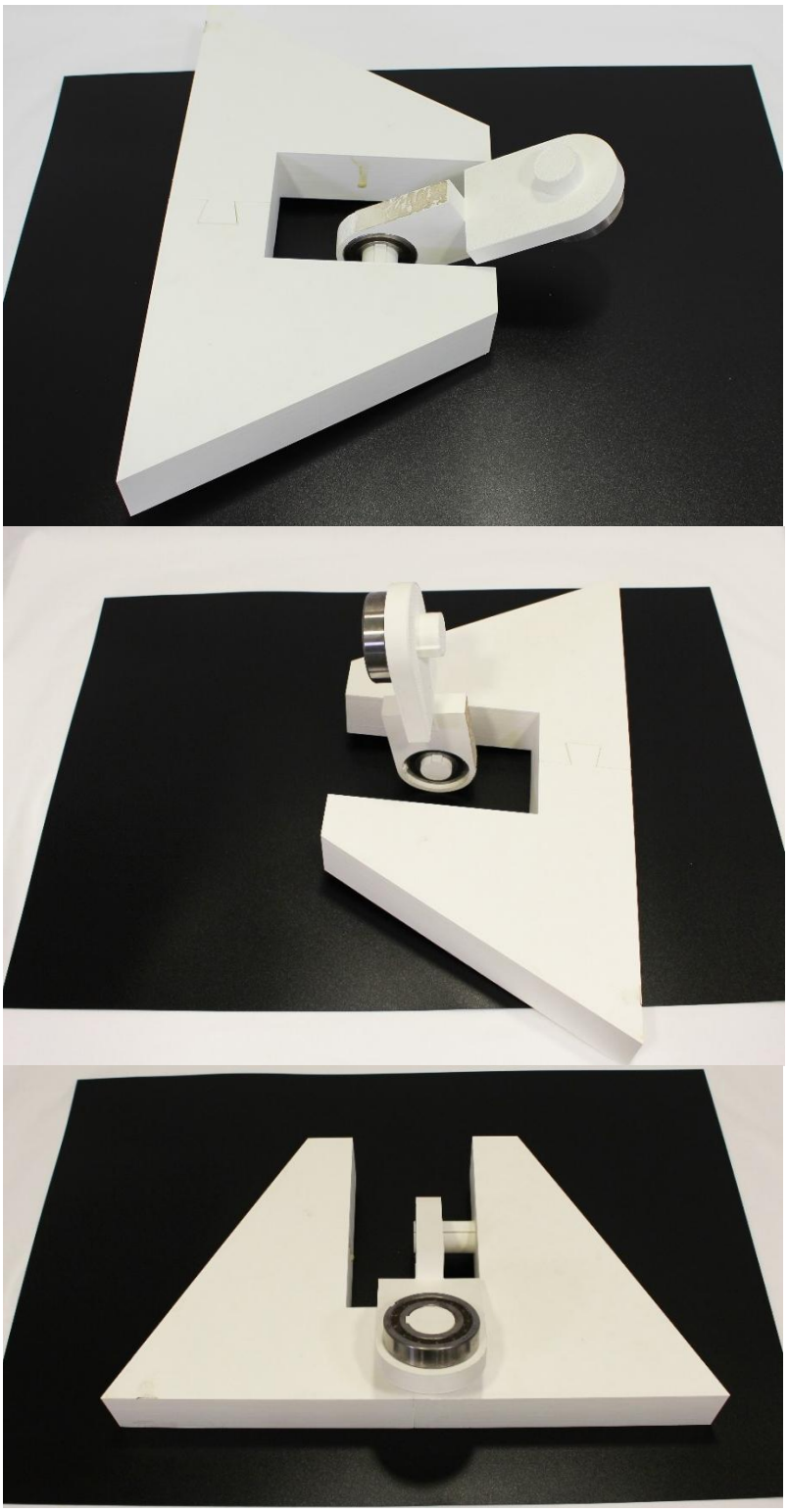

Figure 5.3-23 Pitch rotation check of Dual Axis one way bearing systems- mark 3- assembly type 2

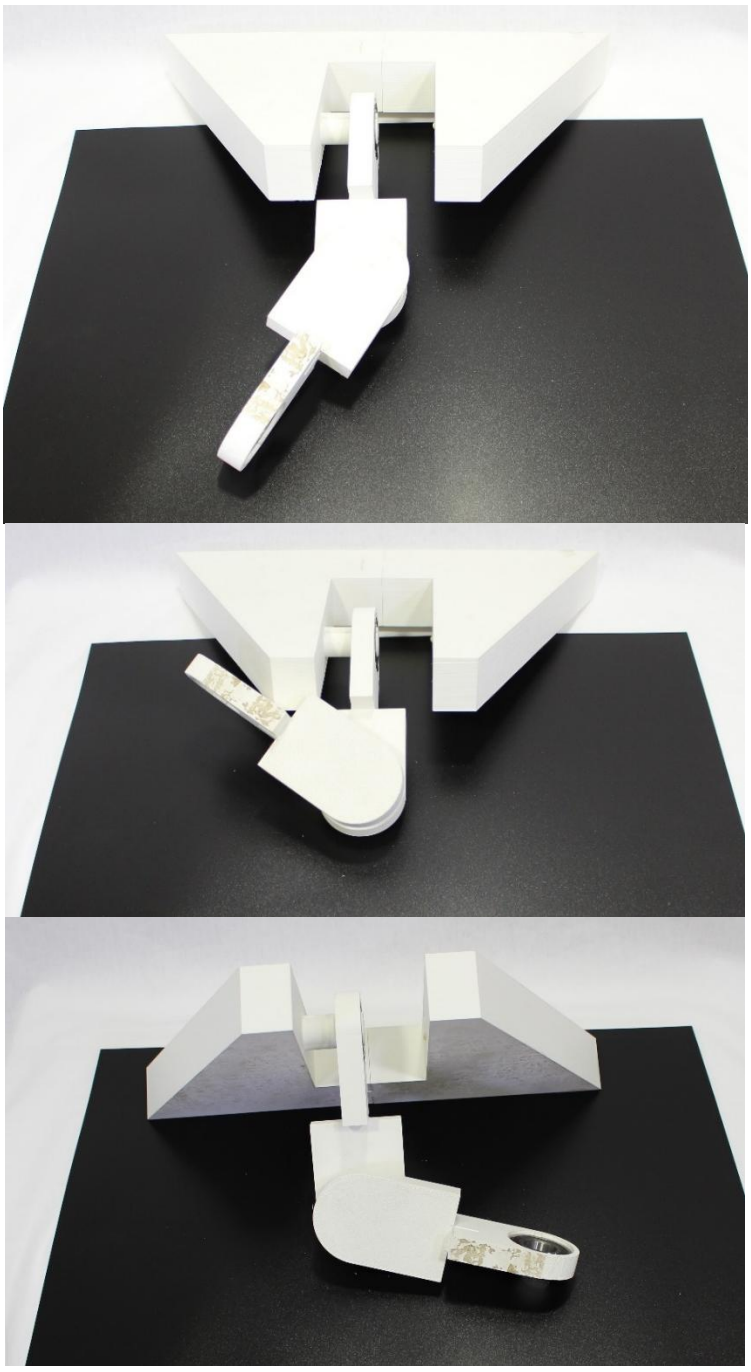

Figure 5.3-24 Yaw and pitch rotation check of Dual Axis one way bearing systems- mark 3- assembly type 3

5.3.5.3 Constraints and Limitations

Despite its improved articulation and compactness, the Mark 3 prototype exhibited several critical limitations that highlighted the inherent trade-offs in its design.

Lack of Reversibility:

Unlike Mark 1 and Mark 2, which incorporated ratchet-based return mechanisms, this version was non-reversible. Once deployed, the one-way clutch bearings locked unidirectionally, preventing smooth retraction. Attempts to force reversal not only undermined deployment efficiency but also compromised the notch integrity of the primary CSK30 bearing, occasionally leading to mechanical failure (Figure 5.3-25). This irreversible nature emerged as the most significant drawback of the Mark 3 system, limiting its adaptability in scenarios requiring repeated cycles of deployment and stowing.

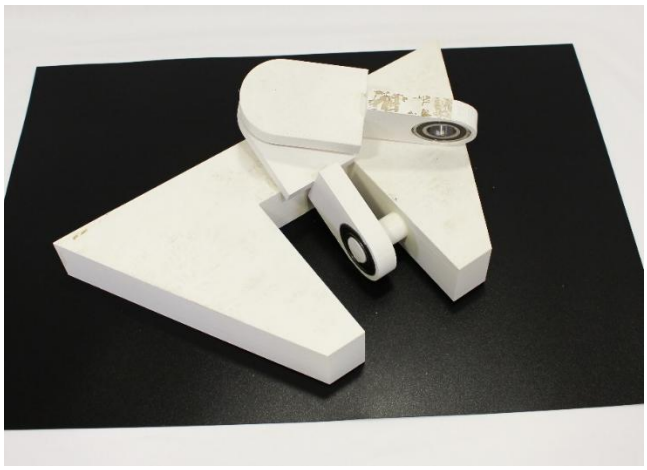

Figure 5.3-25 Mark 3 failure report - lack of reversibility

Bearing Housing Failures:

Structural weaknesses were observed around the bearing housings, particularly at stress-concentrated anchor points. Misalignments, hairline cracks, and occasional delamination were evident even under light loads. These issues stemmed largely from insufficient wall thickness and the limitations of 3D printing resolution. While functional for prototyping, the material and fabrication approach constrained durability, suggesting that future iterations would require either reinforced housings, hybrid material inserts, or higher-precision manufacturing methods.

Angular Overextension:

The increased rotational freedom of the Mark 3 system occasionally resulted in angular overextension (Figure 5.3-23). Along the pitch axis in particular, units exceeded their intended range of motion, leading to partial collapse or structural distortion. The absence of integrated stops or external limiters allowed joints to move beyond controlled boundaries, highlighting a need for built-in safeguards to preserve structural coherence during dynamic deployment.

Comparative Reflections:

When considered alongside Mark 1 (ratchet-spring mechanism) and Mark 2 (dual ratchet with ball joint), Mark 3 represents a significant step forward in integrating rotational behaviours with

greater modularity, precision, and repeatability. Unlike its predecessors, it eliminated backlash and provided a cleaner kinematic profile. However, these gains came at the cost of reversibility, a feature in which Mark 1 and Mark 2 performed considerably better due to their ratchet-based manual return systems. As such, Mark 3 traded operational flexibility for stability and precision. This reinforces the broader conclusion that no single joinery configuration is universally optimal, and each prototype responds differently depending on the deployment requirements, locking conditions, and curvature control strategies of the system.

5.3.5.4 Future Improvements and Opportunities

The observations made during the development and testing of the Mark 3 prototype highlight several promising directions for refinement. These opportunities are not only incremental but also foundational for bridging the gap between proof-of-concept experimentation and deployable architectural application.

Integrating Reversibility:
The lack of reversibility remains the most critical shortcoming of the Mark 3 system. A possible solution lies in embedding a compact flick-switch ratchet or spring-based lock override within the bearing housing. Such a mechanism would allow controlled bidirectional rotation, making it possible to retract and redeploy the system multiple times without damaging the bearing notches. Restoring this capacity would align the prototype more closely with the requirements of deployable systems in practice, where flexibility and repeatability are as important as stability.

Material Upgrade:
Current reliance on PLA for 3D printing proved insufficient in terms of strength and long-term performance, particularly at stress-concentrated regions. A shift to PETG or carbon-fiber-reinforced composites would provide greater durability, higher impact resistance, and improved tolerance to stress. Such a transition would also allow thinner walls without compromising toughness, thereby improving both spatial efficiency and robustness in real-world conditions.

Snap-Fit and Modular Assembly:
Assembly and disassembly remain cumbersome in the present iteration. Introducing snap-fit joints, modular cartridge-style bearing housings, or interlocking features would allow rapid prototyping, quicker replacement of faulty components, and more flexible on-site deployment. This modularity would not only reduce fabrication and testing times but also enable systematic scalability across different structure sizes.

Bearing Angle Calibration:
Fine-tuning the offsets and angular orientations of the Y-axis bearings offers the opportunity to improve compound curvature control. By introducing precise angular restrictions or limiters, the system could achieve smoother and more predictable deformation during dome transitions or shell morphing behaviour. This would directly enhance its suitability for complex architectural geometries requiring adaptive, controlled curvature.

Customised Joinery with Angular Restriction:
While off-the-shelf clutch bearings such as the CSK30 series provided a useful testing baseline, their generic design-imposed limitations on performance. Developing a customised joinery system tailored to reciprocal-auxetic geometries represents a significant opportunity. Such joints could integrate angular restriction features, ensure controlled ranges of motion and prevent overextension or collapse along unintended axes. Unlike commercial bearings, which prioritize industrial generality, a bespoke joint could balance deployability, reversibility, and

load-bearing capacity in a single integrated system, specifically engineered for architectural deployment.

Machine based load Articulations
At this stage, testing was deliberately limited to manual methods, relying on hand-applied pressure and loads to assess movement feasibility and validate basic locking behaviour. Mechanical or machine-based load simulations were not employed, both due to resource constraints and because the immediate objective was to confirm proof of movement rather than full structural performance. However, future investigations could incorporate mechanical testing and advanced load simulations to provide a more comprehensive evaluation of structural integrity and performance under applied stresses

Together, these improvements outline a clear path forward: moving from adaptation of industrial components to the creation of specialised architectural joinery systems. With stronger materials, modular assembly strategies, enhanced angular control, and tailored mechanical designs, future iterations of the DR-STAB framework can evolve from experimental prototypes into robust, versatile, and scalable systems suitable for real-world applications.

5.3.5.5 Conclusion and inference

The Mark 3 prototype marks a significant leap in the development of mechanical joineries for deployable, auxetic structures. By leveraging precision one-way bearings, it achieves multi-axis movement, passive locking, and compact housing, forming the basis for scalable, repeatable modular components. While its non-reversibility poses challenges, its performance in deployment accuracy, structural stability, and component integration signals its readiness for large-scale application with only minor refinements. This prototype thus embodies a critical balance between kinematic performance and architectural usability, reinforcing the thesis ambition of bridging design experimentation with real-world construction potential.

5.3.6 Comparative Analysis of Joinery Prototypes

Table 5.3-1 Non Analytical Comparative table of 3 physical prototypes

Aspect	Mark 1: Ratchet + Spring	Mark 2: Dual Ratchet + Ball Joint	Mark 3: One-Way Bearing System
Primary Function	Yaw movement with passive spring return	Multi-axis control using yaw and pitch mechanisms	Clean multi-axis movement with passive locking
Controlled Axes	Z-axis (Yaw); limited pitch via spring flex	Z-axis (Yaw) and Y-axis (Pitch)	Z-axis (Yaw) and Y-axis (Pitch), better separation
Locking Mechanism	Ratchet with spring-loaded fallback	Dual ratchets with friction locking	One-way bearings restrict reverse movement
Reversibility	Yes – Spring returns to rest position	Yes – Manual locking/unlocking through dual ratchets	No – Movement is locked post-deployment
Component Complexity	Medium – Few moving parts	High – Two ratchets, ball	Medium – Bearings housed

	(ratchet, spring)	joint, more assembly	in compact custom print
Material Used	Steel ratchet and spring, PLA housing	Steel ratchets and ball joint, PLA housing	Steel bearings (CSK30PP & CSK25PP), PLA housing
Yaw Range (Z-axis)	0°–120°	0°–120°	0°–120°
Pitch Range (Y-axis)	<10°, uncontrolled via spring	5°–30° target; collapses at ~90° without stop	0°–30° simulated; crashes after 90°
Articulation	Spring compliance	Ball joint for minor flex (±5°)	Bearing-only articulation, no ball joint
Assembly Size	~150 mm diameter, 80 mm thick	250–300 mm diameter, 100 mm thick	~100 mm diameter, 80–100 mm thick
Deployment Stability	Moderate – Spring tension varies	Low–Moderate – Friction-based locks inconsistent	High – Bearings passively lock, stable form
Fabrication Issues	Spring calibration difficult; some backlash	Bulky; frequent print failures; internal collisions	Early housing delamination; bearing misalignments resolved with iterations
Cycle Testing	5–10 cycles; spring fatigue observed	~5–7 cycles; risk of collapse if over-pitched	~10 cycles; stable performance
Main Advantage	Simple, reversible, fast-to-produce	Multi-axis control and flexible motion	Modular, stable, precise control, ready for scaling
Main Limitation	Weak pitch control and return tension	Too bulky and fragile in pitch articulation	No reverse deployment, failure beyond 90° pitch
Ideal Use Case	Compact reversible joints, temporary pavilions	Experimental systems needing full articulation	Modular deployable shells requiring accuracy and locked form

5.3.7 Overall Insights

The comparative evaluation of the three prototypes (Table 5.3-1) reveals a progressive enhancement in mechanical performance, design logic, and deployability feasibility, with each prototype addressing specific challenges and trade-offs in joinery design for deployable reciprocal-auxetic shells.

Mark 1, the simplest of the three, effectively established the foundational logic for directional movement and passive locking using a ratchet and spring mechanism. Its reversibility, compactness, and ease of fabrication made it ideal for simulating deployable behaviours in early-stage experiments. However, it suffered from a lack of control over pitch movement and required careful spring tuning, which limited its reliability under varying loading conditions.

Mark 2 introduced a more ambitious dual-ratchet and ball joint configuration, enabling multi-axis articulation. It demonstrated improved pitch control and offered a partial load-dampening mechanism through the ball joint, representing a significant conceptual leap. Yet, this advancement came at the cost of mechanical complexity, spatial inefficiency, and locking inconsistency, particularly along the pitch axis due to reliance on off-the-shelf ratchet components.

Mark 3 reflects the most refined iteration, leveraging precision-engineered one-way bearings to achieve clean multi-axis control, passive locking, and modular construction. Its compact design, stable deployment, and low part count make it highly suited for scalable architectural applications. Though it lacks the reversibility offered by Mark 1 and 2, it compensates with robust articulation, repeatability, and resistance to unintended collapse, which are essential qualities for real-world structural systems.

While each prototype contributes uniquely to the research, Mark 3 stands out as the most advanced and practically viable solution. It combines mechanical precision, structural stability, and deployable fluidity in a compact housing, making it ideal for full-scale implementation in reciprocal and auxetic systems. However, it's important to recognize that Mark 1 and Mark 2 introduced critical ideas namely, reversibility, dual-axis experimentation, and manual override capabilities which informed the evolution toward a more robust joinery model. In essence, the development of these three prototypes represents an iterative refinement of principles, where each version has played a distinct and valuable role in shaping the final direction of the thesis.

Full Photo documentation of Mechanical joinery , Building process and kinetic movement documented and reported in Appendix J : Physical Prototype (Testing Mechanisms& Movements)

5.4 Digital Simulations of mechanical joinery

5.4.1 Simulation Logic and Workflow

To evaluate the deployment mechanics of the one-way bearing joinery system Mark 3 , we began by modelling a single-junction network architecture in SolidWorks. This foundational unit was treated as a self-contained mechanical node capable of rotational articulation under defined constraints. Each junction was studied independently to analyze its degrees of freedom, locking behaviour, and interaction dynamics with adjacent nodes.
The simulation progressed through scalable assembly stages, beginning with a 6-unit triangular configuration, which was the first full module tested for synchronized motion. Unlike a bottom-up rigid anchoring strategy, we adopted a push-up actuation logic, where motion was induced from the center or base upwards to mimic the effect of deploying a dome. This method

allowed for organic observation of joint responsiveness and motion propagation across the curved surface.
During this process:

- Each junction node adhered to the Mark 3 bearing logic, with yaw capped at ±120° and pitch capped at 30°.
- The assembly was positioned over a partial dome geometry, and deployment was simulated by physically raising the base units along a Z-axis path to observe how the joints adjusted, locked, or failed under cumulative motion.
- This push-up simulation strategy was selected to resemble real-world expansion mechanics and operator-based deployment methods, enabling observation of emergent spatial behaviour without relying on abstract force application.

Following the 6-unit test, we continued simulation at 2-unit 6 unit and 24-unit scales, analysing motion consistency, angular drift, and constraint integrity at each level. Observations were then compared against physical prototypes and parametric Grasshopper simulations to validate the fidelity of the digital model.

5.4.2 Limitations and considerations Due to Computational Constraints

It is important to acknowledge a significant limitation encountered during the digital simulation phase: computational power constraints significantly restricted the extent of simulated lattice expansion. While theoretically, the auxetic reciprocal lattice structure is capable of expanding up to 2.84 times its original flat, two-dimensional surface area, practical computational limitations in SolidWorks forced the current study to scale down this ambitious target. Consequently, the simulated deployment scenario demonstrated here explores only approximately 15–20% of the lattice's maximum theoretical expansion capacity, corresponding to a surface area expansion factor of approximately 1.32 times (from final results) in a curved, three-dimensional deployment. This limitation was imposed to maintain file stability, prevent solver convergence issues, and ensure manageable computational run-times, thus enabling effective and realistic observation of the fundamental kinematic behaviours within the available computational resources. Nonetheless, this scaled-back simulation provides valuable insights into the system’s mechanical deployment principles and represents a robust foundational step, inviting future research to fully leverage enhanced computational tools or methodologies capable of rigorously exploring the complete potential expansion range.

5.4.2.1 Proxy modelling logic :

To ensure the SolidWorks simulation remained computationally feasible while preserving the essential mechanical behaviour of the deployable joinery system, a proxy modelling approach was adopted. Given the complexity of accurately modelling each joinery component with detailed ratchet teeth profiles, intricate material interactions, and dynamic locking mechanisms, fully resolving these elements in a large assembly would result in prohibitively heavy files and unmanageable simulation runtimes. To address this, a simplified proxy geometry strategy was implemented, wherein each joinery was represented by a cylindrical element embedded with assigned kinematic properties that emulate the intended behaviour. Specifically, these proxy cylinders were configured to allow unidirectional rotation (simulating the bearing’s free movement in one direction) while enforcing a locking condition in the opposite direction, effectively replicating the ratcheting action without geometrically modelling the teeth or internal mechanics. This abstraction allowed for multiple units to be incorporated into the simulation environment while maintaining a light file size and stable assembly performance. The following unit-wise breakdown details how this proxy logic was systematically applied to individual components and assemblies, ensuring that the essential motion dynamics and locking behaviours were accurately simulated despite the geometric simplifications

5.4.2.2 Material choice for simulation inputs

Prior to settling on Stainless Steel 316, we evaluated a range of candidate materials mild steel for its cost-effectiveness and ease of machining, Stainless Steel 304 for its common availability and basic corrosion resistance, aluminum 6061-T6 for its lightweight strength-to-weight ratio, and advanced composites (e.g., carbon-fiber, polymer blends) for their potential weight savings. However, given the DRSTAB system's requirements for durable, precision-machined joineries subject to repeated deployment cycles and exposure to varying environmental conditions, SS 316 emerged as the most balanced choice. Its superior yield strength (290 MPa) and ultimate tensile strength (580 MPa) ensure robust performance under high stress, while its excellent corrosion resistance guarantees long-term reliability. Moreover, SS 316 offers predictable material properties for simulation (high Young's modulus and known Poisson's ratio), straightforward fabrication, and minimal maintenance making it the logical, convincing choice for our deployable mechanical joineries. Table 5.4-1 exhibits a simplified tabular to follow.

Table 5.4-1 property Value assumptions for Digital simulation

Property	Value	Unit
Density (ρ)	8000	kg/m³
Young's Modulus (E)	193	GPa
Poisson's Ratio (ν)	0.3	(dimensionless)
Yield Strength (σy)	290	MPa
Ultimate Tensile Strength (σuts)	580	MPa
Shear Modulus (G)	77	GPa
Thermal Expansion Coefficient	16.0×10^{-6}	mm/mm/°C
Thermal Conductivity	14.6	W/m·K
Specific Heat Capacity	500	J/kg·K

5.4.3 Individual parts – modelling logic

Before embarking on the full kinematic and stress simulations, we first delve into a comprehensive, part-by-part walkthrough of the DRSTAB contraption (Figure 5.4-1 to Figure 5.4-18). In the following sections, each component triangular frame modules, knuckle-joint connectors (Type 1 and Type 2), base rail attachments, bounded hexagonal frame, support poles, and dome cap is examined in detail. For each, we outline the geometric modelling steps in SolidWorks, material and proxy-logic decisions, mating strategies, and key parameter choices made to balance fidelity with computational efficiency. This foundational review ensures that every design decision is transparent and reproducible before integrating the complete assembly into the simulation environment.

5.4.3.1 Unit Triangular Lattice Module (Overall & Corner Detail)

Dimensions & Modelling Logic

The unit is an equilateral triangular frame with 500 mm sides and an internal diagonal span of ~570 mm. The frame body is 89 mm wide with 14 mm thick walls. An 8 mm groove runs along the inner perimeter for alignment clearance. Each vertex features a 27 mm deep pocket topped by a 36 mm vertical extension to house the junction proxy, creating the interface for adjacent modules and providing the necessary free space for kinematic movement (Figure 5.4-1)

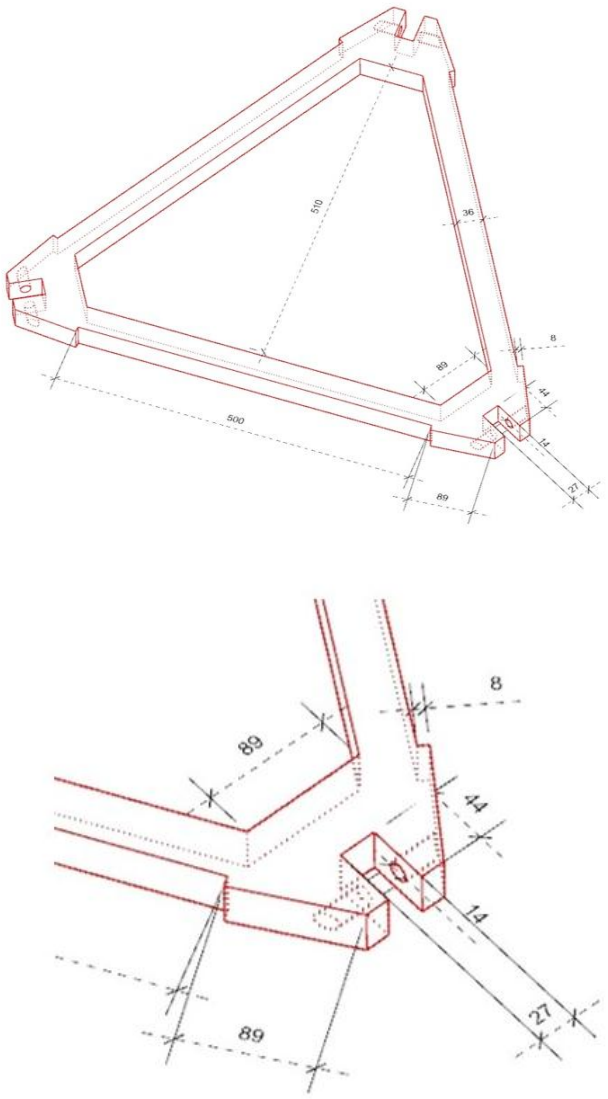

Figure 5.4-1 Unit Triangular Lattice Module

Proxy Logic
To keep the assembly lightweight and simulation stable, each intricate ratchet bearing sub assembly is abstracted as a cylindrical proxy. These proxies carry equivalent mechanical properties allowing unidirectional rotation (free spin in deployment) and instant locking in reverse via custom mate constraints, without modelling individual ratchet teeth.

Working Arrows
Straight arrows along the sides denote the “push up” vector applied to emulate dome deployment (Z axis translation). Circular arrows at each vertex indicate the yaw rotation direction (±120°) and the pitch axis tilt (0–30°, segmented into 0–5°, 5–15°, 16–30° tiers) used during curved deployment scenarios. These arrows clarify how motion is driven and propagated through the lattice.

Technicality
All structural members and proxies are assigned Stainless Steel 316 ($E = 193\,GPa$, $\nu = 0.3$, $\sigma_Y = 290\,MPa$). Detailed tooth geometry and frictional contacts are omitted at this stage rigid body behaviour and mate logic replicate the essential locking and rotational characteristics.

Simulation Setup & Constraints
Solver: Nonlinear kinematic/static study
Mesh: Fine mesh on frame and ultra fine around proxy surfaces and corner fillets
Mates: Concentric Mate for each proxy cylinder
Limit Angle Mates for yaw (±120°) and segmented pitch (0–5°, 5–15°, 16–30°)
Boundary Conditions: Frame base edges fixed on virtual rails; gravity disabled
Motion Drivers:
Z axis "push up" translation applied to base vertices
Angular displacement inputs on proxies to simulate ratchet engagement

5.4.3.2 Junction Type 1 Module

Dimensions & Modelling Logic
The Type 1 knuckle joint connector is built around a 13 mm thick rectangular block that seats within the triangular frame's 27 mm deep pocket. A slim pivot arm extends 100 mm from the block and maintains an 11 mm width, aligning concentrically with the block's cylindrical bore. The center to center distance from the block face to the arm's pivot axis is 53 mm, ensuring proper clearance and leverage when mated to a Type 2 counterpart. All walls and features share a 14 mm nominal thickness to match the frame shell, and generous fillets around the block edges reduce stress concentrations (Figure 5.4-2)

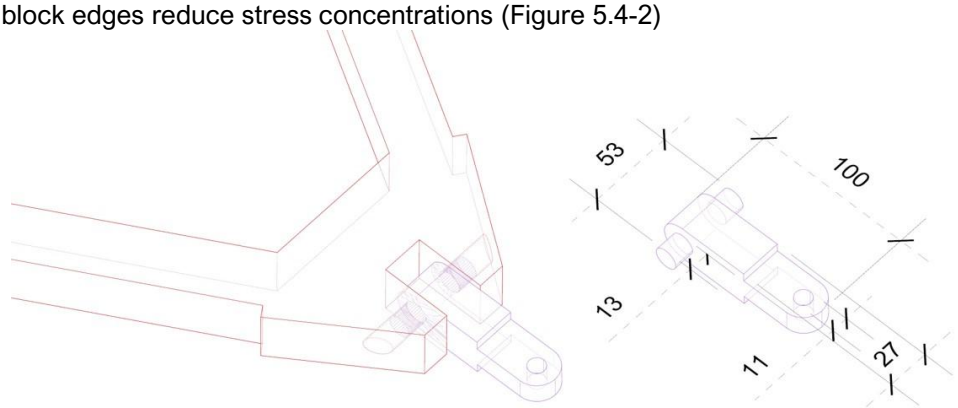

Figure 5.4-2 Junction Type 1 Module

Proxy Logic
Detailed ratchet and bearing geometry are abstracted into two concentric cylindrical proxies:

- A yaw proxy (diameter equals the bore) enforces 0–120° one way rotation via a one way mate.
- A pitch proxy (perpendicular pin) captures 0–30° tilt, segmented into three curvature tiers with limit angle mates.

These proxies replicate the actual joint stiffness and locking behaviour, dramatically reducing part complexity and enabling stable multi unit simulations.

Working Arrows
Red semicircular arrows along the block's top edge illustrate the pitch tilt axis and its allowable range, reflecting how the connector pivots to accommodate dome curvature. Blue circular

arrows around the arm's pivot indicate the yaw rotation and ratchet style reverse lock, visualizing the unidirectional spin that drives sequential deployment (Figure 5.4-3).

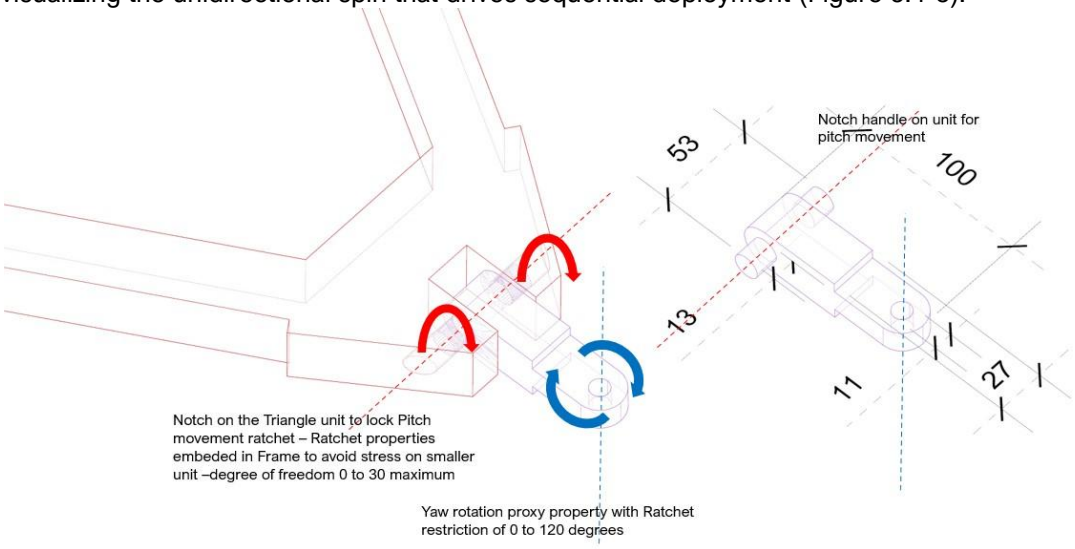

Figure 5.4-3 Junction Type 1 Module - working arrows

Technicality
The entire assembly is assigned Stainless Steel 316 ($E = 193\ GPa$, $\nu = 0.3$, $\sigma_Y = 290\ MPa$). Material stiffness and strength are captured through rigid body proxies and mate constraints, omitting explicit friction or tooth profiles while preserving core mechanical behaviour.

Simulation Setup & Constraints
Solver: Nonlinear kinematic study for large angle movements
Mesh: Fine tetrahedral around proxy interfaces and block fillets; coarser on flat surfaces
Mates:
Concentric Mates for both yaw and pitch proxies
Limit Angle Mates restricting yaw to 0–120° and pitch to segmented ranges (0–5°, 5–15°, 16–30°)
Boundary Conditions: Block base faces fixed to triangular frame; gravity disabled
Motion Drivers:
Prescribed angular displacement on the pitch proxy to simulate curvature engagement
Unidirectional rotation input on yaw proxy to emulate ratchet engagement

5.4.3.3 Junction Type 2 Module

Dimensions & Modelling Logic
The Type 2 knuckle joint connector mirrors its Type 1 counterpart but inverts the mounting orientation to complete the knuckle assembly. It consists of a 13 mm thick block that sits flush against the frame pocket and a 100 mm long, 11 mm wide arm. The pivot block features a 27 mm deep engagement face and aligns concentrically with the arm via a 53 mm center to center spacing from block face to arm pivot. All external walls are 14 mm thick to match the lattice frame, and filleted edges on the block ensure smooth stress flow at the transition (Figure 5.4-4)

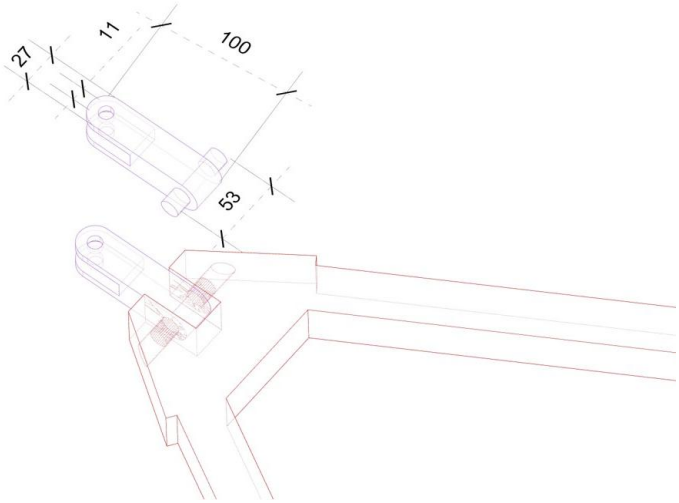

Figure 5.4-4 Junction Type 2 Module

Proxy Logic

As with Type 1, two simplified cylindrical proxies represent the complex ratchet bearing behaviour:

- A yaw proxy cylinder enforces 0–120° one way rotation through a one way mate, simulating the ratchet's locking in reverse.
- A pitch proxy pin provides 0–30° tilt, controlled by segmented limit angle mates corresponding to dome curvature tiers.

These proxies preserve joint stiffness and locking characteristics without detailed tooth geometry, keeping the assembly lightweight and simulation stable.

Working Arrows

Blue circular arrows at the pivot cylinder indicate the yaw rotation direction and ratchet style reverse lock behaviour. Red semicircular arrows at the block's lateral face show the pitch movement axis and its maximum allowable tilt, guiding how Type 2 levers against Type 1 during curved deployment (Figure 5.4-5).

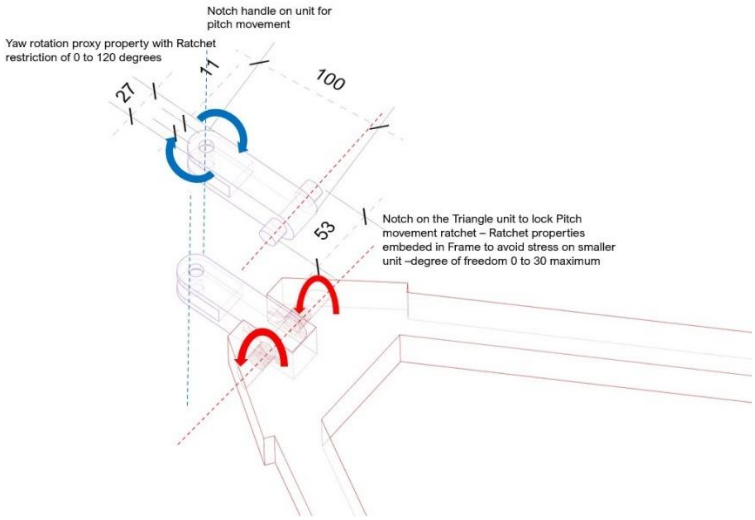

Figure 5.4-5 Junction Type 2 Module - working arrows

Technicality

Both the connector body and proxies are modelled in Stainless Steel 316 (E = 193 GPa, ν = 0.3, σ_Y = 290 MPa). Rigid body proxies with mate logic replace explicit friction or ratchet-tooth modelling, ensuring the critical mechanical interaction is faithfully reproduced.

Simulation Setup & Constraints
Solver: Nonlinear kinematic study for joint articulation
Mesh: Fine elements around proxy cylinders and block fillets; coarser elsewhere
Mates: Concentric Mate for the yaw proxy to the arm
Limit Angle Mates restricting yaw to 0–120° and pitch to segmented tiers (0–5°, 5–15°, 16–30°)
Boundary Conditions: Block base faces fixed to the triangular frame; gravity disabled
Motion Drivers:
Unidirectional rotation input on the yaw proxy to simulate ratchet engagement
Prescribed angular displacement on the pitch proxy to emulate dome curvature tilting

5.4.3.4 Junction 1 – combination of junction 1 and 2 and its movements

In these images we're looking at a single knuckle joint in two extreme positions its relaxed, "closed" stance (Figure 5.4-6)and its fully "deployed" (Figure 5.4-7) end of travel so we can see exactly how the proxy model enforces the intended movement limits.
At the heart of the joint are two concentric cylindrical proxies embedded in the block–arm geometry:

- The yaw proxy, aligned with the arm's pivot axis, permits unidirectional rotation up to a 120° cap. A one way mate simulates the ratchet's free spin in the deployment direction and instant lock on reversal.
- The pitch proxy, oriented perpendicular to the yaw axis, controls the tilt of the arm through 0–30° of motion. This tilt is segmented into three curvature bands (0–5°, 5–15°, 16–30°) via limit angle mates, mimicking how the real ratchet teeth engage in stages.

In the closed state render, the pitch proxy sits at just a few degrees of tilt (red semicircles barely visible) and the yaw proxy is at minimal spin (small blue arrows), so the arm remains nearly flush with the block. In the deployed state render, the arm visually approaches a straight line yet under the hood the yaw proxy is strictly clamped at 120° (large blue arrow) and the pitch proxy at 30° (bold red arcs), preventing any over extension.
By using these simple cylinders instead of detailed tooth geometry, the model stays lightweight enough for large assemblies while still reproducing the authentic ratcheting action. Limit angle mates lock each proxy at its design stop, ensuring the joint's rotation and tilt never exceed the real kinematic bounds.

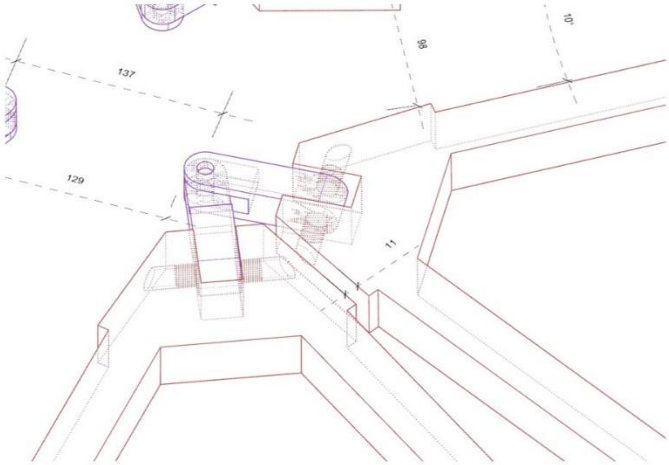

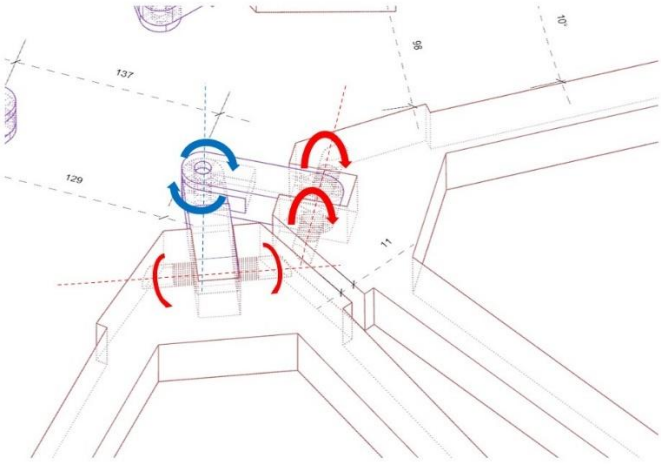

Figure 5.4-6 Junction 1 – combination of junction 1 and 2 and movements

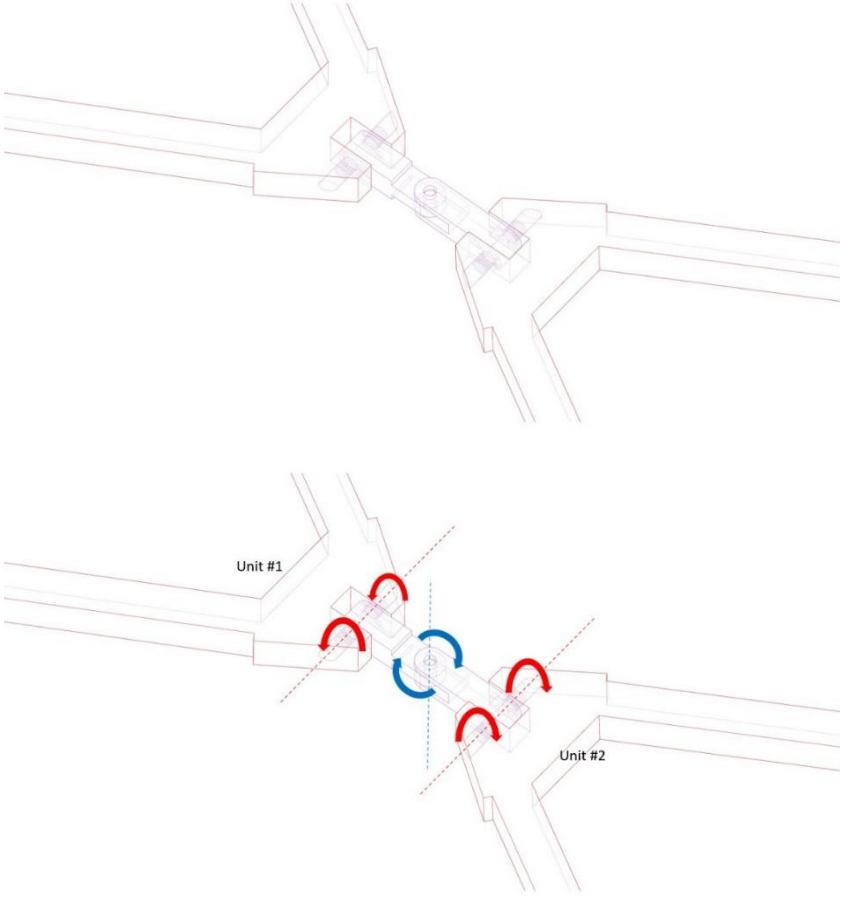

Figure 5.4-7 unction 1 – combination of junction 1 and 2 and movements

Six-unit assembly

Six triangular modules are arranged radially around a central hub, each meeting its neighbors via the Type 1–Type 2 knuckle joints (Figure 5.4-8). Every joint employs the same dual-cylinder proxy logic; a blue yaw proxy enforces one-way rotation up to 120° around the vertical axis, while a red pitch proxy controls tilting in 0–30° stages to accommodate curvature. Limit-angle mates lock each proxy at its design stop, so as you “push up” the ring into a dome shape, each

hinge rotates smoothly in the allowed direction and instantly locks in reverse. The frame bodies remain rigid, with a consistent 500 mm side length and 14 mm wall thickness, but it's the proxy mates that reproduce the ratchet-style kinematics without bogging down performance at this module count.

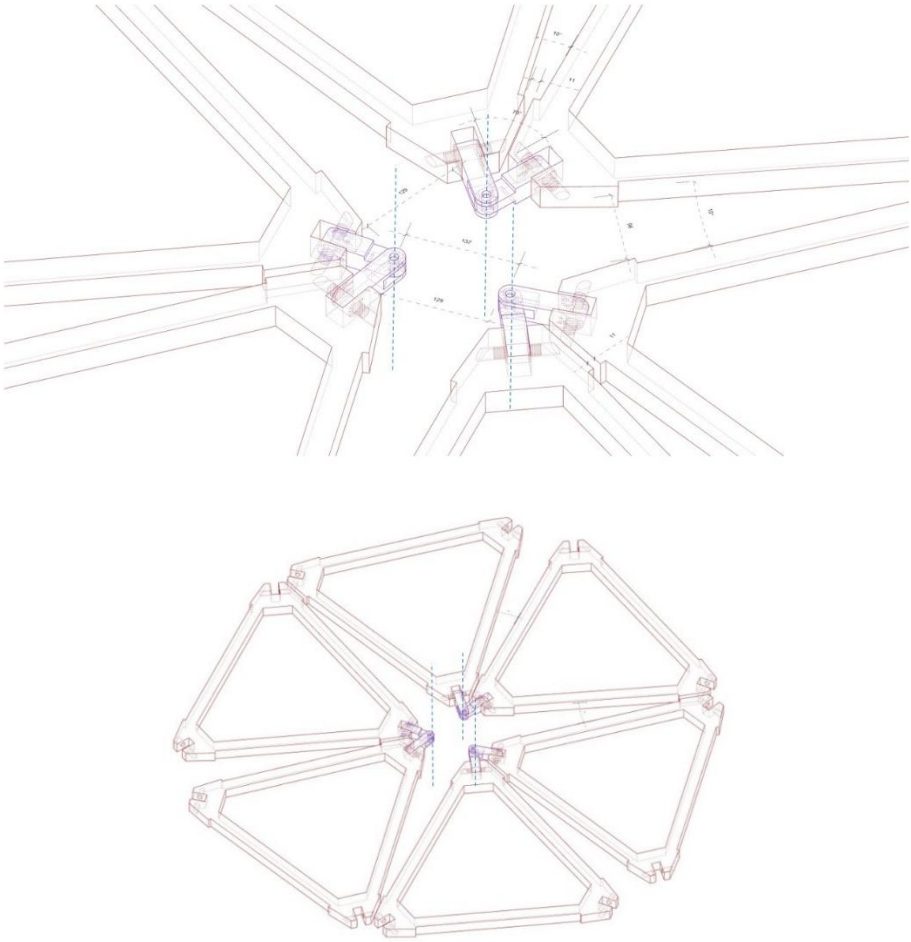

Figure 5.4-8 Six unit assembly

When extending the model to twenty-four units, the same proxy-based joinery logic scales the pattern into a larger hexagonal patch, enabling coordinated yaw and pitch movement across dozens of joints (Figure 5.4-9). Here, you can visualize from prior graphics, the blue yaw axes and red pitch arcs propagating through the network, driving a seamless deployable surface. However, despite using simplified cylinder proxies, the sheer number of mates and bodies pushed the workstation's computing limits: beyond 24 units the simulation became sluggish and prone to errors. Although the original intent was to model a full 32-unit dome, we halted at 24 to maintain file stability. For future iterations, distributing the simulation across higher-performance hardware or further reducing mesh density around noncritical regions could allow us to reach the intended scale.

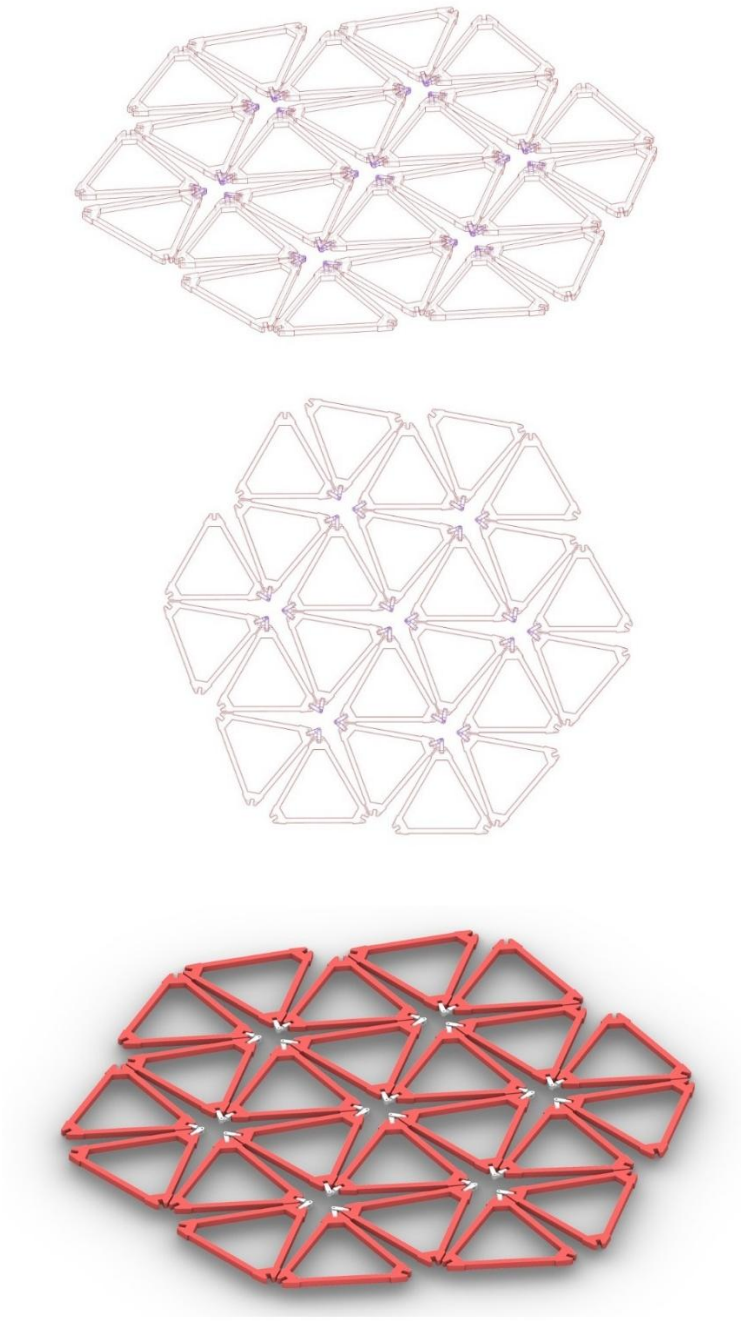

Figure 5.4-9 Twenty four unit assembly

5.4.3.5 Base Rail Attachment System

Dimensions & Modelling Logic

The base connector consists of a 140 mm long main block (13 mm thick) that seats beneath the triangular lattice unit, with an 11 mm-wide extension arm pivoting off one end. A 27 mm deep pocket houses the pivot cylinder, positioned 36 mm from the block face, while a 10 mm diameter hole through the arm aligns with the lattice's Type 1–Type 2 knuckle pin. Opposite

the pivot, a 103 mm long rail slider tab protrudes, sized to slide within a fixed channel. All walls and flanges are consistently 14 mm thick, matching the lattice frames (Figure 5.4-10)

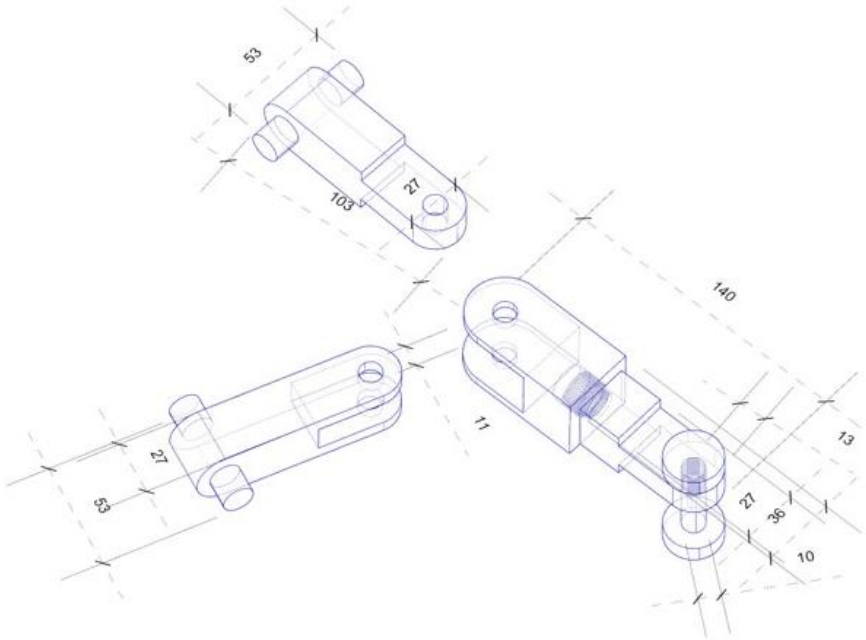

Figure 5.4-10 Base Rail Attachment System

Proxy Logic

To simulate combined angular and linear freedom without heavy geometry, three proxy elements are used:

- A yaw proxy cylinder enforces 0–120° one way rotation at the block–arm joint.
- A pitch proxy pin limits 0–30° tilt between block and frame.
- A linear slider proxy governs the outward rail travel, constrained to the green arrow stroke distance shown.

Each proxy carries equivalent stiffness and locking behaviour through custom mates, eliminating detailed teeth or guide profiles.

Working Arrows

Green straight arrow along the slider tab indicates the allowed linear travel of the base connector, enabling the lattice to “push up” and curve vertically as it expands.

Blue circular arrows at the pivot denote the yaw rotation direction and ratchet style reverse lock, while Red semicircular arrows on the block edges show pitch tilt arcs, illustrating how the unit rocks into curvature as it rides the rail (Figure 5.4-11)

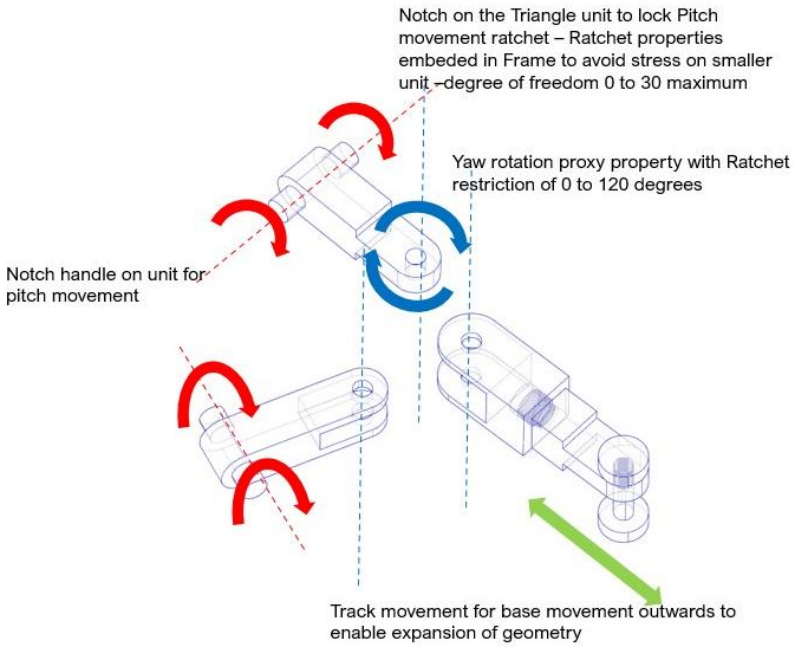

Figure 5.4-11 Base Rail Attachment System - working arrows

Technicality
All components and proxies are assigned Stainless Steel 316 ($E = 193$ GPa, $\nu = 0.3$, $\sigma_Y = 290$ MPa). Rigid body proxy mates replace detailed tooth and guide geometry, preserving the core mechanical response with minimal computational overhead.

Simulation Setup & Constraints
Solver: Nonlinear kinematic/static study
Mesh: Fine around proxy interfaces, coarser on slider tab
Mates: Concentric Mates for yaw and pitch proxies
Limit Angle Mates for yaw (0–120°) and pitch (0–30° tiers)
Slider Mate for linear tab movement, stroke limited to the green arrow distance
Boundary Conditions: Frame block faces fixed to lattice; slider channel walls fixed in world X direction; gravity disabled
Motion Drivers:
Prescribed linear displacement on the slider proxy to emulate rail expansion
Angular displacement inputs on yaw and pitch proxies to simulate ratchet engagement

5.4.3.6 Bounded Hexagonal Base Rail Frame

The adoption of a hexagonal base rail system was determined through an iterative process of trial and failure. The initial attempt employed an open rail configuration, as Chapter 5.4.4.3 Initial 21-Unit Trial Open Railing – Failure Analysis and illustrated in Figure 5.4- 21, which highlights the structural instabilities and lack of constraint that compromised the system's performance. These shortcomings made it clear that a more controlled base condition was required. Although the hexagonal constrictive rail system reduced the degree of predicted expansion compared to the open configuration, its introduction was vital for stabilizing the units, maintaining alignment, and enabling the successful continuation of the simulation process. In effect, the trade-off between expansion capacity and structural coherence became a necessary condition for progression."

Dimensions & Modelling Logic

The Bounded Hexagonal Base Rail Frame is designed as a rigid and robust base to ensure stable support for the DRSTAB lattice assembly during its deployment (Figure 5.4-12). Structurally formed in a hexagonal shape, the frame consists of straight, interconnected segments, each measuring precisely 2144 mm in length. The frame segments have a uniform cross-sectional profile of approximately 89 mm width by 14 mm thickness, providing suitable rigidity to withstand structural and kinetic forces during the deployment phase.

Each segment is integrated with specialized angled notches or guide slots, strategically positioned along its inner edges to securely accommodate and guide the linear sliding motions of the base attachment rail connectors. These angled notches measure approximately 142 mm at the base and taper gently, featuring elongated slots measuring 122 mm in length and 12 mm in width. This geometry facilitates a smooth, linear translation of the base connectors, which allows the DRSTAB triangular lattice modules to expand outwards uniformly. The guide slots ensure consistent directionality of movement, maintaining geometric coherence during deployment.

In total, the hexagonal frame incorporates 12 such angled notches two evenly spaced per segment allowing symmetrical outward movement of the base connectors during the vertical dome-induced deployment process. Due to computational constraints, the current design and simulation intentionally limited the linear translation to within the range defined by these notches, supporting approximately 15–20%

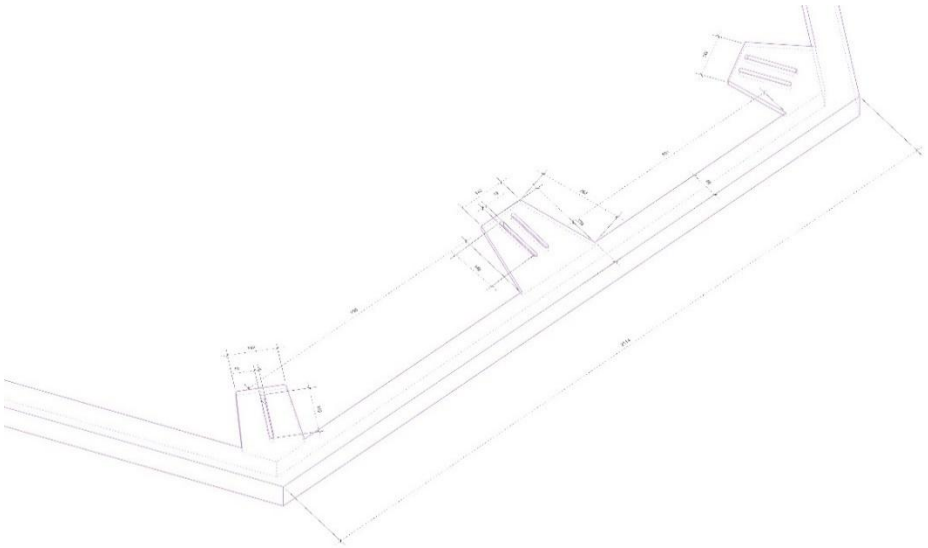

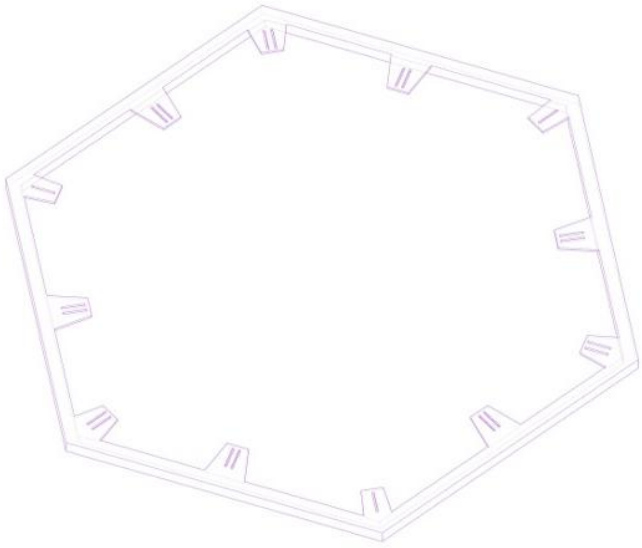

Figure 5.4-12 Bounded Hexagonal Base Rail Frame

Proxy Logic
While the original design envisioned physical rails sliding in ground mounted channels, for simulation we abstract these rails as linear slider proxies. Each notch's guide slots is paired with a one degree of freedom slider mate, enforcing the outward travel without detailed rail geometry. This preserves the intended expansion kinematics without overcomplicating the model.

Working Arrows
Green arrows running along each side illustrate the primary expansion vector: outward linear motion of the lattice modules as the structure "pushes up" into a dome shape. These arrows indicate the direction and extent of slider travel permitted by the proxy mates. (Figure 5.4-15)

Technicality
The entire frame is assigned Stainless Steel 316 ($E = 193$ GPa, $\nu = 0.3$, $\sigma_Y = 290$ MPa). Rail and guide interactions are handled by rigid body slider mates no detailed contact or friction is modelled at this stage.

Simulation Setup & Constraints
Solver: Nonlinear kinematic study
Mesh: Fine along notch walls and proxy slots; coarse elsewhere
Mates:
Slider Mates for each of the twelve guide slots, stroke limited to the notch depth (27 mm)
Boundary Conditions: The hexagon's outer edges are fully fixed; gravity disabled
Motion Drivers: Prescribed linear displacement inputs on each slider proxy to emulate the rail guided outward expansion

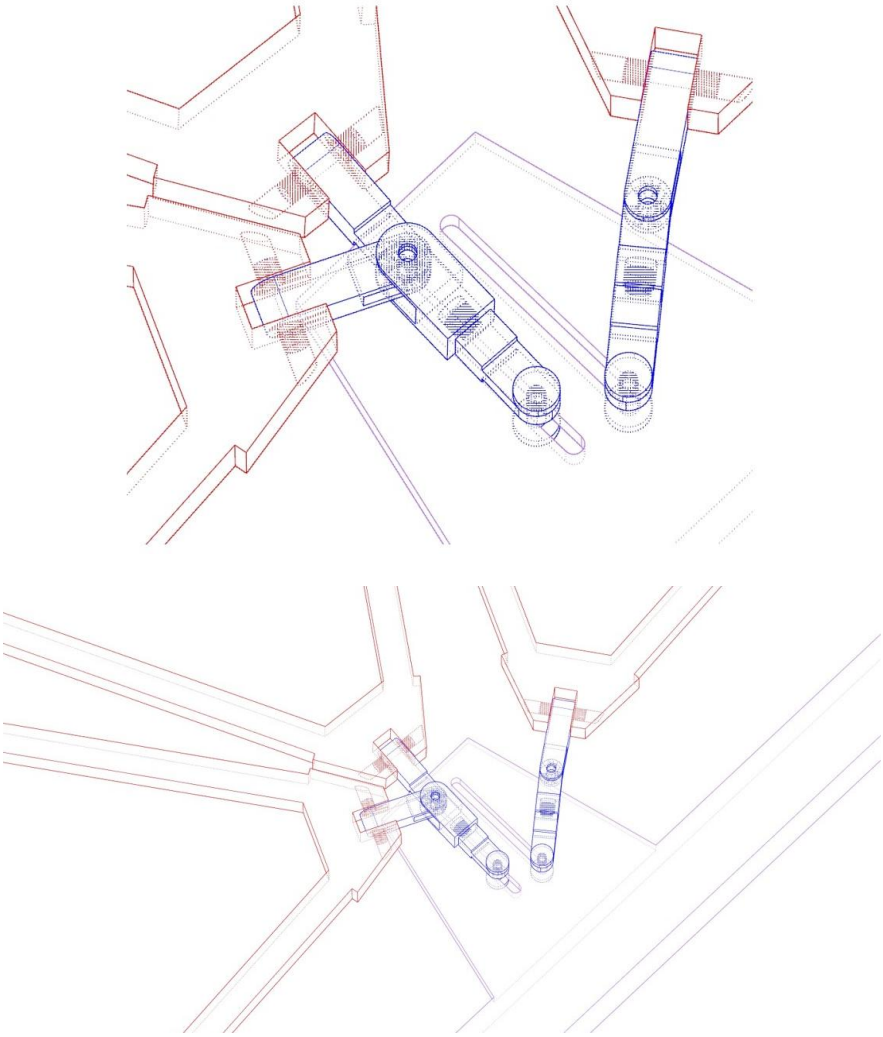

Figure 5.4-13 Base Rail system Frame Assembly

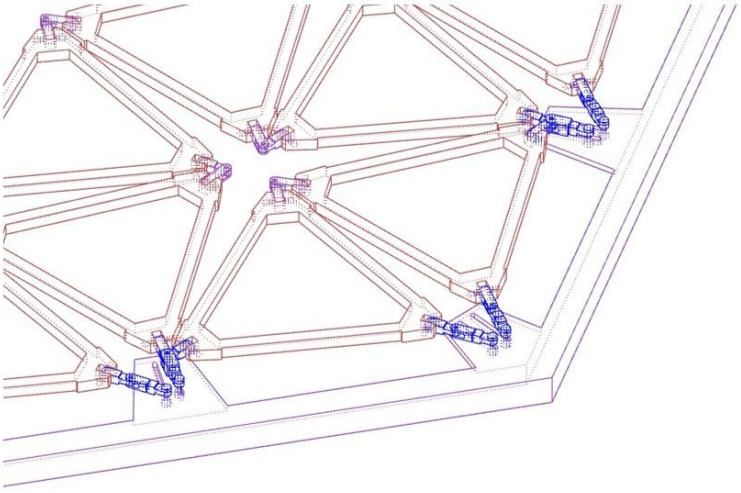

Figure 5.4-14 Base Rail system Frame Assembly

Here, each Base Rail Attachment System is fully engaged with the Bounded Hexagonal Base Rail Frame, creating a self contained, six point kinematic ring (Figure 5.4-13 & Figure 5.4-14). As illustrated in Figure 5.4-15 ,the hexagonal frame's twelve notches precisely cradle the slider tab proxies on each connector, so when a linear slider mate drives a 27 mm outward translation (green arrows), the lattice units collectively push up along the rail. Simultaneously, at each knuckle, the yaw proxy cylinder rotates freely in the deployment direction but instantaneously locks on reversal, thanks to a one way concentric mate capped at 120° (blue arrows). In tandem, the pitch proxy pin allows the connector arm to tilt up to 30° segmented in three curvature tiers via limit angle mates (red arcs) so as the ring lifts, each joint smoothly accommodates the evolving dome curvature. By abstracting the complex ratchet teeth and guide rails into these three simple proxies (slider, yaw, pitch), the model maintains high kinematic fidelity while keeping file size and solver load manageable. This integrated proxy network orchestrates the coordinated outward slide, pivoting yaw, and controlled tilt that transform the planar hexagon into a reliable deployable dome.

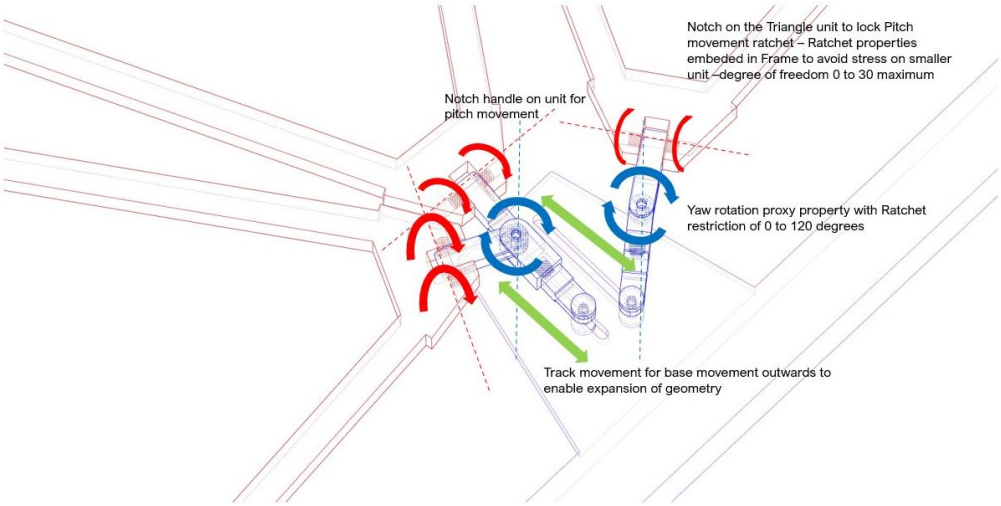

Figure 5.4-15 Base Rail system Frame Assembly- working arrows

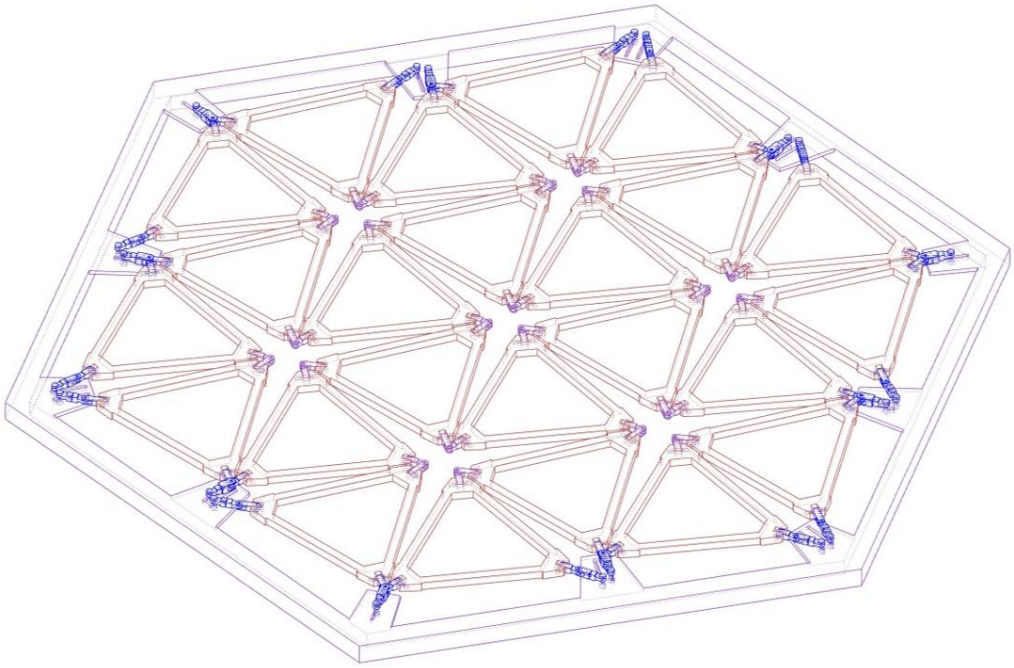

Figure 5.4-16 Overall Full Frame Assembly

5.4.3.7 Hemispherical Dome Rig and Support Poles

Dimensions & Modelling Logic

To emulate the dome's inflation in lieu of a true fluid structure or membrane simulation, a sturdy hemispherical rig was modelled beneath the base joinery ring (Figure 5.4-17) . Two vertical support poles (Ø 358 mm) rise from fixed ground points and terminate in a solid SS 316 dome cap approximately 2 100 mm in diameter. Clearance between the dome and the hexagonal frame notches is set to 10 mm to prevent binding during vertical travel.

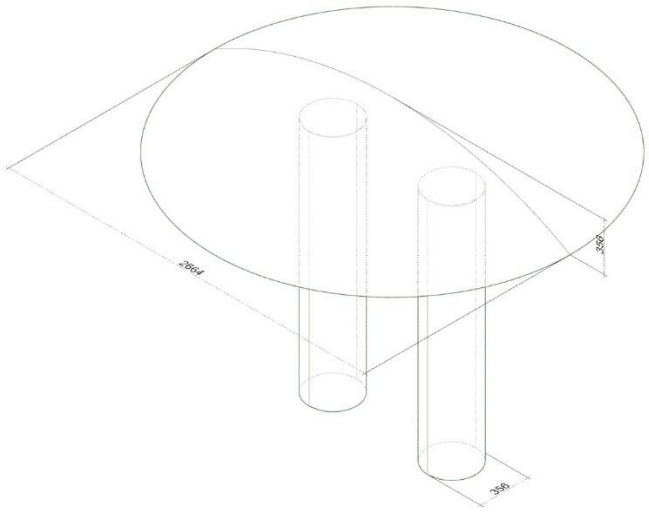

Figure 5.4-17 Hemispherical Dome Rig and Support Poles

Proxy Logic
Because SolidWorks does not natively simulate inflatable membranes, this rigid dome surrogate is abstracted as a single slider proxy. A vertical translation mate prescribes the dome cap's upward motion, which simultaneously drives all twelve base connector slider proxies. As the dome cap rises, each connector's linear slider proxy unlocks for a 27 mm outward stroke, its yaw proxy cylinder pivots up to 120°, and its pitch proxy pin tilts up to 30°, faithfully reproducing the ratchet style and hinge tilt behaviour without modelling membrane inflation.

Working Arrows
Blue upward arrows alongside the support poles indicate the prescribed vertical displacement of the dome cap (Figure 5.4-18). These arrows illustrate how the rigid shell pushes against each base connector's slider tab, initiating the coordinated expansion of the lattice above.

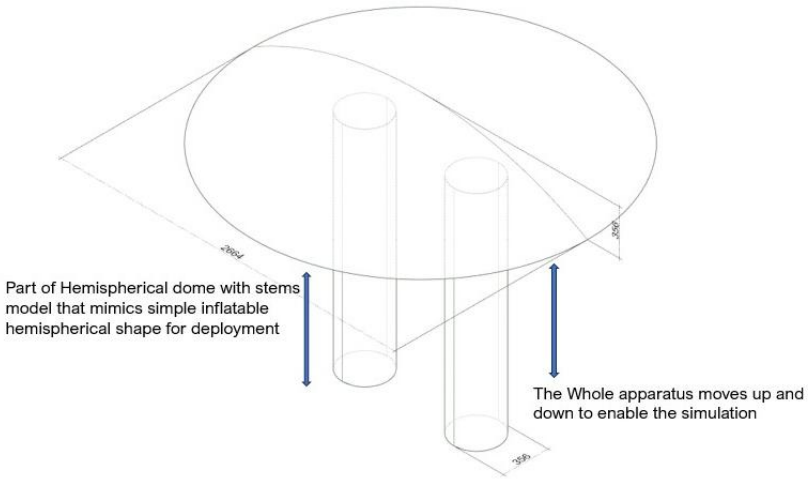

Figure 5.4-18 Hemispherical Dome Rig and Support Poles

Technicality
All dome and pole components are assigned Stainless Steel 316 ($E = 193$ GPa, $\nu = 0.3$, $\sigma_Y = 290$ MPa). The dome is modelled as a rigid solid, omitting any shell or fluid–structure coupling, so that its sole function is to impart motion to the proxy mates beneath.

Simulation Setup & Constraints
Solver: Nonlinear kinematic study
Mesh: Coarse on dome shell; fine around pole bases and slider interfaces
Mates:
Slider Mate for dome cap vertical translation (stroke = 200 mm)
Concentric Mate fixing each pole to its ground mount
Boundary Conditions: Pole bases fully fixed; gravity disabled
Motion Drivers: A prescribed vertical displacement on the dome slider proxy synchronously engages all underlying slider, yaw, and pitch proxies, transforming the planar hexagon into a raised dome without complex inflation dynamics.

5.4.3.8 Overall Assembly

This final assembly view brings every element of the DRSTAB contraption together in one simulation ready model (Figure 5.4-19) . The red triangular lattice composed of 24 equilateral 500 mm side modules sits neatly within the purple bounded hexagonal base frame, its corner knuckle joints and rail attachment connectors (in blue) all engaged in their respective notches and guide slots. Beneath the lattice, the two Ø 358 mm support poles and Ø 2 100 mm SS 316

dome cap rise to push the structure upward, emulating membrane inflation via a single slider proxy. Each junction still relies on its dual cylinder proxies a yaw cylinder capped at 120° and a pitch pin limited to 30° while every base connector houses a linear slider proxy for its 27 mm outward travel. All components share the same material assignment (Stainless Steel 316) and are held together by a network of concentric, limit angle, and slider mates that govern kinematic behaviour. This integrated configuration is now ready for the next phase of analysis: a nonlinear kinematic study to capture the motion sequence of outward sliding, pivoting, and tilting; followed by a static stress simulation to evaluate hinge loads, stress concentrations around proxy interfaces, and overall structural coherence under the dome's upward force. By consolidating geometry, proxy logic, and motion driver mechanics into one comprehensive model, we ensure a seamless transition from deployment animation to detailed performance evaluation.

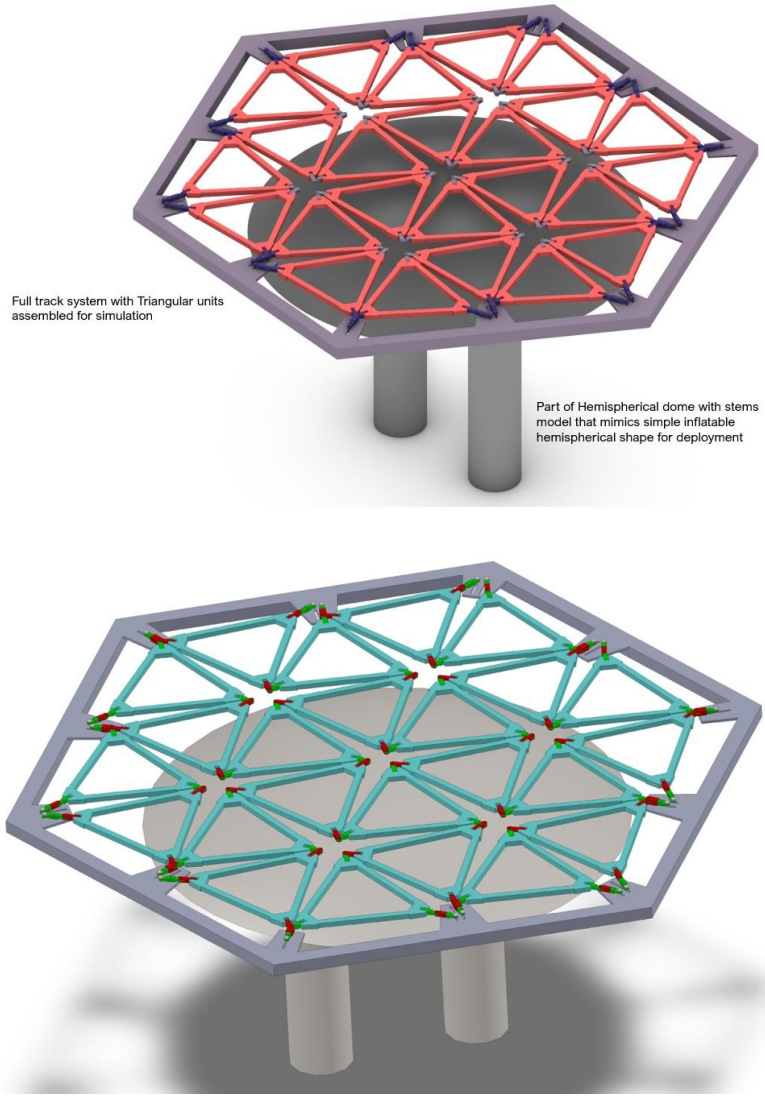

Figure 5.4-19 Overall Full Frame Assembly with Hydraulic poles

5.4.3.9 Overall data of Components and assembly

Table 5.4-2 Data of components and assembly

Component	Count	Volume per Unit (m^3)	Total Volume (m^3)	Mass per Unit (kg)	Total Mass (kg)	% of Total Mass
Triangular Frame Module	24	0.00187	0.0449	14.95	358.80	1.45%
Knuckle Connector (Type 1/2)	36	0.0000162	0.00058	0.13	4.65	0.02%
Base Attachment	24	0.0000347	0.00083	0.28	6.72	0.03%
Hexagonal Base Frame	1	0.01581	0.01581	126.48	126.48	0.51%
Support Pole	2	0.30204	0.60408	2 415.83	4 831.67	19.54%
Solid Dome Cap (hemisphere)	1	2.42400	2.42400	19 392.00	19 392.00	78.47%
Overall Total	–	**3.7372**	**3.0892**	–	**24 720.32**	**100.00%**

An inference from the consolidated data Table 5.4.2 indicates that ,the Dome Cap dominates at 78.4% of the total mass, reflecting its large volume as a solid hemisphere. Support Components (hexagonal frame plus poles) account for 20.1%, providing the rigid backbone and driving mechanics. Lattice Modules (triangular frames, knuckle connectors, base attachments) collectively represent just 1.5%, underscoring their lightweight nature relative to the support structure.

This distribution highlights where material and weight are concentrated guiding future optimization efforts. For instance, exploring lighter alternatives for the dome or poles could dramatically reduce the overall mass, whereas lattice components, though small in mass, are critical to kinematic performance and warrant detailed mechanical analyses.

5.4.3.10 Load distribution per joint under dome weight (for safety factor estimation)

Table 5.4.3 , is an estimated vertical load distribution based on the total mass of the assembly (24 726.52 kg) under standard gravity (9.81 m/s^2), giving a total weight of $\approx$242 567 N. We distribute this load across two sets of joints:

Table 5.4-3 load distribution at joints

Joint Type	Count	Total Load (N)	Load per Joint (N)	Load per Joint (kN)
Knuckle Connector	36	242 567	6 737.98	6.74
Base Attachment	24	242 567	10 106.97	10.11

Notes on Distribution Logic

We assume uniform load sharing among identical joints, recognizing that in practice local geometry and stiffness variations may shift loads slightly. Knuckle connectors carry the weight of the lattice above them, so each experiences roughly 6.74 kN of force in the deployed state.

Base attachments directly interface with the dome rig, hence each supports about 10.11 kN of the upward push required to lift the structure.

These figures provide a first-order estimate of the forces seen by each joint, offering a useful basis for checking joint strength (against SS 316 yield capacity) and guiding future detailed FEA or experimental validation.

5.4.3.11 Moment of Inertia around principal axes (for dynamic studies)

Table 5.4-5, is an approximate moment of inertia for each major sub-assembly about its principal axes, given in kg·m². These values are intended as first-order estimates

Table 5.4-4 Moment of Interia around Principal axis

Sub Assembly	Mass (kg)	I_{xx} (kg·m²)	I_{yy} (kg·m²)	I_{zz} (kg·m²)	Notes / Approximation Method
Triangular Frame Module	14.95	0.31	0.31	0.25	Treated as a thin equilateral triangular lamina (a=0.5 m): Izz≈m·a²/12; Ixx=Iyy≈Izz·(1+sin²(60°)).
Knuckle Connector	0.13	0.00002	0.00002	0.00001	Approximated as a small rectangular prism about its centroid.
Base Attachment	0.28	0.00010	0.00010	0.00004	Rectangular prism assumption for slider tab geometry.
Hexagonal Base Frame	128.23	52.50	52.50	17.76	Approximated as a thin regular hexagonal ring: Izz≈m·R²; R≈0.64 m.
Support Pole (each)	2 415.83	1 833.00	1 833.00	38.65	Solid cylinder h=3 m, r=0.179 m: Ixx=Iyy≈(1/12)m(3r²+h²); Izz=½mr².
Solid Dome Cap (hemisphere)	19 396.19	8 548.00	8 548.00	8 548.00	Solid hemisphere R=1.05 m: Izz≈0.4·m·R²; Ixx=Iyy≈Izz.

Key Assumptions & Methods

- Triangular Frame: Modeled as a uniform triangular plate of side 0.5 m and thickness small compared to in plane dimensions.
- Knuckle & Base Attachments: Small prisms, negligible inertia relative to larger parts.
- Hex Frame: Treated as a thin ring with radius equal to the distance from the center to a side midpoint (≈0.64 m).
- Support Poles: Standard formulas for solid cylinders.
- Dome Cap: Approximated using the moment of inertia for a solid hemisphere about its symmetry axes.

5.4.4 Assembly Simulation in Solidworks

5.4.4.1 Initial Simulation Setup

Fixed Hexagonal Base Frame:
The bounded hexagonal base frame is fully constrained through fixed-geometry mates. This ensures absolute immobility of the base frame, creating a stable reference platform from which the rest of the contraption's kinematic behaviours are accurately observable. All edges and vertices of the hexagonal frame remain stationary, emulating real-world anchorage conditions.

Dome and Support Poles as Motion Drivers:
The rigid, stainless steel (SS 316) dome cap, supported firmly by two robust vertical poles (Ø 358 mm, 3 m height), is employed as the primary actuator. The dome cap, defined as a solid

body, is driven slowly upwards via a precisely controlled linear translation mate, ensuring a gradual, controlled, and realistic vertical displacement. This upward motion provides a proxy for inflation-induced upward force since actual fluid-structure interactions or inflatable simulations are beyond the current SolidWorks capability. The translation is carefully modulated, typically executed over an extended timeframe (e.g., 0–200 mm displacement over several minutes of simulation time), to maintain smoothness and stability in simulation outcomes.

5.4.4.2 Initial trial in 6 units – failure reflection

In our first dome-driven test, a 6-unit triangular lattice was mounted on the bounded hexagonal frame and pushed upward by a rigid dome surrogate (Figure 5.4-20). While the setup was conceptually sound, the prototype failed to deploy as intended. This outcome stemmed from several interconnected issues that quickly became apparent during the trial.

The most immediate limitation was the insufficient rail-slot travel. Even in the modest 6-unit layout, the slider proxies bottomed out almost instantly. The original notch depth and slot length, which had been designed for minimal expansion, proved far too short. As a result, the base connectors could only travel a few millimeters before hitting their limits, leaving the lattice effectively “locked” in place with no meaningful outward expansion.

Another difficulty was the challenge of observing angular motion. With only six units, the theoretical 120° yaw and 30° pitch limits translated into extremely small displacements. In both top-view and side-view video playback, the rotations were so subtle that they were nearly invisible. This made it difficult to verify whether the proxies were behaving as intended and undermined confidence in the validity of the kinematic definitions.

The small number of units also created proximity-induced interference. Because the joints were tightly clustered, connectors frequently attempted to rotate or slide into overlapping spaces. This led to mate conflicts and solver errors that brought the motion study to a halt. Without dedicated collision-avoidance rules or small geometric offsets, the simulation encountered unsolvable constraints almost immediately.

Despite the failure to achieve deployment, these early trials proved invaluable. They demonstrated, first, that the rail-slot depth had to be significantly increased. This insight led us to expand notch lengths from approximately 27 mm to values that could accommodate a full 15–20% expansion in later 24-unit tests. Second, the trials showed that limit-angle thresholds needed to be tuned or staged, so that smaller increments could produce visible motion in low unit counts. Third, they highlighted the necessity of introducing explicit collision-avoidance mates or micro-offsets between adjacent proxies, which we later incorporated as minimal clearances in the refined model.

Armed with these insights, we re-engineered the base frame to a side length of 2144 mm, extended the rail slots accordingly, and reinforced the mate definitions. These targeted improvements directly enabled the subsequent 24-unit deployment simulation, in which smooth and fully constrained expansion was finally realized.

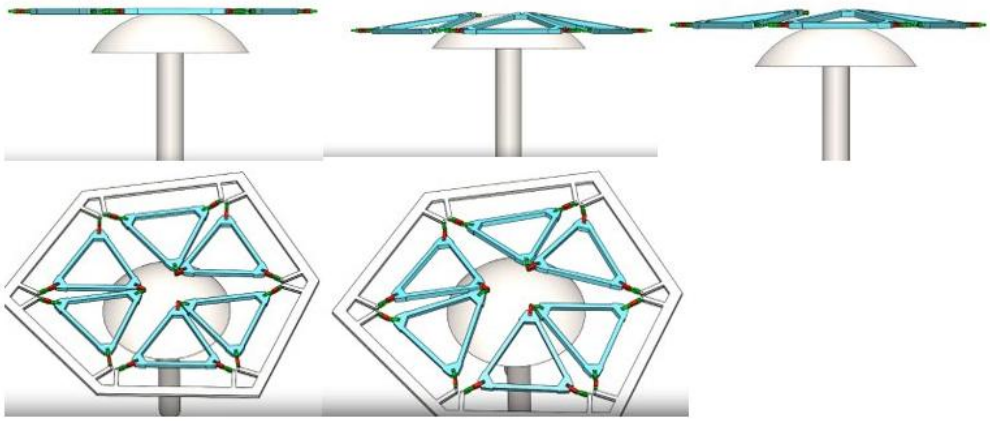

Figure 5.4-20 Assembly simulation of 6 unit system

5.4.4.3 Initial 21-Unit Trial Open railing – Failure Analysis

In our first large-scale kinematic test, we assembled a 21-unit ring on an open-ended rail system directly modelled after the scaled physical prototype. The simulation was recorded as a 15-second video (screenshots shown in Figure 5.4-21) , and the top-view screenshots at 1, 5, 10, and 15 seconds revealed a consistent pattern. While the central modules began to pitch and yaw in line with expectations, the outer units drifted uncontrollably and eventually disengaged from the lattice altogether. This collapse was traced to three primary factors.

The first issue was the unbounded rail geometry. Without clearly defined end stops, the slider proxies on the open rails either bottomed out or drifted laterally. This caused adjacent connectors to misalign and rotate away from their intended paths, breaking the coherence of the motion. The second issue was the absence of adequate collision definitions. Neighboring proxies attempted to move into overlapping spaces, which triggered mate conflicts and solver errors. As the simulation progressed, these conflicts compounded until the assembly could no longer continue. The third issue was the subtlety of the angular displacements. The yaw and pitch limits of 120° and 30°, while appropriate for larger-scale assemblies, produced only minimal visible deformation in the 21-unit ring. This made the movement difficult to observe and equally difficult to verify, reducing confidence in the underlying kinematic setup.

Although the 21-unit test did not achieve stable deployment, it was nonetheless an important step in refining the system. It clearly demonstrated the need for a bounded hexagonal frame, extended rail slots, stricter limit-angle definitions, and explicit collision-avoidance constraints. These lessons directly informed the adjustments that later made the 24-unit deployment simulation smooth, stable, and predictable.

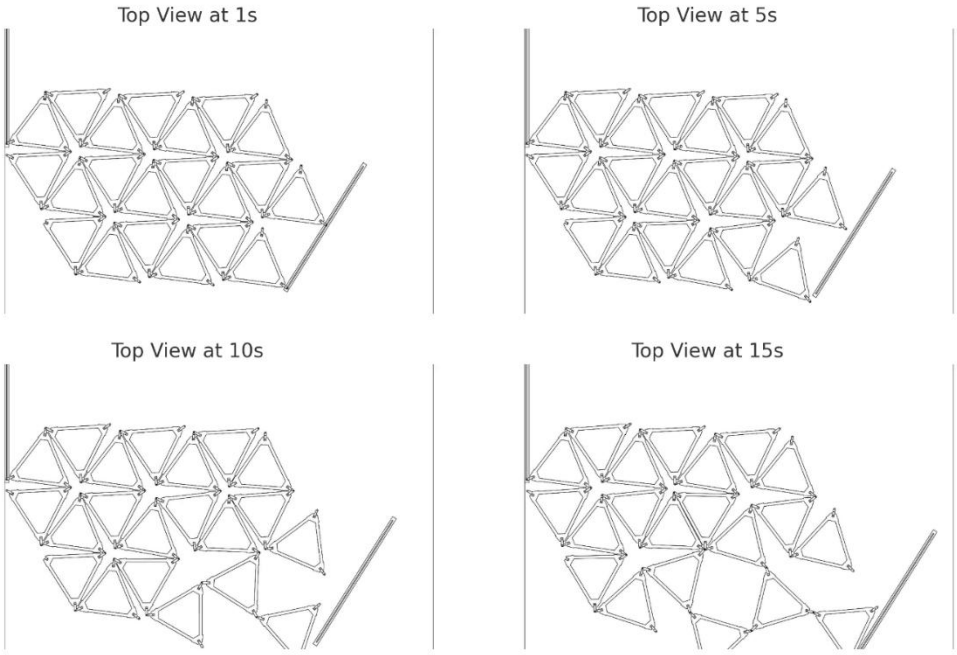

Figure 5.4-21 Assembly simulation of 24 unit - open rail systems

5.4.4.4 Deployment Sequence and Joint Reaction – 24 Units (Expected vs. Observed Outcomes)

The 24-unit deployment simulation was conceived as a definitive test of the system's ability to translate unit-level kinematics into coherent, multi-unit expansion (Figure 5.4-22) . It built upon successful small-scale tests and was expected to demonstrate synchronized pitch and yaw activation through the upward movement of a rigid dome cap. However, while the kinematic logic was sound in theory, the actual simulation revealed critical execution flaws that resulted in complete collapse of the deployable lattice, offering valuable lessons in digital simulation methodology (Figure 5.4-24)

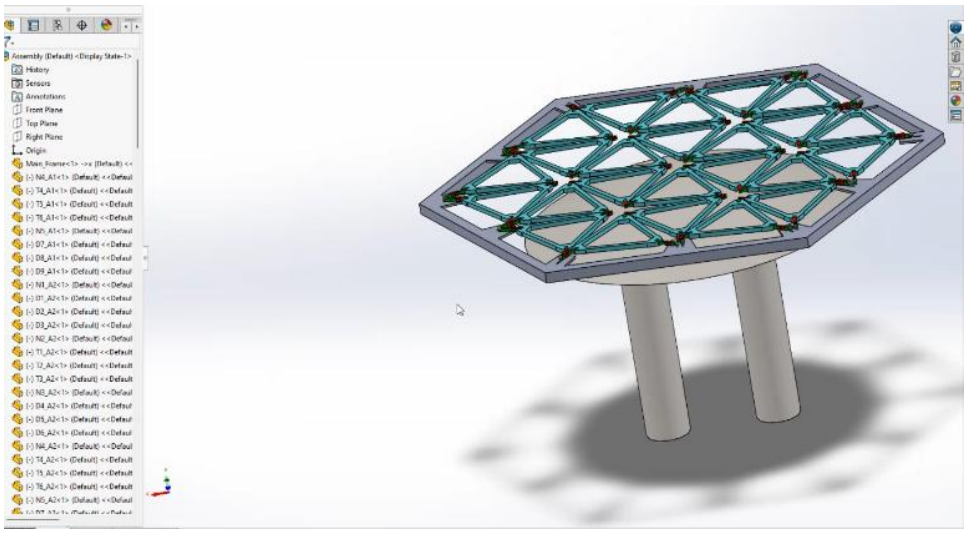

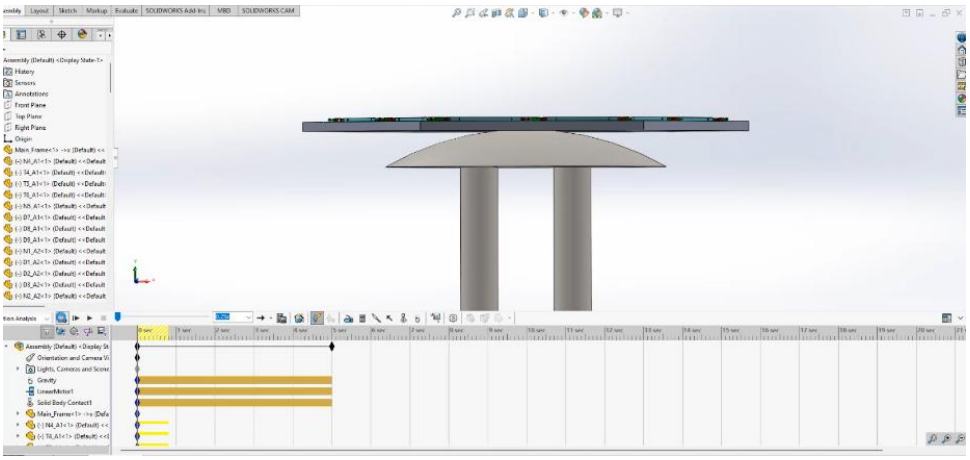

Figure 5.4-22 Overall Full Frame Assembly in motion simulation

Intended Behavior: A Sequential Auxetic Deployment

The simulation was carefully structured to replicate the progressive actuation of each triangular unit within the system, achieved through a combination of linear sliders, pitch-rotation proxies, and yaw ratcheting joints. This setup provided a digital proxy of the mechanical behaviour expected from the physical joinery system (Figure 5.4-23) As the dome cap was lifted vertically along dual support poles, the following sequence of responses was anticipated:

Central Contact and Initiation:
The first point of contact occurred at the central triangular modules. This interaction unlocked the central sliders, initiating the pitch movement of these units at small angles of up to 5°. This early rotation marked the beginning of the dome curvature, establishing the foundational geometry for subsequent transformations.

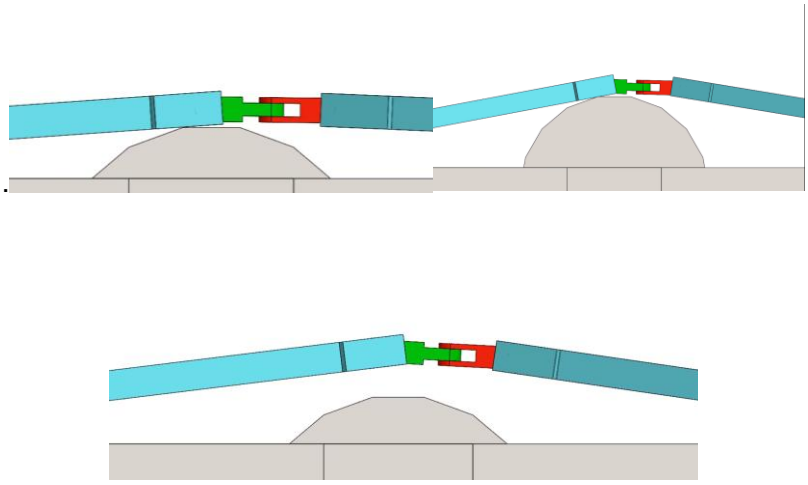

Figure 5.4-23 Singular trial testing of Joinery unit- earlier experiments

Pitch-to-Yaw Transition:
As vertical displacement continued, the central units were expected to extend their pitch angles toward 30°. At this stage, the system introduced controlled yaw rotations capped at 120°, reflecting the intended unidirectional ratchet behaviour of the joints. This transition from pitch to yaw was critical, as it demonstrated the capacity of the joinery to shift seamlessly between degrees of freedom while maintaining structural coherence.

Peripheral Engagement:
The transformations initiated at the center were then designed to propagate radially outward to the neighboring modules. This outward cascade created a coordinated wave of expansion, ensuring that the system's growth respected both structural symmetry and balanced stress distribution. This mechanism was a defining test of whether the auxetic-reciprocal framework could maintain uniformity during large-scale deployment.

Rail Locking and Stabilization:
Once the outermost sliders reached their maximum displacement (27 mm), the structure was programmed to "lock in place." At this stage, the maximum allowable pitch and yaw thresholds were achieved, effectively stabilizing the deployed geometry. The rail system thus acted as both a limiter and a stabilizer, ensuring that expansion did not exceed safe thresholds while preserving the intended dome shape.

Controlled Retraction and Shape Retention:
In the final stage, the dome cap was retracted to evaluate whether the deployed system could hold its shape without continuous external support. This test of retraction was crucial for validating the intrinsic stability of the auxetic-reciprocal design, confirming that once deployed, the geometry could remain self-supporting under its own locked configuration.

Overall, this sequence was designed not only to validate the logical behaviour of the deployable system but also to test the reliability of proxy-based simulation methods in SolidWorks for replicating highly complex mechanical phenomena. By systematically simulating pitch, yaw, and locking transitions, the study was able to evaluate both the theoretical and practical robustness of the joinery framework within a controlled digital environment

Actual Outcome: Collapse Due to Constraint Oversights

Despite this meticulous planning, the simulation failed during execution. Rather than initiating a gradual upward expansion, the lattice collapsed dramatically into the base structure (Figure 5.4-24) . A combination of missing contact definitions and incomplete constraint hierarchies led to a complete structural breakdown, with the system behaving unpredictably under force conditions.

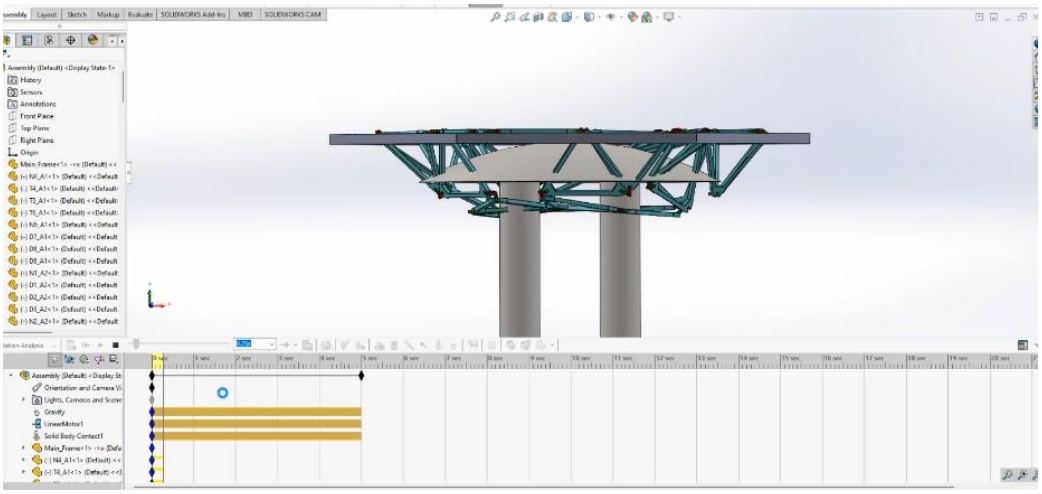

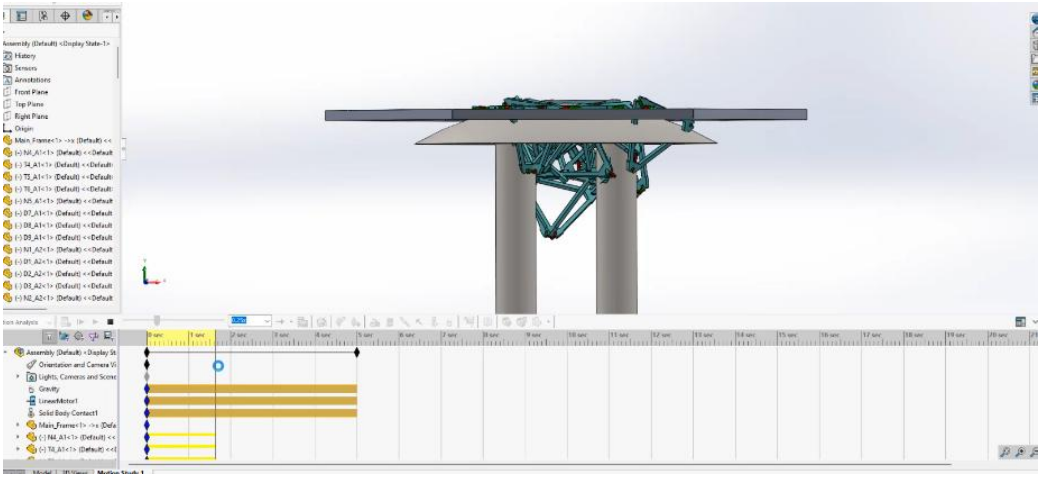

Figure 5.4-24 24-Unit Dome Trial – Failure reporting

Key issues detected :

Absence of Solid Body Contact Definitions

Inferring from Figure 5.4-24 ,One of the most significant shortcomings of the simulation was the absence of solid body contact definitions at the interface between the dome cap's underside and the lattice's top connectors. Instead of being set with "no penetration" or realistic collision-bound constraints, the software allowed the dome to move upward as though the lattice did not exist. This meant the dome passed ghost-like through the structure, completely bypassing the frictional, compressive, and reactive forces that would be present in a real-world deployment scenario. As a result, the intended mechanical interactions that were expected to initiate deformation in the lattice were never triggered, making the simulation meaningless as a predictor of actual behaviour. This error highlighted the importance of establishing robust contact logic in future simulations, as without it, critical load transfers, joint stresses, and system-wide synchronization cannot be validated at any scale.

Support-Pole Geometry Not Interacting

A related issue was the failure of the support-pole geometry to interact meaningfully with the lattice or dome structure. In the intended design logic, these poles were supposed to act as vertical guides, directing the dome's upward trajectory while simultaneously stabilizing the lattice's alignment. However, in the simulation, the poles were defined only as fixed entities at their base without any contact constraints at the dome or lattice interfaces. This left them functionally inert, offering no resistance, boundary conditions, or stabilizing effects. Consequently, the lattice had no physical framework against which to react during the dome's upward motion. Instead of working as a guiding boundary, the dome essentially scooped through the lattice units without restriction. This revealed that structural guide systems in simulation cannot be left as symbolic or placeholder geometries; they must be modelled with accurate solid interactions if they are to replicate the resistance, support, and stability expected in physical reality.

Insufficient Lateral Boundary Conditions

The absence of lateral constraints such as guide pins, stoppers, or rail-based tracks meant that the simulated system lacked positional stability. In practical terms, this deficiency allowed the assembly to drift laterally, destabilizing its geometry under simulated forces. As units lost alignment, internal parts collided, producing cascading failures across multiple joints. This was not an accurate reflection of the intended design but rather an artifact of missing constraint logic. In real-world systems, secondary rails, pins, or lateral supports play a crucial role in distributing loads and preventing uncontrolled geometric drift. Their absence in the simulation

highlighted how even small missing constraints can magnify into system-wide instabilities in computational models. For deployable systems like DRSTAB, where geometric precision and synchronized expansion are critical, lateral stabilization must be explicitly built into both physical prototypes and digital models to ensure accurate behaviour prediction and reliable performance during deployment sequences.

Gravitational Overload on Incomplete Mates

When gravitational forces were applied in the simulation, the shortcomings of incomplete joint definitions became even more evident. Because the upper elements of the lattice failed to engage or lock properly, their weight acted as a destabilizing force, dragging the system downward into itself. Instead of resisting deformation or transferring forces through properly constrained connections, the structure collapsed under its own weight. This outcome did not represent the intended mechanical strategy but rather exposed how the absence of fully defined mates distorted the results. Gravity is a critical factor in architectural-scale simulations, but it must only be introduced after kinematic logic has been validated. Applying it prematurely to an incomplete assembly not only produces misleading outputs but also obscures the system's actual potential. This experience underscored the importance of sequencing simulation steps: validating motion first, then adding gravitational and environmental forces only when joint logic is reliable.

Reflections and Lessons for Future Simulation

Although the simulation failed to validate deployment, the errors themselves became valuable feedback mechanisms. They exposed precisely where digital abstractions diverged from real-world mechanics, particularly in terms of contact detection, inter-part coordination, and boundary condition definitions. These lessons will inform future refinements by emphasizing the necessity of realistic solid body contact, progressively scaled assemblies, and properly sequenced constraints. Importantly, the failures also reinforced the idea that simulations are not endpoints in themselves but iterative testing grounds where missteps provide direction for improvement. Rather than dismissing unsuccessful results as setbacks, they were treated as diagnostic tools that clarified the limitations of the current workflow. This iterative understanding ensures that subsequent efforts will not repeat the same omissions but will instead integrate more robust logic, ultimately moving closer toward digital models that can meaningfully approximate physical deployment.

Restricted Computational Power

A further challenge was the restricted computational power available for running these simulations. Deployable systems with multiple interdependent joints, recursive contacts, and dynamic constraints demand significant processing resources to resolve collision detection, load transfers, and motion hierarchies. In this case, the hardware limitations meant that simulations frequently failed to converge, produced unstable outcomes, or froze mid-sequence. These failures were not indicative of the design itself but of the system's inability to handle the computational demands of such complex assemblies. Limited processing capacity also prevented high-fidelity meshing, which is crucial for detecting localized stress behaviours around joints and connectors. As a result, many analyses were forced to be approximated, lowering their predictive reliability. This underscores the necessity of adopting either more advanced hardware or hybrid workflows, where simulation responsibilities are shared across specialized platforms. For architectural-scale applications, computational efficiency and precision are not optional but essential for validating deployable design systems.

Key learnings from Failures to support Future research :

Proxy Systems Must Be Supplemented with Realistic Contact Logic

The use of proxy systems to represent yaw, pitch, and slider movements proved to be a useful strategy for establishing basic motion at smaller scales. However, when applied to larger assemblies, these simplifications introduced inconsistencies that failed to capture the true complexity of contact interactions, particularly at critical interfaces such as dome–frame transitions and multi-unit joint intersections. Without realistic solid-body contact logic, results tend to overestimate smoothness of motion and overlook issues such as friction buildup, rotational backlash, or tolerance stacking. These omissions create gaps between computational predictions and physical reality. To address this, larger simulations must incorporate full-body contact parameters and collision detection protocols, enabling more accurate analysis of stress transfer and deformation behaviour during deployment. This refinement is especially crucial for scaling up from component-level trials to architectural assemblies, where minor inaccuracies at the joint level can amplify into major synchronization and stability problems.

Assembly Simulation Requires Progressive Scaling

Jumping directly into simulating full 24-unit assemblies proved impractical, as errors and computational overload often disrupted motion pathways before meaningful data could be obtained. A more effective approach involves adopting a progressive scaling method, where simulations are developed incrementally through 6-unit and 12-unit subassemblies. This staged methodology provides opportunities to debug localized motion behaviours, calibrate constraints, and validate load-sharing patterns before attempting full-scale integration. By incrementally scaling complexity, the simulation hierarchy becomes more reliable and less prone to systemic failure. Additionally, progressive scaling allows researchers to isolate issues related to synchronization, rotational bias, or node misalignment at manageable scales, where corrective measures can be quickly applied. This approach not only builds confidence in simulation fidelity but also mirrors the logic of physical prototyping, where smaller mock-ups are often tested before committing resources to larger models. Thus, gradual scaling offers both computational efficiency and greater insight into structural coherence.

Gravity Should Be Temporarily Disabled in Early Motion Tests

In early motion analyses using simplified proxy systems, the inclusion of gravitational forces created distortions that masked the true kinematic behaviour of the assemblies. For instance, sliding and rotational joints were often pulled into unnatural positions or subjected to stresses that exaggerated deflection, leading to false-positive failures during deployment simulations. Temporarily disabling gravity during the initial testing phases provides a clearer framework for mapping motion pathways, aligning unit synchronization, and validating the intended kinematic sequence without the confounding influence of environmental loads. Once these motion behaviours are properly understood and confirmed, gravity and other environmental factors such as wind or live loads can be progressively introduced to test the system's robustness under realistic conditions. This step-by-step inclusion of forces aligns with standard practices in structural simulation, where isolating kinematic logic before adding external constraints ensures greater clarity and prevents premature misinterpretation of system performance.

Simulation Software Limitations Must Be Recognized

Although SolidWorks Motion Study provided a strong starting point for analysing jointed motion, it became evident that the software has limitations when applied to complex, nested assemblies at architectural scales. The software struggled with recursive joint systems, often freezing or producing inconsistent results when multiple rotational and sliding constraints were nested within reciprocal-auxetic frameworks. Additionally, the solver tended to oversimplify or misrepresent scenarios where non-linear behaviours such as backlash, multi-body friction, or large-scale deformation were expected. Recognizing these limitations is essential, as reliance

on a single simulation platform risks misrepresenting both the challenges and the potential of deployable shells. Future explorations would benefit from hybrid strategies, combining SolidWorks for detailed mechanical part analysis with Grasshopper-based plugins such as Kangaroo2 or physics engines better suited for recursive and parametric motion systems. This combination can bridge the gap between mechanical fidelity and architectural scale, ensuring that simulations are both computationally feasible and physically meaningful.

Table 5.4-5 Expected vs observed outcomes of Digital Simulation

Expected (Planned Outcome)	Observed (Actual Outcome)
Dome cap pushes central units upward, triggering smooth radial deployment through yaw and pitch articulation.	Dome cap passed through lattice without contact; central units collapsed downward, causing total system failure.
Controlled yaw rotation of up to 120° achieved progressively via ratchet-like proxy mates.	Yaw proxies not triggered due to premature structural collapse; system never reached angular activation stages.
Linear sliders allow uniform 27 mm horizontal expansion per triangle, reaching maximum extension before locking.	Sliders failed to activate meaningfully; lack of collision constraints allowed parts to pass through each other.
Gradual and stable pitch transition from 0° to 30° across curvature levels as defined by angular zones.	Pitch movement was not observed beyond early initiation; components collapsed before any meaningful inclination was achieved.
Entire structure stabilizes post-deployment with locking mates, dome curvature maintained even after load release.	No stable post-deployment state was achieved due to total collapse; locking logic was never tested.
Minimal post-deployment oscillation due to rigid structural behavior and damping from material and proxy definitions.	No oscillation testing possible; system failed before deployment concluded.
Simulation to serve as proof-of-concept for real-world movement fidelity of mechanical lattice system.	Simulation highlighted critical flaws in constraint definitions and sequencing; proved the need for refinement before real-world testing can be validated.

5.4.4.5 Strategies for Future Researchers: Addressing Simulation Failures in Deployable Systems

The unexpected failure of the 24-unit deployment simulation highlighted both the inherent complexities of multi-joint kinematic behaviour and the limitations of conventional motion study tools when applied to non-linear, architectural-scale mechanisms. Rather than representing a setback, this failure provided crucial insights into the challenges of simulating deployable systems and informed a set of recommendations for future researchers working on similar pathways of simulation, fabrication, and mechanical design in architectural contexts.

One key lesson was the necessity of defining explicit solid body contacts. All interacting surfaces, particularly those driving actuation such as the dome cap, lattice connectors, and guide poles, must be assigned “no-penetration” solid body contacts. Relying solely on mate

constraints without incorporating contact logic can result in unpredictable or ghost-like motion, especially under gravitational influence.

Equally important is the staged validation of assemblies. Complex systems should not be tested at full scale without first verifying smaller clusters, such as 3-unit, 6-unit, or 12-unit sections. Incremental testing allows the confirmation of constraint behaviours and the observation of motion propagation before scaling up, making it easier to isolate errors and debug issues progressively.

Proxy joints, while computationally efficient, must also be supported with realistic interference controls. Limit mates, rail slots, and lock-unlock sequences should emulate real-world joint behaviour, and visual or physical stop elements such as collars, detents, or blocks can help replicate end conditions. Similarly, the premature application of gravity can exaggerate constraint errors, so early motion validation should be conducted in a gravity-free environment, with gravitational forces reintroduced only after the correct sequence of movements and joint responses has been confirmed.

Maintaining structural stability during deployment also requires lateral restraints or guide rails. Guide pins, sliders, or planar supports for critical units help prevent collapse due to drifting or torsional instability, ensuring the lattice remains aligned with its intended movement logic and avoids sideways buckling under actuation. Controlling movement in segments, rather than relying on a single global actuator such as the dome cap, further aids in debugging by allowing the observation of central and peripheral unit responses independently, revealing patterns of failure and propagation.

While SolidWorks provides robust mechanical modelling tools, it can struggle with large, interlinked kinematic chains. Future researchers are encouraged to explore alternative simulation environments for cross-validation, including Grasshopper with Kangaroo2 for real-time physics-based simulation of auxetic behaviour, Unity or Blender physics engines for dynamic proxy testing, and COMSOL Multiphysics or ANSYS for structural stress and constraint analysis under load. However, digital simulations alone are insufficient; physical prototyping remains essential to capture phenomena such as material resistance, joint friction, and tolerance misalignment. Even inexpensive mockups using foamboard, acrylic, or 3D-printed PLA can reveal unanticipated behaviours before committing to higher-fidelity models.

Crucially, failure pathways themselves are valuable data. Documenting cause-and-effect sequences, unexpected behaviours, and corrective strategies provides empirical evidence that informs iterative refinement and the evolution of best practices in architectural kinematics. For researchers working with deployable systems and auxetic structures, digital simulation should be approached as an iterative learning environment rather than a guaranteed predictor of performance. Failures such as the 24-unit collapse illuminate the limits of digital assumptions and clarify mechanical realities, offering a roadmap for building more resilient and verifiable workflows in future studies.

Ultimately, the failure of the 24-unit simulation did not invalidate the design logic (Table 5.4-7). On the contrary, it clarified the mechanical sensitivities of the system and the simulation parameters required to model them accurately. This reflection grounds the digital workflow in pragmatic, test-driven revision and reinforces the importance of mechanical awareness even when using proxy-based simulation environments, ensuring that future deployments can achieve both predictable motion and structural stability.

Table 5.4-6 Lessons and Recommended fixes of digital simulation

Lessons Learned	Fixes and Recommendations for Future Research
Lack of proper collision/contact definitions leads to structural penetration errors in motion studies.	Explicitly define "Solid Body Contact" or "No Penetration" mates between interacting parts like the dome cap and lattice nodes.
Vertical supports alone do not ensure system stability during vertical motion.	Add secondary guide pins or sliders to prevent unintentional lateral or downward movement of the lattice during upward displacement.
Proxy mates (yaw/pitch/slider) were not activated due to premature collapse.	Sequence the simulation with time-based or conditional constraints, so each motion (pitch, yaw, slide) activates in logical order.
Failure to simulate real-world gravitational interactions accurately.	Assign realistic gravity vectors and material weight properties; simulate frame reactions and locking constraints early in the setup.
Dome push-up mechanism failed to "engage" with the lattice.	Define the mating surfaces as colliding or magnetically attracting bodies to ensure synchronized movement initiation.
Over-reliance on perfect geometry in digital models caused overlooked misalignments.	Introduce tolerance gaps and minor imperfections to test robustness of the system under non-ideal conditions.
Simulation output does not guarantee real-world behavior if constrained simplistically.	Validate key digital simulations with scaled physical mockups before advancing to full assembly simulations.
Simulation failure revealed issues not originally considered in the design logic.	Embrace failure as a feedback mechanism; document each failed iteration as a learning opportunity to refine constraints and design logic.
Lack of damping or oscillation control in post-deployment stability phases.	Apply spring damping, rotational friction, or motion limiters to simulate physical inertia and resistance.
System complexity increases significantly beyond 6 units.	Consider modular simulation testing (6-unit, 12-unit, 24-unit) before attempting full-system simulation to reduce cascading error risks.

5.4.5 Movement and Stress Analysis Attempt Using ANSYS – Failure

Since SolidWorks simulations did not yield successful outcomes, particularly in handling contact definitions and complex constraint hierarchies, the study progressed to ANSYS Workbench as an alternative platform (Figure 5.4-25). Unlike SolidWorks Motion Study, ANSYS provides more advanced multi-body dynamics and finite element analysis capabilities, allowing both motion behaviour and stress distribution to be examined within the same environment. Its solver architecture is better suited for handling assemblies with multiple interacting joints and contact surfaces, making it more appropriate for the reciprocal–auxetic system where geometric complexity and recursive motion demand higher fidelity. By importing the SolidWorks mesh into ANSYS, tasks could be simplified through meshing refinements and modular analysis, enabling the exploration of both kinematic deployment sequences and

structural stress pathways ,into ANSYS Workbench to perform Finite Element Analysis (FEA) under various static and dynamic load scenarios.. This approach was aimed not only at evaluating stress concentrations but also at capturing motion behaviour more accurately across the deployable system.

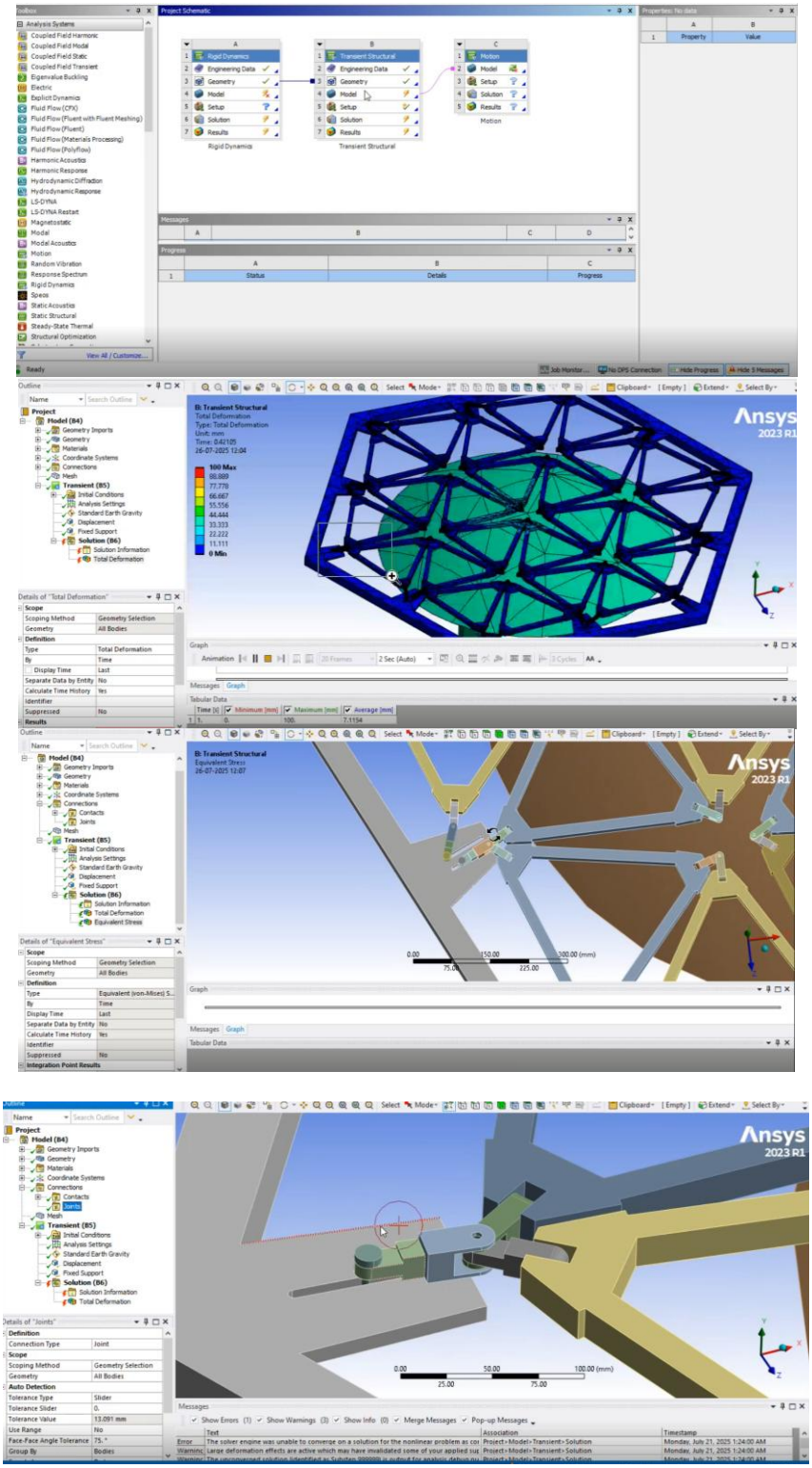

Figure 5.4-25 Trials of Mechanical joinery assembly in ANSYS

However, due to limitations stemming from unresolved interaction conflicts, interrupted part geometries, and incomplete constraint data within the SolidWorks model, the export to ANSYS was not seamless. Although initial attempts were made to convert the model into a meshable format using neutral file types (e.g., STEP or IGES), the system geometry resulted in error messages and incomplete imports within ANSYS. This was largely due to the complex joint system, proxy-based constraints, and overlapping parts that lacked material bonding or shared contact definitions making the model unsuitable for meshing and subsequent simulation. The failure wasn't documented as the error reports couldn't be derived due to file crash.

Despite efforts to resolve these errors through reimporting, remeshing, and simplifying the model, the simulation process failed to initiate, and no meaningful stress maps or results could be obtained. While placeholder images of the model setup and attempted meshing were captured to document the process, the actual stress distribution analysis could not be completed within the current research scope. This limitation, while unfortunate, reinforces the need for future researchers to approach multi-body simulations and structural validation with refined CAD preparation, including explicit contact definitions, simplified assemblies, and tested meshing strategies. Stress and load analyses remain essential for understanding how deployable systems behave under real-world forces, especially at joint junctions and expandable regions. Future studies could significantly benefit from validating digital assumptions using FEA tools like ANSYS, thereby reinforcing the mechanical logic developed throughout the design process and strengthening the argument for real-world applicability.

5.5 Other mechanical joinery design

Apart from the major junctions which is the primary focus of this research , the other parts that is conceptually designed as follows ,these developments are majorly conceptual future directions derived or implied from the masters thesis, Jayachandran.S (2019)

5.5.1 Base rail system- Controlled Planar Expansion and Positional Locking

As part of the broader mechanical strategy for the DRSTAB (Deployable Reciprocal Shells Through Auxetic Behaviour) system, the base rail system acts as a foundational support and control mechanism, enabling guided horizontal expansion during deployment and structural stabilization post-expansion. Initially conceived as a conceptual framework in Jayachandran (2019), this rail mechanism was further refined through simulation-based explorations in the current research, offering a clear pathway toward precision-controlled expansion, particularly for dome or freeform curvatures formed from auxetic-reciprocal geometries.

The base rail comprises a network of radial or linear guide tracks, onto which each module or anchor point of the patterned sheet is fixed via sliding connectors or glider nodes (Figure 5.5-1) . During deployment whether through dome push-up, pneumatic inflation, or mechanical pull the rails allow for controlled XY planar displacement, effectively enabling the structure to grow outward while maintaining pattern alignment and modular coordination. This controlled expansion is critical for managing the auxetic effect, which often leads to rapid dimensional changes under minimal force if not properly constrained.

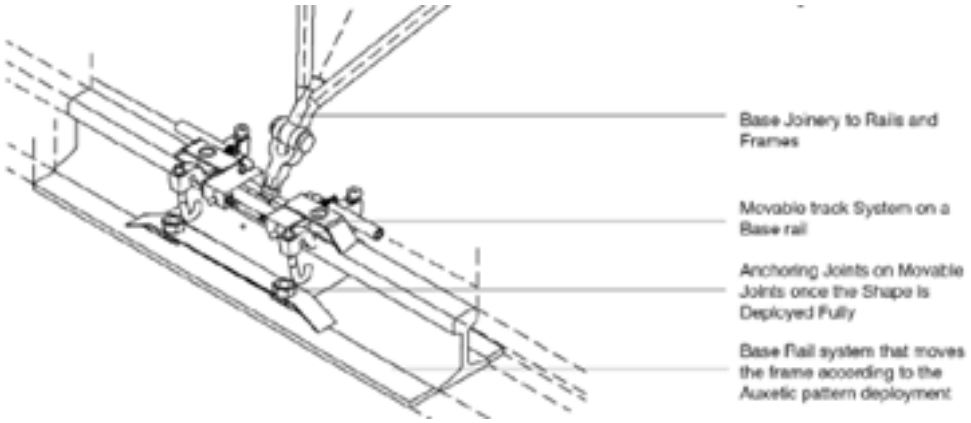

Figure 5.5-1 Conceptual design of Base Rail system

Note: From , *Deployable reciprocal shells through auxetic behaviour: Architectural hypothesis to fabricate double-curved structures* by *Jayachandran, S. (2019).*

Based on digital simulation trials and the predicted movement envelopes, the rails are pre-positioned with precision to align with expected expansion vectors. Each rail is modularly fixed into the base frame, with allowances for dynamic adjustment during setup. As the deployment progresses, the glider nodes slide along the tracks, enabling the required curvature transformation and outward spread of the reciprocal lattice. Once the system reaches its fully deployed state, each glider or anchor point is manually locked into position using a mechanical fastener, ratchet pin, or notch-lock mechanism. This ensures that no backward slippage or uncontrolled contraction can occur due to environmental loading or post-deployment disturbance. The manual locking stage serves as a critical safety measure, converting the dynamic lattice into a stable architectural form.

In addition to the base locking mechanism, the system allows for the integration of secondary reinforcements, such as perimeter braces, cross-stiffeners, or spring-dampers, which can be selectively added to support high-stress zones or maintain form under lateral loads. These reinforcements further stabilize the rail system, distributing load more evenly and mitigating stress concentrations, especially near boundary conditions.

This base rail concept thus offers a multi-functional platform: it guides movement, supports deployment, locks structure, and enables modular resetting. It is especially valuable in real-world architectural scenarios where deployability, repositioning, and reuse are desired traits. Though not physically prototyped in this phase, it remains a critical future direction, with immediate feasibility through laser-cut assemblies, composite rail elements, or modular extrusions. As demonstrated in simulation visualizations, its inclusion could significantly enhance both predictability and robustness in deployable reciprocal auxetic systems. Future researchers are encouraged to build upon this base system by experimenting with low-friction materials, snap-lock mechanisms, or automated rail extension systems that respond dynamically to deployment pressures or pattern behaviour.

5.5.2 Junction cover nodes- Flexible Caps for Post-Deployment Reinforcement

To complement the dynamic performance of the DRSTAB system and address long-term structural durability, the concept of Junction Cover Nodes is introduced as a secondary, post-deployment intervention. These components are designed to provide reinforcement and protective encapsulation at each of the critical joinery points in the lattice once deployment has been completed.

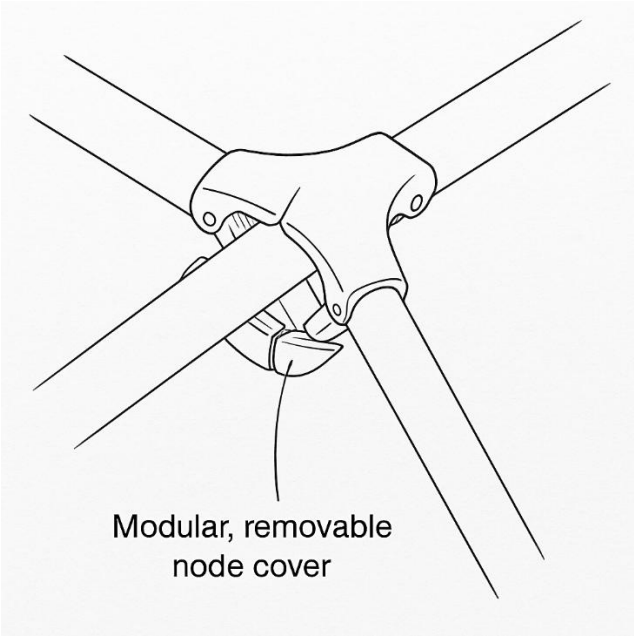

Figure 5.5-2 Conceptual design of Junction cover nodes

Each junction cover node is conceived as a two-part modular component that can be manually attached around the mechanical joints after the structure has reached its fully expanded configuration. These nodes act like protective cups or flexible collars that wrap around the connection points where triangular modules meet especially at regions experiencing compounded curvature or intersecting movements (Figure 5.5-2)

Because the triangular modules within a reciprocal-auxetic system take on varied orientations and angular relationships, the cover nodes are fabricated from flexible or semi-flexible materials, such as thin PETG, silicone composites, or rubberized polymer blends. This elasticity allows the cover node arms to adapt to different surface curvatures and embrace joints from multiple directions, ensuring full contact without compromising the intended geometry or obstructing deployment movement.

Once installed, these junction covers act as load-sharing devices, transferring a portion of the static and dynamic stresses away from the primary mechanical joints and into the wider support mesh. This mechanism significantly reduces wear and tear on the moving parts, particularly at high-traffic rotational junctions like the yaw and pitch axes. Over time, this can extend the lifespan of the mechanical system and minimize the need for frequent maintenance or replacement especially crucial in architectural applications where access may be limited. In addition to their protective function, these covers can also serve aesthetic or climatic roles, such as shielding joints from dust, moisture, or UV exposure in outdoor installations. They can

be colour-coded or fabricated with lightweight reinforcement ribs to match the visual language of the overall design.

During reverse deployment, the cover nodes are removed in a carefully coordinated sequence, potentially with the support of scaffolding or external stabilizers, to prevent destabilization during disassembly. The modular snap-fit or fastener design ensures they can be installed and removed without tools, aiding in rapid redeployment or transport. This strategy introduces a non-permanent reinforcement system that works in harmony with the adaptive, reconfigurable ethos of DRSTAB, offering structural support without compromising flexibility or scalability. Although not prototyped in full, the conceptual basis for junction cover nodes opens up new directions for adaptive architecture, where post-deployment augmentation plays a critical role in performance and longevity.

5.5.3 Deployment techniques or system -conceptual

Building on the bottom-up hydraulic push-up or pull up technique explored in the masters thesis ,Jayachandran (2019). this section examines four additional deployment strategies hydraulic push-up, crane pull-up, top-down lay-down, and pneumatic inflation each inspired by precedents in grid shell construction and auxetic structure research Jayachandran (2019). While the point hydraulic method formed the basis of our Chapter 5 SolidWorks simulations, strategic crane lifting, scaffold-guided lay-down, and inflatable formwork offer alternative means of achieving the complex, doubly-curved geometry inherent to deployable lattices. Drawing on historical examples from Otto's early elastic grid shells (1962–67) and contemporary Metastructures studies, these concepts propose varied mechanical advantages and highlight key considerations in synchronization, load distribution, and formwork design. Together, they chart a comprehensive landscape of erection methodologies for future digital and physical prototyping.

5.5.3.1 Point Hydraulic Push up

The point hydraulic push-up method adopted as the deployment strategy in our SolidWorks kinematic simulations (Author 2025) uses multiple vertical towers fitted with hydraulic jacks to lift the lattice from its base. In the simulation, each jack is mated to key connector nodes via linear slider and tension-cable proxies, driving an upward displacement that mimics real-world erection sequences. To prevent uncontrolled "bell-mouthing" during lift, a network of tensioned cables is threaded through the lattice members and incrementally tensioned in concert with jack extension, imposing a controlled flexure analogous to a catenary arc (Otto 1978).

Historically, a single-jack arrangement was used for the Toledo Municipal Garden gridshell, where one central tower raised the entire shell in a bottom-up sequence (Otto 1978). For larger spans most famously Frei Otto's Multihalle in Mannheim a ring of towers was arranged along a 9 m radius, with each jack spaced to induce predictable bending between adjacent lift points (Otto 1975). By emulating this arrangement in Chapter 5, our SolidWorks model synchronizes multiple jacks around a virtual 9 m-radius frame, coupling jack-stroke definitions with no-penetration contact mates to reproduce the gradual, uniform dome geometry achieved in these landmark hydraulically erected grid shells (Figure 5.5-3)

Key Components & Considerations:

Hydraulic Jacks & Towers: High-pressure cylinders sized for the total dead load plus safety factor; towers must be plumb and rigidly fixed to foundations.
Adapter Plates & Mating Geometry: Precision-machined interfaces to distribute jack loads across connector nodes without inducing stress concentrations.
Cable Network & Tensioning System: Steel cables or high-strength webbing routed through lattice members, tensioned via turnbuckles or hydraulic tensioners to maintain uniform flexure.
Control & Synchronization: Hydraulic manifold with proportional valves and electronic feedback to ensure simultaneous jack extension, preventing uneven lift and grid distortion.

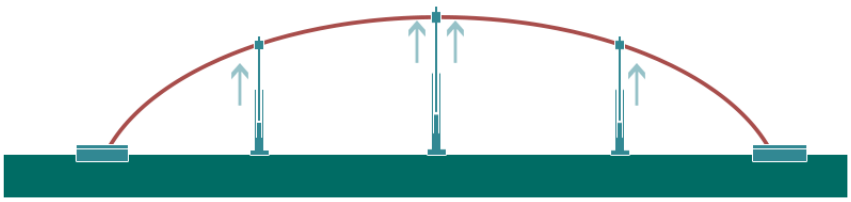

Figure 5.5-3 Hydraulic Point push up deployment technique

Advantages & Drawbacks:

Pros: Fine control over lift sequence and curvature; minimal temporary scaffolding; direct replication in SolidWorks via slider and cable proxies.

Cons: High equipment cost; complex synchronization required; potential for hydraulic leaks necessitating fail-safe check valves and redundancy.

5.5.3.2 Strategic Crane pull up

The crane pull-up method employed in the 1:5-scale prototype tests reported in Chapter 4 uses an overhead crane or gantry hoist to lift the lattice from above. In this approach, reinforced lifting points are temporarily affixed to the lattice's apex nodes, and slings or spreader beams distribute the load to prevent local overstress. As the crane hoist raises the grid, self-weight and gentle bending induce the membrane-like curvature required for the final shell form (Figure 5.5-4)

Frei Otto's seminal 1962 experimental grid shell in Essen pioneered this technique, erecting an elastic timber lattice with a single mobile crane and scaffold towers positioned around the perimeter (Otto 1965). A similar strategy was applied at Expo 67 in Montreal, where suspension cables from an existing structure hoisted pavilion modules into place (Otto 1967). The chief advantage of crane erection lies in its rapid deployment structures can be formed in hours rather than days because the crane applies a pure vertical uplift without imposing horizontal constraints, allowing the lattice to flex freely into its intended form.

However, this freedom comes at a cost. Cable anchor points introduce concentrated static loads that can exceed local bearing capacities, and unchecked bending of out-of-plane elements may push members to their stress limits (Otto 1965). Furthermore, the absence of horizontal restraint permits sudden distortions under load, necessitating slow, incremental lifts and constant monitoring to avoid peak-load damage. Consequently, while crane pull-up is highly effective for small-scale prototypes and training exercises, its practical application to

full-size shells requires careful load-control protocols and temporary bracing to manage joint stresses and maintain structural integrity.

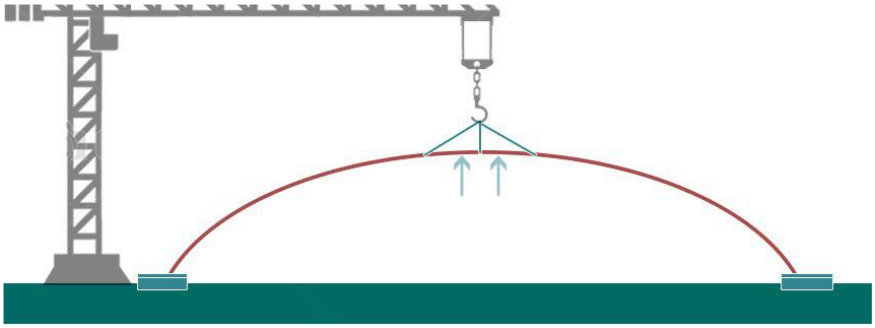

Figure 5.5-4 Crane pull up deployment technique

Key Components & Considerations:

Overhead Crane/Gantry System: Must provide sufficient hook-block clearance and rated capacity to exceed the lattice's dead and live loads.
Spreader Beams & Slings: Custom spreaders to prevent local overstress and maintain level lifting; synthetic slings or steel cables sized for working load limits.
Temporary Lifting Rings: Welded or bolted plates designed to interface with lattice connectors and resist multi-axial loads during lift.
Dynamic Load Control: Slow, incremental hoist operation with load-monitoring to avoid pendulum effects and peak-load spikes.

Advantages & Drawbacks:

Pros: Rapid deployment; minimal ground-based equipment footprint; easy adjustment of lift points to fine-tune curvature.

Cons: Concentrated point loads at lift rings; risk of over-bending at unsupported spans; requires detailed monitoring to prevent sudden deformation or overload.

5.5.3.3 Laydown from top

In the lay-down method (Figure 5.5-5) , the pre-assembled lattice remains flat as it is elevated to a predetermined elevation by temporary scaffolding or shoring, then progressively "laid down" onto the final form using controlled downward displacements at free edges (Author 2023). This technique was successfully demonstrated in reduced-scale PETG laser-cut auxetic prototypes in Chapter 4, and has been employed at full scale by Buro Happold for the Downland Grid shell, Savill Garden Gridshell, and the Japan Pavilion. In each case, an array of scaffold supports spanned the coverage area; the flat grid was raised uniformly and then flexed into the doubly-curved geometry by incrementally lowering the free edges along calibrated displacement strips or slide rails (Smith and Jones 2010).

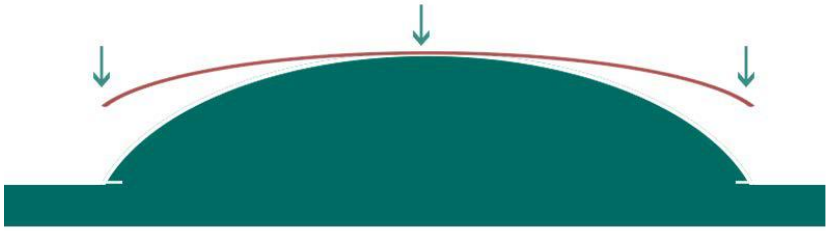

Figure 5.5-5 Laydown from top deployment technique

Key Components & Considerations:

Scaffolding & Shoring: A network of scaffold poles and platforms must provide uniform support beneath the entire lattice during lift. In full-scale projects, tubular steel “innocent” scaffold pipes form the primary elevation structure (Smith and Jones 2010).
Displacement Strips & Guide Rails: Precisely machined rails or adjustable chutes guide the lattice edges as they descend. These guides incorporate low-friction liners and incremental locking stops to control down-stroke rates and prevent sudden collapse.
Control Protocols: Lay-down demands meticulous sequencing. Physical scale models are indispensable for planning the sequence of supports to drop and rails to engage, ensuring that each cell deforms within elastic limits (Brown et al. 2015).
Load Management: As the edges descend, tensile forces develop across the spans; guide rails must resist these forces without excessive friction or wear. Hydraulic dampers or foam buffers are often used at end stops to absorb impact energy.

Advantages & Drawbacks:

Pros: Gravity-assisted deployment reduces reliance on heavy jacks or cranes, and the absence of horizontal restraints allows the grid to adopt its natural curvature seamlessly.

Cons: Requires extensive temporary scaffolding and precise guide machining; impact loads at the conclusion of each down-stroke must be managed to avoid overstressing the lattice.

5.5.3.4 Inflation method

The inflation-based expansion technique uses an airtight pneumatic cushion placed beneath the flat lattice, functioning as a living formwork that uniformly lifts and shapes the grid (Figure 5.5-6) . As air pressure increases within the membrane, the cushion transmits a homogenized uplift to the lattice members, eliminating the concentrated point loads inherent in point-hydraulic or crane-based methods. This synchronized elevation ensures that the shell and its supporting formwork deform in unison, mirroring the stress states anticipated during the design phase (Lutes 1971).

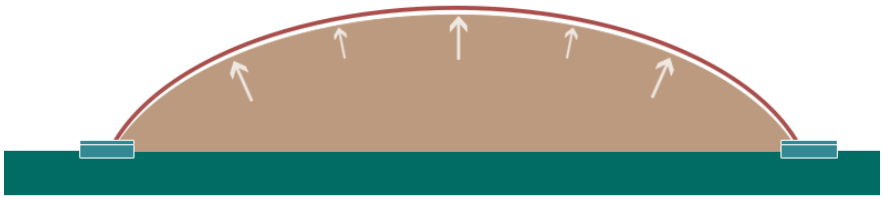

Figure 5.5-6 Inflation deployment technique

Key Components & Considerations:

Pneumatic Membrane: A custom-fabricated PVC- or TPU-coated nylon bladder sized to the lattice footprint. Must exhibit high tear resistance and low creep under sustained pressure.
Air Supply & Regulation: Continuous-flow blowers or compressors with proportional pressure control, pressure-relief valves, and feedback from multiple pressure sensors to maintain a stable inflation profile.
Perimeter Clamping System: Rigid frames or clamping tracks anchor the membrane edges to the hexagonal base frame, ensuring an airtight seal and uniform pressure distribution.
Dynamic Load Management: Rapidly varying external loads (wind, thermal expansion) can alter internal pressure requirements; integration with HVAC systems or automated waste-gate dampers is advisable to adjust cushion pressure in real time.

Advantages & Drawbacks:

Pros: Provides exceptionally uniform lift, minimizes local overstressing of joints, and replicates the idealized formwork assumed in structural design without complex mechanical lifts.

Cons: Requires airtight sealing and robust secondary supports to handle dynamic loads; membrane failure or puncture can lead to catastrophic collapse; less feasible for outdoor or unprotected environments without backup inflation redundancies.

5.5.4 Cladding systems-Integration Between Triangular Modules

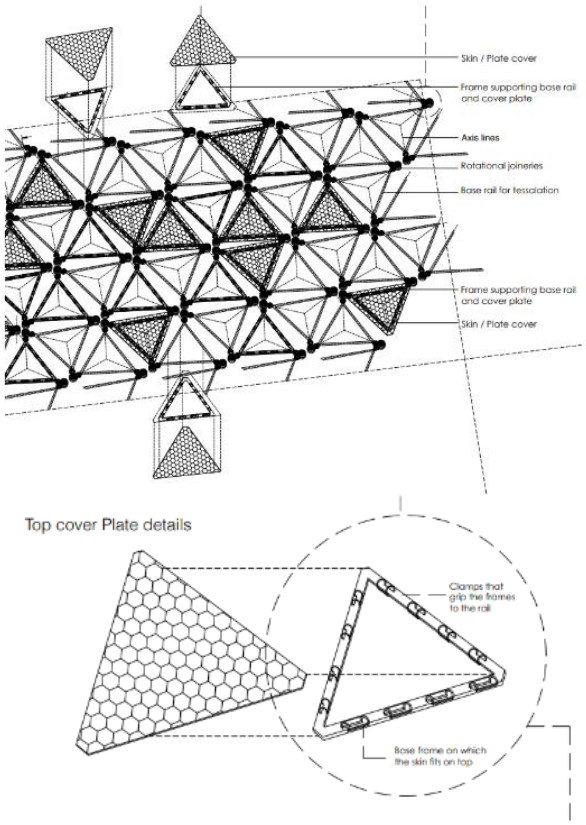

Figure 5.5-7 Cladding systems addons between Modules

As illustrated in ,Figure 5.5-7, the structural tessellation of triangular modules allows for the integration of a secondary skin or cladding system layered on top of the deployable framework. These cladding elements indicated as "skin/plate cover" can be affixed to the triangular faces or the supporting frame once full deployment is achieved. Their modular nature permits alignment with the underlying geometric logic, enabling selective shading, insulation, or weather protection without obstructing mechanical movement. The cladding can also act as a visual finish or architectural expression layer, transforming the structural shell into a fully enclosed envelope. This approach ensures that the deployable structure is not only functional but also contextually responsive to environmental and aesthetic requirements.

5.6 Summary of Chapter 5

Chapter 5 synthesizes the experimental and computational efforts undertaken to transform the geometric and material insights from earlier chapters into functional mechanical systems. This stage focuses on bridging digital abstraction with material and mechanical realities, addressing RQ3 by developing, testing, and refining joinery mechanisms that enable the deployability of the Tristar–reciprocal auxetic shell system. The investigations in this chapter highlight how mechanical articulation determines the success of architectural deployables, particularly in mediating between geometric intent and real-world motion. Through iterative prototyping, three mechanical assemblies (Mark 1–3) were explored, each introducing a progressive enhancement in rotational control, locking precision, and structural stability. The Mark 3 prototype, incorporating one-way clutch bearings and refined ratchet mechanisms, exemplifies how controlled pitch–yaw coordination can yield repeatable and coherent deployment. However, the chapter also identifies persistent challenges, such as synchronization loss in larger assemblies, uneven load distribution, and digital simulation limitations, which collectively underscore the complexity of modeling kinetic reciprocity through conventional tools like SolidWorks (Pellegrino, 2001; Norton, 2020; Shigley et al., 2004).

Through these findings, Chapter 5 establishes that mechanical joinery is not a secondary consideration but a structural intelligence embedded within the system. The study demonstrates that hybridized joints combining rotational freedom with passive locking (as in ratchet–bearing systems) can effectively translate auxetic geometry into large-scale architectural motion without compromising stability or modular coherence. These insights confirm that successful deployment in reciprocal auxetic shells requires an integrated design logic, where geometry, mechanics, and material act synergistically rather than hierarchically.

In doing so, this chapter contributes a framework for understanding how precision-engineered mechanical joints can transform conceptual auxetic geometries into real, buildable, and adaptive systems. The outcomes directly answer RQ3 by providing empirical and design evidence that bespoke joinery design rather than generic mechanical replication is key to scaling deployable auxetic architectures for practical application. The lessons drawn here form the foundation for the final synthesis in Chapter 6, where the broader architectural and theoretical implications of the Deployable Reciprocal Shells through Auxetic Behaviour (DRSTAB) system are consolidated.

Chapter #6

Insights / Gaps / Possibilities

Research Answers

Limitations & Inference

Future Possibilities

6 Conclusion

This chapter consolidates the outcomes of the study by addressing the research questions individually, reflecting on the limitations that shaped the scope and outcomes of the investigation, and outlining potential directions for future inquiry. By structuring the discussion around the core research questions, the chapter highlights how reciprocal and auxetic principles were integrated, how simulations and physical prototypes informed adaptive shell design, and how mechanical joineries were developed and tested to enable controlled deployment. The limitations section provides a critical reflection on methodological, material, and computational constraints, acknowledging where the study's ambitions could not be fully realized. Finally, the forward-looking discussion presents pathways for extending this work through full-scale testing, material innovation, advanced simulation, and interdisciplinary collaboration. Together, these sections situate the contribution of the thesis within the broader context of deployable architectural research while pointing toward its continuing evolution.

6.1 Research Questions Answered

This section summarizes how the core research questions posed at the start of this thesis have been addressed through the various chapters. It highlights key findings and insights related to the adaptability of mechanical joinery systems, the effectiveness of digital simulations compared to physical prototypes, and the validation of deployable architectural mechanisms. Emphasis is placed on the contribution to understanding how auxetic geometries combined with advanced joinery enable new possibilities in kinetic structures. The discussion also reflects on the success in bridging theory and practice, confirming which hypotheses were supported and where unexpected results emerged.

RQ1: How can reciprocal and auxetic principles be combined to design deployable, double-curved architectural shells?

Findings and Answers :
The study demonstrated that reciprocal frames and auxetic systems can be effectively combined when their complementary properties are harnessed. Reciprocal structures provide distributed stability, modular adaptability, and load sharing, while auxetic patterns contribute predictable surface expansion and contraction. Studies in Chapter 2.2 (Literature Review of Reciprocal and Auxetic Systems) lay the base work for the wider exploration of reciprocal and Auxetics in use of the system. Inferences From Chapter 3.1 informs that RF patterns with hexagon and triangle are the best choice for consideration .Chapter 3.2 ,comparative breakdowns of Auxetic identified the Tristar as the most suitable geometry due to its ability to expand uniformly and adapt to convex, concave, and saddle-shaped surfaces. Geometric CAD-based analyses (Chapter 3.3) and physical PETG prototyping (Chapter 4.2) confirmed its adaptability, though localized buckling, junction pile-ups, and edge instability highlighted the need for mechanical articulation. Collectively, these findings established in Chapters 3 and 4 confirm that reciprocal frameworks paired with Tristar auxetic modules provide a coherent structural logic for deployable double-curved shells, but also emphasize that their practical realization depends on the development of specialized joinery systems..

RQ2. How can physical testing and digital simulations of the Tristar auxetic pattern inform the design of adaptive and deployable shell geometries?

Findings and Answers :
Computational simulations in Chapter 4.4 (Parametric Simulations in Rhino/Grasshopper) successfully mapped deployment directionality, anchoring behaviour, and global curvature adaptability, but remained limited to geometric abstraction without incorporating material

friction or joint mechanics. Physical testing of laser-cut PETG prototypes (documented in Chapter 4.2) revealed real-world adaptability across multiple curvatures while also exposing issues such as buckling, boundary lift, and reliance on manual intervention. The scale prototype explored in Chapter 4.5 not only supported the versatility factor of the Tristar further, but also extended its expandability factor with mimicked mechanical articulations

Together, the digital and physical approaches complemented one another: digital simulations defined potential deployment sequences, while prototypes revealed practical constraints that must be resolved mechanically. While this limited validation at system scale, these failures were instructive, clarifying the complexity of modelling recursive joint behaviour and highlighting the need for hybrid workflows that combine geometry-driven design tools with high-fidelity multi-physics solvers. The key insights distilled across Chapters 3, 4 show that simulation and prototyping together perform well for shell geometry design, even though predictive validation at architectural scale remains incomplete.

RQ3. How can mechanical joinery systems be designed, prototyped, and simulated to support the controlled deployment of auxetic-reciprocal architectural shells?

Findings and Answers :
The decisive contribution of this study lies in the iterative exploration of mechanical joinery systems, documented in Chapter 5.3 (Joinery Prototyping). Three successive prototypes were developed, each addressing specific shortcomings of its predecessor. Mark 1 employed compact ratchet mechanisms to achieve unidirectional yaw rotation, proving that deployable locking could be embedded into architectural joints. However, this version lacked pitch control and suffered from wear and spring inaccuracy, limiting reliability. Mark 2 introduced dual ratchets for yaw and pitch in combination with a universal ball joint, expanding articulation but resulting in inconsistent locking due to the tolerances of off-the-shelf parts. Mark 3 advanced the system by embedding one-way clutch bearings to stabilize yaw, supported by refined ratchet locks for pitch. This iteration offered smoother angular performance and the most stable deployment observed, extending movement beyond the 60° threshold established in PETG tests. Despite these improvements, challenges persisted, including incomplete synchronization and over extensions of joineries

Mechanical simulations of these joints, detailed in Chapter 5.4, further exposed the difficulty of validation. Attempts in SolidWorks failed to yield accurate results, primarily due to missing contact definitions, constraint-setting errors, and computational limitations. While this limited predictive accuracy at the system scale, the failures were instructive. They highlighted the complexity of modelling recursive joint behaviour and confirmed that off-the-shelf digital proxies cannot fully represent custom kinetic joints. Together, these findings underscore that bespoke, precision-engineered joineries are indispensable for translating the Tristar–reciprocal logic into controlled and scalable architectural deployment. The study therefore points toward hybrid workflows that combine geometry-driven design tools with high-fidelity multi-physics solvers as the most viable path forward.

6.2 Limitations of the PhD Research

Here, the inherent limitations of the research are critically examined. This includes constraints such as the scale and materials of physical prototypes, the fidelity and assumptions within digital simulation tools, and the scope of mechanical joinery options explored. Practical challenges encountered during fabrication and testing, such as precision tolerances, wear factors, and assembly complexities, are acknowledged. Additionally, methodological limitations, including the absence of full-scale deployments or long-term durability studies, are

discussed. Recognizing these limitations contextualizes the findings and provides transparency regarding the extent to which conclusions can be generalized.

Scope and Scale of Testing

One of the primary limitations of this research lies in the scale at which the simulations and physical prototypes were executed. Due to constraints in both resources and time, the majority of investigations were conducted using reduced-scale models and simplified factorial conditions. While these prototypes successfully demonstrated fundamental geometric logics, they did not account for real-world structural forces such as wind pressure, seismic activity, or sustained live loading conditions. The absence of these critical forces means that the results, while indicative of spatial and geometric potential, cannot be directly extrapolated to full-scale architectural applications without significant assumptions. Furthermore, small-scale models tend to exaggerate flexibility and tolerance, masking issues that would become pronounced at building scale, such as joint friction, buckling thresholds, or load redistribution. Therefore, the limited scope of testing should be understood as a conceptual exploration rather than a performance validation, highlighting the need for future full-scale trials under realistic environmental conditions.

Material Constraints and Selection

Another significant limitation arises from the material palette employed during physical prototyping. The research primarily relied on PETG sheets, acrylic, leather straps, and steel screws due to their affordability, availability, and ease of fabrication at model scale. While effective for demonstrating movement logics, these materials exhibit behaviours that are unlikely to translate seamlessly into architectural-scale applications. For example, PETG and acrylic were prone to localized buckling and stress concentrations, while leather elements stretched unpredictably under repeated loading, introducing inconsistencies in joint behaviour. Additionally, while steel screws provided satisfactory performance as connectors, they did not replicate the precise tolerances or angular restrictions expected from custom-engineered joints. The decision to exclude 3D-printed components, largely due to budgetary and time constraints, further limited the exploration of optimized material systems. Consequently, while the materials served as functional stand-ins for proof-of-concept testing, they inevitably restricted the structural accuracy of outcomes. Future research should therefore investigate stiffer, more robust materials such as composites, alloys, or engineered polymers.

Simulation and Modelling Constraints

The computational modelling phase represents one of the most critical limitations of this research, with SolidWorks simulations ultimately producing unsuccessful outcomes. While simplified CAD breakdowns and proxy-based assemblies provided initial insights, the mechanical simulations in SolidWorks failed to yield viable results. Key issues included the absence of solid body contact definitions, incomplete boundary constraints, and difficulties in simulating realistic joint mechanics. These problems, compounded by limited computational power and the researcher's developing proficiency in the software, meant that simulated assemblies collapsed prematurely, often producing results that bore little resemblance to the intended mechanical logic. As a consequence, no reliable conclusions regarding stress–strain behaviour, angular tolerances, or deployment sequences could be drawn from the simulations. This outcome reflects both the technical limitations of the software when handling recursive, nested systems at architectural scales, and the methodological gap between digital abstraction and physical mechanics. Future research should employ hybrid workflows, combining physics engines like Kangaroo2 with high-fidelity engineering simulations, to achieve more accurate and representative digital outcomes.

Mechanical Joinery Limitations

The development of mechanical joineries within this research was also subject to notable constraints, particularly in terms of precision and validation. The prototypes primarily relied on standard, commercially available components such as Chicago screws, ball joints, and off-the-shelf clutch bearings. While these elements facilitated basic rotational movements and offered a convenient means to test proof-of-concept assemblies, they imposed specific angular limitations that hindered performance. For example, yaw rotation was constrained to approximately 120°, and pitch movement rarely exceeded 30°. Moreover, the lack of integrated locking mechanisms meant that movement was not always predictable or repeatable, requiring manual intervention during deployment trials. Because the SolidWorks simulations could not provide reliable validation of joint behaviour, the experimental results were limited to partial observations rather than comprehensive verification. Customized joinery systems, designed specifically for the angular and load requirements of deployable shells, are therefore essential for future iterations. The inability to prototype or simulate these joints at a high level remains a major limitation of this work.

Deployment and Synchronization Challenges

The physical testing phase also revealed persistent challenges in achieving synchronized deployment across the system. While the deploy–retract cycles were attempted successfully in principle, the prototypes frequently required manual intervention to maintain alignment and prevent collapse. Uniform deployment was rarely sustained throughout the system, with uneven stresses and irregular joint behaviour causing distortions and localized instabilities. Furthermore, long-term durability testing was not conducted, meaning that the capacity of these prototypes to withstand repeated cycles or environmental wear remains unknown. The inherent material constraints and assembly tolerances compounded this issue, as minor misalignments became amplified during transformation. As a result, the system demonstrated functional adaptability but could not establish reliability across repeated operations. These observations indicate that future research must investigate automated or guided deployment systems, perhaps through rails or motorized actuators, to ensure consistent synchronization. The absence of such systems in the current research remains a critical limitation that prevents direct application in real-world architectural contexts.

Time and Resource Constraints

Time and resource constraints shaped the boundaries of this research in significant ways. Given the breadth of the investigation, spanning geometric logic, physical prototyping, and mechanical joinery, certain planned aspects remained incomplete. Notably, the intended structural simulations using SolidWorks and ANSYS could not be carried through to completion, as repeated attempts resulted in failure due to technical limitations and researcher proficiency gaps. Although logically robust in design, the inability to achieve working simulations deprived the research of a critical layer of validation. This issue was compounded by limited access to advanced fabrication facilities, specialist hardware, and interdisciplinary collaboration, all of which might have mitigated some of the challenges encountered. While extensive data were collected, the inability to complete certain simulations and advanced prototyping stages means that the findings must be read as exploratory rather than conclusive. Future research will need to build upon these partial outcomes with expanded resources and technical expertise.

Gaps Between Digital and Physical Outcomes

Another limitation observed throughout this research was the discrepancy between digital predictions and physical prototypes. Digital simulations often assumed idealized conditions of

material uniformity, perfect contact, and frictionless joints, whereas physical prototypes revealed unexpected behaviours such as edge buckling, joint friction, and localized deformation. These discrepancies became especially clear during deployment testing, where the theoretically smooth unfolding process was disrupted by real-world factors such as slippage, uneven tension, and non-uniform expansion. The divergence between digital and physical outcomes underscores the difficulty of translating abstract computational models into functioning prototypes, particularly for highly interdependent systems like deployable shells. While these mismatches highlight the limitations of the current research, they also serve as valuable feedback for refining future workflows. A closer integration of digital and physical testing, with iterative feedback loops to reconcile discrepancies, will be essential for achieving greater alignment between predictive modelling and real-world performance.

Pattern Selection and Overlap Analysis

The approach to pattern selection and overlap analysis in this research also had inherent limitations. Most analyses were carried out through CAD-based geometric breakdowns and comparative visual assessments rather than through advanced, data-driven computational methods. While this approach provided useful insights into the geometric and structural logic of auxetic and reciprocal systems, it lacked the rigor and quantification necessary to establish definitive conclusions about optimal pattern performance. Specifically, overlaps, stress concentrations, and interaction effects between patterns were not systematically measured or simulated, leaving potential weaknesses unexplored. This limitation highlights the need for integrating advanced analytical tools, such as finite element methods or parametric optimization algorithms, to generate more rigorous and quantified evidence. By doing so, future research could validate not only which patterns are theoretically adaptable but also which configurations perform best under real-world conditions. The absence of such an approach in the current work must therefore be acknowledged as a methodological limitation.

Mechanical Joinery and Conceptual Proposals

Finally, while this research introduced several conceptual proposals related to mechanical joinery and deployment strategies, these ideas were not comprehensively developed or tested. Concepts such as rail-based deployment, reinforcement junctions, and alternative actuation techniques were outlined as promising directions but remained largely theoretical. The lack of simulation or physical prototyping meant that these proposals could not be evaluated in terms of feasibility, scalability, or structural efficiency. Although they represent important avenues for future exploration, their absence in the current research reflects both time limitations and the prioritization of core investigations into auxetic–reciprocal integration. Future studies should build upon these proposals by subjecting them to rigorous technical development, including computational testing and scaled prototyping. Until such validation is achieved, these ideas remain speculative, though they hold potential to address several of the limitations encountered in the present research.

6.3 Possibilities and scope for Future Research

This section outlines potential avenues to expand and deepen the research. Suggestions include exploring alternative materials and fabrication methods to enhance joinery durability and ease of assembly, integrating sensor technologies for real-time monitoring of mechanical stresses, and advancing simulation models to better capture complex multi-physics interactions. Further work might investigate full-scale prototypes and diverse geometric configurations beyond the Tri-Star auxetic framework. Interdisciplinary collaborations could also explore the architectural and environmental implications of deployable structures.

Ultimately, this forward-looking discussion aims to inspire continued innovation and practical application in kinetic architectural systems.

Full-Scale Structural and Environmental Testing

One of the most pressing directions for future research is the transition from scaled prototypes and small assemblies to full-scale structural and environmental testing. In the current work, testing was limited to small- and medium-scale models under laboratory conditions, meaning that real-world structural forces such as wind, seismic activity, snow, and live loading were not accounted for. These conditions will play a decisive role in validating the practicality of reciprocal–auxetic deployable shells at an architectural scale. Future research should include full-scale prototypes tested under site-specific climate conditions and topographic variations, which would reveal important insights into structural resilience and adaptability. Rigorous testing would also allow researchers to fine-tune joinery tolerances and evaluate performance under repeated load cycles, ensuring safety and functionality in real deployment scenarios. Integrating these full-scale studies into design workflows would transform the conceptual system into an architecture-ready solution capable of addressing emergency housing, mobile infrastructure, and sustainable pavilions.

Material Innovation and Optimization

Material limitations in the present study highlight another promising research path. Current prototypes used PETG, acrylic, leather, and steel screws, which were cost-effective and easy to fabricate but unsuitable for long-term or full-scale applications. These materials demonstrated localized buckling, wear, and stress concentrations that would be unacceptable at architectural scales. Future investigations should experiment with advanced composites such as carbon fiber, glass-reinforced polymers, and shape-memory alloys, which offer superior strength-to-weight ratios and long-term resilience. Additive manufacturing can play a pivotal role in this pursuit, enabling the production of custom joint components with precision tolerances that small-scale fabrication could not achieve in this research. Optimizing material thickness, elasticity, and thermal properties would refine the system's fatigue resistance and long-term performance. Such innovations would move the system away from fragile, short-lived prototypes toward robust architectural assemblies capable of repeated deployment without degradation, thereby bridging the current gap between conceptual demonstration and functional application.

Advanced Digital Simulation and Validation

A critical limitation of this research was the failure of SolidWorks mechanical simulations to produce viable results. Inadequate computational power, incomplete contact definitions, and lack of expertise prevented reliable digital validation of movement, stress–strain behaviour, or angular tolerances. This failure represents both a limitation and a major opportunity for future work. Advanced digital simulation should focus on resolving these shortcomings by employing high-fidelity software such as ANSYS for nonlinear finite element analysis and Grasshopper physics plugins like Kangaroo2 for parametric motion studies. Future simulations should integrate real material behaviours, frictional contacts, and dynamic loading scenarios to approximate real-world conditions. Importantly, hybrid workflows that combine computational geometry with mechanical simulation would help overcome the complexity of recursive auxetic systems. By addressing the shortcomings of this research and producing validated digital models, future studies would gain predictive accuracy, reduce reliance on trial-and-error prototyping, and significantly strengthen the reliability of deployable auxetic–reciprocal shells.

Custom Mechanical Joinery and Actuation Systems

The limitations of off-the-shelf joineries revealed in this study underscore the urgent need for custom-designed mechanical joints. Chicago screws, ball joints, and clutch bearings provided basic rotational movements but could not reliably achieve the required yaw (120°) and pitch (30°) tolerances, nor could they support consistent locking and unlocking sequences. The lack of validated simulations further limited the ability to refine joint performance. Future research should prioritize the development of bespoke mechanical joineries tailored to the specific requirements of deployable reciprocal–auxetic shells. Precision ratchets, adaptive clutch bearings, or even joints inspired by robotics could be designed to provide smooth, reliable articulation. Integration of semi-automated actuation systems, such as pneumatic actuators or linear motors, could enhance control and synchronization, reducing the reliance on manual deployment. Smart materials or embedded sensors might further enable self-monitoring joints capable of adjusting in real time, ensuring both reliability and responsiveness in architectural contexts.

Lifecycle and Fatigue Analysis

The present research demonstrated deploy–retract cycles at the prototype level but did not investigate fatigue or long-term durability. The fragility of materials, combined with inconsistencies in joint behaviour, meant that repeated cycling would likely lead to rapid degradation. Future studies must therefore investigate lifecycle performance in depth, conducting repeated deployments to measure wear, material fatigue, and mechanical failure points. Testing should include thousands of cycles under varied environmental conditions, including exposure to moisture, UV radiation, and temperature fluctuations. Such research would provide valuable data for developing maintenance strategies, replacement intervals, and reliability standards. Without this knowledge, deployable shells cannot transition from conceptual systems to practical architectural products. Understanding fatigue behaviour would also guide the selection of advanced materials and joint configurations, ensuring durability over years of use rather than weeks of experimentation. Establishing lifecycle analysis is thus critical for proving long-term feasibility and integrating these systems into real-world architectural practice.

Comparative Studies of Auxetic Patterns

While this research focused on the Tristar auxetic pattern, numerous alternative configurations such as re-entrant, rotating squares, Miura, and chiral patterns remain underexplored. Each auxetic system demonstrates unique expansion behaviours, energy absorption properties, and directional adaptability that could significantly impact deployable architectural design. Future research should undertake systematic comparative studies of these patterns, using both computational simulations and physical prototypes. Comparative evaluations should include metrics such as expansion ratios, surface coverage efficiency, load-bearing capacity, and ease of integration with reciprocal frames. Such studies would enrich the knowledge base and help identify the optimal pattern for specific architectural applications, whether temporary shelters, kinetic pavilions, or adaptive facades. By expanding beyond the Tristar framework, researchers can create a library of deployable auxetic geometries, ensuring that solutions are not limited by a single pattern but are adaptable to varied design contexts and environmental demands.

In-Depth Analysis of Pattern Overlaps and Tessellations

Another area requiring further exploration is the study of overlaps and tessellations between auxetic and reciprocal systems. In this research, analyses were primarily limited to CAD-based breakdowns without employing data-driven computational methods to quantify efficiency or stress distribution. Future research should incorporate advanced numerical tools, such as

genetic algorithms, machine learning models, or parametric optimization, to investigate overlapping geometries systematically. By analysing how different tessellations distribute loads, reduce joint counts, or optimize material use, researchers can identify configurations that maximize efficiency while minimizing fabrication complexity. This approach would also allow for the identification of weak points where overlaps could create stress concentrations or failure zones. A more rigorous understanding of tessellation performance would not only improve geometric efficiency but also inform fabrication strategies, leading to more robust and scalable deployable shells. The absence of such advanced methods in this research highlights a critical gap that future work can fill.

Detailed Exploration of Deployment and Rail-Based Mechanisms

The concept of rail-based guidance systems introduced in this research was only discussed at a conceptual level, without technical validation or physical prototyping. However, these systems hold significant promise for overcoming synchronization issues observed during manual deployments. Future research should design, prototype, and test rail-based deployment systems at architectural scale, evaluating their ability to ensure smooth, uniform transformations across large assemblies. These mechanisms could prevent localized buckling, improve alignment, and distribute loads more effectively during deployment and retraction cycles. Incorporating rails or guided tracks would also reduce reliance on manual intervention, making the system more reliable and user-friendly. In disaster-relief scenarios, for example, such systems could enable rapid assembly by non-experts, ensuring stability and safety. Rail-based deployment strategies could therefore transform the system from an experimental model into a practical, deployable architecture with real-world functionality, significantly advancing the current state of kinetic and temporary structures.

Advanced Computational and Physical Integration

Closing the gap between digital and physical testing remains one of the most critical challenges. The failure of SolidWorks simulations to align with physical prototypes highlights the need for more integrated workflows that combine computational models with real-time feedback. Future research could employ digital twin technologies, where embedded sensors in prototypes continuously transmit data to refine computational models. This approach would allow real-world behaviours, such as joint friction, material fatigue, or deployment irregularities, to be integrated into predictive simulations, creating more reliable digital outcomes. Iterative feedback loops between physical prototypes and computational models could significantly reduce mismatches and improve predictive accuracy. Furthermore, combining advanced parametric design with real-time sensing could lead to adaptive systems capable of recalibrating themselves in response to external stimuli. Such integration would not only refine current methodologies but also set the foundation for highly responsive, intelligent deployable systems.

Interdisciplinary Collaboration

Finally, the future of deployable reciprocal–auxetic systems lies in robust interdisciplinary collaboration. This research highlighted how architectural design, mechanical joinery, computational modelling, and material science intersect but also where expertise gaps remain. Collaborations between architects, structural engineers, computational designers, materials scientists, and mechanical engineers would provide the technical depth needed to overcome current limitations. For instance, mechanical engineers could refine custom joint designs, materials scientists could test novel composites, and computational experts could develop hybrid simulation environments. Beyond technical integration, interdisciplinary teams could also explore the environmental, cultural, and social implications of deployable systems, ensuring their adoption in diverse architectural contexts. Such collaborations would accelerate

innovation, expand the scope of practical applications, and help translate experimental prototypes into deployable, industry-ready systems. Without interdisciplinary engagement, progress risks remaining siloed and incremental rather than transformative.

6.4 Proposed Workflows and Possible Implications

6.4.1 Proposed Workflow for DRSTAB System Deployment

Computational Design and Feasibility Simulation

The workflow of the DRSTAB system begins with a computationally driven design phase, where project inputs such as span, height, curvature, and spatial requirements are defined. These parameters are processed through a parametric modelling environment (Rhino–Grasshopper), which generates the underlying tessellation logic and evaluates feasible geometric configurations. Due to the inherent constraints of reciprocal–auxetic systems, particular attention is given to curvature behaviour, module interaction, and rotational limits. At this stage, simulations are used to identify potential issues such as module clustering, overlap, or excessive rotational stress that may compromise deployment.

In parallel, preliminary structural approximations may be integrated into the workflow to indicate zones of stress concentration or areas requiring reinforcement. While detailed structural validation is beyond the scope of this research, this stage establishes a critical decision-making layer, similar to digital workflows in industrialised systems such as XFrame or FrameCAD, where design, validation, and fabrication data are closely linked. The output of this phase is a coordinated digital model that informs fabrication logic, assembly sequencing, and deployment strategy.

Fabrication Logic and Pre-Assembly Strategy

Following design validation, the system transitions into a fabrication-informed stage where module dimensions, joinery details, and assembly sequences are rationalised. Similar to prefabrication workflows in light-gauge steel systems, the DRSTAB framework can be partially pre-assembled in controlled factory conditions to improve precision and reduce on-site complexity. Components are produced and labelled according to a predefined sequence, allowing for systematic assembly akin to CNC-based or kit-of-parts construction methodologies.

Depending on transport constraints and project scale, the system may be delivered as partially assembled modules or as discrete components for final on-site integration. This flexibility reflects a hybrid approach between fully prefabricated systems and adaptable modular construction.

Logistics and Transportation Planning

The transport phase involves the coordinated delivery of DRSTAB modules, base systems, and auxiliary components to the site. Due to the system's deployable nature, compact storage and efficient packing strategies can be leveraged to minimise transportation volume. Additional elements such as base rail systems, pneumatic scaffolding (in the case of inflation-based deployment), and façade or covering systems are also included at this stage. While these auxiliary systems remain conceptual within the research, their integration highlights the need for a coordinated logistics strategy similar to industrial modular construction workflows.

Site Preparation and Base System Integration

Upon arrival on site, the workflow shifts to ground preparation and base system installation. The site is marked according to the predefined layout, and the base rail system is anchored, forming the primary interface between the deployable structure and the ground. This stage is critical in ensuring alignment accuracy and structural stability during deployment.

For inflation-based deployment strategies, the pneumatic scaffolding system is positioned and anchored in its deflated state beneath or within the DRSTAB assembly. The preparation of this system, including anchoring and alignment, directly influences the success and precision of the deployment process.

System Assembly and Deployment Execution

The DRSTAB modules are then positioned and connected to the base rail system using specialised joinery designed for controlled movement and locking. If required, additional module connections are completed on site to achieve the final configuration. Once the system is secured, the deployment process is initiated.

In the case of pneumatic deployment, gradual inflation activates the expansion of the system, allowing it to transition from a compact state to its final form. Assisted deployment mechanisms, such as tension anchors or guided lifting points, may be used to ensure controlled movement. Continuous monitoring during this stage is essential to identify anomalies such as misalignment, uneven expansion, or mechanical resistance. Adjustments and troubleshooting are carried out in real time, reflecting the iterative and responsive nature of deployable systems.

A simplified graphics of DRSTAB as shown in Figure 6.4.1, has a workflow inspired and has conceptual similarities with industrialised construction systems (such as XFrame and FrameCAD) , particularly in its emphasis on digital-to-physical integration, prefabrication, and assembly sequencing. However, while conventioanl systems systems ,rely on standardised light-gauge steel framing and linear assembly processes, DRSTAB introduces a non-linear, deployable logic driven by geometric transformation and mechanical articulation.

Unlike conventional framing systems that achieve form through static assembly, DRSTAB achieves form through controlled deployment, requiring additional layers of simulation, tolerance management, and real-time adjustment. This positions the system closer to advanced deployable or kinetic architectures, while still maintaining compatibility with prefabrication principles.

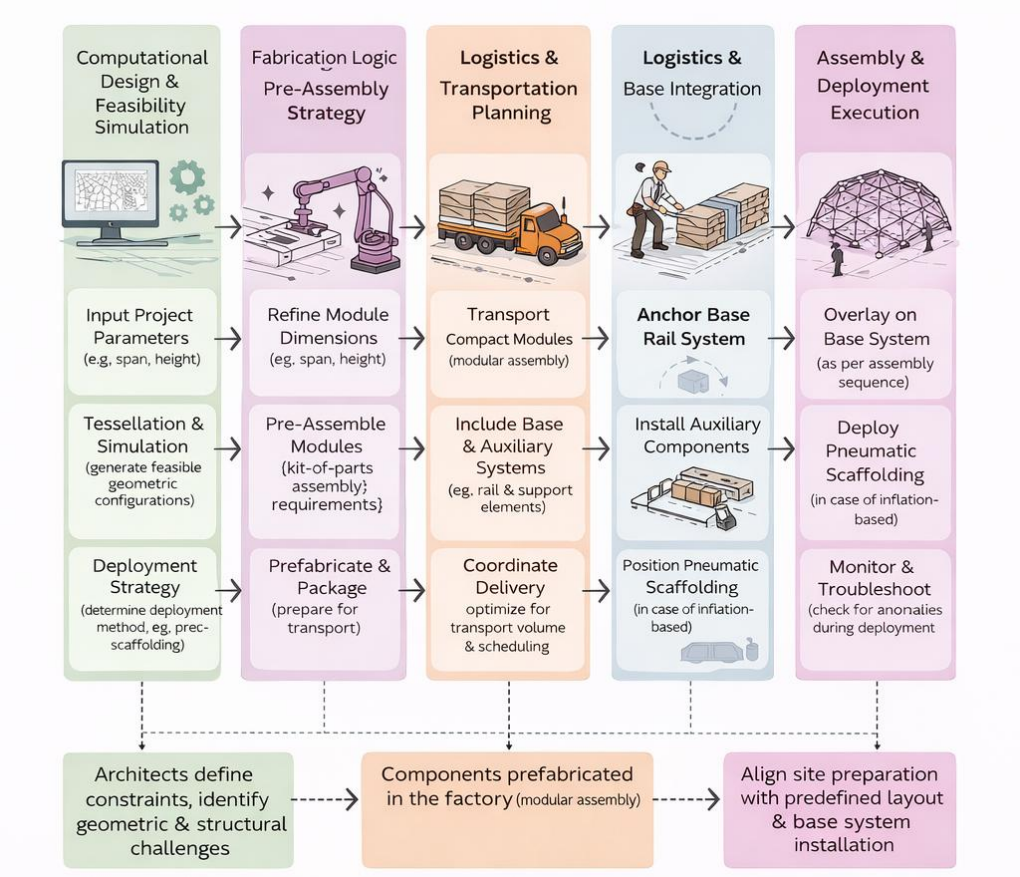

Figure 6.4-1 Simplified graphics of the Workflow of DRSTAB system

Note: Flowchart graphics Generated through OpenAI and Canva

Role of the Architect and Computational Designer

Design Orchestration and System Intelligence : Within the DRSTAB workflow, the role of the architect extends beyond conventional spatial design into that of a computational orchestrator. The architect or computational designer is responsible for defining parametric rules, managing geometric constraints, and interpreting simulation feedback to guide feasible design outcomes. This requires a high level of proficiency in digital modelling, scripting, and troubleshooting, as design decisions are directly linked to fabrication and deployment performance.

Integration Across Design, Fabrication, and Deployment : The architect also acts as a mediator between design intent and technical execution, ensuring alignment between computational models, fabrication logic, and on-site deployment strategies. This role is particularly critical in identifying potential failure points during early simulation stages and translating these insights into actionable design adjustments. In contrast to traditional workflows where roles are segmented, the DRSTAB system demands a more integrated approach, where the architect actively engages with engineering logic, material constraints, and assembly processes.

Facilitating Adaptive and Responsive Systems : Ultimately, the architect's role evolves into that of a systems designer, enabling the creation of adaptive, responsive, and reconfigurable structures. By leveraging computational tools and engaging with mechanical logic, the architect contributes not only to form-making but also to the operational intelligence of the system, ensuring that the DRSTAB framework performs effectively across its lifecycle.

6.4.2 Future Architecture implications of DRSTAB system

Expanded Architectural and Structural Applications

While this research has primarily focused on the ground deployment of reciprocal–auxetic shell structures, the DRSTAB system demonstrates significant potential across a broader range of architectural and engineering applications (Jayachandran, 2019). With further refinement of mechanical joinery, material optimisation, and deployment strategies, the system could evolve into a versatile framework adaptable to multiple contexts and scales. One immediate extension lies in dome and large-span spaceframe structures, where controlled expansion and curvature enable lightweight, self-supporting enclosures with minimal reliance on temporary support systems. The integration of reciprocal load distribution and auxetic adaptability enhances both structural efficiency and geometric flexibility, allowing the system to respond to varying spatial and functional requirements.

Temporary, Adaptive, and Infrastructure Systems

The system also presents strong potential in scaffolding and temporary structural frameworks, where its modular and deployable nature allows rapid assembly, disassembly, and reconfiguration in response to complex site conditions. This adaptability is particularly beneficial in construction environments that require flexibility around irregular geometries. Additionally, DRSTAB can function as a flat-expansion framework capable of bridging gaps, forming temporary platforms, or supporting transitional infrastructure. Such applications are especially relevant in post-disaster reconstruction, temporary urban interventions, and rapidly deployable field conditions. Its compact storage, transport efficiency, and repeatable deployment cycles further strengthen its suitability for event structures, emergency shelters, and mobile installations.

Facade Systems and Future Extensions

At the architectural scale, DRSTAB may operate as an adaptive façade framework, capable of conforming to complex double-curved geometries while supporting dynamic environmental responses such as shading, ventilation, and vibration dampening. Beyond conventional architectural applications, the system also suggests potential in extreme or mobile environments, including remote or resource-constrained contexts. These directions highlight its broader relevance as a lightweight, reconfigurable, and scalable structural system, extending its applicability beyond deployable shells into a wider family of adaptive construction solutions.

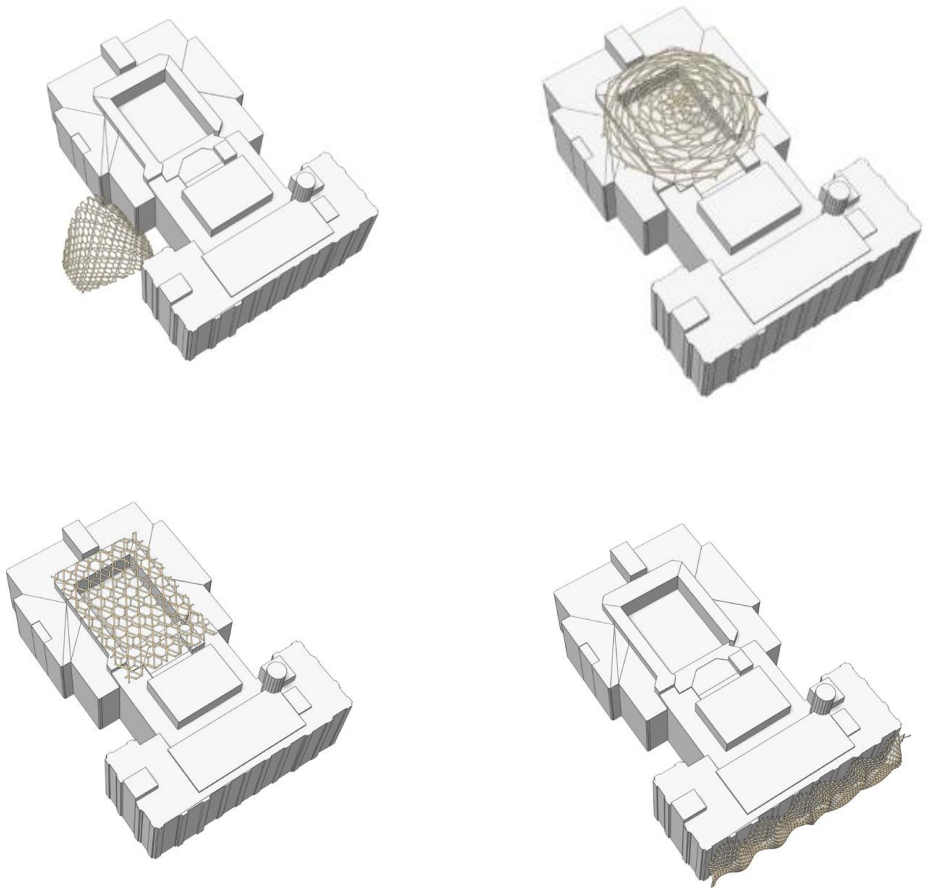

Figure 6.4-2 Future Implications for DR STAB system- Pavillions, Domes , Spaceframes & Façade systems

Note: From , *Deployable reciprocal shells through auxetic behaviour: Architectural hypothesis to fabricate double-curved structures* by *Jayachandran, S. (2019).*

Scafolding Framework and facades for Interior Spaces

Although the primary focus of this research is on large-scale architectural shells, the underlying auxetic principles can also inspire smaller-scale interior applications (Figure 6.3-2) Similar patterns and deployment logics can be adapted to develop versatile interior installations, where dynamic form and reconfigurability are desired. At this scale, auxetic structures could be fabricated using alternative materials whose properties allow for localized actuation. For instance, heating or cooling specific regions of the system could trigger expansion, contraction, or shape transformation, effectively enabling adaptive partitions, shading devices, or sculptural ceiling elements. Experimentation with material composition such as shape-memory polymers, thermally responsive composites, or hybrid textiles would allow these systems to change state in response to environmental or programmed cues. Such applications not only extend the DR-STAB framework beyond structural shells but also demonstrate its potential to influence interior spatial experience, where adaptability and responsiveness are increasingly valued in contemporary design

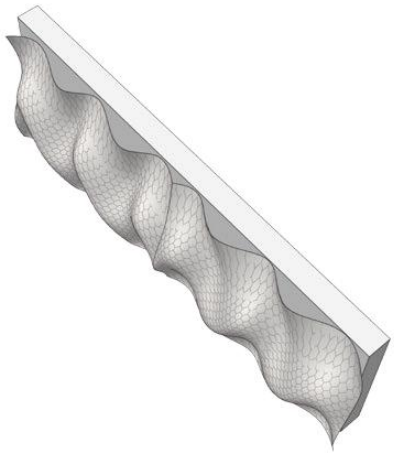

Figure 6.4-3 Future Implications for DR STAB system- interiors
Note: From , *Deployable reciprocal shells through auxetic behaviour: Architectural hypothesis to fabricate double-curved structures* by *Jayachandran, S. (2019).*

6.5 Overall concluding statements

This thesis has advanced the exploration of deployable architectural systems by integrating reciprocal structural logic with auxetic patterning to develop transformable, double-curved shells. The study set out to address a central challenge in contemporary architecture: how to design construction systems that are lightweight, reconfigurable, and capable of adapting to complex geometries while remaining structurally coherent. Through a design-led process combining literature synthesis, geometric analysis, physical prototyping, and mechanical experimentation, the research established the Tristar auxetic pattern, in combination with reciprocal framing, as a highly promising foundation for such systems.

At its core, this research demonstrates that reciprocal frameworks and auxetic logics are not simply parallel structural concepts but mutually reinforcing strategies. Reciprocal frames provide distributed stability and material efficiency, while auxetic patterns contribute controlled deformation and directional adaptability. Their integration, when linked with deployability, offers a design grammar that redefines how shells can be conceived, transported, and assembled. The Tristar pattern in particular proved to be the most adaptable geometry, offering uniform expansion and contraction across multiple curvatures, thereby overcoming limitations of other auxetic systems such as Miura or re-entrant lattices.

Scaled prototypes confirmed the feasibility of the system's geometric adaptability. PETG laser-cut modules and 3D-printed assemblies successfully demonstrated deployment across concave, convex, and saddle-like surfaces, validating the concept of controlled auxetic expansion embedded within reciprocal scaffolds. These experiments also revealed inherent weaknesses, including localized buckling, boundary instabilities, and synchronization challenges, underscoring the need for refined mechanical articulation. Importantly, these prototypes provided physical evidence that deployable auxetic–reciprocal shells could adapt to a wide range of geometries without requiring bespoke formwork or static prefabrication.

The exploration of mechanical joinery systems further highlighted the bridge between conceptual geometry and architectural application. Off-the-shelf components such as Chicago screws, ball joints, and clutch bearings enabled proof-of-concept demonstrations of rotational behaviour, but their limitations confirmed that bespoke mechanical solutions are essential. Angular restrictions, wear, and inconsistent locking emphasized the necessity of joints

engineered specifically for deployable auxetic behaviour. The progression from basic joints to conceptual proposals for ratchet-like and rail-based systems laid the groundwork for future development of reliable, scalable joinery mechanisms.

One of the major limitations of this research was the failure of high-fidelity mechanical simulations. SolidWorks models did not produce viable outcomes, collapsing under incomplete contact definitions and computational constraints. While disappointing, these failures were instructive, exposing the complexity of simulating recursive systems and pointing directly to the need for more advanced hybrid workflows and interdisciplinary collaboration. The inability to digitally validate joinery behaviours reinforced the role of physical experimentation in this research while simultaneously setting a clear agenda for future computational development.

Despite these limitations, the thesis makes a substantive contribution to architectural research. It establishes a framework for integrating geometry, mechanics, and deployability into a coherent structural logic. By articulating both the strengths and weaknesses of reciprocal–auxetic shells, it offers future researchers a roadmap that is transparent about methodological shortcomings while clear about the opportunities for advancement. The findings reaffirm that deployable systems are not merely engineering novelties but hold genuine architectural promise: enabling lightweight, reconfigurable, and sustainable structures that can adapt to diverse contexts, from temporary pavilions to emergency shelters.

Looking forward, the work suggests several key trajectories. Full-scale prototypes must be built and tested under realistic environmental conditions to validate structural viability. Advanced materials such as composites or shape-memory alloys should replace scaled plastics to ensure durability. Hybrid simulation workflows that integrate parametric modelling, finite-element analysis, and real-time sensing are essential to bridging digital predictions and physical performance. Finally, custom mechanical joineries must be designed and fabricated to unlock the full potential of the Tristar auxetic–reciprocal framework.

In conclusion, this thesis contributes a conceptual and methodological foundation for deployable shells that combine reciprocal and auxetic systems. It demonstrates both the promise and the challenges of such structures, showing that while the geometric logic is robust and scalable, the mechanical realization requires further refinement. By situating this research at the intersection of architecture, engineering, and materials science, the work not only advances theoretical discourse but also provides practical insights for future innovation. The vision of dynamic, reconfigurable architecture is not yet fully realized, but this thesis has taken an important step toward making it a tangible reality.

6.6 References

1. Alderson, A., Alderson, K. L., Attard, D., Evans, K. E., Gatt, R., Grima, J. N., ... & Zied, K. (2010). How to make auxetic fibre reinforced composites. *Physica Status Solidi (B)*, *247*(3), 706–718. https://doi.org/10.1002/pssb.200945481
2. Albag, O., Anishchenko, M., Grassi, G., & Paoletti, I. (2020). Adaptive skins: Towards new material systems. In *Proceedings of the International Conference on Adaptive Architecture* (pp. 1–12). Springer. https://doi.org/10.1007/978-3-030-33570-0_19
3. Babaee, S., Shim, J., Weaver, J. C., Chen, E. R., Patel, N., & Bertoldi, K. (2013). 3D soft metamaterials with negative Poisson's ratio. *Advanced Materials*, *25*(36), 5044–5049. https://doi.org/10.1002/adma.201301986
4. Baverel, O., Nooshin, H., & Langman, B. (2000). Nexorades: A family of interwoven space structures. *International Journal of Space Structures*, *15*(2), 155–159. https://doi.org/10.1260/0266351001495970
5. Bertoldi, K., Vitelli, V., Christensen, J., & van Hecke, M. (2017). Flexible mechanical metamaterials. *Nature Reviews Materials*, *2*, 17066. https://doi.org/10.1038/natrevmats.2017.66
6. Borgström, O. (2019). *That which tends to increase: Architectural application of auxetic systems* [Master's thesis, Chalmers University of Technology]. Chalmers Open Digital Repository. https://odr.chalmers.se/items/962cda52-087a-4ea4-8b89-ed0be59f3cfc/full
7. Carneiro, V., Meireles, J., & Puga, H. (2013). Auxetic materials: A review. *Materials Science-Poland*, *31*(3), 561–571. https://doi.org/10.2478/s13536-013-0140-6
8. Chilton, J., Popovic Larsen, O., & Hayes, R. (2015). Reciprocal frame structures in contemporary architecture. *Engineering Structures*, *101*, 750–760. https://doi.org/10.1016/j.engstruct.2015.07.036
9. Collins, J. A. (2009). *Mechanical design of machine elements and machines* (2nd ed.). Wiley.
10. Dong, S., & Hu, H. (2023). Sensors based on auxetic materials and structures: A review. *Materials*, *16*(9), 3603. https://doi.org/10.3390/ma16093603
11. Douthe, C., & Baverel, O. (2009). Design of reciprocal frame structures with timber plates. *International Journal of Space Structures*, *24*(4), 231–240. https://doi.org/10.1260/026635109790426974
12. Eguchi, S., Okabe, C., Ohira, M., & Tanaka, H. (2022). Pneumatic auxetics: Inverse design and 3D printing of auxetic pattern for pneumatic morphing. In *Proceedings of the CHI Conference on Human Factors in Computing Systems (CHI '22)* (pp. 1–7). https://doi.org/10.1145/3491101.3519801
13. Evans, K. E., & Alderson, A. (2000). Auxetic materials: Functional materials and structures from lateral thinking! *Advanced Materials*, *12*(9), 617–628. https://doi.org/10.1002/(SICI)1521-4095(200005)12:9<617::AID-ADMA617>3.0.CO;2-2
14. Fenci, G. E., & Currie, N. G. R. (2017). Deployable structures classification: A review. *International Journal of Space Structures*, *32*(2–3), 112–130. https://doi.org/10.1177/0266351117738254
15. Feng, H., Ma, J., Chen, Y., & You, Z. (2018). Twist of tubular mechanical metamaterials based on waterbomb origami. *Scientific Reports*, *8*(1), 1–10. https://doi.org/10.1038/s41598-018-27877-1

16. Gíslason, E. (2010). *Reciprocal frame structures: A guide for design and construction*. University of Iceland Press.
17. Grima, J. N., & Evans, K. E. (2006). Auxetic behavior from rotating squares. *Journal of Materials Science Letters*, *25*(15), 1383–1385. https://doi.org/10.1007/s10853-006-0310-x
18. Halderman, J. D. (2011). *Automotive suspensions and steering systems* (4th ed.). Pearson.
19. Gantes, C.J. (2001). Deployable Structures : Analysis and Design.
20. Harris, T. A. (2001). *Rolling bearing analysis* (4th ed.). Wiley.
21. Jackson, P. (2011). *Folding techniques for designers: From sheet to form*. Laurence King Publishing.
22. JAYACHANDRAN, S. (2019). Deployable reciprocal shells through auxetic behavior. Architectural hypothesis to fabricate double curve structures. Polimi.it. http://hdl.handle.net/10589/147499
23. Konaković, M., Crane, K., Deng, B., Bouaziz, S., Piker, D., & Pauly, M. (2016). Beyond developable. ACM Transactions on Graphics, 35(4), 1–11. https://doi.org/10.1145/2897824.2925944
24. Kwan, A. S. K., & Pellegrino, S. (1994). A New Concept for Large Deployable Space Frames. International Journal of Space Structures, 9(3), 153–162. https://doi.org/10.1177/026635119400900304
25. Lakes, R. (1987). Foam structures with a negative Poisson's ratio. *Science*, *235*(4792), 1038–1040. https://doi.org/10.1126/science.235.4792.1038
26. Larsen, N. M. (2008). *Reciprocal frame structures: Design and build*. BIS Publishers.
27. Lim, T.-C. (2015). *Auxetic materials and structures*. Springer. https://doi.org/10.1007/978-3-319-13776-5
28. Liu, H., Kollosche, M., Yan, J., Zellner, E., Bentil, S., Rivero, I., Wiersema, C., & Laflamme, S. (2020). Numerical investigation of auxetic textured soft strain gauge for monitoring animal skin. *Sensors*, *20*(15), 4185. https://doi.org/10.3390/s20154185
29. Lu, C., Hsieh, M., Huang, Z., Zhang, C., Lin, Y., Shen, Q., Chen, F., & Zhang, L. (2022). Architectural design and additive manufacturing of mechanical metamaterials. *Materials & Design*, *218*, 110703. https://doi.org/10.1016/j.matdes.2022.110703
30. Mir, M., Ali, M. N., Sami, J., & Ansari, U. (2019). Auxetic systems for architectural applications. *Materials & Design*, *167*, 107634. https://doi.org/10.1016/j.matdes.2019.107634
31. Mott, R. L. (2014). *Machine elements in mechanical design* (6th ed.). Pearson.
32. Naboni, R., Sartori, S., & Mirante, L. (2017). Adaptive-curvature structures with auxetic materials. In *Proceedings of ACADIA 2017* (pp. 368–375).
33. Nasiri, S. (2024). Auxetic grammars: An application of shape grammar using shape machine to generate auxetic metamaterial geometries for fabricating sustainable kinetic panels. In *Proceedings of the International Conference on Computational Design and Fabrication*. Springer. https://doi.org/10.1007/978-981-99-8405-3_10
34. Norton, R. L. (2020). *Machine design: An integrated approach* (6th ed.). Pearson.
35. Orthwein, W. C. (2004). *Clutches and brakes: Design and selection* (2nd ed.). Marcel Dekker.
36. Pahl, G., Beitz, W., Feldhusen, J., & Grote, K. H. (2007). *Engineering design: A systematic approach* (3rd ed.). Springer. https://doi.org/10.1007/978-1-84628-319-2

37. Panetta, J., Isvoranu, F., Chen, T., Siéfert, E., Roman, B., & Pauly, M. (2021). Computational inverse design of surface-based inflatables. *ACM Transactions on Graphics*, *40*(4), 71:1–17. https://doi.org/10.1145/3450626.3459813
38. Parigi, D., & Kirkegaard, P. H. (2014). Reciprocal structures: Statics, kinematics, and design. *Journal of the IASS*, *55*(3), 165–176.
39. Panetta, J., Konaković-Luković, M., Florin Isvoranu, E. Bouleau, & Pauly, M. V. (2019). X-Shells. 38(4), 1–15. https://doi.org/10.1145/3306346.3323040
40. Pellegrino, S. (2001). Deployable Structures in Engineering. 1–35. https://doi.org/10.1007/978-3-7091-2584-7_1
41. Pereira, F., Henrique, P., Monteiro, S. N., & Fabio, L. (2023). Development and applications of 3D printing-processed auxetic structures for high-velocity impact protection: A review. *Eng*, *4*(1), 903–940. https://doi.org/10.3390/eng4010054
42. Popovic Larsen, O. (2008). Reciprocal frame structures in nature and architecture. *Architectural Design*, *78*(2), 24–31.
43. Prawoto, Y. (2012). Seeing auxetic materials from the mechanics point of view. *Computational Materials Science*, *58*, 140–153. https://doi.org/10.1016/j.commatsci.2012.01.009
44. Rivas-Adrover, E. (2017). Classification of geometry for deployable structures used for innovation: Design of new surfaces with scissor 2 bar, and form generation method of relative ratios. *International Journal of Space Structures*, *32*(2–3), 89–99. https://doi.org/10.1177/0266351117736000
45. Ron Resch Tessellation - Parametric House. (2019, November 26). *Parametric House*. https://parametrichouse.com/ron-resch-tessellation/
46. Saxena, K. K., Das, R., & Calius, E. P. (2016). Three decades of auxetics research: Materials with negative Poisson's ratio – A review. *Advanced Engineering Materials*, *18*(11), 1847–1870. https://doi.org/10.1002/adem.201600053
47. Schenk, M., & Guest, S. D. (2013). Geometry of Miura-folded metamaterials. *Proceedings of the National Academy of Sciences*, *110*(9), 3276–3281. https://doi.org/10.1073/pnas.1217998110
48. Sclater, N. (2011). *Mechanisms and mechanical devices sourcebook* (5th ed.). McGraw-Hill.
49. Shigley, J. E., Mischke, C. R., & Budynas, R. G. (2004). *Standard handbook of machine design* (3rd ed.). McGraw-Hill.
50. Tachi Lab Artifacts. (2010, August 11). *Freeform Origami* [Video]. YouTube. https://www.youtube.com/watch?v=T35So_88mio&list=PL7847CD99F92C491D&index=9
51. Uicker, J. J., Pennock, G. R., & Shigley, J. E. (2017). *Theory of machines and mechanisms* (5th ed.). Oxford University Press.
52. Veenendaal, D., Block, P., & Adriaenssens, S. (2011). Reciprocal frame structures as deployable systems. *International Journal of Architectural Computing*, *9*(4), 375–396. https://doi.org/10.1260/1478-0771.9.4.375

53. Volkov, V. S., Makhnenko, O. V., Kandala, S. M., Volkova, O. A., & Borovyk, Y. V. (2021). Compactness variability of metal deployable load-carrying shell structures. *Engineering Structures*, *241*, 112477. https://doi.org/10.1016/j.engstruct.2021.112477
54. Zhang, J., Lu, G., & You, Z. (2020). Large deformation and energy absorption of additively manufactured auxetic materials and structures: A review. *Composites Part B: Engineering*, *183*, 107683. https://doi.org/10.1016/j.compositesb.2019.107683
55. Zhang, X., Ren, X., Jiang, W., Zhang, X., Luo, C., Zhang, Y., & Xie, Y. (2021). A novel auxetic chiral lattice composite: Experimental and numerical study. *Composite Structures*, *282*, 115043. https://doi.org/10.1016/j.compstruct.2021.115043
56. Zhang, Z., Wen, Q., Li, P., & Hu, H. (2021). Application of double arrowhead auxetic honeycomb structure in displacement measurement. *Sensors and Actuators A: Physical*, *333*, 113218. https://doi.org/10.1016/j.sna.2021.113218

Artificial intelligence (AI) tools were employed throughout this research process in accordance with the *AUT Postgraduate Handbook* 2025 , AI Guidelines for AUT PG (p. 81–82) New AI Guidelines for AUT PG Researchers – Thesislink).

OpenAI's ChatGPT models (GPT-4, GPT-4o, and GPT-5) were utilised to support writing development, grammar refinement, rephrasing for clarity, identifying relevant research references, genreating basic graphics and processing large datasets. All AI-assisted outputs were critically reviewed, edited, and verified by the researcher to ensure accuracy, originality, and alignment with academic integrity standards mentioned in the *AUT Postgraduate Handbook* 2025.

6.7 Appendices

6.7.1 Appendix A : Reciprocal pattern Analysis

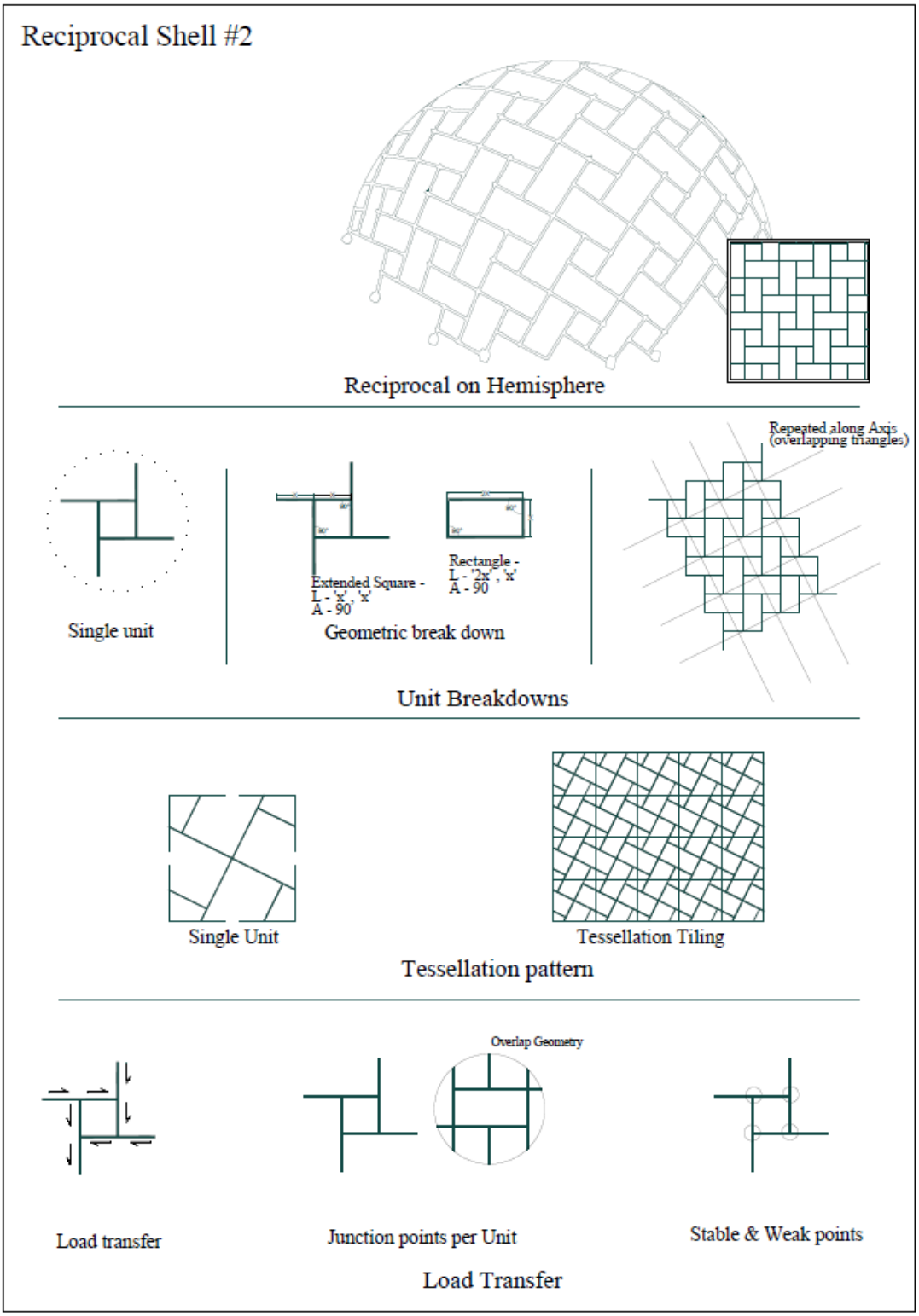

Figure 6.7-1 Reciprocal Analysis breakdown of RF pattern #2

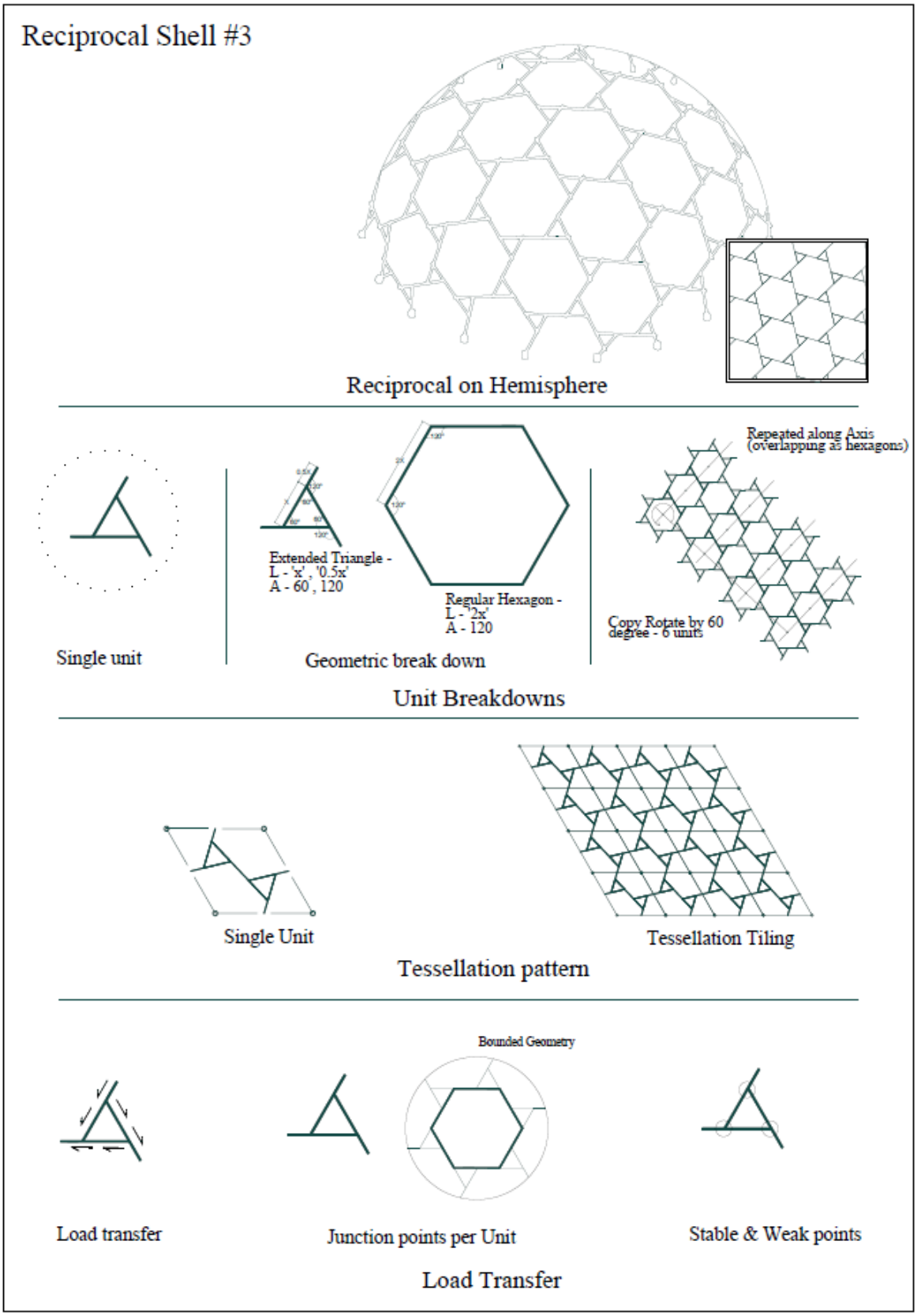

Figure 6.7-2 Reciprocal Analysis breakdown of RF pattern #3

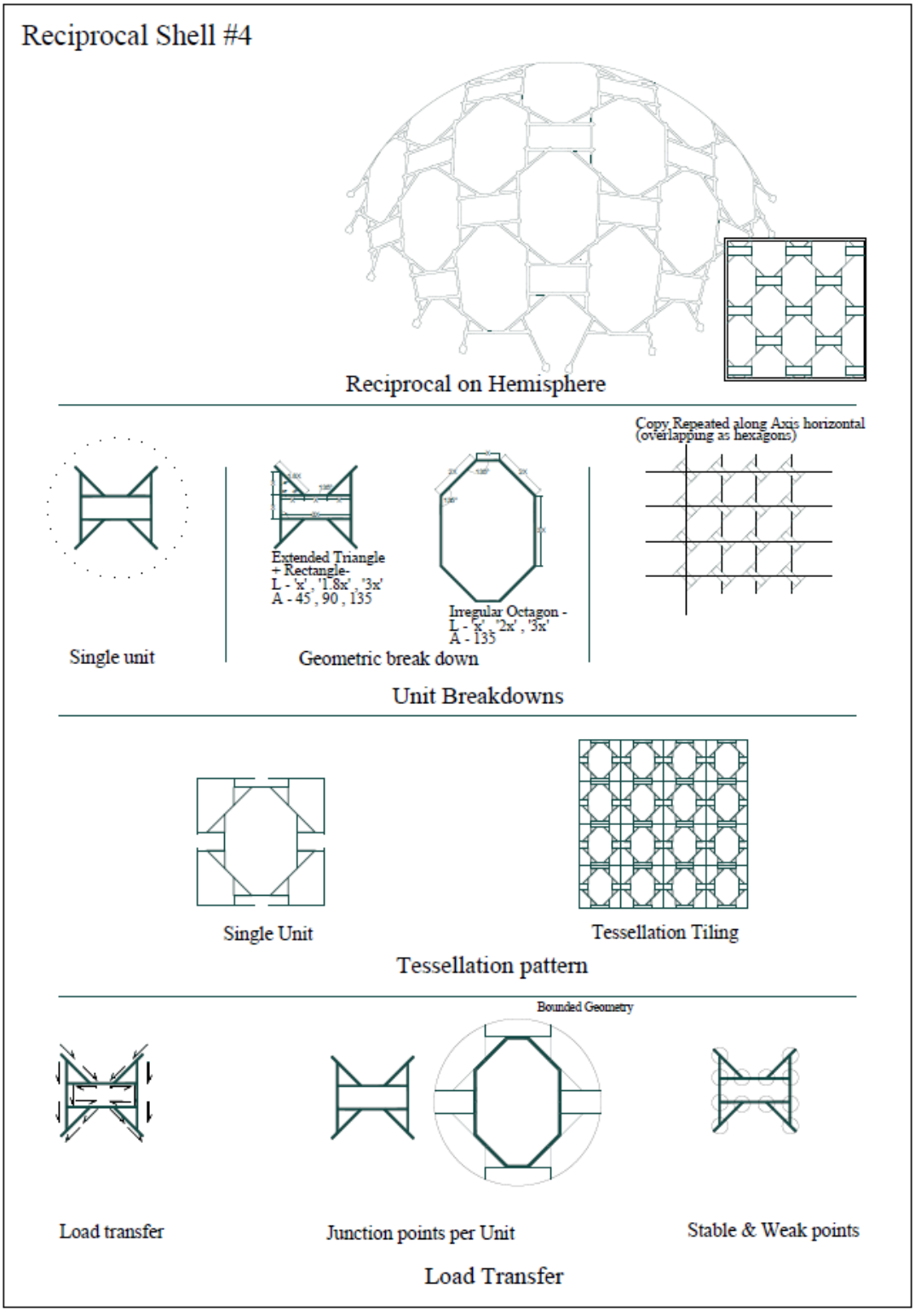

Figure 6.7-3 Reciprocal Analysis breakdown of RF pattern #4

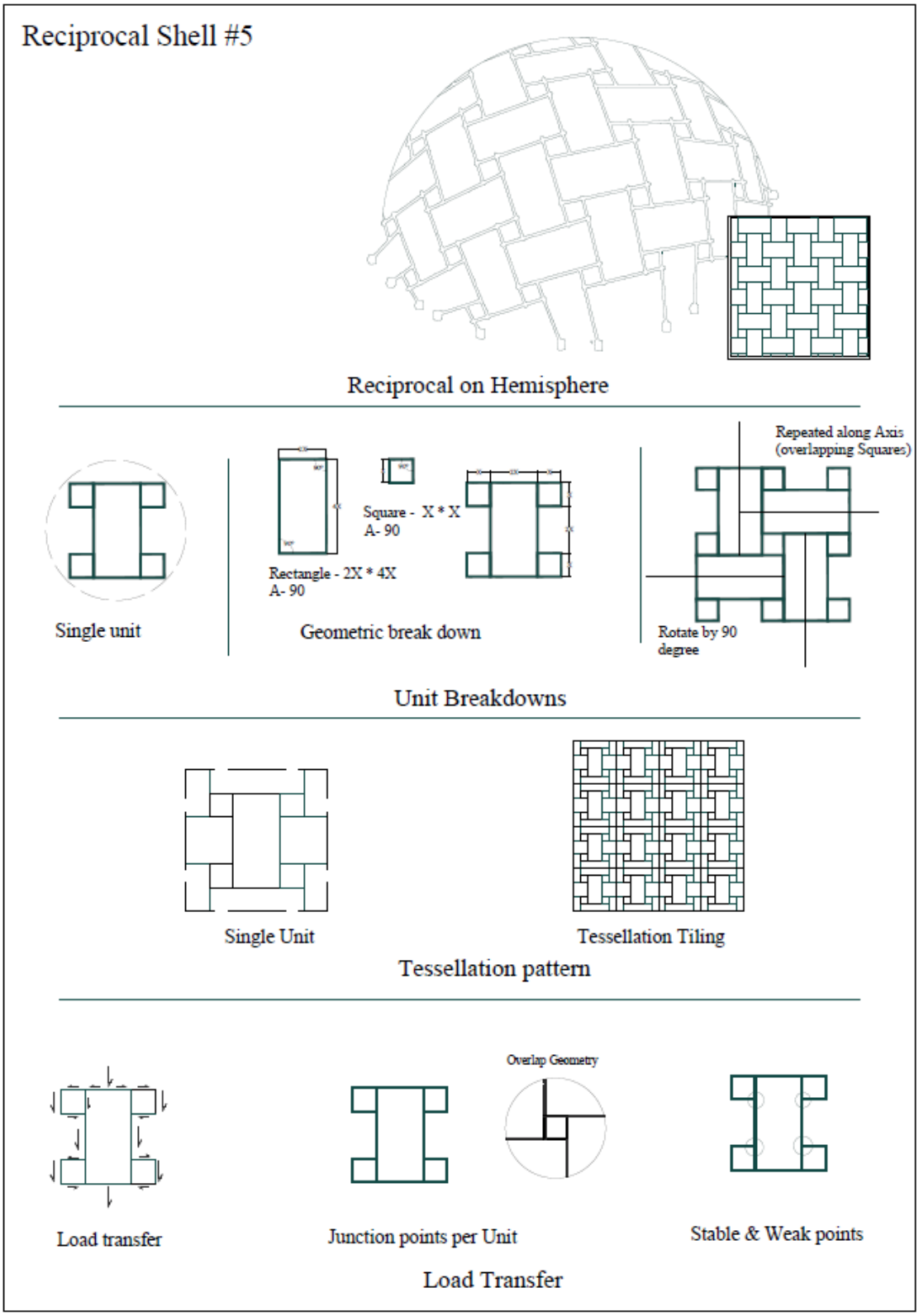

Figure 6.7-4 Reciprocal Analysis breakdown of RF pattern #5

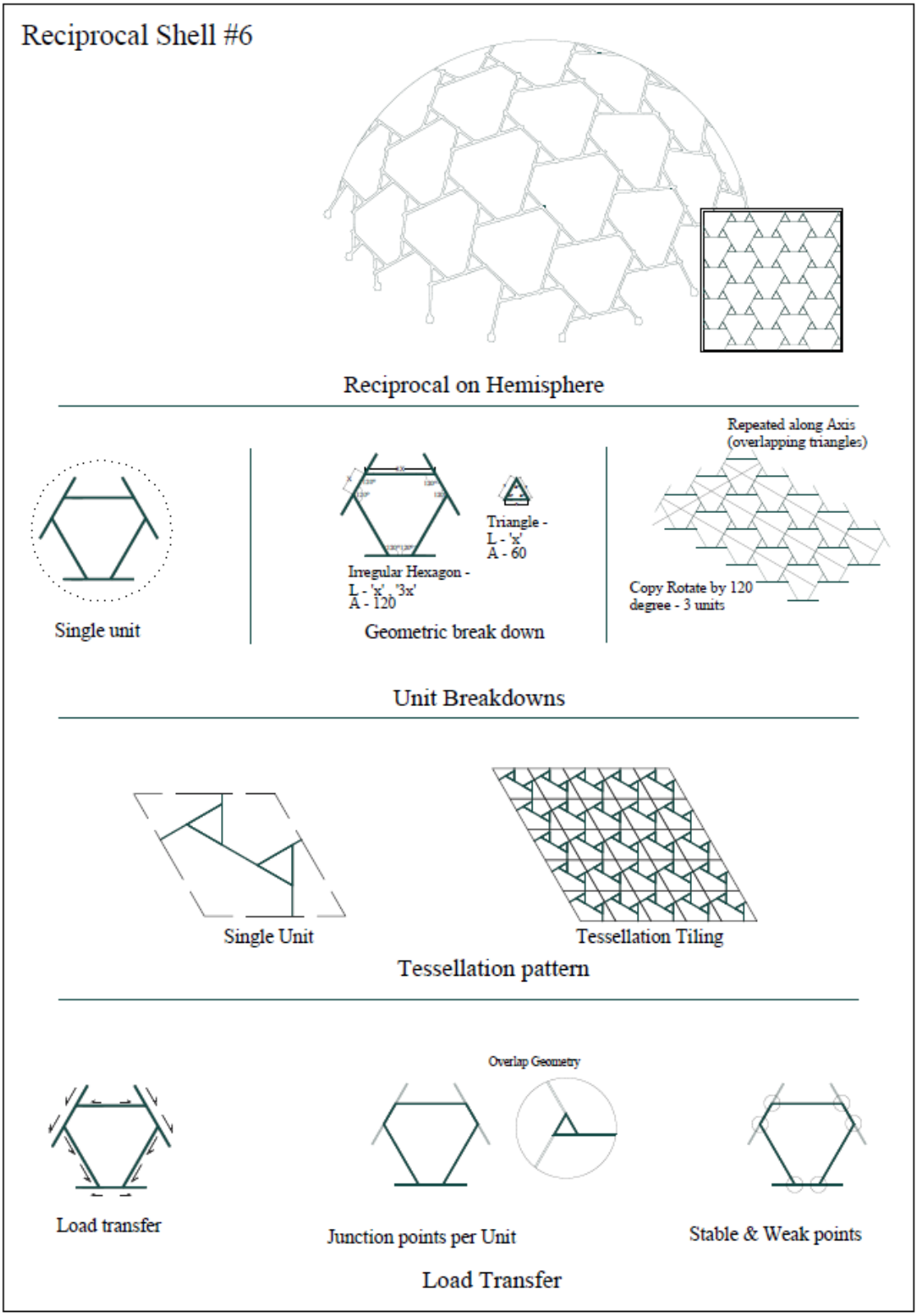

Figure 6.7-5 Reciprocal Analysis breakdown of RF pattern #6

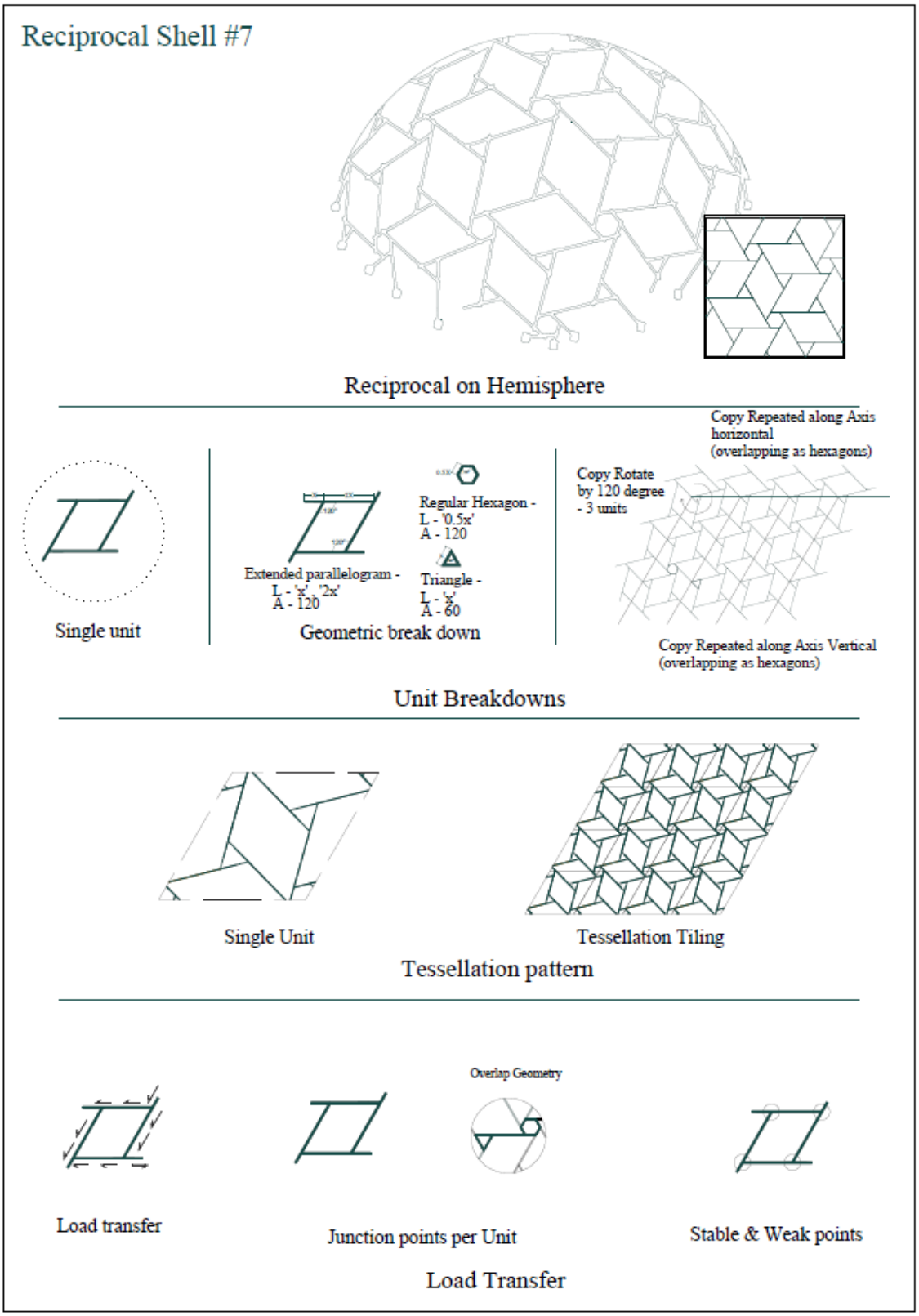

Figure 6.7-6 Reciprocal Analysis breakdown of RF pattern #7

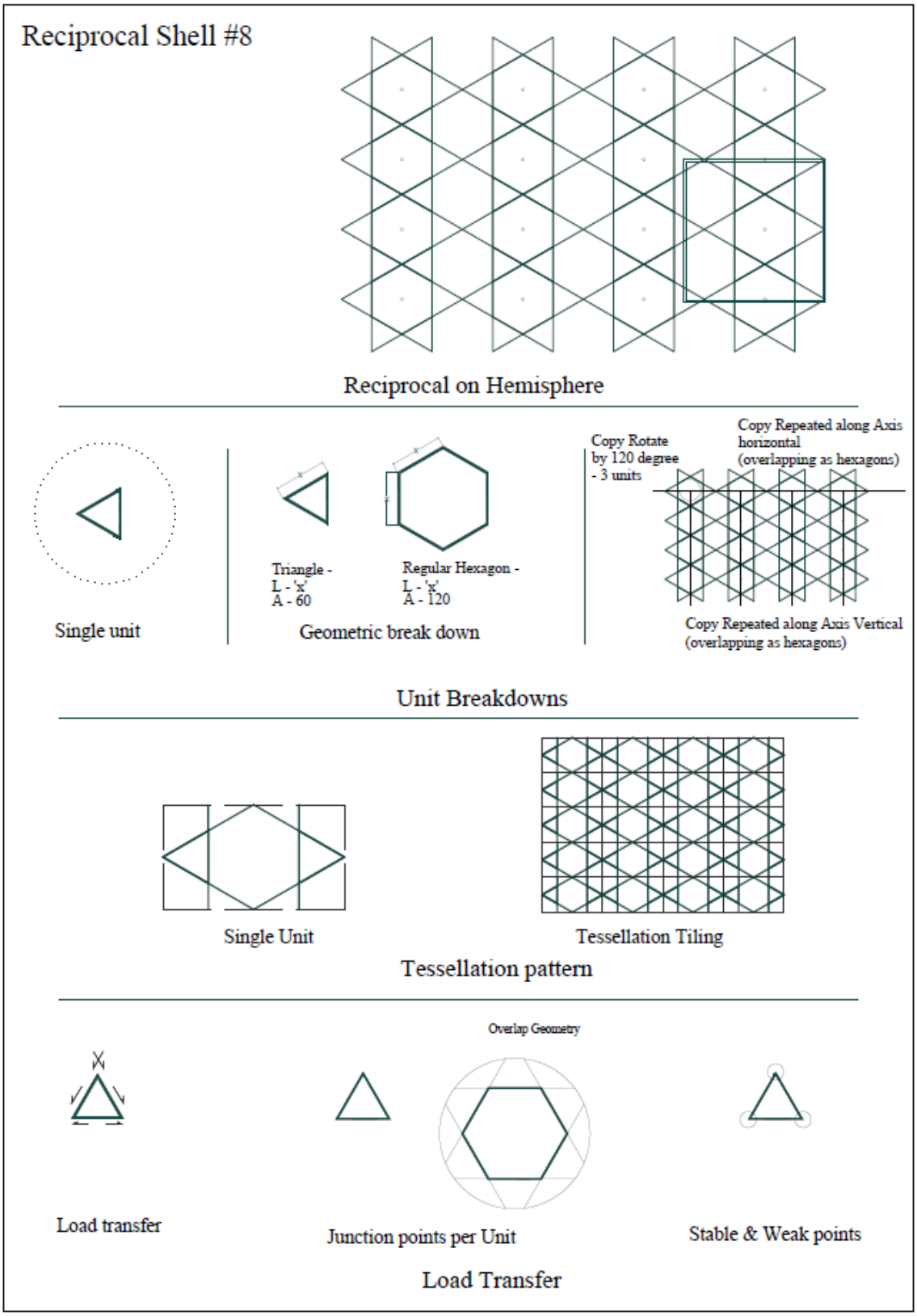

Figure 6.7-7 Reciprocal Analysis breakdown of RF pattern #8

6.7.2 Appendix B : Classification Of Auxetics from Literature

The auxetic patterns analyzed in Chapter 3.2 (2D Pattern Analysis) and Chapter 4.3 (3D Auxetic Pattern Adaptation and Spatial Behaviour) are based on established studies, including Evans & Alderson (2000), Grima & Evans (2006), Lakes (1987), Alderson et al. (2010), and Lim (2015).

6.7.2.1 Re-entrant Structures

Re-entrant Honeycomb (Pattern A)

This classic re-entrant hexagonal geometry features inward-angled cell walls (θ) that open outward under tensile strain, producing a negative Poisson's ratio. It is widely used as a foundational auxetic topology for its simple yet effective mechanism of lateral expansion .

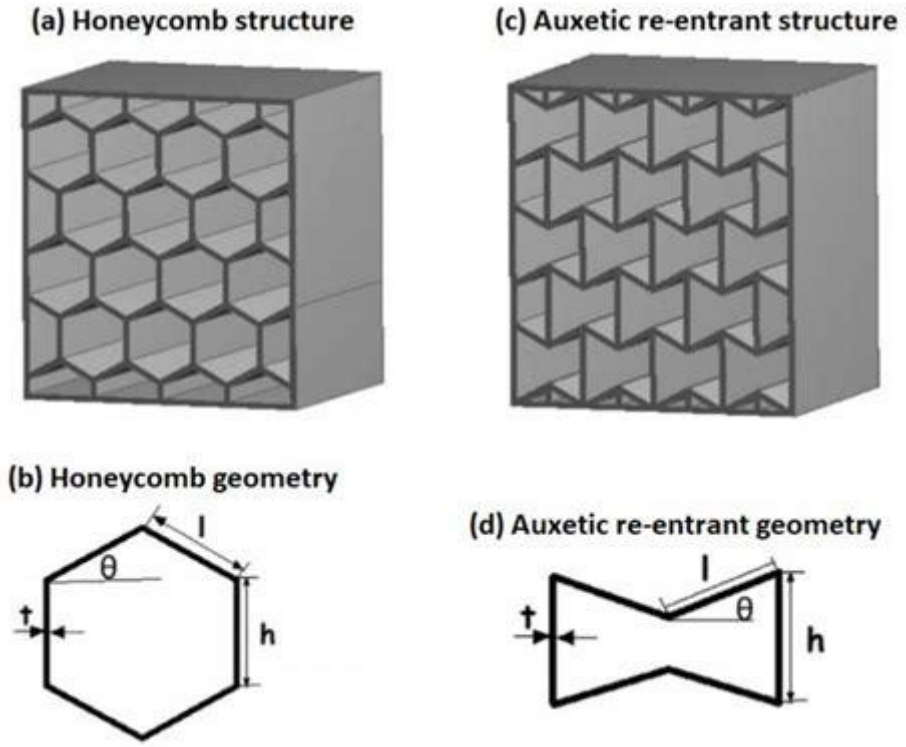

Figure 6.7-8 Re-entrant Honeycomb Auxetic structures
Note: From *Auxetic materials - A review* by *Carneiro, Vitor & Meireles, José & Puga, Hélder. (2013).*

Re-entrant Triangular & Star-Shaped Systems (Patterns B & C)

The triangular-shaped honeycomb (Pattern B) and its star-shaped variant (Pattern C) introduce pointed cell junctions that accentuate anisotropic auxetic behavior. Under load, the vertices hinge open, amplifying lateral strain and offering tunable stiffness through adjustments in cell angle and arm length .

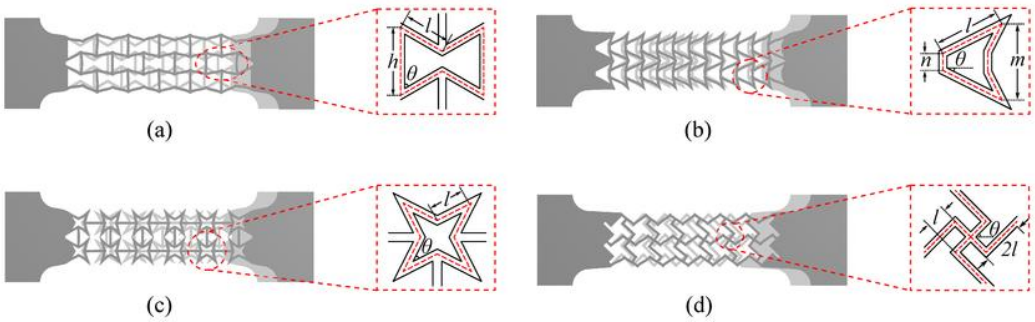

Figure 6.7-9 Re-entrant triangle Auxetic structures

Note : From *Numerical Investigation of Auxetic Textured Soft Strain Gauge for Monitoring Animal Skin. Sensors* by *Liu, Han & Kollosche, Matthias & Yan, Jin & Zellner, Eric & Bentil, Sarah & Rivero, Iris & Wiersema, Colin & Laflamme, Simon. (2020).*

Missing-Rib Model

In the missing-rib configuration, alternating ribs are omitted to create hinging joints at beam intersections. This design harnesses spring-like rotation (angle θ) around these hinges, achieving auxetic response without complex re-entrant geometry. It's especially favored in melt-electrowritten polymer patches for biomedical applications .

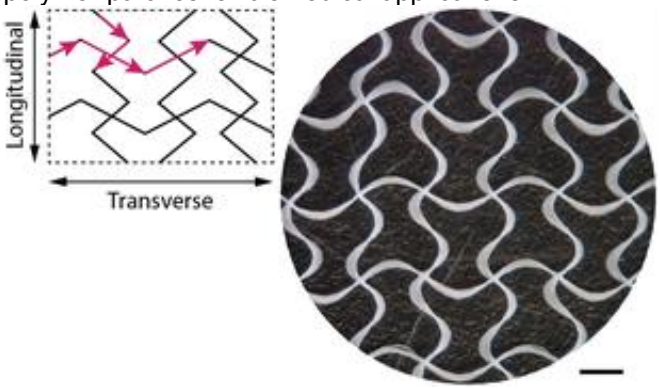

Figure 6.7-10 Re-entrant Missing rib Auxetic structures

Note : From *A novel auxetic chiral lattice composite: Experimental and numerical study. Composite Structures* by *Zhang, Xuegang & Ren, Xin & Jiang, Wei & Zhang, Xiangyu & Luo, Chen & Zhang, Yi & Xie, Yi. (2021).*

Double-Arrowhead Structure

The double-arrowhead unit cell combines two opposing arrowheads back-to-back, creating a highly compliant, tunable auxetic lattice. Axial tension causes both arrow tips to rotate outward, resulting in significant lateral expansion and customizable mechanical properties for

load-bearing scaffold designs

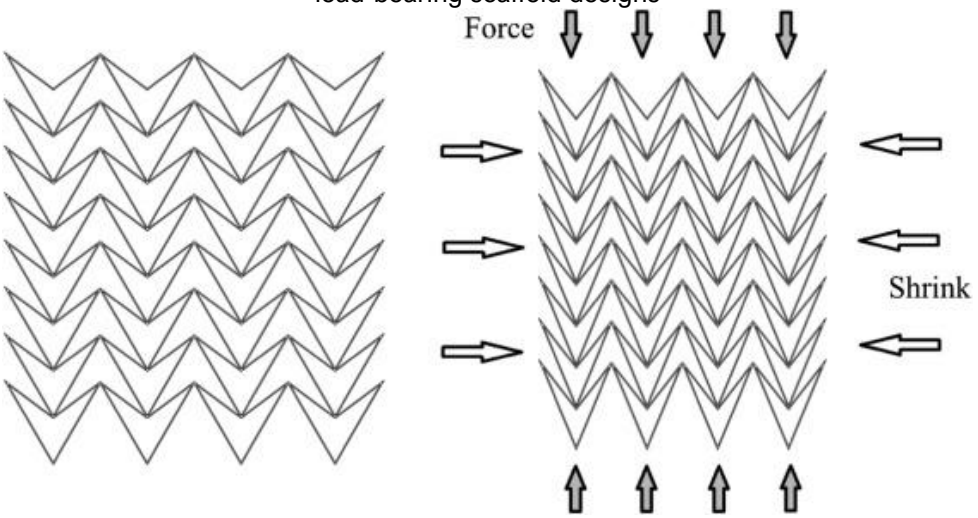

Figure 6.7-11 Re-entrant double head arrow Auxetic structures

Note : From *Application of double arrowhead auxetic honeycomb structure in displacement measurement. Sensors and Actuators A: Physical* by *Zhang, Z., Wen, Q., Li, P., & Hu, H. (2021).*

6.7.2.2 Rotating Units

Rotating Squares

In this pattern, each square unit pivots about its corners, opening like a flower under tensile strain. As the squares rotate, voids form and expand laterally, producing a pronounced negative Poisson's ratio without requiring complex hinge mechanisms.

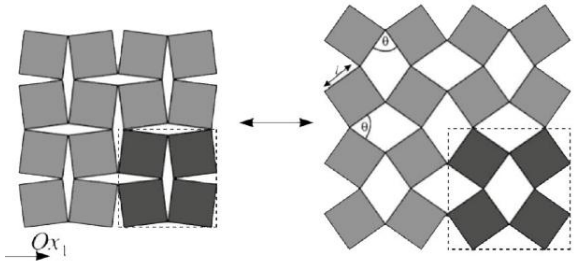

Figure 6.7-12 Rotating Squares Auxetic structures

From : From A*uxetic Grammars: An Application of Shape Grammar Using Shape Machine to Generate Auxetic Metamaterial Geometries for Fabricating Sustainable Kinetic Panels* by *Nasiri, Simin. (2024).*

Rotating Triangles

Here, equilateral triangles are connected at their vertices by pivots. Under tension, the triangles swing outward in a coordinated fashion, creating a star-like expansion that increases the lattice's overall footprint.

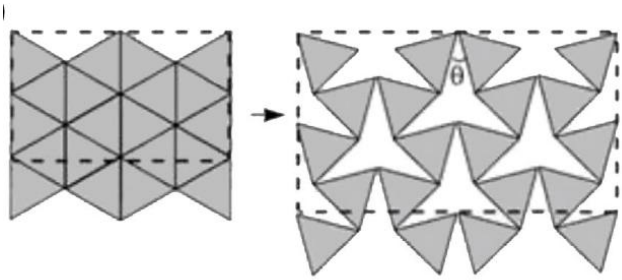

Figure 6.7-13 Rotating triangle Auxetic structures

Note : From *Sensors Based on Auxetic Materials and Structures: A Review. Materials*, by *Dong, S., & Hu, H. (2023).*

Rotating Rectangles

Rectangular units with a>b side ratios rotate rigidly around embedded pivots. Adjusting the rectangle aspect ratio and pivot offset (x) tunes the degree of lateral expansion and the critical strain at which auxetic behavior emerges.

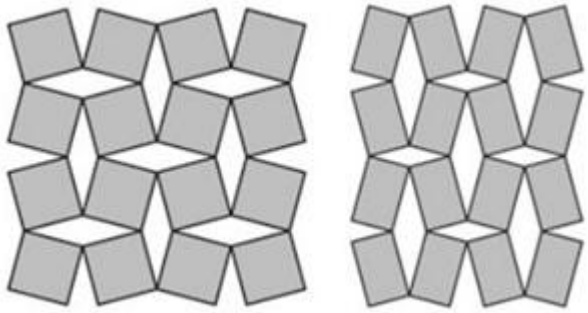

Figure 6.7-14 Rotating rectangle Auxetic structures

Note : From *Sensors Based on Auxetic Materials and Structures: A Review. Materials*, by *Dong, S., & Hu, H. (2023).*

Rotating Rhombi & Parallelograms

These patterns feature rhombic or parallelogram cells that hinge at opposing corners. Under load, each cell deforms by rotating its acute and obtuse angles, enabling broad tunability in mechanical response and offering both Type I and Type II configurations for varied auxetic performance.

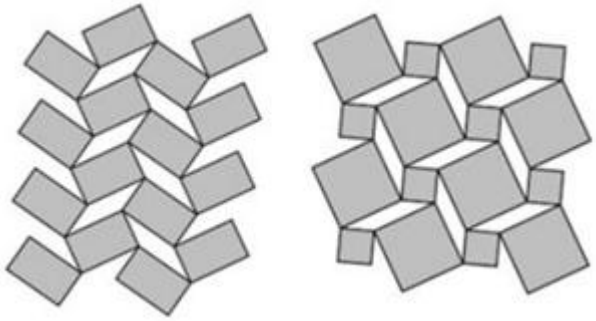

Figure 6.7-15 Rotating rhombi Auxetic structures

Note : From *Sensors Based on Auxetic Materials and Structures: A Review. Materials*, by *Dong, S., & Hu, H. (2023).*

6.7.2.3 Chiral Structures

Hexachiral Lattice

Each node (ring) connects to six ligaments arranged in a hexagonal pattern. Under tension, the ligaments bend and the rings rotate, creating a pronounced negative Poisson's ratio and isotropic auxetic response in two dimensions.

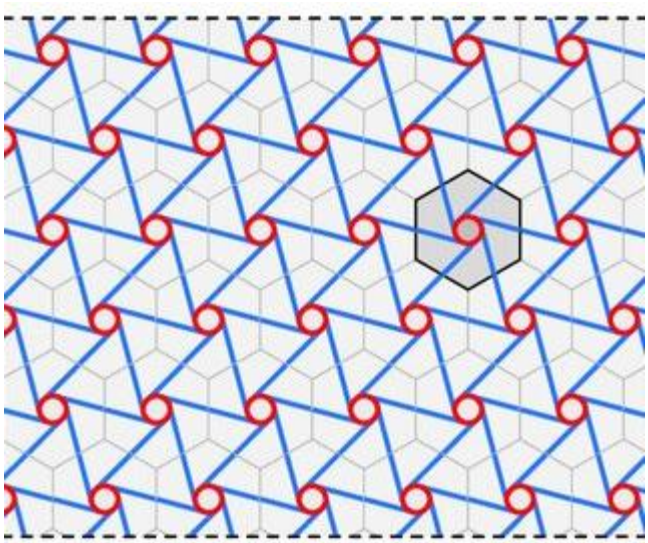

Figure 6.7-16 Hexachiral Auxetic structures

Note : *Development and Applications of 3D Printing-Processed Auxetic Structures for High-Velocity Impact Protection: A Review* by *Pereira, F., Henrique, P., Lucas, Sergio Neves Monteiro, & Fabio, L. (2023).*

Tetrachiral Lattice

This topology features circular nodes linked by four tangential beams. When stretched, nodes rotate and beams realign, yielding lateral expansion. The tetrachiral design offers directional tuning based on beam length and node radius.

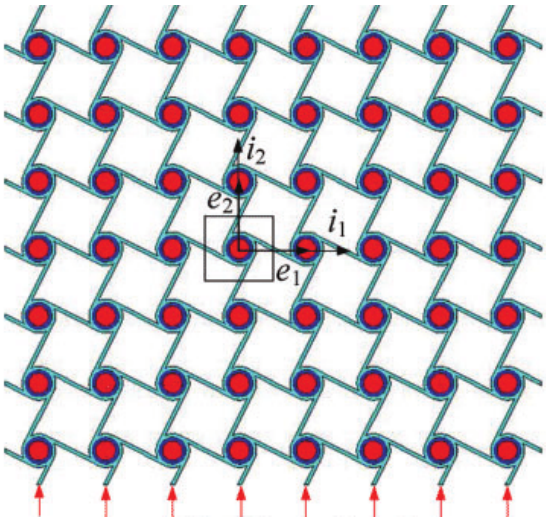

Figure 6.7-17 Tetrachiral lattice Auxetic structures

Note : *Development and Applications of 3D Printing-Processed Auxetic Structures for High-Velocity Impact Protection: A Review* by *Pereira, F., Henrique, P., Lucas, Sergio Neves Monteiro, & Fabio, L. (2023).*

Anti-Chiral Hexagons

In the anti-chiral arrangement, circular nodes connect via curved ligaments that wrap around each node center. Loading causes the nodes to translate without rotation, providing a softer auxetic response compared to chiral variants.

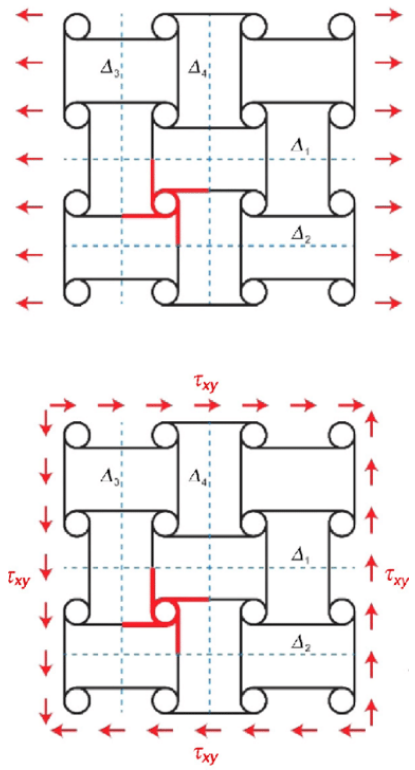

Figure 6.7-18 Antichiral hexagons Auxetic structures

Note : *Development and Applications of 3D Printing-Processed Auxetic Structures for High-Velocity Impact Protection: A Review* by *Pereira, F., Henrique, P., Lucas, Sergio Neves Monteiro, & Fabio, L. (2023).*

Mixed Chiral-Anti-Chiral ("Bi-Chiral") Patterns

Combining elements of chiral-3 and anti-chiral-3 honeycombs, these hybrid lattices feature both rotating rings and fixed hinge points. The resulting structure exhibits complex tension–torsion coupling and customizable auxetic behavior through geometric parameter adjustments.

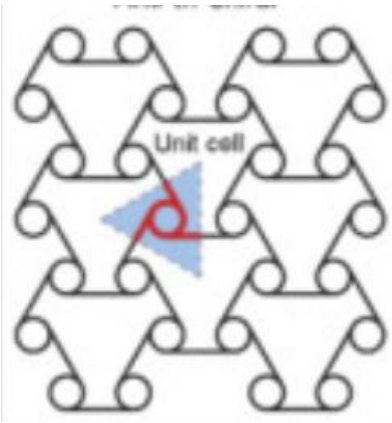

Figure 6.7-19 Mixed Chiral Auxetic structures

Note : *Development and Applications of 3D Printing-Processed Auxetic Structures for High-Velocity Impact Protection: A Review* by *Pereira, F., Henrique, P., Lucas, Sergio Neves Monteiro, & Fabio, L. (2023).*

6.7.2.4 Origami-Based

Miura-ori

A classic origami tessellation of parallelograms connected by alternating mountain and valley folds, the Miura-ori pattern allows a sheet to expand and contract uniformly. Under tension it flattens while creating a saddle-shaped curvature when loaded off-axis.

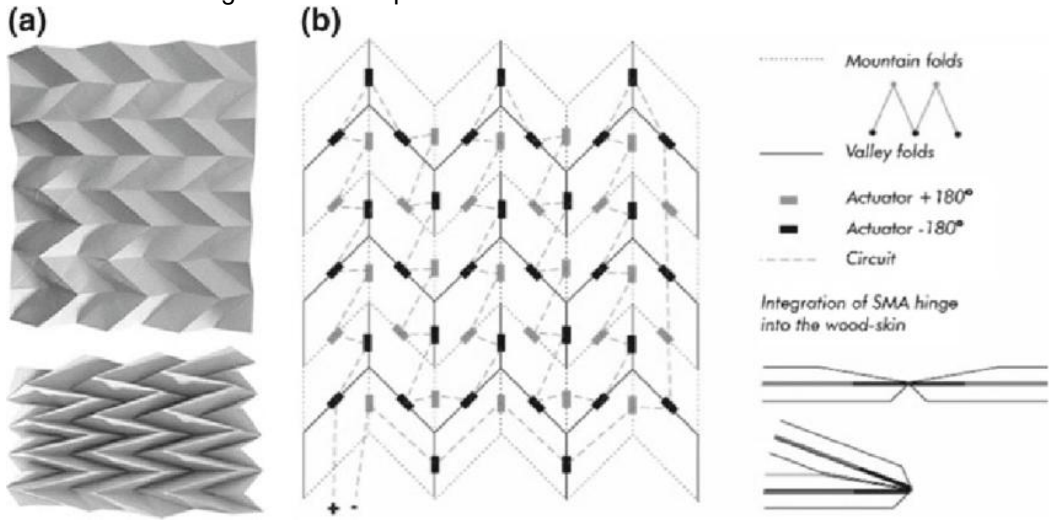

Figure 6.7-20 Miura ori Auxetic structures

Note : From *Adaptive Skins: Towards New Material Systems*. By *Albag, Ofir & Anishchenko, Maria & Grassi, Giulia & Paoletti, Ingrid. (2020).*

Ron Resch Tessellation

Developed by Ron Resch, this pattern uses triangular cells that interlock in a curved, petal-like layout. As the sheet deforms, the petals rotate and translate, yielding a flexible, deployable structure with smooth curvature transitions.

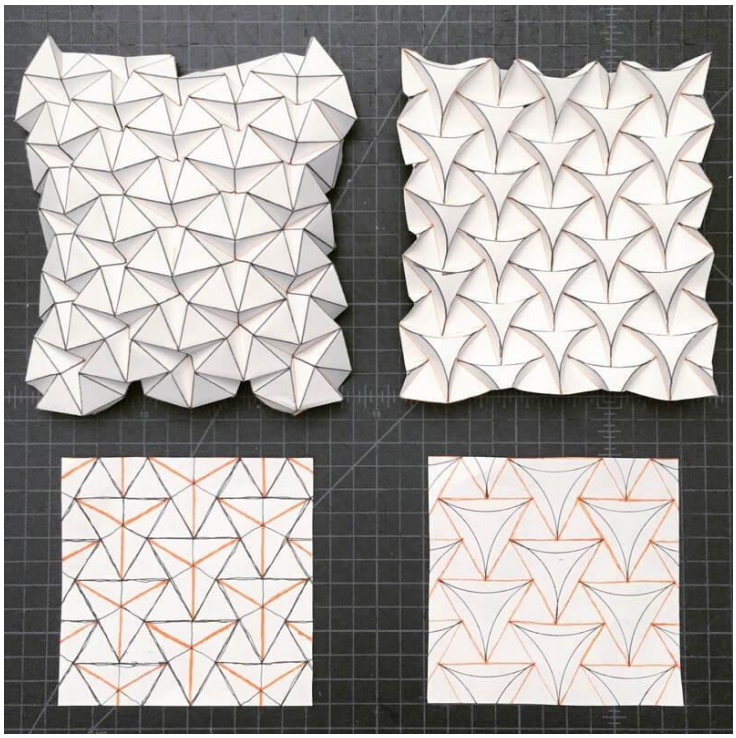

Figure 6.7-21 Ron Resch Auxetic structures

Note : From Ron Resch Tessellation - Parametric House. (2019). Parametric House.

Waterbomb Base

The Waterbomb base is formed from a simple grid of alternating mountain and valley folds, creating a collapsible cell structure. When expanded, the cells open symmetrically in both principal directions, producing a pronounced auxetic response.

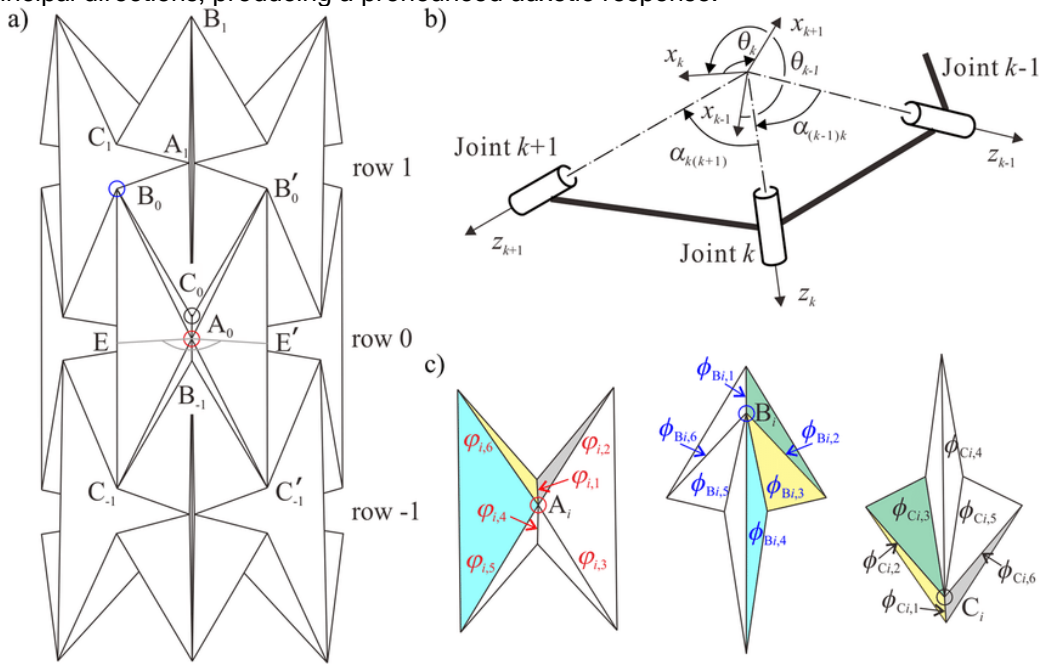

Figure 6.7-22 Waterbomb base Auxetic structures

Note : From *Twist of Tubular Mechanical Metamaterials Based on Waterbomb Origami.* by *Feng, Huijuan & Ma, Jiayao & Chen, Yan & You, Zhong. (2018).*

Kresling Pattern

Composed of alternating mountain-valley zigzags on a cylinder, the Kresling pattern contracts radially and extends axially under twist, behaving like a compressible spring. Its unique rotational deployment makes it ideal for cylindrical actuators.

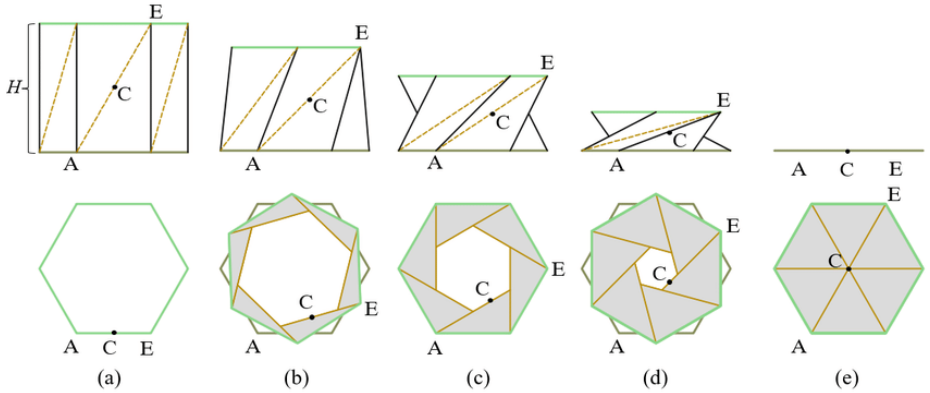

Figure 6.7-23 Kresling Auxetic structures

Note: From *A Novel Radially Closable Tubular Origami Structure* by *Ye, Siyuan & Zhao, Pengyuan & Zhao, Yinjun & Kavousi, Fatemeh & Feng, Huijuan & Hao, Guangbo. (2022).*

Tachi Freeform ("Tachi Fold")

Based on Tomohiro Tachi's Freeform Origami, this pattern uses smoothly curved crease lines ("lens tessellation") to generate complex 3D surfaces from a flat sheet. Under deformation, the curved creases guide the sheet into doubly curved geometries without stretching the paper.

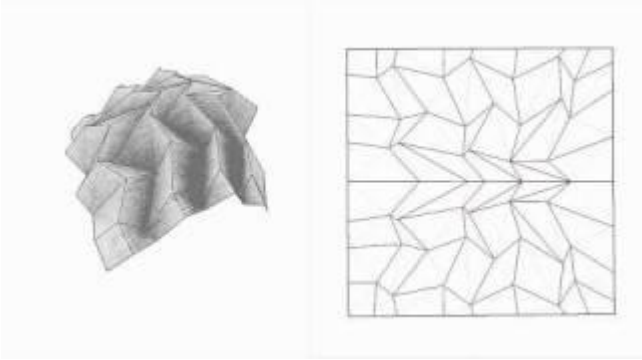

Figure 6.7-24 Tachi freeform Auxetic structures

Note : From Tachi Lab Artifacts. (2010, August 11). Freeform Origami. YouTube.

6.7.2.5 Perforated Sheets

Diamond-Cut Sheet

Regular arrays of rhombus-shaped perforations when stretched, the diamond apertures open and rotate, causing the sheet to expand laterally and exhibit auxetic behaviour .

Circular-Cut Pattern

Tessellated circular holes connected by narrow ligaments deform under tension by ligament bending, producing a modest negative Poisson's ratio and smooth expansion .

Star-Shaped Cuts

Star or petal-like holes arranged in a grid hinge open at the points under load, generating pronounced lateral expansion and anisotropic mechanical response .

Hierarchical Perforations

Multi-scale perforation patterns larger primary holes interspersed with smaller secondary cuts create hierarchical hinge mechanisms that magnify auxetic effects across scales .

6.7.2.6 Tensegrity Structures

Re-entrant Tensegrity Prism (Expanded Octahedron / T3-Prism)
This classic T3-prism comprises two three-strut layers joined in an octahedral arrangement. When axial forces are applied along its central axis, the structure exhibits conditional auxetic behavior its girth narrows under tension but widens under compression highlighting the subtleties of re-entrant tensegrity auxetics .

3-Strut DNA Tensegrity Prism
Constructed at the nanoscale using DNA origami, this prestressed prism demonstrates tensegrity principles in a molecular framework. The three struts and ssDNA springs balance tension and compression, providing a precise, tunable example of tensegrity-based auxetic architecture .

Colorful Tensegrity Sphere (Non-Auxetic Demonstrator)
A multistrut geodesic tensegrity sphere assembled from colored rods and elastic cables. Although primarily non-auxetic under unidirectional loads, this model illustrates how tensegrity lattices can be tuned through node geometry and tensioning to approach auxetic responses in specific orientations .

DIY Tensegrity T3-Prism Tutorial
This instructional model shows a simple three-strut tensegrity prism built from readily available materials. It highlights fundamental construction techniques and visualizes the balance of forces that govern tensegrity stability an essential hands-on reference for prototyping auxetic tensegrity structures .

6.7.2.7 3D Auxetic Networks

Cubic Auxetic Networks
In this $4 \times 4 \times 3$ arrangement of s-hinge unit cells, rigid faces flex at hinge-lines to yield a negative Poisson's ratio in all three axes. Under axial load, the network contracts in the loading direction while expanding laterally .

Tetrahedral Re-entrant Frameworks
By extruding 2D re-entrant bow-tie cells into three dimensions, this lattice of interconnected tetrahedral units produces auxetic behaviour via coordinated hinge rotation of struts under tension .

3D Rotating Cube Networks

Although originally conceptualized for dynamic studies, a cubic grid of pivoting beams (analogous to harmonic oscillators) can be adapted so that each cube rotates at its edges under load, opening the network outward in all directions .

Modified Strut-Based Unit Cell
This design uses thick struts hinged with central nodes; by tuning strut angles and “waist” dimensions, the cell exhibits controlled auxetic expansion in 3D, with applications in high-stiffness metamaterials .

6.7.2.8 Composite / Hybrid Auxetics

Mixed-Mode Chiral–Re-entrant Hybrid
This pattern layers re-entrant units onto a chiral prism backbone, combining inward-angled ribs with rotating node rings. Under tension, the chiral rings rotate while the re-entrant cells hinge open, producing enhanced, directionally tunable auxetic response.

Rotating–Origami Hybrid Surface
Origami-inspired triangular panels are integrated with pivoting rigid units. As the surface deforms, panels fold along curved creases while discrete rigid blocks rotate, yielding a smoothly morphing, multi-state deployable structure.

Hierarchical Layered Auxetic System
Multiple scales of rotating rigid units are nested within one another (levels 0, 1, 2), forming a fractal-like lattice. Each hierarchy level unlocks additional degrees of expansion, allowing complex deformation patterns and graded mechanical properties.

Composite Hybrid Auxetic Sandwich Panel
This composite integrates layers of auxetic core (e.g., re-entrant honeycomb) between conventional facings. The hybrid design leverages both auxetic expansion and sandwich mechanics, achieving superior energy absorption and blast-resistance characteristics.

6.7.2.9 Advanced Metastructures

Foldable Kirigami-Based Auxetics
This pattern uses strategic cuts and rotations of polygonal facets to open the sheet under tension. As the facets unfold (angle η increases), the structure transitions through negative, zero, and positive Poisson’s ratio regimes, showcasing versatile mechanical responses.

Programmable Gear-Based Mechanical Metamaterials
A lattice of meshing gears and hinging struts allows in-situ tuning of stiffness and deformation mode. By adjusting gear cluster arrangements or engaging/disengaging meshing, the metamaterial’s Young’s modulus and auxetic response can be programmed on demand.

Auxetic Origami Tubes
Origami-inspired tubular structures employ folding patterns (e.g., waterbomb and Miura bases) rolled into cylindrical form. Under axial strain, the tube’s cross-section expands radially, making these designs promising for deployable stents and adaptive pipelines.

Chiral Mechanical Metastructure with Shear Coupling
This 3D lattice combines chiral nodes and connecting beams to produce extension–twist coupling. Under load, nodes rotate while beams bend, yielding a unique auxetic effect that couples shear deformation with lateral expansion, ideal for multifunctional smart materials.

6.7.3 Appendix C : Auxetic Pattern Analysis

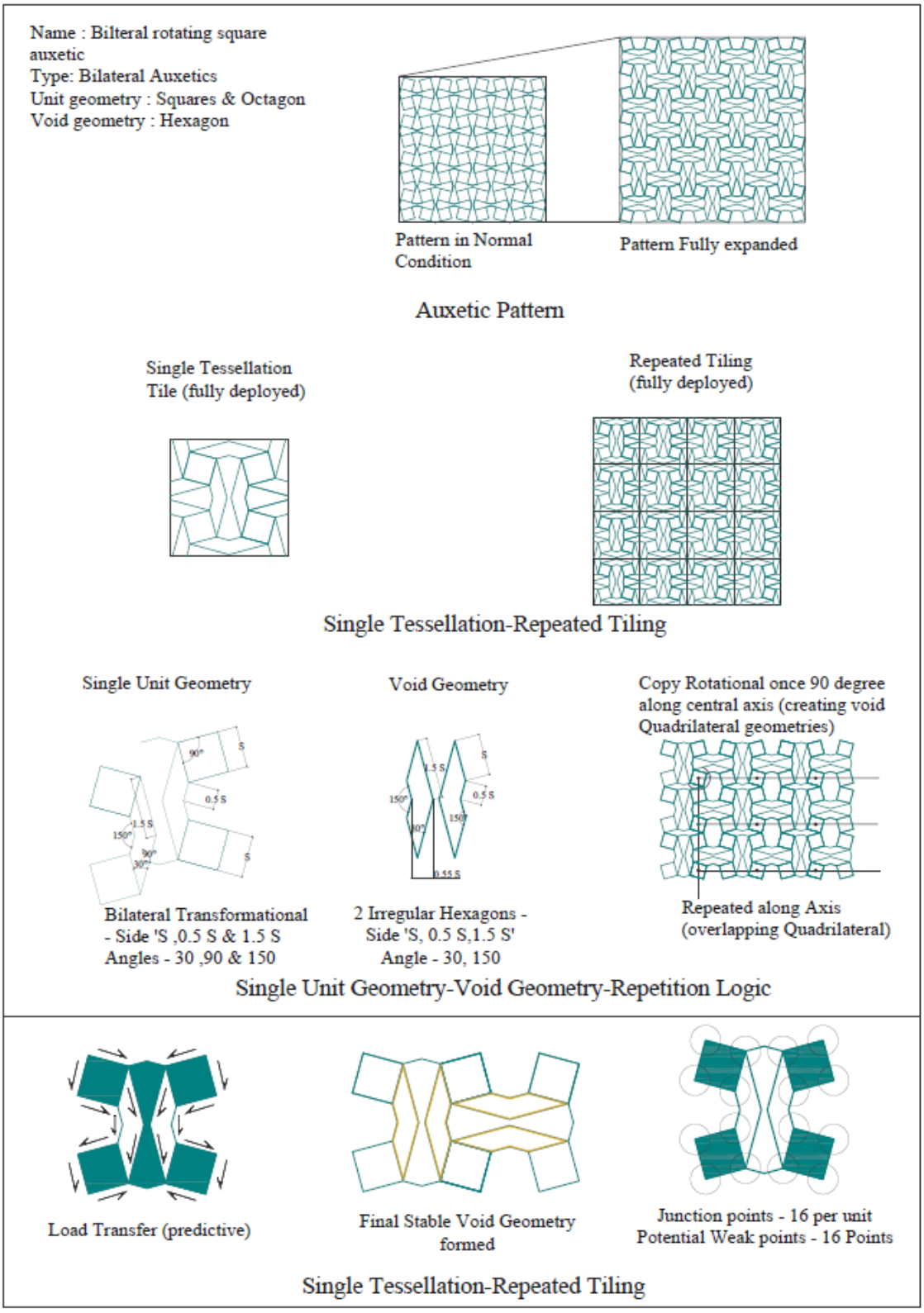

Figure 6.7-25 Analysis of Bilateral Rotating square Auxetic

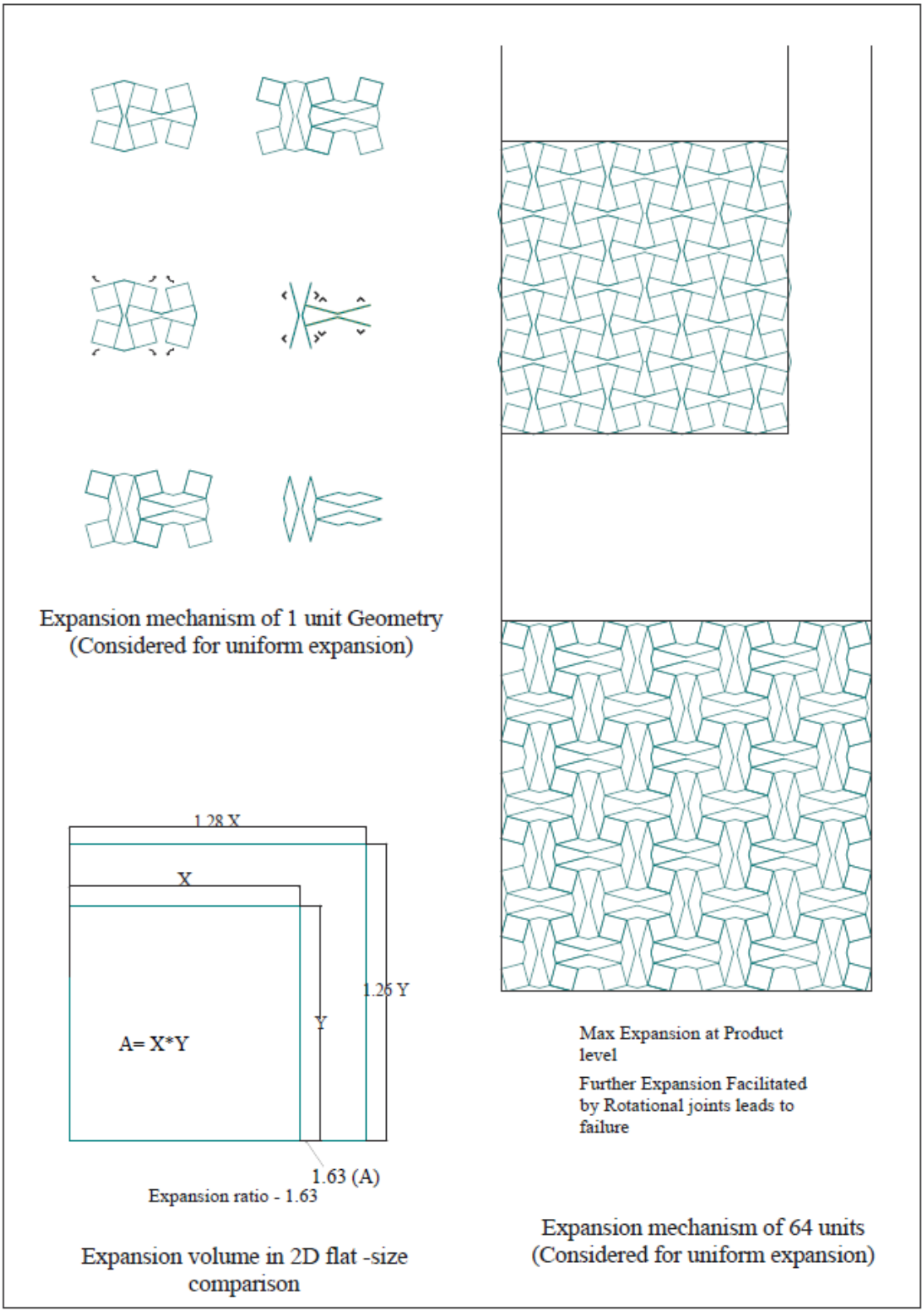

Figure 6.7-26 Analysis of Bilateral Rotating square Auxetic

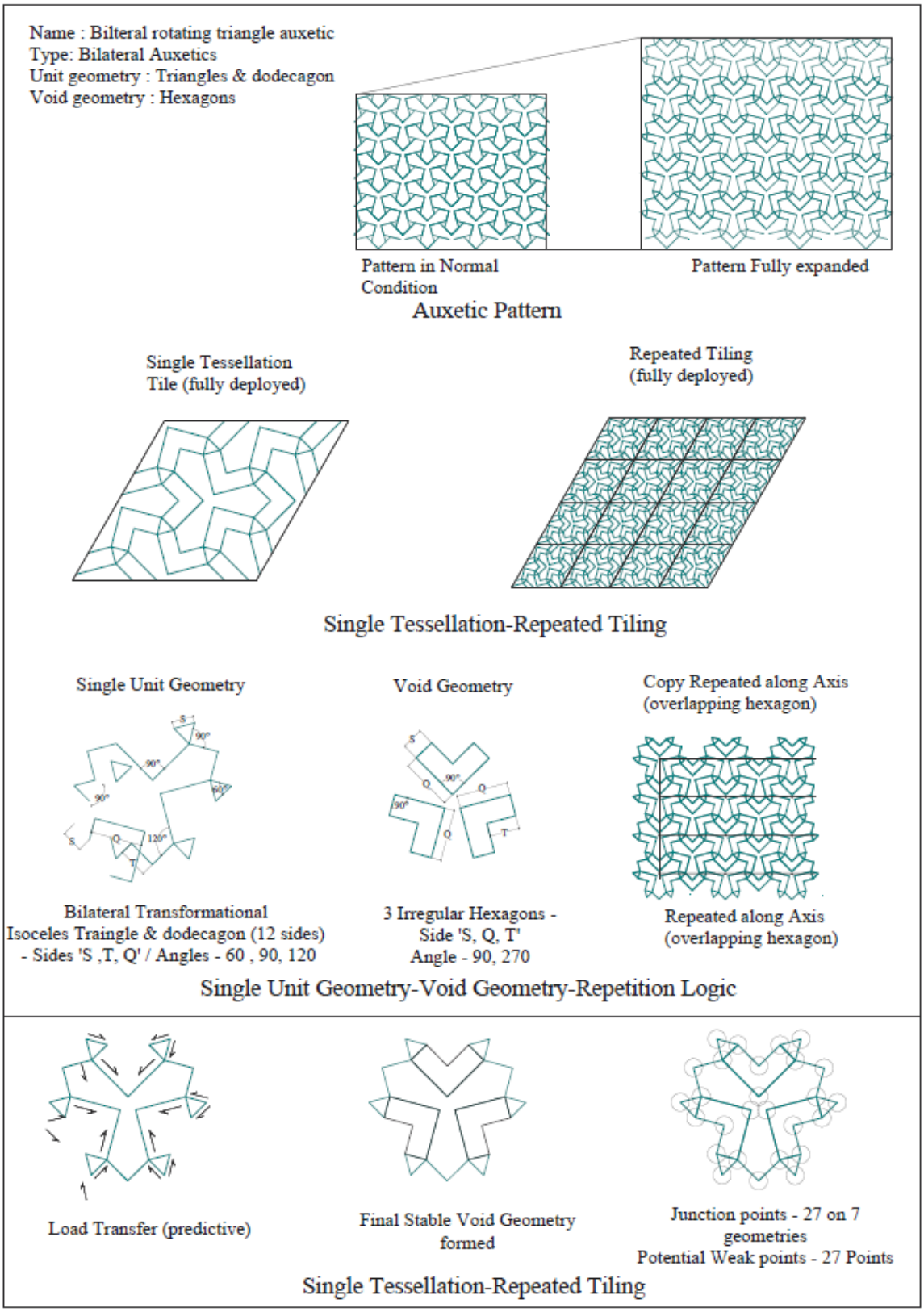

Figure 6.7-27 Analysis of Bilateral Rotating triangle Auxetic

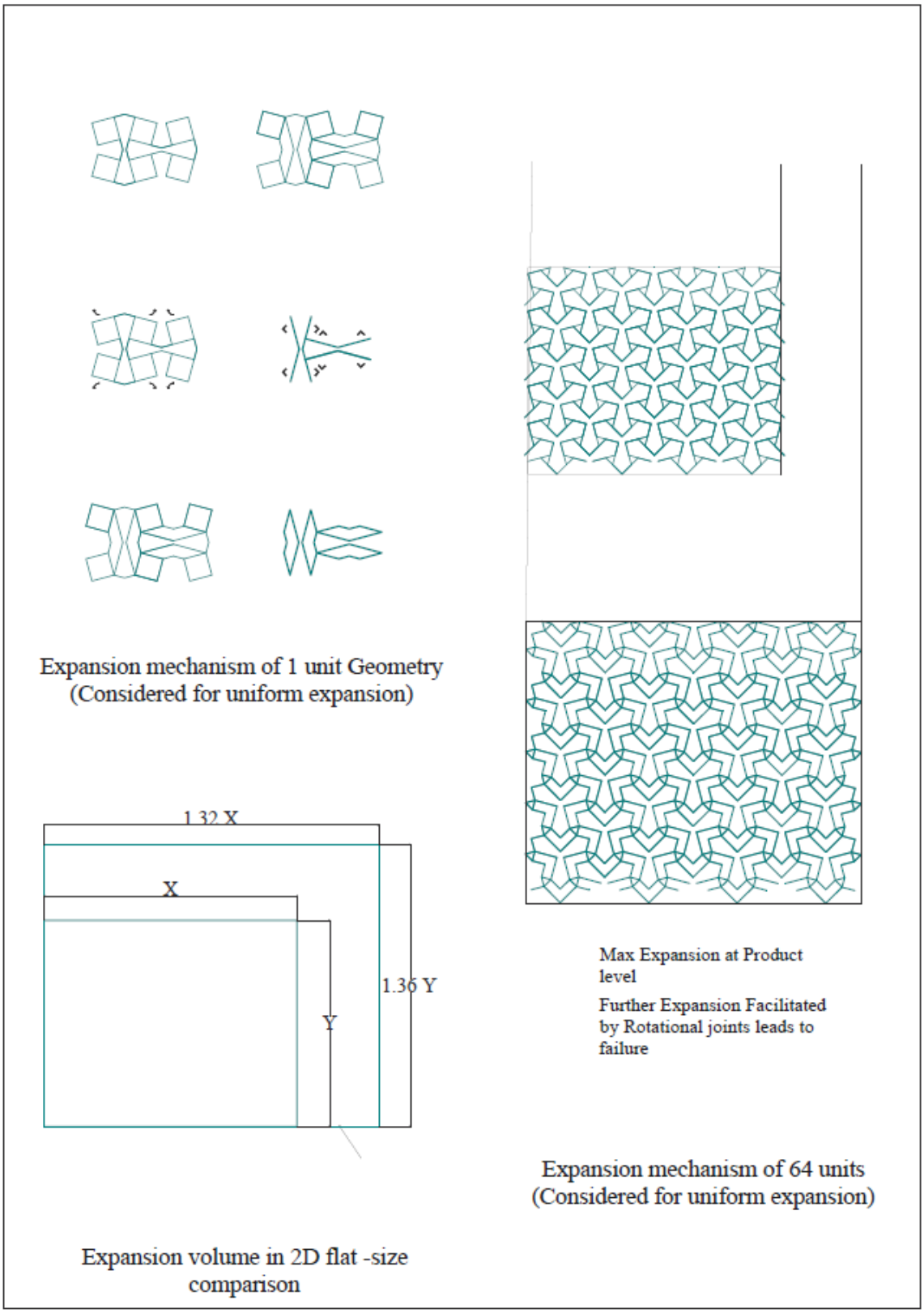

Figure 6.7-28 Analysis of Bilateral Rotating triangle Auxetic

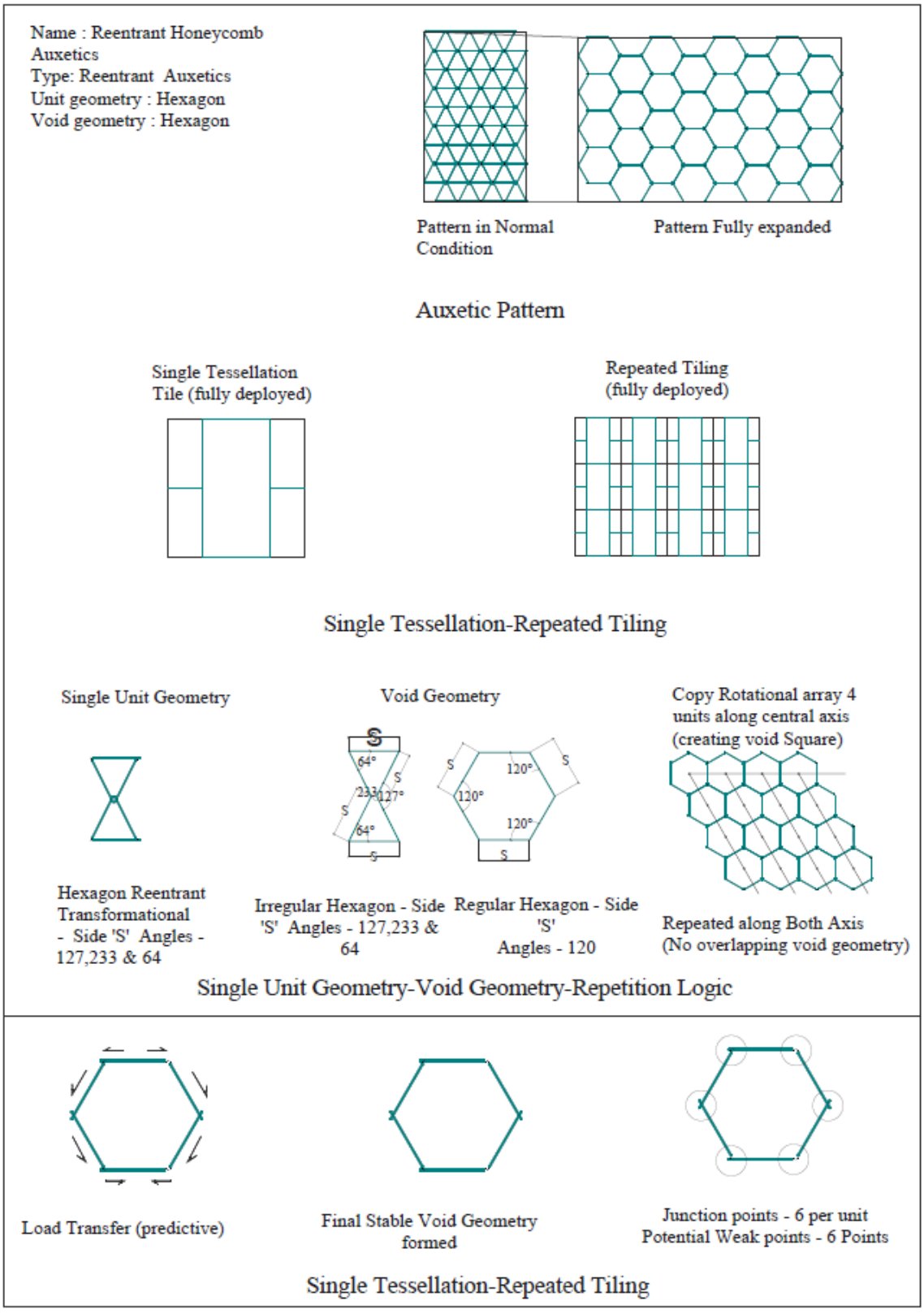

Figure 6.7-29 Analysis of Reentrant honeycomb Auxetic

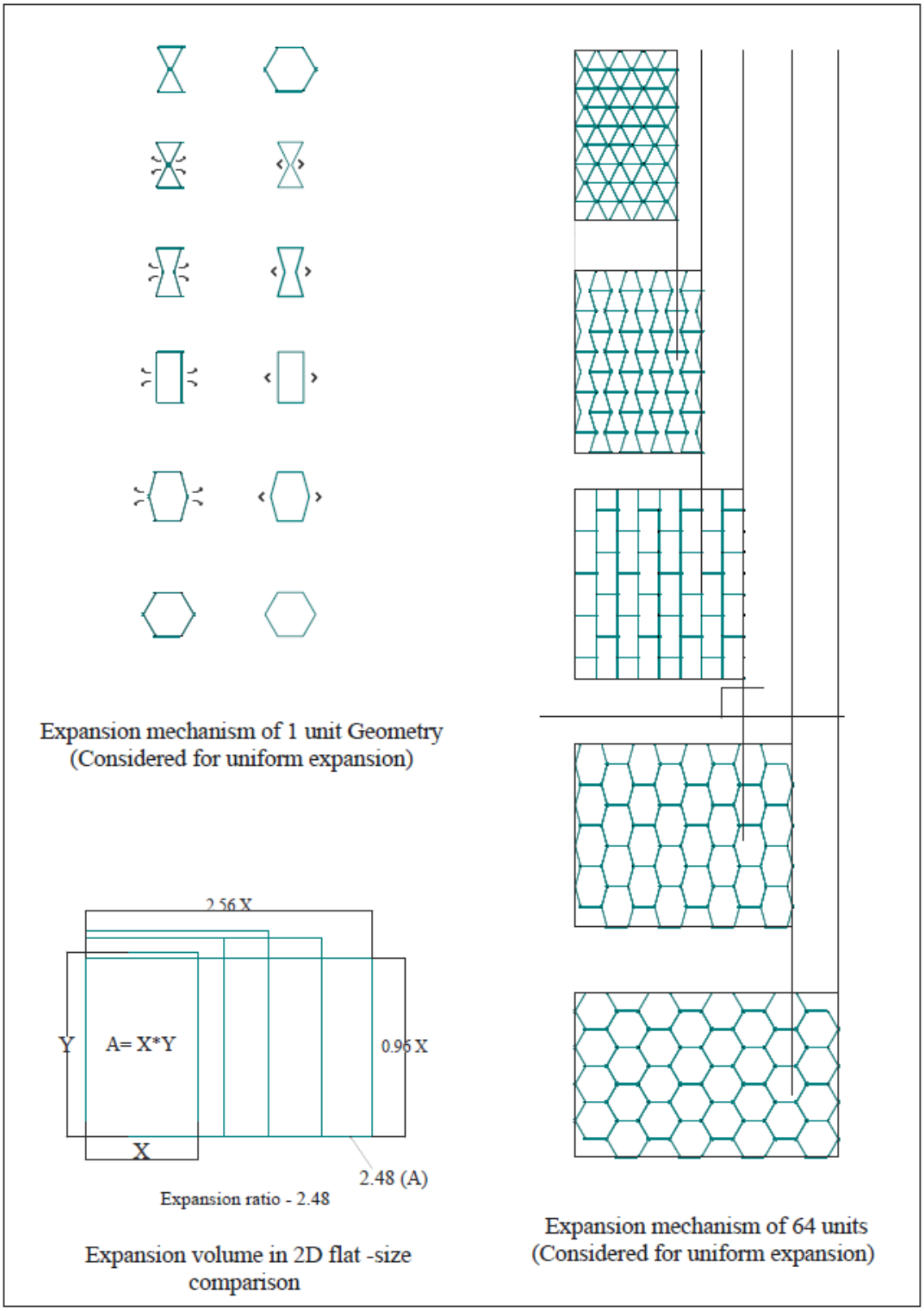

Figure 6.7-30 Analysis of Reentrant honeycomb Auxetic

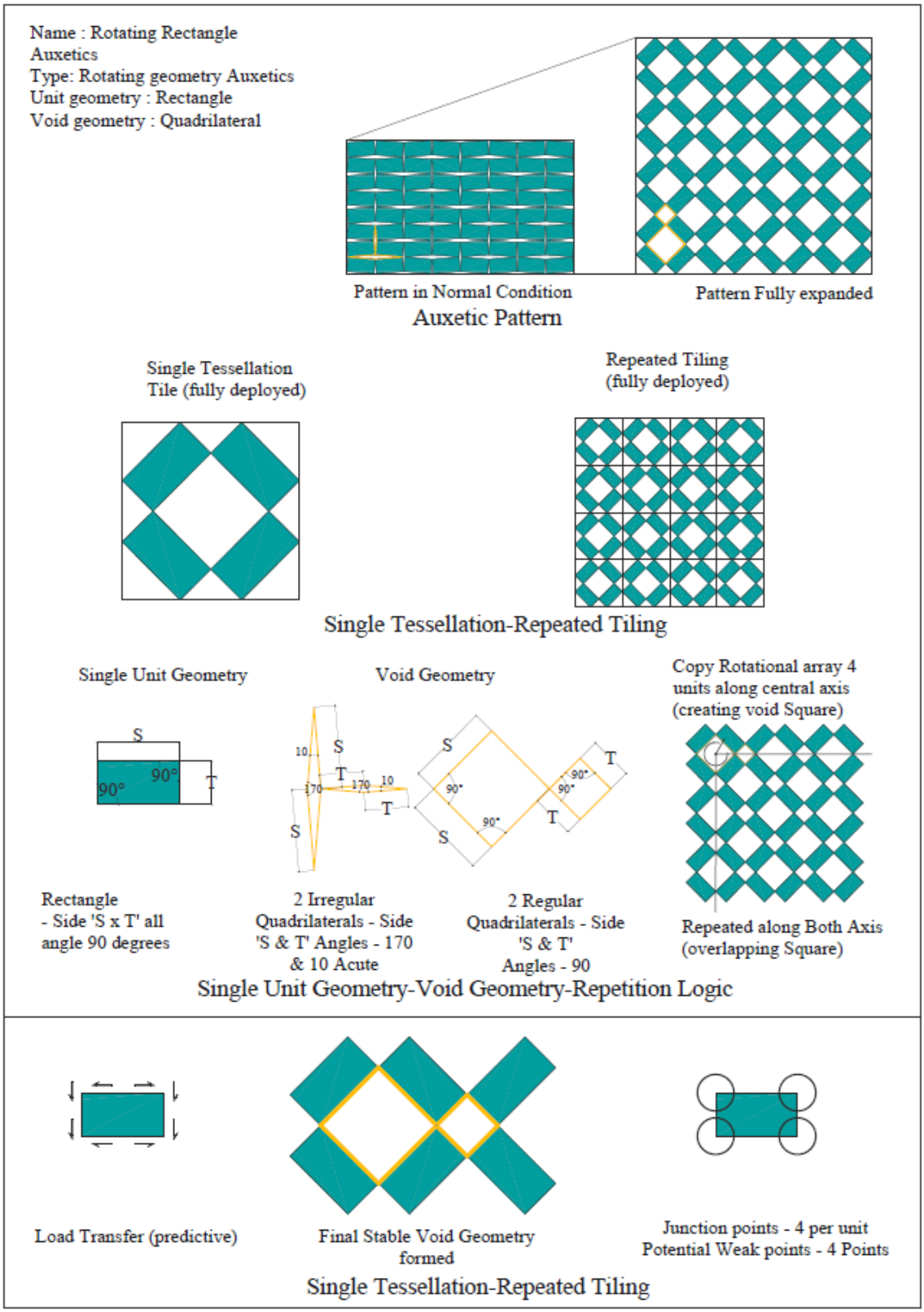

Figure 6.7-31 Analysis of Rotating Rectangle Auxetics

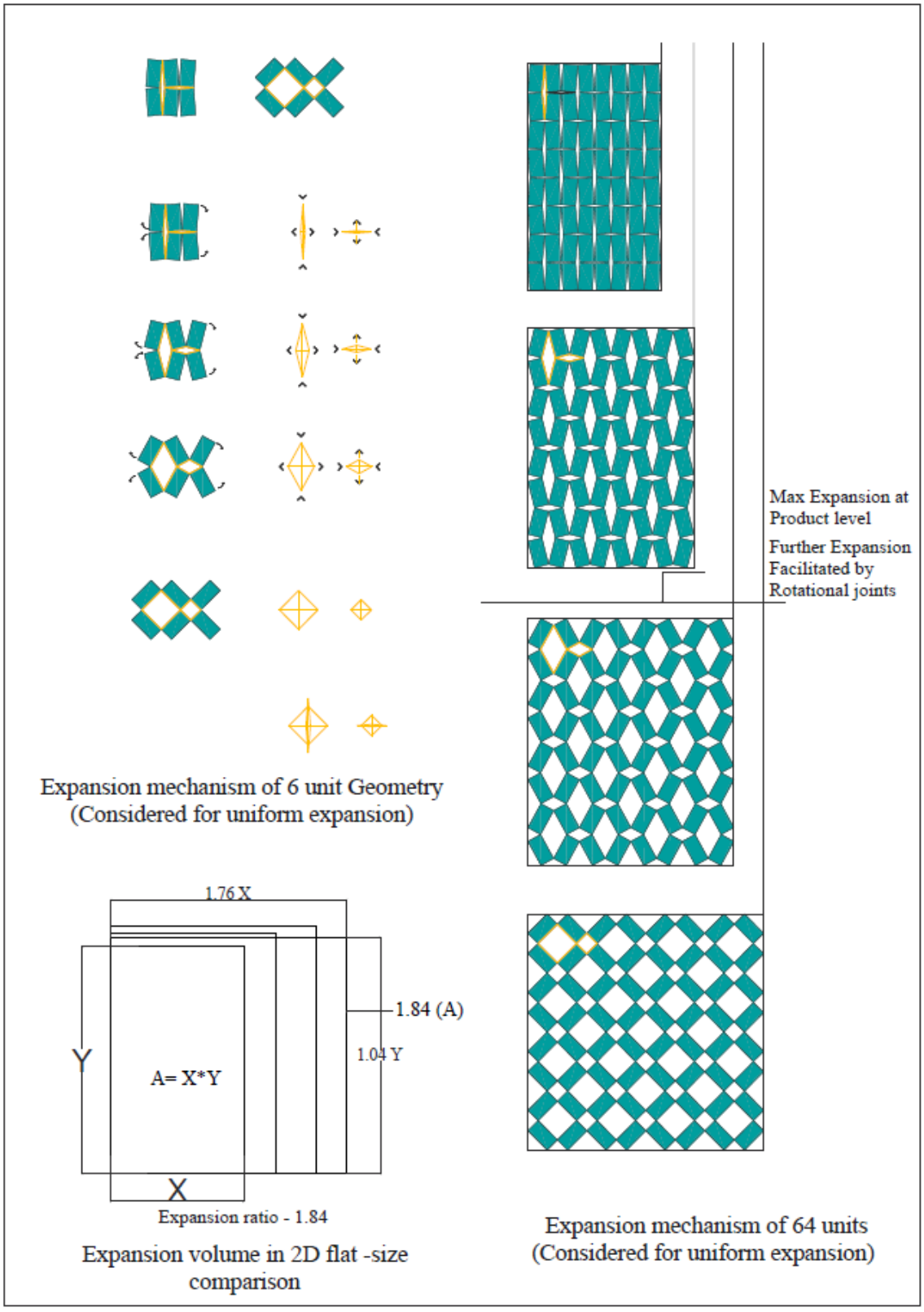

Figure 6.7-32 Auxetic Analysis of Rotating Rectangle auxetics

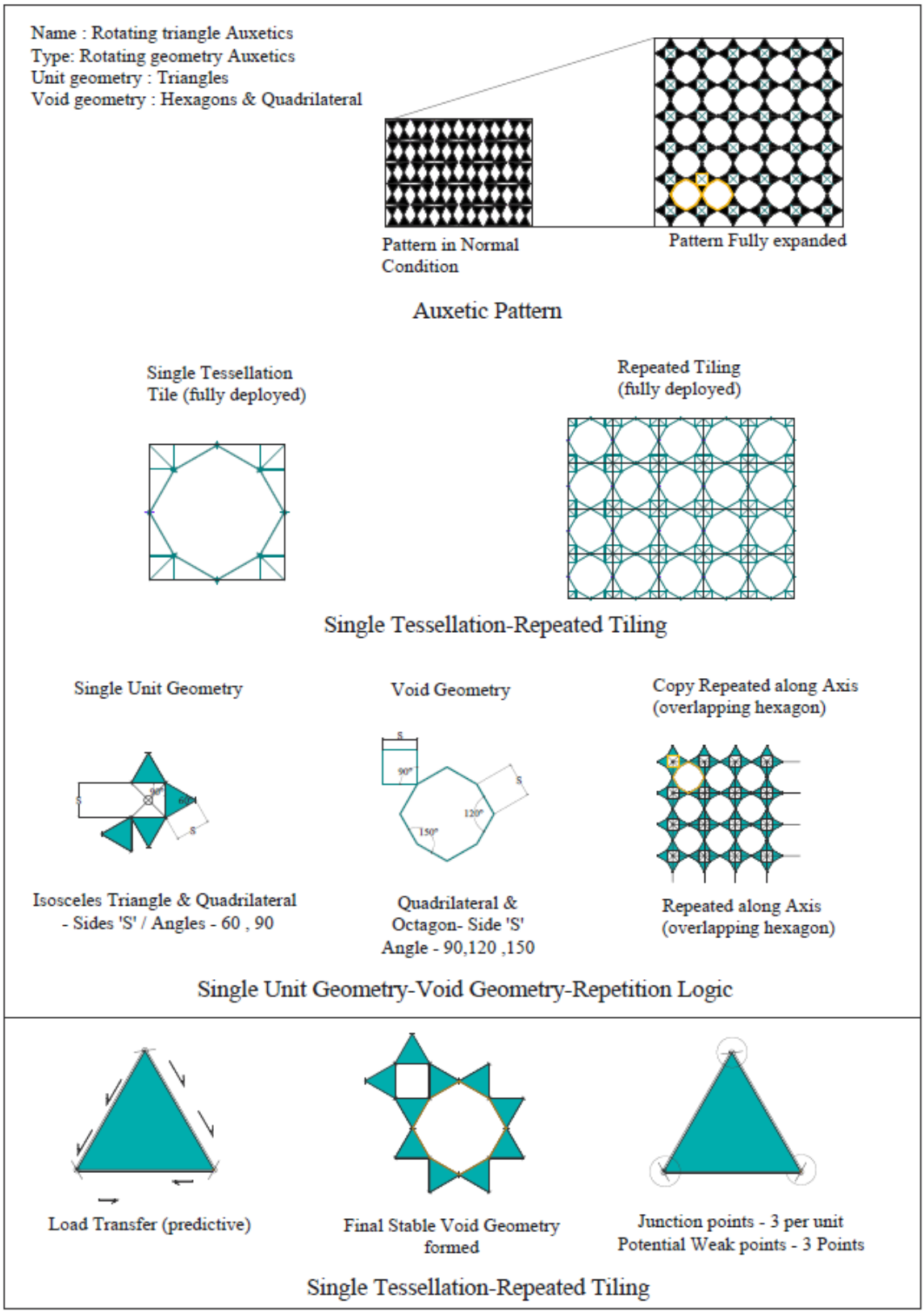

Figure 6.7-33 Auxetic Analysis of Rotating triangle auxetics

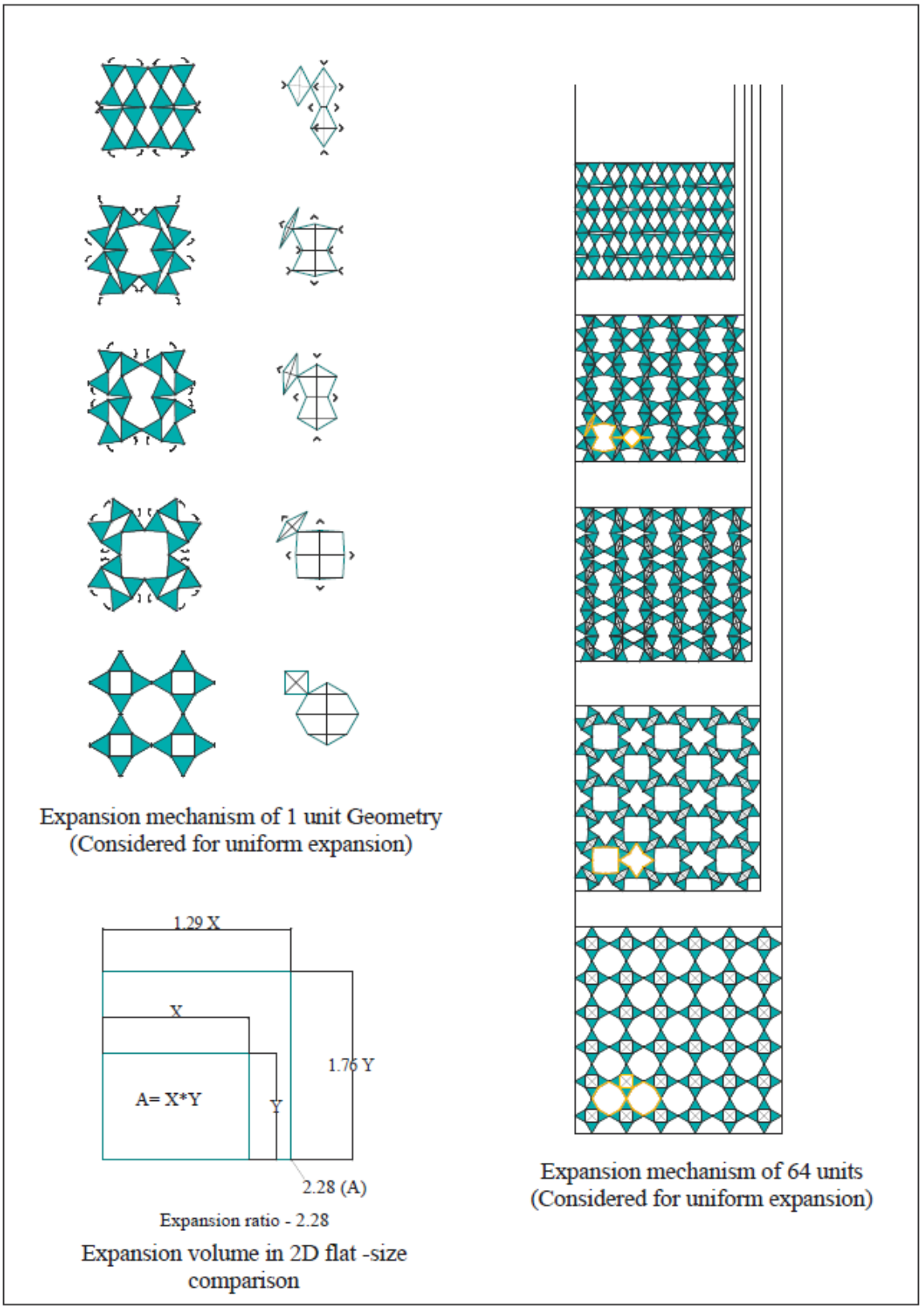

Figure 6.7-34 Auxetic Analysis of Rotating triangle auxetics

6.7.4 Appendix D : Laser-Cut PET Prototypes of Each Geometry

6.7.4.1 Tristar – Rotating Triangle

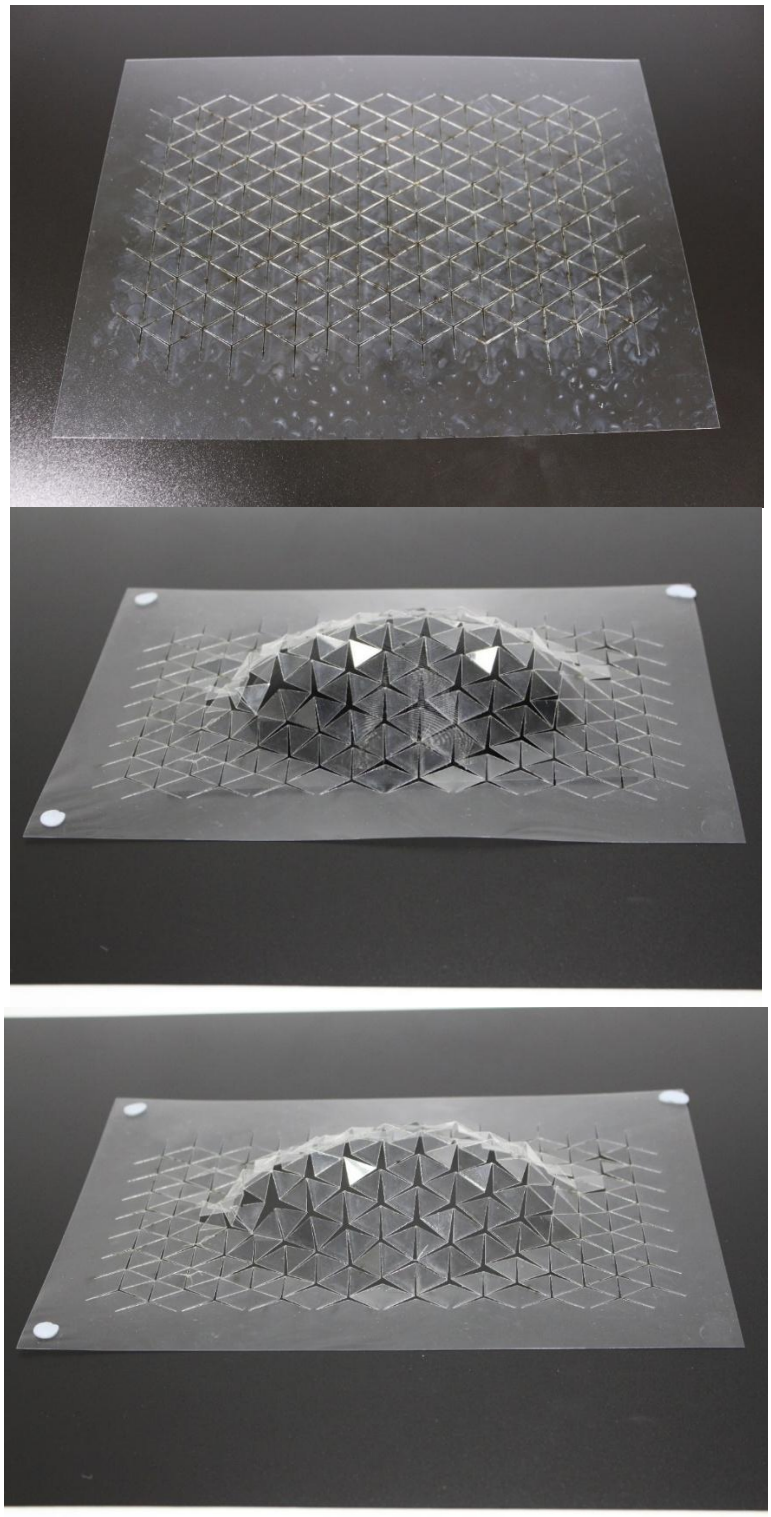

Figure 6.7-35 PETG- Lasercut trial of Tristar Auxetic on Ellipsoid Dome Flat lasercut , laid on dome , dome removed

6.7.4.2 Rotating rectangles

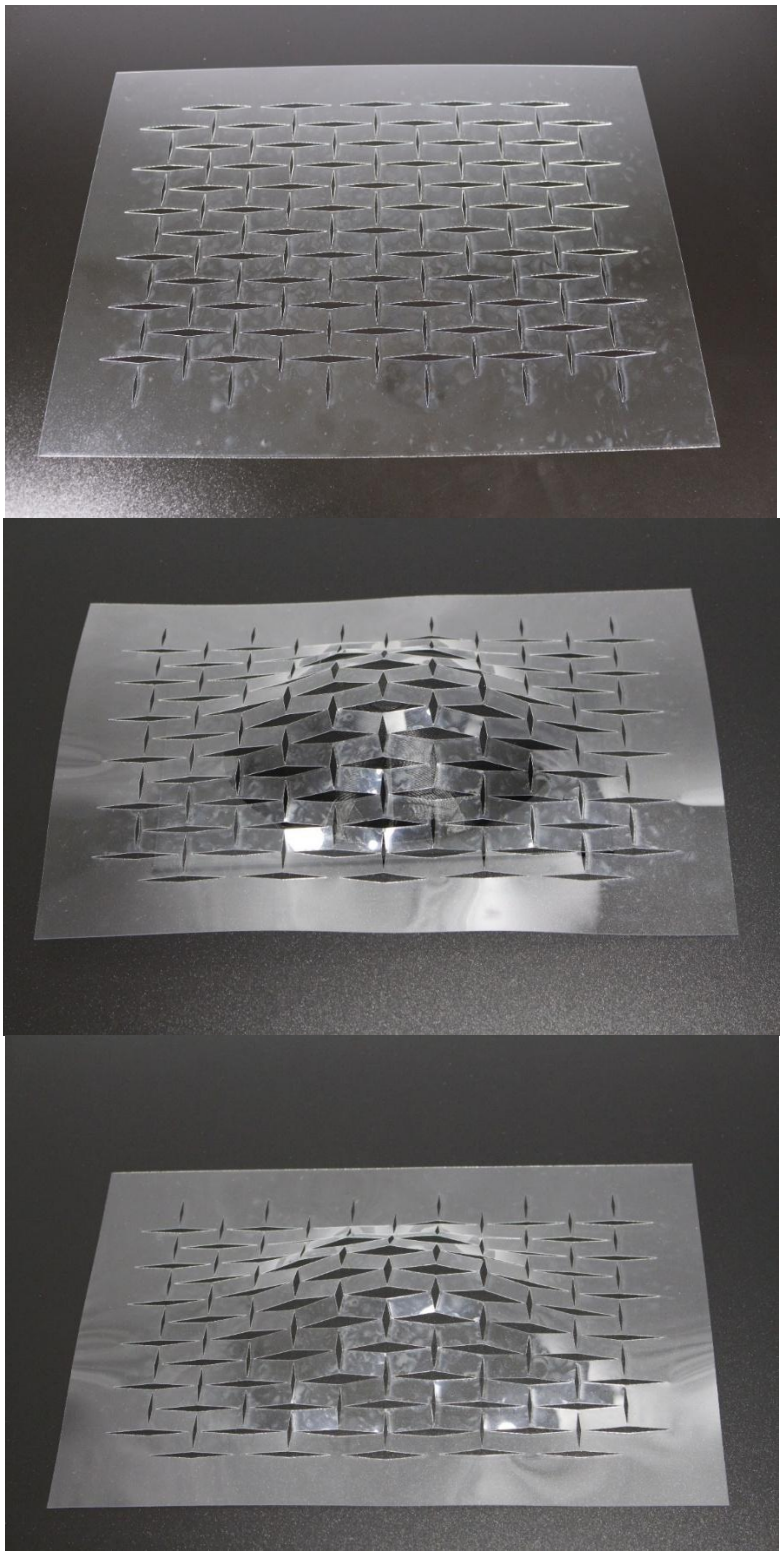

Figure 6.7-36 PETG- Lasercut trial of Rotating rectangle Auxetic on Ellipsoid Dome Flat lasercut , laid on dome , dome removed

6.7.4.3 Bilateral Rotating Square

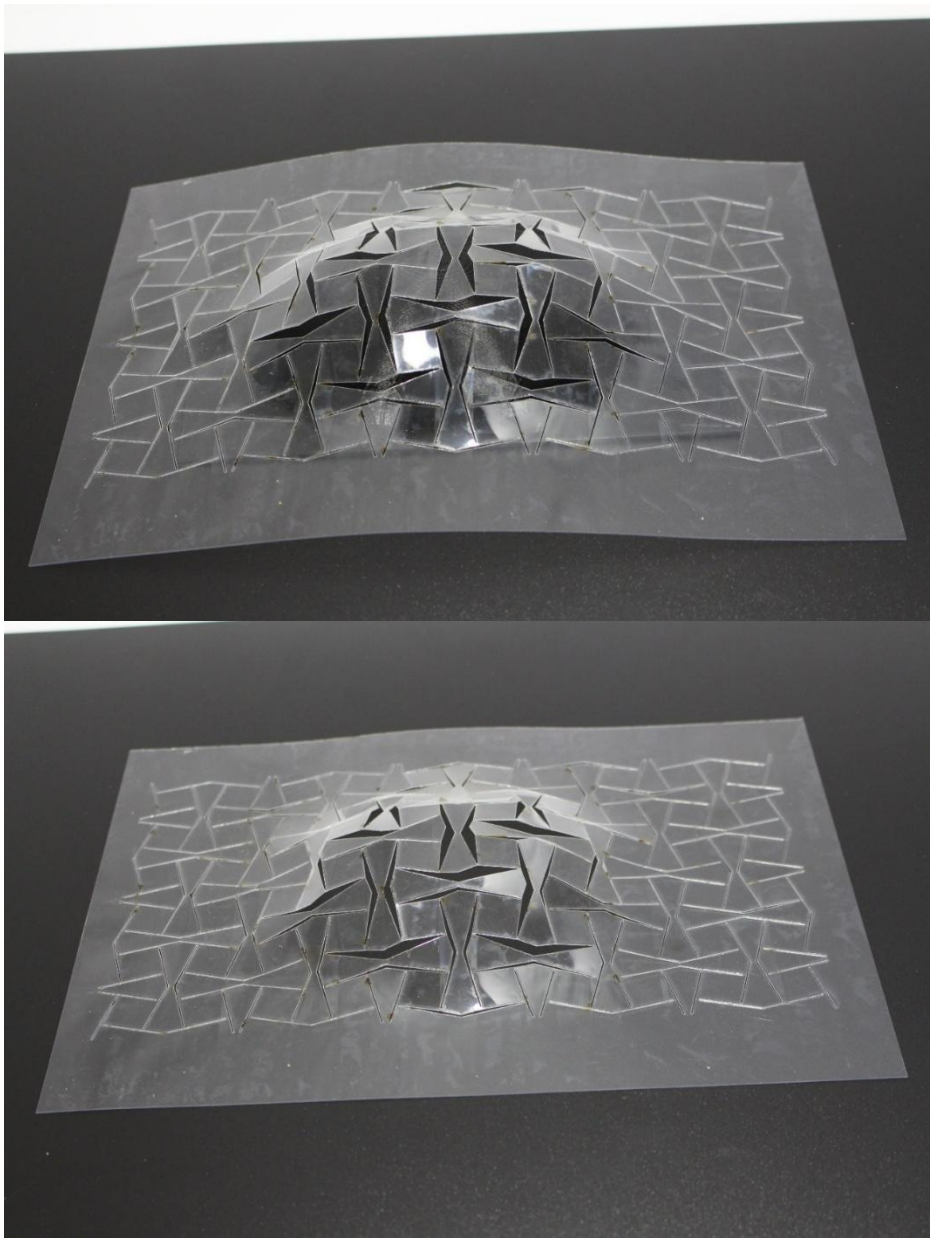

Figure 6.7-37 PETG- Lasercut trial of Rotating Square Auxetic on Ellipsoid Dome , laid on dome , dome removed

6.7.4.4 Bilateral Rotating triangle

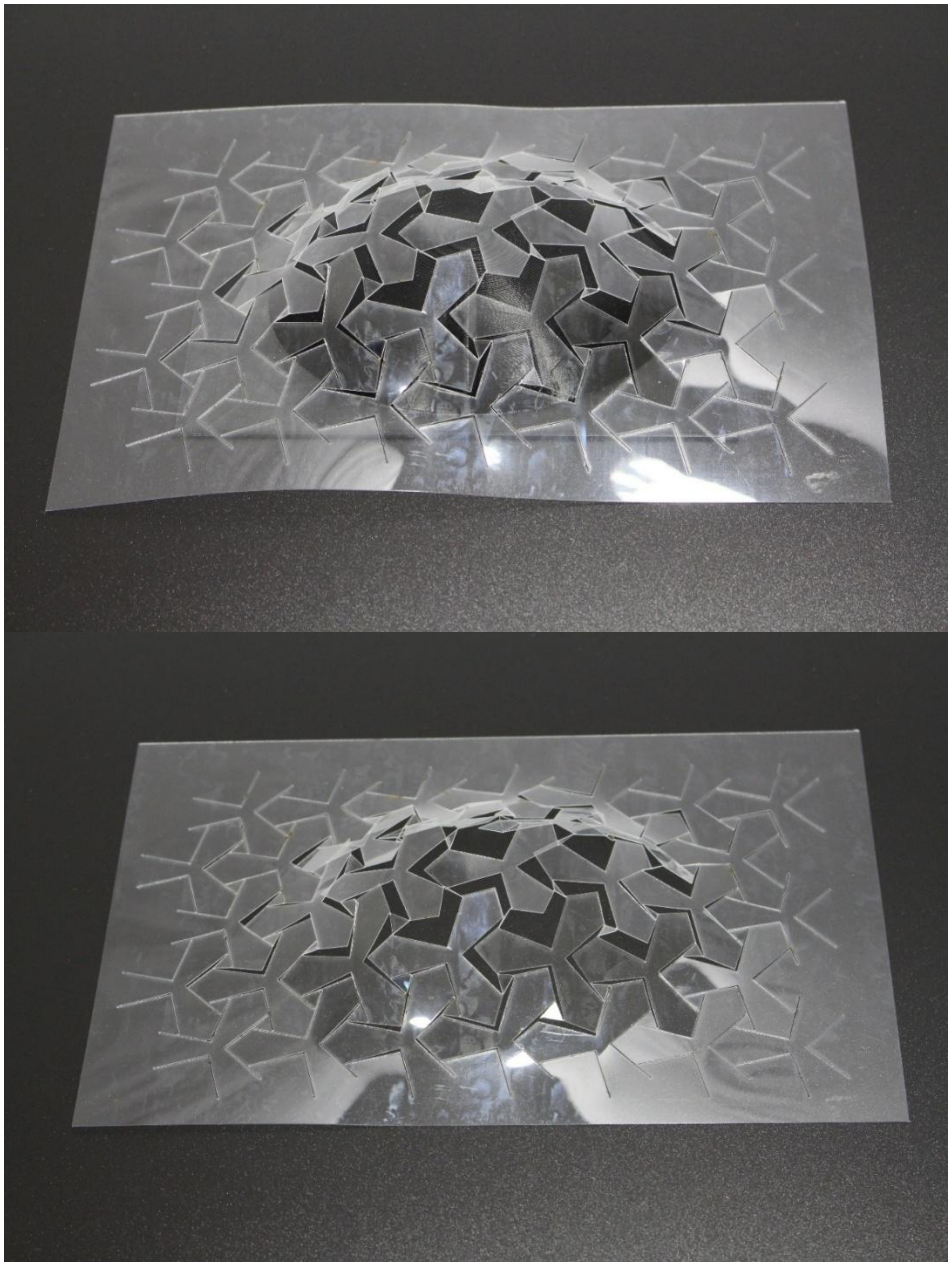

Figure 6.7-38 Lasercut trial of Rotating triangle Auxetic on Ellipsoid Dome , laid on dome , dome removed

6.7.4.5 Rotating Triangle 2

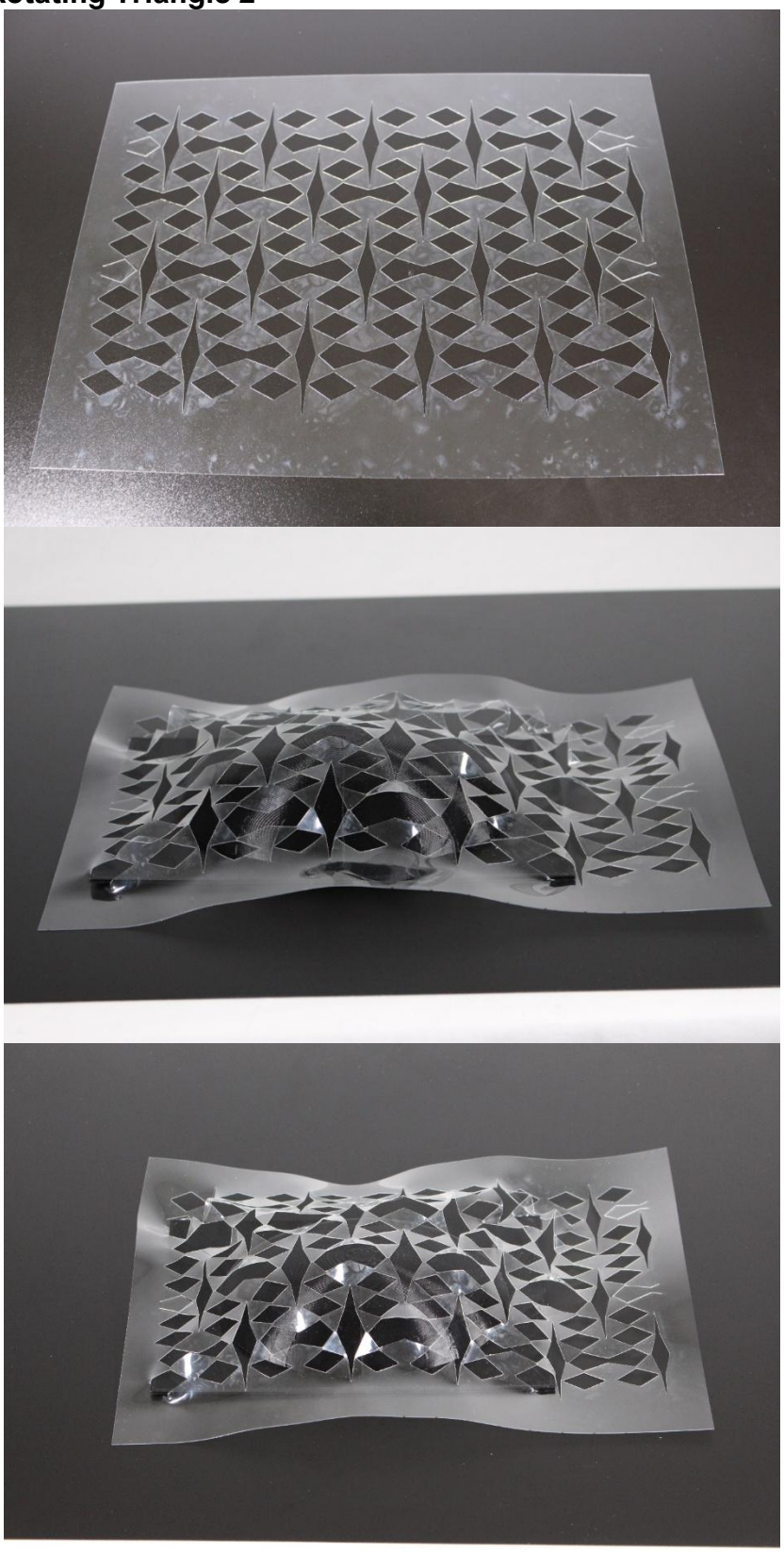

Figure 6.7-39 Lasercut trial of Rotating triangle Auxetic on Ellipsoid Dome , laid on dome , dome removed

6.7.5 Appendix E : Testing of Tristar laser cuts in PETG on 3D printed forms

The Following is the documentation of Tristar laser cut on PETG laid on 3d forms

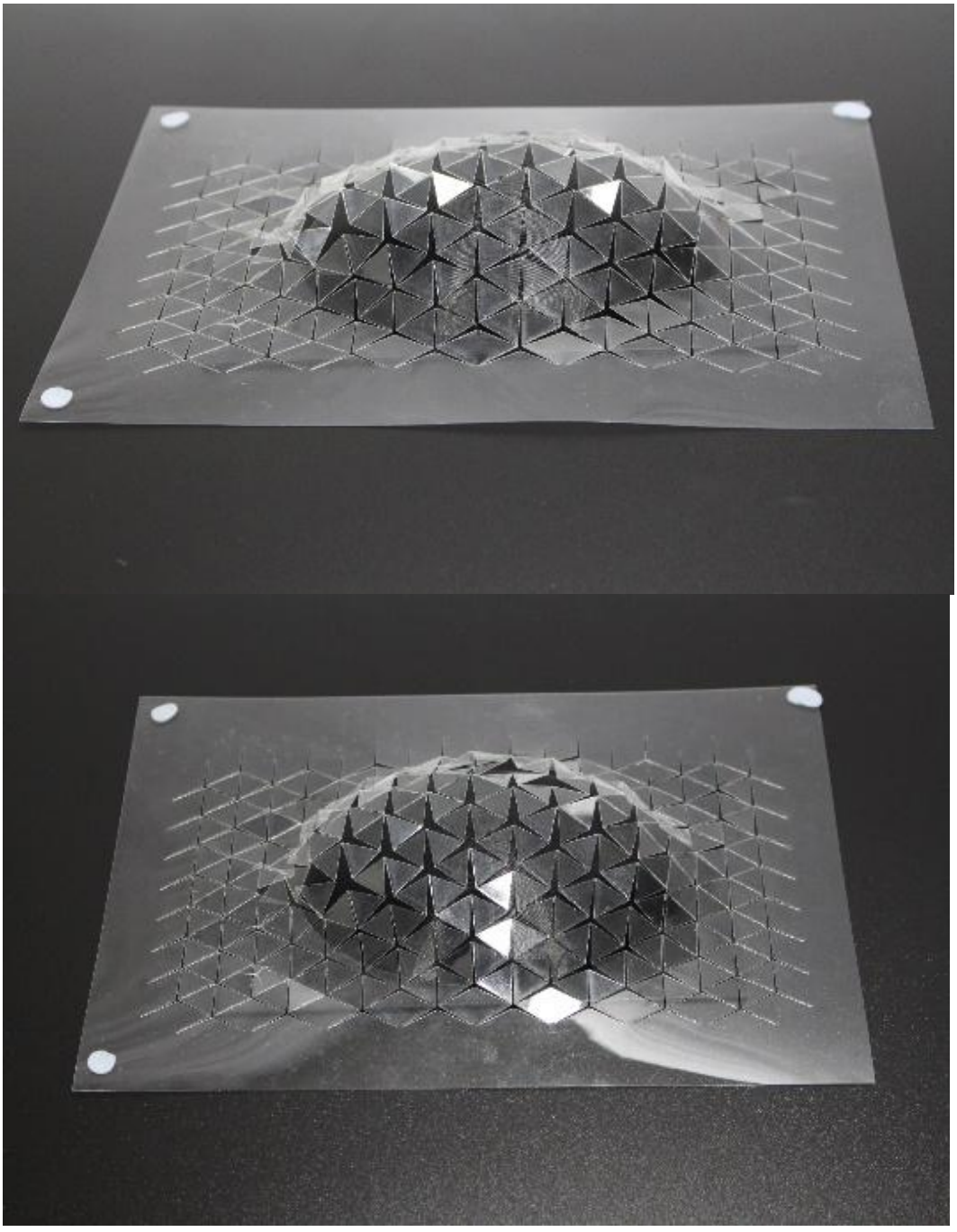

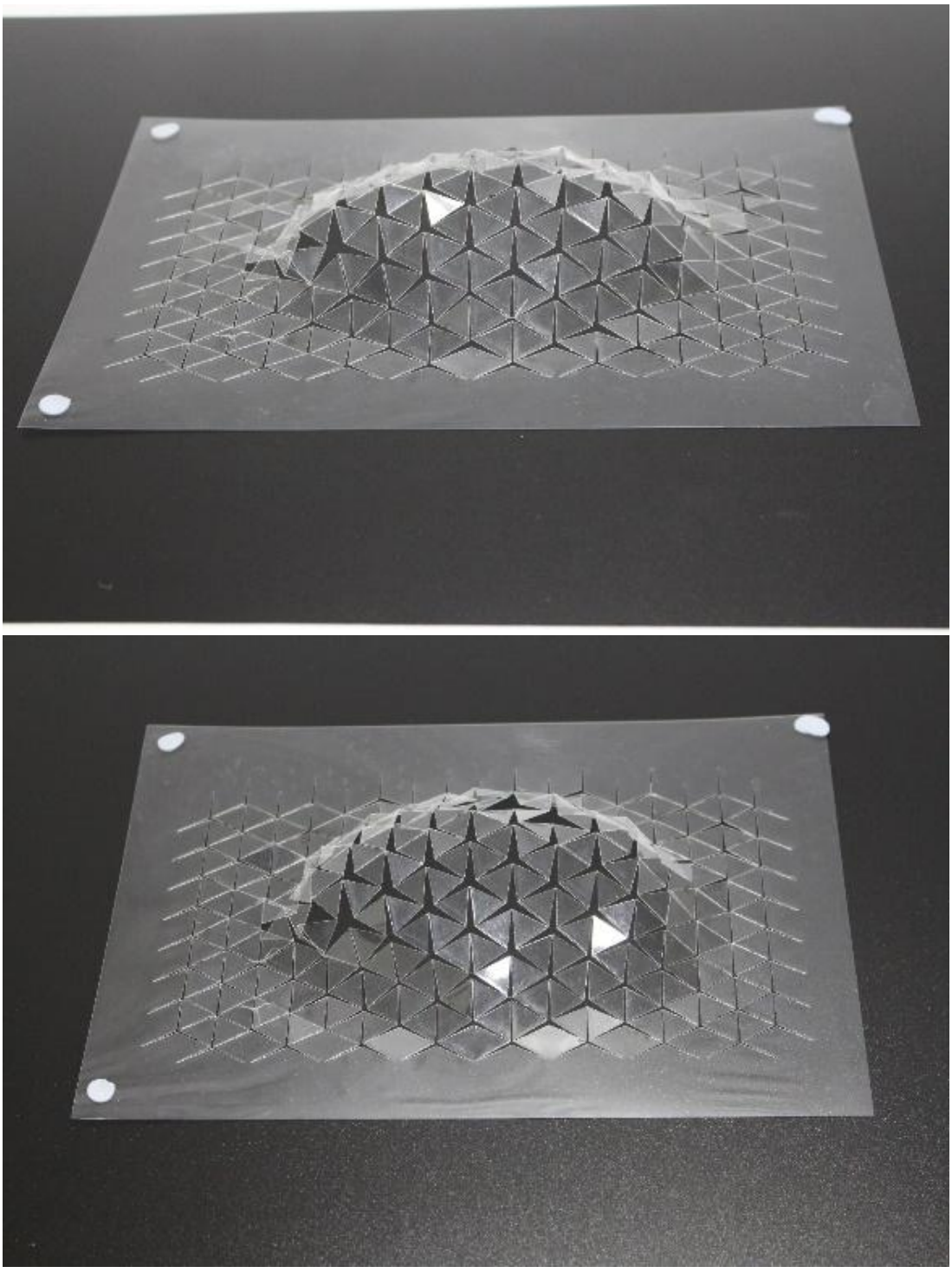

Figure 6.7-40 Tristar PETG on Ellipsoid Dome - – laid on Form and free standing

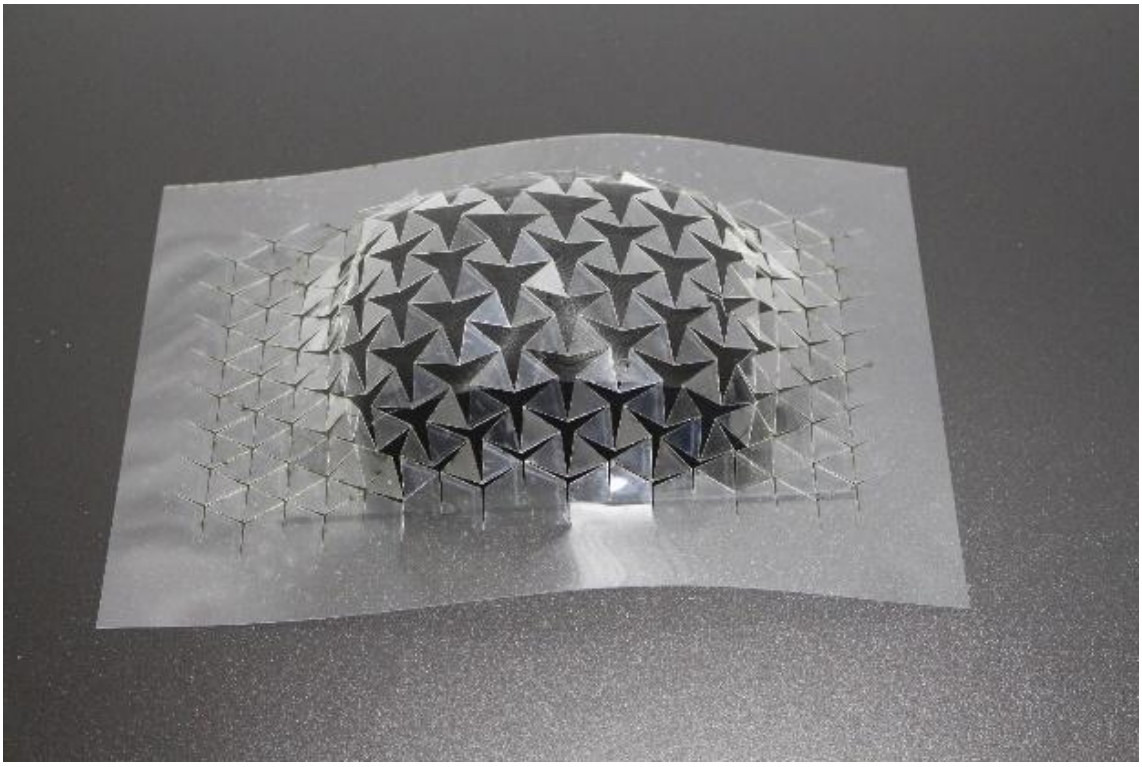

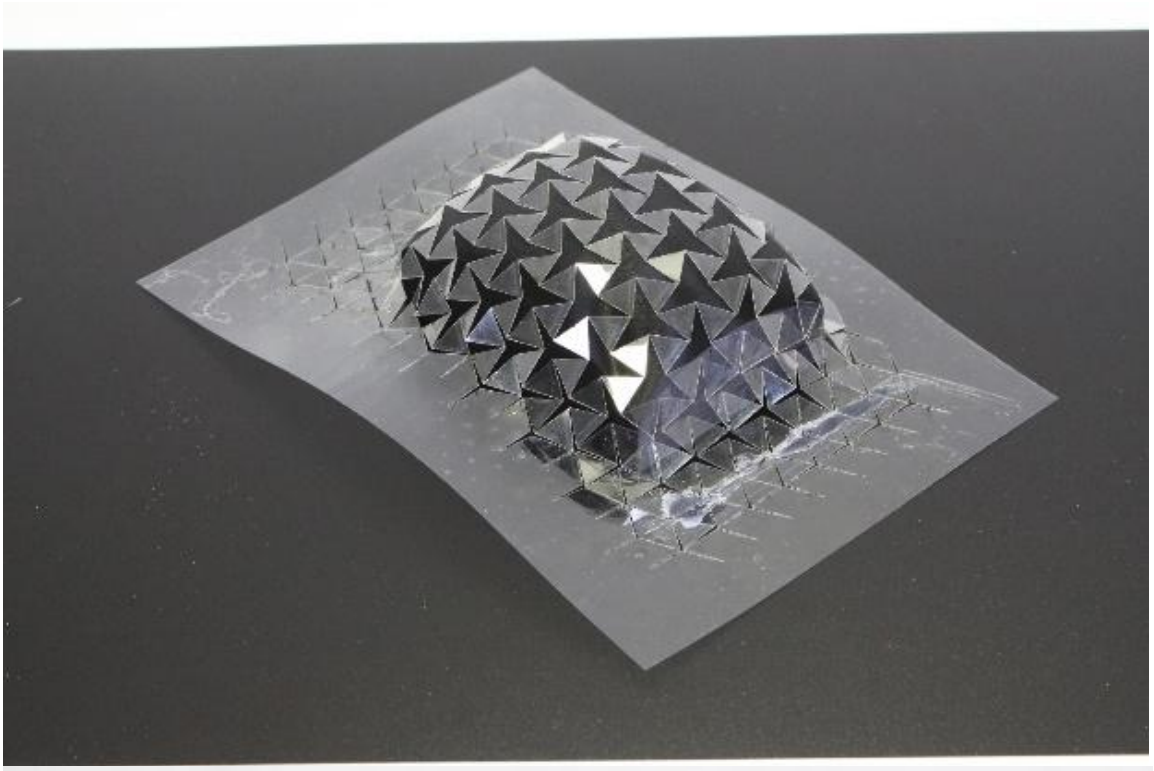

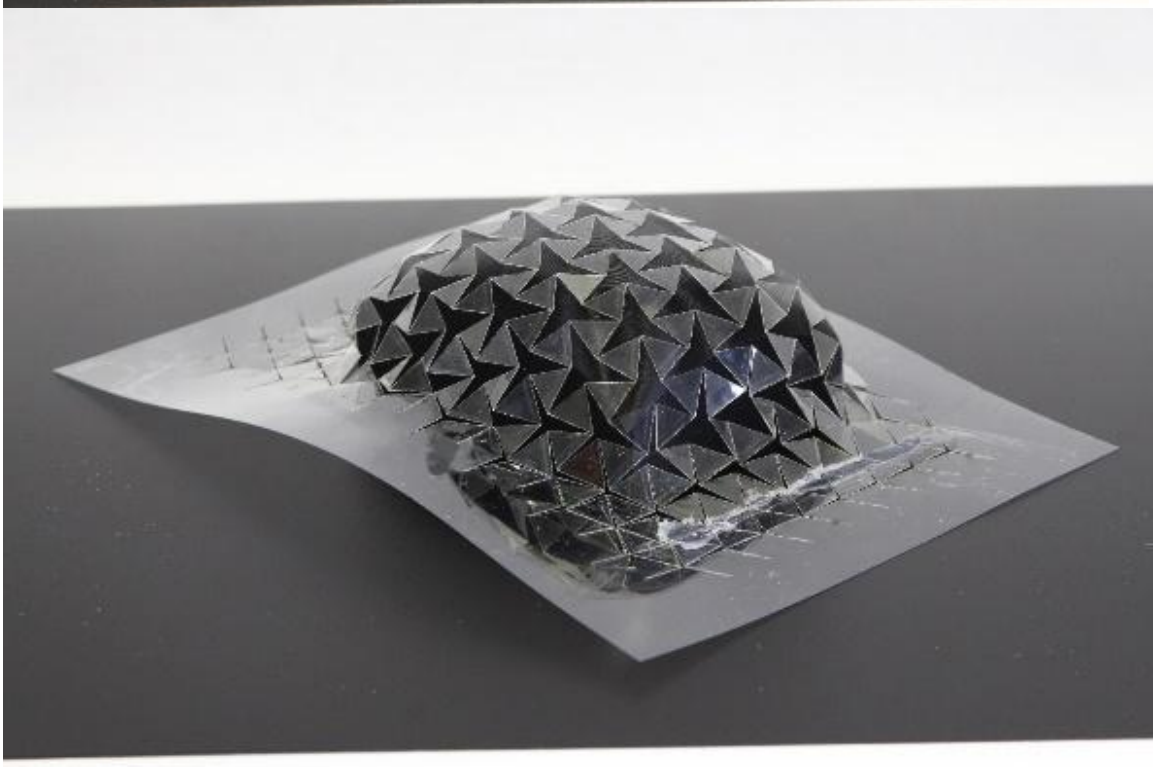

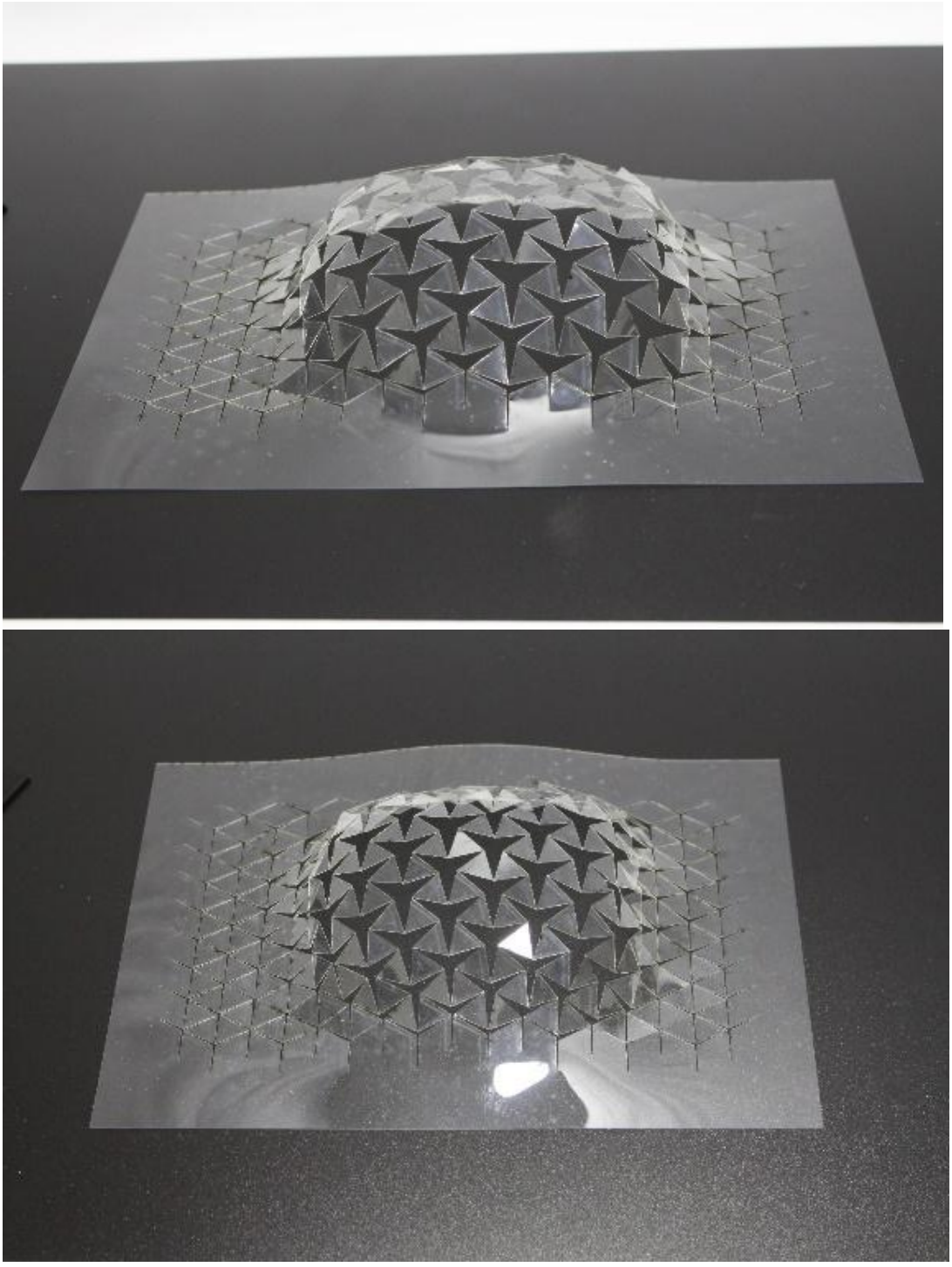

Figure 6.7-41 Tristar PETG on parabolic paraboloid – laid on Form and free standing

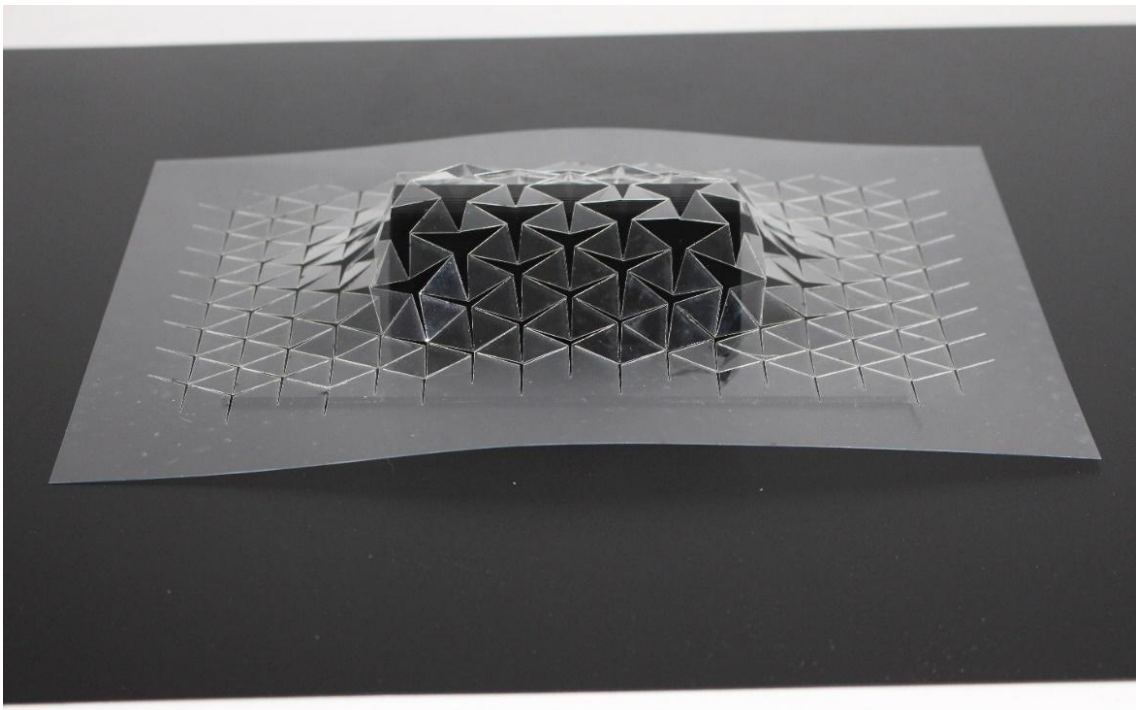

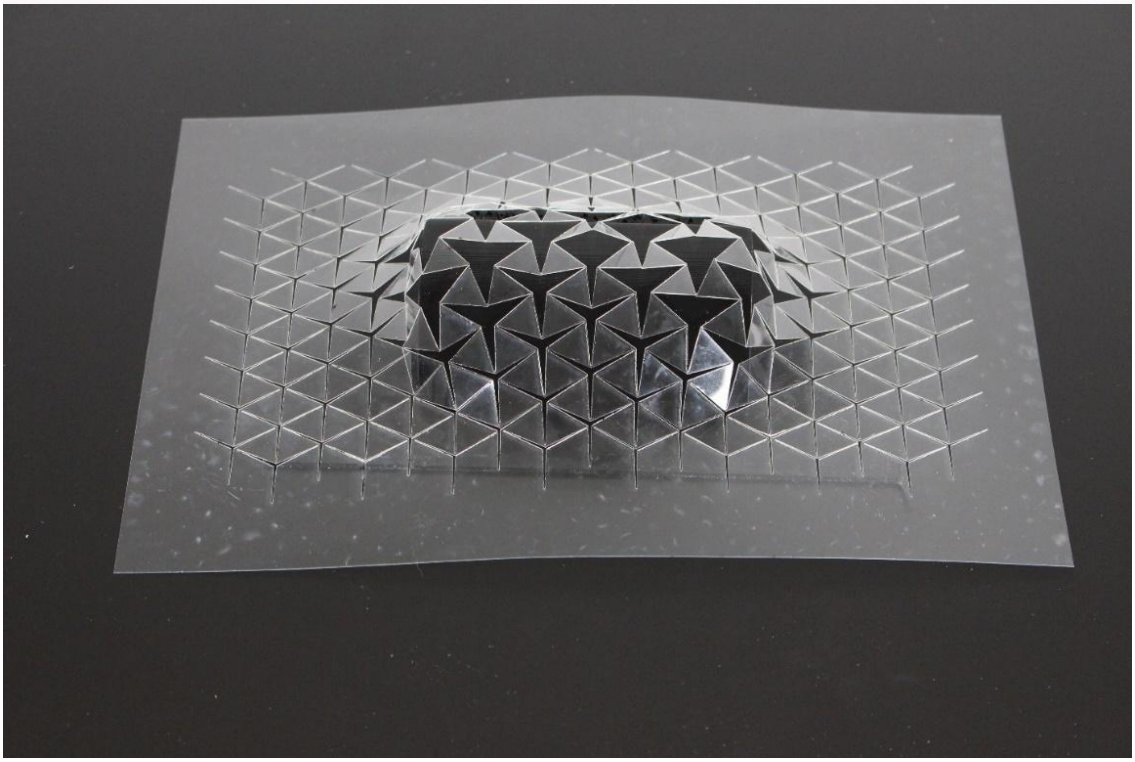

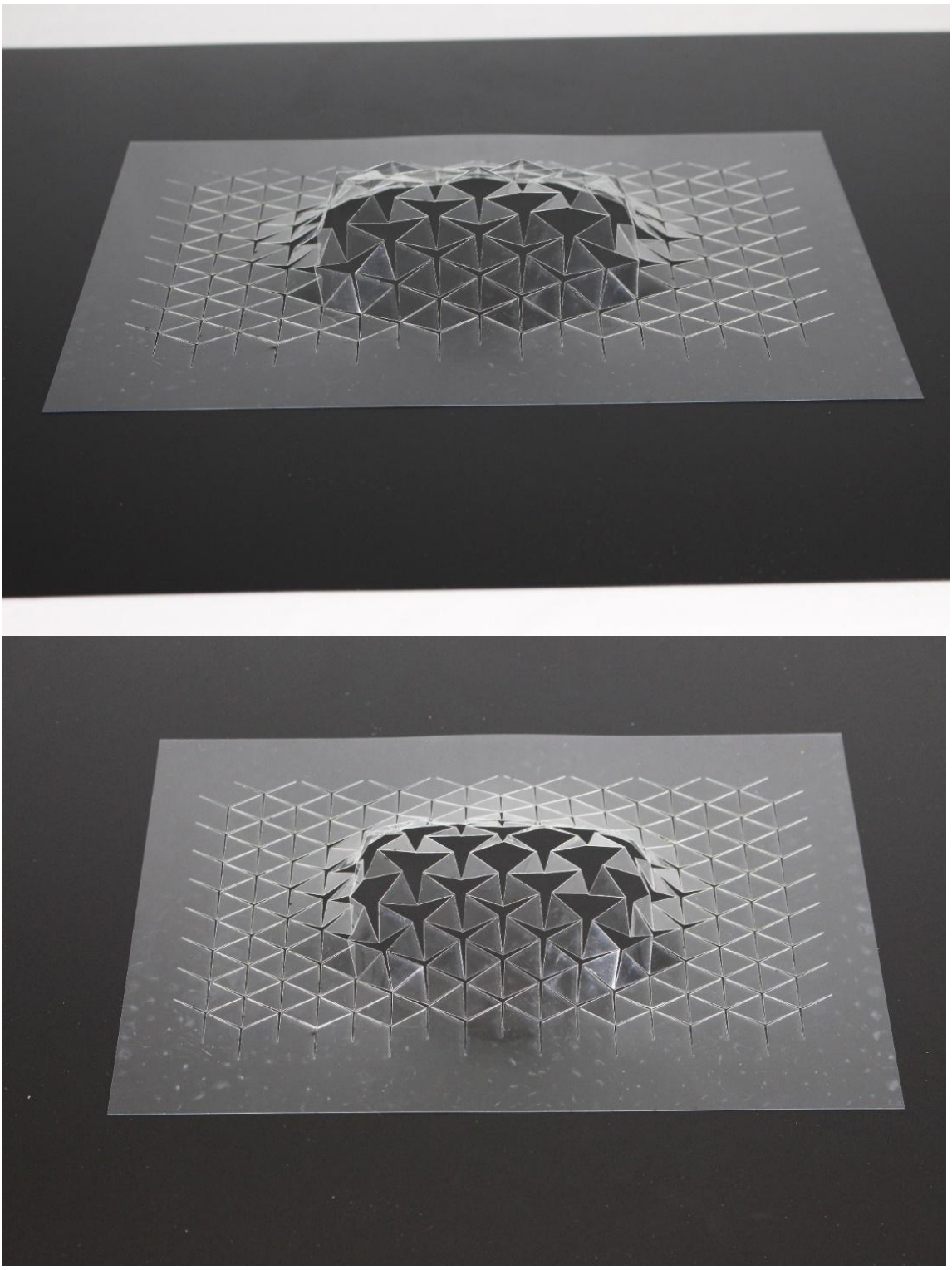

Figure 6.7-42 Tristar PETG on simple Vault – laid on Form and free standing

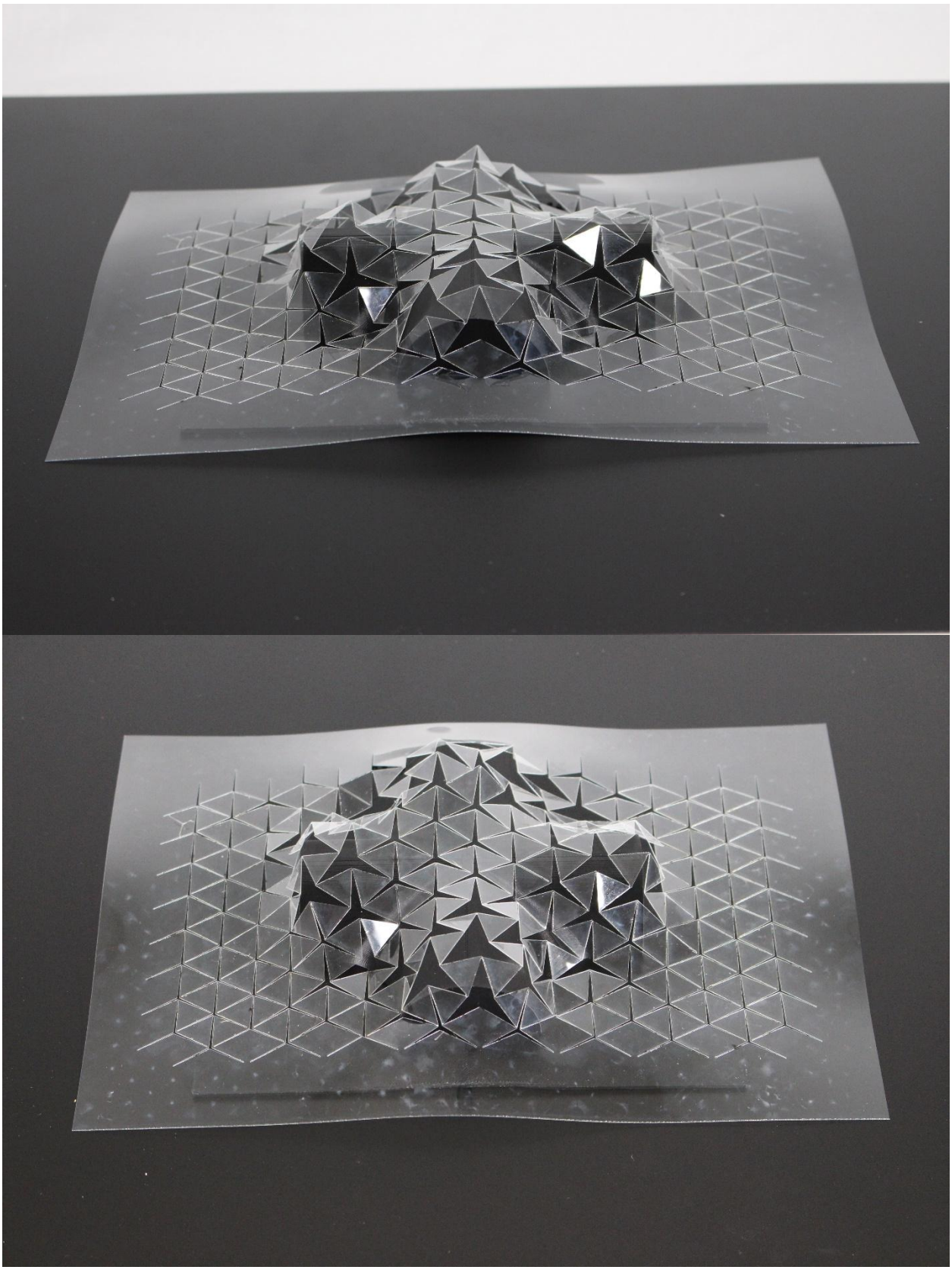

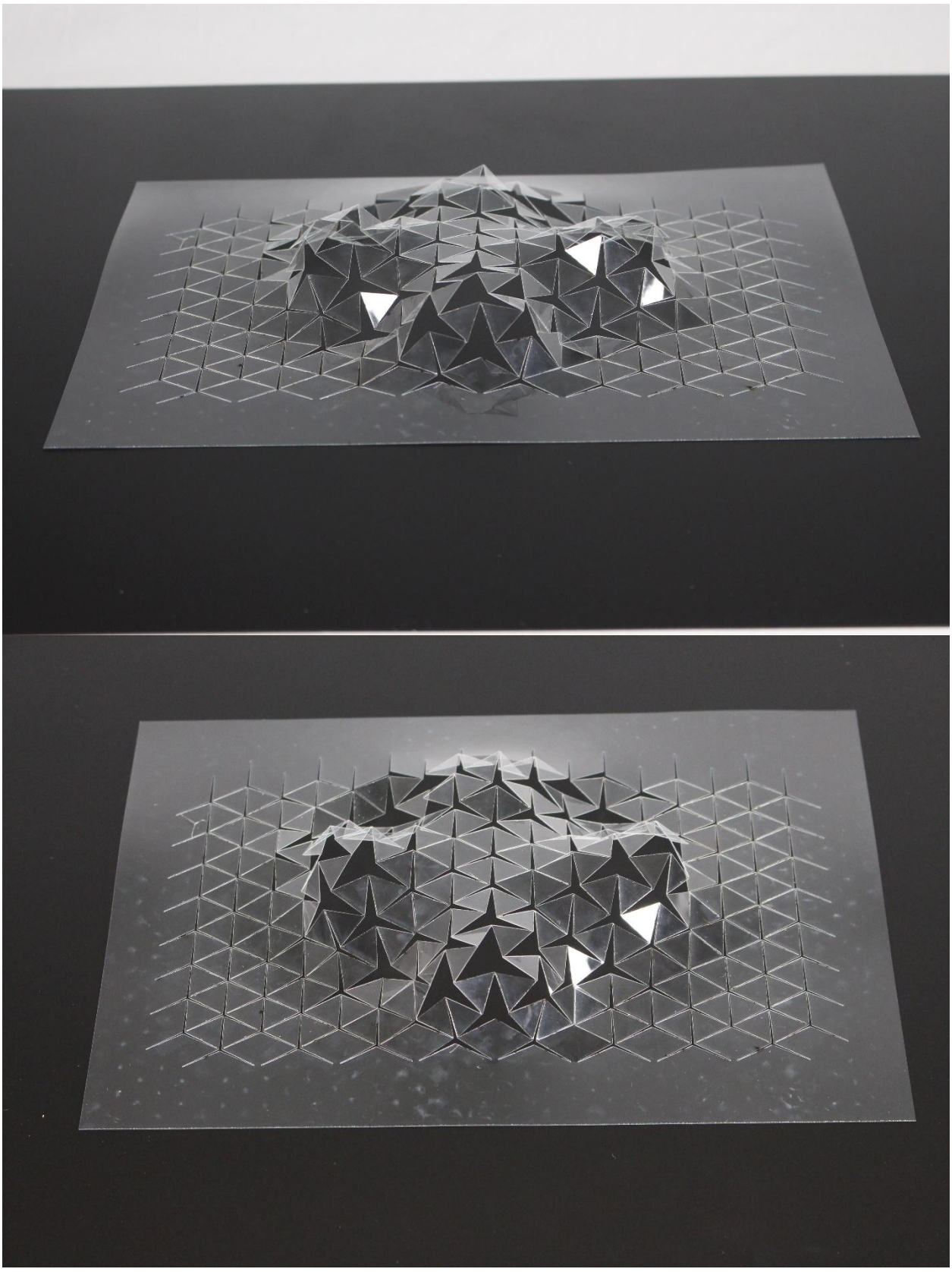

Figure 6.7-43 Tristar PETG on Double cross Vault – laid on Form and free standing

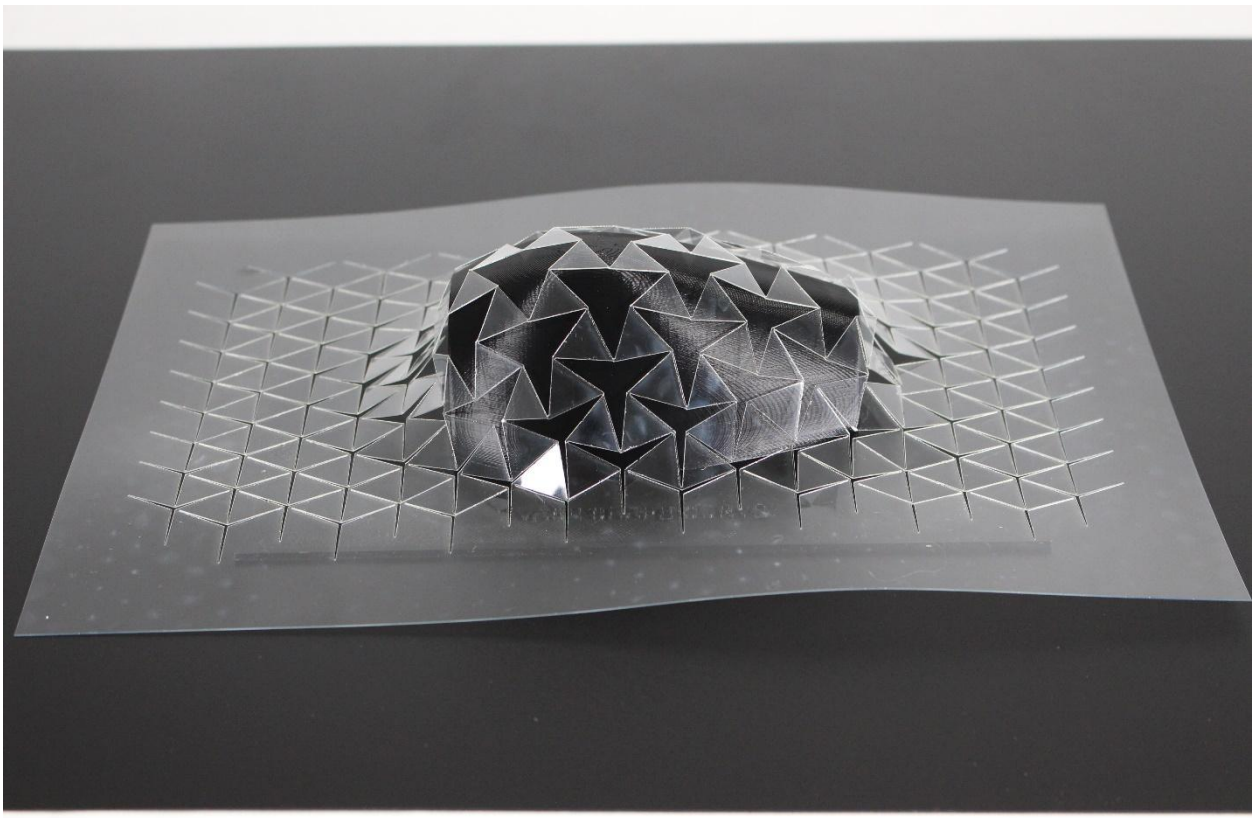

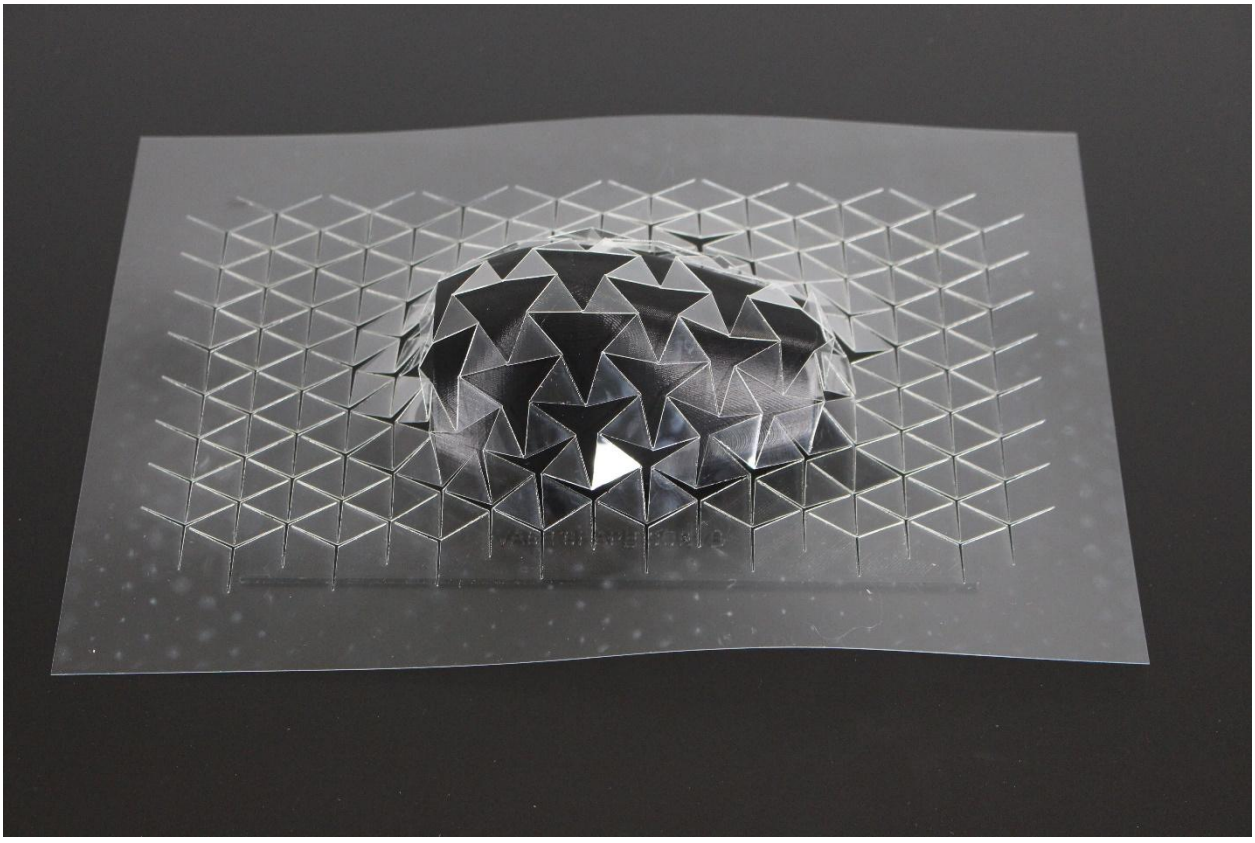

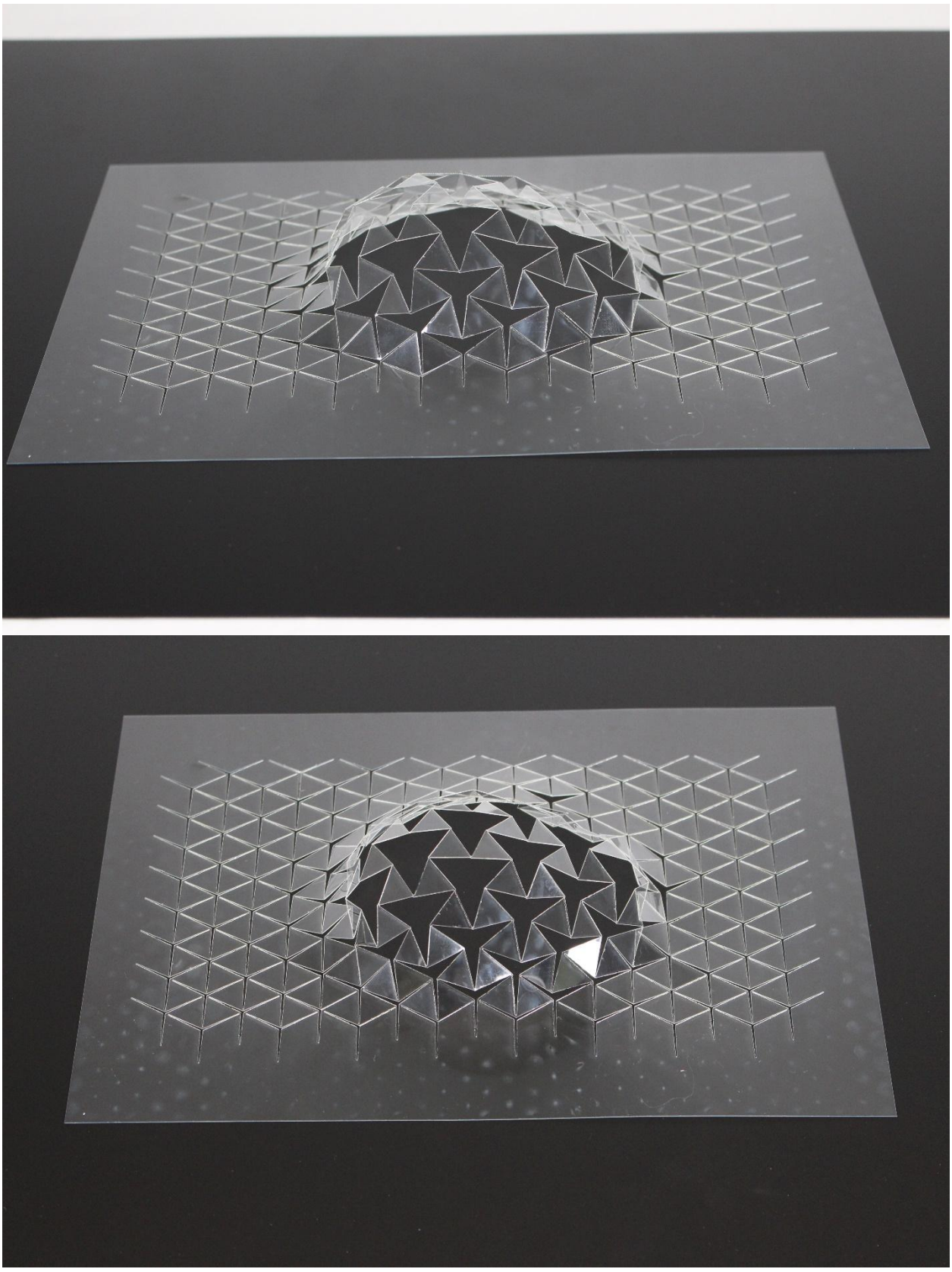

Figure 6.7-44 Tristar PETG on Simple Vase shape – laid on Form and free standing

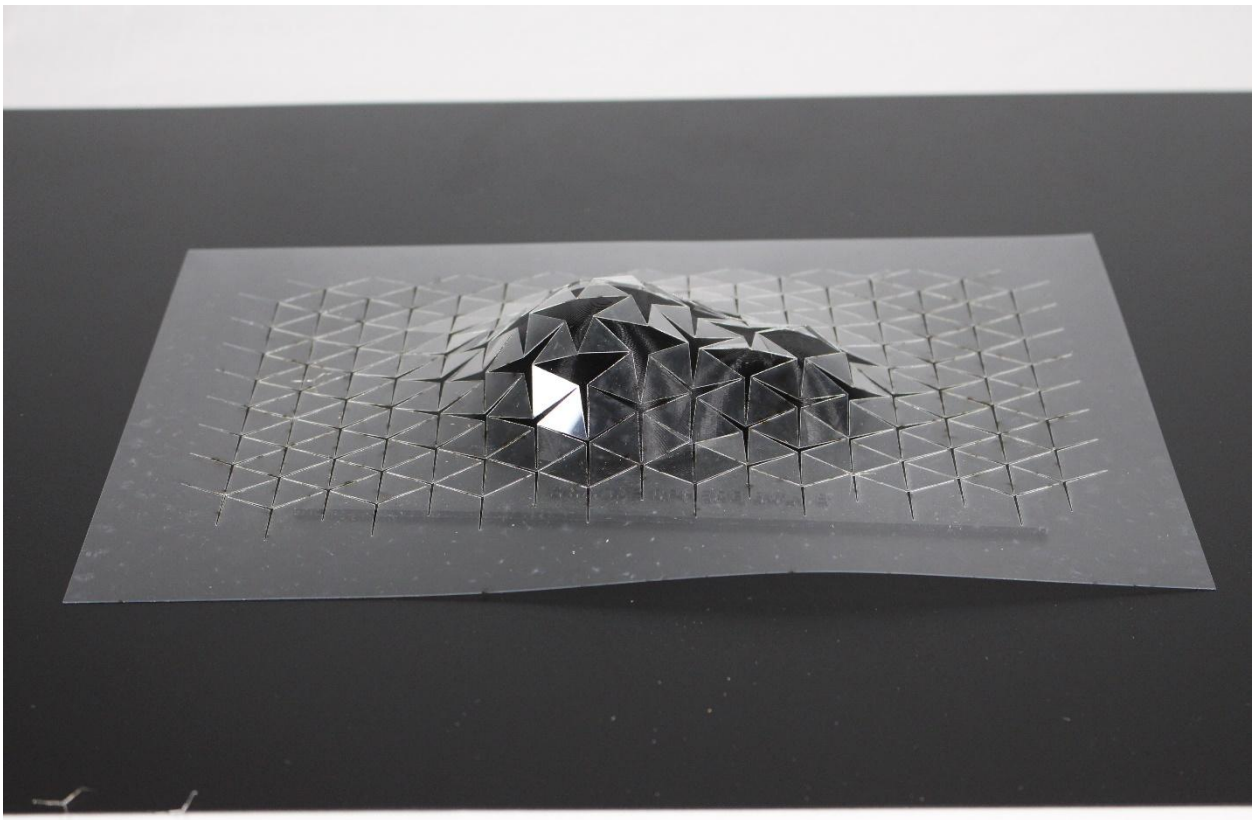

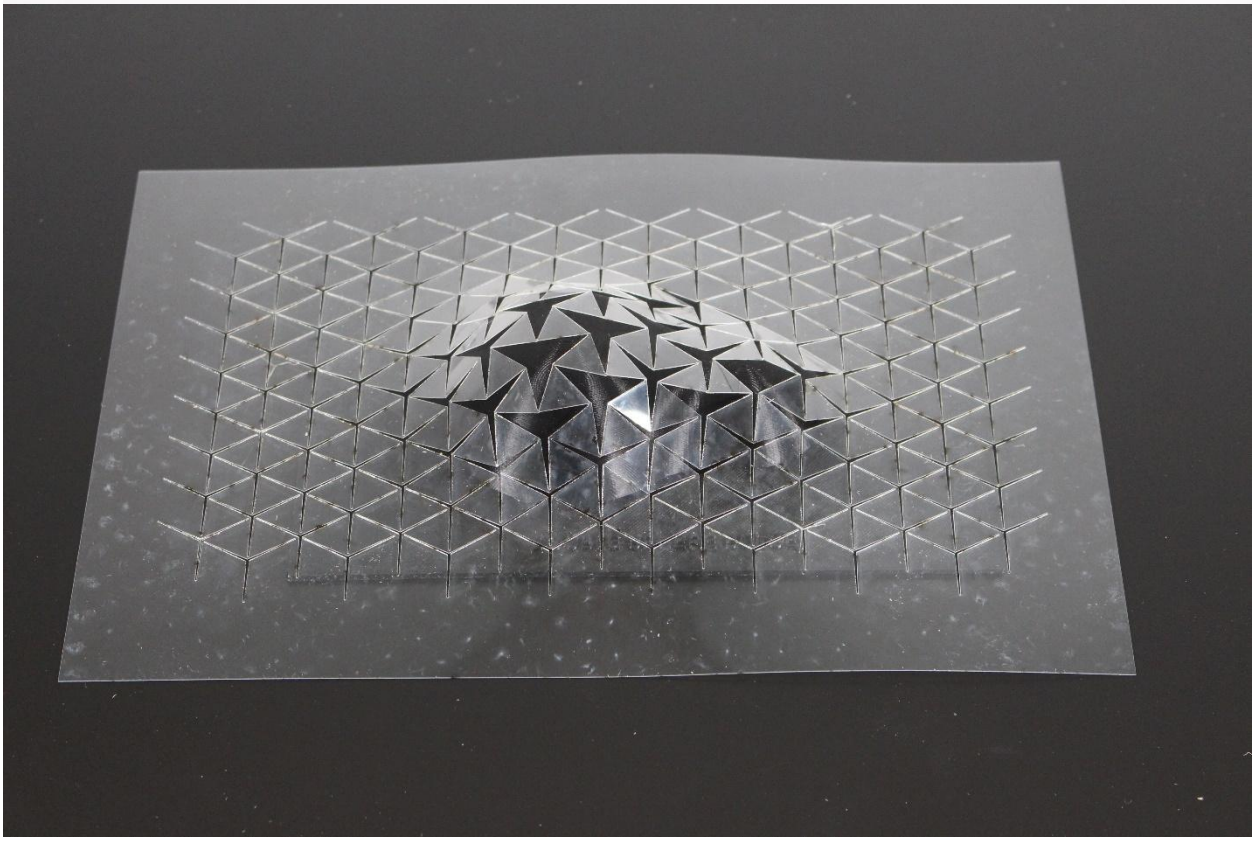

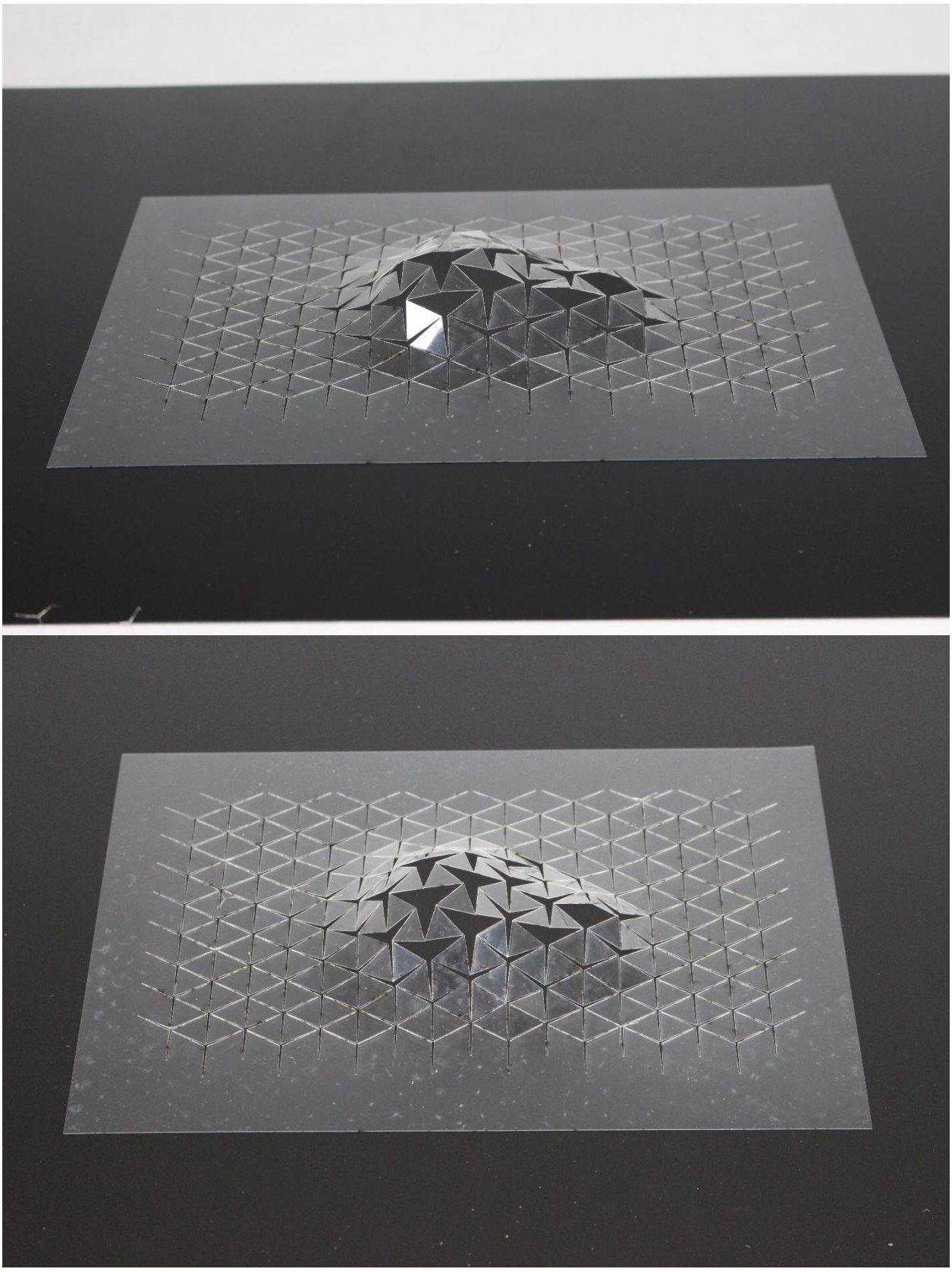

Figure 6.7-45 Tristar PETG on Double Dome Structure – laid on Form and free standing

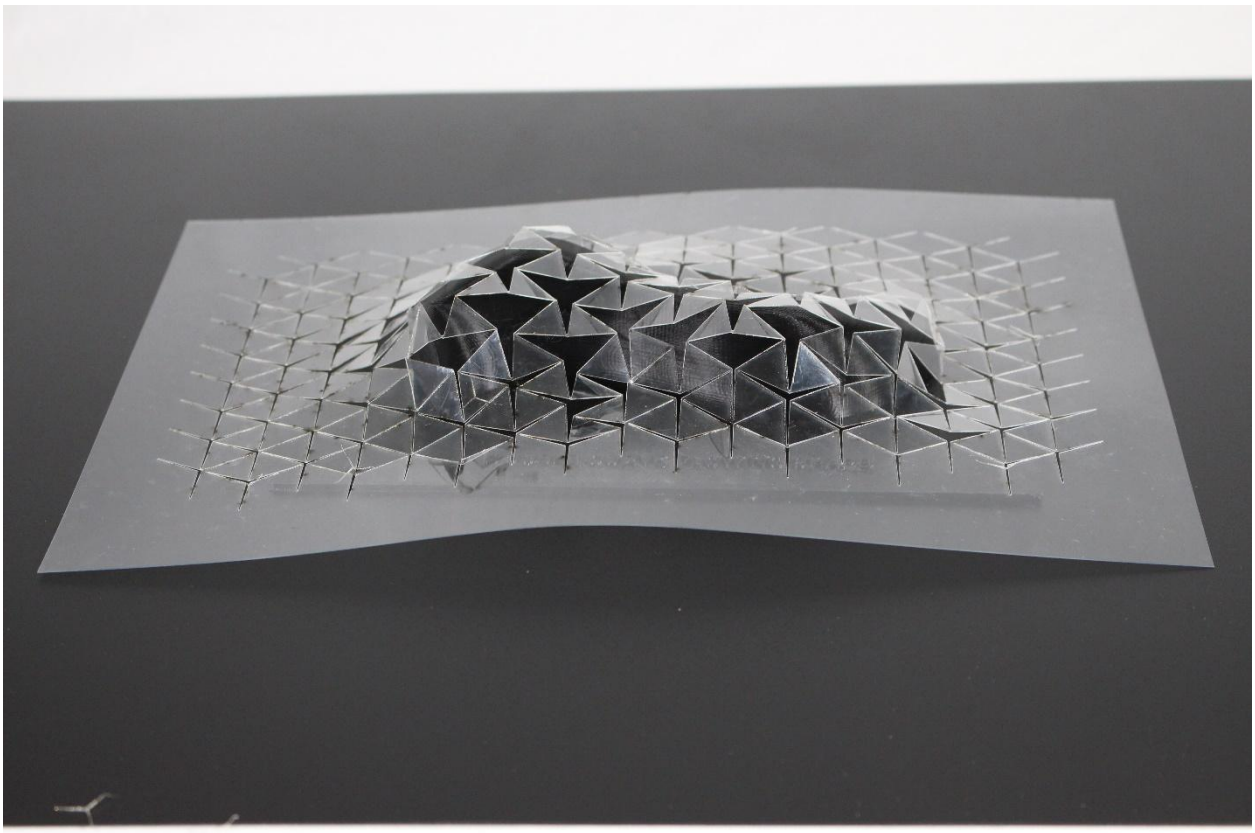

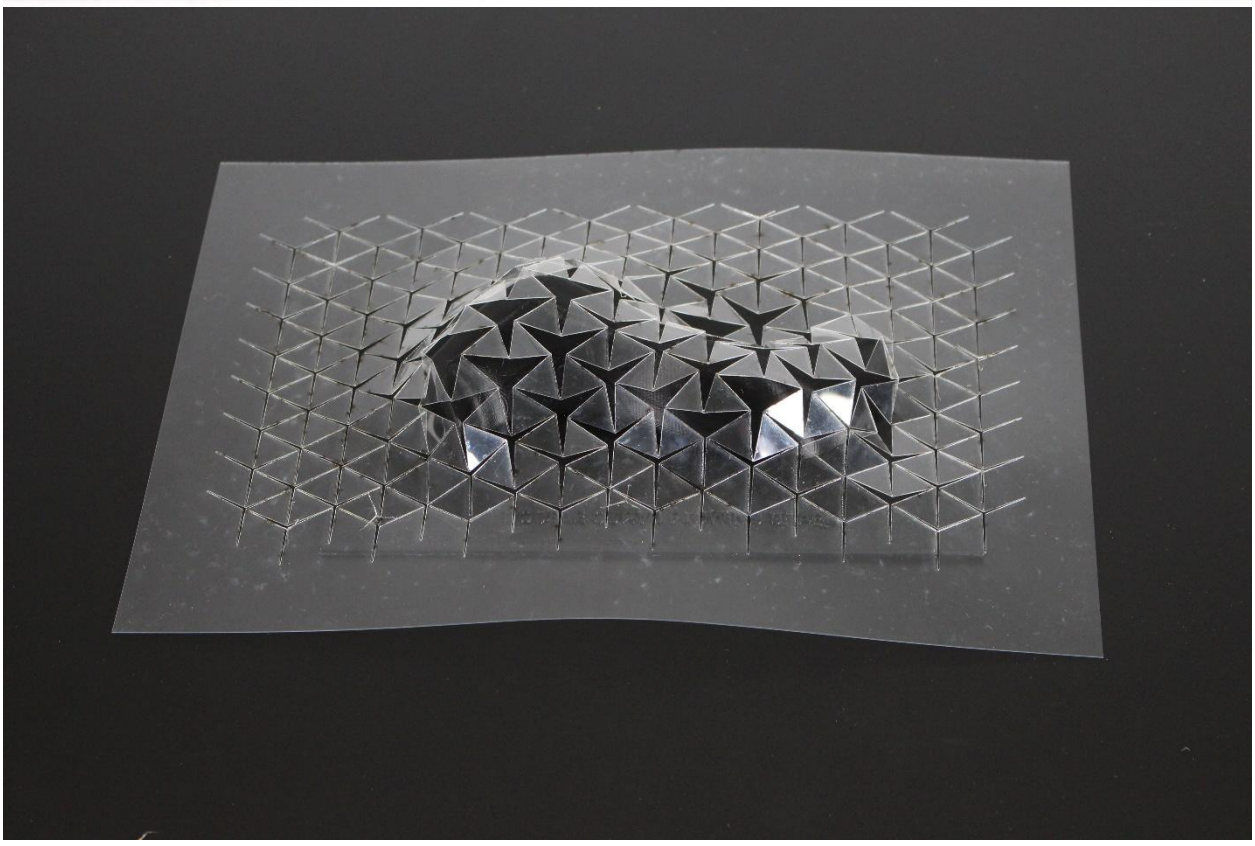

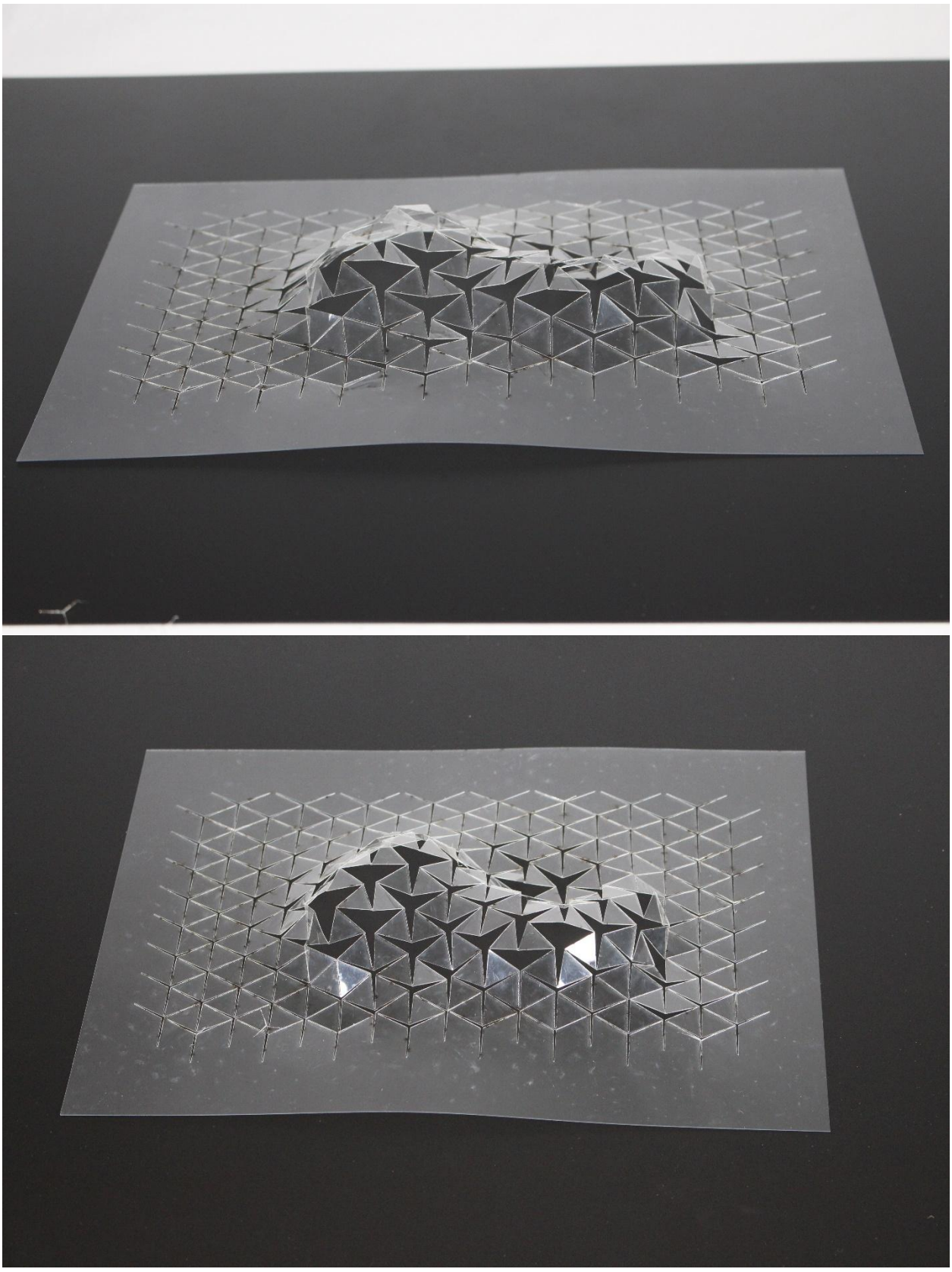

Figure 6.7-46 Tristar PETG on Double curve free flowing form – laid on Form and free standing

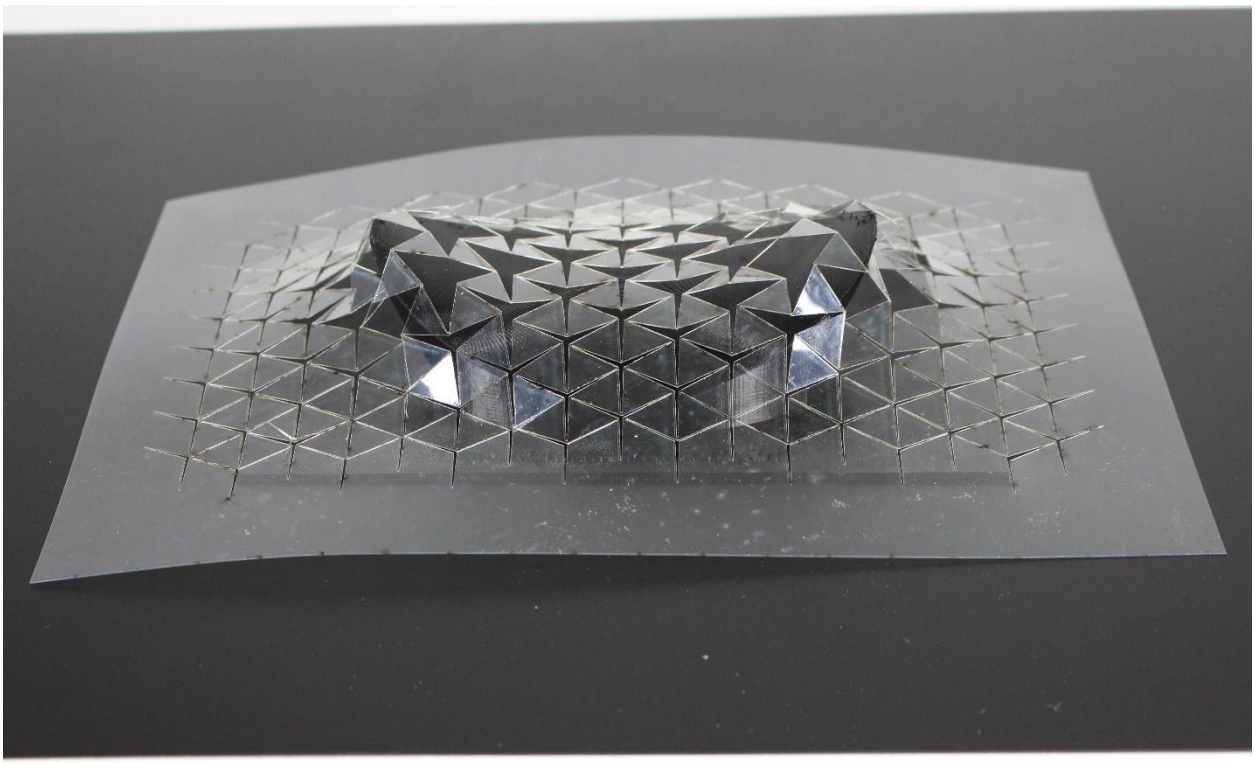

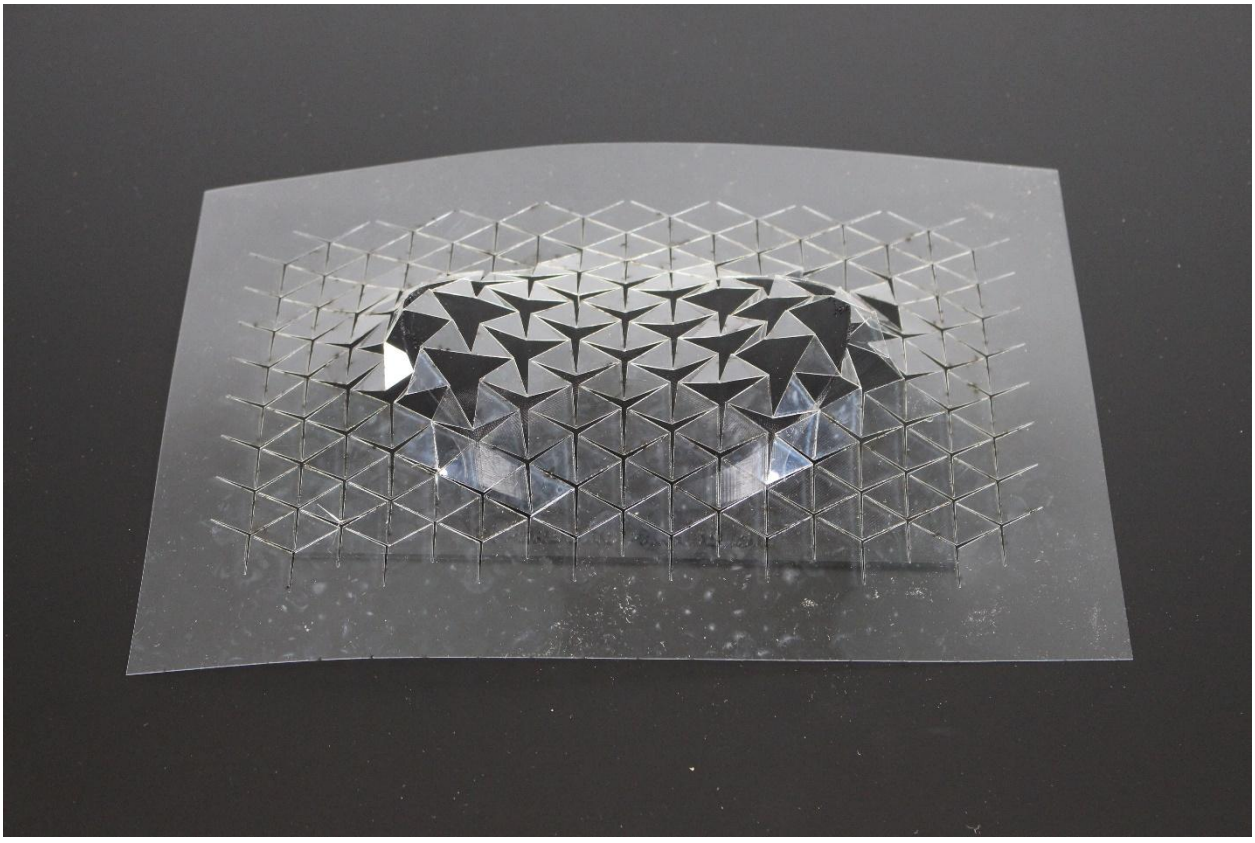

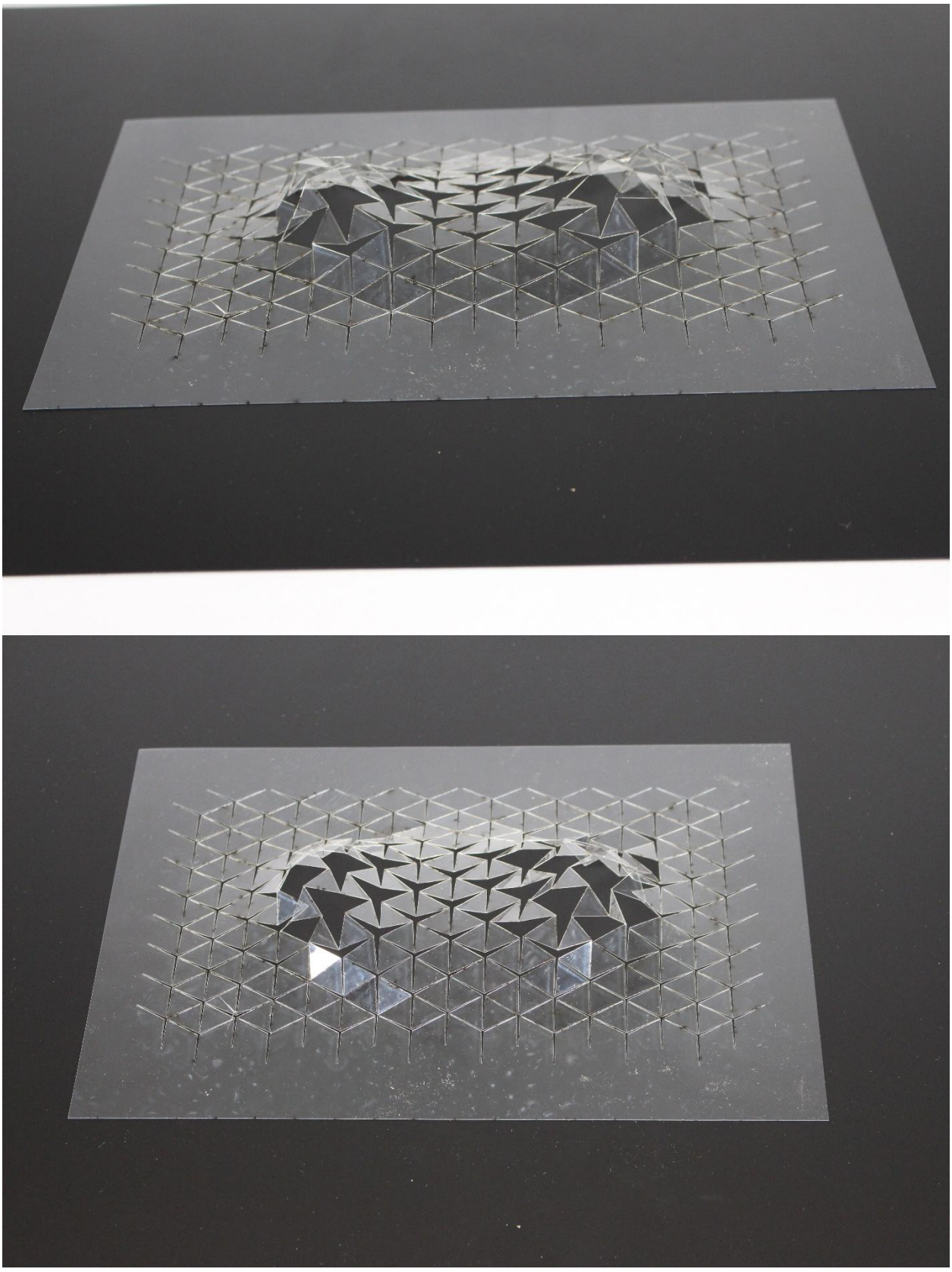

Figure 6.7-47 Tristar PETG on Hyperboloid paraboloid – laid on Form and free standing

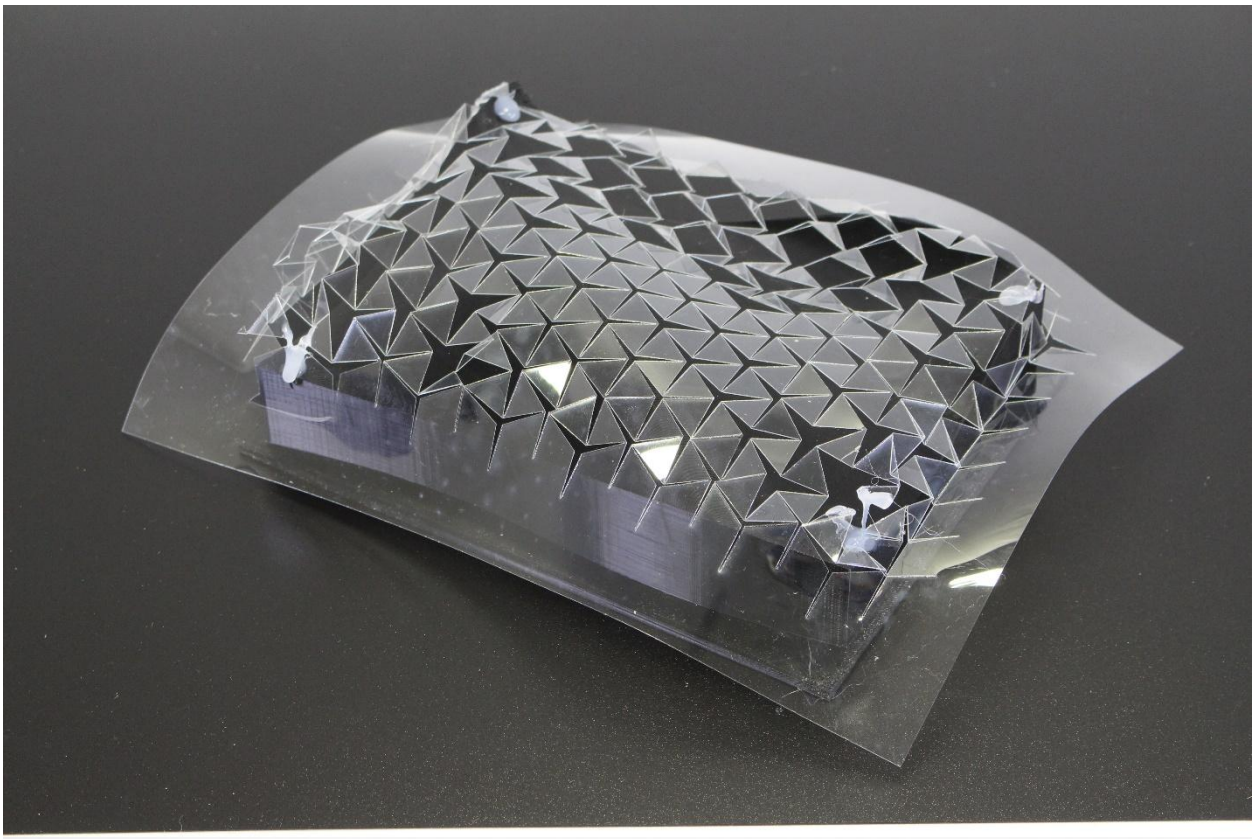

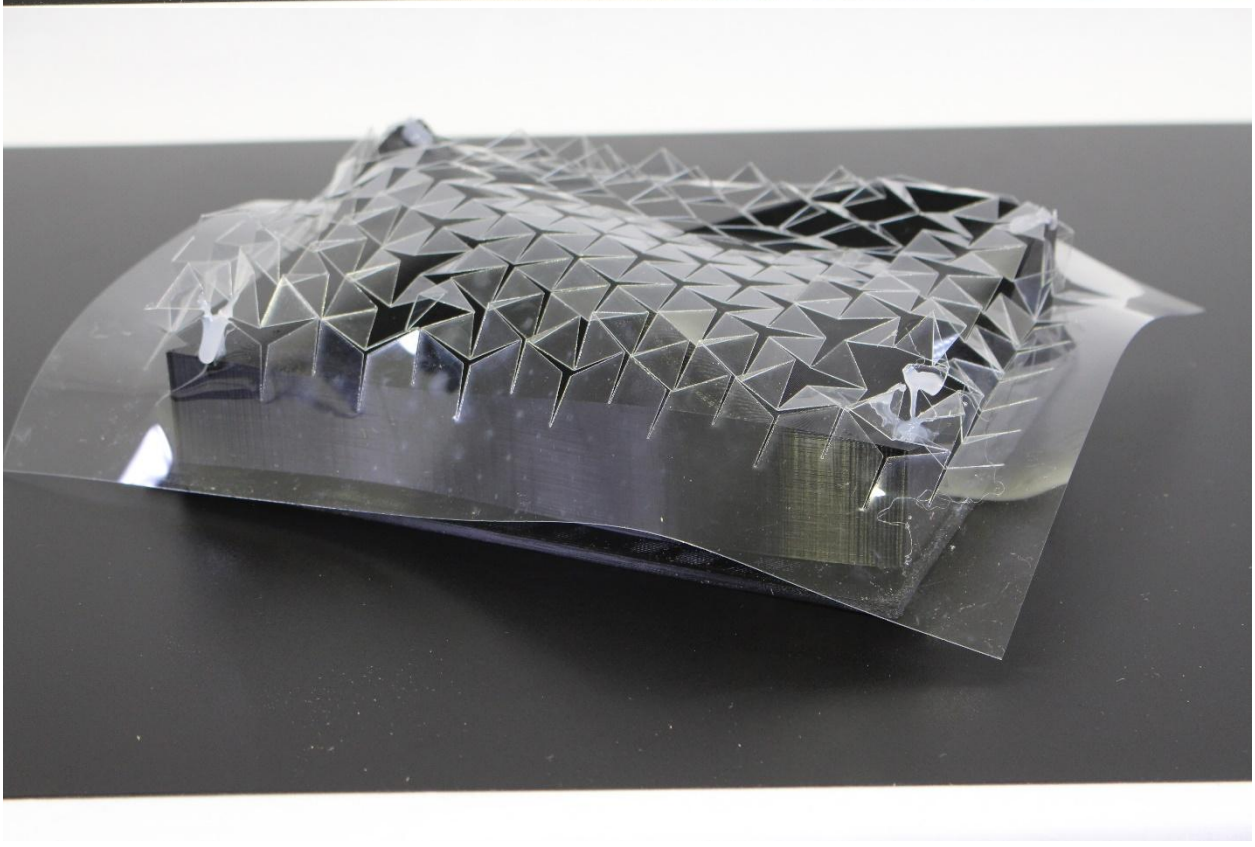

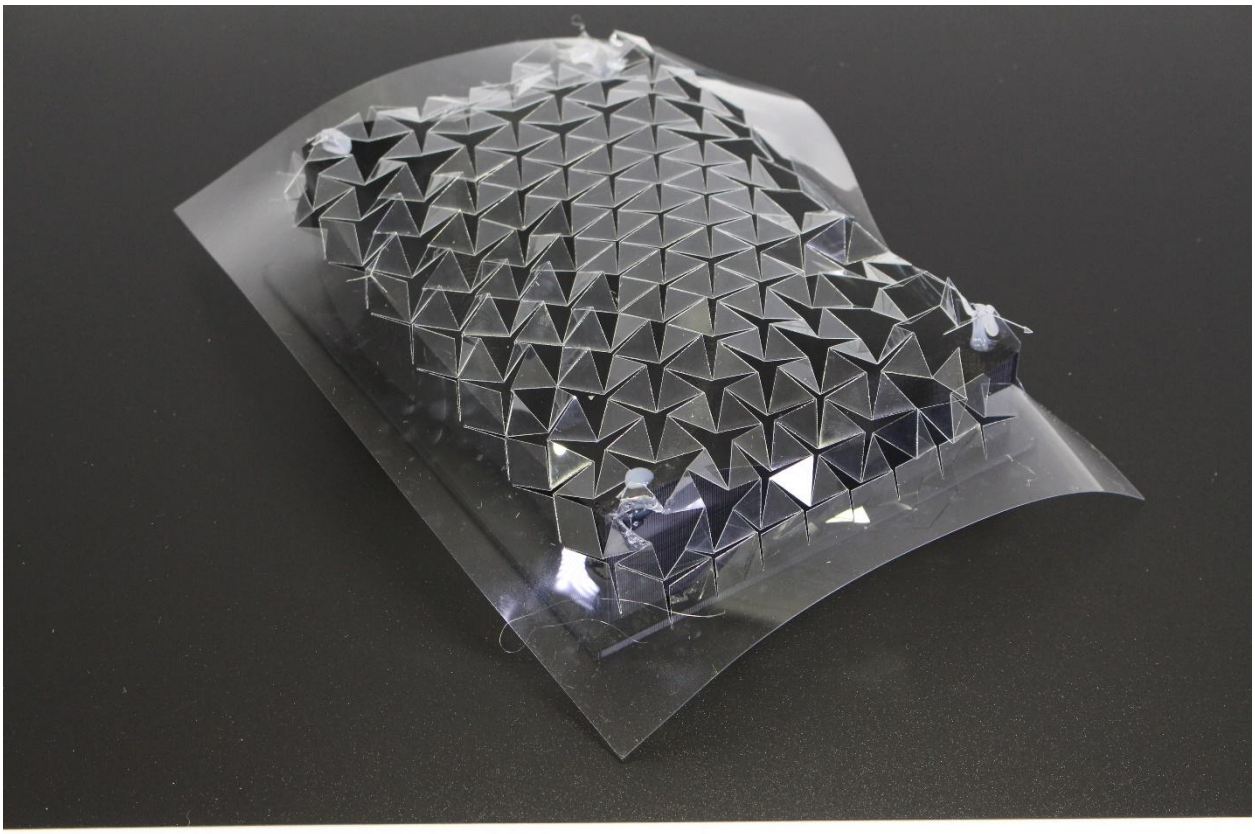

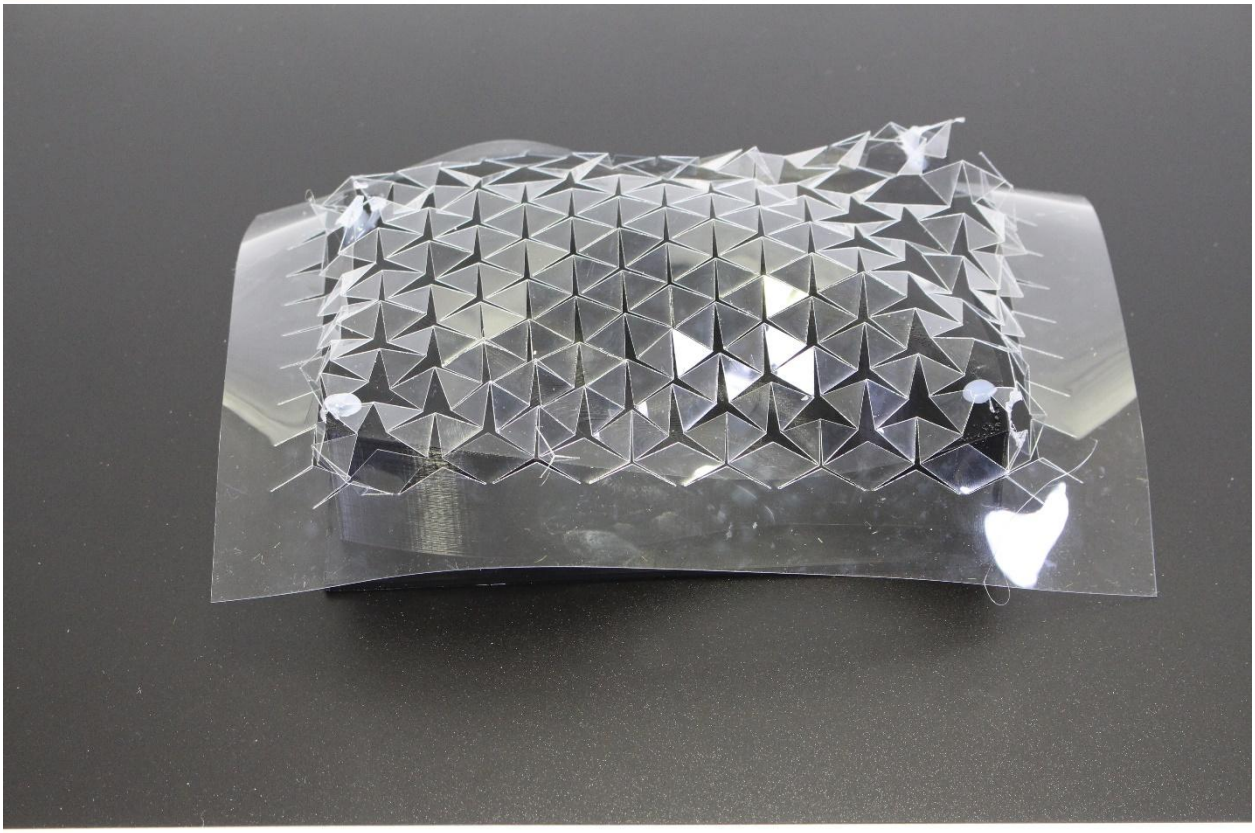

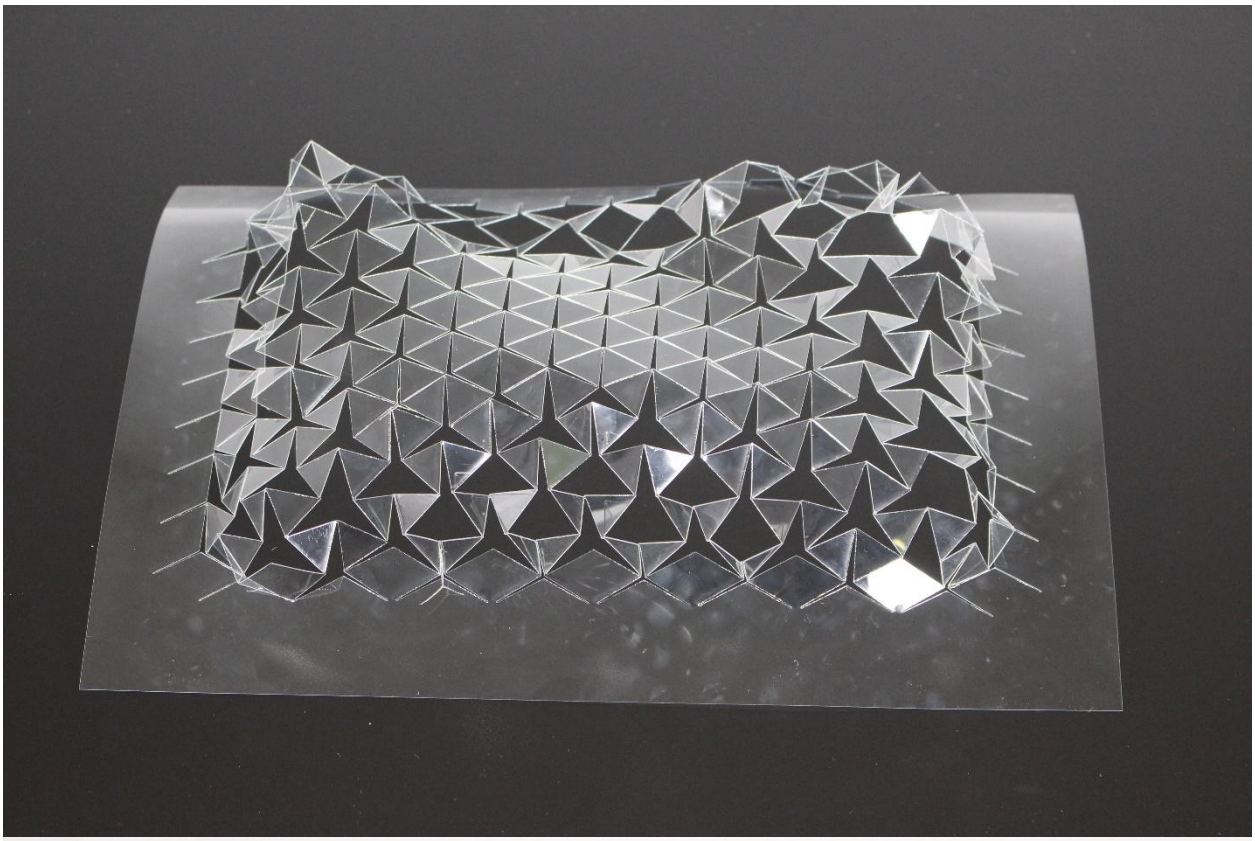

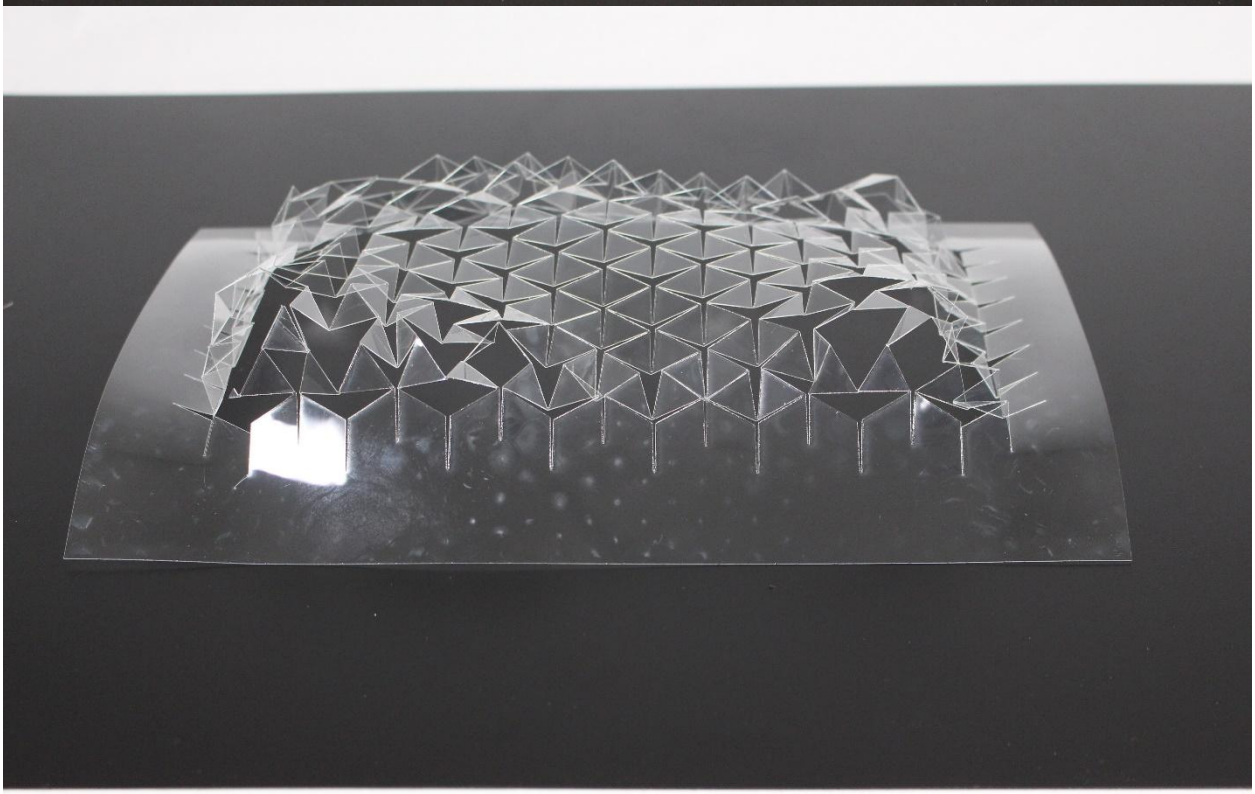

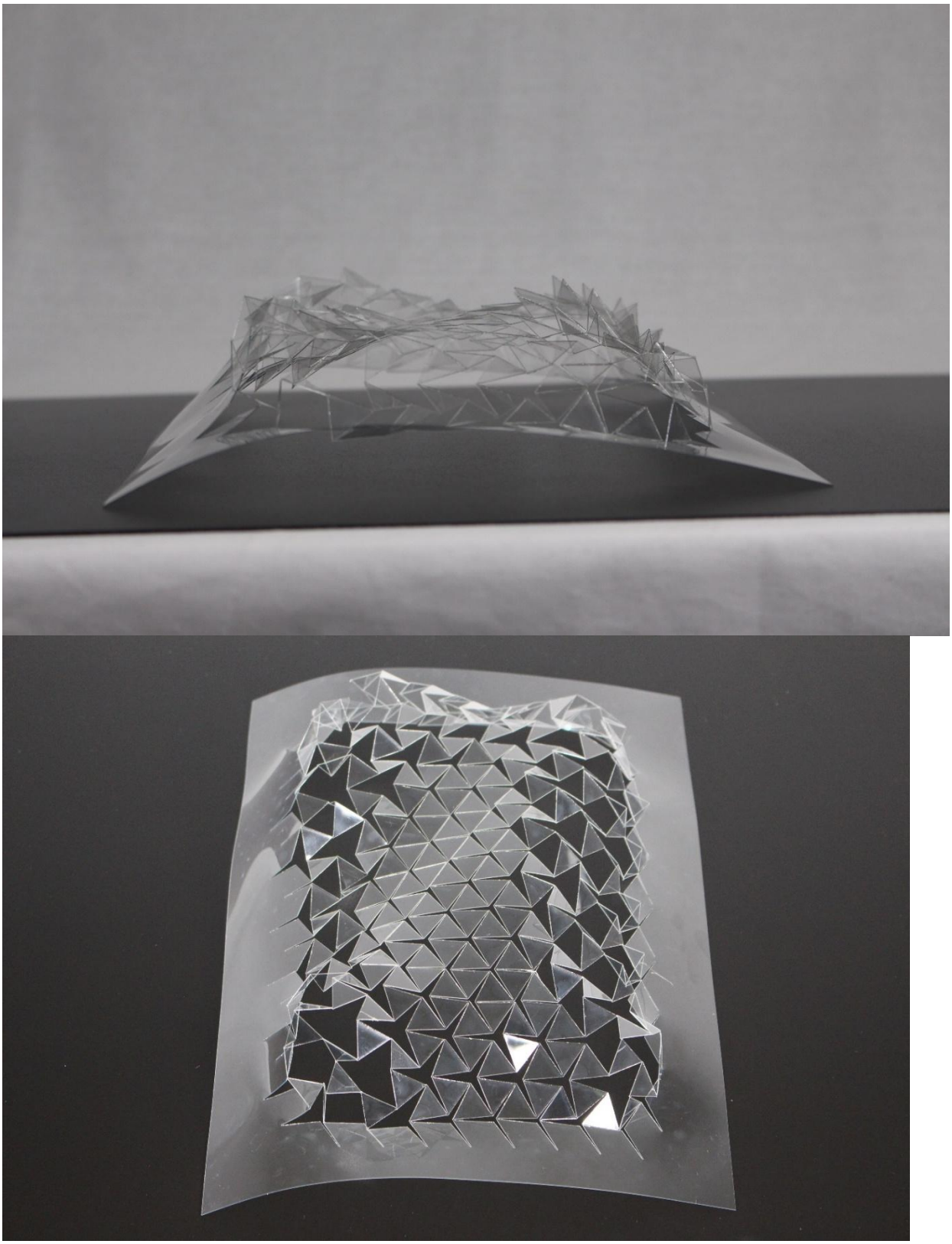

Figure 6.7-48 Tristar PETG on Free flowing double curve – laid on Form

6.7.5.1 Free Form testing

After testing with the 3D printed forms , some experiments with free forming with hands was trialled out , random forms were tried to be pulled and the PetG stayed in the forms , this showcases the pull up technique of deployment discussed earlier

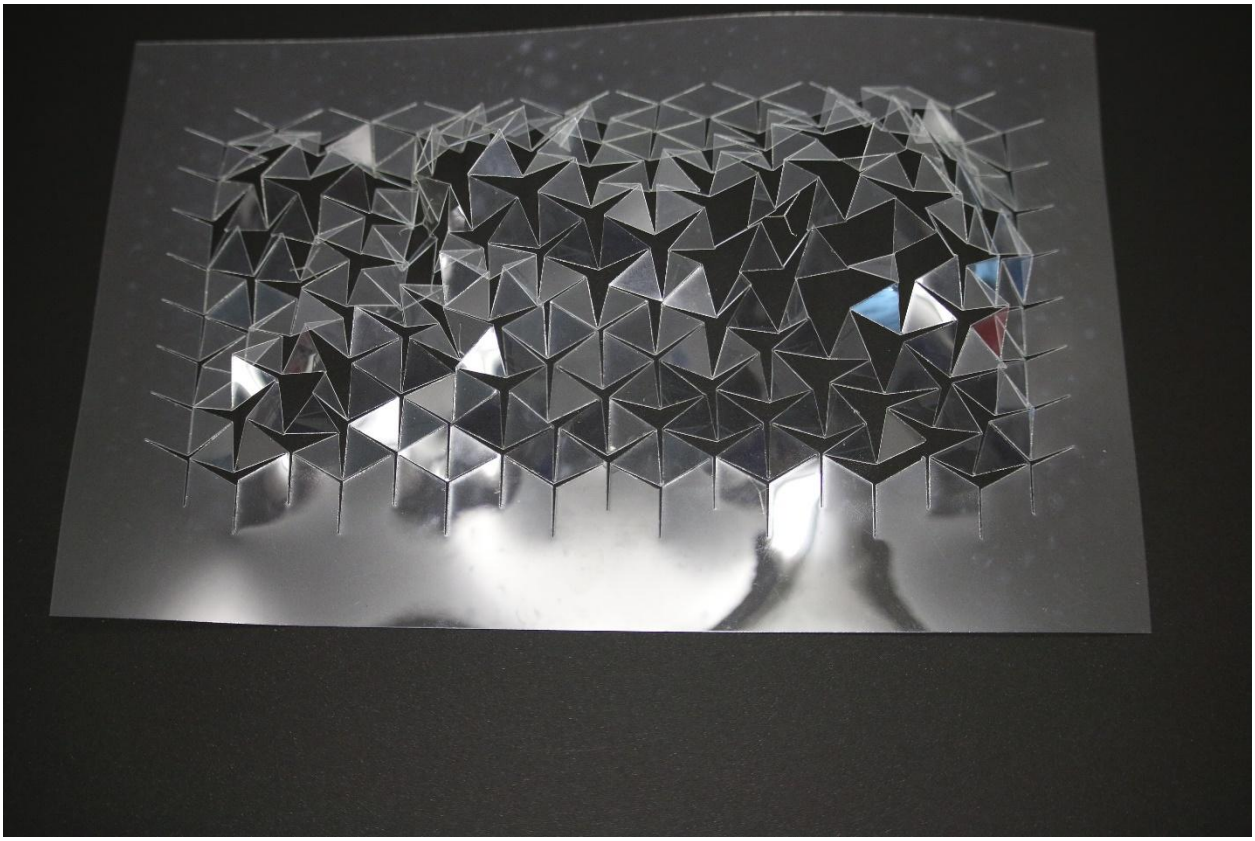

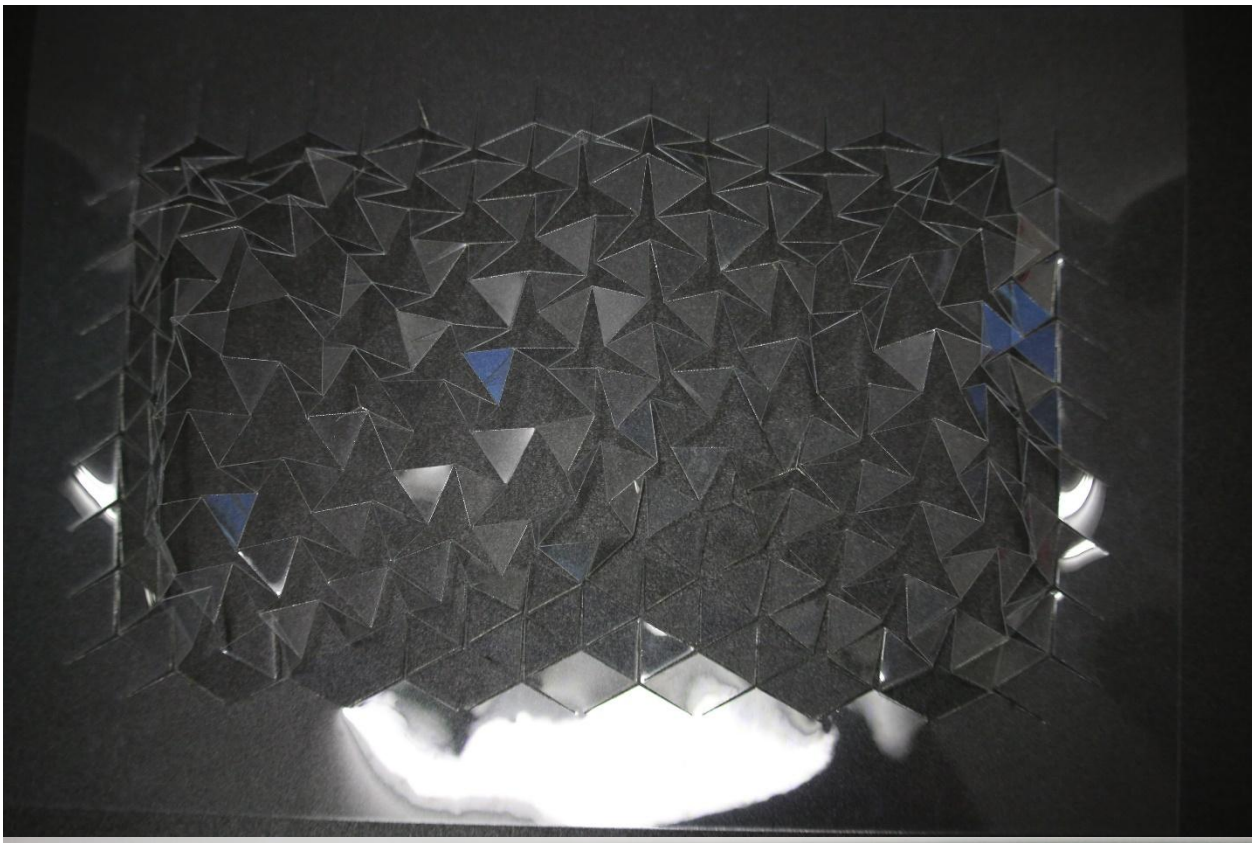

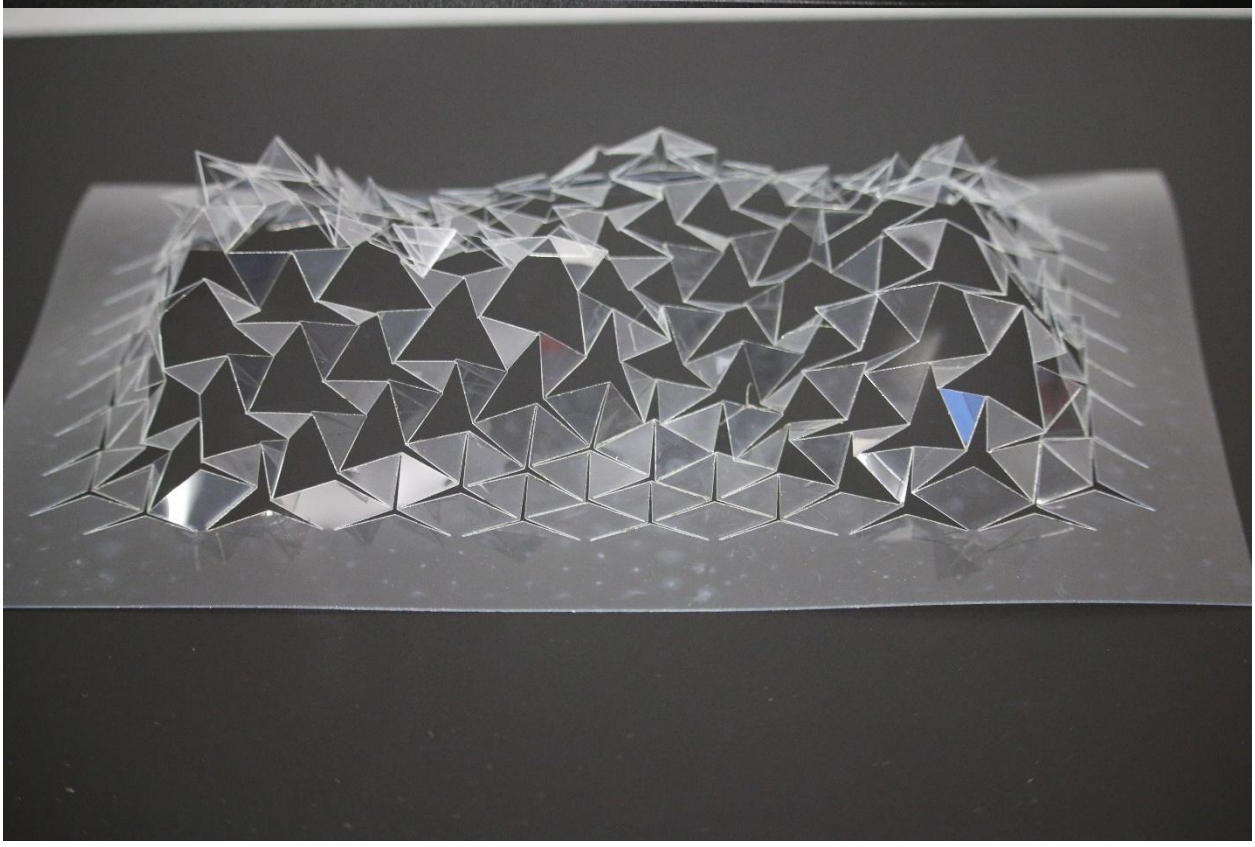

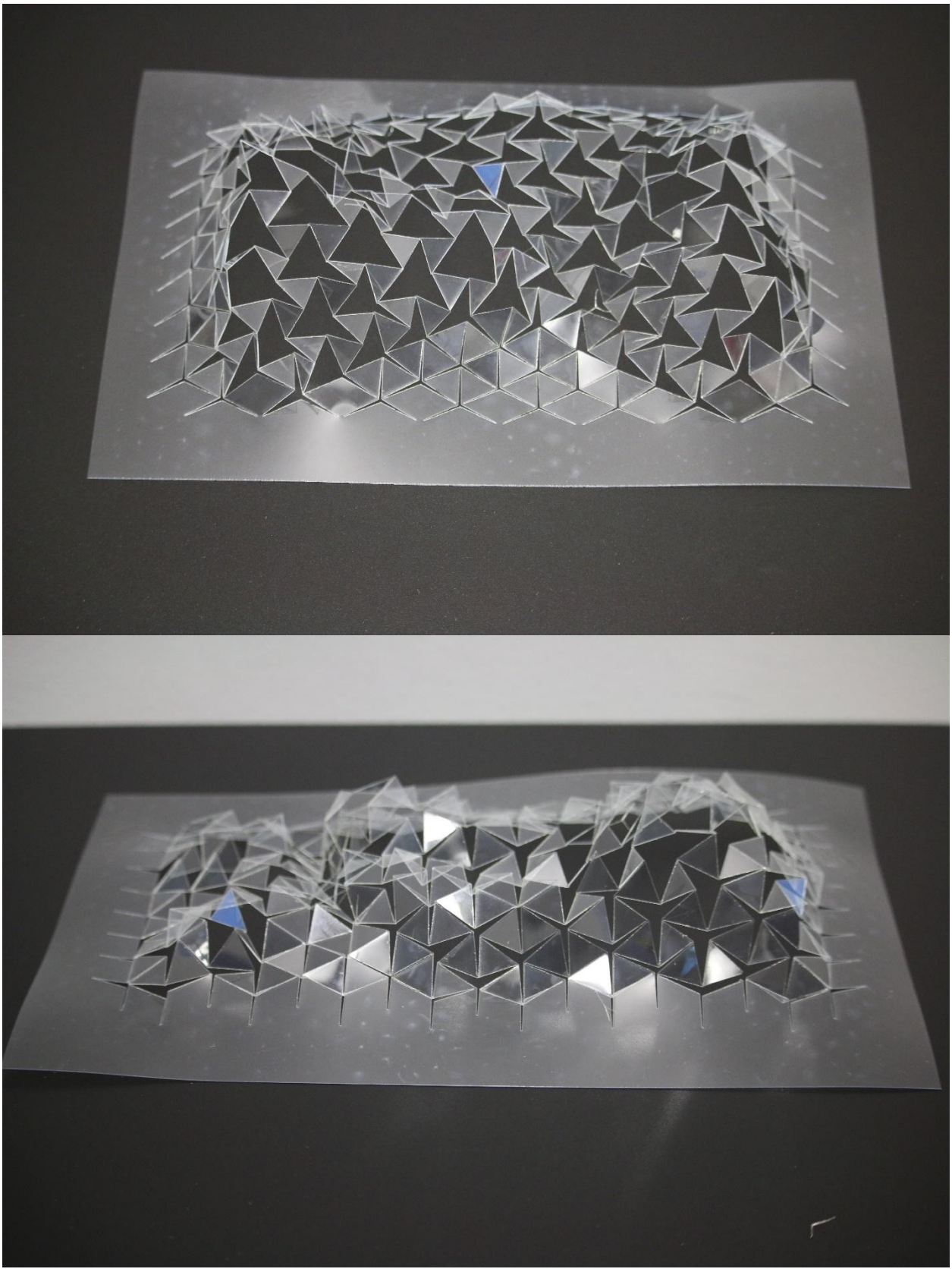

Figure 6.7-49 Freeform testing of Pet G lasercut

6.7.6 Appendix F : Simulation Trials and outcomes

6.7.6.1 Trial 1 - Uniform redistribution on flat surface- simulation

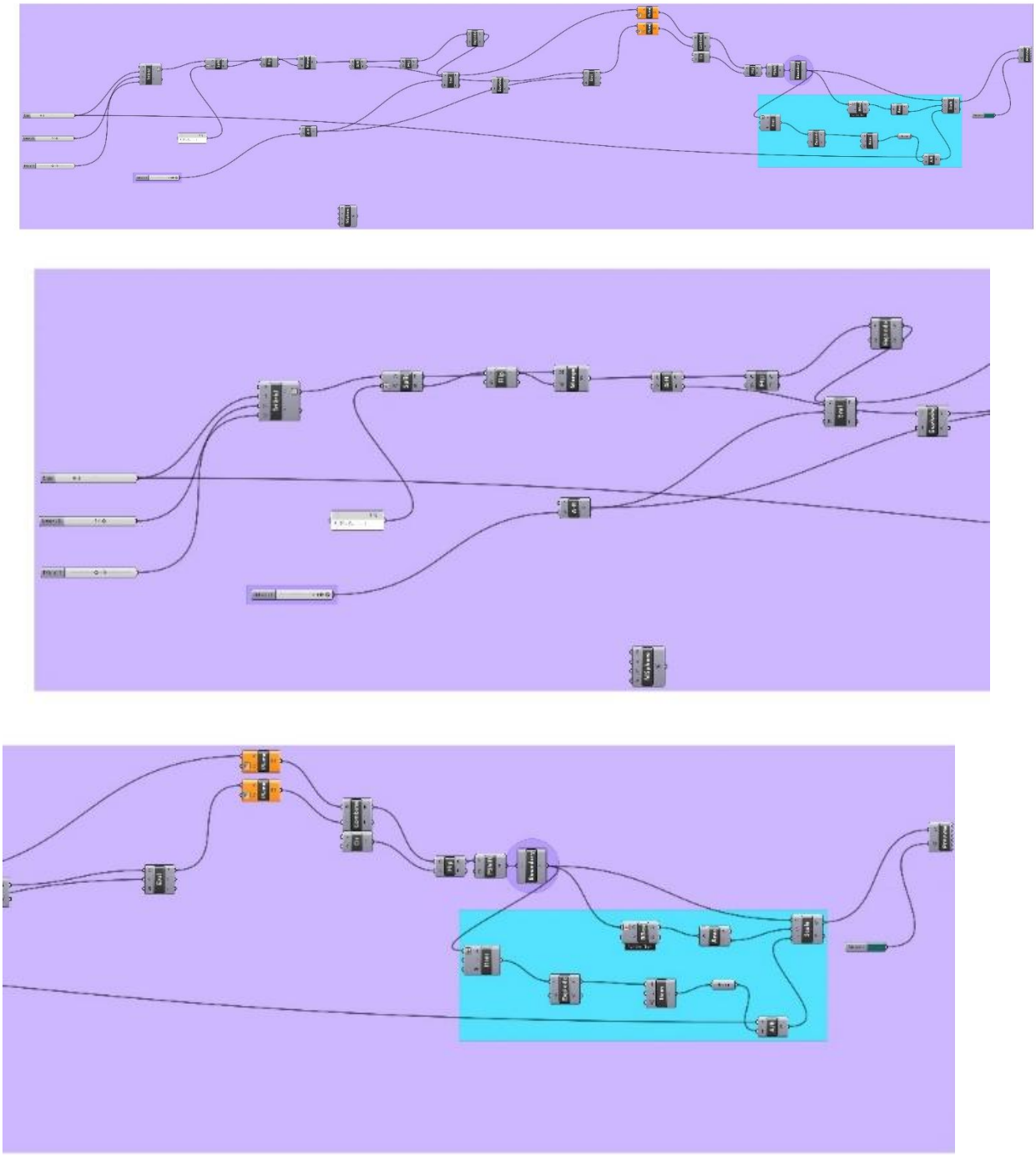

Figure 6.7-50 Grasshopper coding for Uniform rotation in XY plan

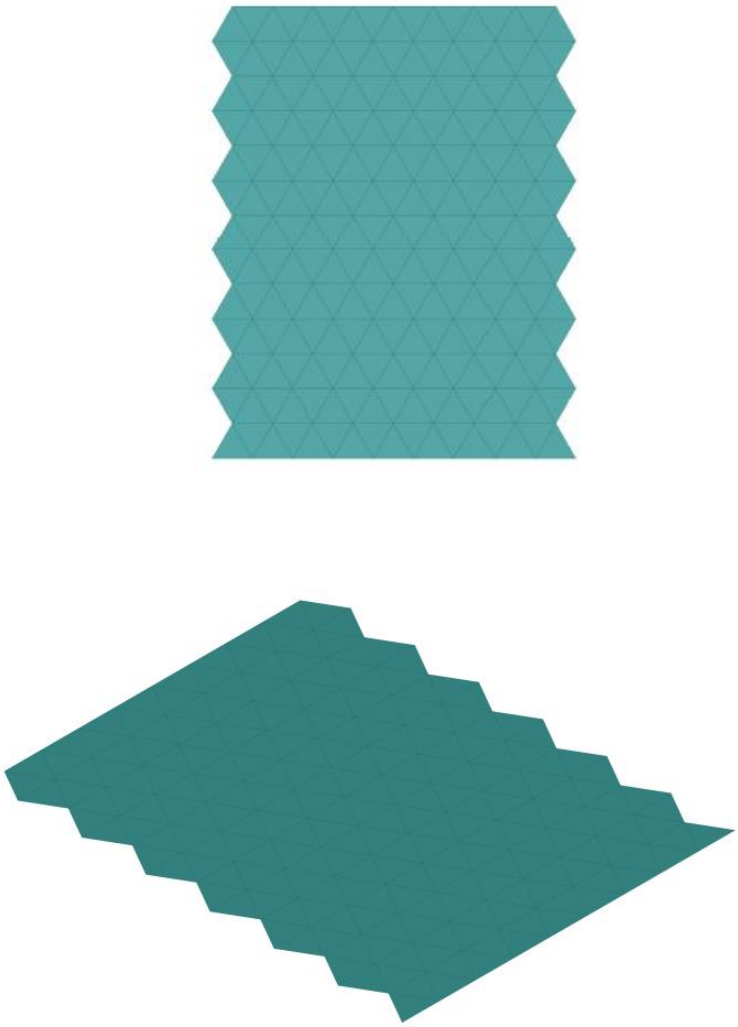

Figure 6.7-51 Results - GH code with Uniform rotation - at angle 0 – Top view and Iso View

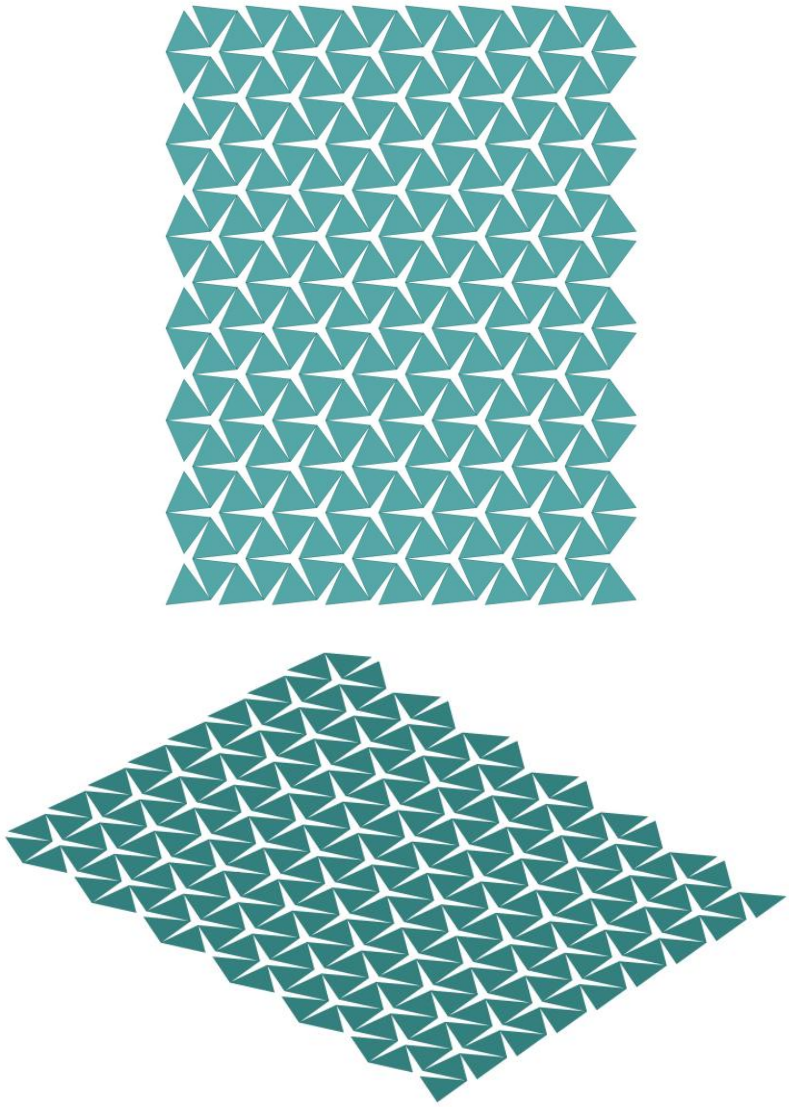

Figure 6.7-52 Results - GH code with Uniform rotation - at angle 30 – Top view and Iso View

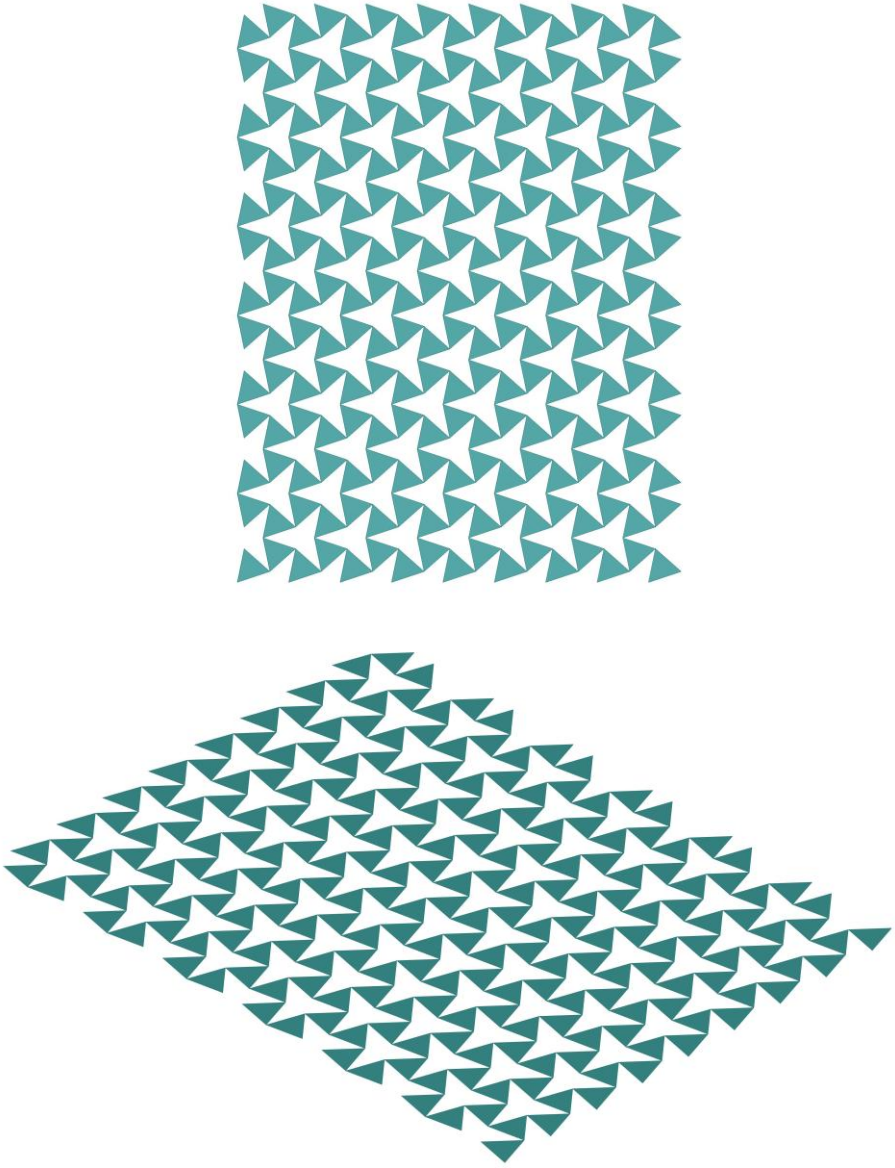

Figure 6.7-53 Results - GH code with Uniform rotation - at angle 60 – Top view and Iso View

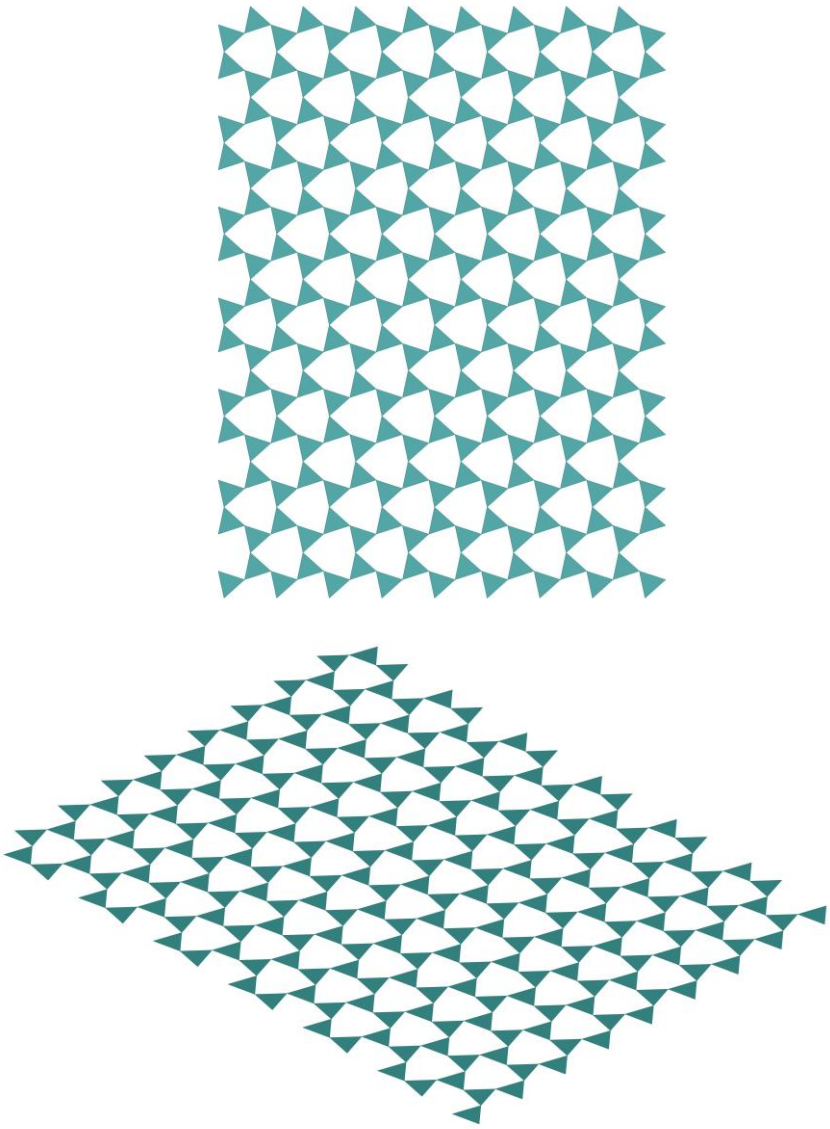

Figure 6.7-54 Results - GH code with Uniform rotation - at angle 90 – Top view and Iso View

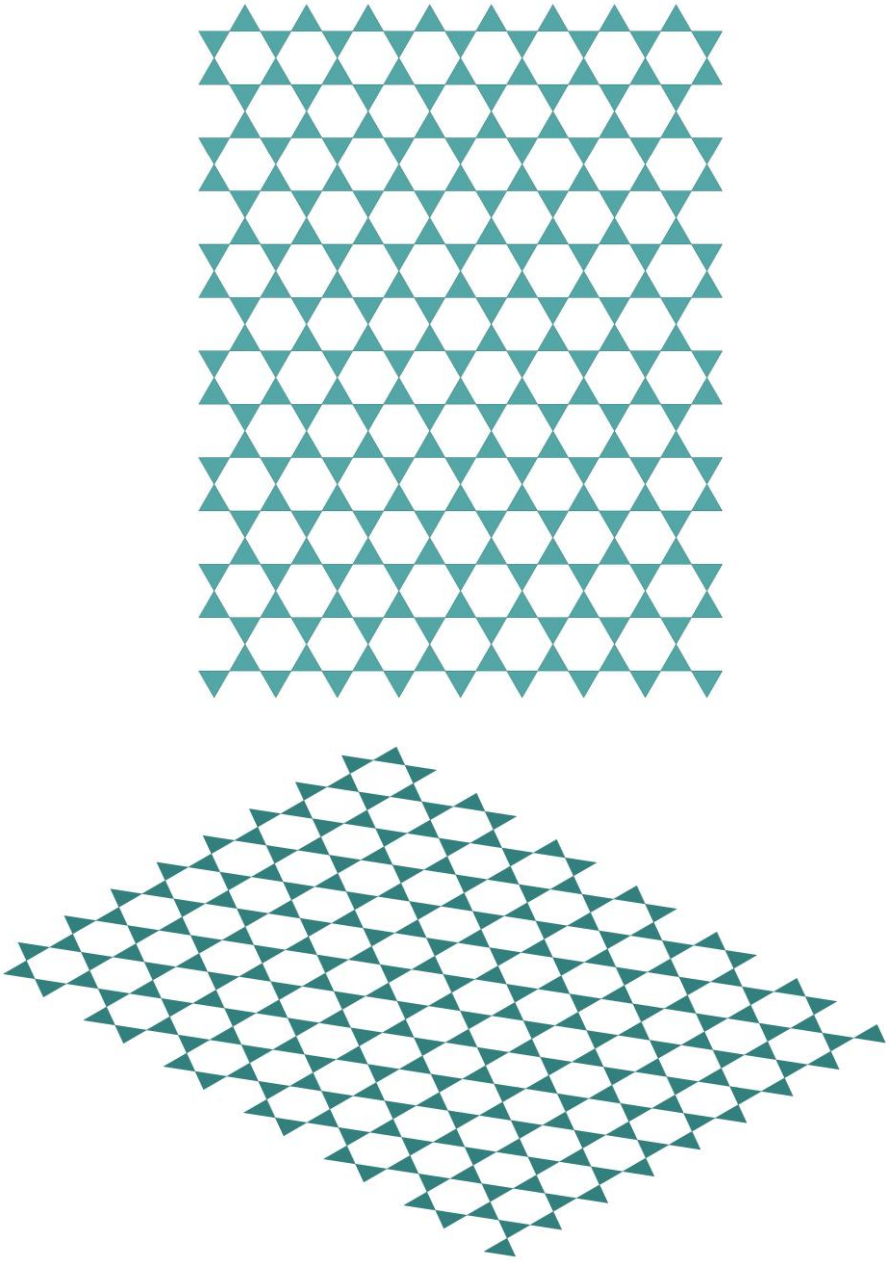

Figure 6.7-55 Results - GH code with Uniform rotation - at angle 120 – Top view and Iso View

6.7.6.2 Responsive Expansion Using Attractor Point Logic on a Flat Surface

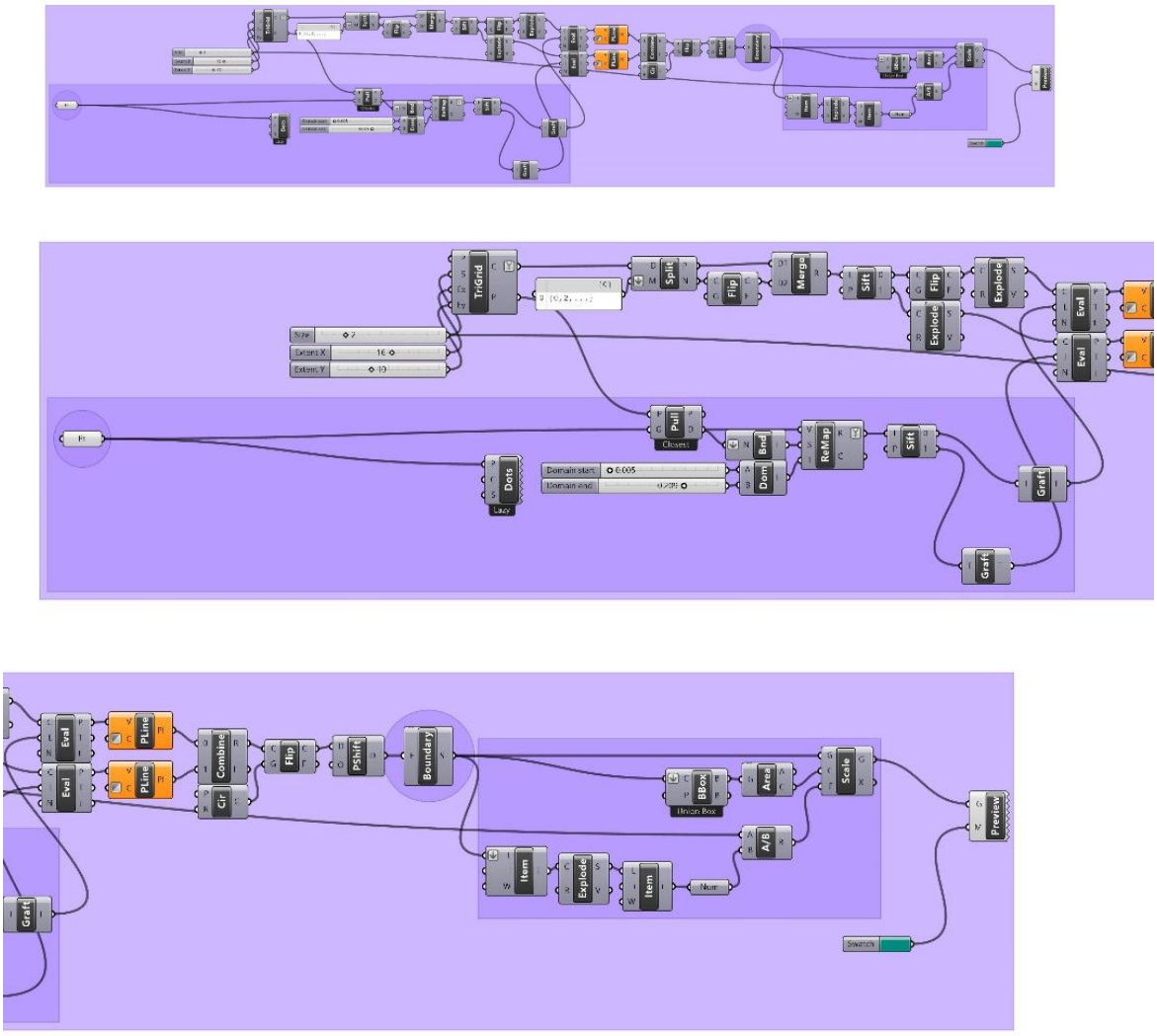

Figure 6.7-56 GH code for Auxetic movement with single 2D attractor point

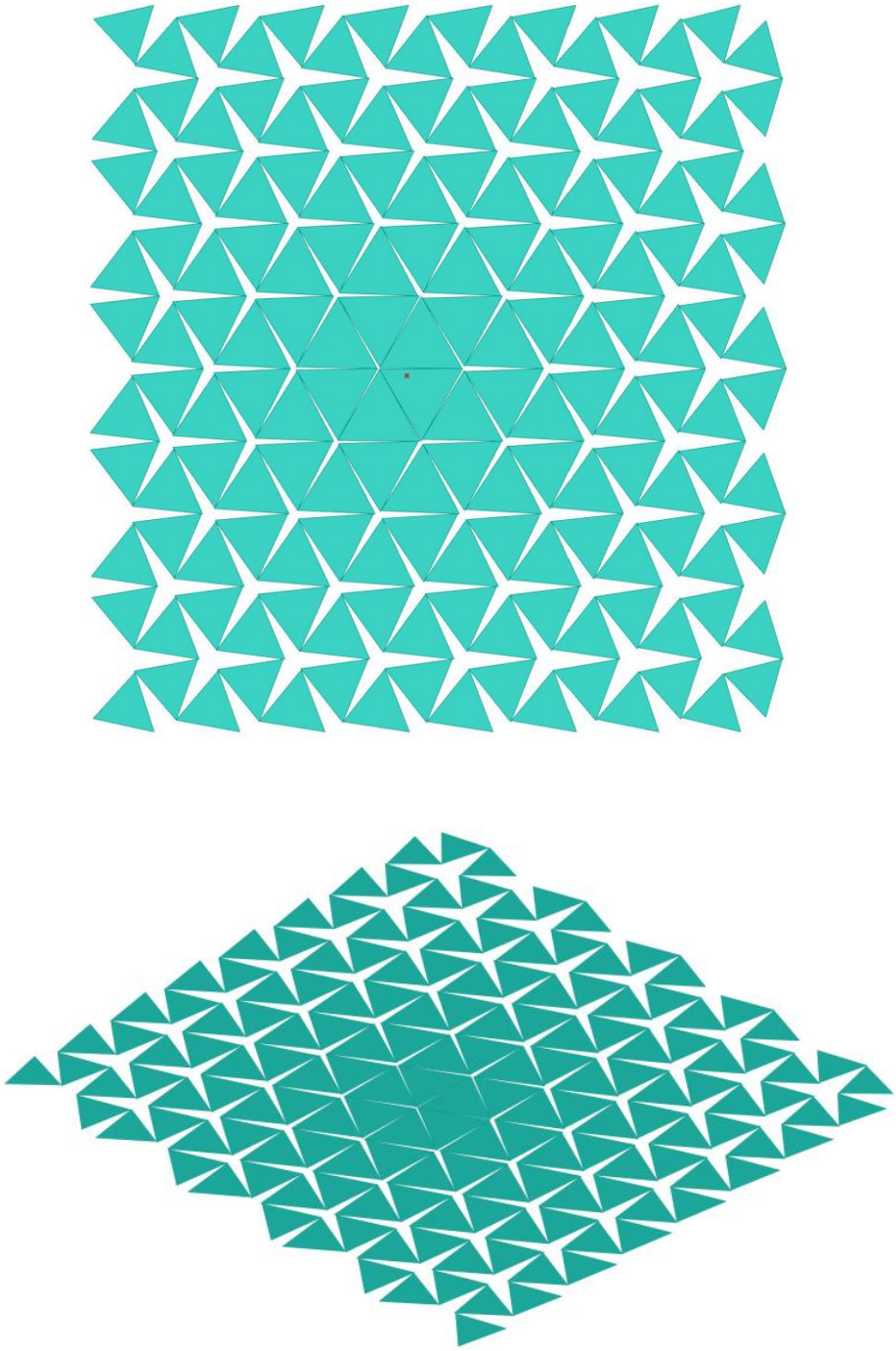

Figure 6.7-57 Results - GH code attractor point- Top and iso view- variation 1

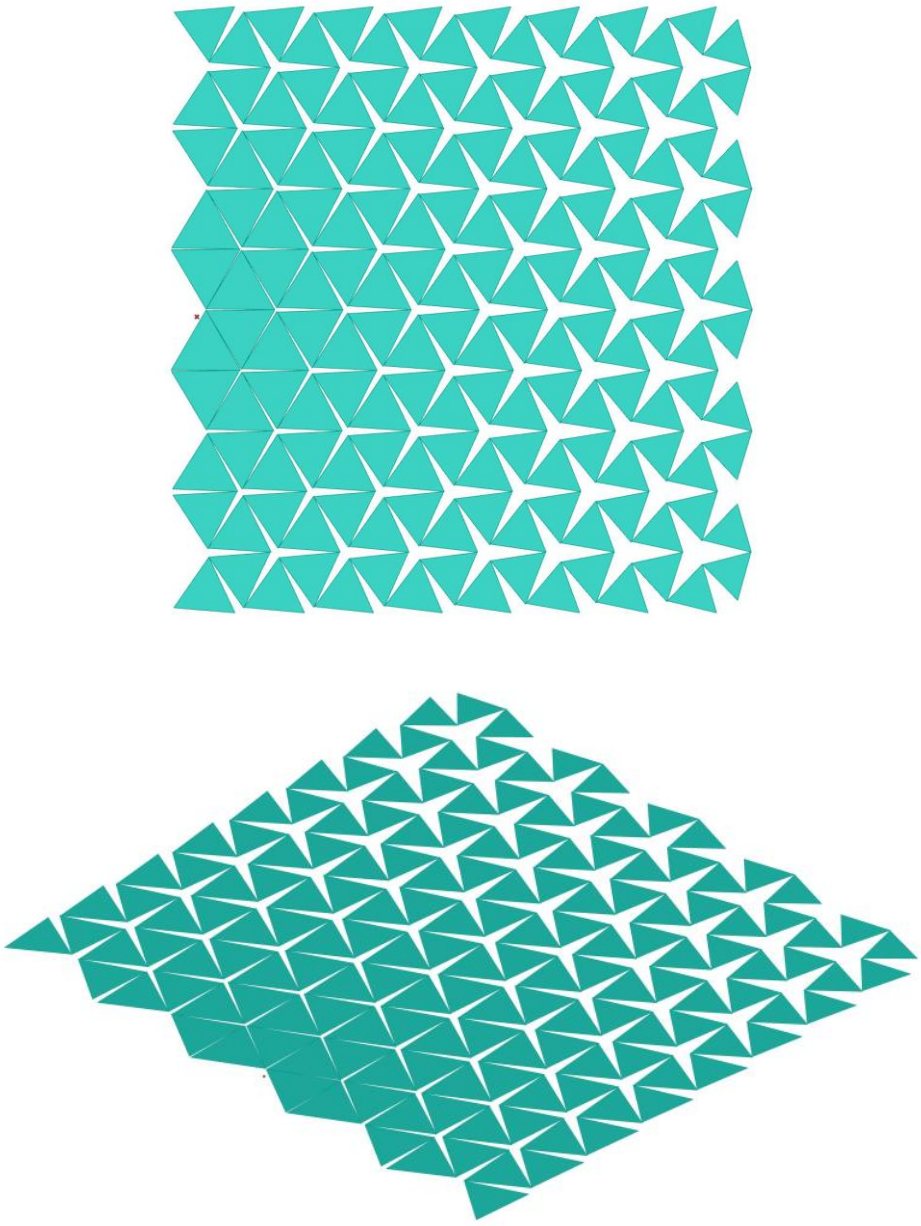

Figure 6.7-58 Results - GH code attractor point- Top and iso view- variation 2

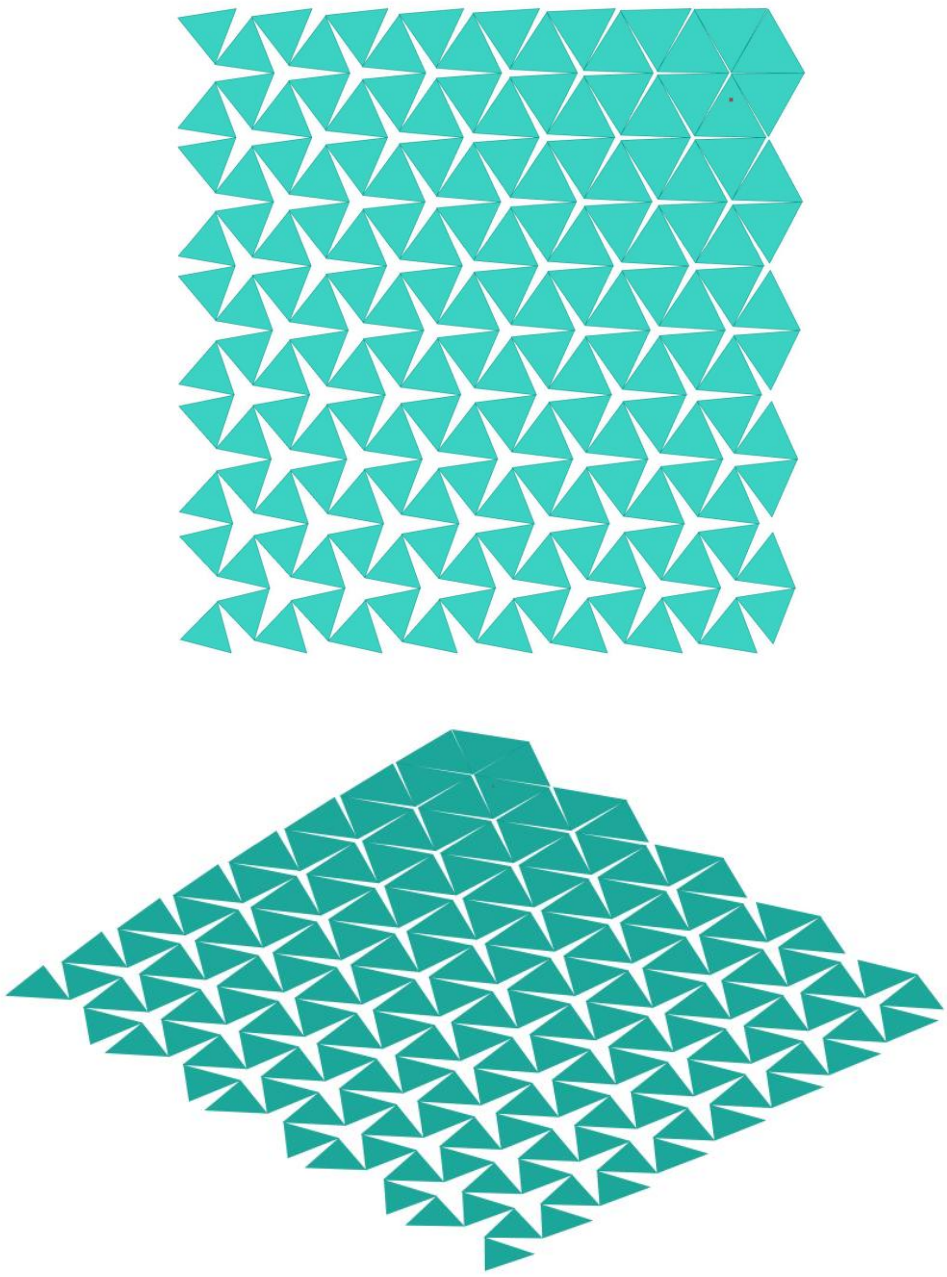

Figure 6.7-59 Results - GH code attractor point- Top and iso view- variation 3

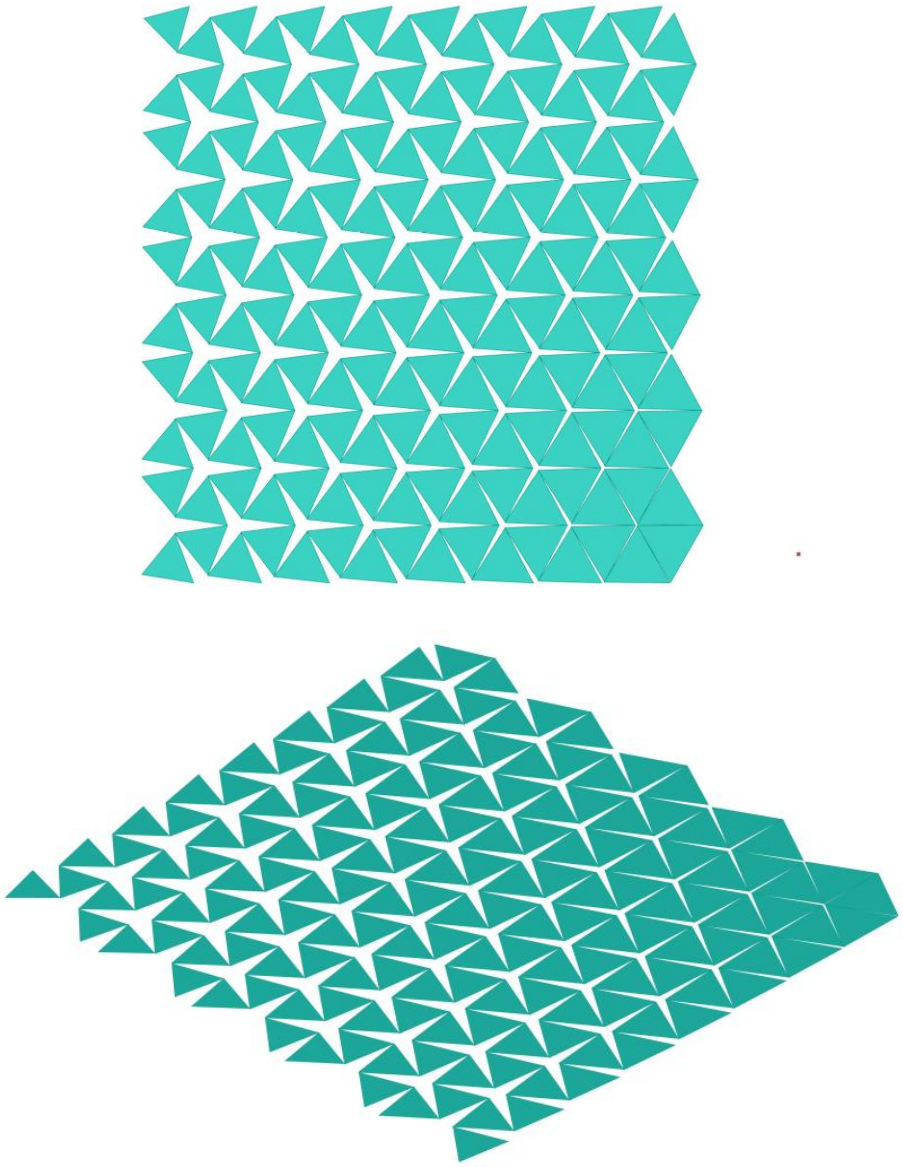

Figure 6.7-60 Results - GH code attractor point- Top and iso view- variation 4

6.7.6.3 Rotating expansion based on XYZ displacement conformal mapping - Simulation trial #5

Grasshopper code -rational and logic

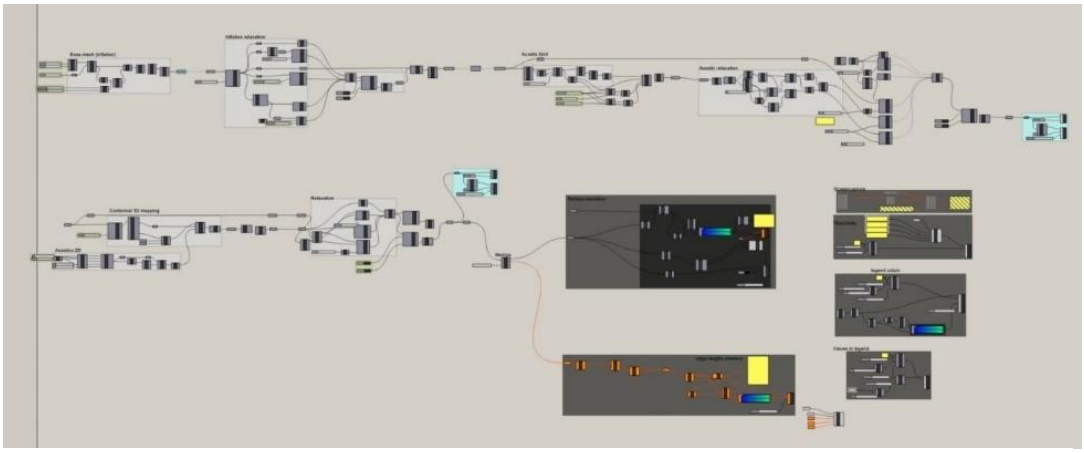

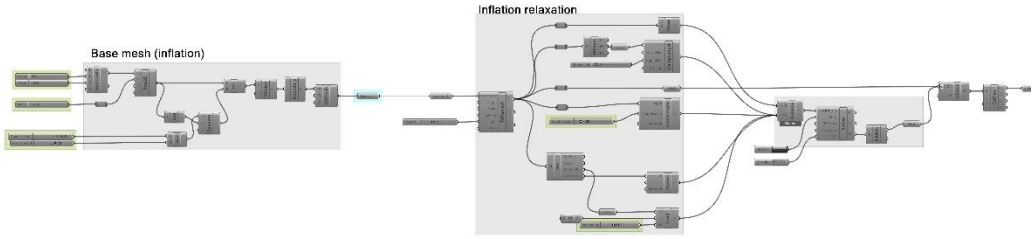

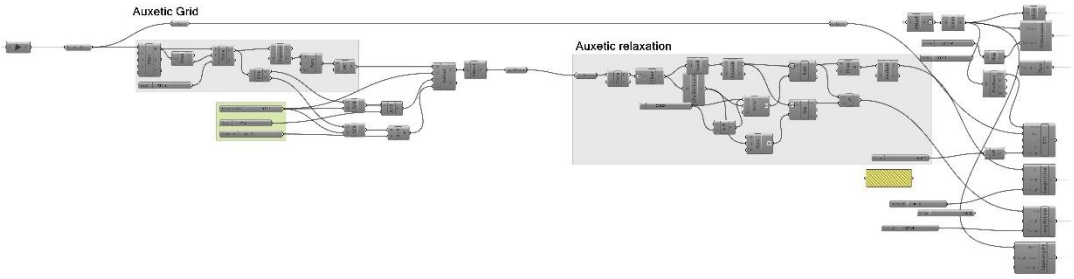

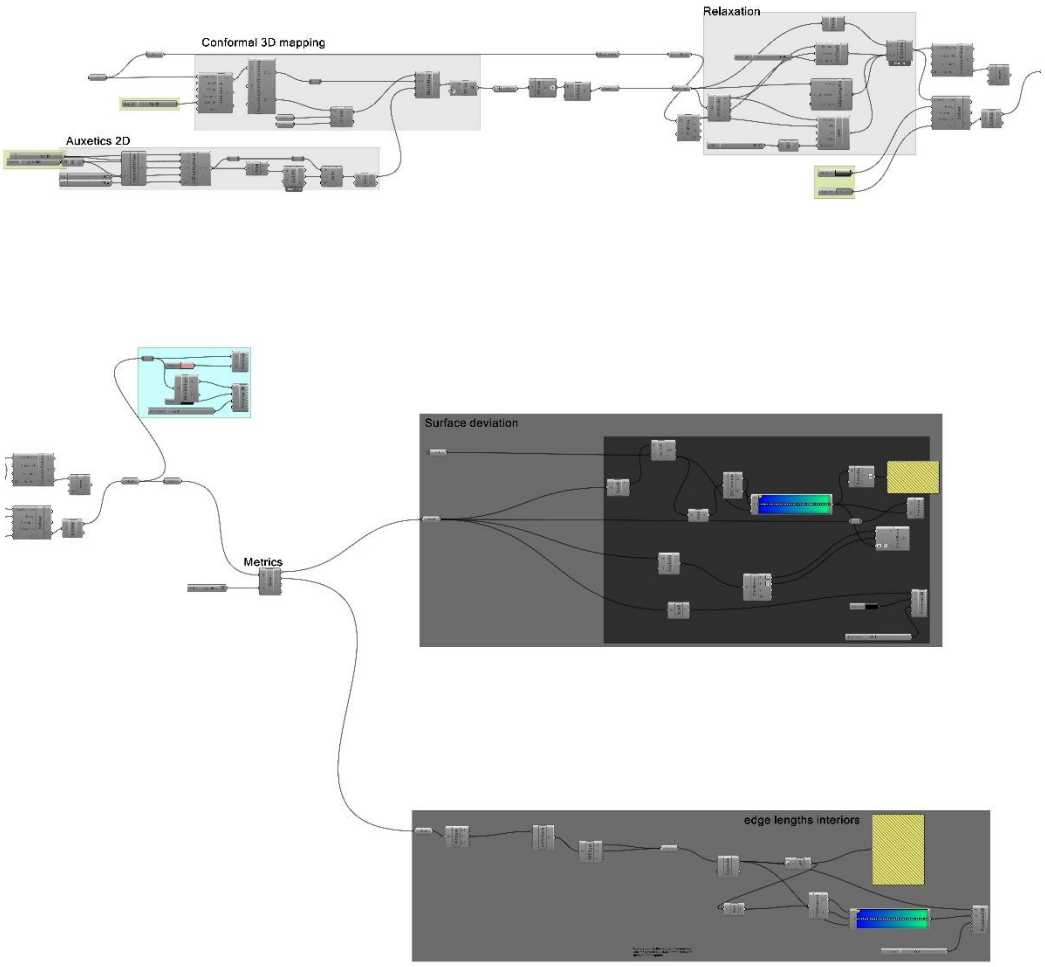
Relaxation
Conformal 3D mapping
Auxetics 2D
Surface deviation
Metrics
edge lengths interiors

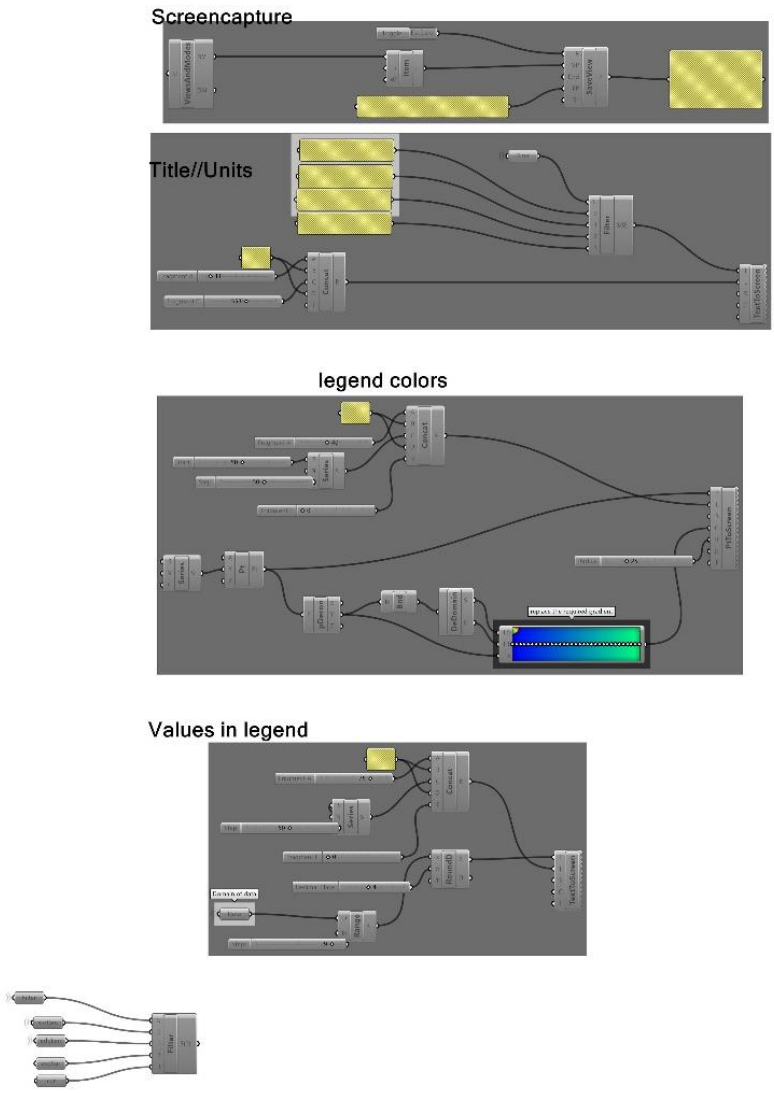

Figure 6.7-61 Grasshopper simulation for 3D expansion based on XYZ axis conformal mapping displacement – iteration #5

Results:

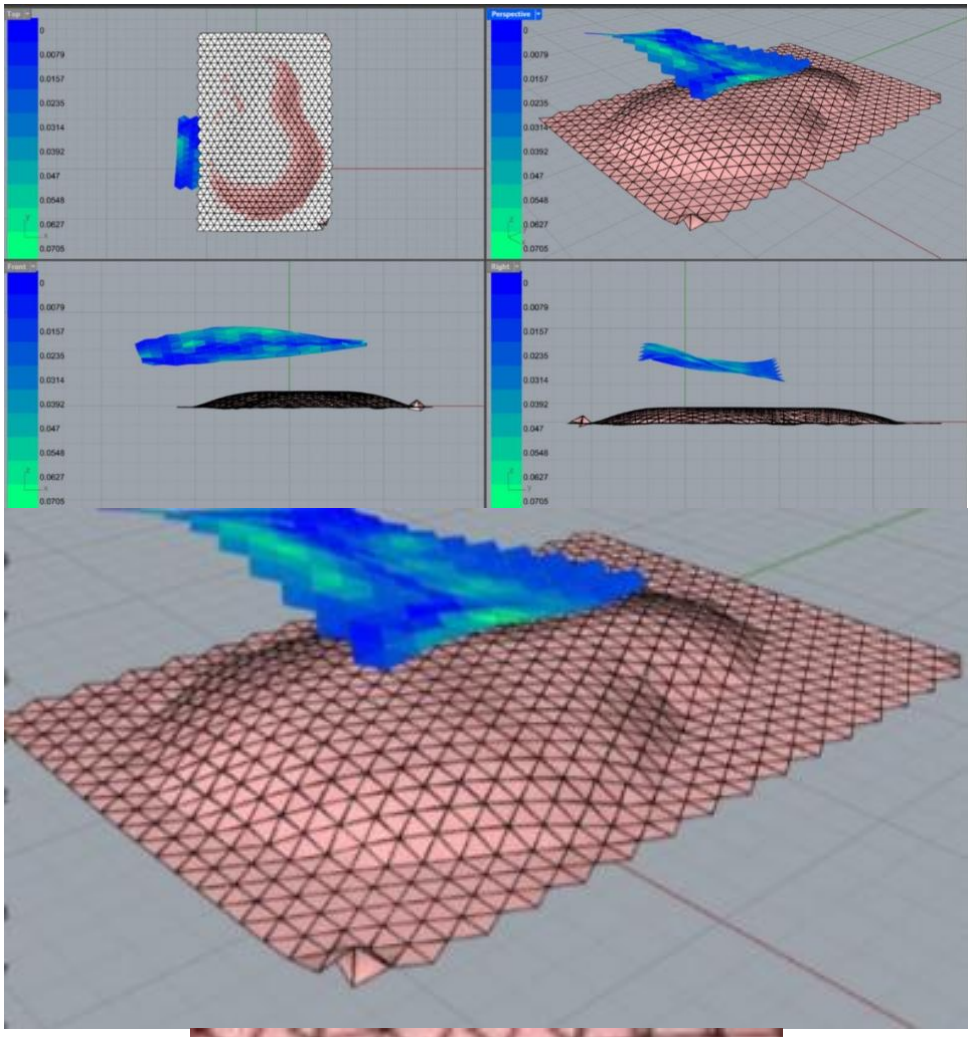

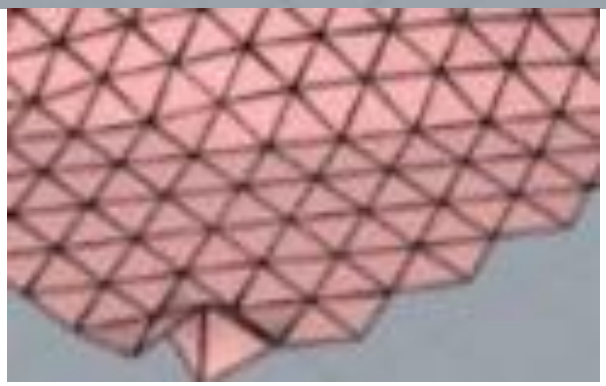

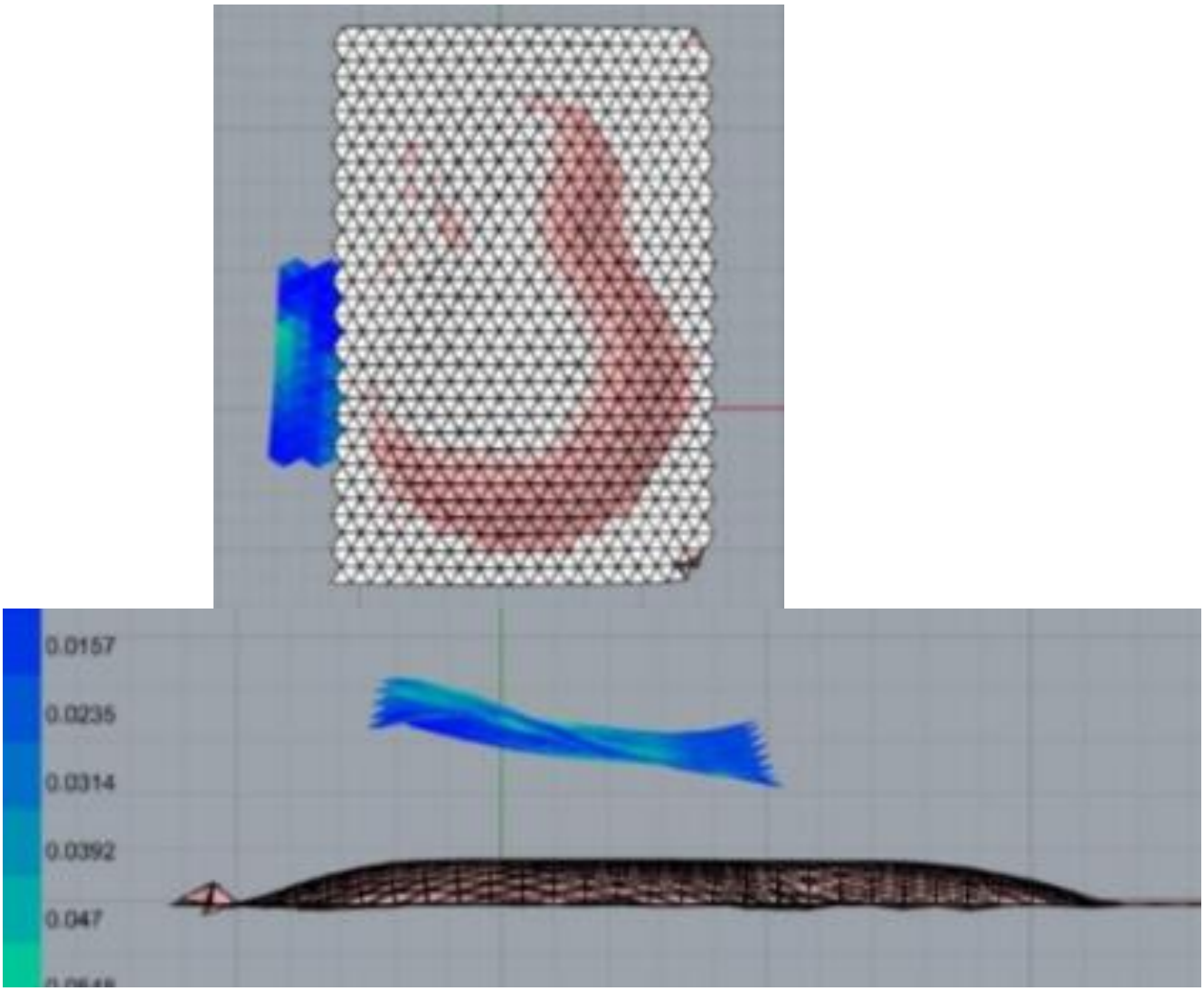

Figure 6.7-62 Isometric view of Outcomes from GH code , Tristar pattern laid on a simple double curve form. Redistribution and rotation based on the XYZ coordinates of the curvature

6.7.6.4 Iterative Rotating expansion based on XYZ displacement conformal mapping – simulation trial #17

Grasshopper code -rational and logic

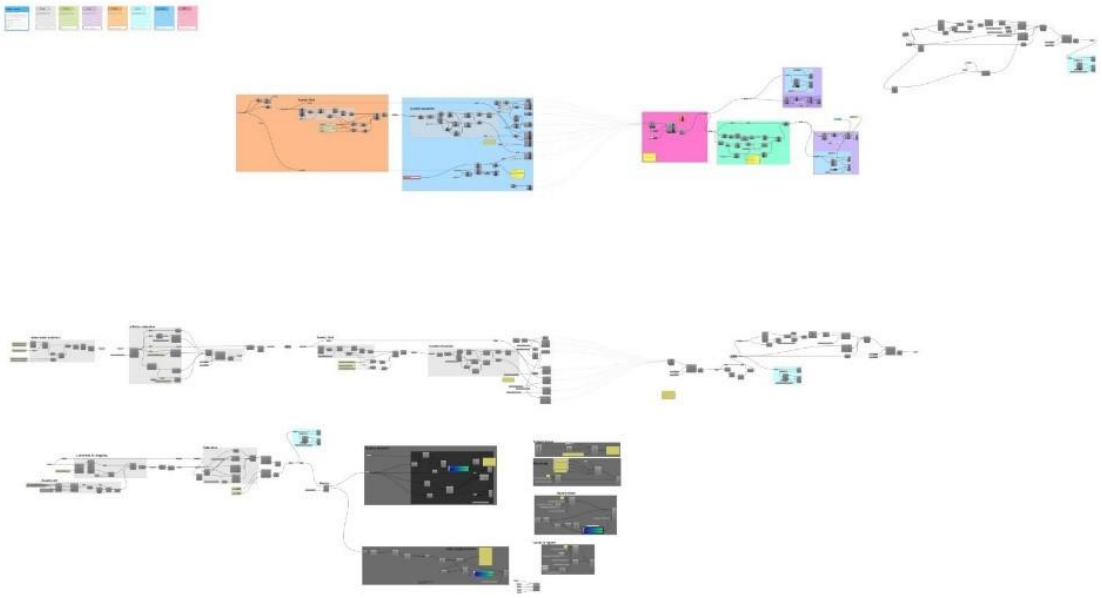

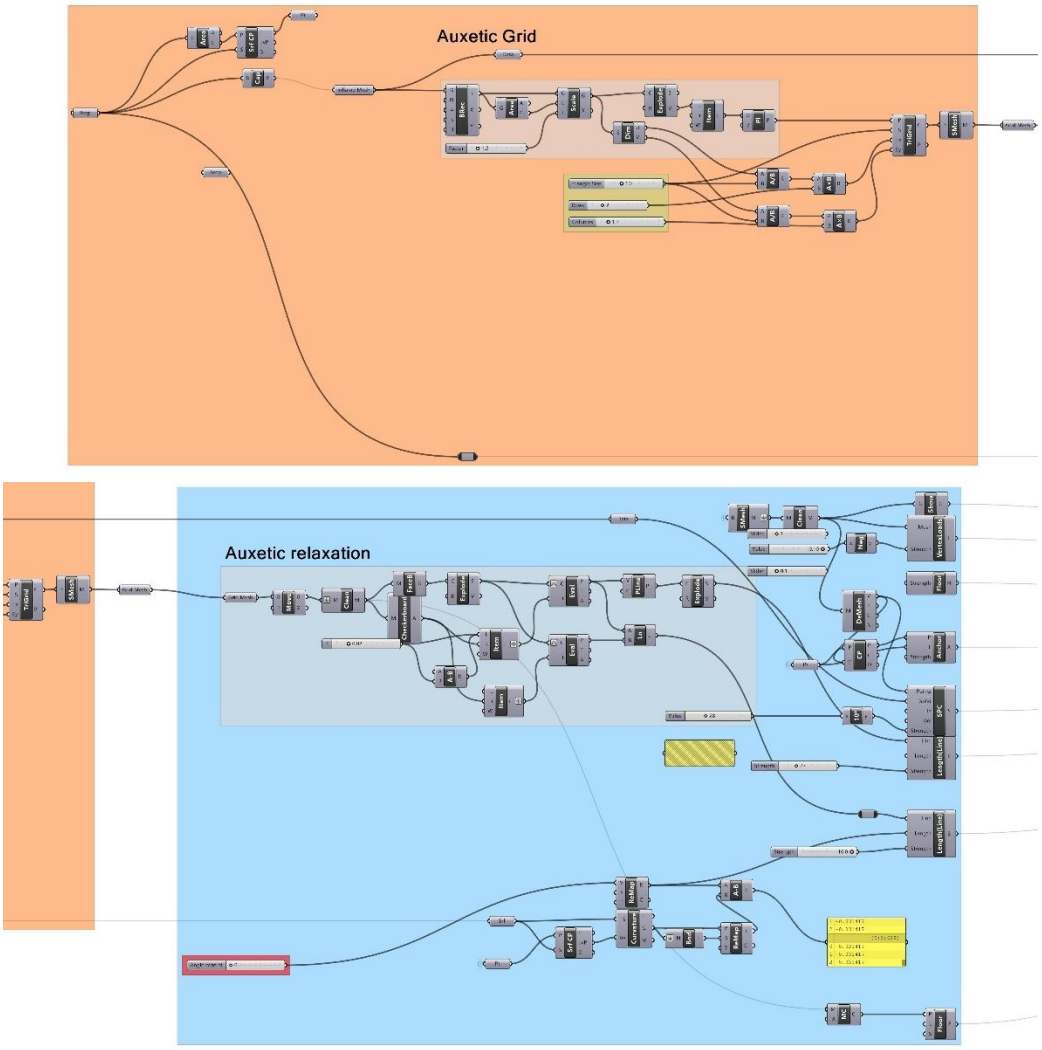
Auxetic Grid
Auxetic relaxation

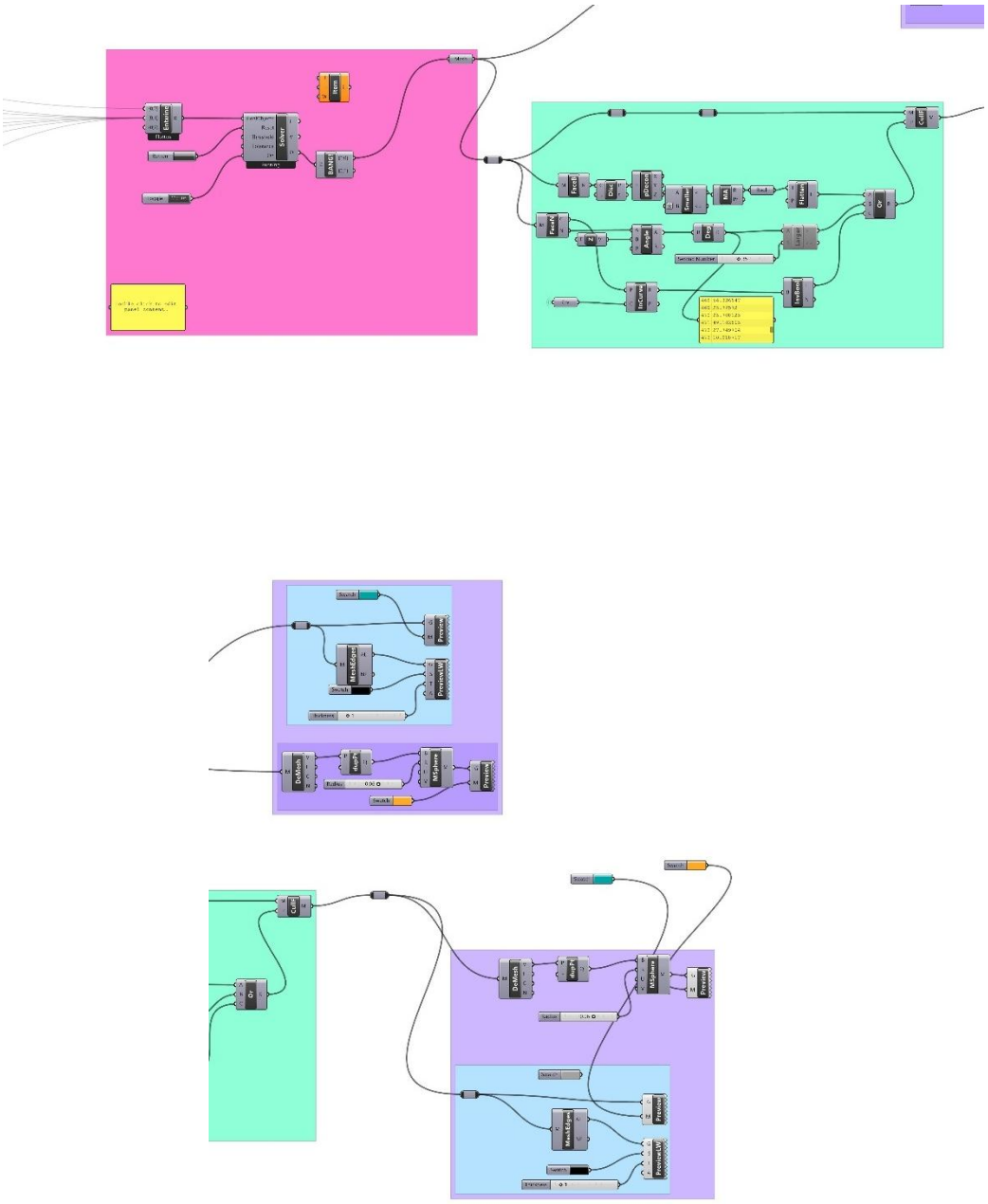

Figure 6.7-63 Grasshopper iterative simulations for 3D expansion based on XYZ axis conformal mapping displacement – Trial #23

Results in different angles

The following are the results as we change the logic between 0 ,30 ,60, 90 & 120

At angle 0 :
Laid on the curve but with 0 degree of restriction factor

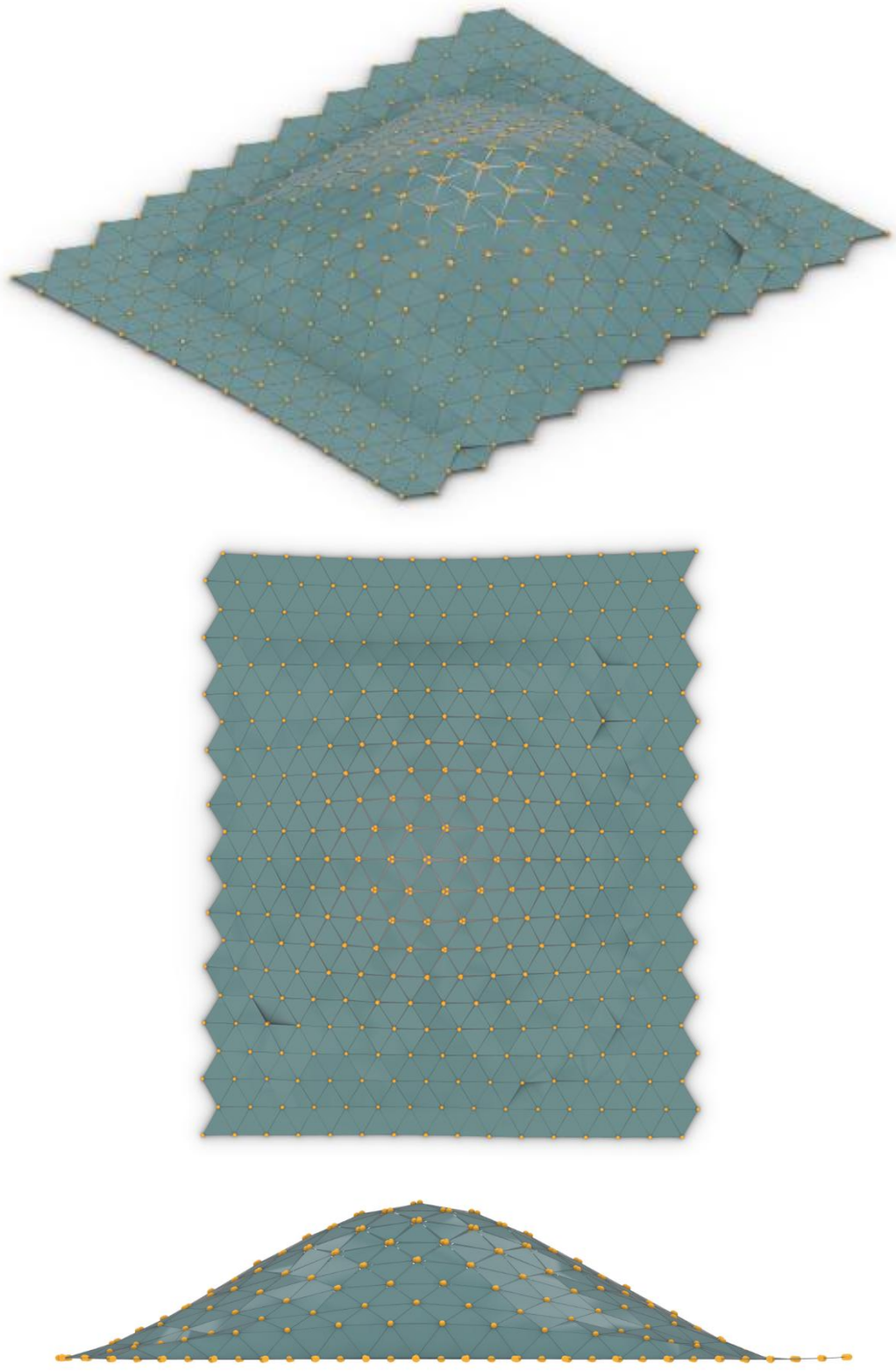

Figure 6.7-64 Displacement conformal mapping results - 0 degree restricting factor- isometric , top and front views

At angle 30 :
Laid on the curve but with 30 degree of restriction factor

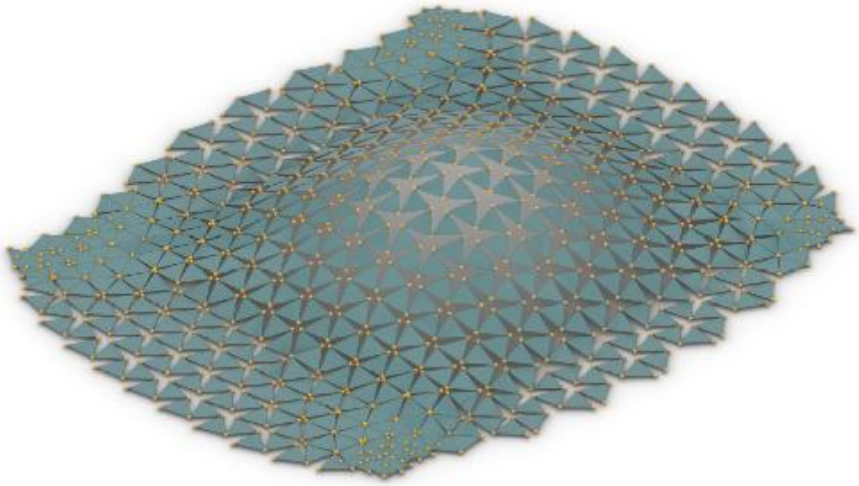

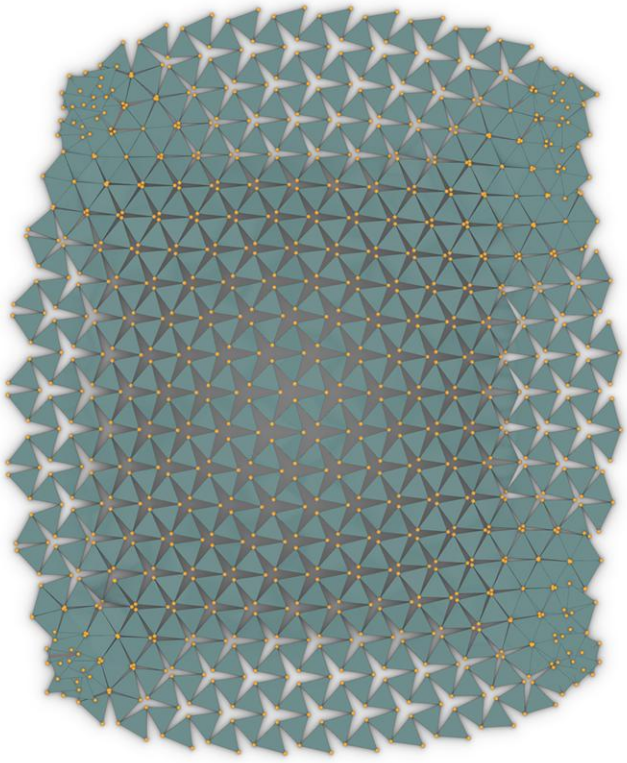

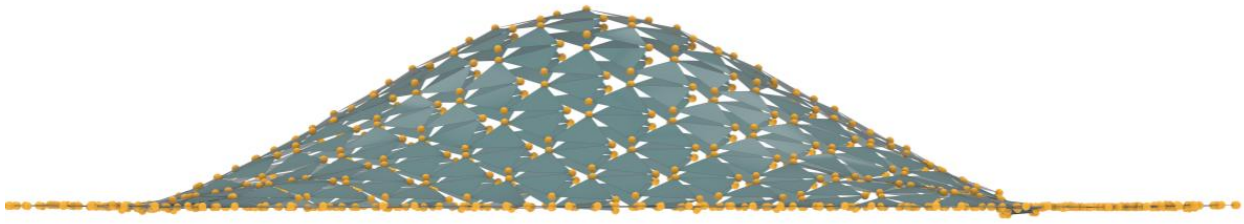

Figure 6.7-65 Displacement conformal mapping results - 30 degree restricting factor- isometric , top and front views

At angle 60 :
Laid on the curve but with 60 degree of restriction factor

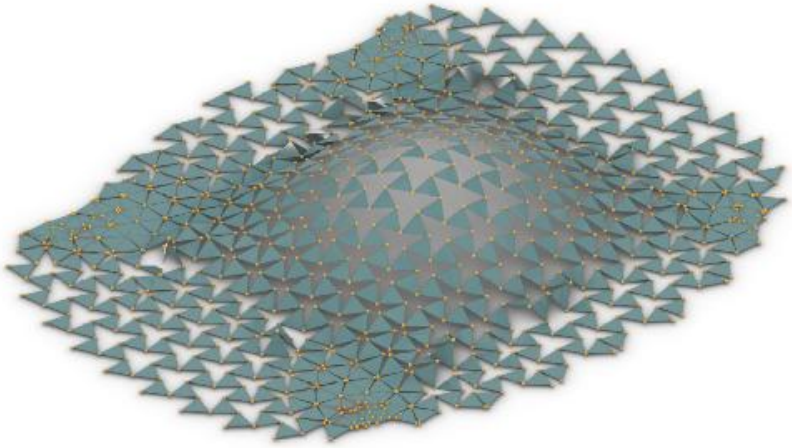

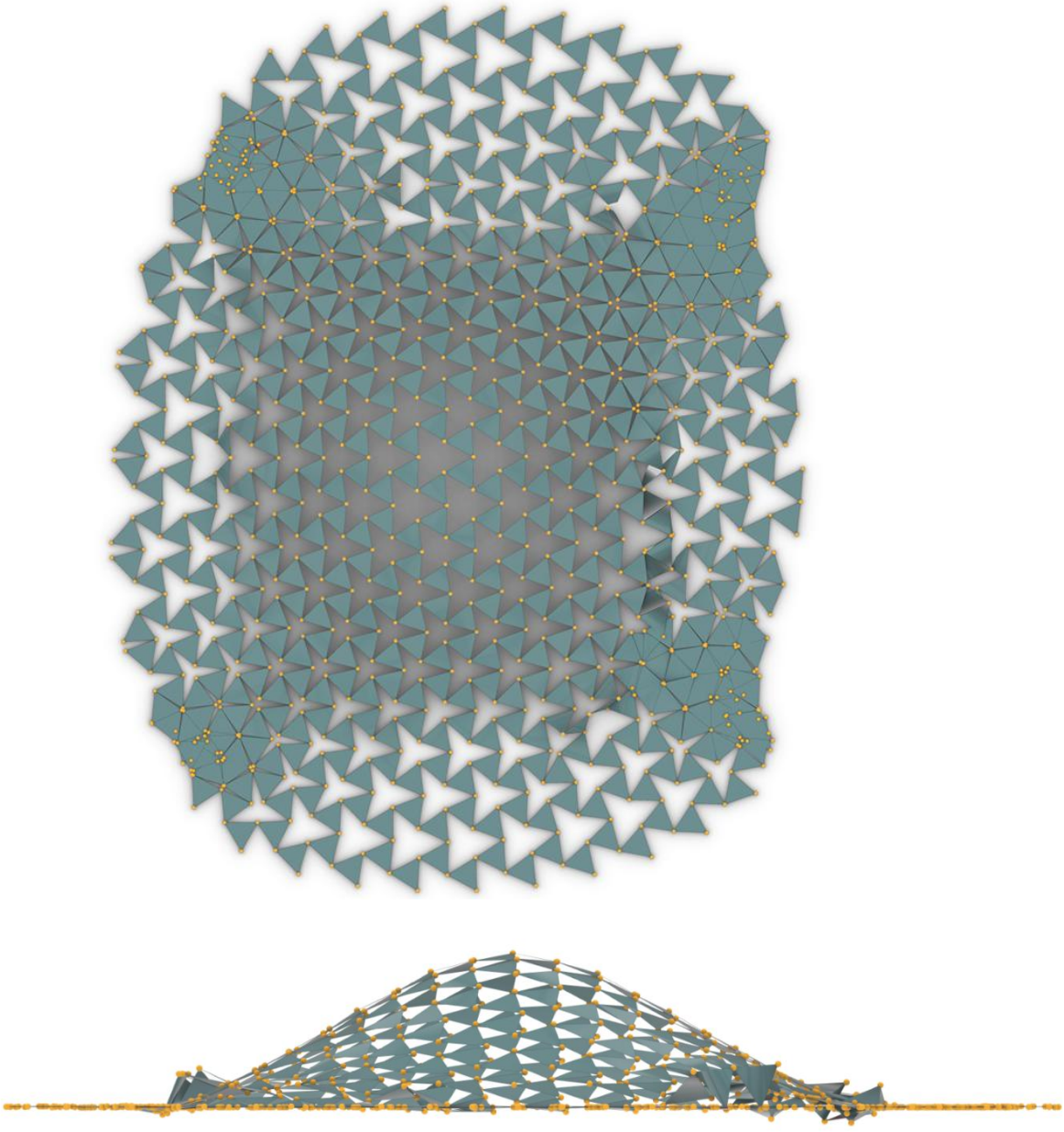

Figure 6.7-66 Displacement conformal mapping results - 60 degree restricting factor- isometric , top and front views

At angle 90 :
Laid on the curve but with 90 degree of restriction factor

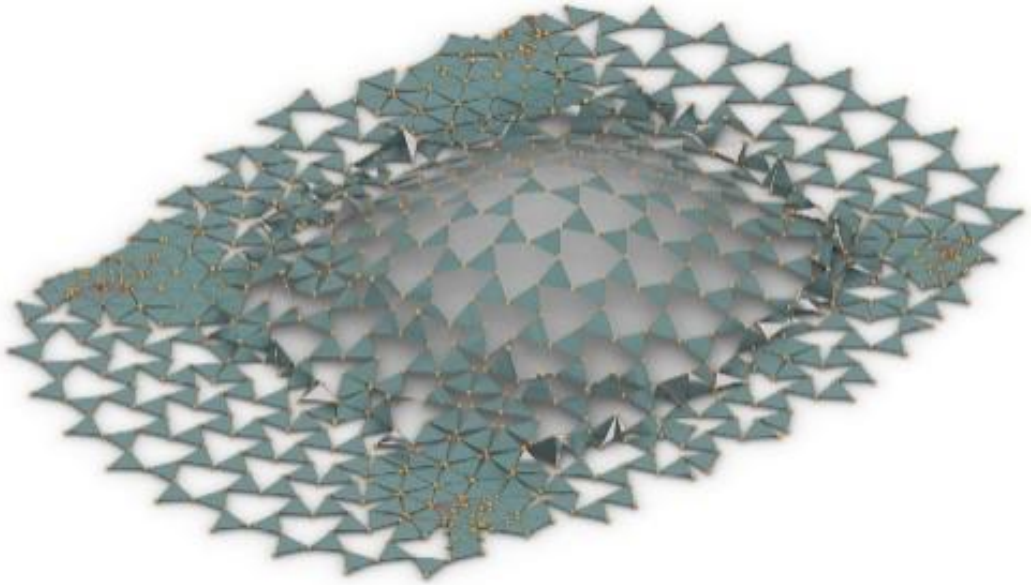

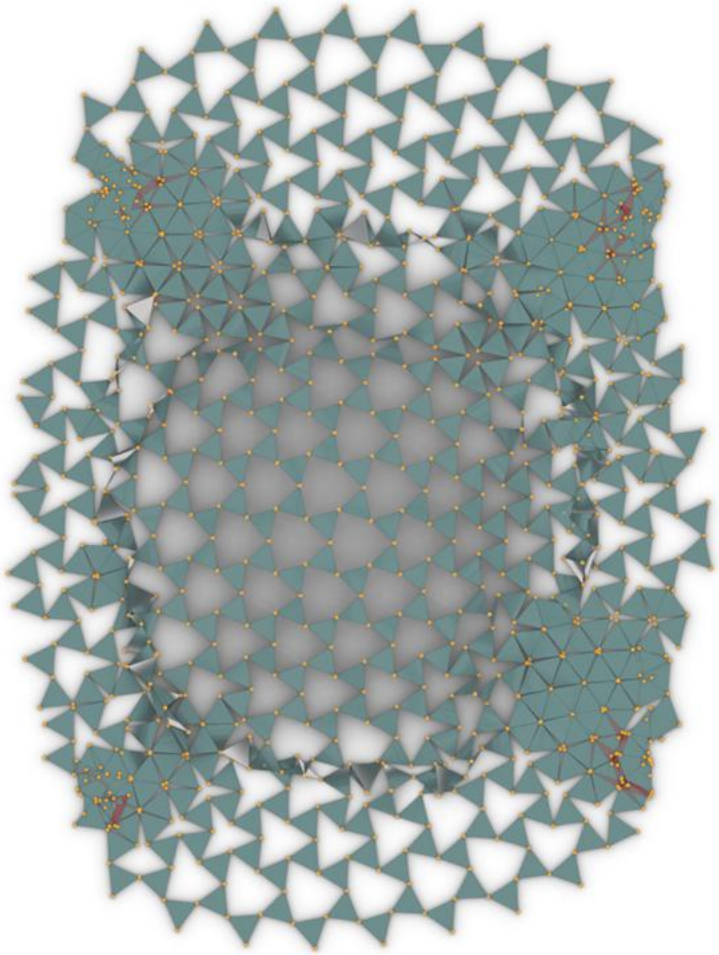

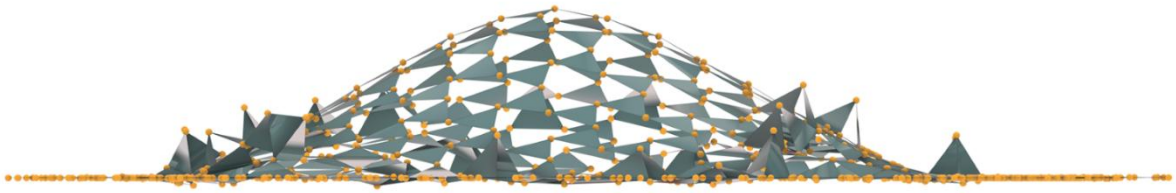

Figure 6.7-67 Displacement conformal mapping results - 90 degree restricting factor- isometric , top and front views

At angle 120 :
Laid on the curve but with 120 degree of restriction factor

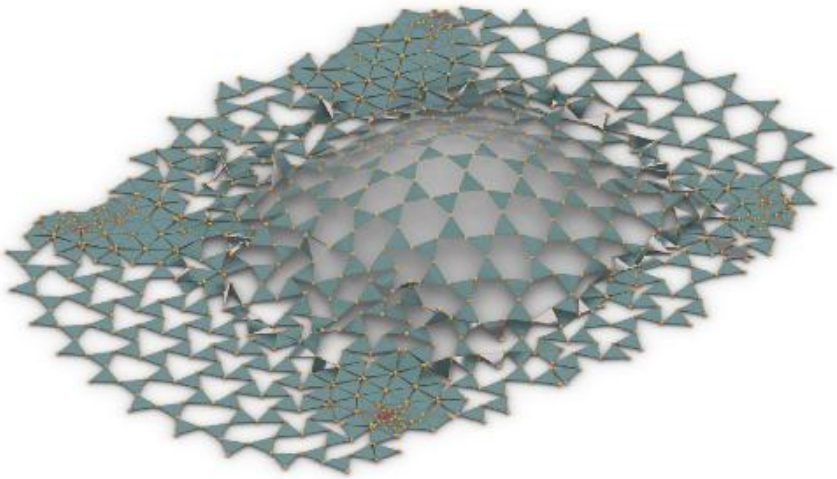

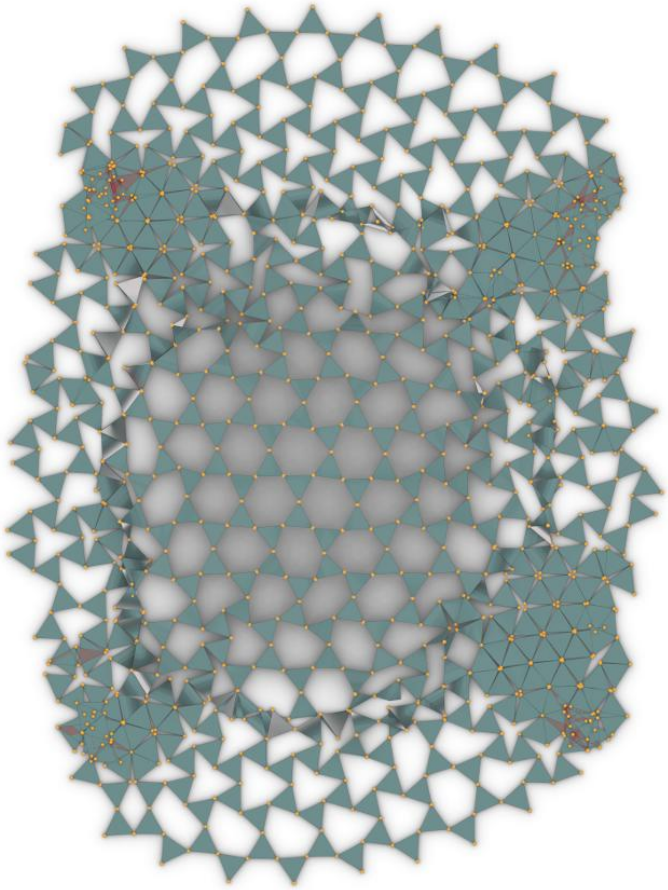

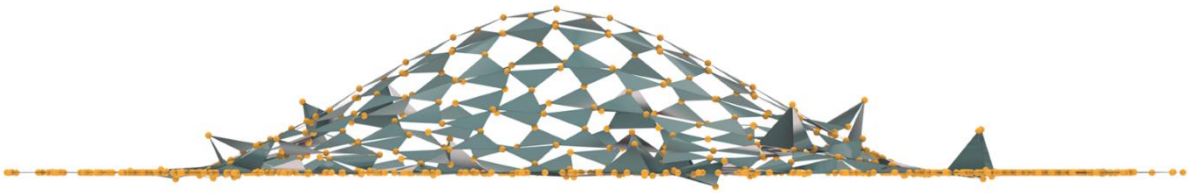

Figure 6.7-68 Displacement conformal mapping results - 120 degree restricting factor- isometric , top and front views

The Full expansion gives us the understanding of the working of code but a few parts are exhibiting undesired results , so to check the accuracy of the curvature adaptation within bounds we apply a Cull logic to hide or cut off the unit triangles outside the bounding edges of the curve form .

This gave a clear delineation of unexpected reactions within the curvature bounds

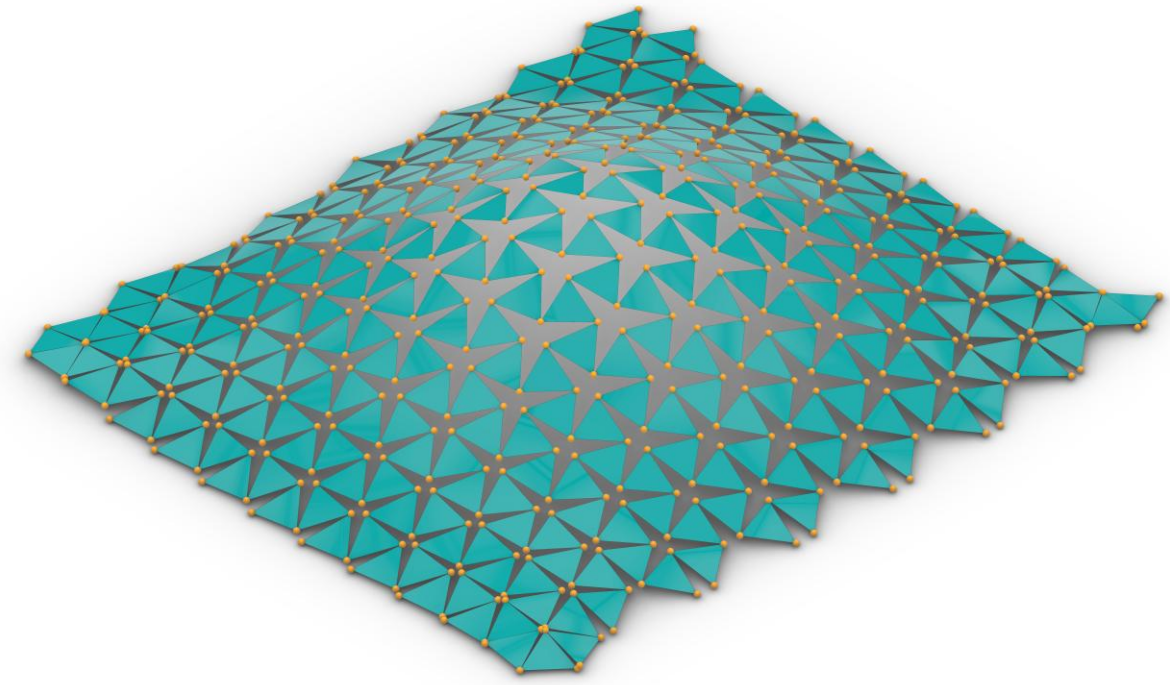

Figure 6.7-69 Displacement conformal mapping results - 30 degree restricting factor- isometric Culled outside geometry results

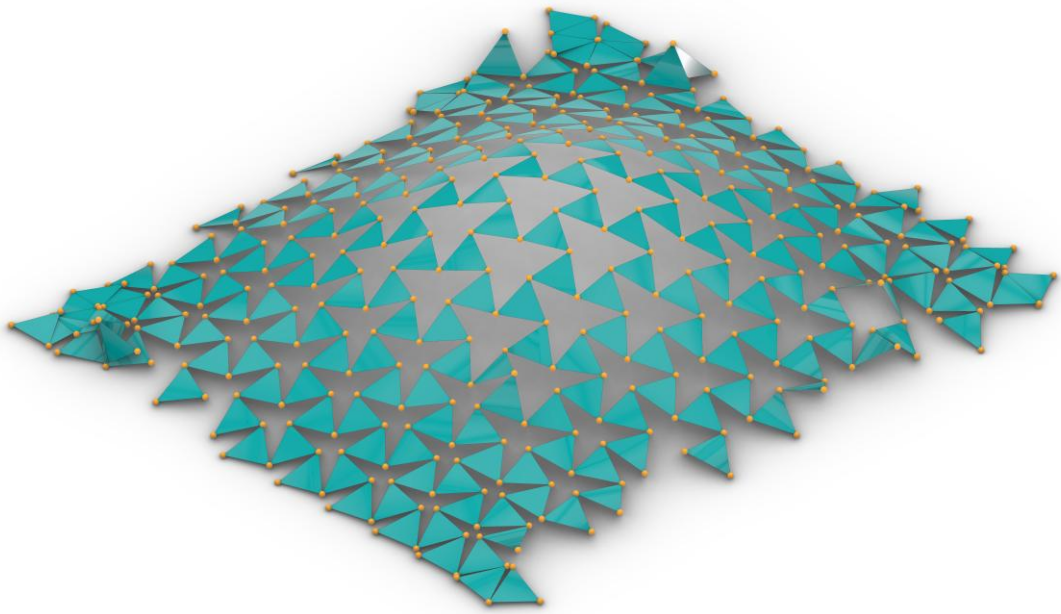

Figure 6.7-70 Displacement conformal mapping results - 60 degree restricting factor-isometric Culled outside geometry results

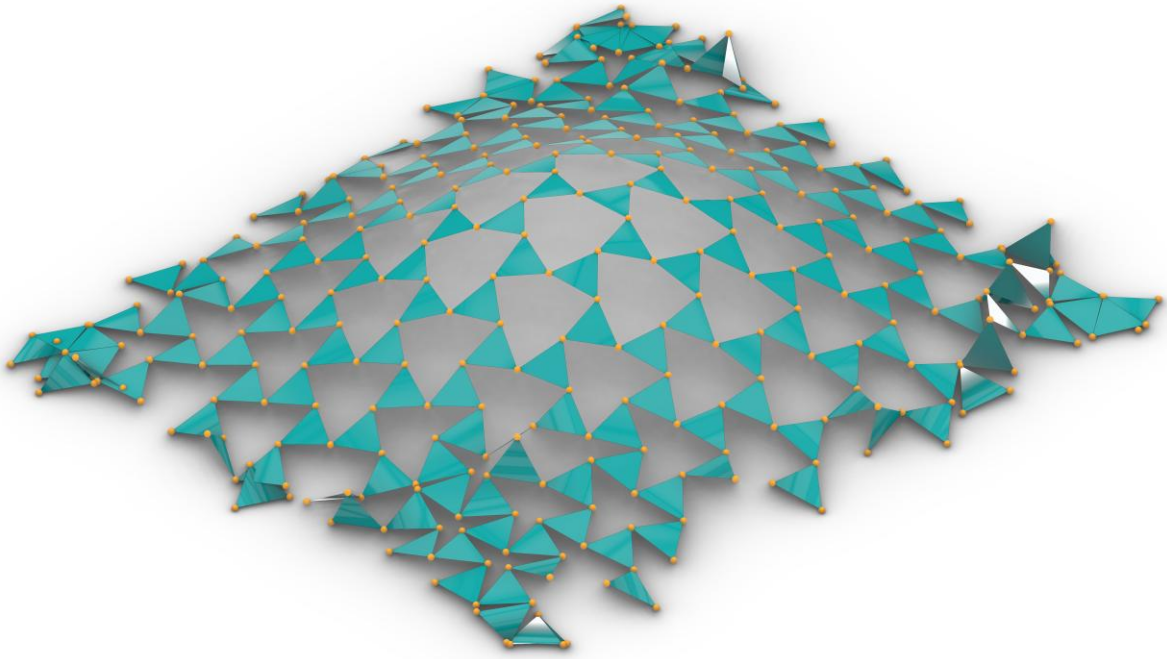

Figure 6.7-71 Displacement conformal mapping results - 90 degree restricting factor-isometric Culled outside geometry results

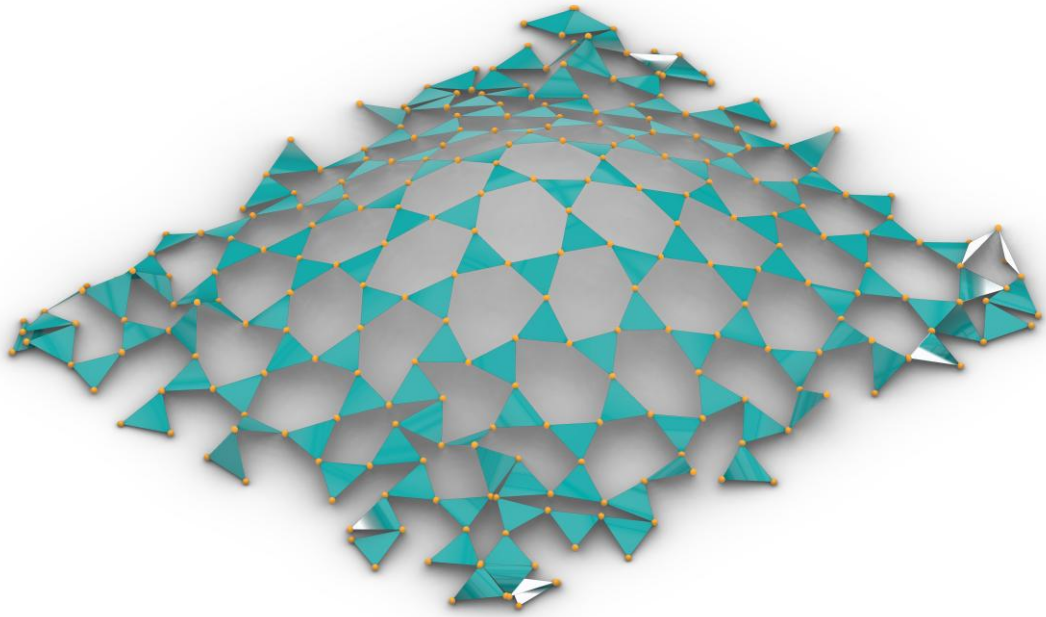

Figure 6.7-72 Displacement conformal mapping results - 120 degree restricting factor-isometric Culled outside geometry results

6.7.7 Appendix G : Building the model – Process documentation

6.7.7.1 Scale and Geometric Basis

The prototype was constructed at a 1:5 scale, enabling a manageable balance between precision and portability. The original unit geometry was derived from an equilateral triangle with a 500 mm side length. In the scaled-down version, each triangle measured 100 mm, retaining the proportional integrity of the system while making it suitable for laser cutting and manual assembly. The rotational factoring units, representing the range of joint-based angular movement, were scaled to approximately 100–150 mm, depending on nodal spacing and pivot distribution.

This setup allowed for an accurate physical replication of the Tristar grid, enabling the testing of both 2D and 3D deformation logics, as explored in the computational simulations.

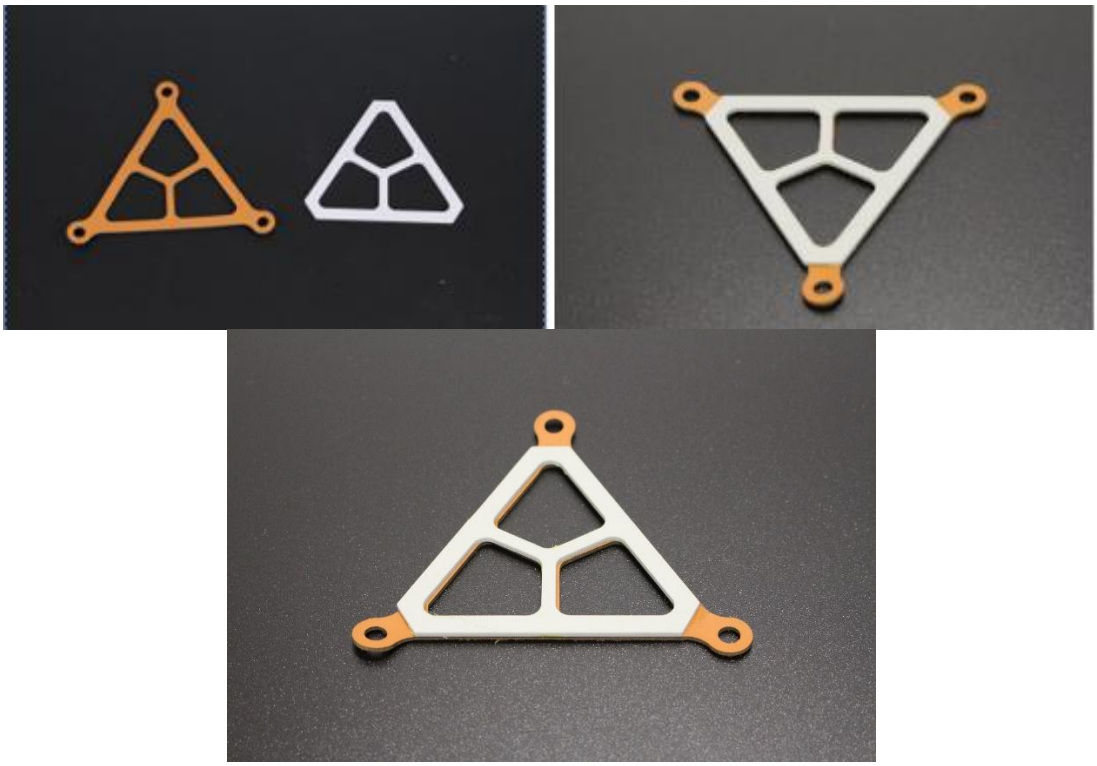

Figure 6.7-73 Single unit of scaled prototype

6.7.7.2 Material Logic and Joint Strategy

Each triangular unit was composed of a laser-cut leather element, selected for its inherent flexibility and suitability for pitch rotation (rotation along the Y-axis). The leather components acted as compliant joints between adjacent modules, enabling deformation without requiring complex hinge assemblies. However, the material's natural pliability also meant that pitch rotation was not precisely limited to the 30° threshold observed in simulations. As a result, minor deviations in angular behaviour were expected and observed during testing.

To reinforce the structure without compromising its flexibility, each leather triangle was laminated with a thin acrylic overlay. This provided additional rigidity, helped distribute applied loads across the surface, and preserved the planar integrity of the units, especially during full expansion states.

Binder screws were employed as the yaw rotation pivots, enabling controlled rotation between units around the Z-axis. While they effectively facilitated the mechanical behaviour of yaw, they did not include built-in limiters, allowing some units to rotate beyond the 120° cap defined in digital constraints. This introduced useful insights into the practical limitations of free pivots and the importance of rotational regulation in future full-scale applications.

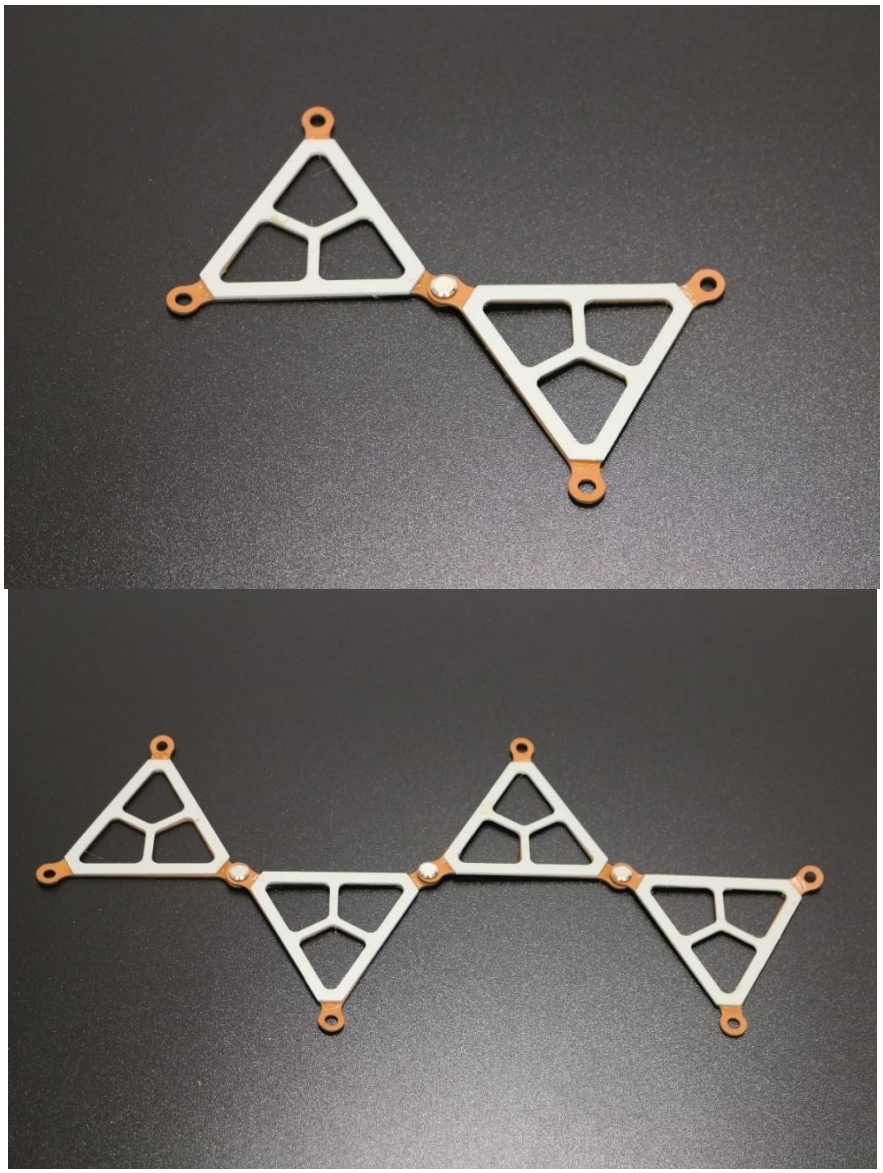

Figure 6.7-74 Multiple units Co-joint with Chicago screws

6.7.7.3 Assembly and Grid Configuration

The prototype consisted of 132 interconnected triangular modules, arranged in a planar Tristar tessellation pattern. This configuration mimicked the same connectivity logic as modelled in Rhino-Grasshopper environments, allowing for consistent comparison across digital and physical behaviours. The assembly process included:

Laser cutting of components

Manual lamination of leather and acrylic elements

Alignment and connection via binder screws

Mounting onto a flexible nylon string matrix for curvature testing

The modular system ensured that movement and deformation could be distributed evenly, and localized responses to curvature could be observed in real time.

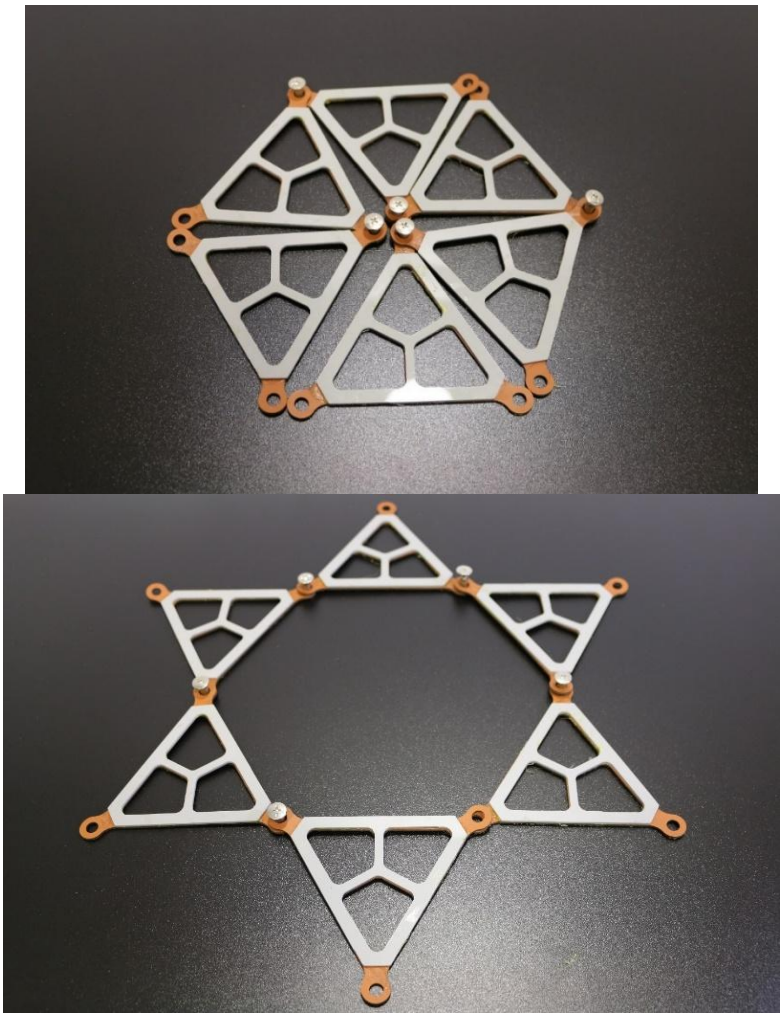

Figure 6.7-75 Multiple units Co-joint with Chicago screws- Rotation and behaviour

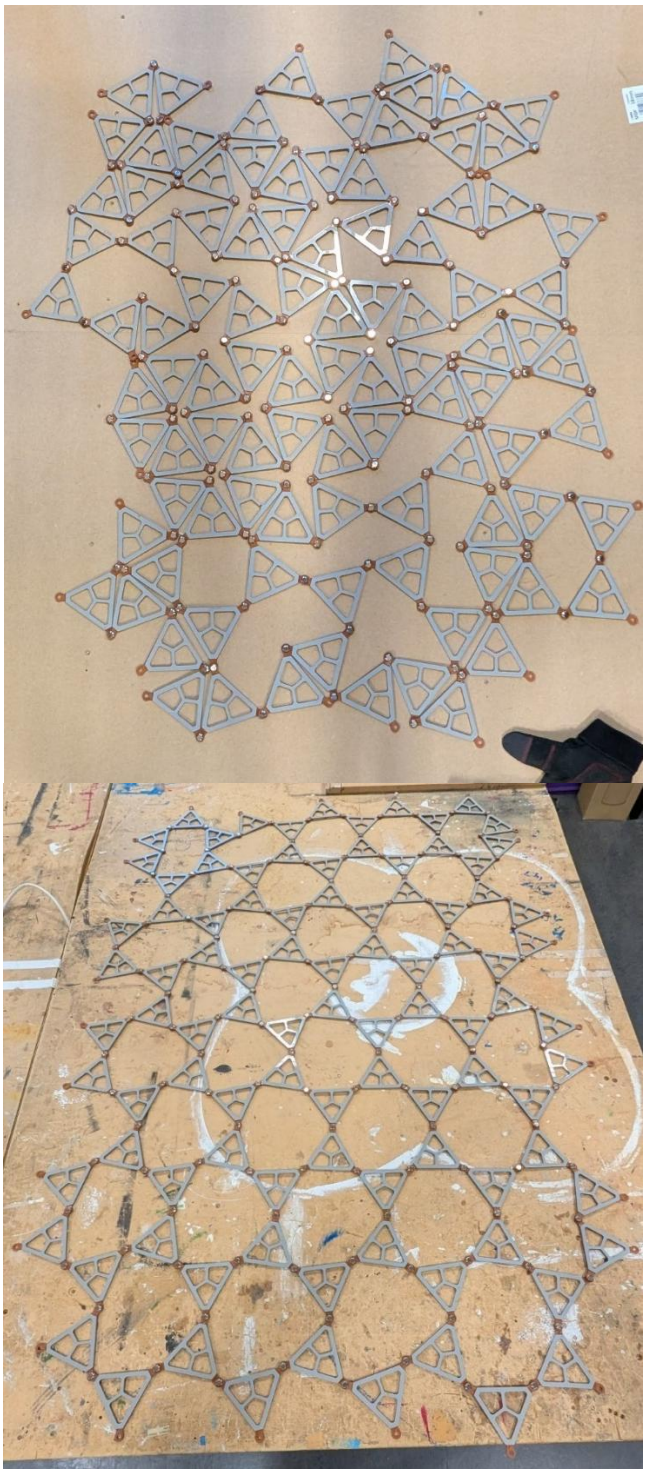

Figure 6.7-76 Auxetic Assembly expanded

6.7.7.4 Deployment Base Design and Control Mechanism

To physically replicate the complex deformation logic observed in simulation especially the vertical expansion and conformal adaptation of the auxetic sheet a custom mechanical base and deployment frame was constructed. This physical setup serves not only as a stable platform but also as an active control rig that facilitates the movement and manipulation of the prototype in three dimensions.

Structural Platform and Dimensions
The base of the deployment system was fabricated using sturdy MDF sheets, selected for their rigidity and ease of fabrication. The platform measures 1800 mm in length by 1200 mm in width, providing sufficient surface area to house the full 132-unit Tristar auxetic grid in its contracted state while allowing space for full expansion.

Four vertical support poles, each 900 mm in height, are mounted securely on the corners of the base. These standing poles act as the primary suspension points for the upward movement of the sheet and are crucial for introducing controlled vertical displacement. Their height is calibrated to match the approximate Z-axis range required to simulate double-curved shell transformations at this 1:5 scale.

Figure 6.7-77 Wooden frame Work in Progress

Marionette-Inspired Central Control System
In addition to the corner supports, the system incorporates four internal support poles arranged near the center of the base. These serve as active tension control points, mimicking a marionette-inspired movement system. By strategically pulling from these inner poles, the sheet can be manipulated to create various local curvature forms such as domes, valleys, or saddles simulating the same differential displacements applied in the digital attractor or XYZ conformal simulations.

Each internal pole connects to a rotational gear mechanism, which was custom-designed and 3D printed. These gears are fixed atop the poles and contain integrated slots for winding nylon strings, which are anchored to metal hooks at their free ends. These hooks are inserted into selected nodal points of the auxetic grid to lift or deform local regions of the sheet. By turning the gear manually, tension is applied gradually and with control, allowing fine-tuned vertical expansion from multiple points.

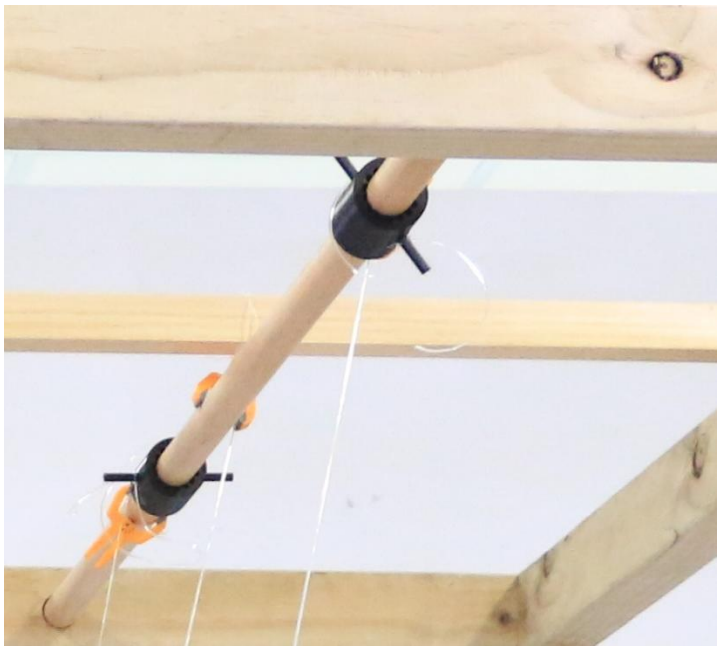

Figure 6.7-78 Marionette contraption - 3d printed parts

Figure 6.7-79 Marionette contraption - 3d printed parts assembled in frame

Base-Level Zip-Track Expansion System

While vertical displacement is critical, horizontal movement across the XY plane is equally important for realizing the complete spatial behaviour of the Tristar system. To achieve this, a base track system was introduced, positioned beneath the main auxetic assembly. This component was also 3D printed, featuring a zip-track or ratchet-tooth system that enables gradual outward expansion of anchor points.

The track system functions as a sliding base anchor, allowing the grid's perimeter nodes to shift outward as the system expands. This is essential because vertical movement in the Tristar logic is not purely linear it is interdependent with base-level planar expansion. Without allowing the base to open, the grid cannot unfold properly in the Z-direction, as the triangles need lateral separation in order to rotate and achieve the auxetic spread.

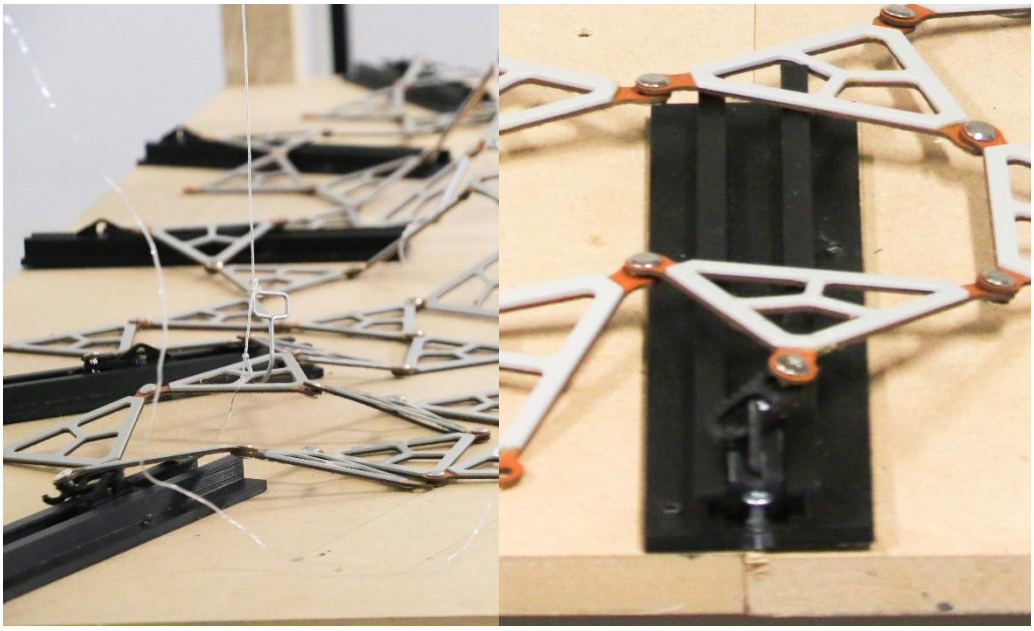

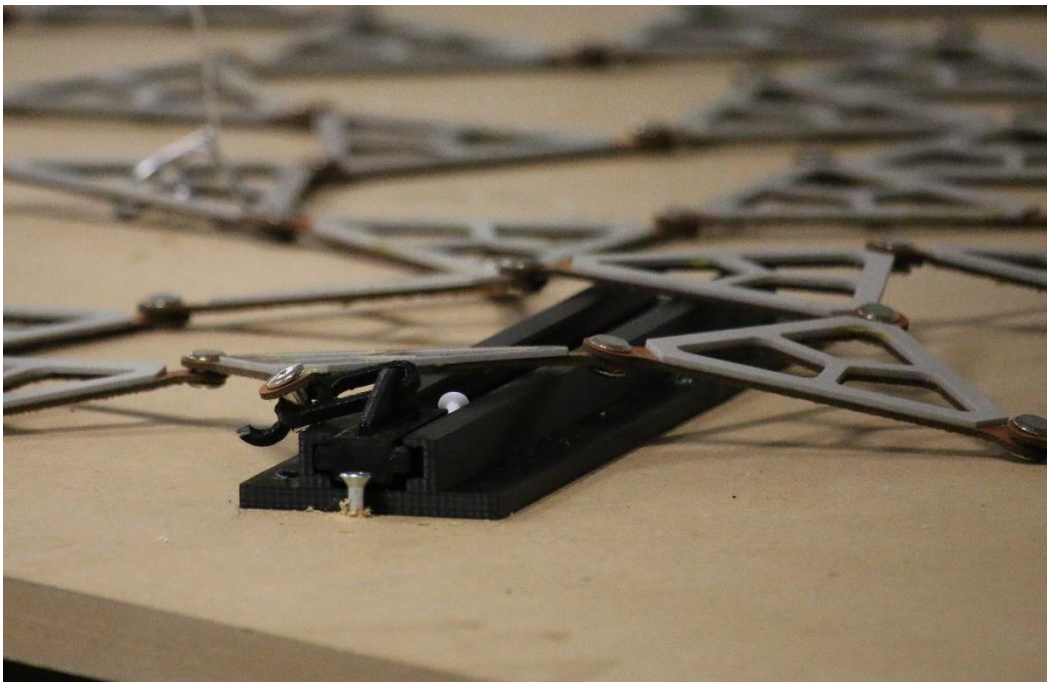

Figure 6.7-80 3D printed Rail track systems

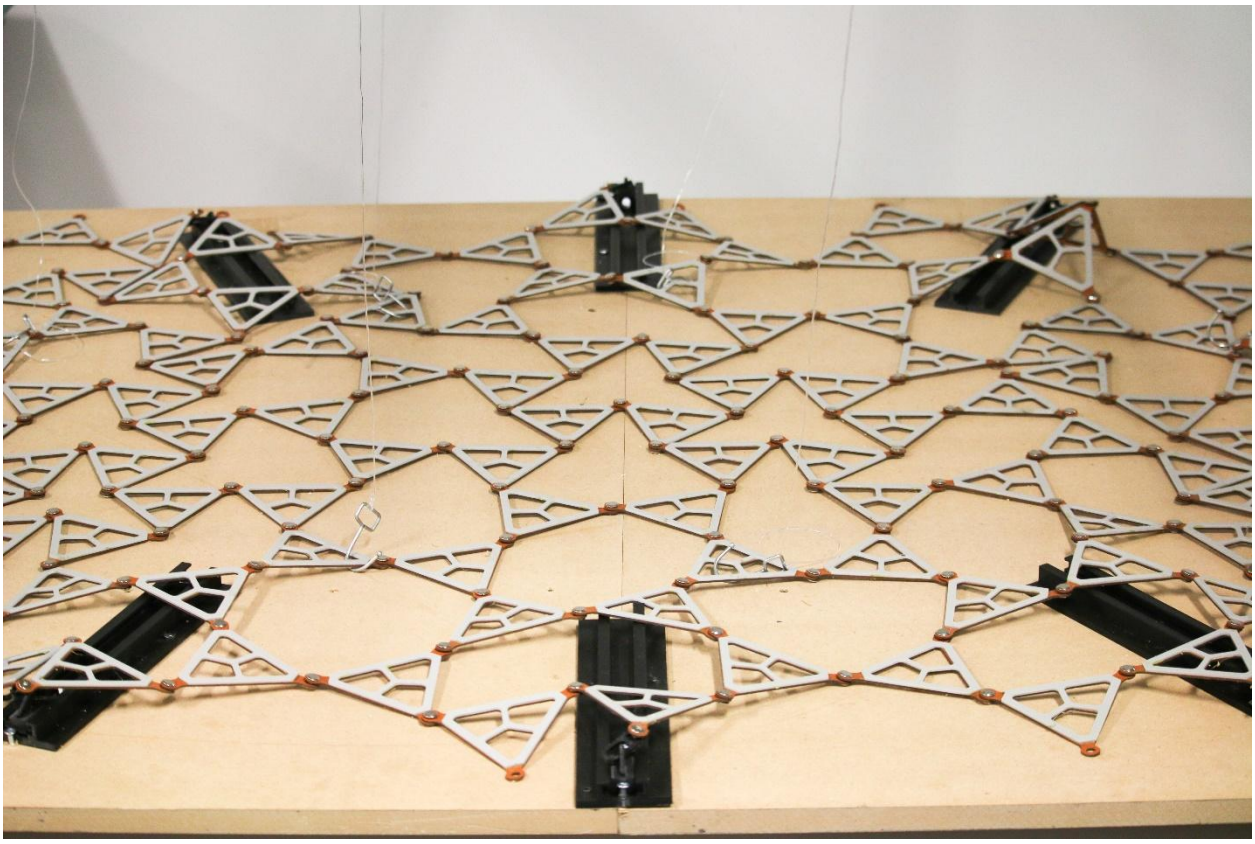

Figure 6.7-81 3D printed Rail track systems with Auxetic system

Thus, the base expansion mechanism mirrors the parametric logic from the simulations, where 3D conformal mapping required both vertical and horizontal deformation to create doubly-curved forms. The zip system ensures controlled, incremental planar movement that synchronizes with the vertical lifting mechanism, allowing a coordinated, realistic deployment sequence.

Assembly process documentation

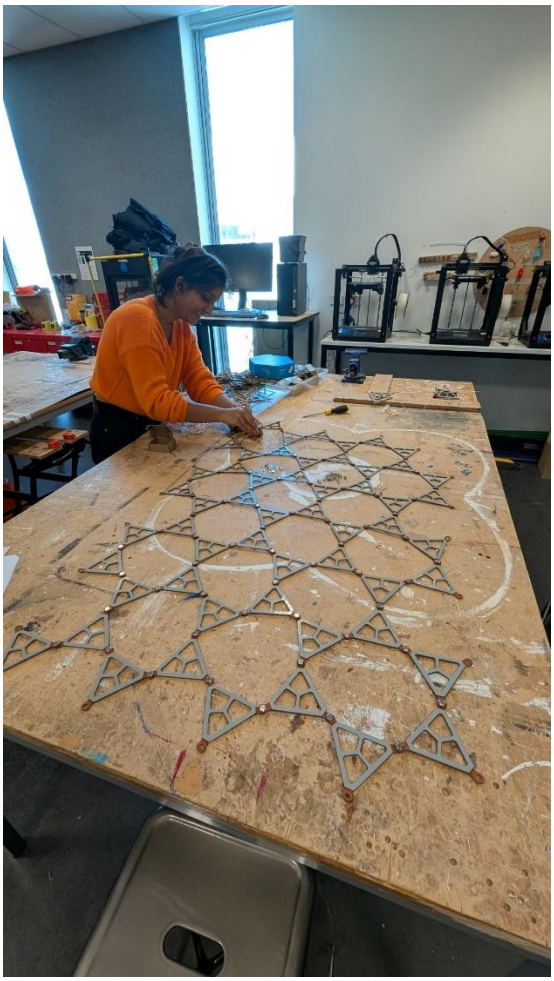

Figure 6.7-82 WIP for assembly of patterns

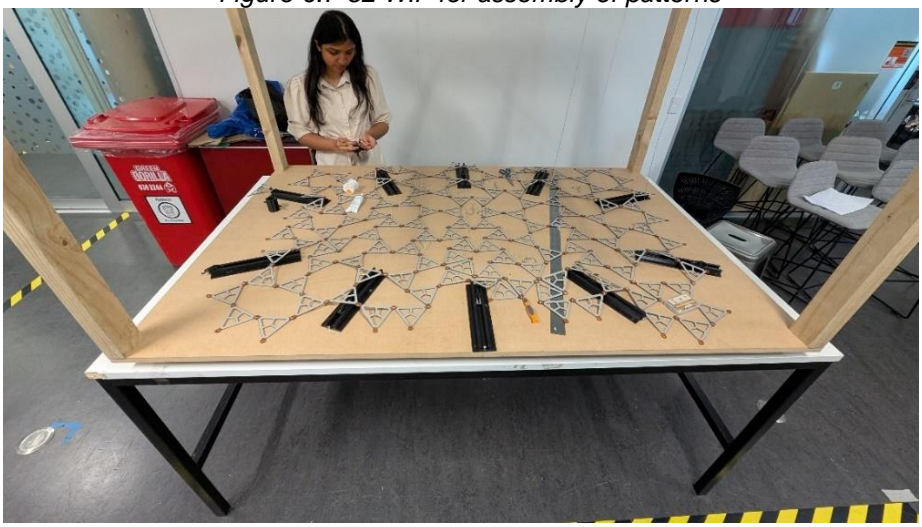

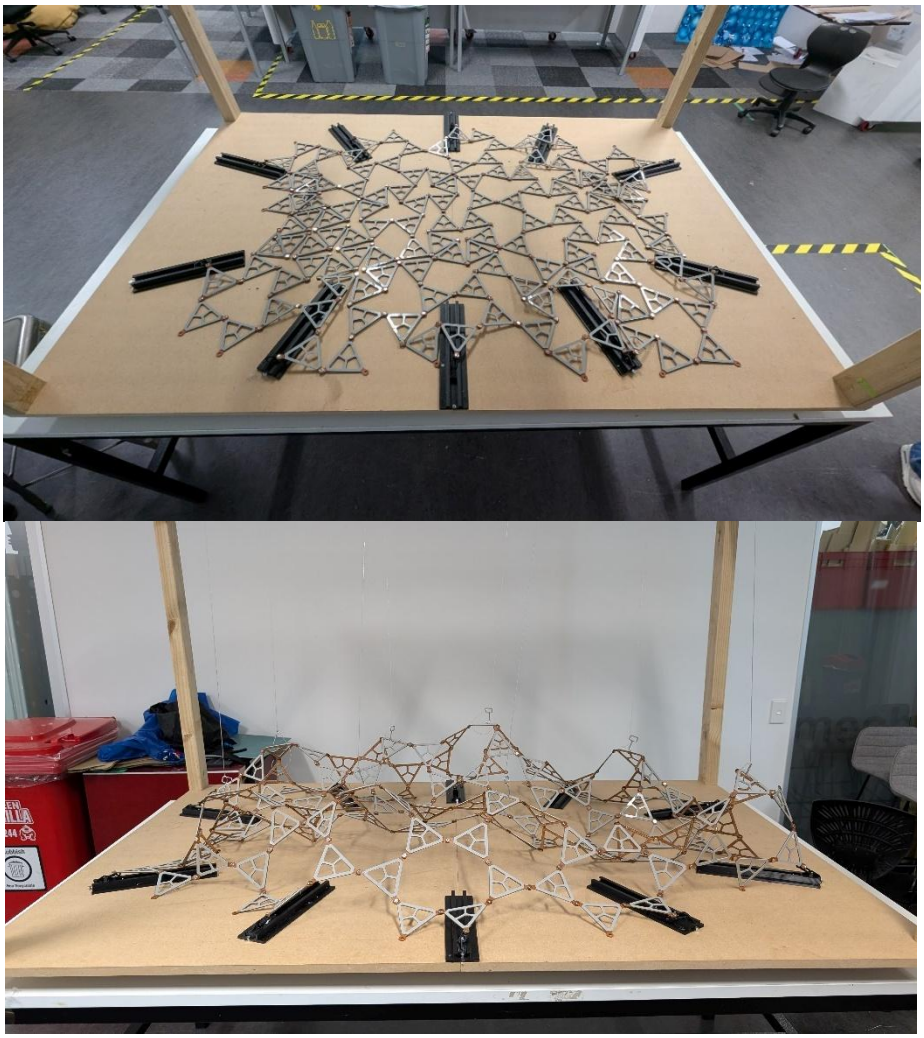

Figure 6.7-83 WIP assembly of full system -initial testing

6.7.8 Appendix H : Deployment Behaviour and Motion Testing

Stage 1 - Fully retracted and compressed

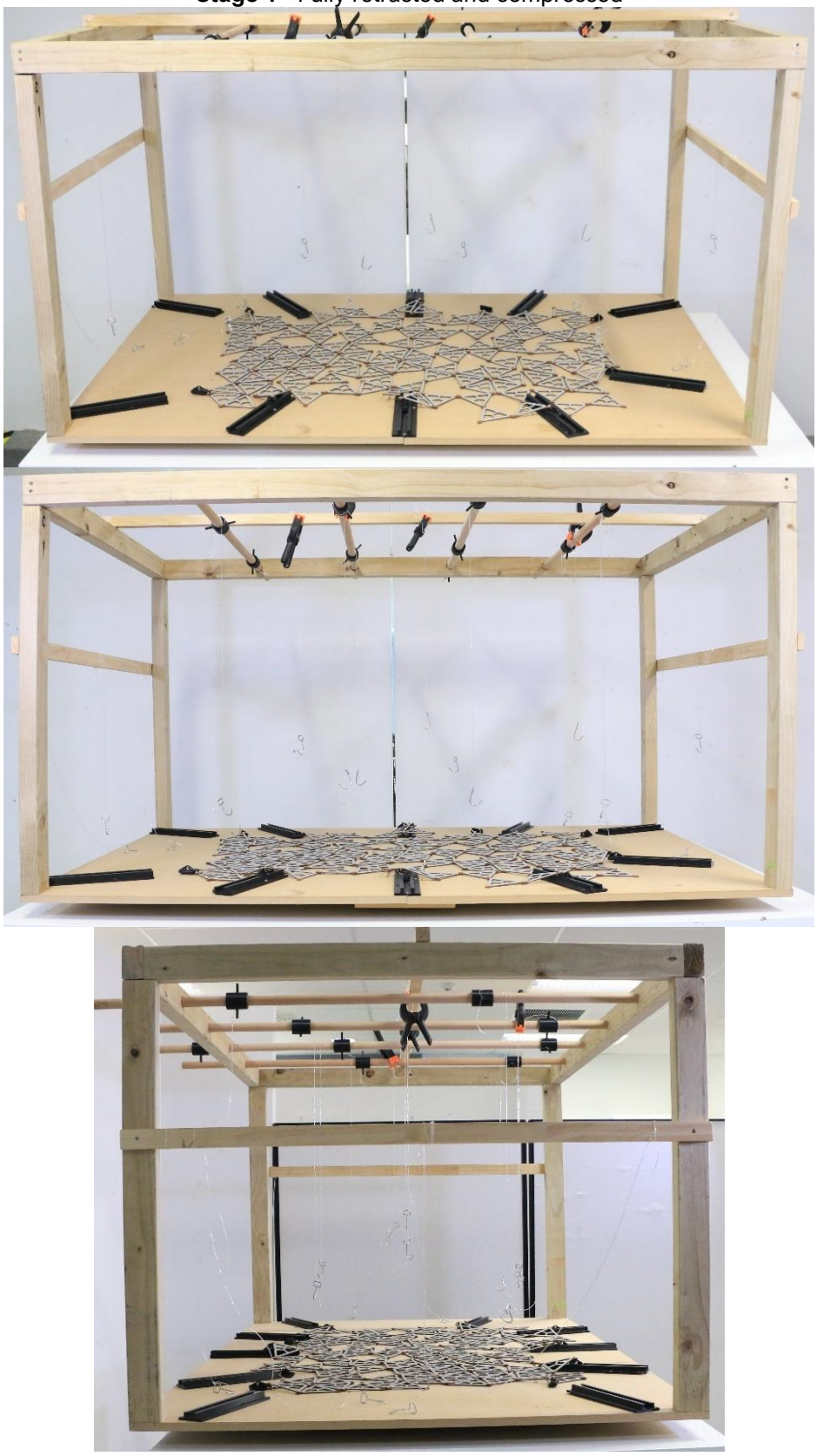

Figure 6.7-84 Deployment behaviour and analysis of Scaled prototype- Stage 1

Stage 2 -base rail moved outward by 30 mm to 50 mm center lifted by 100 mm

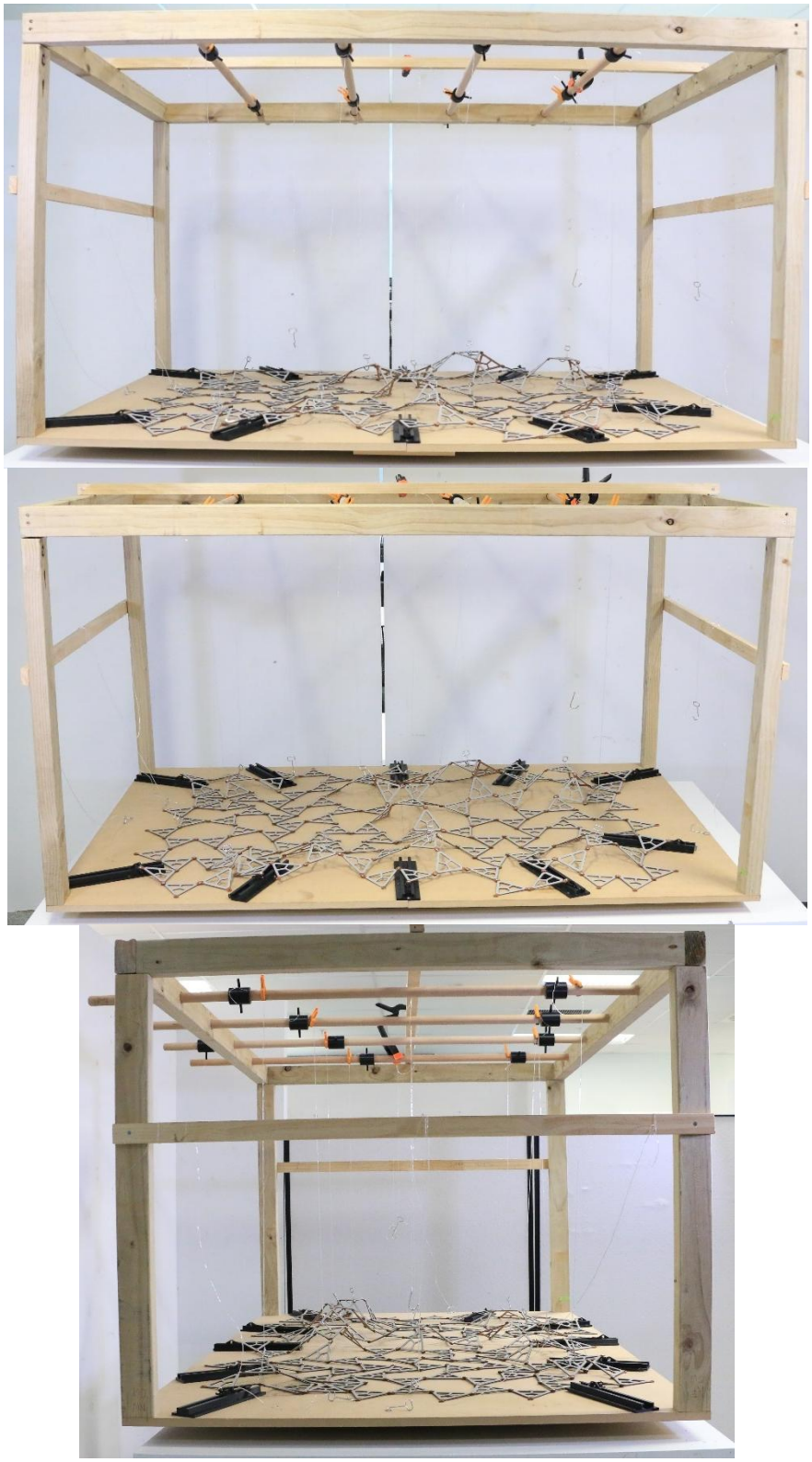

Figure 6.7-85 Deployment behaviour and analysis of Scaled prototype- Stage 2

Stage 3- Base rail moved outward by 30 mm to 50 mm centre lifted by 200 mm

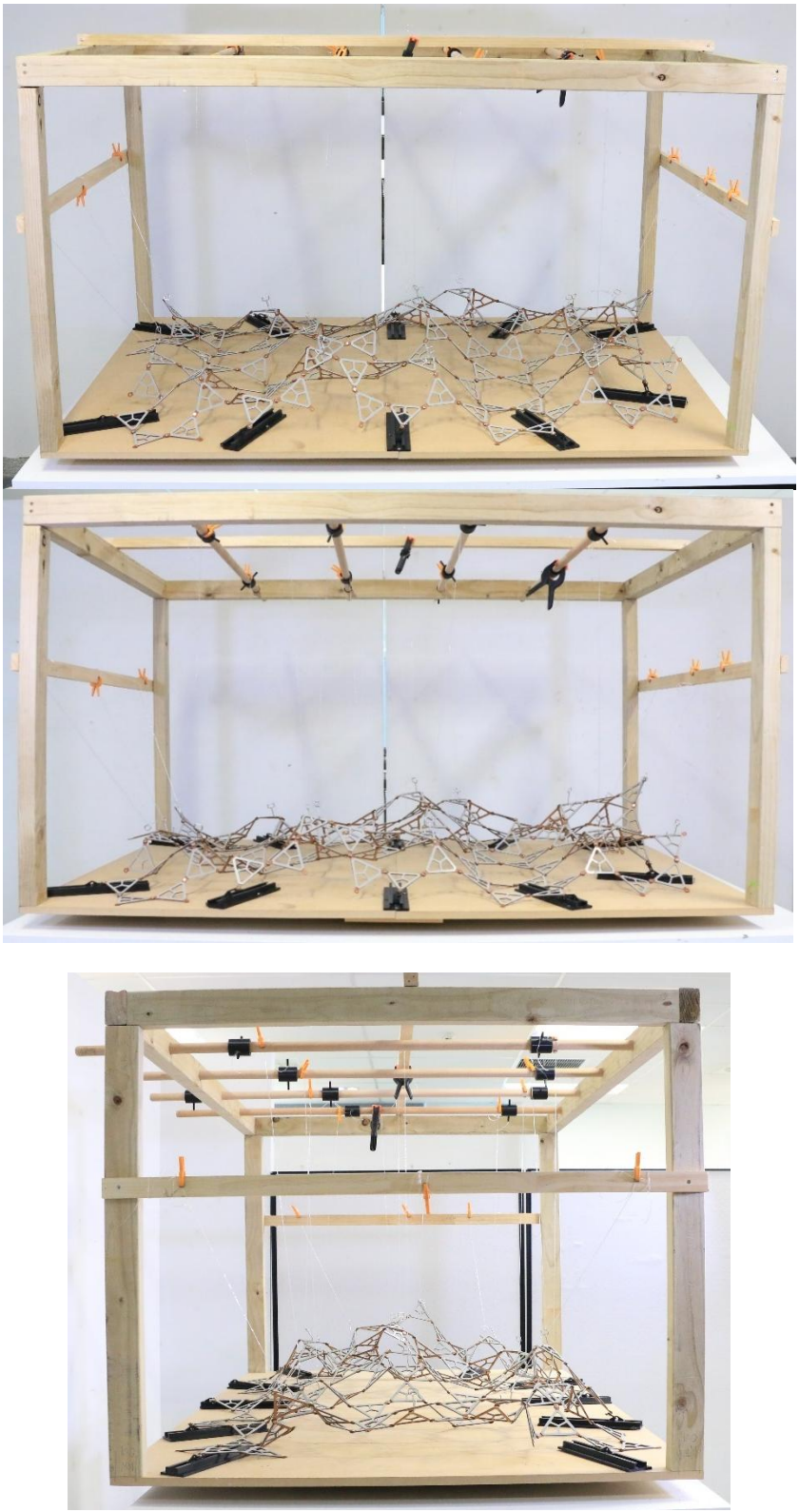

Figure 6.7-86 Deployment behaviour and analysis of Scaled prototype- Stage 3

Stage 4- base rail moved outward by 30 mm to 50 mm centre lifted by 300 mm

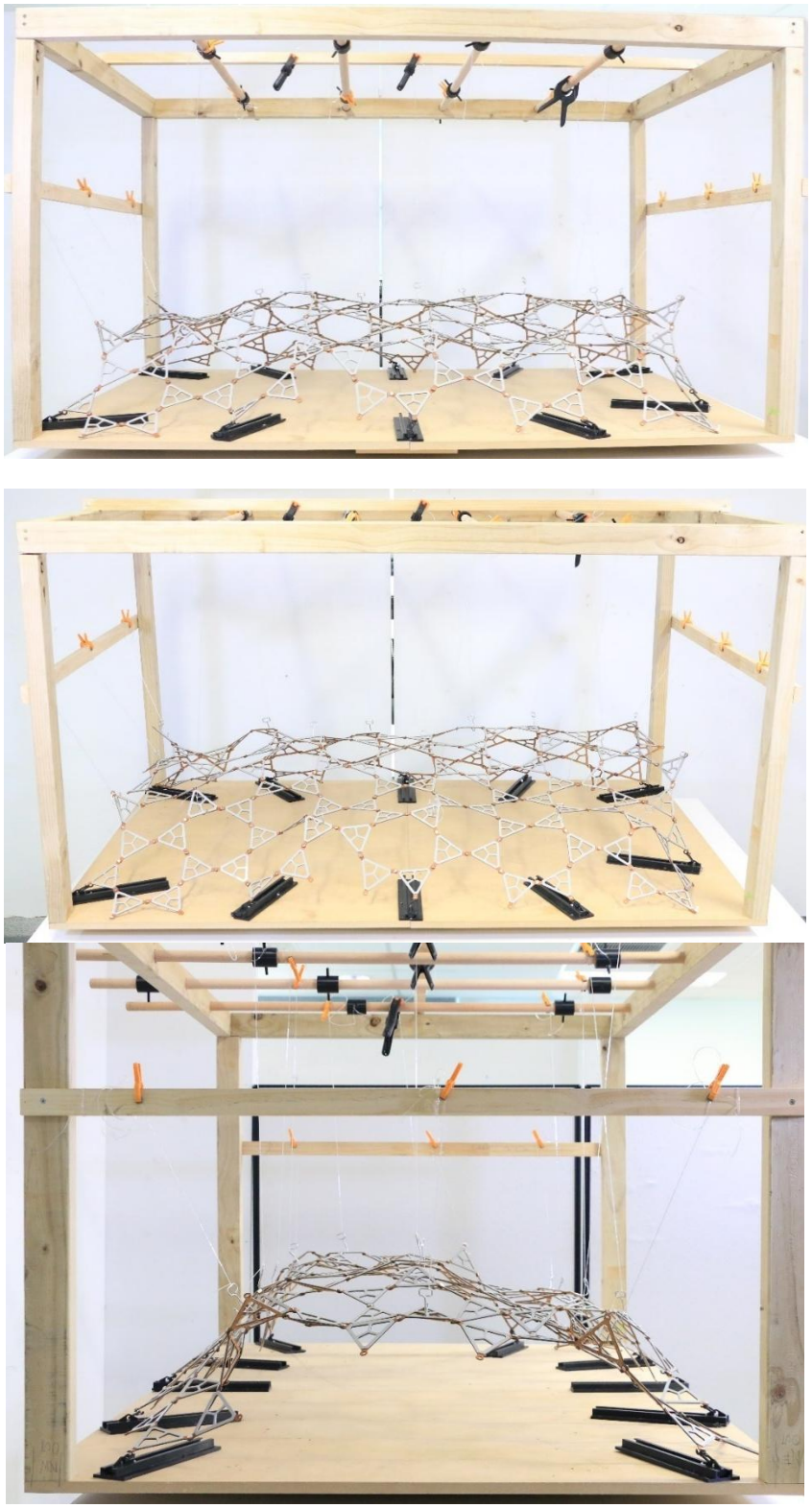

Figure 6.7-87 Deployment behaviour and analysis of Scaled prototype- Stage 4

6.7.9 Appendix I : Versatility in Shape Conformance

A defining test for the tristar auxetic system was its capacity to conform to a variety of three-dimensional geometries. In architectural contexts, deployable surfaces are rarely planar or uniform; instead, they must negotiate double-curved topologies that combine compression, stretching, and directional bending. Evaluating how the system responds to these curvatures was therefore essential to understanding its true adaptability. By referencing the catalogue of 3D printed forms developed earlier in the study, the auxetic sheet was manipulated across a series of controlled geometric trials, replicating as closely as possible the complex morphologies that had already been digitally and physically modelled.

The first trial involved concave bowl-like configurations, where the sheet was pressed inward to evaluate how the units responded to compression along the Z-axis. This geometry tested the ability of the joints to stabilize under inward pulling forces while maintaining continuous surface logic.

The second set of experiments focused on convex dome formations, which inverted the stress conditions and required the auxetic sheet to expand outward smoothly. The dome trials were particularly significant as they align with many natural and architectural precedents, testing the system's strength in resisting pull-back while ensuring directional expansion.

The system was also tested against asymmetric warps and saddle-like hyperbolic paraboloid geometries, both of which are challenging due to their non-uniform stress distributions. These trials examined whether the differentiated expansion of the auxetic sheet could align itself to complex directional pulls and twisting forces without introducing distortions or vertical piling.

Across all these experiments, the sheet demonstrated reliable conformity, closely mimicking the performance observed in the earlier PETG laser cut prototypes. The differentiated expansion across the pattern responded accurately to local stress variations, allowing the structure to adapt dynamically to each form. This adaptability validated the system's potential for architectural use, confirming that the auxetic pattern could accommodate a broad spectrum of double-curved geometries with structural coherence and minimal additional intervention.

Shape 1

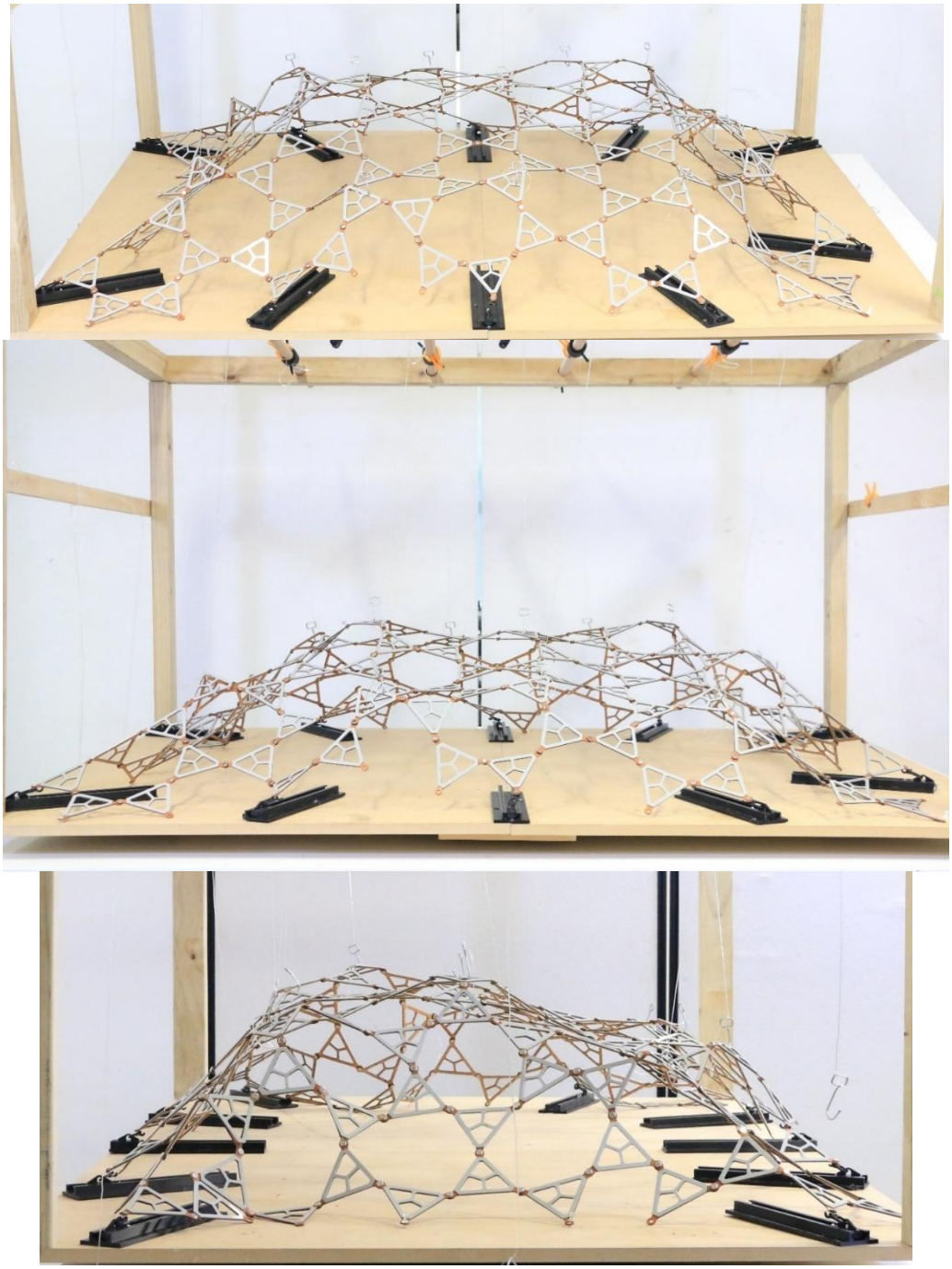

Figure 6.7-88 Scaled prototype check for versatility - shape 1

Shape 2

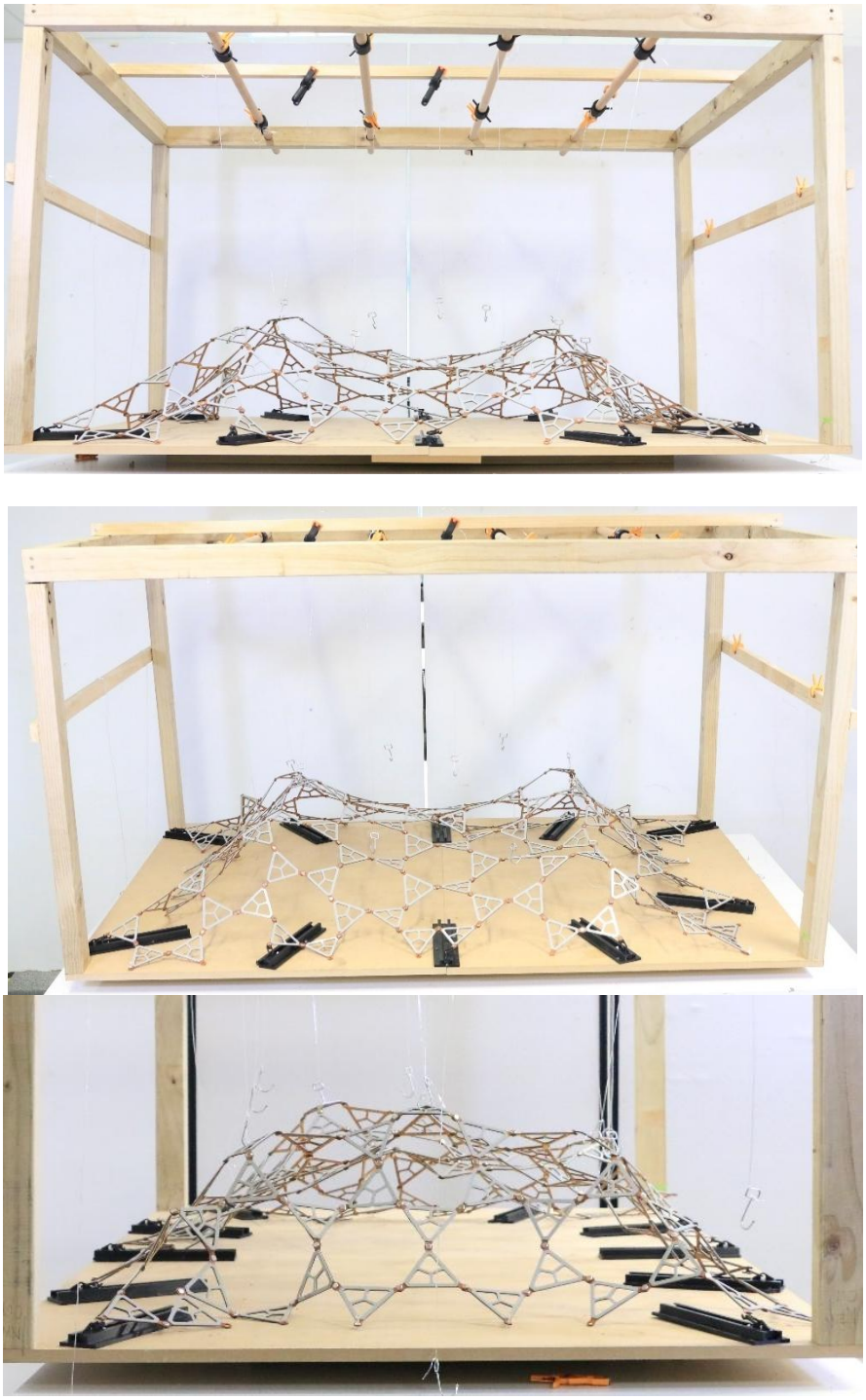

Figure 6.7-89 Scaled prototype check for versatility - shape 2

Shape 3

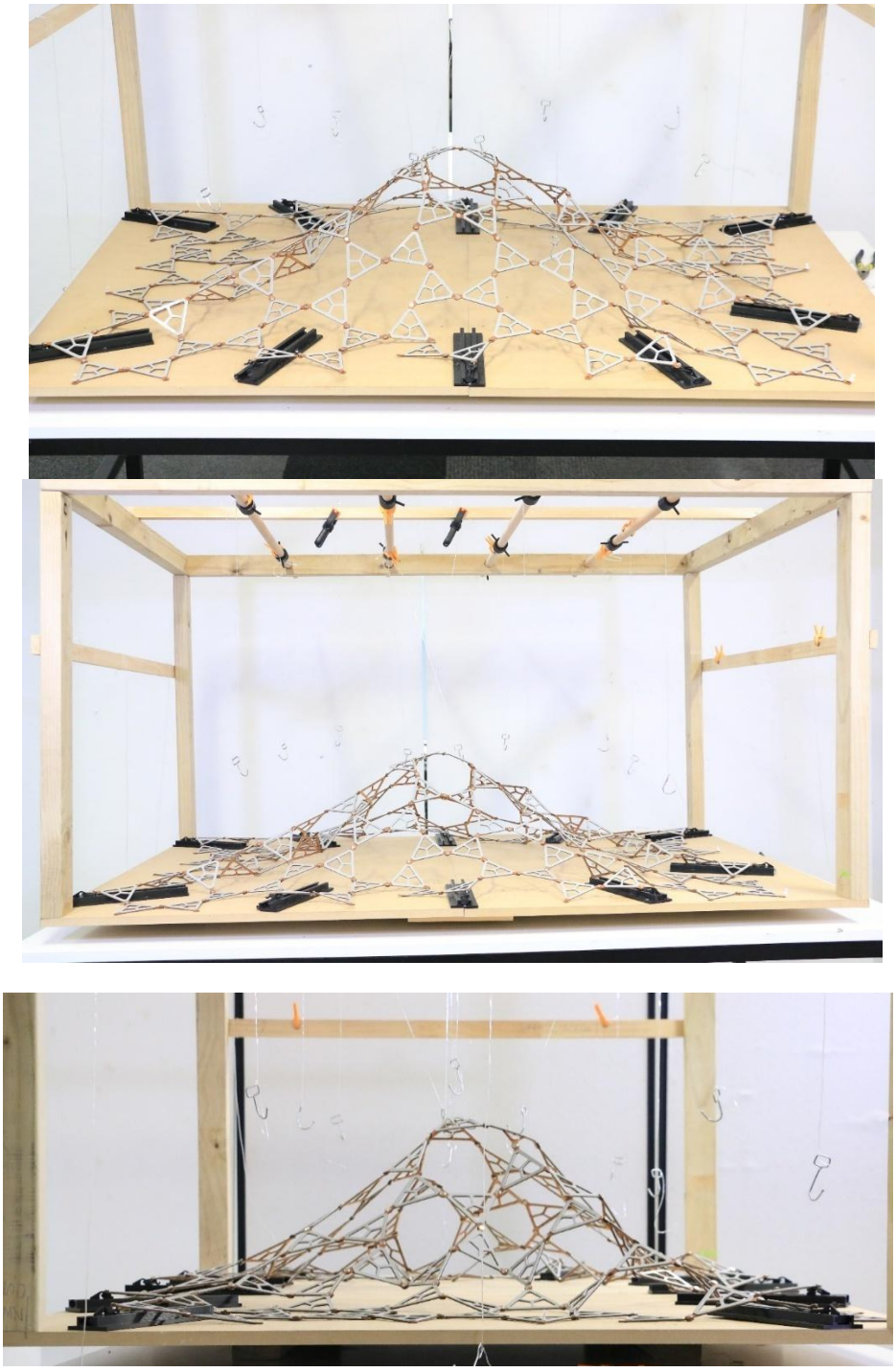

Figure 6.7-90 Scaled prototype check for versatility - shape 3

Shape 4

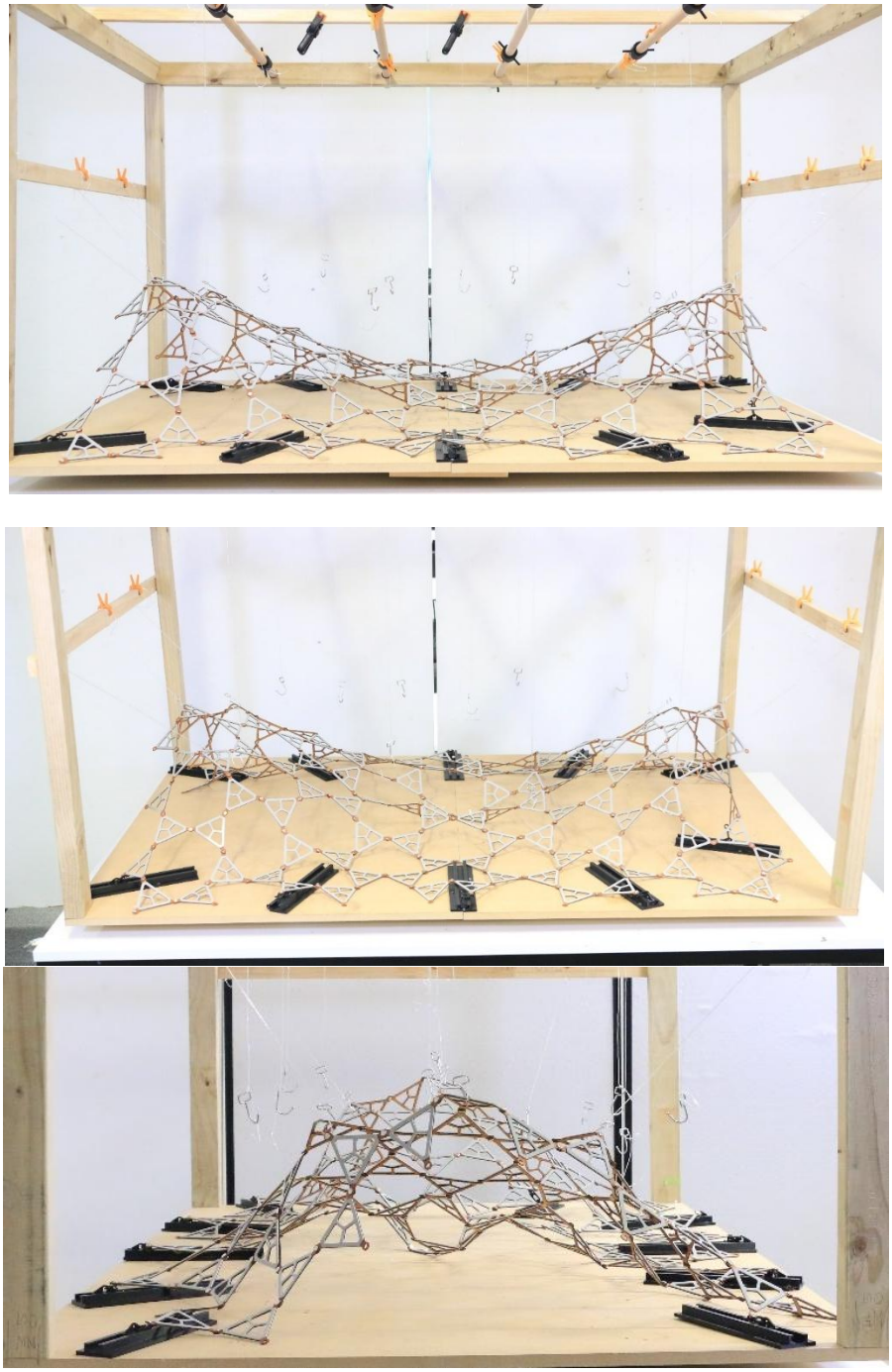

Figure 6.7-91 Scaled prototype check for versatility - shape 4

Shape 5

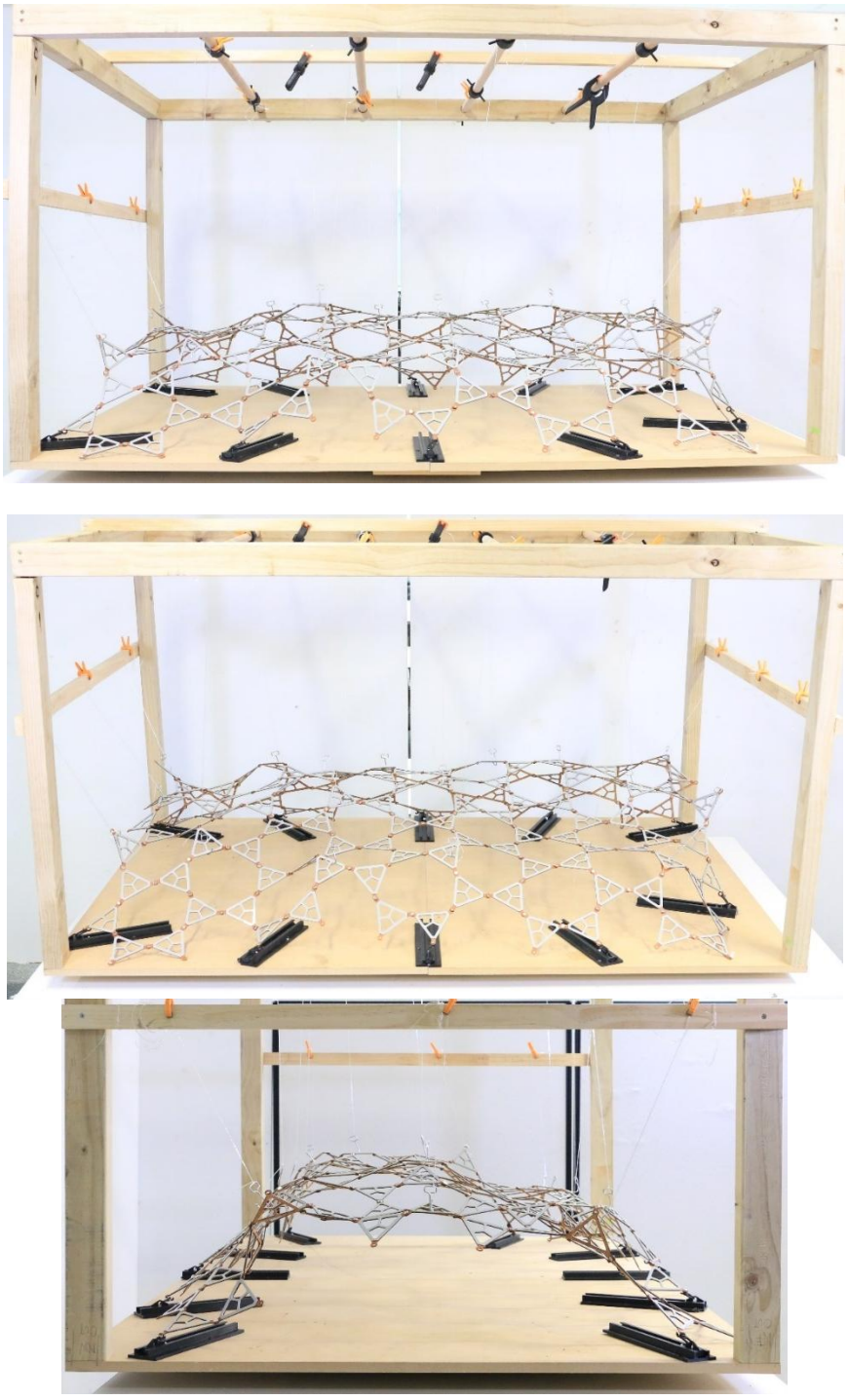

Figure 6.7-92 Scaled prototype check for versatility - shape 5

Shape 6

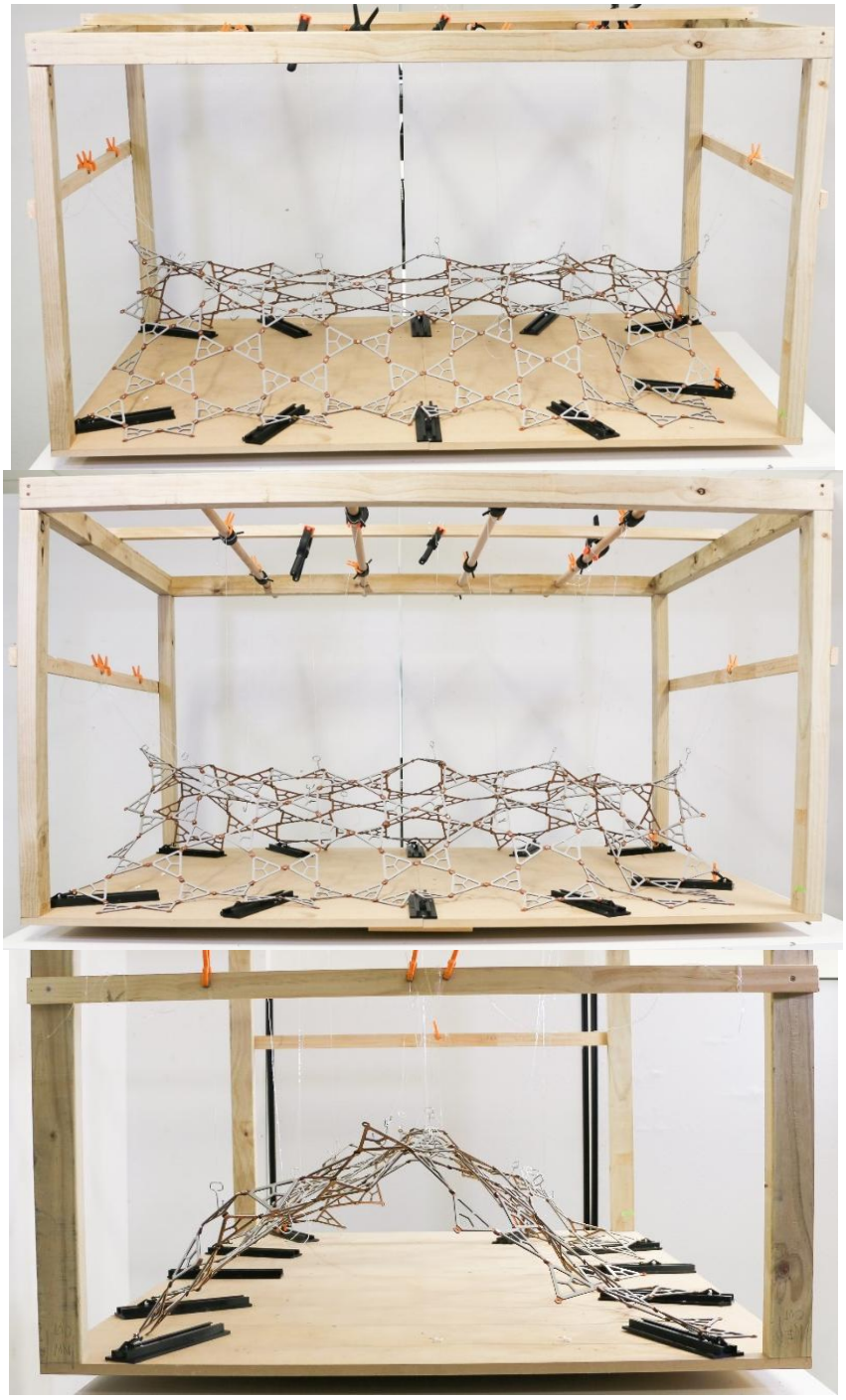

Figure 6.7-93 Scaled prototype check for versatility - shape 6

Shape 7

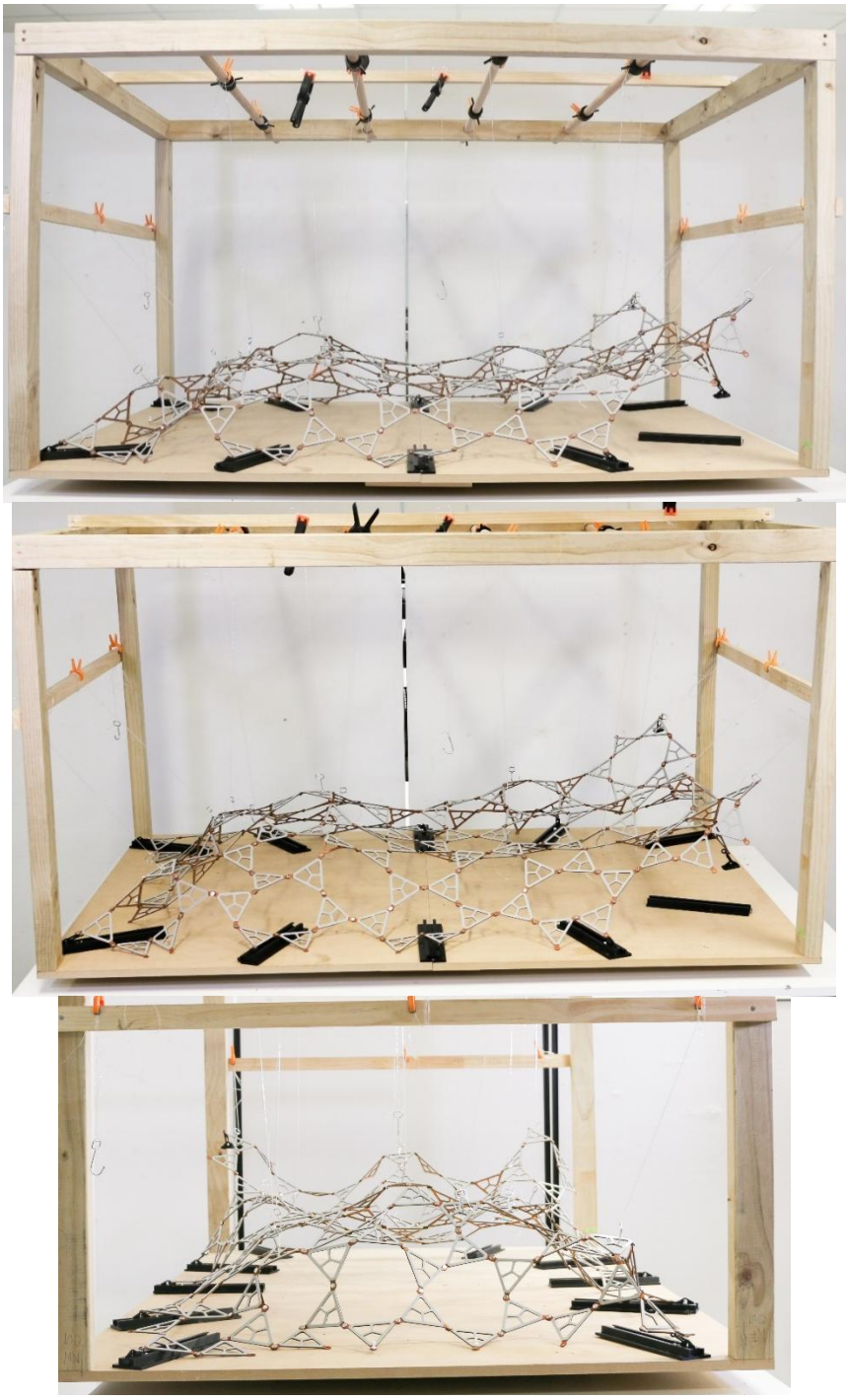

Figure 6.7-94 Scaled prototype check for versatility - shape 7

Shape 8

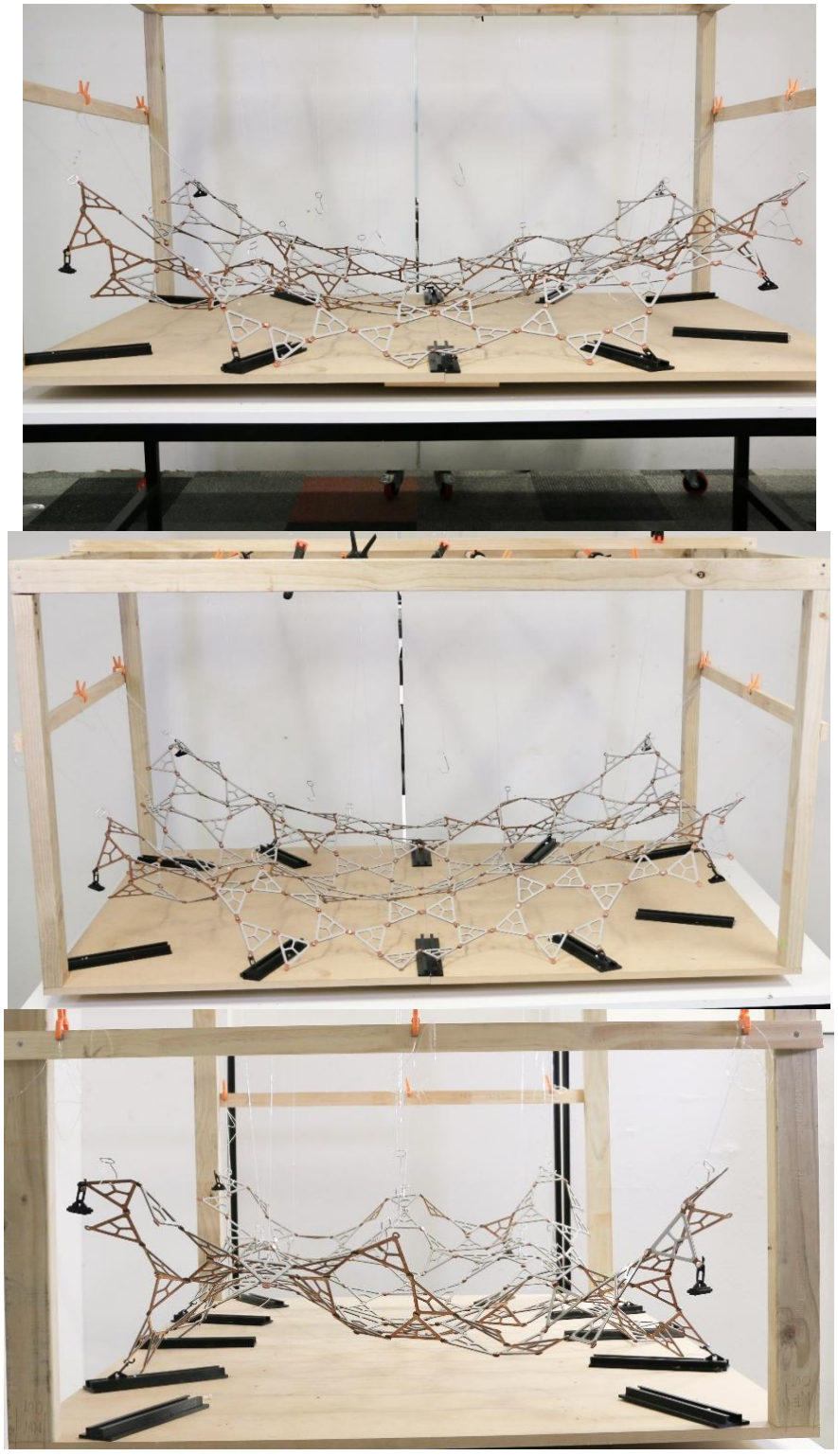

Figure 6.7-95 Scaled prototype check for versatility - shape 8

Shape 9

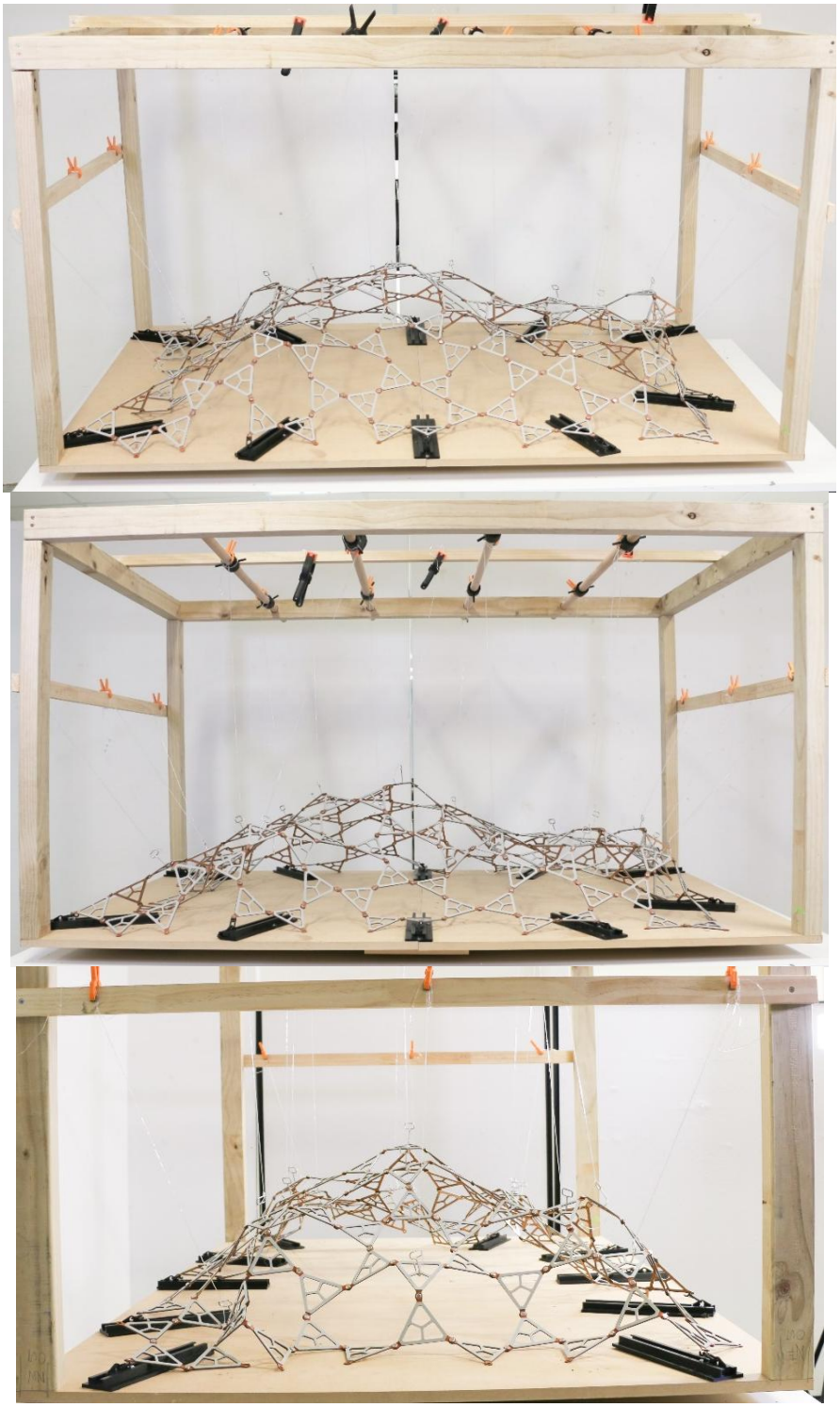

Figure 6.7-96 Scaled prototype check for versatility - shape 9

Shape 10

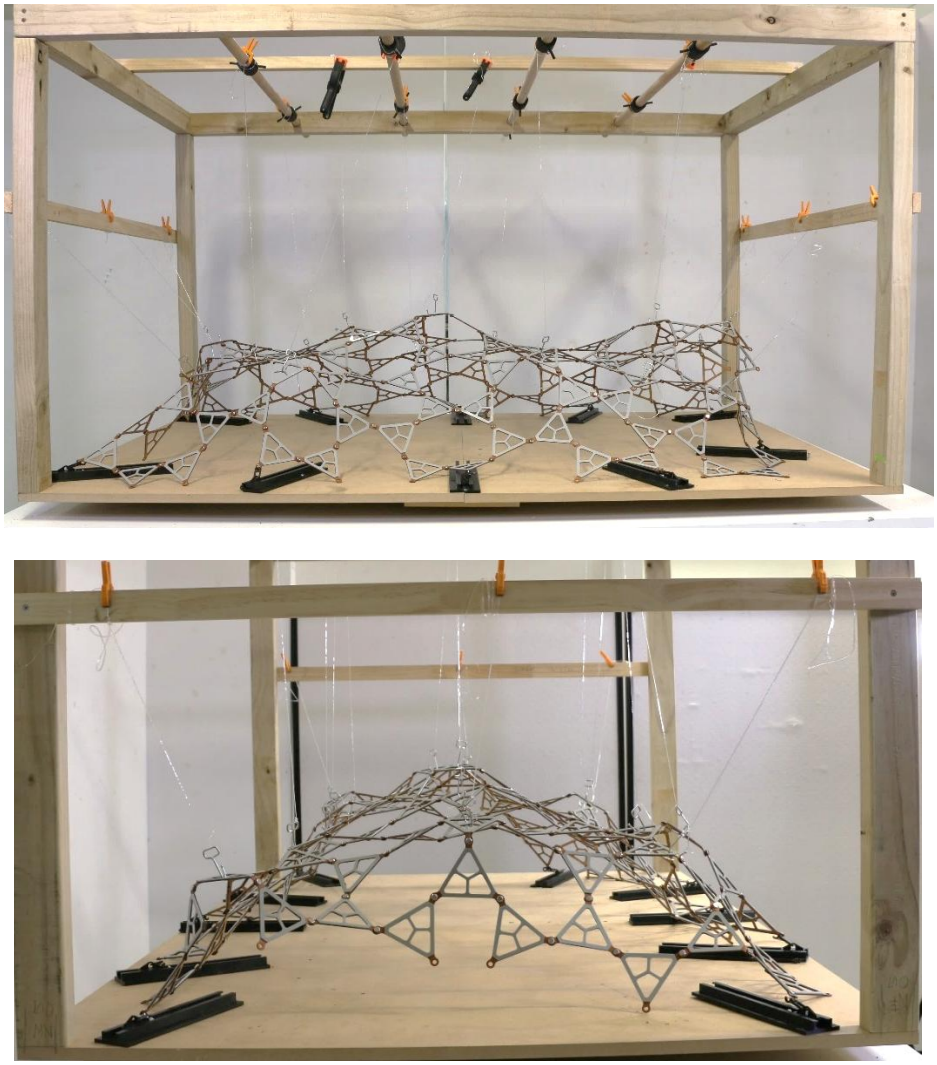

Figure 6.7-97 Scaled prototype check for versatility - shape 10

6.7.10 Appendix J : Physical Prototype (Testing Mechanisms& Movements)

6.7.10.1 Mark 1 Prototype: Ratchet-and-Spring-Based Mechanical Joinery

Kinematic Behavior and Movement Analysis

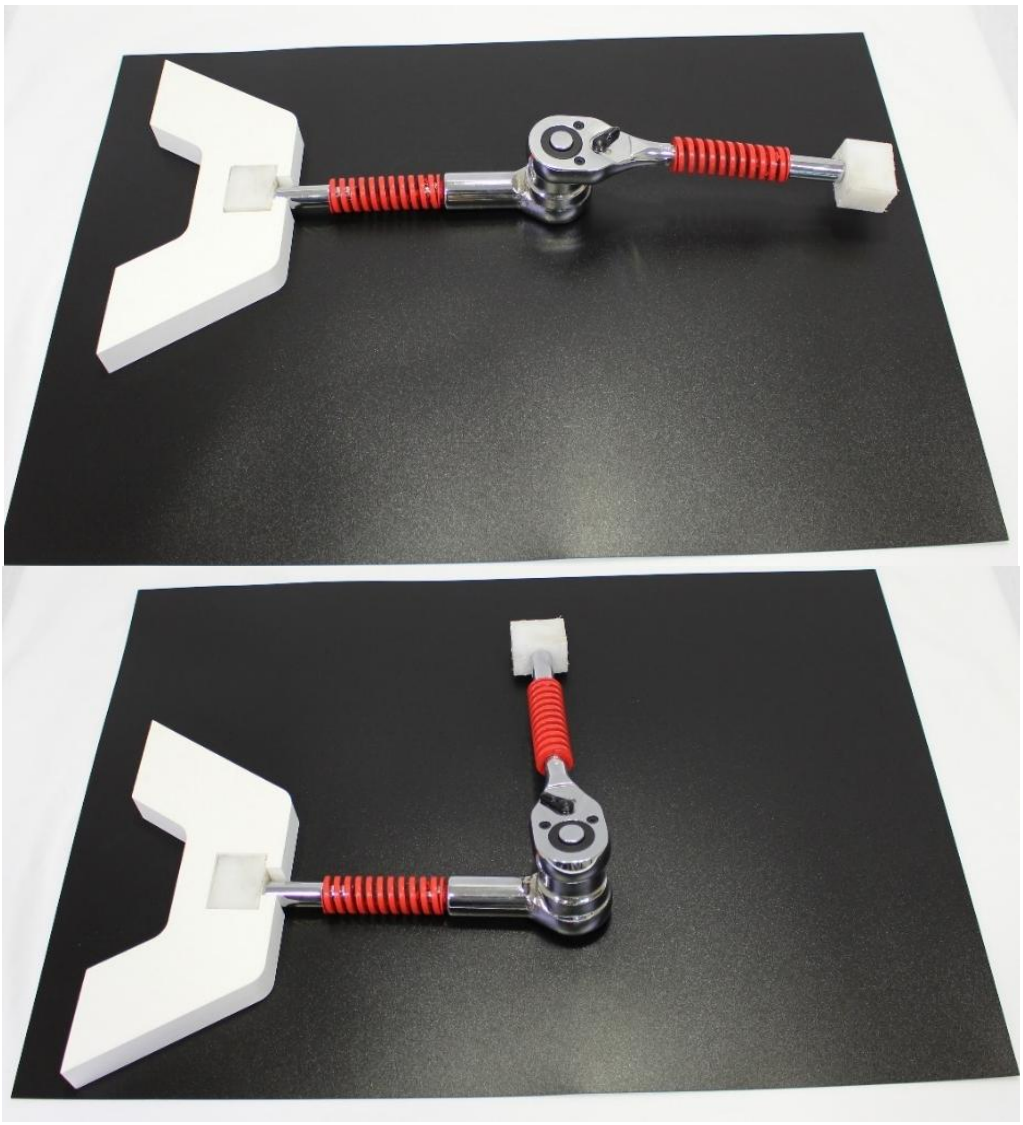

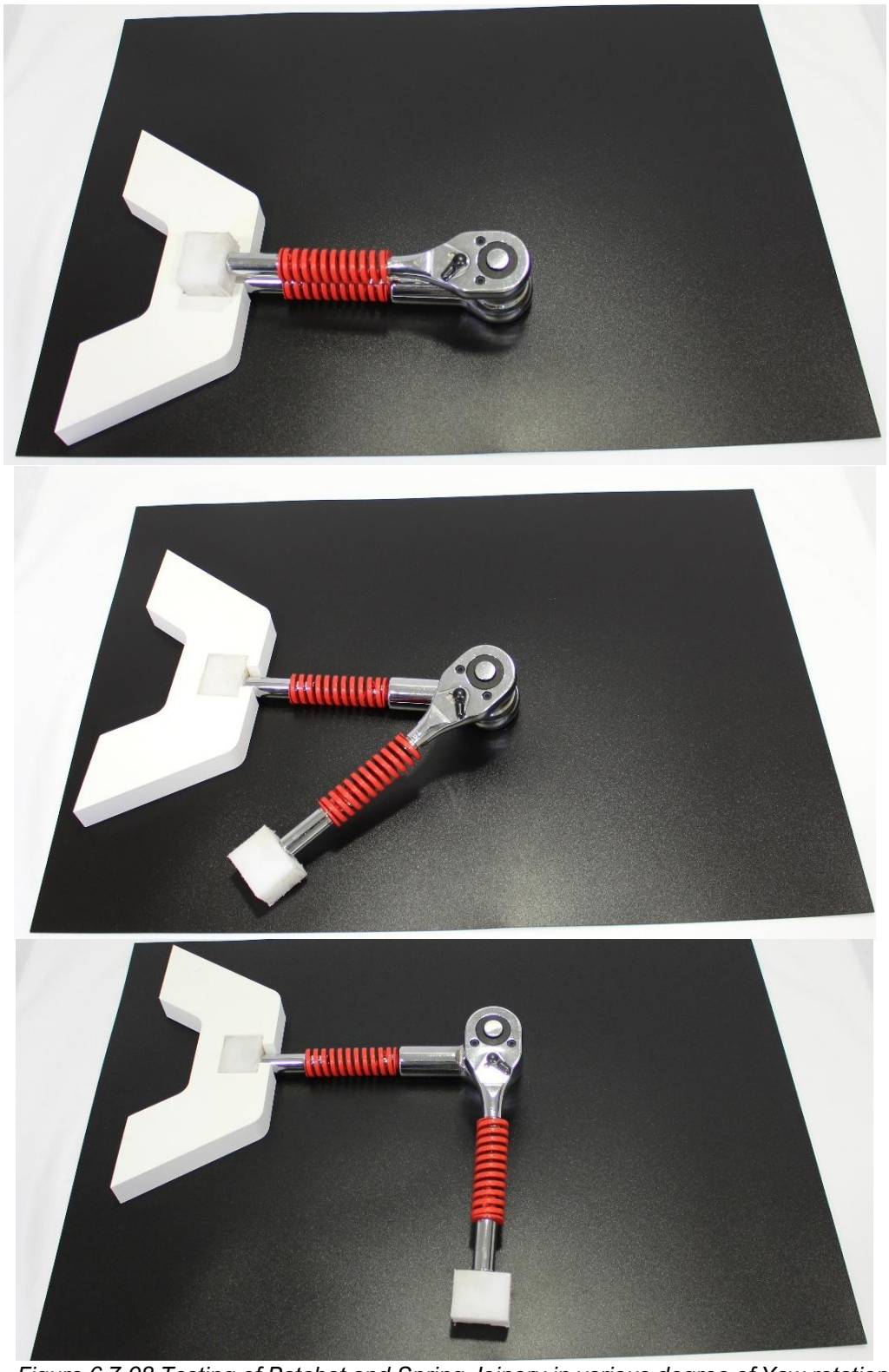

Figure 6.7-98 Testing of Ratchet and Spring Joinery in various degree of Yaw rotation

6.7.10.2 Mark 2 Prototype: Dual-Ratchet Joinery System with Integrated Ball Joint

Kinematic Behaviour and Performance

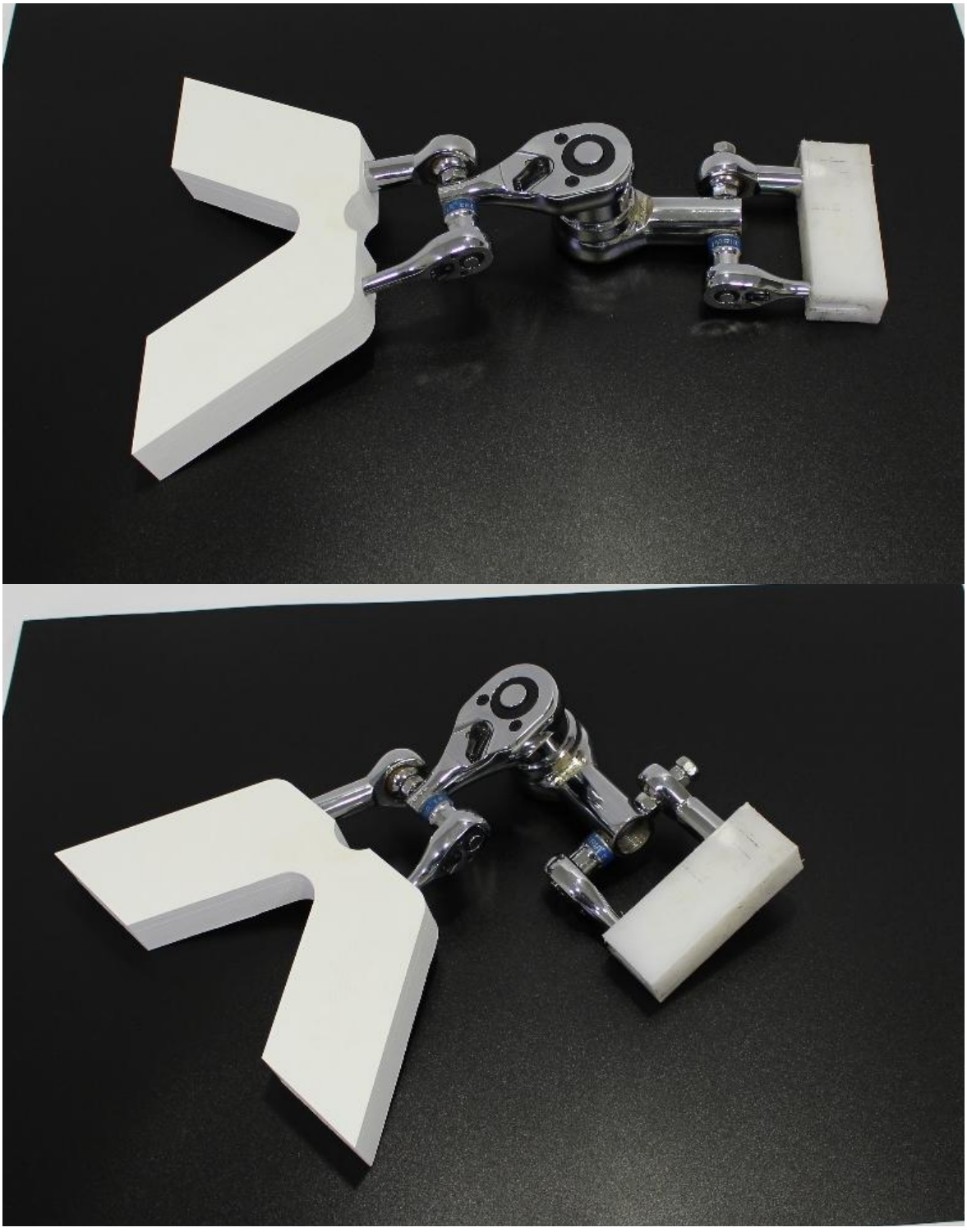

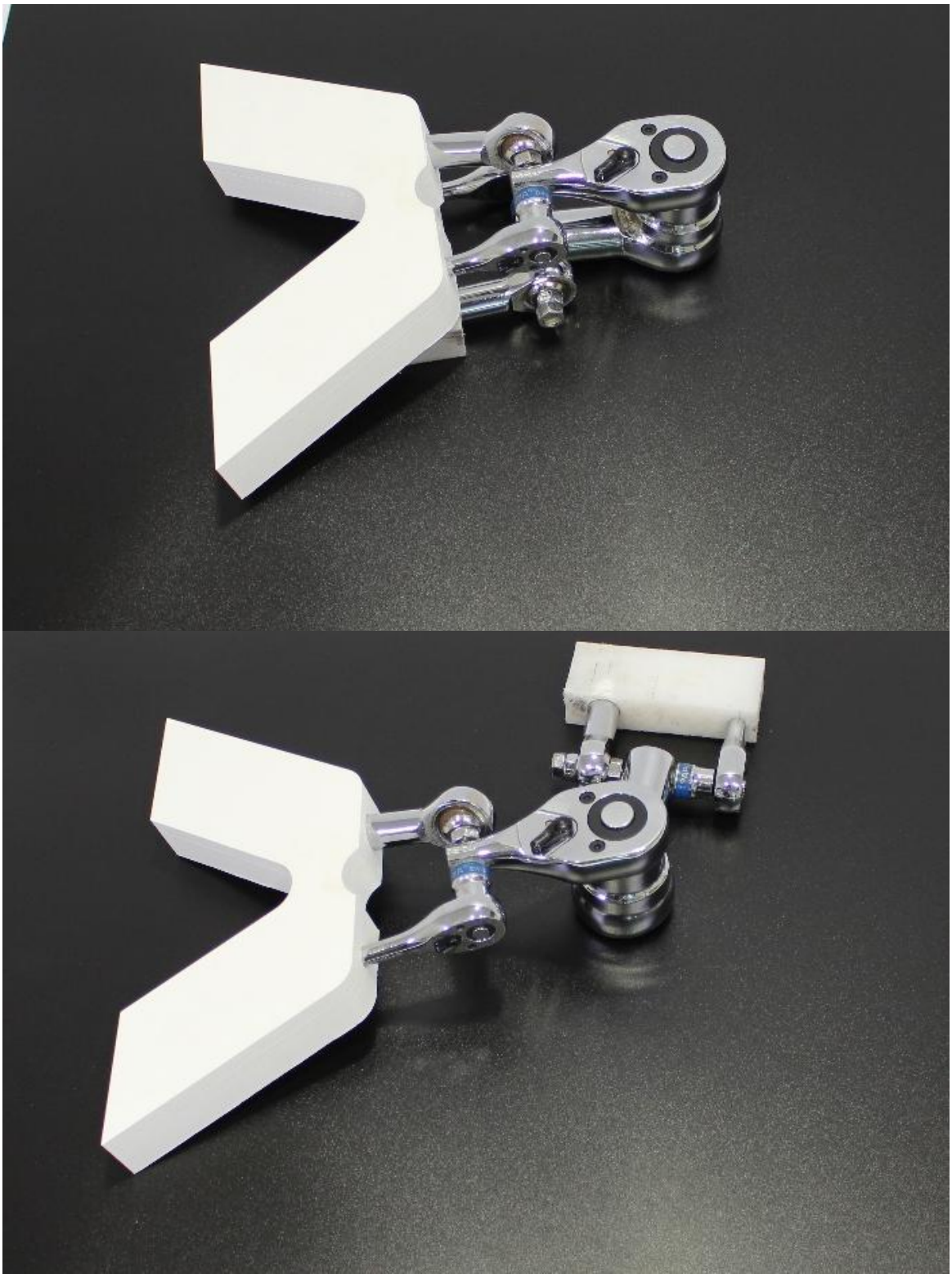

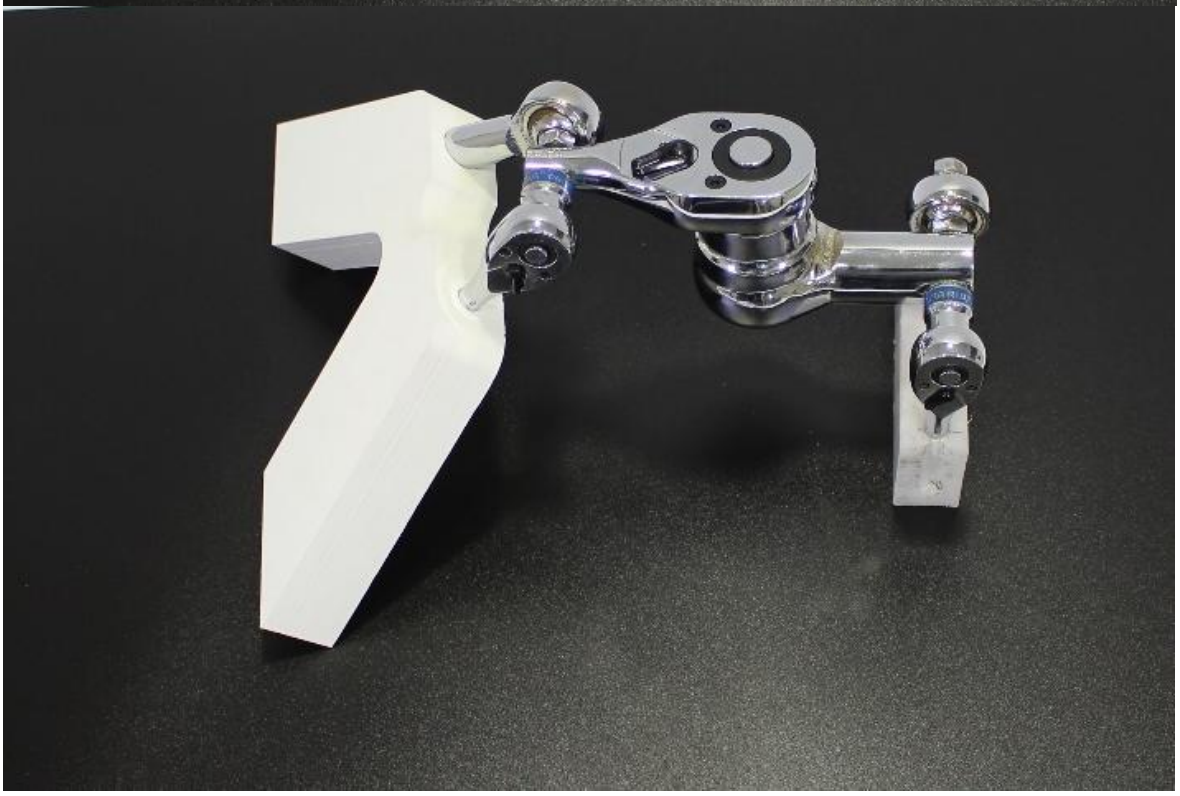

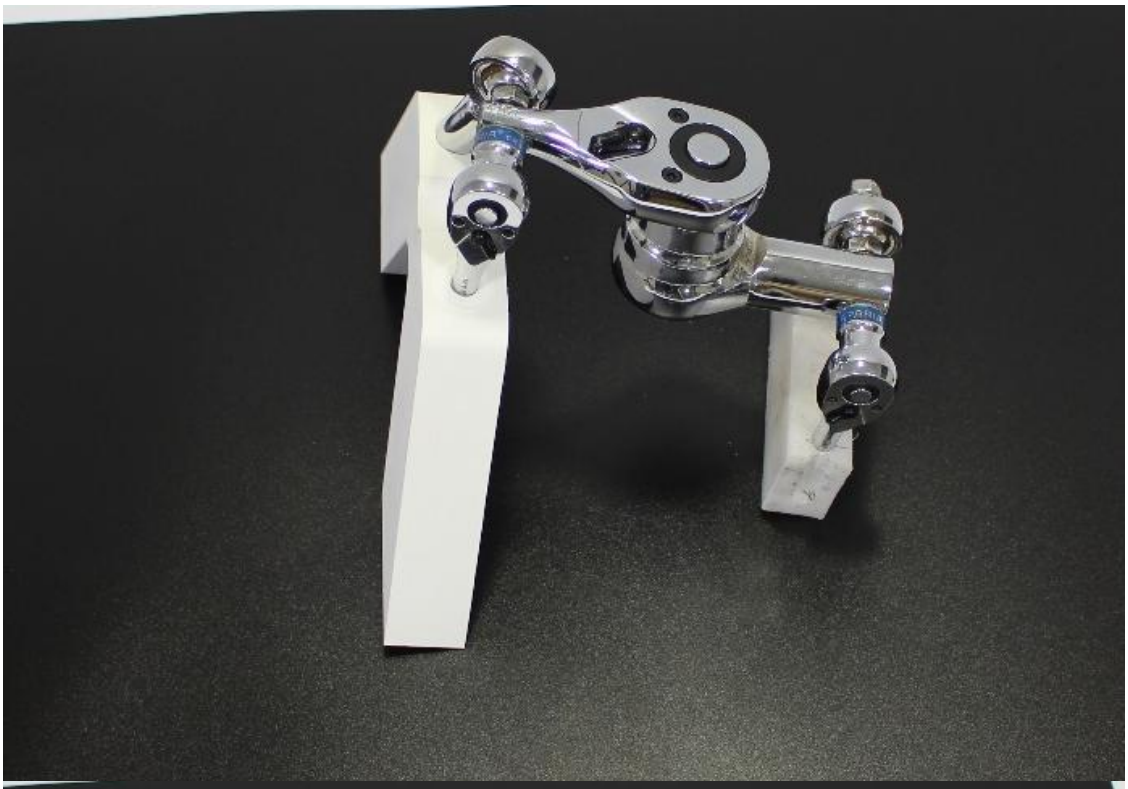

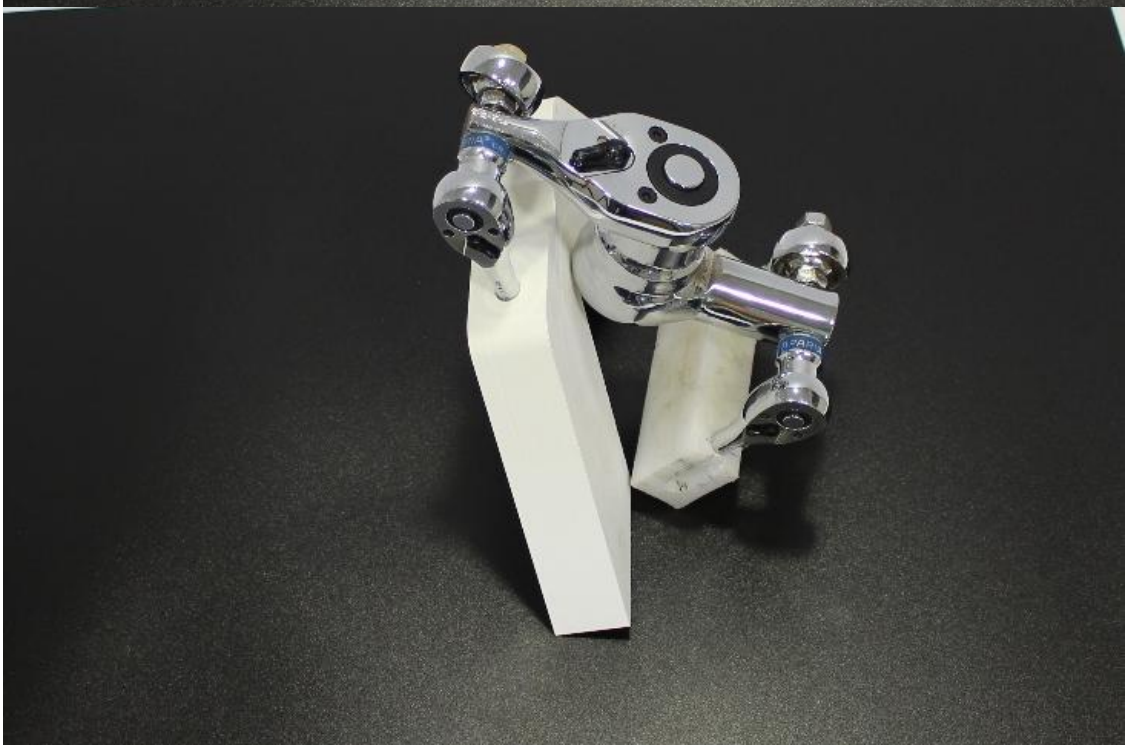

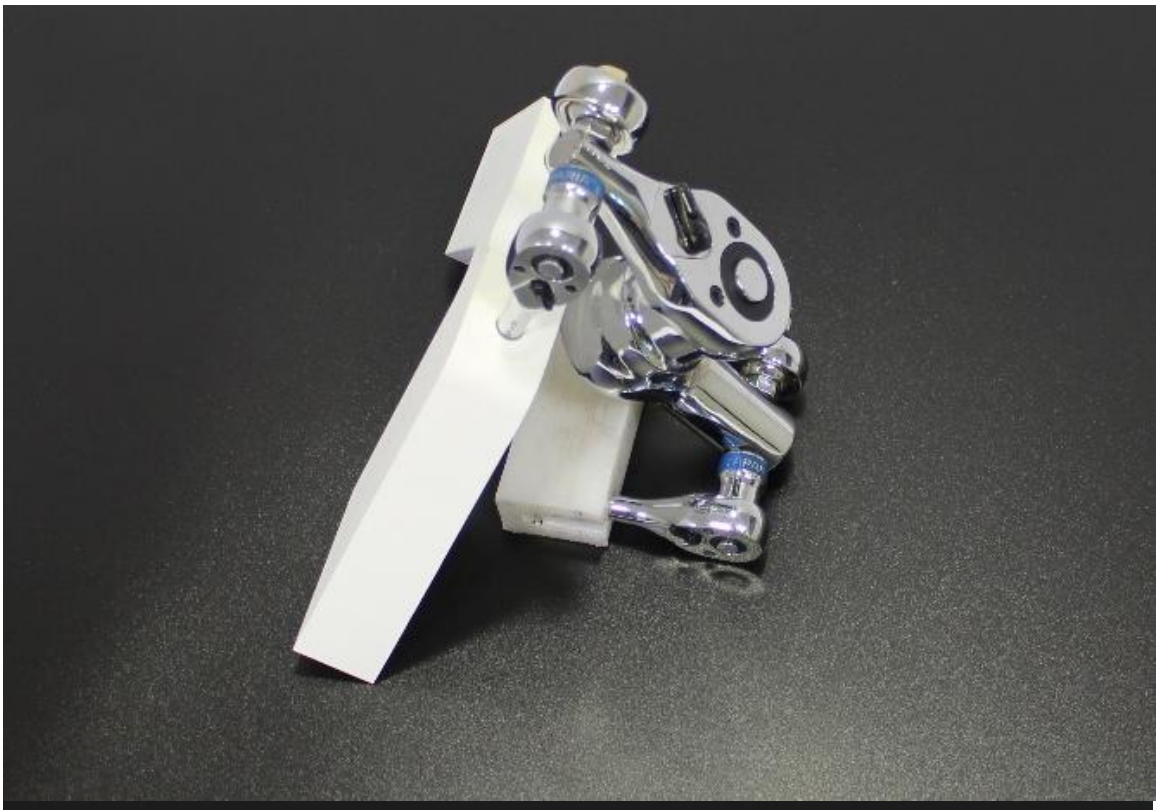

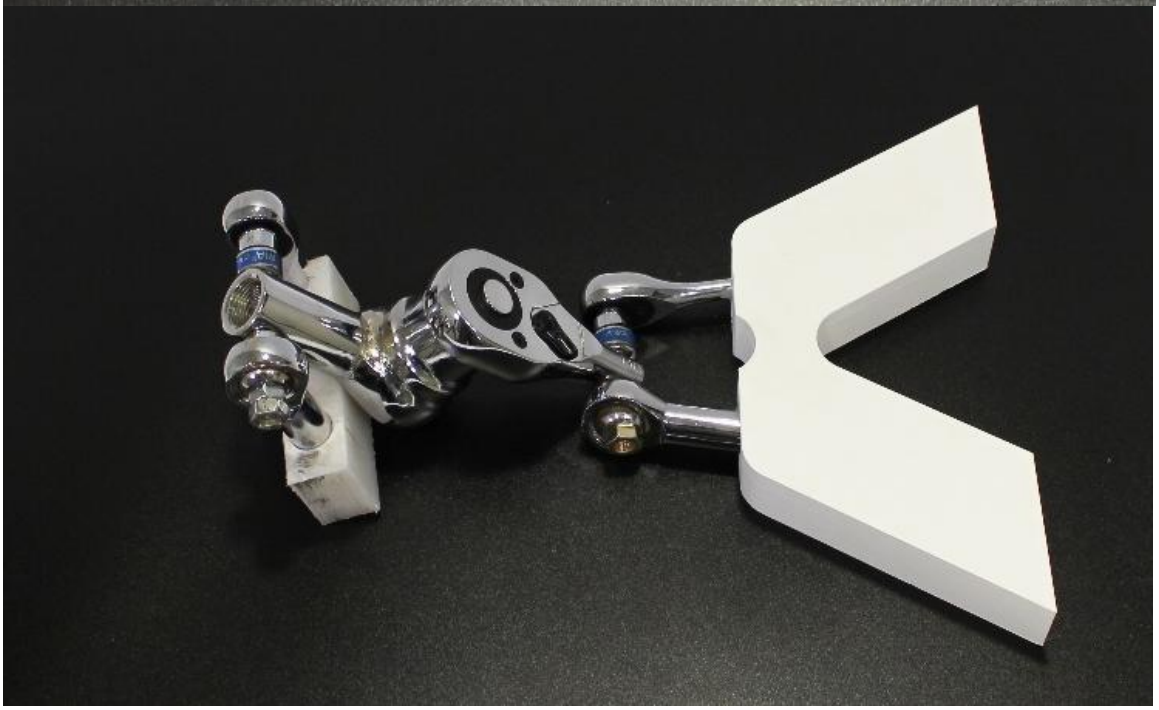

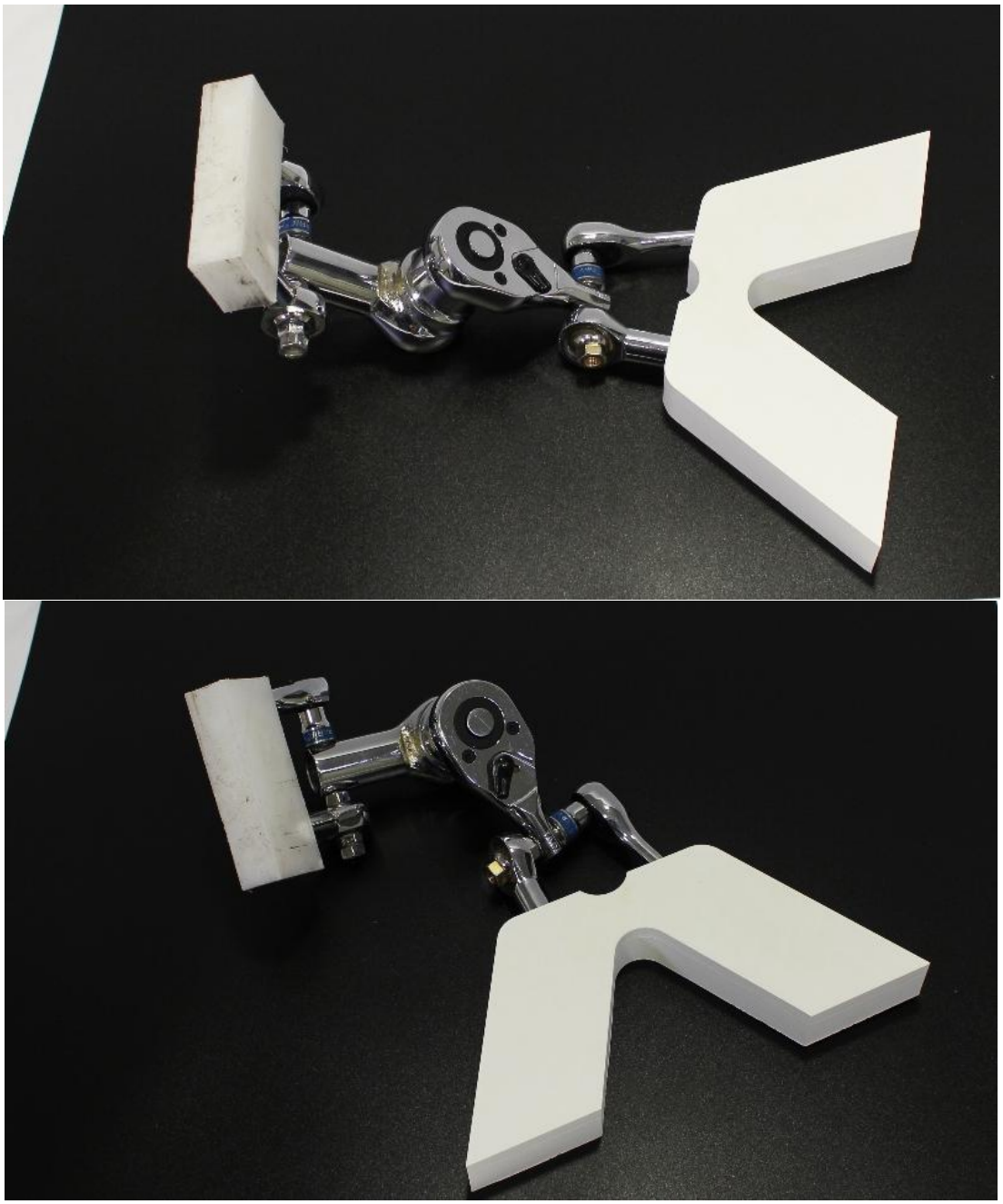

Figure 6.7-99 Testing of Dual ratchet system- mark 2 with various Yaw and Pitch movemnts

6.7.10.3 Mark 3 Prototype: Dual-Axis One-Way Bearing Joinery System

Kinematic Behaviour and Movement Characteristics

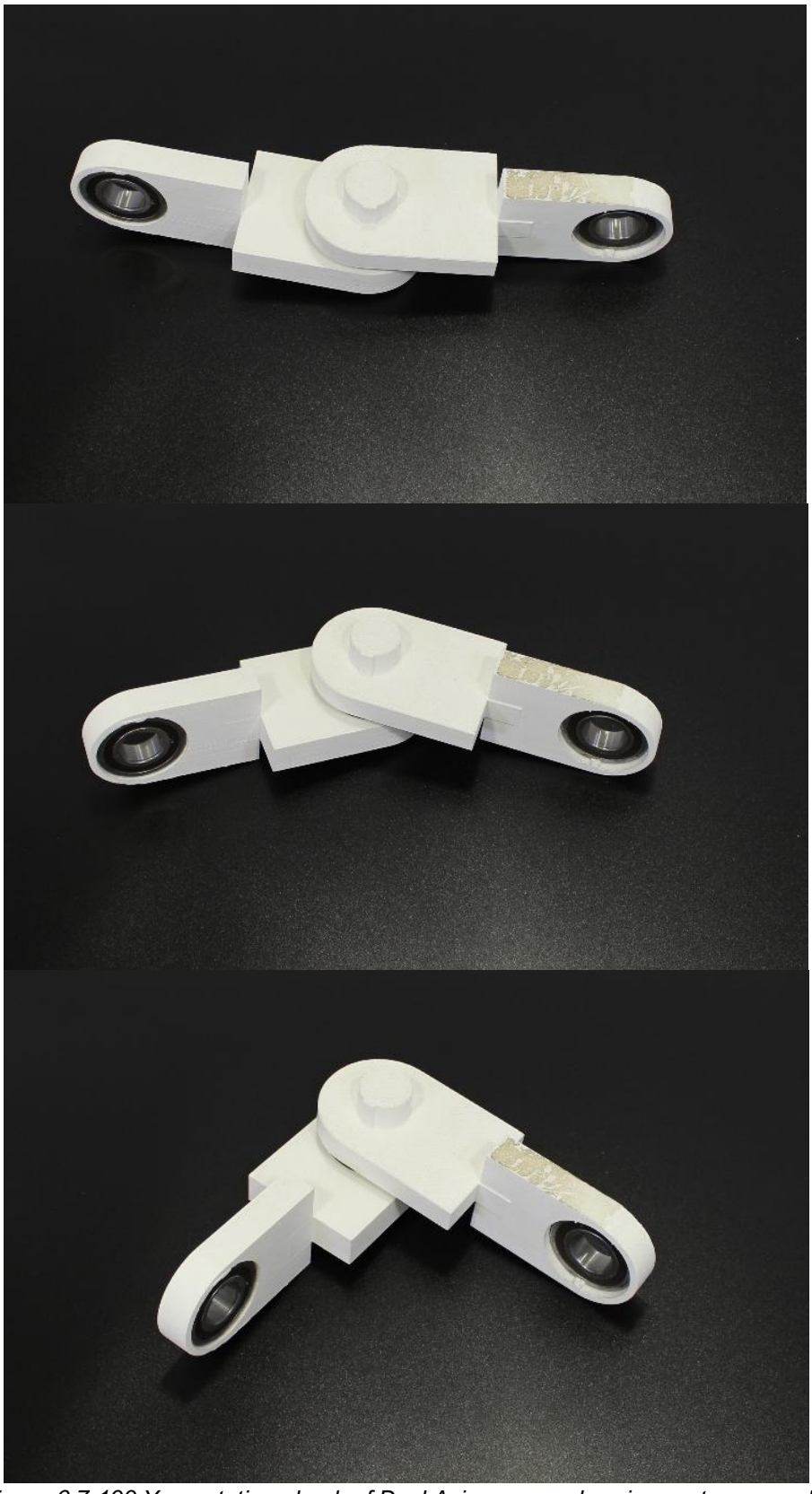

Figure 6.7-100 Yaw rotation check of Dual Axis one way bearing systems- mark 3- assembly type 1

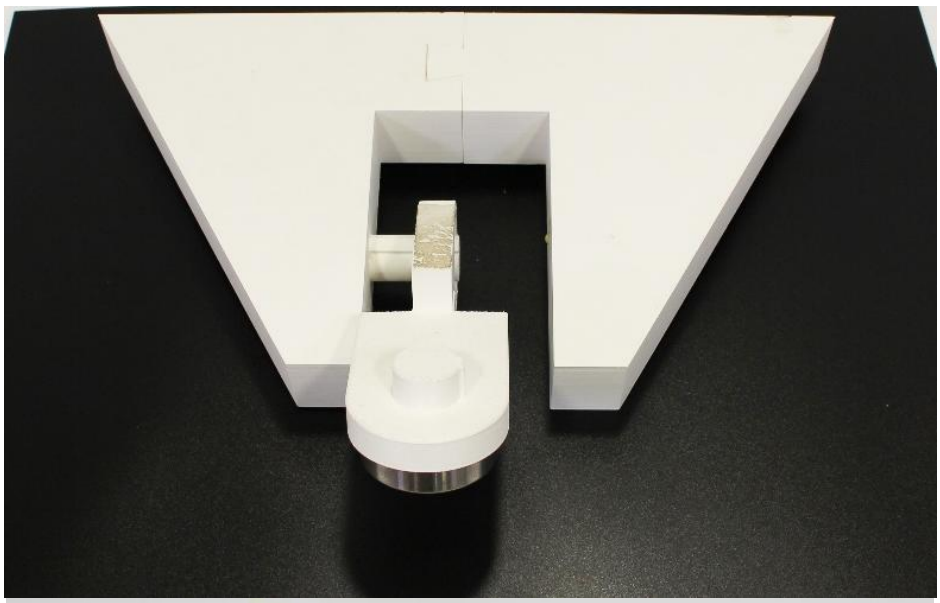

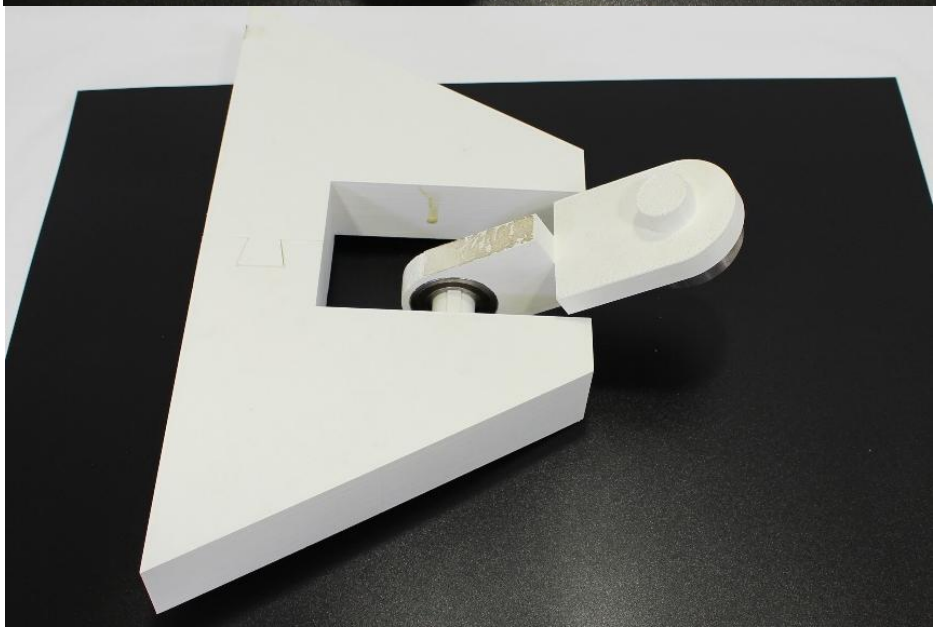

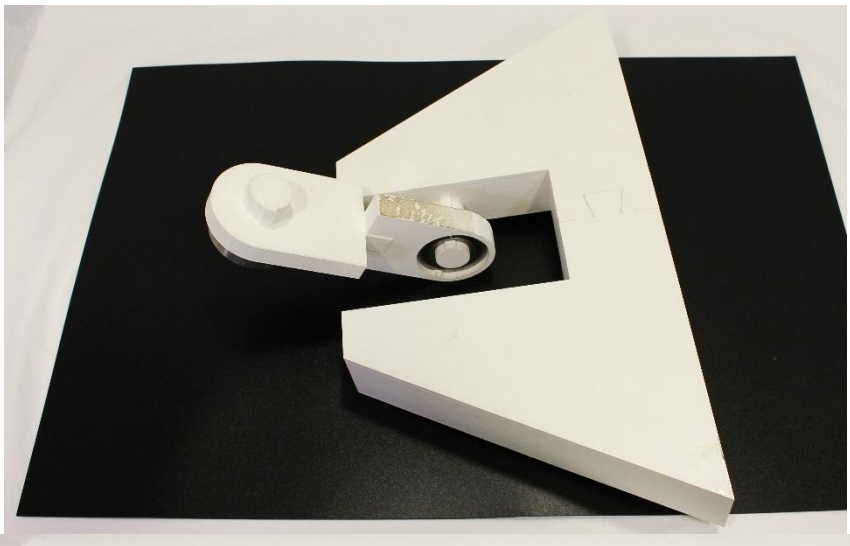

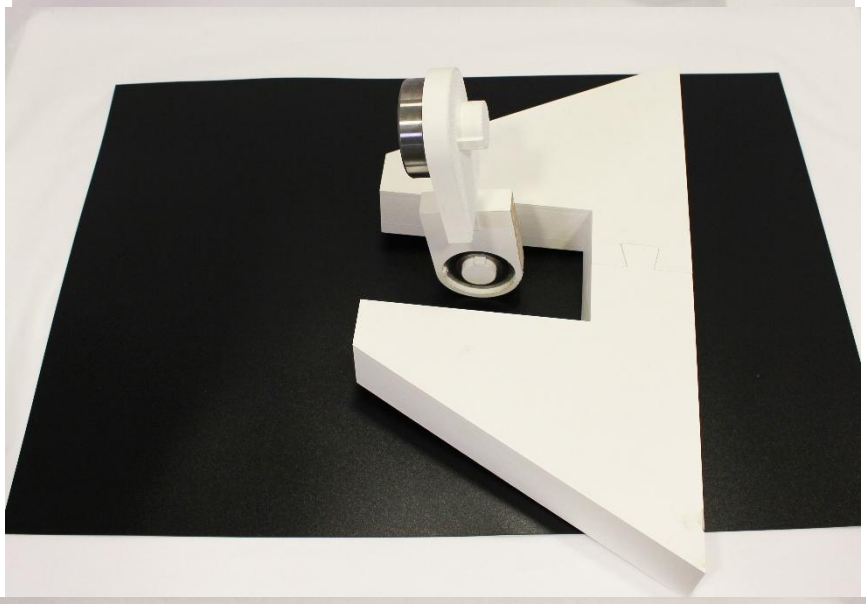

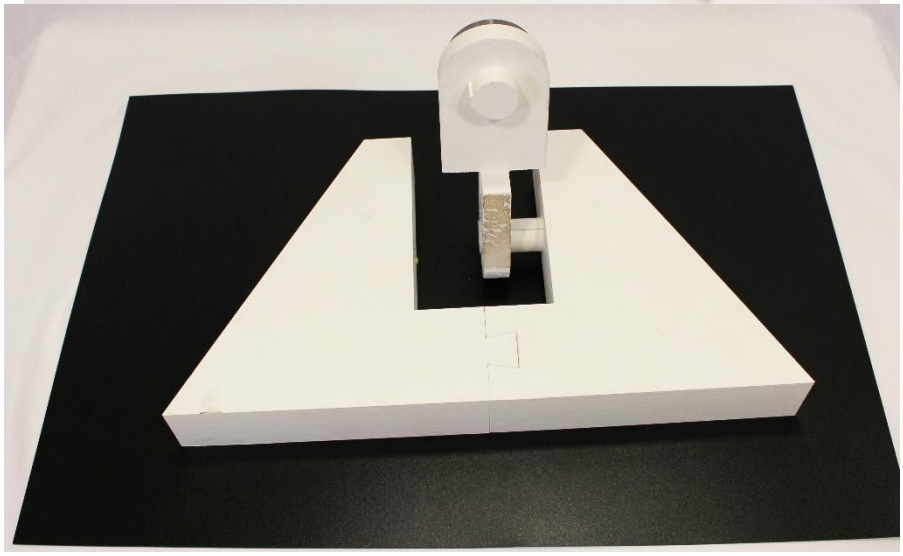

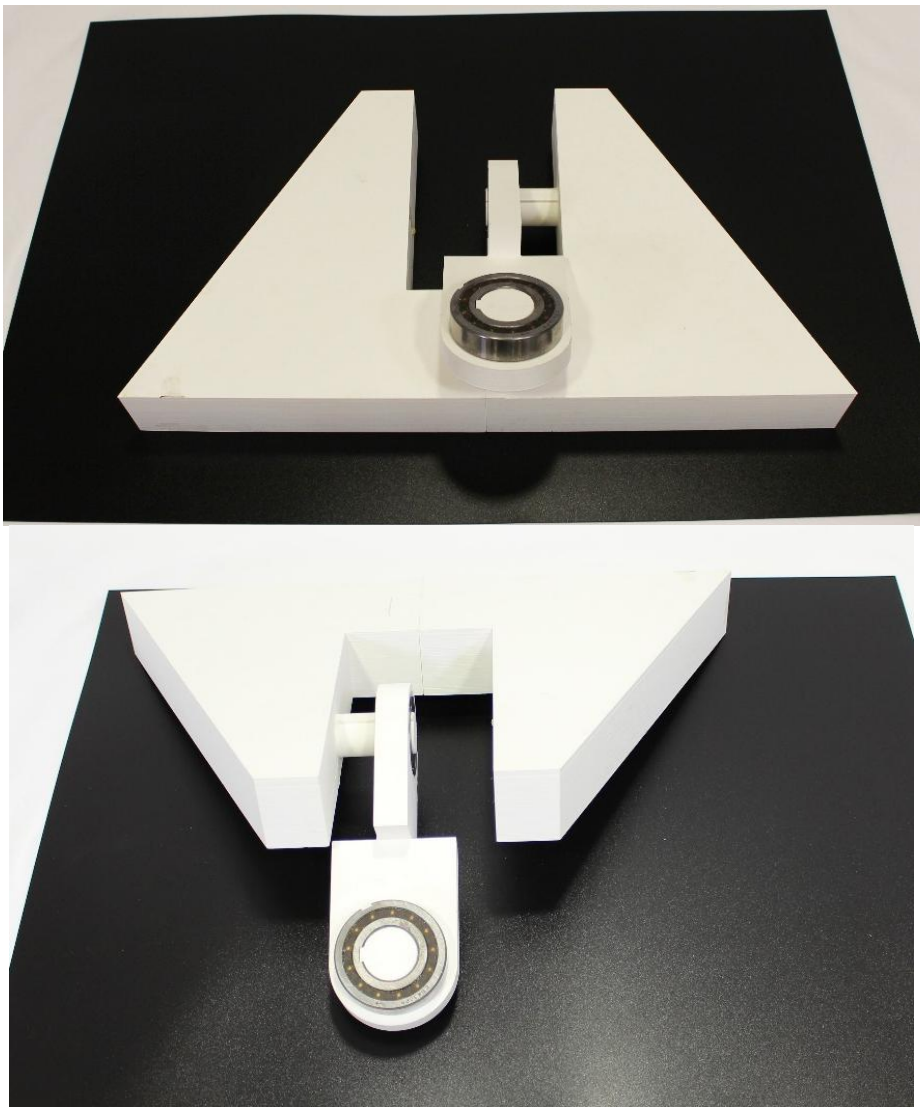

Figure 6.7-101 Pitch rotation check of Dual Axis one way bearing systems- mark 3- assembly type 2

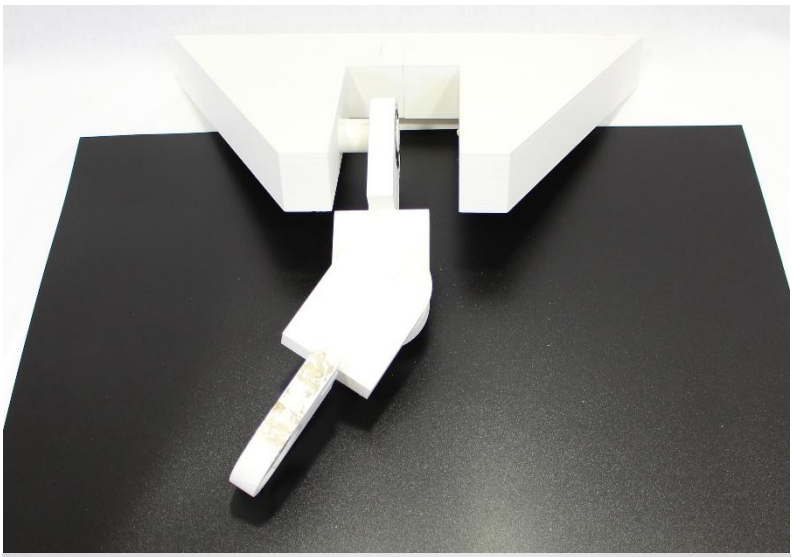

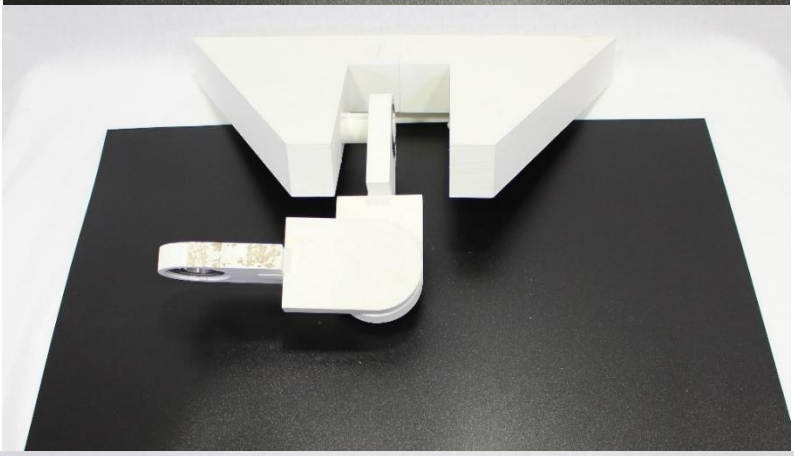

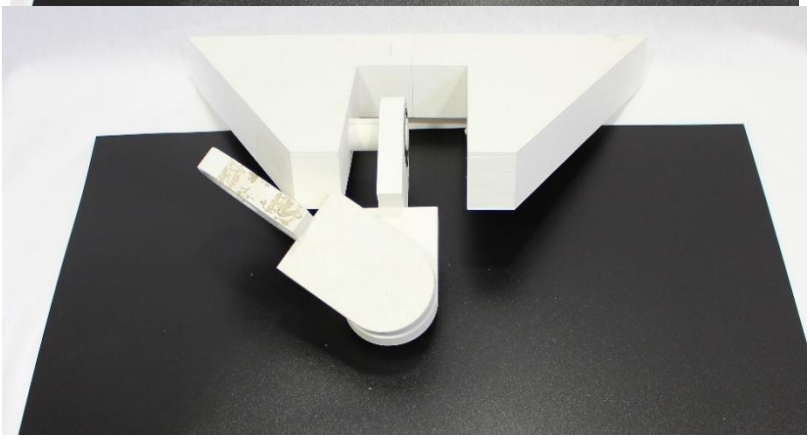

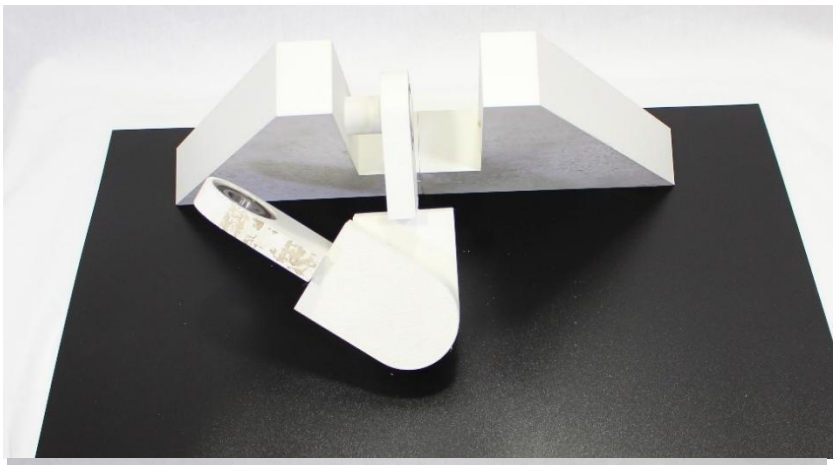

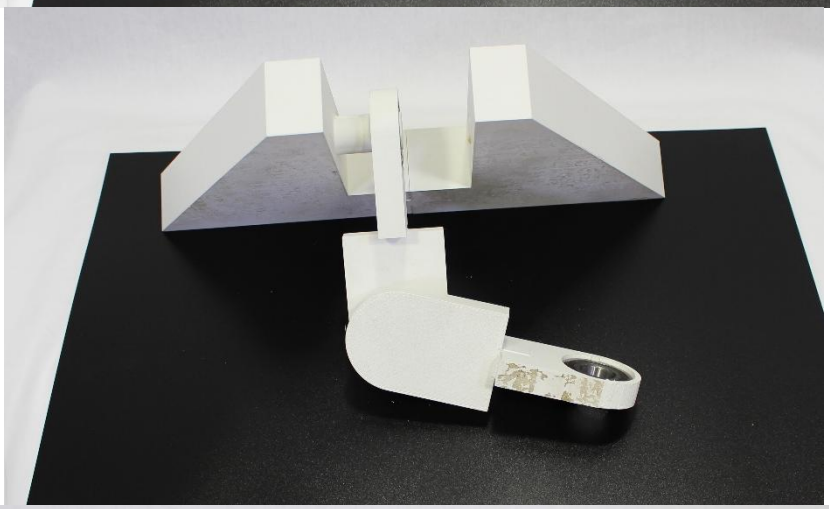

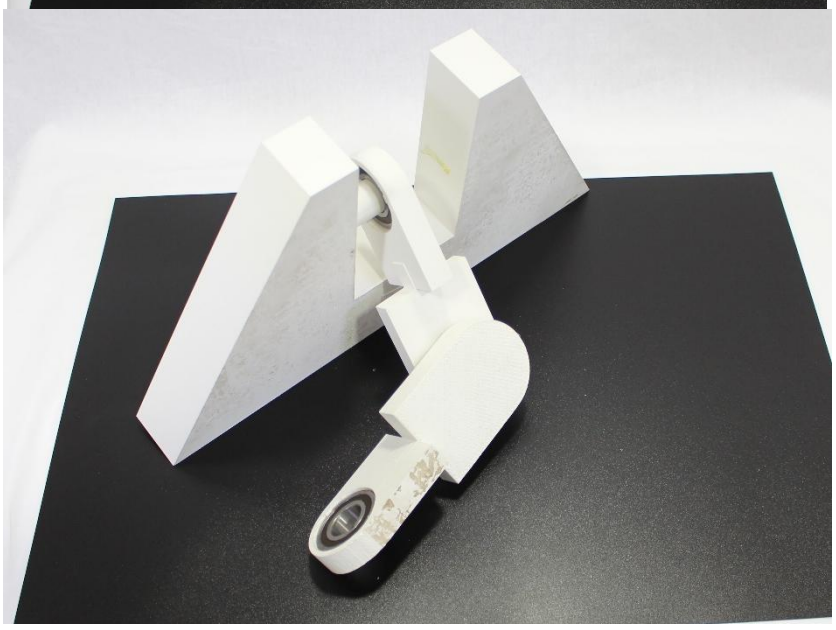

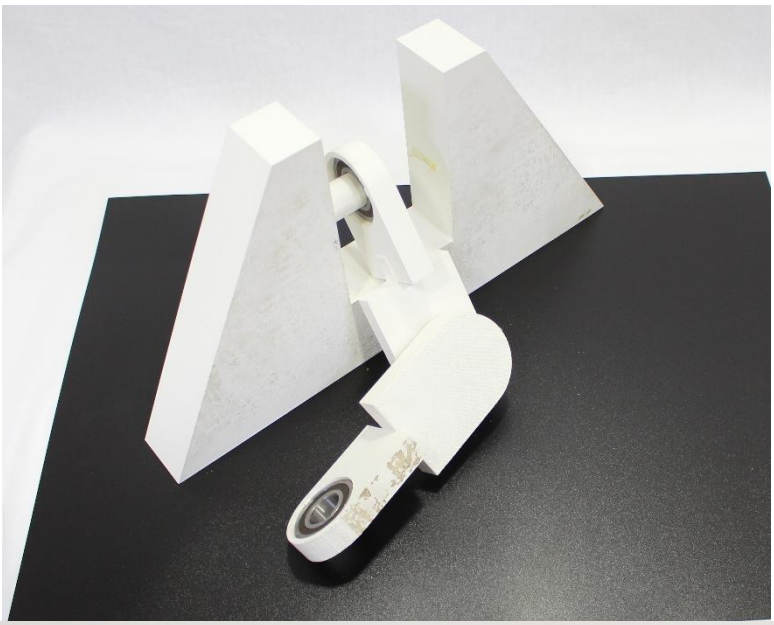

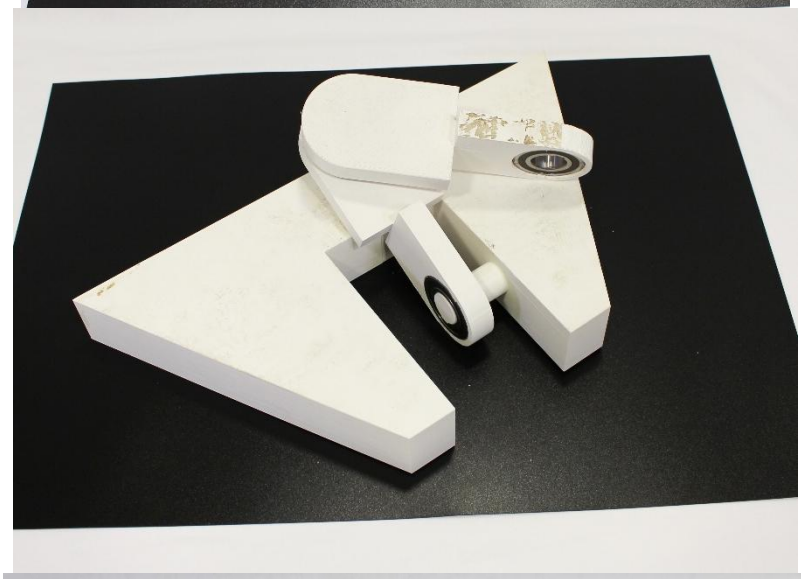

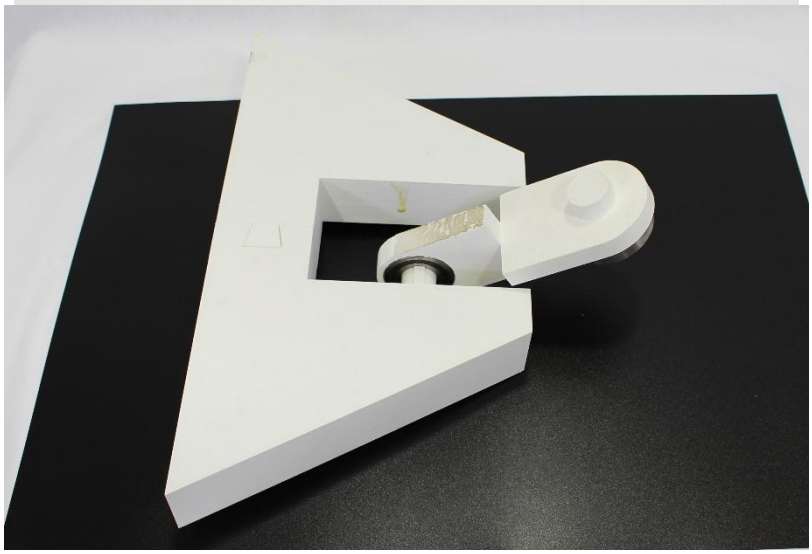

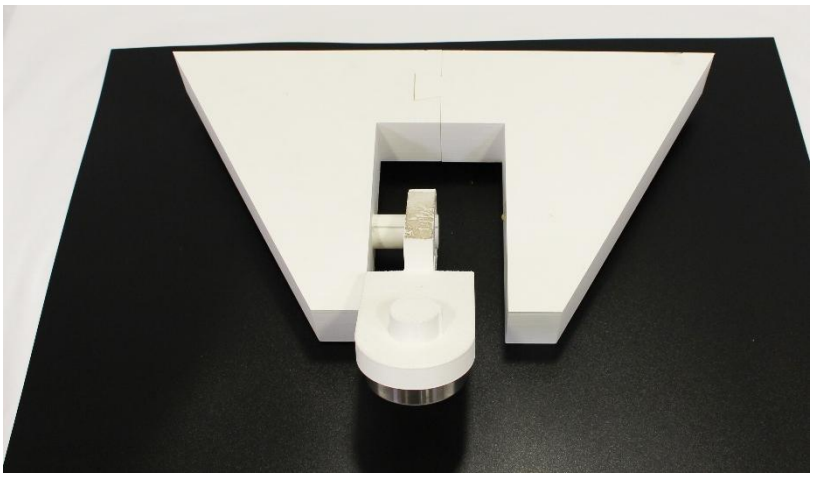

Figure 6.7-102 Yaw and pitch rotation check of Dual Axis one way bearing systems- mark 3- assembly type 3

This concludes the appendices supporting this research. The supplementary materials provided here are intended to complement the discussions in the main chapters and offer additional technical and visual clarification if and when needed. Furthermore these could be of reference for Future researches.

Mechanical Joineries for Deployable Reciprocal Shells Through Auxetic Behaviour (DR STAB)

Surendar Jayachandran
[0009-0003-1565-5384]

Supervised by:

Prof. Charles Walker [0009-0000-3307-7301]
&
Prof. Dermott Mcmeel [0000-0002-3790-3444]

A thesis submitted to Auckland University of Technology in fulfilment of the requirements for the degree of Doctor of Philosophy (PhD) - 2025